

Alma Mater Studiorum – Università di Bologna

DOTTORATO DI RICERCA IN

CHIMICA

Ciclo: XXXII

Settore Concorsuale: 03/C1

Settore Scientifico Disciplinare: CHIM/06

**GOLD CATALYZED FUNCTIONALIZATION OF ALKYNES AND
ALLENAMIDES**

TITOLO TESI

Presentata da: JUZENG AN

Coordinatore Dottorato

Supervisore

Prof. DOMENICA TONELLI

Prof. MARCO BANDINI



Esame finale anno 2020

Acknowledgments

At this meaningful moment, I wish I could present my grateful to my supervisor Prof. Marco Bandini for his kind guidance during the whole PhD research work and also China Scholarship Council for the funding support. In the past three years, there are many thing and feeling which are worth to memorise and I do not even know where to start now. As a PhD candidate, staying in lab almost occupied most of my time. In the lab, I met a lot of difficulties about my research work and I am greatly thankful for the guidance and encouragement from Prof. Marco Bandini. And I also have to appreciate the help from my boss when I am in trouble out of the lab. Thank you very much.

Besides my boss, I secondly thank for the cooperation with Adriano Parodi on my first research project. You are a very nice guy and I am very proud and happy to have this experience working together. I am also happy you will start your PhD life soon this year and wish you have a nice journey in research life.

Thirdly, I would also want to show my thanks to my second partner Lorenzo Lombardi. I have to say that working with you really is very relax and efficient too. I am proud of you and wish you a great and lucky PhD life in our group. In addition, thanks you and Alessandro Cerveri for helping me to enjoy Italy life and culture very much. It is necessary to mention that Alessandro Cerveri is a really funny and friend guy. I also want to show my respect and thanks to you about your accompany.

In addition, I need to thank Riccardo Pedrazzani for your help on the successful synthesis of new chiral catalyst and you impressed me a lot. I wish you also have a great PhD life in the next three years in our group.

Moreover, I am proud of the cooperation with Prof. Carlos Silva Lopez, Prof. Magda Monari, Dr. Stefano Grilli and Dr. Marta Casti ãeira Reis. I am also thankful for their contribution on the corresponding work.

In the meantime, I also want to give my thanks to Dr. Yang Liu, Dr. Lucia Ferrazzano, Dr. Giulia Martelli, Junwei Zhao, Demetra Giuri, Dario Corbisiero and Dr. Michele Anselmi for their kind help during the stay in Bologna. I also felt very pity that the time length with Dr. Assunta De Nisi and Elisabetta Manoni is very short. I will memorise the interesting moment of staying with all of you. At the same time, I appreciate the kind remind of wearing the glass in the lab from Prof. P.G. Cozzi in the past three years.

Moreover, I want to give my thanks to the funding support from Marco Polo program from chemistry department of Bologna University. I spent a grateful time in the group of Prof. David Procter in Manchester University. Besides Prof. David gave me strong guidance on the SmI_2 induced cascade reaction, all the colleagues in this group are very nice and helped me a lot and I really want to tell you all that I am very grateful and happy to meet you. And I really wish to read more and more promising work from you. Good luck to your life and research in the future.

I am proud of being in Bologna University and working with you everyone together. I wish chemistry department become more and more strong and competitive in the world.

At last, I really want to give my thanks to my family and all my good friends for their generous supports and respect for everything in my whole life. Thank you all for your company and encouragement and offering me a very love life no matter what happens. I am proud and grateful to have you around me.

Abstract

The gold(I)-catalyzed chemoselective dearomatization of β -naphthols is reported through a straightforward approach via [3,3]-sigmatropic rearrangement /allene-cyclyzation cascade processes. Easily accessed naphthyl-propargyl ethers and derivatives in this work are employed as starting materials. Delightfully, an array of dearomatized dihydrofuryl -naphthalen-2(*1H*)-ones featured densely functional groups are obtained in high yields (up to 98%) in 10 min reaction time under extremely mild reaction conditions like reagent grade solvent and exposure to air. The potential of accessing to high enantioselectivity on the dearomatized dihydrofuryl-naphthalen-2(*1H*)-ones is also approved by the good ee (65%) relying on (*R*)-xylyl-BINAP(AuCl)₂. In addition, complete theoretical elucidation of the reaction pathway is also proposed which addresses a rationale for essential motivation such as regio- and chemoselectivity.

Moreover, an efficient gold catalyzed intermolecular dearomatization of substituted β -naphthols with allenamides is presented here. PPh₃AuTFA (5 mol %) approves the efficient dearomatively allylation protocol under mild conditions and exhibits high tolerance on substrates scope (24 examples) in good to excellent yield accompanied with high regioselectivity and stereoselectivity. Moreover, the synergistic catalytic system also highlight the synergistic function between the [PPh₃Au]⁺ (π -acid) and TFA⁻ (Lewis base). At last, a new chiral BINOL phosphoric acid silver salt is successfully synthesized and used as the chiral counter anion, which strongly promotes the enantioselectivity (up to 92%).

At last but not least, crucially, SmI₂ induced enantioselective formal synthesis of strychnine, a complex alkaloid and a classical target used to benchmark new synthetic methods is developed. Building on Reissig's formal synthesis of racemic strychnine, we propose that ketoester will undergo an enantioselective radical cascade in the presence of an optimised chiral ligand to give enantiomerically enriched, complex intermediate. The radical cascade will proceed via ketyl radical in which the right hand ester moiety binds to Sm(III). Enantioselective dearomatising radical cyclisation on to the indole unit and further ET will then give organosamarium that is quenched diastereoselectively by the ester to deliver Strychnine in 7 steps. Since it has not been finished, this work is not presented in this thesis.

Table of Contents

1. Introduction	1
1.1. Gold catalysis	1
1.1.1 Gold(I) catalyzed activation of alkene	12
1.1.2. Gold(I) catalyzed activation of alkyne	27
1.1.3. Gold(I) catalyzed activation of allenamide	47
1.2. Catalytic asymmetric dearomatization reaction	60
1.2.1. Dearomatization of Heteroaromatic Compounds	61
1.2.2. Dearomatization of Phenol and Derivatives	74
2. Gold(I) Catalyzed Dearomatization of 2-Naphthols with Alkynes	93
2.1 Abstrsct	93
2.2 Introduction	94
2.3 Experiment and Results	95
2.4 Summary	104
2.5 Reference	105
2.6 Supplement	107
3. PPh₃AuTFA Catalyzed intermolecular Dearomatization of 2-Naphthols with Allenamides	179
3.1 Abstrsct	179
3.2 Introduction	180
3.3 Experiment and Results	181
3.4 Summary	188
3.5 Reference	189
3.6 Supplement	191
4. Conclusion	243

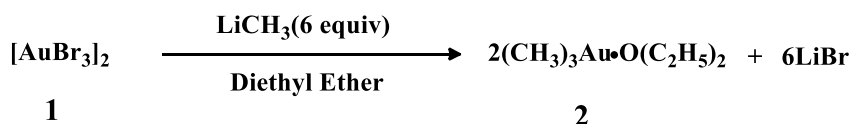
Abbreviations

Ac	Acetyl	bis(trifluoromethyl)phenyl]borate	
Ar	Aryl	NHC	Nitrogen-heterocyclic carbene
Ad	Adamantyl	Oct	Octyl
Bn	Bencyl	Piv	2, 2-dimethylpropanoyl
Bz	Benzoyl	PMP	<i>p</i> -Methoxyphenyl
<i>t</i> Bu	tert-Butyl	Ph	Phenyl
Boc	tert-Butyloxy carbonyl	RT	Room temperature
Cy	Cyclohexyl	T	Temperature
Cbz	Carboxy benzyl	Ts	Toluenesulfonyl
COD	1,5-Cyclooctadiene	Tf	Trifluoromethanesulfonate
Dr	Diastereomeric ratio		
dppm	dis(diphenylphosphino) methane	Tol	Tolyl
DMF	<i>N,N</i> -Dimethyl formamide	TES	Triethylsilyl
EDG	Electron donating group	TFE	Trifluoroethanol
EDG	Electron donating group	TFA	Trifluoroacetic acid
EWG	Electron withdrawing group	NTf	bis(trifluoromethane sulfonyl)imide
Ee	Enantiomeric excess	THF	Tetrahydrofuran
Et	Ethyl	THP	Tetrahydropyran
HOMO	Highest occupied molecular orbital	TIPS	Triisopropylsilyl
IPr	[1,3-bis(2,6-Diisopropyl phenyl)imidazol-2-ylidene]	TMS	Trimethylsilyl
L	Ligand		
LUMO	Lowest unoccupied molecular orbital	TBAF	Tetrabutylammonium fluoride
MS	Molecular sieves	TBDPS	tert-Butyldiphenylsilyl
Me	Methyl		
MOM	Methoxymethyl		
NaBARF	Sodium tetrakis[3,5-		

Introduction

1.1. Gold catalysis

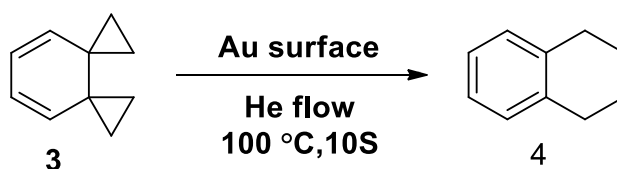
Gold has already been used as a member of monetary systems all over the world thousand years ago relying on its various advantage such as its stability, plasticity and rarity. On the other hand, gold also was used as decoration and medicine^[1] since its beauty and nontoxicity. In this trend, gold is not considered to be a transition metal catalyst in chemistry world as inertness of elemental gold. However, the chemical character would be greatly different when elemental gold exists in the form of ion rather than atom. Actually, gold catalyst^[2] has been used as a greatly important catalyst followed with other noble metal catalyst^[3] since last century and showed their promising ability in synthetic chemistry. In 1943, H. Gilman group^[4] firstly synthesized the trimethyl gold(III) compounds in diethyl ether with tribromogold **1** and methylithium (**Scheme 1**). This work clearly proved that organogold complex could be synthesized in the lab. However, it can not exist for long time even at -40 to -35 °C as the ether donor ligand was not sufficient to stabilize complex. To isolate the stable organogold compound, phosphine^[5] and nitro donor^[4b] ligands were used and tested.



Scheme 1. synthesis of organocatalysis

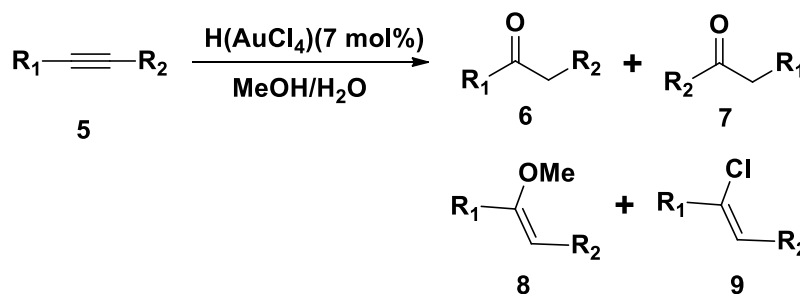
Fortunately, the stable organogold was isolated and could be preserved easily even at room temperature. Under this encouragement, various gold compounds^[6] were synthesized successfully which made the strong foundation for the further development in synthetic chemistry. However, even various kinds of gold compounds were prepared successfully in the lab, gold catalysis was mainly focused on heterogeneous catalysis such as the oxidation of carbon monoxide^[7] and the reduction of nitrogen monoxide with carbon monoxide and hydrogen to give nitrogen, carbondioxide, and water. In 1976, De Meijere group reported the heterogeneous gold catalyzed aromatization^[9] of the dispirocycle **3** to afford tetrahydronaphthalene **4** at 100 °C in few seconds (**Scheme 2**). Until the end of 20th century, only about 2% papers were about homogeneous gold catalysis among 230,000 papers on gold catalysis.^[10] Electron distribution of gold is $[\text{Xe}]4f^{14}5d^{10}$

$6s^1$ and gold(I) and gold(III) are formed via removing one and three electrons respectively (oxidation process). For homogenous gold catalysis, the investigation of gold catalysis was certainly focused on Au(I) and Au(III) catalysts with studying the property respectively. In 1976, C. Barry Thomas group^[11] firstly reported the gold(III) catalyzed hydrochlorination of alkyne derivatives (**Scheme 3**). Even though he got four major products



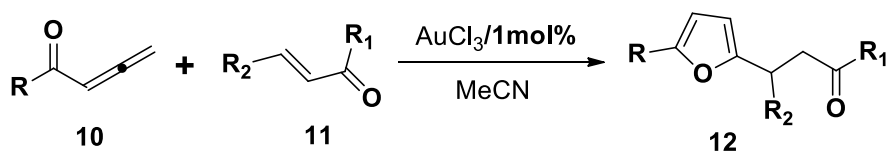
Scheme 2 aromatization transformation

which due to the low regioselectivity and various competence between four nucleophiles in this condition. This work clearly approved the property of gold catalyst being an electrophile. Soon after, in 1987, K Utimoto and H Nozaki^[12] extended the research to intramolecular activation of alkynes with other kind of nucleophile like amino group.



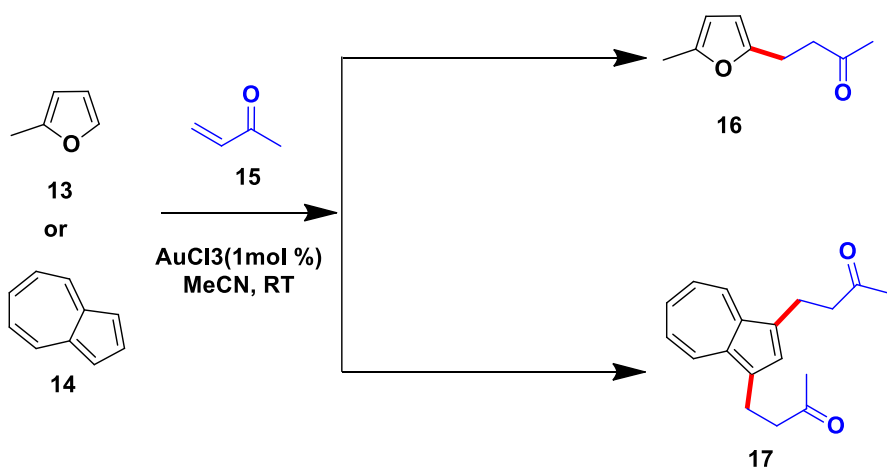
Scheme 3 alkoxylation of alkyne

Besides alkyne substrate, the other π -electron rich compound allene was also considered as the suitable candidate for gold(III) catalyst. In 2000, S. K. Hashmi^[13] group successfully obtained the furan product **12** through cyclization and Michael addition between allenyl ketones **10** and α,β -unsaturated ketones **11** (**Scheme 4**). Actually, this reaction has been reported catalyzed by Ag^[14] and Pd(II)^[15]. However, the result showed that gold gave better activating ability and the condition with gold(III) was more moderate at room temperature with lower loading amount of gold due to its Pd(II)-like d8 orbital and same electron attribution in the out sphere like Ag(I). In addition, gold(III) could also be used to obtain the functionalization of arene compounds via



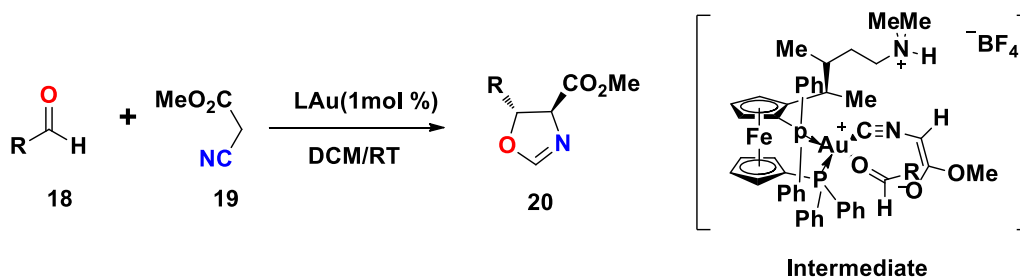
Scheme 4 synthesis of furan

activating C-H bond and Michael addition reaction. In 2003, A.S.K. Hashimi group^[16] applied gold(III) catalyst to functionalize the electron rich arene like furans **13** and azulene **14** with vinyl ketone to afford compounds **16** and **17**, respectively (Scheme 5). In this work, acetonitrile guaranteed the reaction to choose the functionalization pathway selectively rather than other typical decomposition and polymerization reactions, especially for furan compounds.



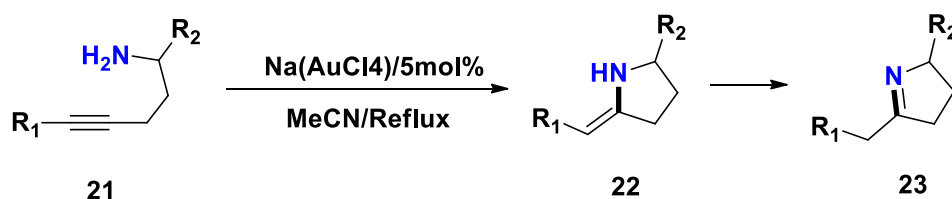
Scheme 5. C-H activation

On the other hand, the first landmark in gold(I) catalysis was reported by Ito and Hayashi^[17] group in 1986. Aldehydes **18** and isocyanoacetate **19** were activated via organogold catalyst which underwent the intermediate conformation (Scheme 6). Ferrocenylphosphane-gold(I) complex showed promising catalytic reactivity in this transformation even without any assistance from additives. In the meantime, the ligand^[18] also approved its function on adjusting the property of



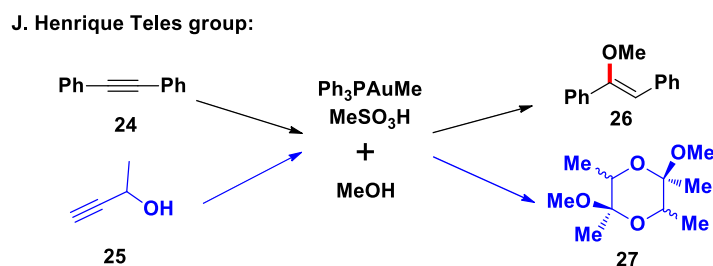
Scheme 6 Au(I) catalyzed activation on ketyl group

gold cation. In 1991, K. Utimoto published their research^[15] on the preparation of 2,3,4,5-tetrahydropyridines **22** from 5-alkynylamines **21** via gold(III) salt (**Scheme 7**) under reflux conditions. However, the study^[16] by T. E. Muller group showed that Au(I) was more efficient than that Au(III) for the title protocol. The conversion with the cationic $[\text{AuCl}(\text{triphos})](\text{NO}_3)_2$ catalyst was up to initial TOF of 212 h^{-1} in refluxing acetonitrile.



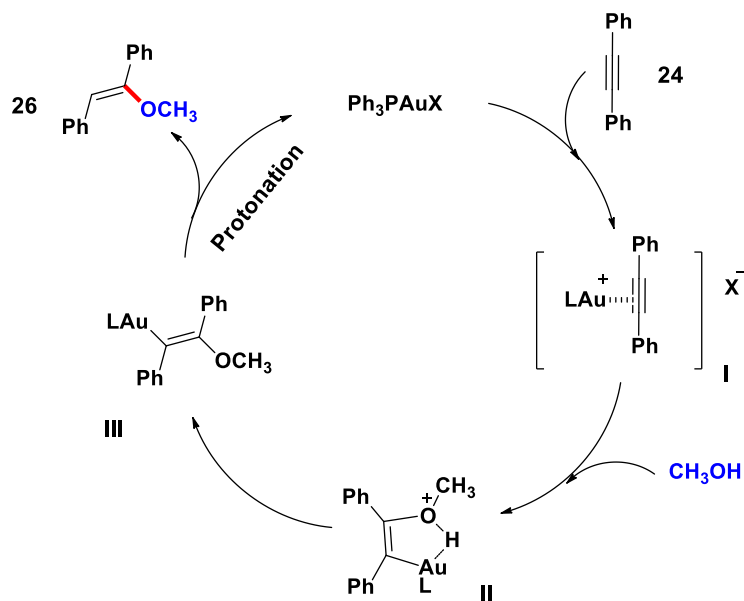
Scheme 7 amination of alkyne

In 1998, J. Henrique Teles group^[17] showed that gold could transfer the alkyne compounds into an nucleophilic substrate as a π -ligand. (**Scheme 8**). Then, nucleophilic attack of the alcohol to the sp hybridized carbon of alkyne **24** from the back face delivered the product **25**. On the other hand, when another nucleophile was introduced on the substrates **26**, the reaction would be motivated to sequent addition step to afford product **27**. In comparison to mercury(II)^[18] and Au(III)^[19] mediated water/methanol addition to unactivated alkynes, Au(I) showed its various advantages such as the lower loading (TON up to 105, TOF up to 5400 h^{-1}) and higher thermal stability.



Scheme 8 alkoxylation of alkyne

In the meantime, this work discovered the considerable influence from phosphorous ligands. As a matter of fact, when electron deficient ligands were used, the activity of gold catalyst increased correspondingly. In addition, stabilizing anions also proved to be a vital factor regarding the catalytic activity of gold complex. Based on the above results, the authors proposed the catalytic model proposed in **Scheme 9**.^[20]



Firstly, they proposed that gold cation will coordinate to **24** in solution delivering the intermediate **I**. Then nucleophilic methanol attacked this intermediate via interacting with gold center at first in syn-conformation. This interaction then went through electron transfer and gave the gold compound **III** which would be quenched by protonation process. At last, product **26** was synthesized and gold complex restored in solution.

Since then, the study on gold(I) catalysis has attracted chemists' attention all over the world. In particular, across years 2000, the number of published paper regarding gold catalysis faces a sharp increase (**Figure 1**).^[21]

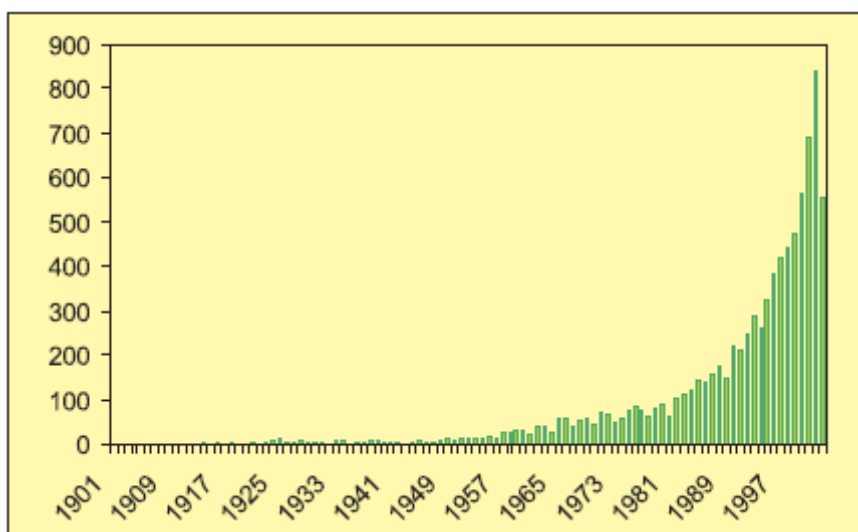


Figure 1. Total number of publications on gold catalysis per year

Under this background, to figure out the way gold(I) worked also became the first mission for chemists so that the application area of gold(I) could be extended in more fields. On this work, assisted by theoretical chemistry, F. Dean Toste group^[22] and Alois Furstner^[23] group shed the light into the essential character of gold(I) which provided strong guidance on the new transformation in synthetic chemistry via gold catalysis which enriched the accesses to valued compounds^[24].

As showed above, phosphine ligand plays a very important role on the activity of gold cation^[18]. In 2003, P. Schwerdtfeger group^[25] did the study on stability of the gold(I)-phosphine complexes using quantum theoretical methods. This study approved that the most stable coordination number of gold(I) is two and further coordination will become weaker. The comparison of crystal structure of two relative gold complexes (**Figure 2-3**) provides detailed information. $[\text{Ph}_3\text{PAuCl}]$ **28** exists in linear ($\alpha=179.6^\circ$) conformation while the bond length of Au-P and Au-Cl are 2.235 Å and 2.279 Å respectively.

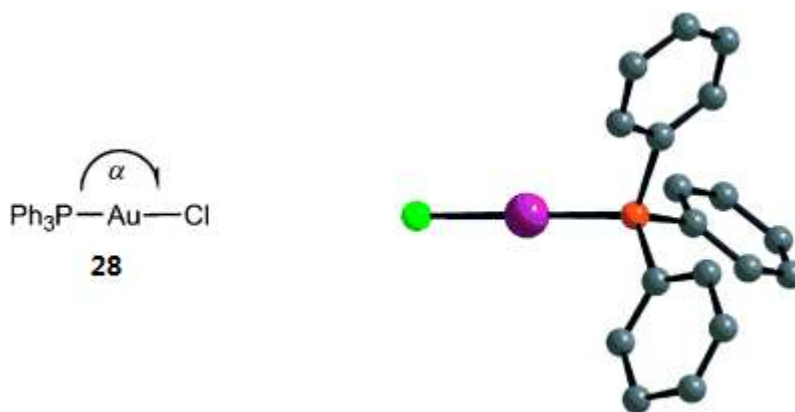


Figure 2. $\alpha=179.6^\circ$; $r_{\text{Au}-\text{P}}=2.235 \text{ \AA}$, $r_{\text{Au}-\text{Cl}}= 2.279 \text{ \AA}$

If $[\text{Ph}_3\text{PAuCl}]$ coordinates another molecule of Ph_3P , the bend of P-Au-Cl will happen from repulsion of second Ph_3P ligand. The angle of P1-Au-Cl becomes from 179.6° to 115.1° and another angle of P2-Au-Cl is 108.1° .

However, the difference of strength between two P-Au bond is very large which is presented clearly via the length of P-Au bond which are $r_{\text{Au}-\text{P1}}=2.230 \text{ \AA}$ and $r_{\text{Au}-\text{P2}}=2.313$ respectively. The longer length bond is weaker which means the third ligand only coordinated to Au(I) loosely^[25].

On the other hand, the bond length of Au-Cl also increases from 2.279 Å to 2.526 Å which decreases the bond strength on the other hand. Moreover, when another *s*-donating ligand (*i.e.* PCy₃) which is added, chloro anion would be replaced by forming the linear Cy₃P-Au-PCy₃ (Figure 4).^[26]

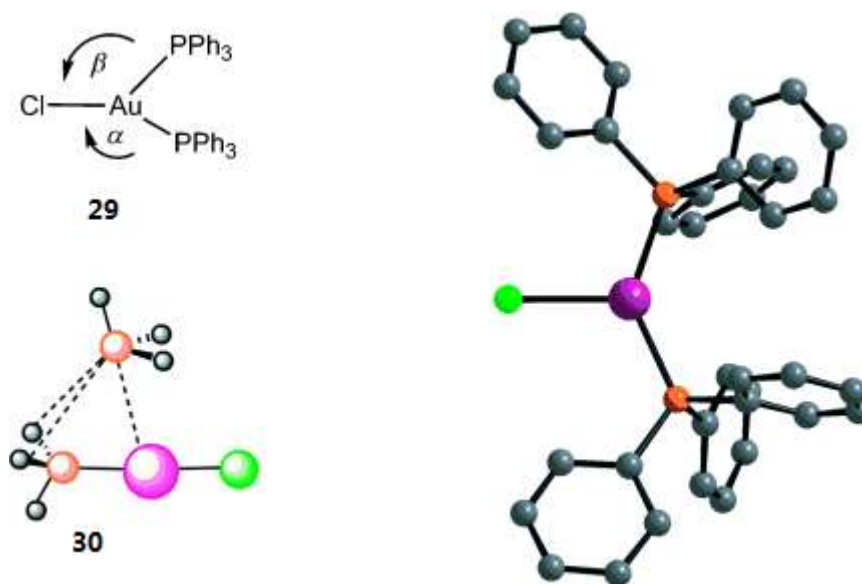


Figure 3. $\alpha = 115.1^\circ$, $\beta = 108.1^\circ$, $r_{\text{Au-P1}} = 2.230 \text{ \AA}$, $r_{\text{Au-P2}} = 2.313 \text{ \AA}$, $r_{\text{Au-Cl}} = 2.526 \text{ \AA}$) and comparison with the computed structure of $[\text{AuCl}(\text{PH}_3)_2]$ **30**

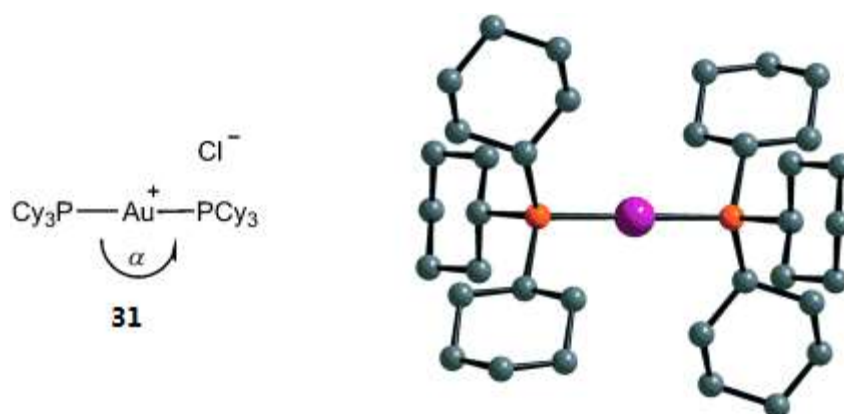


Figure 4. Structure of $[\text{AuCl}(\text{PCy}_3)_2]$ (**31**) in the solid state together with a schematic representation; α

$= 180^\circ$

The relation between structure and function of gold(I) catalyst usually cannot be described separately. Inversely, considering both aspects and their relation has become the research model in chemistry area. Numerous works have verified that gold(I) showed the promising property on activation of alkenes, alkynes and allenes and other π -system. Besides the study on the coordination form which decides the conformation of interacting π ligand, what decides the reactivity of these species also aroused chemists' curiosity. Assisted by theoretical studies on gold^[23,24], the essence of catalytic property is disclosed. Catalytic attitude and unique behavior can be explained based on its electronic configuration. Generally, the bonding model for transition-metal complex interacting π -electron follows the Dewar–Chatt–Duncanson (DCD) model^[27] which is applicable to gold(I) as well. The bond formed between gold(I) and π -ligand is considered as donor-accepter interaction. In this model, π -ligand will form a new σ bond with gold(I) by overlapping the π electron with empty metal orbitals of suitable symmetry. In the meantime, the back-donating process of electron density proceeds from a filled d orbital into an anti-bonding π^* orbital of the corresponding π -ligand.^[27]

In addition, the electrostatic interactions in the total bonding also slowly was figured out by

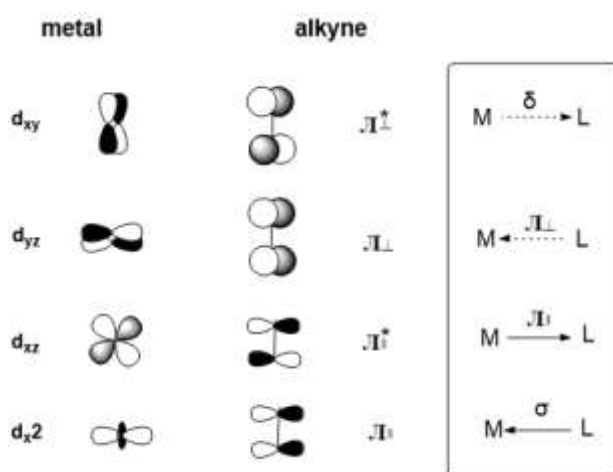


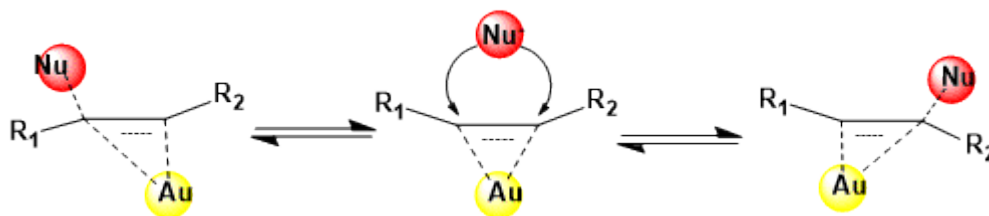
Figure 5. Qualitative orbital diagram showing the interaction between a transition metal and an alkyne ligand^[29]

chemists and computational study with high level of theory approved that almost half contribution on the interaction was donated by electrostatic in nature^[28]. Alois Furstner^[23] described the details of electronic structure of the bond of transition metal with alkynes. The bond formation benefited from four principle components (**Figure 5**). The in-plane π_{II} orbitals are responsible for a

σ -symmetric $M \leftarrow L$ donation and the anti-bond orbitals of $\pi_{||}$ are ready for $M \rightarrow L$ electron back-donation. On the other hand, the orthogonal, out-plane π_{\perp} orbitals then engage in $M \leftarrow L$ π donation and an occupied d orbital of the metal and the empty anti- π_{\perp} orbital of alkyne interacts to form an additional $M \rightarrow L$ back donation which is only weak overlap so that lead to a short time contribution to the bonding.

In addition, the analyzed result is supported by higher level computational methods which strengthen this electron structure model strongly. For example, with Au^+ -acetylene complex ($[Au^+(C_2H_2)]$), the σ interaction contributed largest electron density to the orbital term which is 65% while other three components contributed 27%, 7%, 1% respectively. This data may conclude that π -ligands are strong two-electron σ donor but weak π accepters for Au(I).

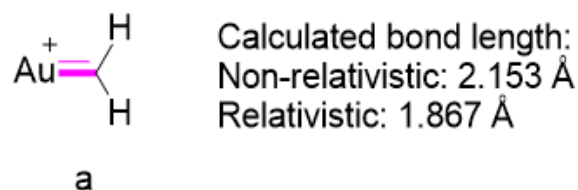
When the electron density shift between gold(I) and π -ligand, the π -ligand goes through distortion to be ready for the nucleophile. Hence, more detailed information about this transition state such as metal-alkyne needs to be dug more. Now it gets agreement in chemistry community on gold that metal fragment is flexible and walking along the axis of π electron functional group back and forth (**Scheme 10**) and the nucleophile attacked from the opposite site of gold. During this process, gold(I) cation dived into the π -electron sink, as “ π acid”, and causes the change of the bond length which becomes longer and lower energy barrier of rotation of the ligand around gold-ligand centroid axis. In the meantime, the π ligand is transformed from nucleophile to electrophile resulting in a new platform to form new chemical bonds by reacting with another nucleophile.



Scheme 10 Schematic representation of the redistribution of electrons upon nucleophilic attack onto an alkene bound to a pacidic metal template

In the meantime, this “soft” character of large and polarizable gold(I) makes itself more affinity to substrate and provides the milder reaction condition compared to Brønsted acid. The reason why

gold(I) cation exhibits so brilliant Lewis acid property should belong to a relatively low-lying lowest unoccupied molecular orbital. What is more, compared with other group 11 metals, gold(I)



Scheme 11. Au-alkylidene

exhibits more electron affinity as the relativistic contraction of the valence 6s and 6p orbitals. Besides these characters, the study which has been done by Irikura & Goddard discovered that Au-CH_2^+ not only featured the σ bond character, but was it revealed the multiple bond property which the π bond is formed from backbonding from Au^+ to methylene (**Scheme 11**)^[30] and the model is showed in **Figure 6**. The calculation^[31] on gold(I)-ethylene and gold(I)-ethyne complexes showed contrary results toward Dewar–Chatt–Duncanson (DCD) model bonding because the energy of antibonding orbitals is so high that it is not suitable to receive the backdonating electron density. However, the lower-energy non-bonding p orbitals become a more competitive candidate to overlap with the filled 5d orbitals of gold(I). In this mode, another

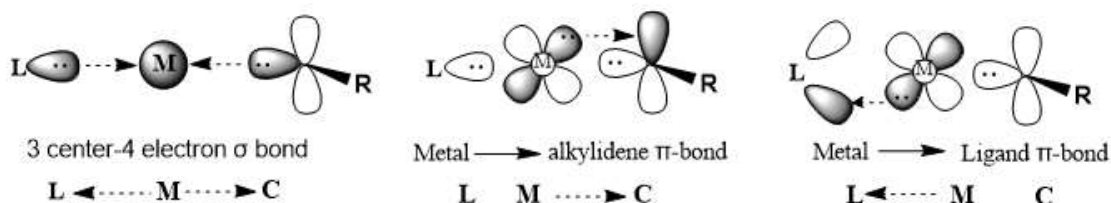
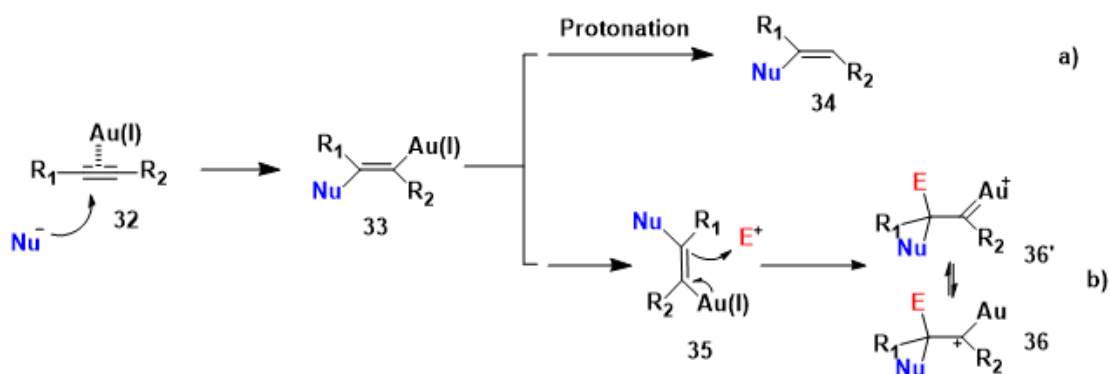


Figure 6. Model of important bonding interactions in L-Au(I)-CR_2 species

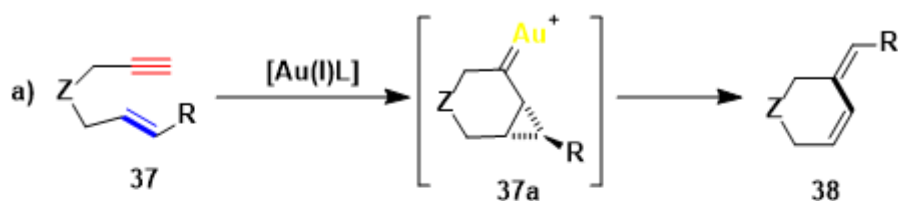


Scheme 12. a) protonation. b) The Au 5d electrons back-bond into conjugated empty carbon p orbitals.

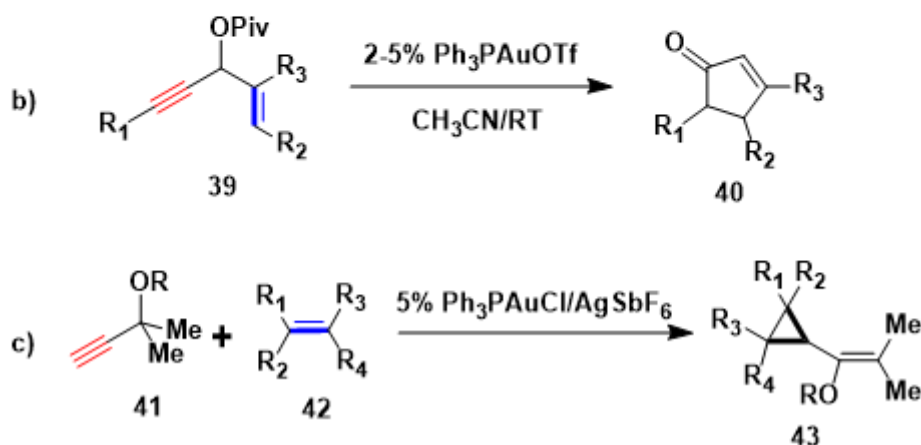
reaction pathway came into chemists' horizon which provides various transformation opportunities in advanced organic chemistry (**Scheme 12b**).

The gold-alkyne intermediate **33** can proceed through two possible pathways, the direct protonation process to achieve addition reaction or electron back-donation into conjugated empty carbon *p* orbitals which formed Au-C π bond **36'** accompanied with formation of a new electrophile.

Antonio M. Echavarren, 2004



F. Dean Toste, 2005



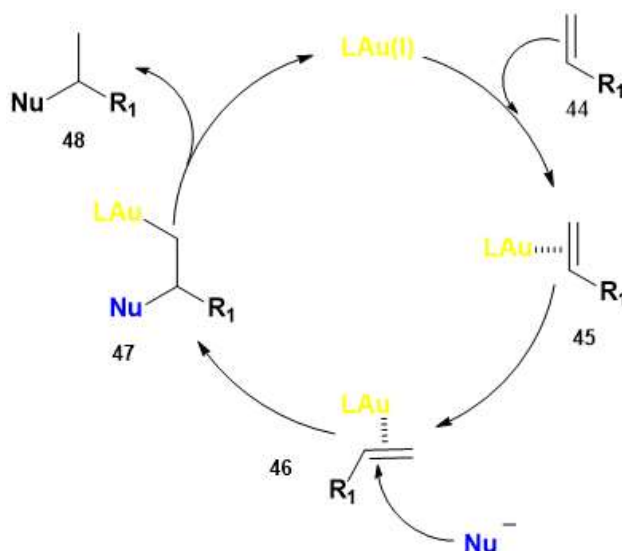
Scheme 13 example of application of carbene gold intermediate

Intermediate **36** was studied that it exists in two conformations between gold-stabilized carbocation and gold-stabilized carbene^[32] which could be adjusted by modulating the adjacent vinyl group and ligand. Based on these studies cyclization and isomerization of enynes have been published (**Scheme 13**) in the Echavarren group,^[33] the Furstner group^[34] and the Toste group^[35] which strengthened gold-carbene intermediate theory.

1.1.1 Gold catalyzed activation of alkene

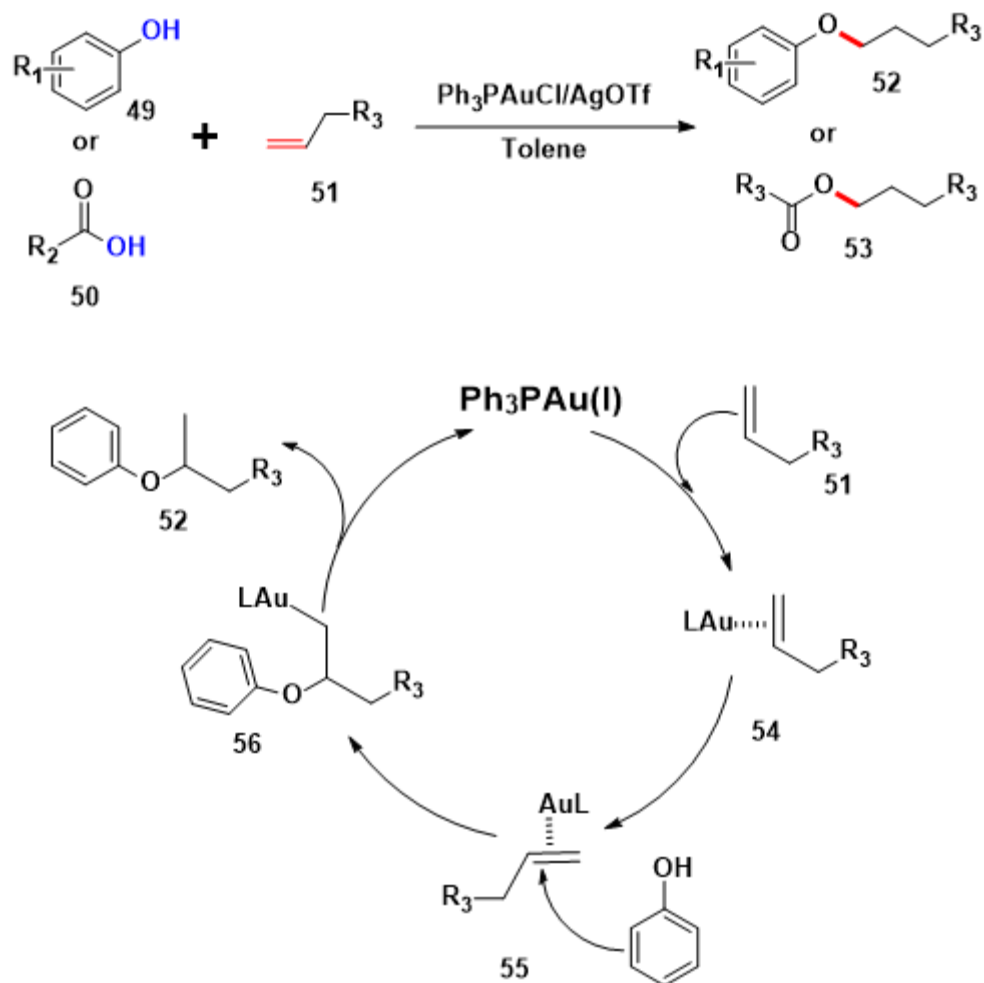
Alkene compounds have shown its valuable application being an functional unite in the synthesis of natural and pharmaceutical compounds via metal^[36] and organo- catalysis^[37] based on the electron rich character. Along with the application of Pd, Rh on activation of alkene functional groups, gold catalyst showed its advantages like mild reaction conditions, high efficiency and high tolerance toward hash reaction conditions.

The alkene function group contains a π -bond and it could easily coordinate to gold which has been proved a great soft π acid. In this process between gold and the π ligand, alkene could be induced into electrophilic property which could accept the attack of nucleophile which is exhibited in **Scheme 14** in linear model. Then the gold-alkyl intermediate **48** would go through protodeauration process by releasing gold catalyst to recycle in the next catalytic cycle.^[38]



Scheme 14. Model of activation on alkene

In the past decades, various nucleophiles have been developed all over the world triggered by gold catalyst to form new C-X (C-O, C-S, C-C and C-N) bond and construct more novel molecules^[39]. The initial study on the activation via gold catalyst to form the C-O bond was accomplished in C-He group^[40]. In this work, *in situ* catalyst $\text{Ph}_3\text{PAuCl}/\text{AgOTf}$ expressed its unique ability compared to triflic acid, ZnOTf_2 and AgOTf on the activation of alkene and achieved the Markovnikov-like addition of phenols and carboxylic acids to C=C under mild reaction conditions. Besides high yield and high tolerance on functional group, this catalytic system could also be applicable on

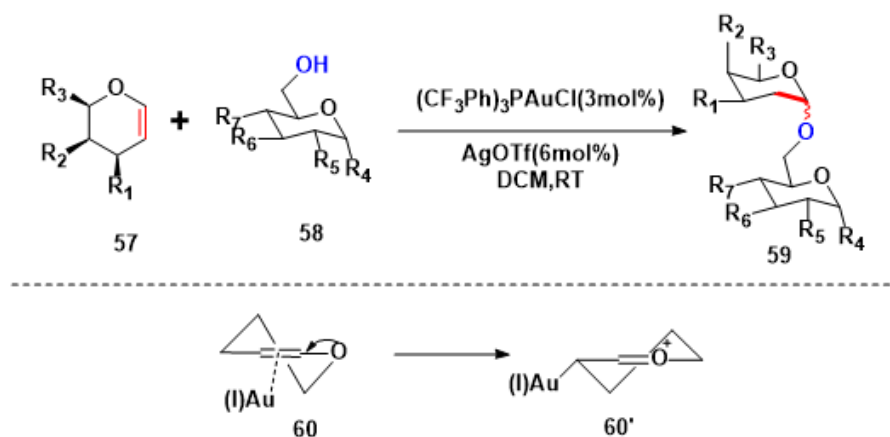


Scheme 15. Alkoxylation of alkene and mechanism

intramolecular reaction. In addition, this promising result could be supportive on the proposed gold catalyzed activation of alkene (**Scheme 15**). In 2017, M. Carmen Galan group^[41] successfully reported the gold(I) catalyzed directly stereoselective synthesis of deoxyglycosides with glycals **58** (**Scheme 16**). This work presented the further potential application on the functionalization of more challenge molecule and approved the potential value on the synthesis of functional compounds.

In this work, [(pCF₃Ph)₃P]AuCl] and AgOTf were used to be the optimized catalyst which could gave high yield and high stereoselectivity on the α carbon. It was worth to notify that the loading and ratio of gold complex and silver salt could change the result greatly. Furthermore, with this catalytic method, the cascade synthesis of di-, tri- and tetrasaccharides could be obtained accompanied with good stereoselectivity and moderate yield. On the other hand, the mechanistic

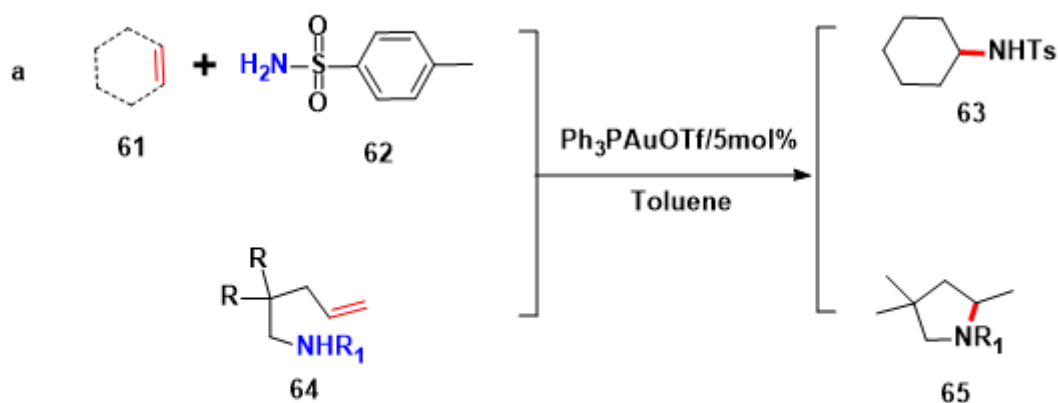
study proposed that the oxygen was involved in a conjugation system with the double bond which formed ketyl group having oxygen Onium **60'**. Then it can accept the attack of alcohol **58** to form



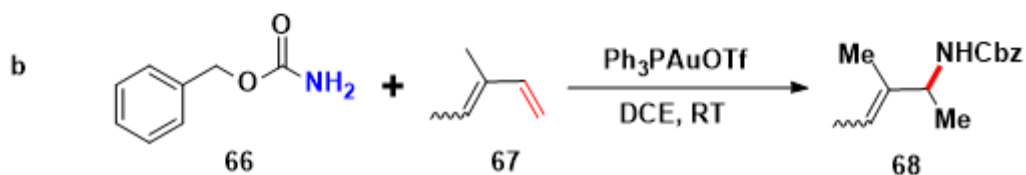
Scheme 16. Synthesis of deoxyglycosides

the deoxyglycosides **59**. On the other hand, constructing C-N bond in efficient and friend method also were developed via gold catalysis. In 2016, Chuan He group^[42] developed the gold catalyzed hydroamination of alkenes (intra and inter) and diene respectively (**Scheme 17**). In the work of activation on alkene, p-toluenesulfonamide **62** was chose to be the nucleophile to construct acyclic

Chuan He, 2006



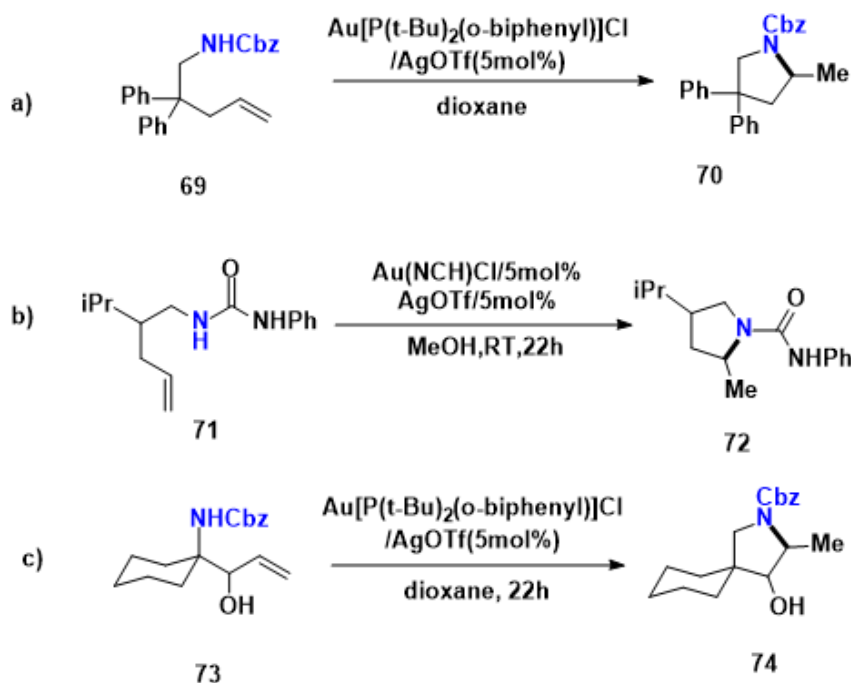
Chuan He, 2006



Scheme 17. Amination of alkene

or cyclic nitrogen-containing molecules which have potential applications in human health. This methodology firstly approved the ability of gold cation to afford C-N bond since the high tolerance of substrate bearing various functional group and wide application in inter and intra hydroamination reaction. In addition, when the alkene substrates were replaced by dienes compounds **67**, benzyl carbamate **66** being the nucleophile, the results were still promising and inspiring (Scheme 17b). Even though the diene substrates are more reactive than alkene compounds, the selectivity arises as a new challenge in front of chemists. However, this catalytic system afforded high selectivity between two double bonds.

Ross A. Widenhoefer, 2006



Ross A. Widenhoefer, 2008

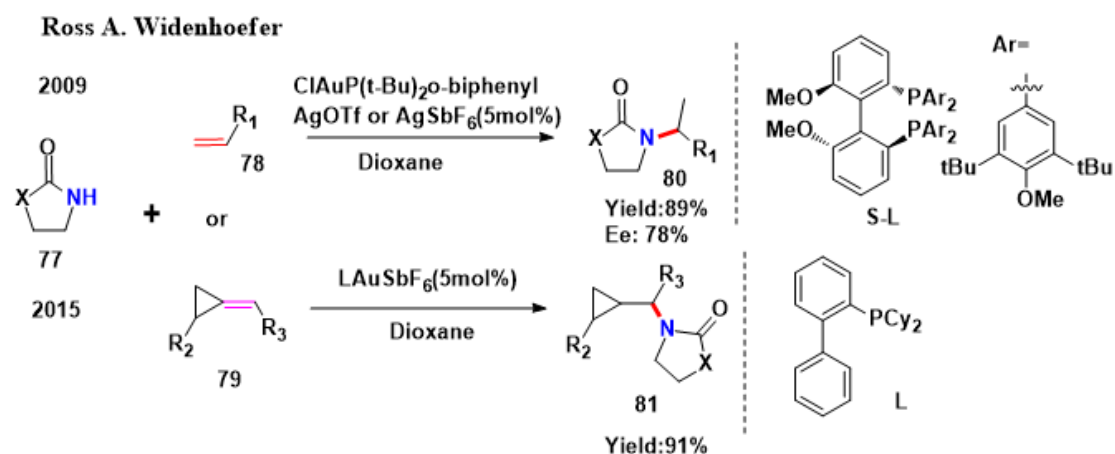


Scheme 18 Intramolecular amination of alkene

In the same year (2006), Ross A. Widenhoefer group^[43] studied the hydroamination of alkene compounds

catalyzed by gold catalysis. He designed firstly alkenyl carbamates **69** as the examination object to form protected pyrrolidines, piperidines, and heterobicyclic compounds **70** assisted by in situ catalysis of Au[P(t-Bu)₂(o-biphenyl)]Cl and AgOTf (5 mol%) in dioxane at 60 °C (**Scheme 18a**). In the meantime, various kinds of substrates bearing harsh substituents were very friend to this catalytic system and offered corresponding product smoothly. Based on this work, they kept working on other studies by adjusting the protection group of nitrogen with ureas **71**, carboxamides **73** and ammonium salts **75** (**Scheme 18 b, c, d**). By adjusting the ligand, promising results could be obtained which meant ligands played very important role to manage the property of gold(I) to fit different substrates.

Besides, Ross A. Widenhoefer group did not stop to explore more applicable hydroamination reaction of olefins. They turned attention on the intermolecular hydroamination with gold(I) catalysis. Firstly, in 2009, cyclic ureas **77** was selected as the nucleophile and the catalytic



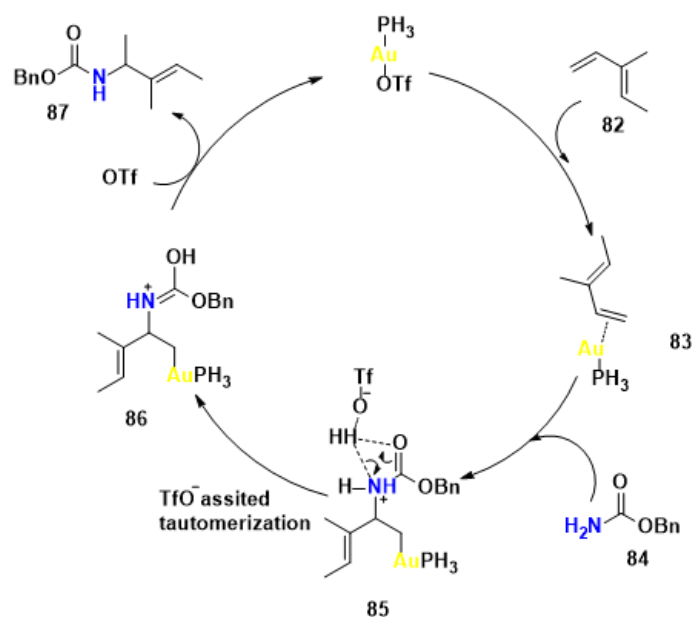
Scheme 19. Intermolecular amination of alkene

condition was based on the previous work using in situ catalysis of Au[P(t-Bu)₂(o-biphenyl)]Cl and AgOTf (5 mol%) in dioxane but at higher temperature (100 °C). In the meantime, the challenge of high enantioselectivity was tackled by designing and examined different phosphine ligand, the result proved that [(S)-4](AuCl)₂ [(S)-L(S)-3,5-t-Bu-4-MeO-MeOBIPHEP] ligand could afford almost 78% ee in this work (**Scheme 19**, 2009).^[44]

Based on the analysis of the above results, the products were all the Markovnikov hydroamination. Widenhoefer developed the alkylidenecyclopropanes which is a kind of attractive substrates for the synthesis of functionalized cyclopropanes owing to the strain-driven reactivity to achieve the

goal that harvesting the anti-Markovnikov hydroamination product (**Scheme 19**, 2015).^[45] Gold complex with **L** ligand and SbF_6^- anion was chosen to be the best catalyst to selectively collect the anti-Markovnikov hydroamination products instead of passing through ring opening process and Markovnikov hydroamination pathway. This work represents both the first examples of the transition-metal-catalyzed hydroamination of an ACP without ring opening and the first examples of the transition-metal-catalyzed *anti*-Markovnikov hydroamination of an aliphatic, non-cumulated alkene compared with previous relative works.

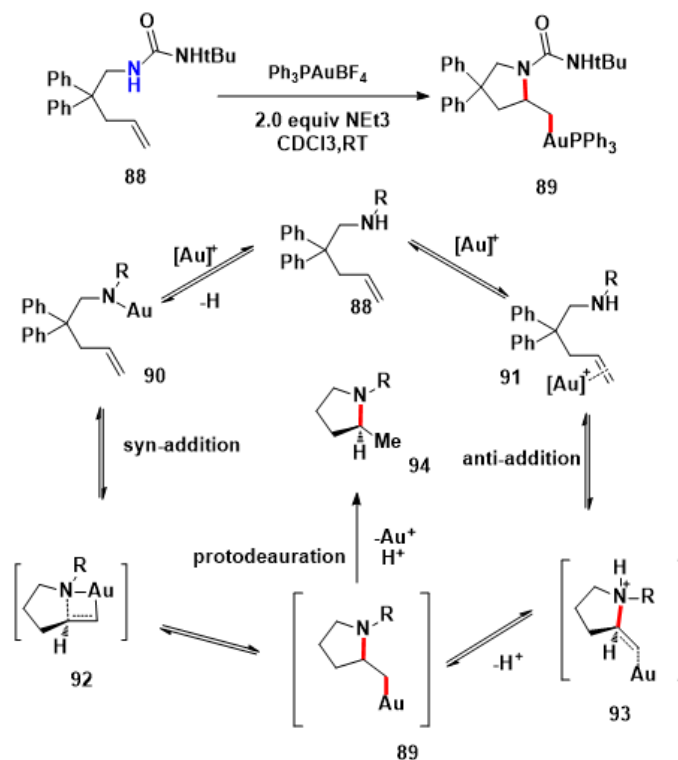
The study of the mechanism on the gold catalyzed hydroamination has been proposed in above promising work, however the role of counteranion was almost neglected in the catalytic cycle. In 2007, Agust Lledos^[46] shed the light and dug more details about the role of counteranion assisted with computational studies in the addition reaction of benzyl carbamate to dienes (**Scheme 20**). Firstly, the OTf^- counter anion would be replaced by the diene ligand and the format of coordination with gold preferred the η^2 -type which only one double bond was coordinated with gold(I). Benzyl carbamate then came to attack the olefin from the back face led to gold-alkyl intermediate **85**. At this step, OTf^- counter anion joined in the next step which assisted the tautomerization to form **86** intermediate which could be quenched during the protodeauration process.



Scheme 20. The function of counter anion

In 2010, F. Dean Toste^[47] successfully obtained the alkyl gold complexes by the intramolecular

aminoauration of unactivated alkenes. It was proposed two possible catalytic pathways including *syn*-addition and *anti*-addition (**Scheme 21**). When aminoauration product **89** was formed, it could



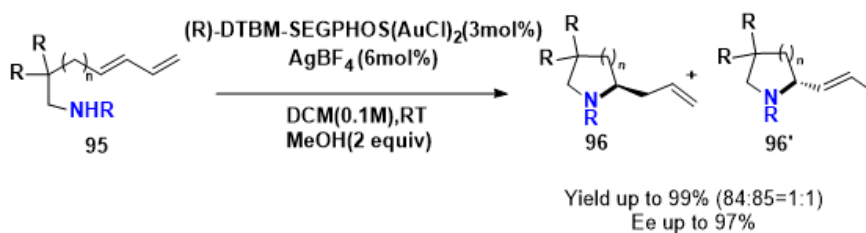
Scheme 21. Synthesis of alkyl gold complex

be isolated or undergo the protodeauration process with external proton source. Between these two possibilities, the experiments provided the convinced experimental evidence for the elementary step of gold-drove nucleophilic addition to olefin. Deuterium-labeling studies and X-ray crystals structure also gave the strong support for the *anti*-addition model of the amino nucleophile to the gold activated alkene. On the other hand, DFT analysis also was consistent with the experiment truth.

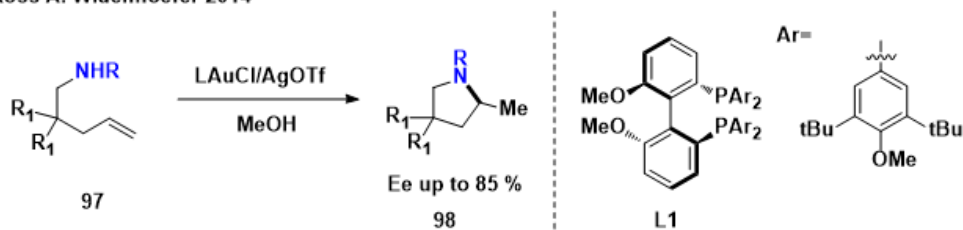
What is more, asymmetric hydroamination reaction of alkene became the other challenge of gold catalysis since the large diameter of gold and the linear coordination style. Efforts have been invested greatly on this area by adjusting the ligand. In 2011, F. Dean Toste^[48] developed regio- and enantioselective hydroamination of dienes **95** with in situ (*R*)-DTBM-SEGPHOS(AuCl)₂ and AgBF_4 in DCM at room temperature. (**Scheme 22**). To control the regioselectivity and enantioselectivity of the reaction, chiral ligand is the very important factor and the other important reason is that the addition of methanol as a cocatalyst which could act as a Brønsted acid when coordinated to the gold catalyst. Soon after, in 2014, Widenhoefer^[49] reported the enantioselective

intramolecular hydroamination of unactivated alkenes **97** based on their previous racemic work by introducing the (*S*)-DTBM-MeO-BIPHEP] ligand and silver tetrafluoro borate (AgBF₄) in methanol. Eventually, the ee was almost 85% which attributed to the chiral ligand and the additives methanol (**Scheme 22**).

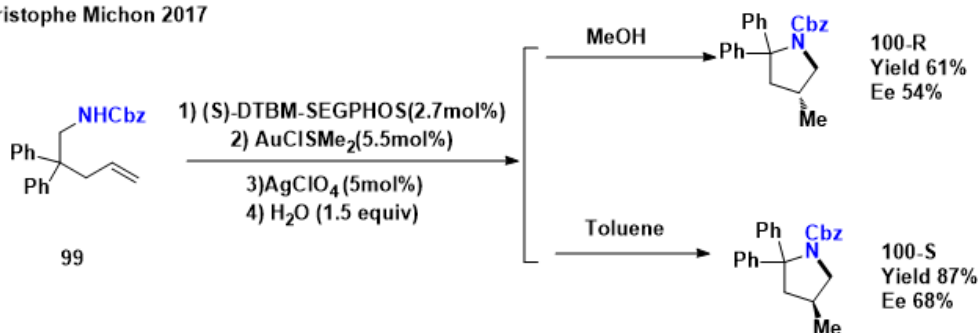
F. Dean Toste 2011



Ross A. Widenhoefer 2014



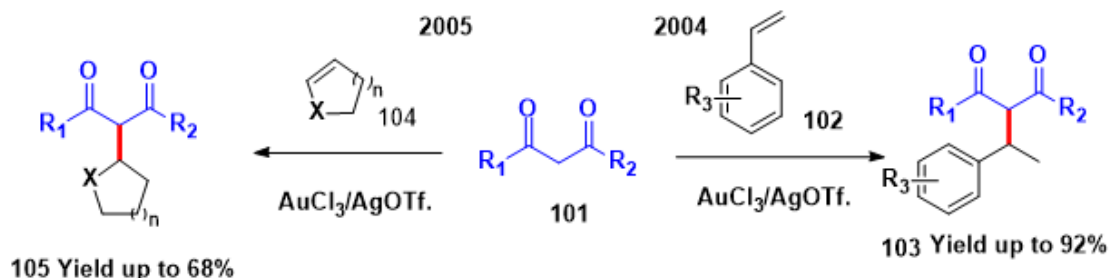
Christophe Michon 2017



Scheme 22

Then in 2017, Michon^[50] realized that using single chiral binuclear gold(I) chloride complex and AgClO₄ can achieve enantioselective control of hydroamination of alkene **99** and afford both enantiomers of the product (**Scheme 22**, **100-R** and **100-S**) by just changing the solvent. All the results obtained above disclosed the clue to design the suitable catalytic system and provided the guidance for the creative work for chemists who worked on gold catalysis in organic synthesis, especially for enantioselective control.

Besides nitrogen nucleophile, carbon could also act as a very useful nucleophile which can form C-C bond combined with activation of alkenes catalyzed by gold catalyst. Actually, compared to nitrogen nucleophile, carbon is less nucleophilic and usually need harsh reaction condition to drive the reaction. Under this reality, more active methylene was chose to be the candidate of carbon



Scheme 23. C-C bond construction

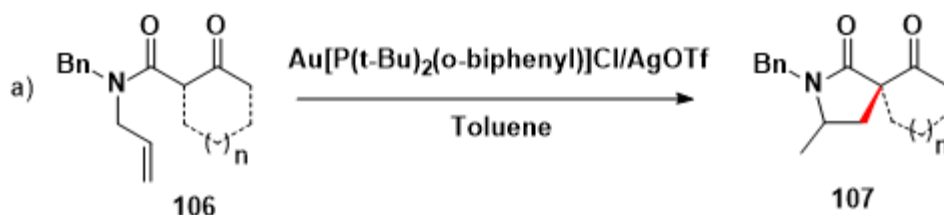
nucleophile firstly. In 2004, Chaojun Li group^[51] originally reported the C-C construction through activation of alkene **102** via gold catalysis and addition reaction of methylene **101** by forming the addition product **103** while the yield was up to 92% (**Scheme 23**). After testing various substrates with this method, AuCl₃/AgOTf showed its high efficiency and high tolerance on the functional group.

Next year (2005), this group^[52] extent this catalytic system to dienes, triene, and cyclic enol ethers (**Scheme 23**) substrate **104** which successfully got high regioselectivity to form the carbocycles and heterocycles **105** through a highly atom-economical carbon-carbon bond formation.

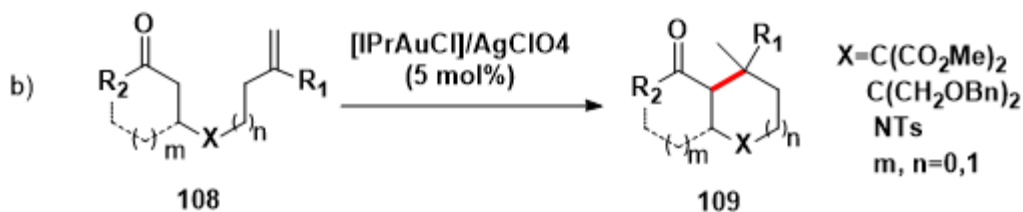
Those two works encouraged chemists to explore more common carbon nucleophile to construct C-C bond with alkene derivatives catalyzed by gold catalyst. In 2007, Chi-Miing Che group^[53] developed intramolecular addition of β -Ketoamide to unactivated alkenes **106** activated by 5 mol % of Au[P(t-Bu)₂(o-biphenyl)]Cl/AgOTf at 50 °C (**Scheme 24a**). Even though all the results approved the value of gold catalysis on the activation of alkenes and construction of C-C bond, the carbon nucleophiles were mainly focused on the activated carbon like 1,3-diketone compounds.

To break this limitation of substrates, in 2011, Chi-Ming Che group^[54] achieved the direct intra-molecular hydroalkylation of unactivated alkenes with α -ketones **108** (**Scheme 24b**). In this work, stronger catalyst of iPrAuCl/AgClO₄ worked very well which belonged to its strong electron deficiency property. In addition, this catalytic system allowed various substituents to be introduced without compromise of decreasing the yield.

Chi-Ming Che, 2007



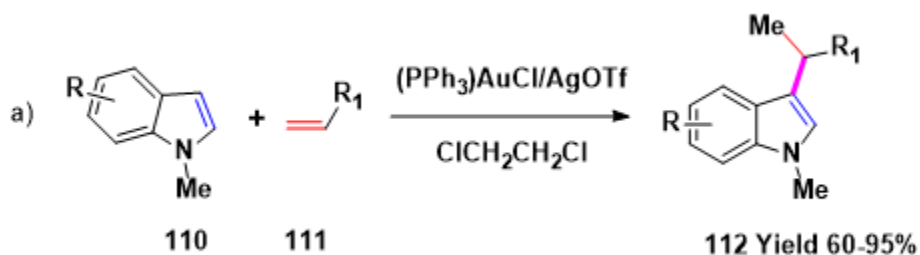
Chi-Ming Che, 2011



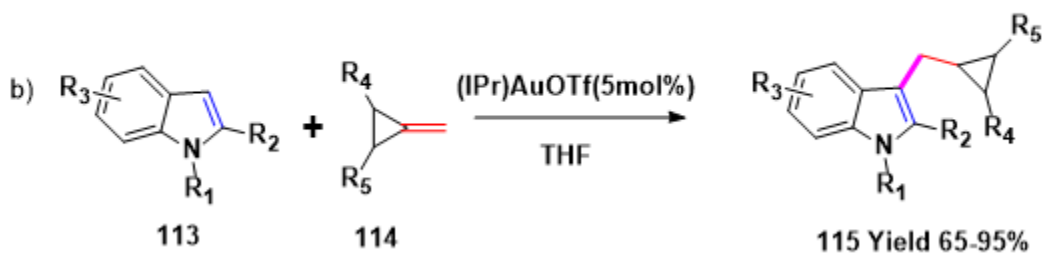
Scheme 24. Intramolecular C-C bond construction

Besides gold catalyzed hydroalkylation of alkenes, construction of C-C on the activation of alkene by gold catalyst can also be achieved through hydroarylation of olefin with arenes compounds. In 2008, Chi-Ming Che group^[55] reported their work of intermolecular hydroarylation of alkenes **111** with indoles **110** at 80 °C in toluene (Scheme 25a). Compared to previous work, this method provided more moderate reaction conditions and surprisingly expanded largely wide scope of substrates (more than 45 substrates).

Chi-Ming Che, 2008



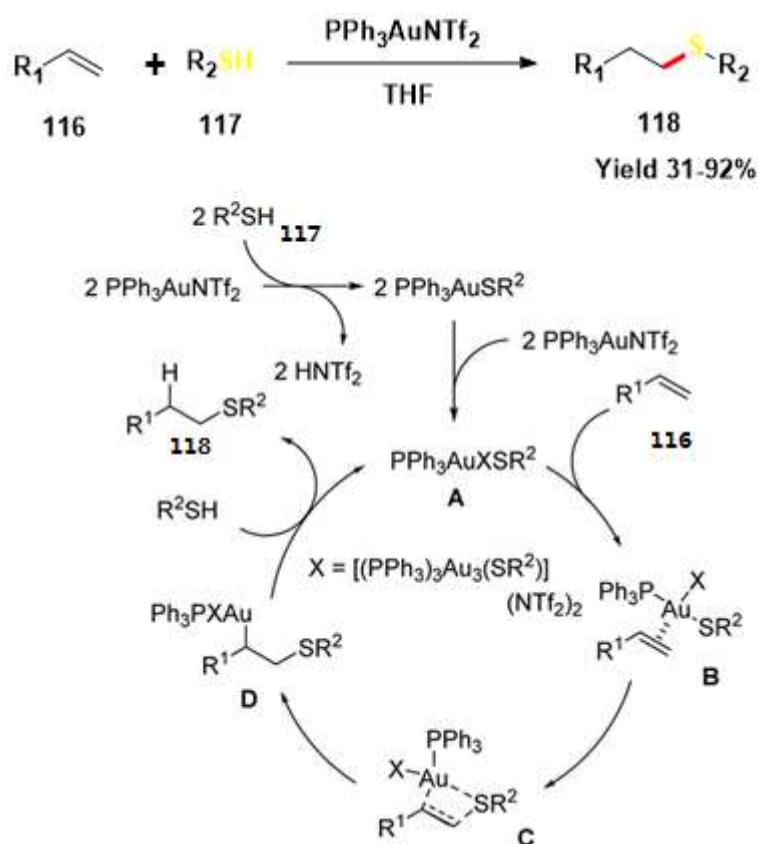
Ross A. Widenhoefer 2016



Scheme 25.

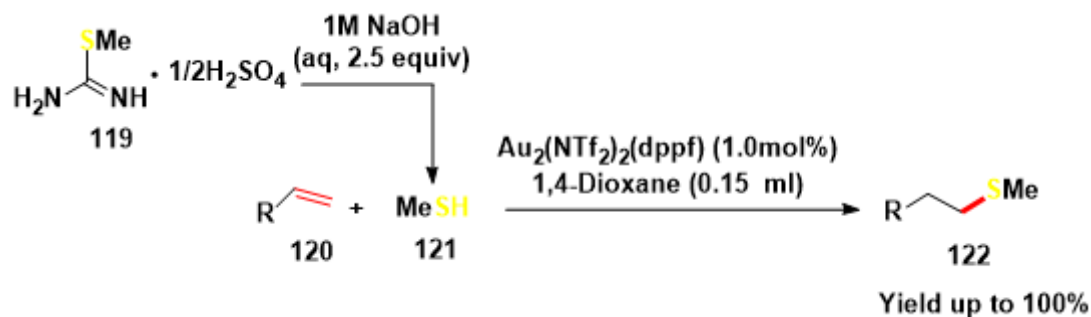
On the other hand, high regioselectivity and promising yield can be obtained. In 2016, Widenhoefer^[56] developed another method (**Scheme 25b**) to get the anti-Markovnikov product **115** with indol derivatives **113** and methylenecyclopropanes **114**, which approved the flexibility of gold catalysis by adjusting the state of gold with different ligand and solvent.

Compared with the nucleophiles like carbon, nitrogen and oxygen, the study of organosulfur is really rare since it is known to poison transition-metal catalysts. However, it does not mean that organosulfur is impossible to be a nucleophile in gold catalysis. In 2016, Akiya Ogawa group^[57] successfully reported the gold catalyzed Anti-Markovnikov selective hydrothiolation of unactivated alkenes in THF at moderate temperature (**Scheme 26**). This work not only gave high yield, high selectivity and high tolerance on functional group, it also provided another possible catalytic model which was different with the common style. In this work, it was proposed that organosulfur **117** will coordinate to gold by replacing NTf₂ counter anion to form the Ph₃PAuSR₂. Then it reacted with PPh₃AuNTf₂ to form tetranuclear gold complex **A** which will activate alkene



Scheme 26. C-S bond construction

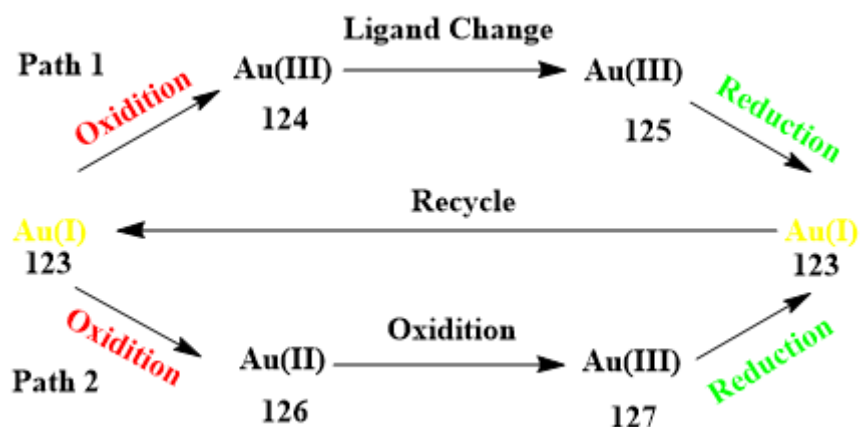
116 by coordination and subsequent addition of the Au–S species into the double bond of the unactivated alkene affords gold–alkene complex D. The last step of protodeauration by the thiol provides the anti-Markovnikov hydrothiolation product selectively, with the regeneration of A.



Scheme 27. C-S bond construction

Soon after in 2018, Troels Skrydstrup group^[58] (**Scheme 27**) developed another protocol to construct C-S bond with alkene catalyzed by gold(I) catalyst using ex situ formation of methanethiol which formed from inexpensive S-methylisothiourea hemisulfate salt. This protocol enriched the methodologies about the construction of C-S bond with simple sulfur source and avoided the dangerous manipulation of it.

At last, the new creative study^[59] on gold catalysis proved that gold(I) can not only work as Lewis acid to activate multiple bond, it can also pass through Au(I)/Au(III) redox catalytic cycle by adding oxidants and merging visible light photoredox. In general, in this redox catalytic cycle of gold, there are mainly two pathways^[60] (**Scheme 28**).

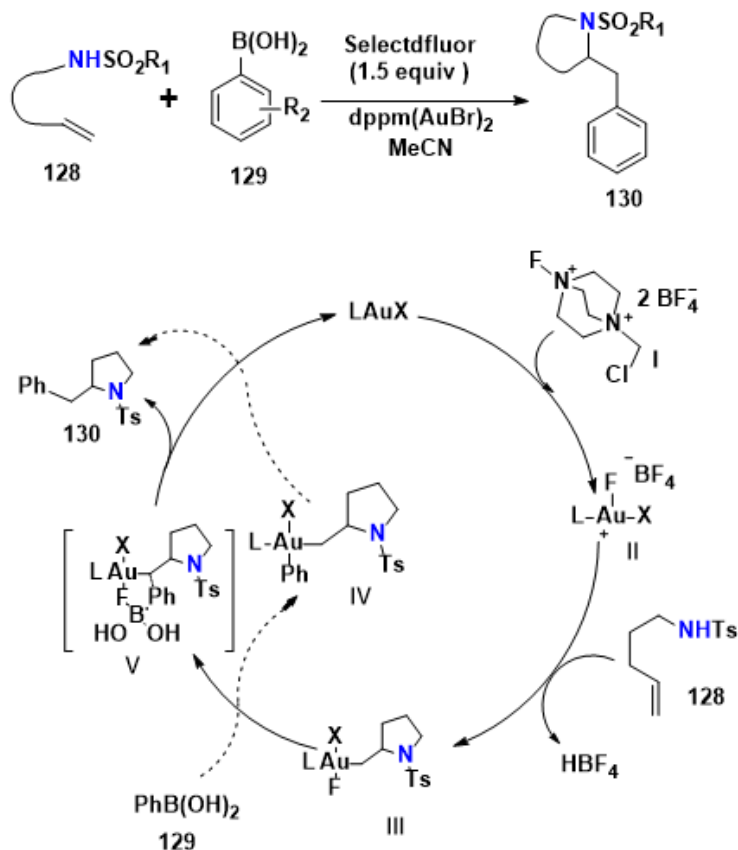


Scheme 28

In path I, gold(I) will be oxidized directly by oxidative addition into gold(III) **124** which undergoes a ligand exchange process with another substrate to be ready for the next reductive elimination process by gold(III) **125** to afford the final product and release the gold(I) **123**. Another path II, gold(I) will firstly be oxidized in to gold(II) **126** and it will be oxidized again into gold(III) **127** which experiences reductive elimination to give the final product and release the gold(I).

In 2010, F. Dean Toste group^[61] reported their work about intra-molecular amino arylation of alkenes making use of the Au(I)/Au(III) catalytic cycle. In this reaction, selectfluor acted as an external oxidants to oxidize gold(I) into gold(III) which then went through ligand exchange with starting material **128** (Scheme 29). When the gold(III)-alkyl intermediate **II** formed, based on previous work^[62], it was thought that gold(III)-alkyl will interact with phenylboronic acid and form the intermediate **IV** which experienced reductive elimination to afford the final product. But further controlled experiments show that intermediate **IV** cannot be formed in this reaction and it

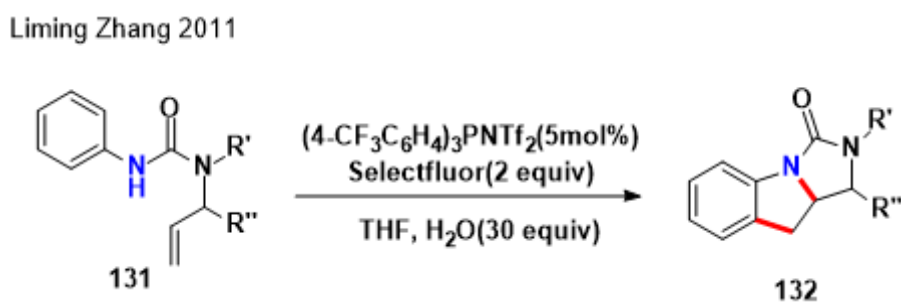
F. Dean Toste 2010



Scheme 29. Amination and phenylation of alkene

was proposed that intermediate **III** was transferred into **V** which induces a bimolecular reductive elimination to afford the final bifunctionalized product **130**. In this mechanism, the B-F interaction was greatly vital for the reductive elimination step, because it increases the nucleophilicity of the boronic acid and the electrophilicity of the carbon gold(III) moiety. In the same year, Liming Zhang^[62] also published relative work which extended the nucleophile to oxygen and also high yield were obtained. On the other hand, Cristina Nevado group^[63] enriched the application of this catalytic model by achieving the gold catalyzed aminoxygenation of alkenes and a novel alkene aminoamidation by gold activation of nitriles was also successful.

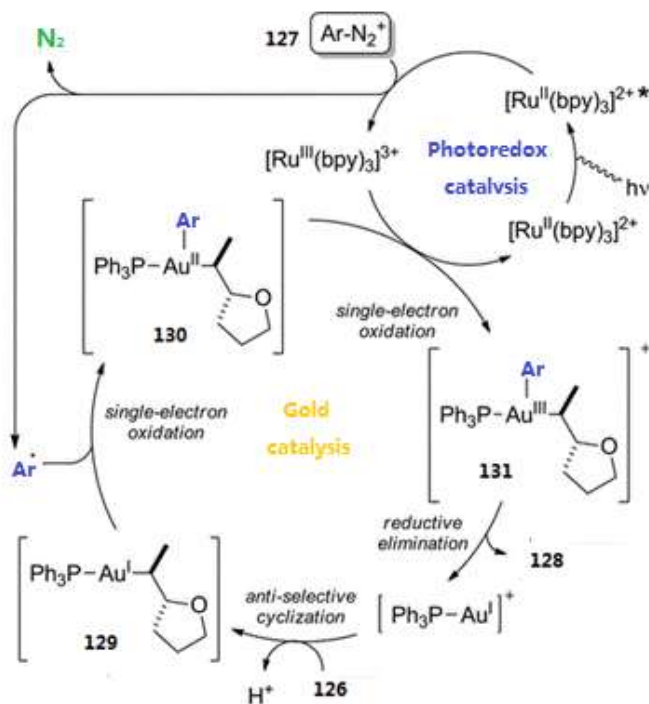
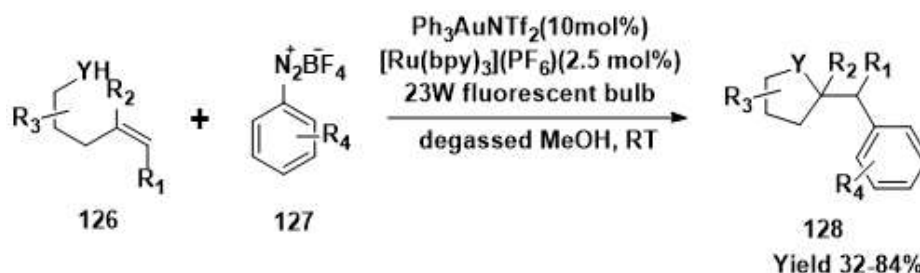
In 2011, Liming Zhang group^[64] combined gold(I)/gold(III) catalysis and C-H functionalization into one work(**Scheme 30**). By coupling with the aminoauration intermediate, the electrophilic aromatic compounds completed an intramolecular [3+2] annulation process in **131** to afford tricyclic indolines **132**. Deuterium labeling and kinetic isotope effect studies also strongly approved the subsequent inner-sphere concerted reductive mechanism.



Scheme 30. Alkylation and amination of alkene

In addition to adding oxidants to drive the Au(I)/Au(III) catalytic cycle, merging visible light photo-catalyst can also force this Au(I)/Au(III) catalytic cycle to happen effectively. In 2013, Frank Glorius group^[65] published the visible light-mediated oxy- and aminoarylation of alkenes via the synergistic catalysis between gold and photo-catalyst (**Scheme 31**). Aryldiazonium salts **134** are known as a good radical source of phenyl radical-activated by visible light. The most challenge task in this work is that the aminated intermediate **A** could catch the phenyl radical **B** and gold(II) complex **C** could also be oxidized into gold(III) complex **D**.

The experiment proved that this challenge has been conquered excellently. In the meantime, no matter the nucleophile is oxygen or nitrogen, this catalytic system worked smoothly. In the



Scheme 31. Au(I)/ Au(III) catalytic cycle

mechanism they proposed, the alkene firstly did the *anti*-selective cyclization and afforded alkyl-gold(I) **A**. Then phenyl radical **B** formed from the reduction of aryldiazonium salts **134** reduced by Ru(II) catalyst was captured by **A** to give the gold(II) intermediate **C** via single electron oxidation process. Then gold(II) intermediate kept being oxidized into gold(III) **D** complex by the oxidized Ru(III) catalyst. At last, gold(III) **D** complex went through reductive elimination to offer the final product and released gold(I) catalyst to be recycled. Besides this work, more and more works based on this catalytic system have been published in the following year^[66].

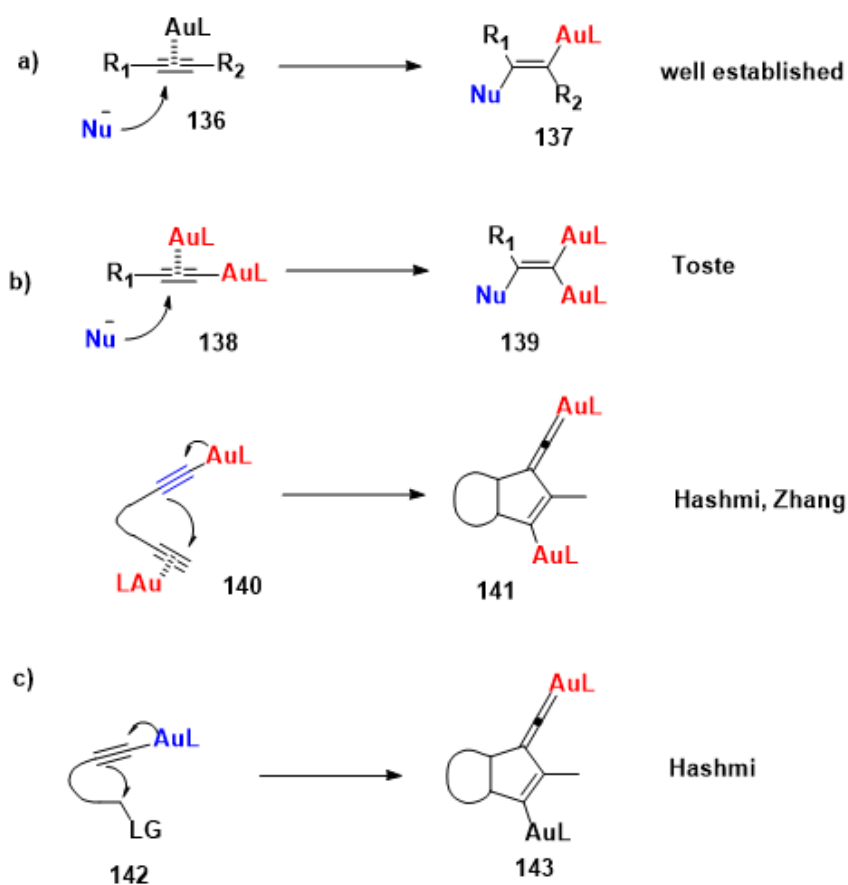
All the works summarized above have shown that the activation of alkene by gold(I) provide colorful synthetic tools for chemists to synthesize more valuable compounds. In addition, the study on this area also builds strong foundation for further research on gold catalysis and alkenes compounds. It will motivate chemists come up with more creative and friendly study in the future.

1.1.2 Gold catalyzed activation of alkyne

Alkyne compounds^[67] have become star compounds for transition metal catalyst to form various functionalized molecules in the past years. Gold catalyst also raised up to a talented member of activating alkyne compounds^[67c,d] in the past decades since its character of π -electron affinity and the adjustable ability on the spatial structure and electron property.

So far, the activation models of alkyne by gold are classified based on the work reported by Toste, Zhang and Hashmi, respectively (Scheme 32). The first one: π -activation mode (Scheme 32a) occurs by the coordination with gold and the nucleophile attacked the alkyne to form the gold-akenyl intermediate 137.

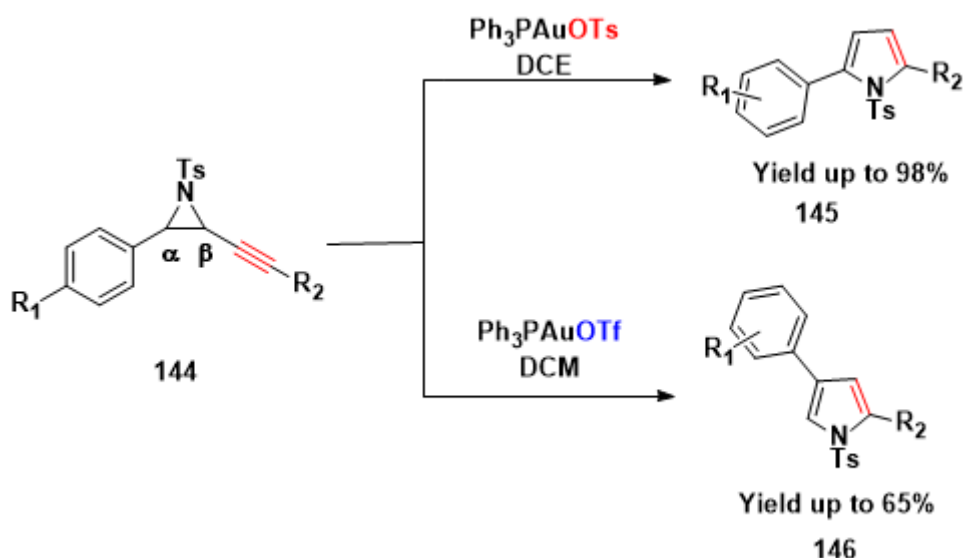
The second catalytic model is called dual σ , π -activation mode which was proposed by F. D. Toste,^[68] Hashmi and Zhang^[69] (Scheme 32b). This mode proposed that one alkyne was activated by π -coordination and σ -coordination or when the substrate contained two alkyne groups, one



Scheme 32

alkyne moiety was activated by gold catalyst through π -coordination while the other one was activated by gold catalyst in σ -coordination. In addition to above two modes, in 2014, Hashmi group^[70] developed the σ -activation mode (**Scheme 32c**). In this mode, the alkyne part of substrate was activated by σ -coordination format with gold catalyst leading to the increase of nucleophilicity of β -carbon atom of **142**. These catalytic models provide effective and efficient theoretic foundation for the gold catalysis accessing to numerous valued compounds by constructing C-C, C-X bond.

Amination of alkyne catalyzed has been a very useful approach accessing to C-N construction since nitrogen played very important role in pharmaceuticals. Gold catalyzed amination of alkyne has already provided numerous of method to construct nitrogen-including molecules. In 2009, Paul W. Davies group^[71] established an approach to access to synthesis of pyrroles from alkynyl aziridines **144** catalyzed by gold catalyst (**Scheme 33**). Relying on the activation of gold, N-tosyl

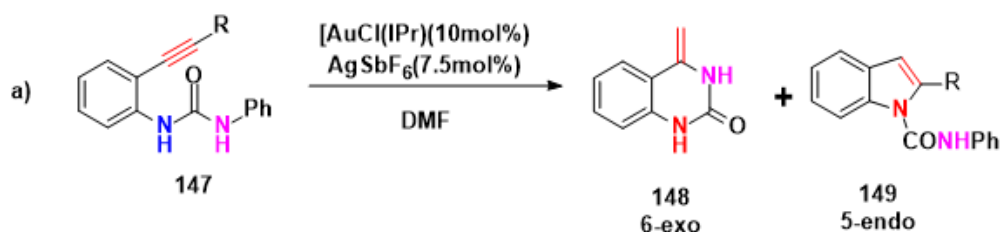


Scheme 33. Synthesis of pyrrol derivatives

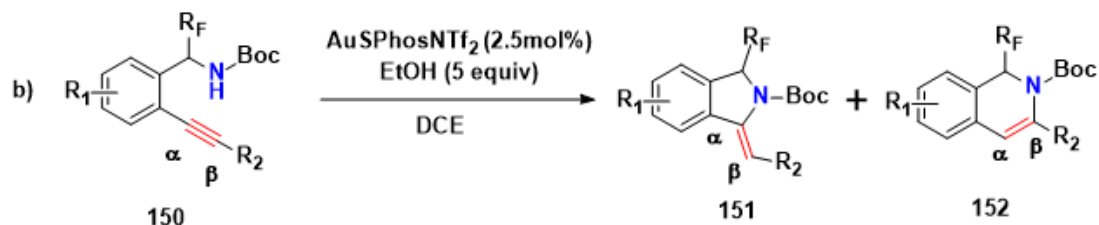
alkynyl aziridines underwent ring opening process and the nitrogen atom as a nucleophile attacked the alkyne from the opposite direction to form the C-N bond. On the other hand, the effect of the counterion on the reaction site of α and β was demonstrated. When the counterion was ^-OTs , the reaction pathway went to afford 2, 5-substituted pyrroles and when the counterion was ^-OTf , 2,4-substituted pyrroles were formed.

In 2010, Asensio ^[72a] developed NHC-stabilized Gold(I) catalyzed 6-*exo*-dig or 5-*endo*-dig cyclization of 3-substituted 1-(*o*-ethynylaryl)ureas **147** by adjusting ligand and substituents of **147** (Scheme 34a). In this work, the most difficult challenge was the selectivity of two N nucleophiles (N1 and N3). With the optimized reaction condition, 6-*exo*-dig **148** or 5-*endo*-dig **149** cyclized product almost obtained high yield which were 96% and 92% respectively. In the meantime, the substituents at terminal carbon of alkyne and N3 position could also affect the reaction pathway which means that spatial structure of substrates could also control the reaction mode.

Gregorio Asensio 2010



Silvia catalan 2013

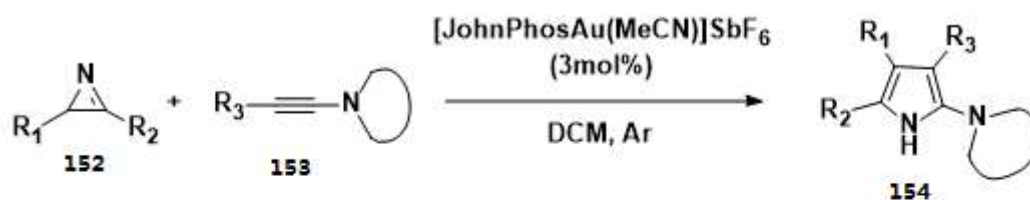


Scheme 34. Amination of alkyne

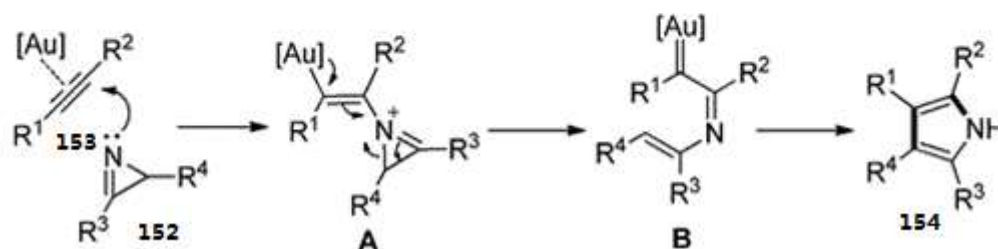
This new protocol also made the synthesis of 4-methylene -3,4- dihydroquinazolin -2- one core easier and economic.

In 2013, Silvia Catalan group ^[72b] chose a different strategy to obtain enantiomerically pure isoindoline **151** and dihydroisoquinoline **152** scaffolds by using an enantiomerically pure starting material **150** (Scheme 34b). There are also two possible reacting sites on alkyne group. The result showed that R₂ substituents could improve the selectivity between α and β carbon. Results showed that electron-donating alkyne substitution led preferably to 6-*endo*-dig cyclization, while an electron-withdrawing effect favored isoindoline formation. As well as the R_F substituent contributed a lot to the regioselectivity.

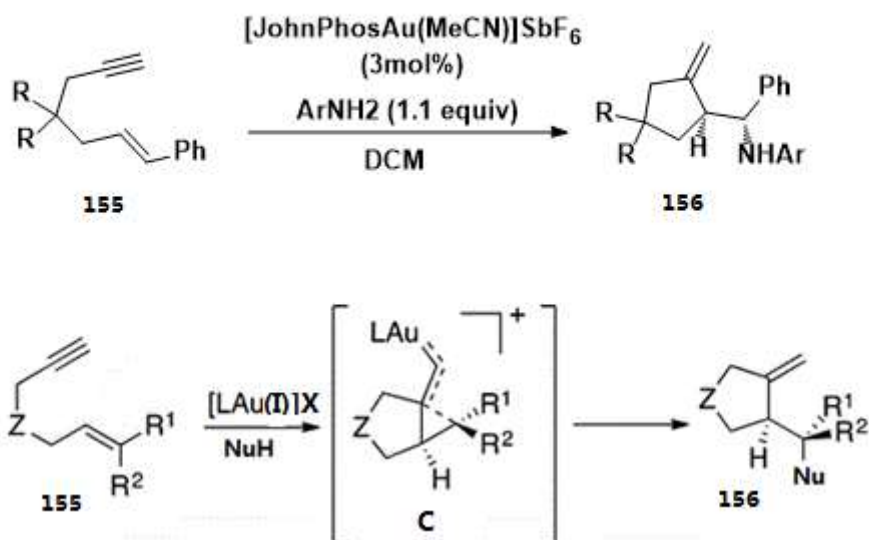
Xueliang Huang 2015



Proposed mechanism



Antonio M. Echavarren, 2016



Scheme 35. Application of carben gold intermediate

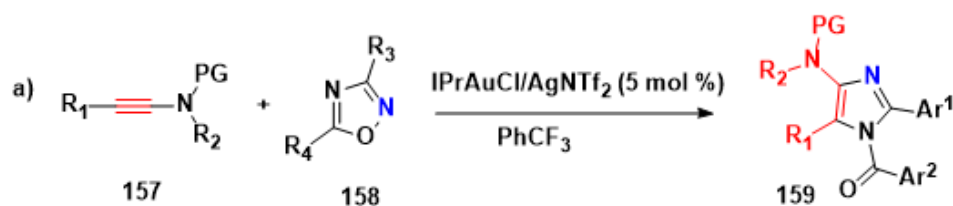
Besides intramolecular amination of alkynes, intermolecular type reactions also were achieved successfully. In 2015, Xueliang Huang group^[73] used 2H-azirines **152** and ynamides **153** as the starting material to synthesize highly substituted pyrroles **154** in a direct method (Scheme 35). In this reaction, $[\text{JohnPhosAu}(\text{MeCN})]\text{SbF}_6$ (3 mol%) was optimized as the best catalyst which could work in moderate conditions and gave the final pyrroles **154** in good to excellent yield. On the other hand, the loading of the gold catalyst was very low together with high scope of substrates. At

last, they proposed a mechanism consistent with π coordination model (**Scheme 32a**). Then gold-carbenoid **B** (**Scheme 35**) pathway was preferred.

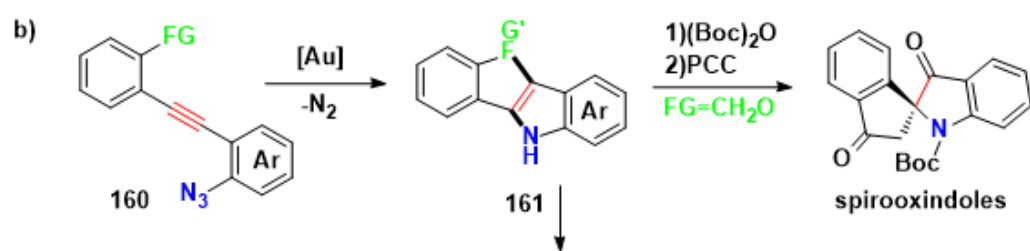
One year later, Antonio M. Echavarren group^[74] achieved aminocyclized product **156** from enynes **155** with high yield (up to 98%) and high tolerance on functional group catalyzed by JohnPhosAu(I) complex in DCM (**Scheme 35**). In this catalytic system, carbenoid gold intermediated was proposed and accepted the attack of aniline compounds to form the heteroatom cyclized product **156**.

Along with the development of gold catalyzed C-N construction by activating alkynes with gold, more and more complicate and creative reactions were also designed. In 2017, A. Stephen K. Hashmi group^[75] (**Scheme 36**) reported synthetic strategy to fully substituted 4-aminoimidazoles

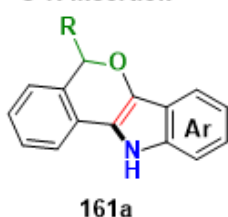
A. Stephen K. Hashmi 2017



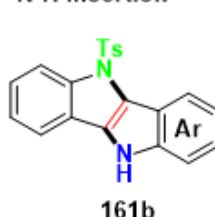
Xinfang Xu 2018



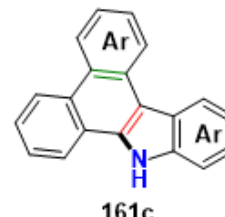
FG=CHROH
O-H insertion



FG=NHTs
N-H insertion



FG=Ar, aromatic substitution



Scheme 36. Synthesis of heterocompounds

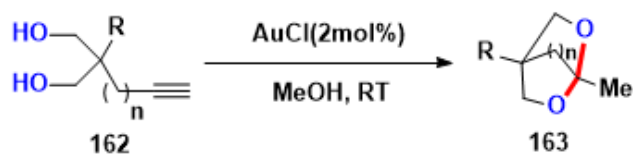
through selective [3 + 2] annulation of 1,2,4-oxadiazoles **158** with ynamides **157** in the presence of IPrAuCl/AgNTf₂ (5 mol %) in PhCF₃. This method disclosed a new chapter for the atom-economic synthesis of polysubstituted 4-aminoimidazole derivatives **159**. They tested more than twenty substrates bearing various substituents and the results were very acceptable. In the meantime, gram-scale synthesis reaction was also set up and the tolerance of this catalytic system was very promising. After this work, they also kept expanding the different nucleophiles to construct the C-N bond ^[75b,c] by gold(III) catalyst which have obtained promising results.

In 2018, Xinfang Xu group^[76] designed a new alkynylazide **160** (**Scheme 36b**) capable of delivering bicyclized product **161**. Under the assistance of gold catalyst, the fused indoles in good to high yields under mild reaction conditions were collected successfully. This reaction started with a gold catalyzed 5-*endo*-dig cyclization to form the α -imino carbenoid which was pivotal step for the second step of O-H **161a**, N-H insertion **161b**, and electrophilic aromatic substitution **161c** to yield the corresponding polycyclic *N*-heterocycles. The product obtained could be further transformed into spirooxindoles with high yield.

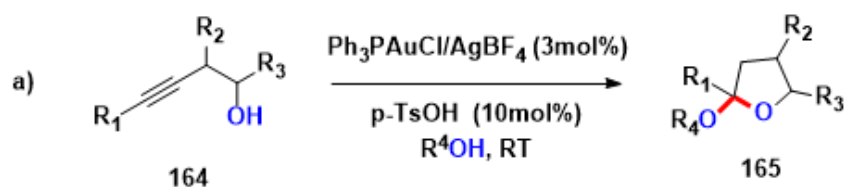
The strategy to construct C-N bond catalyzed by gold(I) complex with alkyne is not limited to the work above. As a matter of fact, anthranils^[77], indazoles^[78] and others^[79] have also been used as nitrogen sources for the annulation with alkynes to synthesize the corresponding C-N bond-included products.

Besides construction of C-N, alkyne can also be catalyzed to construct C-O bond by accepting attack of oxygen as the nucleophile. In 2005, Jean-Pierre Genet group^[80] made use of bis-homopropargylic alcohol **162** as the tested target and AuCl as the catalyst to form the bicyclized product **163** in methanol (**Scheme 37a**). Under optimized conditions, the functional group tolerance was very good in corresponding yield of good to excellent (74% to 99%) while the loading of catalyst was only 2 mol%. Besides this intramolecular hydroalkoxylation of alkyne, Norbert Krause group^[81], in 2006, developed the intermolecular version of tandem hydroalkoxylation of alkyne derivatives (**Scheme 37b**). To obtain the dihydroalkoxylation process, external alcohol was added to interact with the carbon cation intermediate formed by the first step of hydroalkoxylation catalyzed by Ph₃PAuCl/AgBF₄ system. The addition of *p*-TsOH assisted also

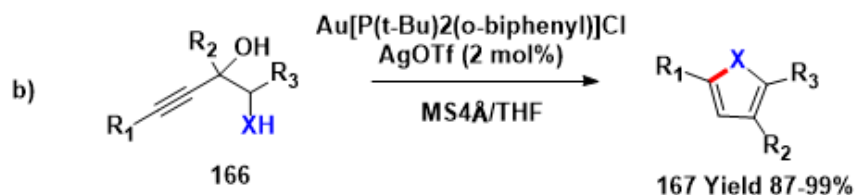
Jean-Pierre Genet 2005



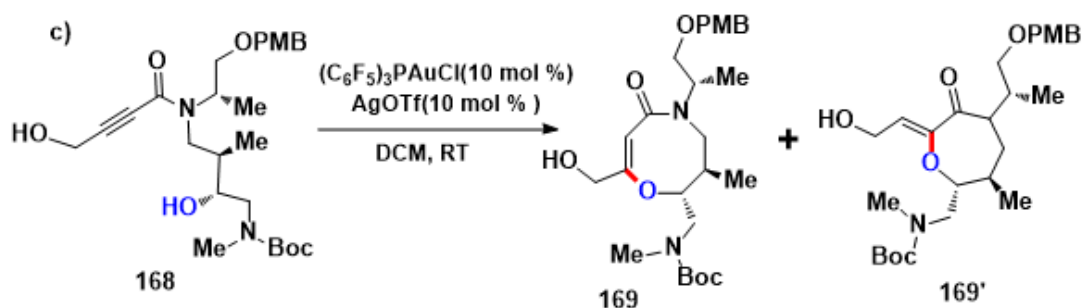
Norbert Krause 2006



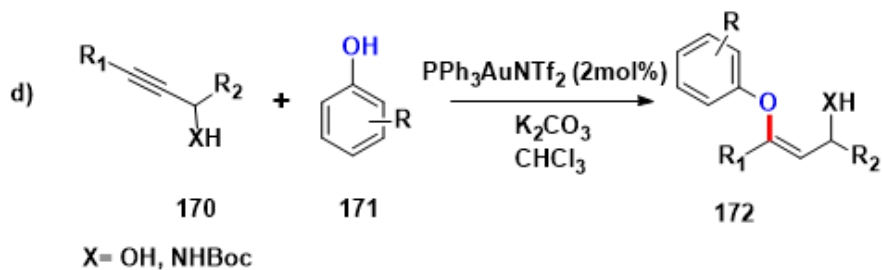
Aaron Aponick/Shuji Akai 2009



Stuart L. Schreiber 2015



Tom D. Sheppard 2019



Scheme 37. C-O bond construction

the second cycle to force alkene into alkyl cation which was ready for external alcohol compounds. This work successfully combined gold catalysis and Brønsted acid catalysis into one reaction and approved the high compatibility with not only functionalized substrates, but other kinds of catalyst.

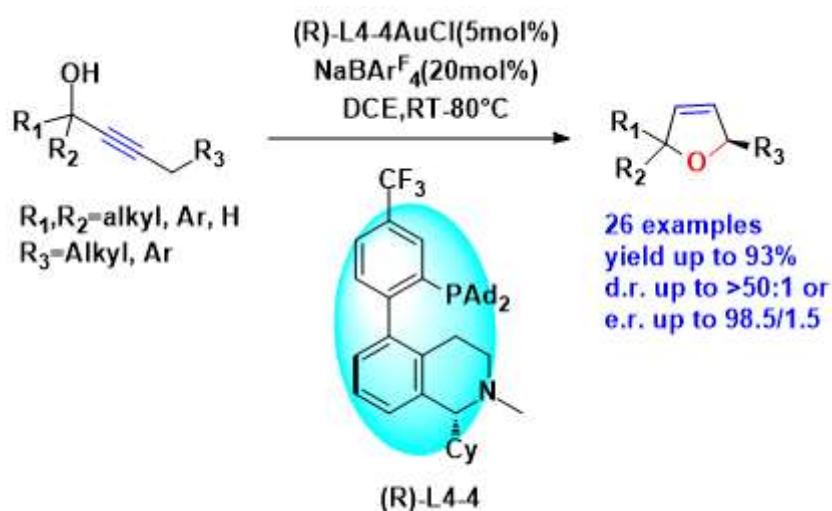
After these two works, in 2009, Aaron Aponick group and Shuji Akai group developed the synthesis of furans and pyrroles **167**^[82] catalyzed by Au[P(t-Bu)₂(o-biphenyl)]Cl/AgOTf (**Scheme 37c**). They introduced a second hydroxyl group which could go through dehydrative process and promoted the whole catalytic cycle. Surprisingly, this hydroxyl group did not compete with the hydroxyl nucleophile and afforded the desired product in excellent yield (87-99%). In this work, molecular sieves were necessary for removing the dehydrated water.

Besides the study on simple molecular, in 2015, Stuart L. Schreiber group (**Scheme 37c**) applied strategy of hydroalkoxylation of alkyne on alkynamides to synthesize the oxazocenones **169** selectively catalyzed by gold in 8-*endo*-dig version. After screening the reaction condition, the electron deficient ligand (C₆F₅)₃P gave the best yield (up to 84%) and 8-*endo*-dig cyclization selectively **169** rather than 7-*exo*-dig cyclization **169'**. In the meantime, this catalytic system showed its high application although the substrate was high structural complexity which also has bioactive characteristic.

Based on the development of relative work on gold catalyzed hydroalkoxylation of alkyne, extension to aliphatic alcohol and aromatic alcohols was envisioned. In 2019, Tom D. Sheppard group^[83] (**Scheme 37d**) synthesized phenyl enol ethers **172** in a chemo-, regio-, and stereoselective fashion in high yield catalyzed by PPh₃AuNTf₂ (2 mol%). K₂CO₃ was necessary to be added as base to increase the nucleophile and it was thought helpful on the selectivity. On the other hand, 50 substrates bearing various functional groups were tested and offered good to excellent yield.

Most gold catalyzed hydroalkoxylation of alkynes mainly focused on the racemic transformation since the difficulty on the asymmetric version controlled by the ligand. Even though facing great challenge on the design of asymmetric transformation catalyzed by gold, Liming Zhang group^[84] still focused on the design and synthesis of chiral ligand. In 2019, Zhang group^[84a] designed chiral

bifunctional phosphine ligand which enabled synthesis of 2,5-dihydrofuran **174** by cascade steps of asymmetric isomerization of alkyne **173** to allene and cyclization (Scheme 38). By the introduced amino group on the ligand, it can promote the isomerization of (R)-dodec-3-yn-2-ol derivatives and formed σ -allenylgold species^[84c] as a catalytic intermediate which underwent cyclization to give the final product in high yield and diastereoselectivity.



Scheme 38. C-H activation and cyclization

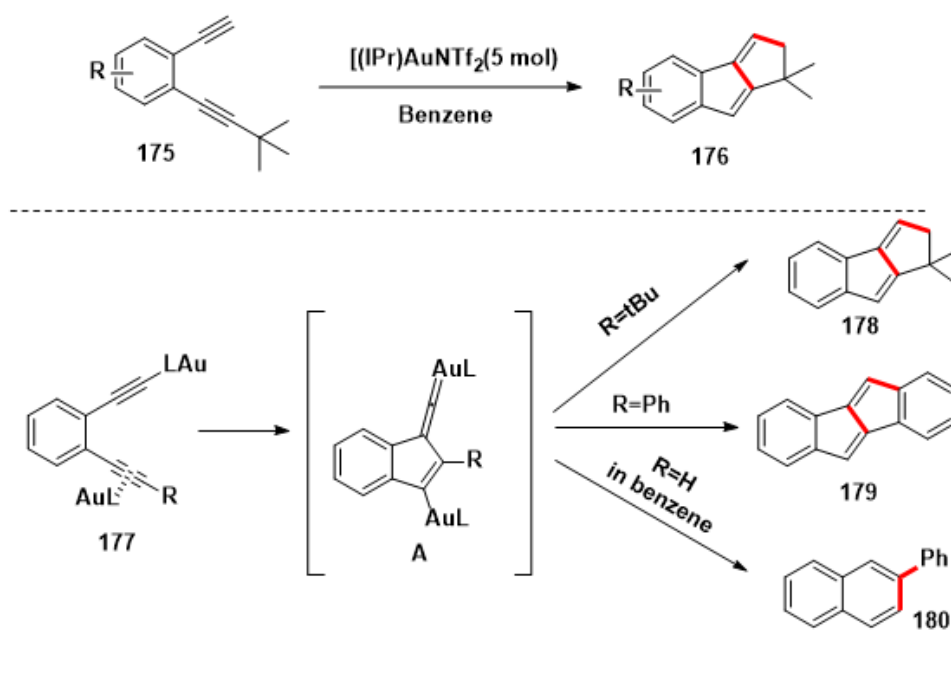
This work offered a promising guideline to make asymmetric transformations by gold catalysis to construct more valuable compounds and expanded the potential application of gold catalysts in synthetic chemistry.

Besides the form of C-X bond via gold catalysis in π activation of alkyne (Scheme 32a), C-C bond could also be formed via this catalytic model with carbon nucleophile^[85] such as alkenes in Dean F. Toste group, Antonio M. Echavarren group. However, not limited to this catalytic mode, the construction of C-C bond can be achieved via forming diactivated species as “Instant Dual-Activation” which was called σ , π -activation mode (Scheme 32b). Firstly, gold catalyzed σ coordination of alkyne is transferred to a nucleophile to attack another electrophilic alkyne unit activated by second gold catalyst through π coordination.

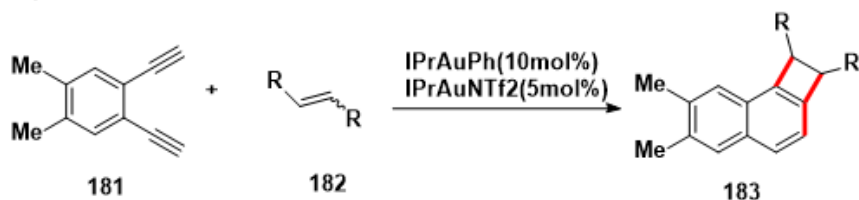
In 2012, A. Stephen K. Hashmi group^[86] reported their work of synthesis of benzofulvenes **176** via dual-gold catalysis mode (Scheme 39a). (IPr)AuNTf₂ was screened out as the best catalyst to drive this reaction with 5mol% loading. Further study on this process was also done to enrich its

application. After the digold intermediates **A** with a gold(I) vinylidene substructure were formed, entirely new reaction pathways were achieved by intramolecular sp^3 C-H and sp^2 C-H insertion pathways to form **178** and **179**^[87a] products. Furthermore, di-terminal alkynes when R was H can be transformed to β -substituted naphthaleneproduct **179**^[87b] After the functionalization^[86b, 88] of

a) A. Stephen K. Hashmi, 2012



b) A. Stephen K. Hashmi, 2012



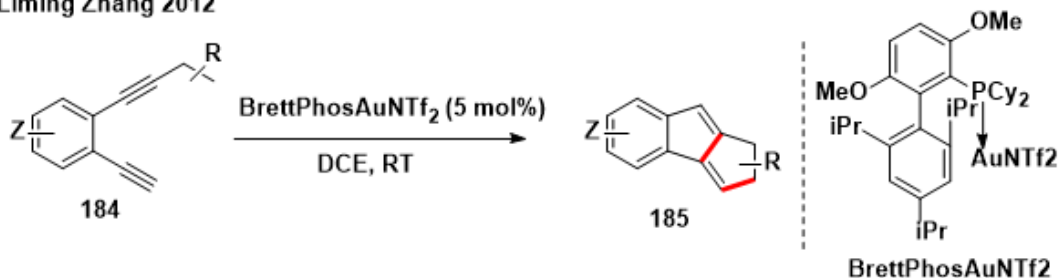
Scheme 39. σ , π -activation

vinylidene gold **A** with various intermolecular sp^3 C-H and sp^2 C-H partners were exploited maturely, alkenes **182** as more-reactive partners was also exploited in A. Stephen K. Hashmi group^[86b] (Scheme 39b). Catalyzed by a mixture of 5 mol% IPrAuNTf_2 and 10 mol% IPrAuPh , **183** was synthesized in good to excellent yield. This work showed the advantages of dual gold catalysis and made more creative reaction on the road.

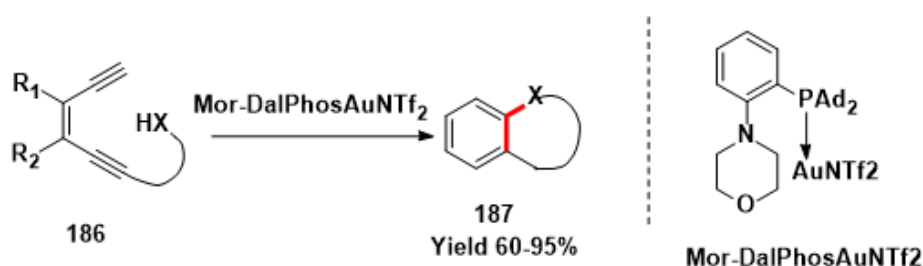
Almost at the same time with A. Stephen K. Hashmi group, Liming Zhang group also developed the sp^3 C-H insertion to the gold vinylidenes intermediates formed by two molecules of

rettPhosAuNTf₂ catalysis^[89a] (**Scheme 40a**) to form the tricyclic indenenes **185** in mostly good yields.

a) Liming Zhang 2012



b) Liming Zhang 2013



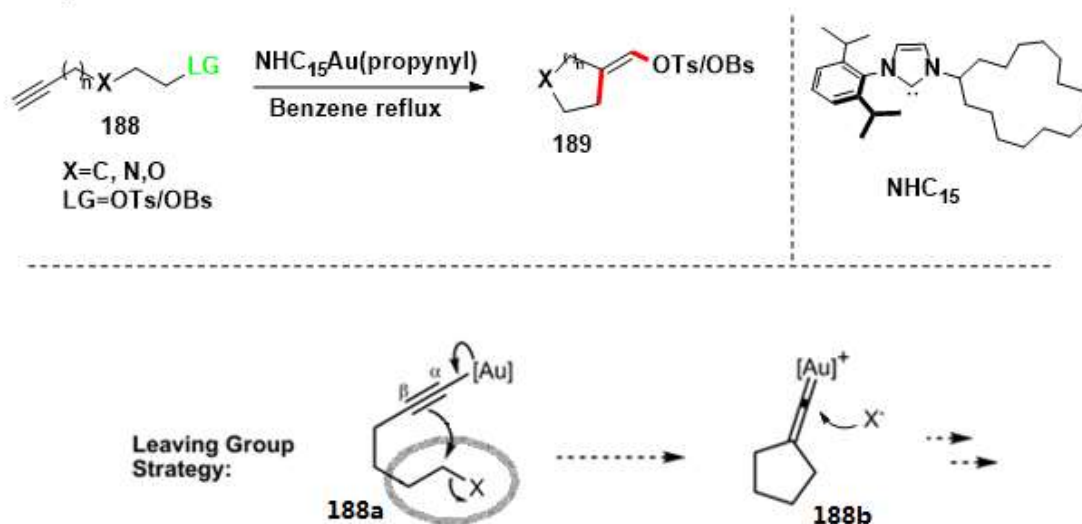
Scheme 40.

Besides sp³ C-H insertion, O-H and N-H insertions can also happen smoothly just by adjusting the ligand with Mor-DalPhos^[89b] to form the heterocycle products **187** (**Scheme 40b**) in good to excellent yield and high selectivity between 5-endo-dig and 6-endo-dig path in the bifurcation. Consistent with the experiments results in hand, gold vinylidene was most likely approved as one of the reaction intermediates on the basis of both mechanistic studies and theoretical calculations.

For single gold catalysis, besides π - activation mode, there is also another catalytic mode named σ -activation mode (**Scheme 32c**) which a gold-alkyne σ bond was formed as an intermediate (like **188a**). In 2013, A. Stephen K. Hashmi group successfully developed σ -activation mode catalysis by gold (**Scheme 41**). Terminal alkynes that bear sulfonate leaving groups **186** at an appropriate distance were chose to be model substrate and were transformed to give cyclized product **187** by optimized catalyst NHC₁₅Au(propynyl) with 5mol%. In the catalytic cycle, intermediate **188a** was produced at first. When electron was donated to α carbon from gold, β carbon increased its nucleophilicity and then went through S_N2 substitution reaction and constructed C-C bond and formed gold vinylidene **188b** intermediate. At last, another nucleophile (could be leaving group) came to quench this gold vinylidene to give final product **189**. The result of application test was

promising which can tolerate differently substituted sulfonates in good to excellent yield. This work also gave the possibility of formation of gold acetylides not just dependent on dual-gold activation.

A. Stephen K. Hashmi 2014



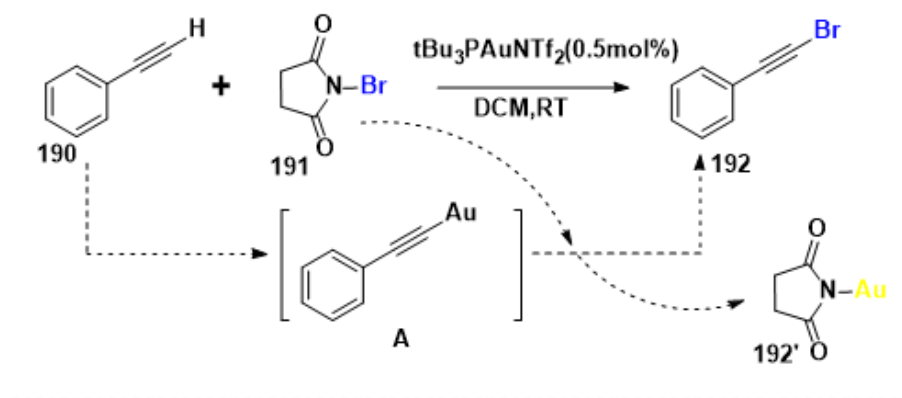
Scheme 41. σ activation of alkyne bearing the leaving group

Compared to C-N, C-O, C-C bond construction catalyzed by gold catalyst, C-X (X= Br, Cl) is more challenging since the halogen atom has high affinity between cationic gold and halogen^[91]. However, attracted by the efficiency and moderate reaction condition of gold catalysis, chemists kept focusing on their attention on this kind reaction with gold catalyst.

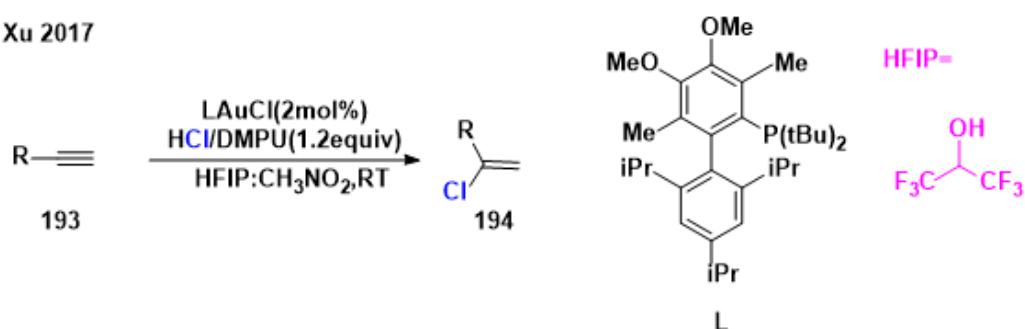
In 2011, on the basis of σ -activation mode of gold catalysis, Avelino Corma group^[92] published the gold catalyzes ω -bromination of terminal alkynes with N-bromosuccinimide (NBS)(**Scheme 42a**). Firstly, alkynyl gold intermediate **A** was formed and interacted with NBS by exchange process to give brominated product **192** and gold complex **192'**.

On the other hand, with another version of π coordination, in 2017, Bo Xu group^[93] reported regioselective hydrochlorination of alkynes. In this reaction, the most promising part was that HCl reacted as nucleophile which usually was not compatible with gold cation. Because the addition of HFIP can generate strong hydrogen bond donor network which could act stabilized counter anion to activate gold cation(**Scheme 42b**).

a) Avelino Corma 2011



b) Bo Xu 2017



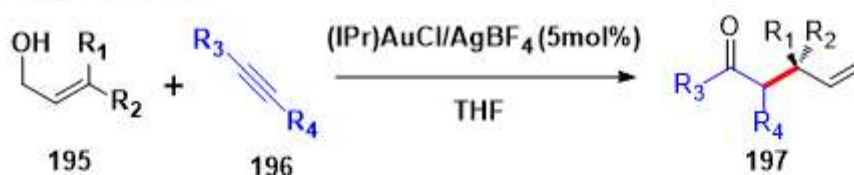
Scheme 42. Halogenation of alkyne

Beyond the above normal C-N, C-O, C-C C-X (Cl, Br) bonds construction assisted by gold catalysis, chemists have not satisfied with using the mechanism above to just construct simple new chemical bond in simple molecular. They attempted to combine all the activation version into one strategy to construct complicated molecules by forming various chemical bonds one-pot.

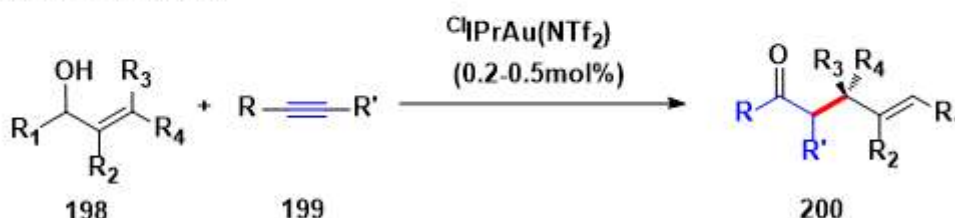
Encouraged by the accumulation of gold catalysis, in 2013, Aaron Aponick group^[94] reported gold catalyzed hydroalkoxylation of alkynes **196** with allyl alcohol **195** and the formed allyl vinyl ethers (like **204**) then underwent Claisen rearrangement process to facilitate the direct formation of γ,δ -unsaturated ketones **197** rather than the direct protodeauration process to give the ether products. This catalytic system can not only tolerate various functional groups on the alkynes **196**, it can offer surprisingly high yield and diastereoselectivity (Scheme 43).

The next year, in 2014, Steven P. Nolan group^[95] kept enriching this catalytic system (Scheme 43) by decreasing the catalytic loading of gold catalyst (0.2-0.5 mol%) and performed this reaction in solvent-free conditions. In the meantime, then expanded the allyl alcohol substrates to poly-substituted allyl alcohol **198** and without big influence on the yield of γ,δ -unsaturated

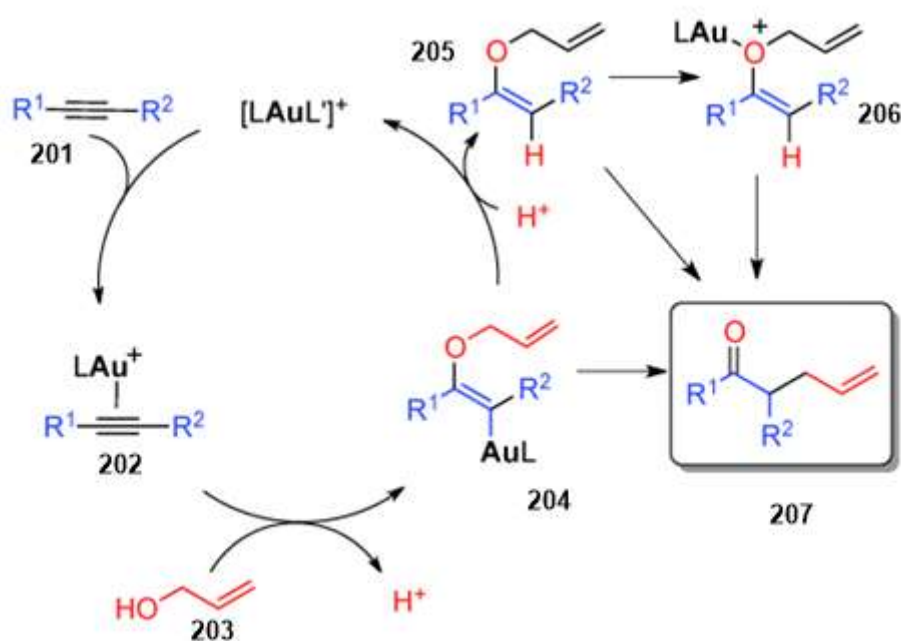
Aaron Aponick 2013



Steven P. Nolan 2014



Antonio M. Echavarren 2015

**Scheme 43.** Intermolecular C-C construction

ketones **200**. Furthermore, solvent-free system provided more environment-friendly and healthy platform.

For the details of hydroalkoxylation/Claisen rearrangement, Nolan group and Antonio M. Echavarren group tried their best to propose the mechanism (**Scheme 43**) assisted by high level computational studies. So far, it was accepted that allyl vinyl ethers **204** was formed through traditional π activation and anti-addition of allyl alcohol. But the last step can not have unambiguous conclusion on whether the final step proceeded by simple thermal [3,3]-sigmatropic

rearrangement(204 to 207), or if it was promoted by gold(I) through decreasing the activation energy by coordinating to the enol ether oxygen (206-207).

No matter which path it goes, this method has become the best method for the synthesis of a wide variety of homoallylic ketones from inexpensive and commercially available materials considering catalytic efficiency and simplicity.

On the other hand, Liming Zhang group keeps working on designing new ligand^[96] to expand the application of gold catalyst. In 2018, they designed biphenyl-2-yl phosphine ligand^[97] (Scheme 44) by featuring a remote basic tertiary amine. Using terminally silylated alkynes **208** as substrates, they proposed that the silyl group can promote the deprotonation process with the assistance of amine on the ligand and led to allenyl gold intermediate **211**. At this step, a competitive electrophile aldehyde **209** would be captured by this intermediate and led to homopargylic alcohol **212**. At last, intramolecular cyclization of **212** happened to afford dihydrofuran **210** product. The condition screening result also showed that the counter anion $\text{NaBAR}_4^{\text{F}}$ played a very important role to abstract chloride and excess amount of $\text{NaBAR}_4^{\text{F}}$ was also necessary to accelerate the

Liming Zhang 2018



Scheme 44.

reaction rate. With this optimized condition, various substituents on alkynes and aldehyde were examined and the tolerance of functional group showed very satisfied result. This work gave a

new direction on the design of gold catalyzed transformation and also expanded the future application on asymmetric transformation by synthesizing multiple functionalized ligand.

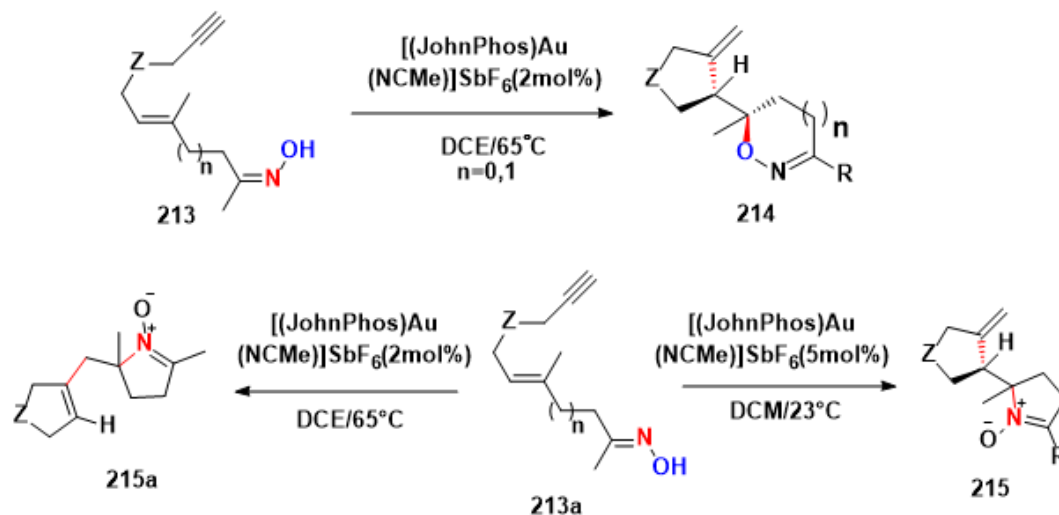
Besides study on the ligand of gold catalyst, chemists also put great attention on designing new transformation of organic molecules to prepare more complicated products which have more potential applicable value. In 2018, Antonio M. Echavarren group^[98] reported their work named “Diastereospecific Gold(I)-Catalyzed Cyclization Cascade for the Controlled Preparation of N- and N,O-Heterocycles”(Scheme 45). They prepared oxime compounds **213** as the substrate and treated it with [(JohnPhos)Au(NCMe)]SbF₆ as catalyst (2mol%) in DCE at 65 °C. Delightfully, dihydro-4H-1,2-oxazines **214** was formed in high yield in cascade cyclization process and functional group could also be featured in this product. More surprisingly, when the isomer oxime **213a** of **213** was used as substrate, under almost same catalytic condition, various dihydropyrrole N-oxides **215a** was afforded as a single diastereomer. Moreover, when the solvent was changed into DCM and the temperature was decreased to room temperature, the isomeric dihydropyrrole N-oxide **215** was then obtained in good yield.

Next year, in 2019, Gaëlle Blond group^[99] synthesized complex molecules having furopyran skeleton via hetero-Diels-Alder cascade process forced by [(JohnPhos)Au(NCMe)]SbF₆ with microwave condition (Scheme 45). In the whole reaction process, dienophile **216a** and diene **216b** were formed concomitantly started from the same starting material **216**. Then these two molecules would interact with each other via Hetero-Diels-Alder reaction to give the polyheterocyclic products **217** in good yield from 32% to 73%. In addition, there were four heterocycles, six bonds including four controlled stereogenic centers formed in this catalytic condition just by gold catalyst.

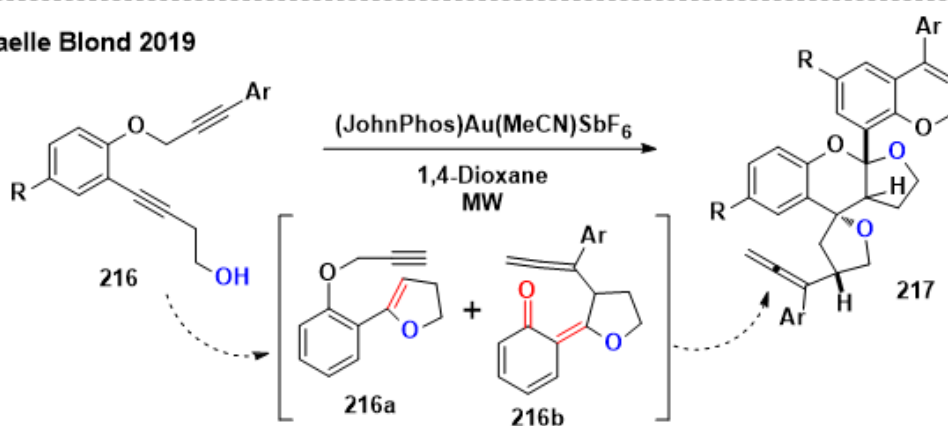
In the same year (2019), Zhenghu Xu group^[100] (Scheme 45) also synthesized polysubstituted spiro cyclopenta[c]furans diastereoselectively in cascade version catalyzed just by Ph₃PAuNTf₂ in mild condition. Alkynyl alcohol **218** and alkynyl enone **219** were picked which both featured several functional group like hydroxyl, alkene, alkyne and ketyl groups to perform this transformation. Like the work of Gaëlle Blond group above, the two starting material would be catalyzed by gold catalyst and afford the corresponding intermediates which then interacted with

each other to lead to final highly polycyclized product **220** in good to excellent yield (up to 94%) and high tolerance (23 examples).

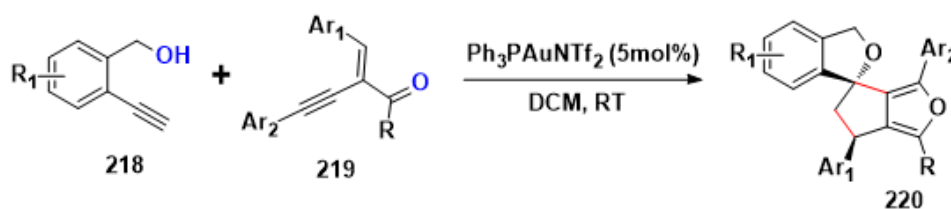
Antonio M. Echavarren 2018



Gaëlle Blond 2019



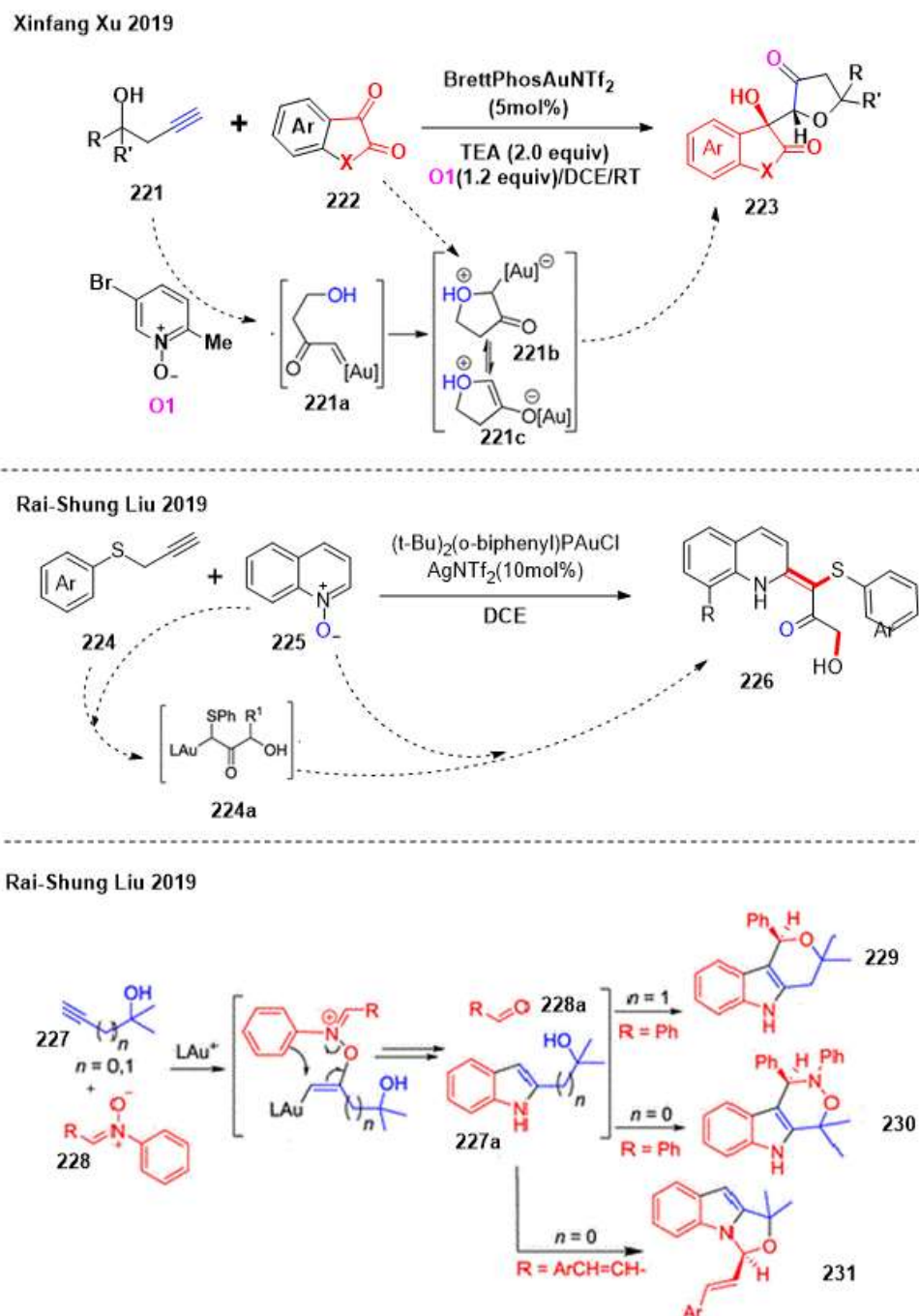
Zhenghu Xu 2019



Scheme 45

In addition to strategies described above, gold catalyzed oxidation of alkyne also possessed important position in chemical transformation to form the new bond by α -oxo gold carbene species. Making use of this intermediate, in 2019, Xinfang Xu group^[101] (**Scheme 46**) completed

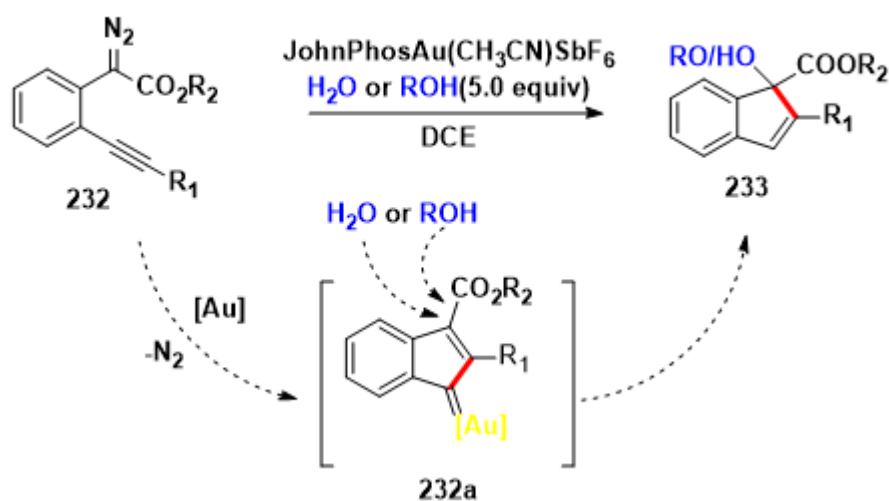
their work about gold catalyzed oxidative cyclization/aldol addition of homopropargyl alcohols **221** with isatins **222**. Homopropargyl alcohols **221** firstly was oxidized into α -oxo gold carbene species **221a** and then was attacked by hydroxyl group to give ylide **221b** or its enolate form **221c**. At last, isatins **222** got involved and captured the intermediate to form the final product **223** via aldol addition process. This work provides an efficient methodology to directly construct oxindole derivatives equipped with two vicinal stereocenters in high yields with high diastereoselectivities.



Scheme 46

Moreover, in the same year (2019), Rai-Shung Liu group^[102] expanded the application of N-oxides compounds which mainly used as oxygen donor to take part in reacting with other starting material after the formation of α -oxo gold carbene species (**Scheme 46**). Firstly, they achieved the work^[102a] on gold catalyzed oxidative functionalization of propargyl aryl thioethers with quinolone N-Oxides via 1,3-sulfur migration reaction. In this work, besides the formation of α -oxo gold carbene species, the different point with the work of Xinfang Xu group was that when PhS attacked the gold carbene functionality produced with one molecular quinolone N-Oxides, 1,3-sulfur migration happened to give the intermediate **224a**. Finally, it reacted with another one molecular quinolone N-Oxides and synthesized 3-hydroxy-1-alkylidene phenylthioprop-2-ones **226** which also could be decorated with various substituents in good yield. Moreover, they also successfully synthesized distinct fused indoles bearing heterocyclic ring^[102b] (**Scheme 46**). Interestingly, by adjusting the carbon line length of **227** between alkyne group and hydroxyl group and changing the substituents of nitrones **228**. However, instead of forming α -oxo gold carbene species, it passed through a C-H insertion and afforded two new species **227a** and **228a**. When arrived at this step, the reaction pathway was diverted into three directions: when R was phenyl group and n equaled 1, tetrahydropyrano[4,3-b]indole **229** was prepared and tetrahydro-[1,2]oxazino[5,4-b]indoles **230** was formed while n equaled 0 and when the R group was styryl group, n equaled 0, dihydrooxazolo[3,4-a]indole **231** was obtained distantly.

Xinfang Xu 2019



Scheme 47. Application of carben gold complex

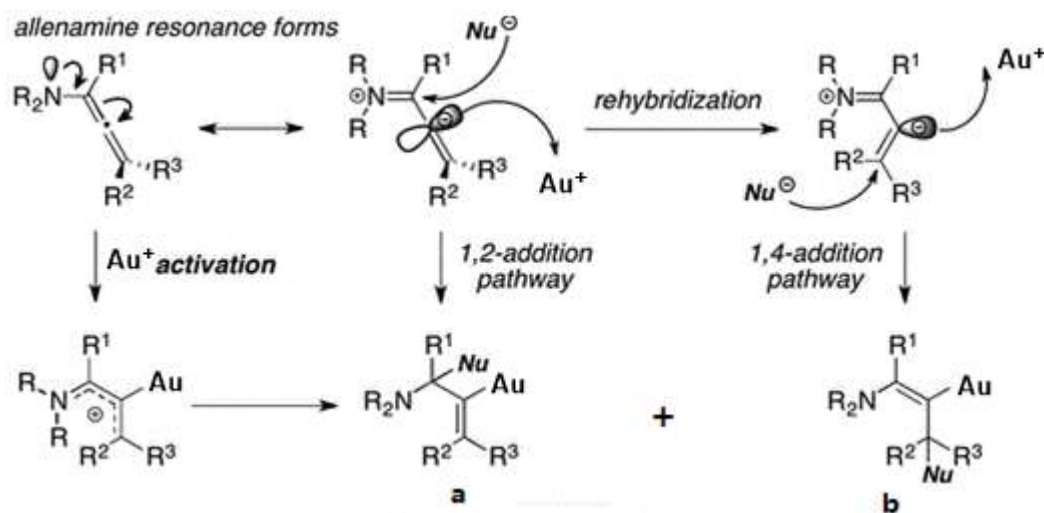
Chapter 1

As gold-carbene intermediate is a very practical tool to access to create more valued compounds, in addition to preparing it by adding additives like *N*-oxides, using diazo compounds to form the gold carbene intermediate by leaving N₂ has also become one of important method. In 2019, Xinfang Xu group^[102] developed a direct strategy by interacting [(JohnPhos)Au(NCMe)] catalyst with alkyne-tethered diazo **232** to form the gold carbene intermediate along with releasing N₂ (**Scheme 47**). However, it was not stable so that it reacted once it was formed with alkyne group via 5-*endo*-dig carbocyclization to lead to the key intermediate vinyl gold carbene **232a**. In this work, water and alcohol were chosen to react with this intermediate followed forming indenols **233** in excellent yield. Surprisingly, various protic nucleophiles such as water, commercially available alcohols, menthol, steroid, etc., were all well tolerated under these conditions to produce the corresponding indenol derivatives.

In summary, alkynes compounds have shown their high application value to construct tons of new compounds catalyzed by gold catalyst. By adjusting the ligand and other elements like solvent, counter anion and temperature, the new transformation can happen smoothly to form the aimed products from various alkyne compounds. Assisted with gold, region and stereoselectivity could also be obtained with promising result. Along with the accumulation of knowledge of gold catalysis on alkyne, there must be more great and creative work coming to our community.

1.1.3. Gold(I) catalyzed activation of allenamide

Being another member of π -electron rich compounds like alkyne and alkene, allenamides^[104] has also arisen up a kind of useful synthetic cells in organic chemistry since it was prepared and characterized in 1968 by Viehe^[105]. The activation model of allenamides is consistent with π -coordination of alkyne (**Scheme 48**). The existence of nitrogen promoted electron rich property allenamides through electron back-donating from nitrogen to allene which led to itself easier to be activated via gold complex compared to alenes. Through the resonance form of allenamines, regioselectivity can be obtained by adjusting the catalyst and using different reagents to direct to three pathways like cation activation which could offer 1 or 3 electrophilic position (afford **a** and **b** product), 1,2-addition and 1,4-addition. In the meantime, the presence of nitrogen atom also brings more advantages than simple allenes compounds. Firstly, it provides an anchor point to afford stereochemical transformation by

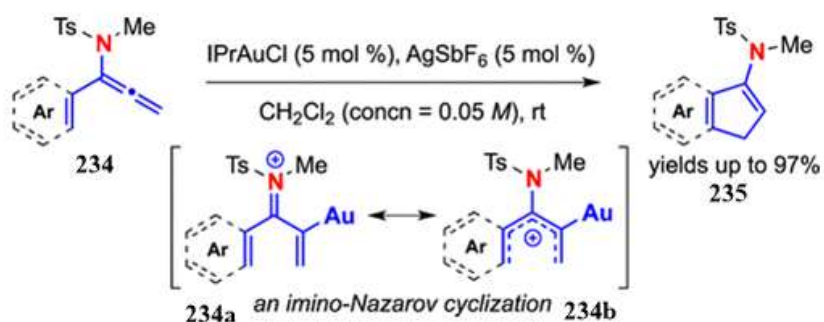


Scheme 48

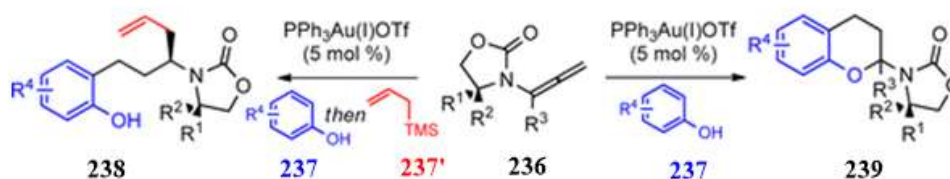
designing new ligand and directive substrates. In addition, it provides more flexible access to develop intramolecular reaction or cascade conversion than oxygen- or sulfur-substituted allenes. Moreover, nitrogen atom also shows great potential value and application in natural compounds and pharmaceutical. When combined with gold catalyst, more and more promising transformations have been published and keep inspiring chemists figure our more creative chemistry synthesis art.

In 2012, Richard P. Hsung^[106] documented the intramolecular imino-Nazarov cascade cyclization catalyzed by gold via producing **234a** and **234b** transition state (Scheme 49a). At first, this reaction showed also the dimerized product as the byproduct. By adjusting the ligand, IPr ligand offered the best selectivity and excellent yield of **235** (up to 97%).

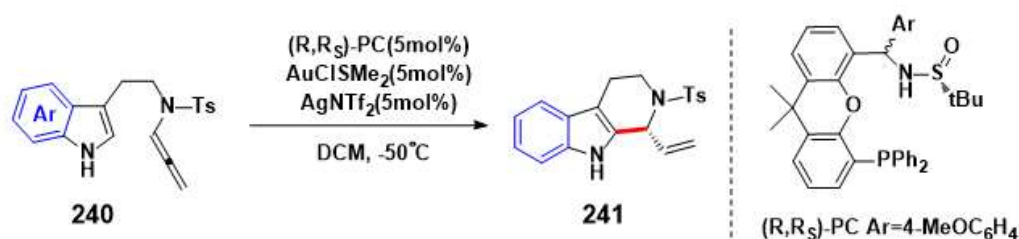
a) Richard P. Hsung 2012



b) Marc C. Kimber 2014



c) Junliang Zhang 2017

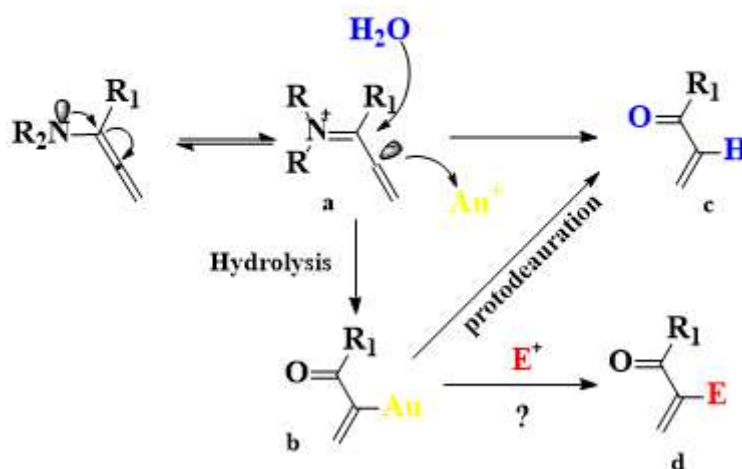


Scheme 49.

Not long from this work, in 2014, Marc C. Kimber^[107] group published the work on synthesis of Chromanes **239** from **236** through di-addition on the α and γ position of allene section with carbon and oxygen activated by gold catalyst (Scheme 49b). In this process, the counter anion ⁻OTf acted a very important function to enhance the nucleophilicity of aromatic carbon and activate the enamide intermediate. More interestingly, when allyl trimethylsilane **237'** was added, the reaction pathway was easily switched to allylation rather than hydroxylation process which meant that the iminium intermediate was very controllable to capture various nucleophiles.

Besides these great synthetic transformations, chemists also devoted their attention on the control of enantioselectivity by designing new chiral ligand. In 2017, Junliang Zhang group^[108] designed and synthesized chiral ligand (R,R)-PC ligand (**Scheme 49c**). To examine its ability, intramolecular N-allenamide **240** was chosen to form chiral tetrahydrocarbolines **241**. Without disappointment, high enantioselectivity (up to 97%) was achieved and it also exhibited promising functional group tolerance with excellent yield.

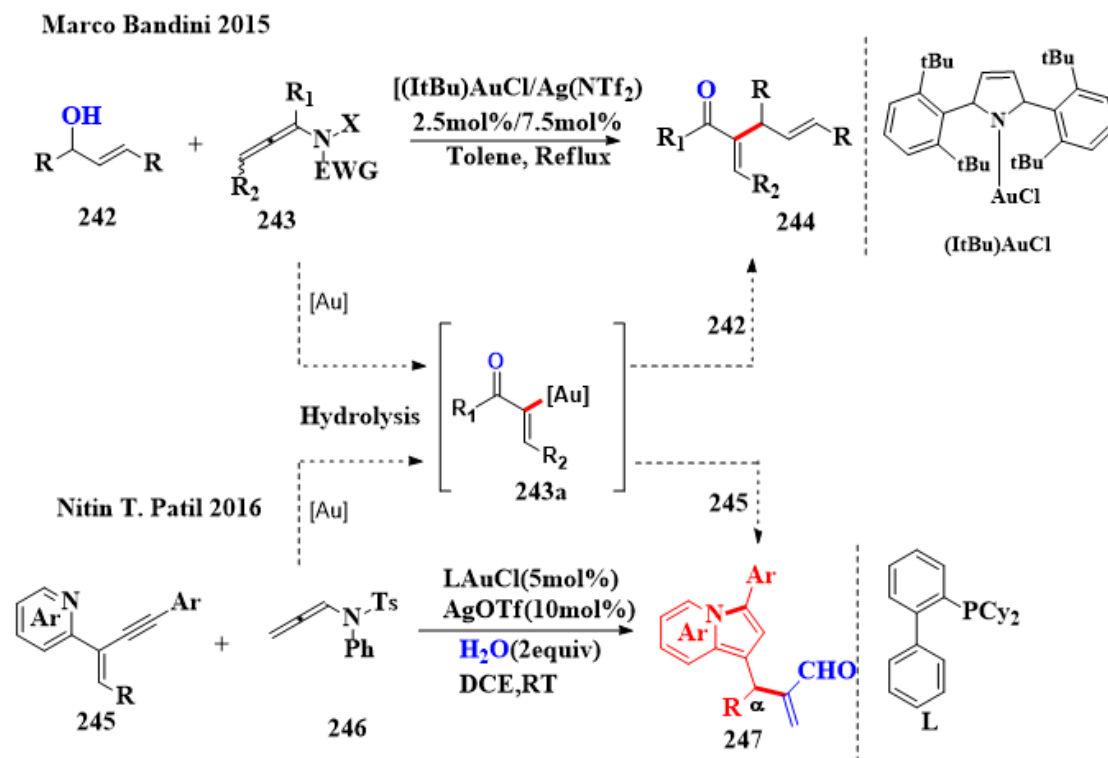
Allenamine resonance form



Scheme 50

Besides this reaction pathway, allenamides can also undergo hydrolysis process with water (**Scheme 50**). When water existed, resonance form of **a** would be hydrolyzed by leaving amine compounds and formed alkeny gold complex **b** which experienced protodeauration process to give the product **c**. However, chemists want to capture the alkeny gold complex **b** with another electrophile so that prepare more new compounds.

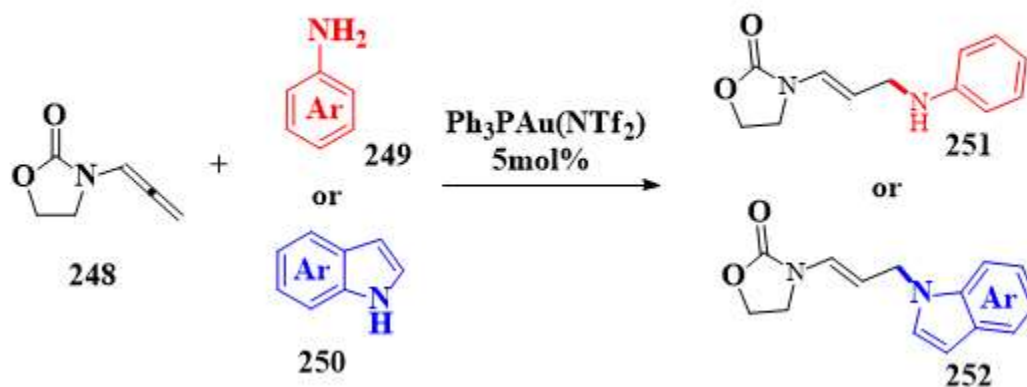
To achieve this target, our group^[109] firstly in 2015 captured this intermediate with allyl alcohol **242** catalyzed by gold and silver dual-catalyzed (**Scheme 51**). At first, we realized that when AgNTf₂ was excess, a marked improvement in chemical yield was collected. To figure this reason out, control experiment was done and the result showed that the excess AgNTf₂ could promoted the dewater condensation between two molecular allyl alcohol with forming allyl ether which also could take part in the next reaction. The water formed before would hydrolyze allenamides **243** to produce the gold complex **243a**. At last, allyl alcohol or ether got involved to react with **243a** and form the allylated product **244** with excellent yield.



Inspired by this work in our group, in 2016, Nitin T. Patil group^[110] (**Scheme 51**) developed another gold(I) and Ag(I) catalyzed synergistically transformation by capturing enal-gold complex **243a**. In this work, excess AgOTf converted starting material **245** into an intermediate with the α carbon cation (red section of **247**) which successfully trapped enal-gold complex **243a** by forming product **247** in mild reaction condition.

For constructing single chemical bond, besides C-C and C-O bond, amines could also be the good candidate to be nucleophiles to form C-N bond with allenamides. On this area, in 2010, Marc C. Kimber group^[111] have successfully documented their work in intramolecular version (**Scheme 52**). Reacting with allenamides **248**, nomatter primary amine or secondary amine, product **251** and **252** with high yield and high regioselectivity could always be collected in very mild condition. On the other hand, these two works also approved the stability and advantage of gold catalysis compared with other sensitive transition metal catalysis. This reaction version also proceeded through π -activation and wait for the attack by nucleophile of amines which was rather traditional reaction style. However, the amination of allenamides was mainly focused on intramolecular version partly belong to the difficulty of synthesis and unstable characteristic.

Marc C. Kimber 2010



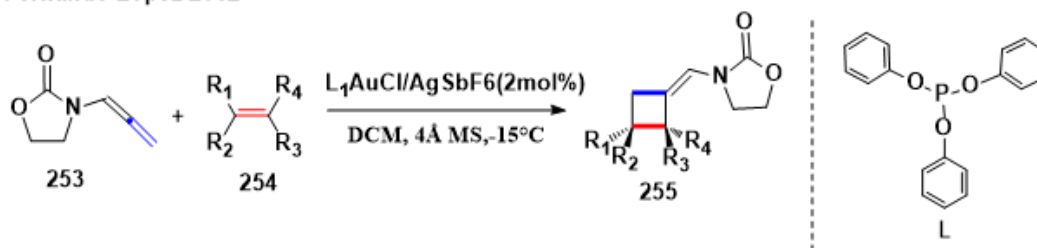
Scheme 52

Besides forming single chemical bond by simple nucleophilic addition pathway, allenamides can be used to proceed cascade reaction with cycloaddition gesture^[112] such as [2+2], [3+2], [4+2] and so on since direct cyclization reaction is always a strong tools to prepare polycyclized compounds which have numerous application and value. On the other hand, different with other starting material, allenamides can bring into hetero atom into the aimed compounds which again improved its value and attracted tons attention of chemists all over the world.

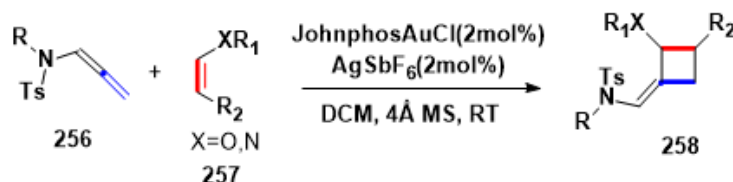
On the gold catalyzed cyclization of allenamides, Fernando Lopez group already contributed many inspiring works and showed us numerous possibilities accessing to stereo-diverse compounds. In 2012, Fernando Lopez and Jose L. Mascarenas group cooperatively reported gold catalyzed [2+2] cyclization of allenamides **253** with alkenes **254** (Scheme 53)^[113]. After examining the reaction condition, the triphenyl phosphite **L** was picked to be the best ligand which afforded cyclobutane derivatives **255** in good to excellent yield (up to 96%). In addition, this catalytic model can embrace tons of kinds of substrate. For alkenes, ont only electron rich alkenes gave promising yield, electron deficient alkenes can also react with allenamides greatly by leading to yield from 42% to 96%. Moreover, the performance on regioselectivity also was surprising. But in this work, there were no other allenamides which were not examined.

To expand the study on [2+2] cyclization of allenamides, in the same year, Zili Chen group and Jose M. Gonzalez group (Scheme 53) reported^[114] the synthesis of cyclobutane derivatives **258** through [2+2] cyclization of substituted allenamides **256** with electron rich alkenes **257** by introducing oxygen or nitrogen atom close to double bond. In this work, Johnphos phosphine

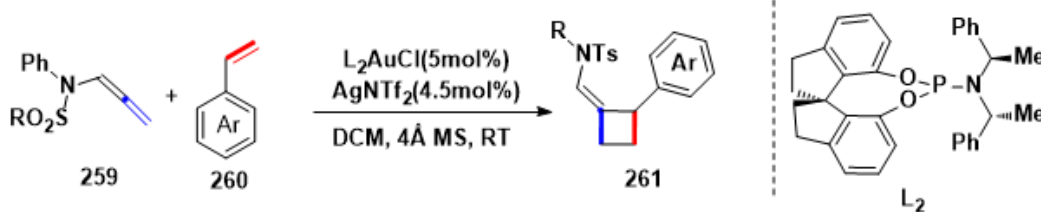
Fernando Lopez 2012



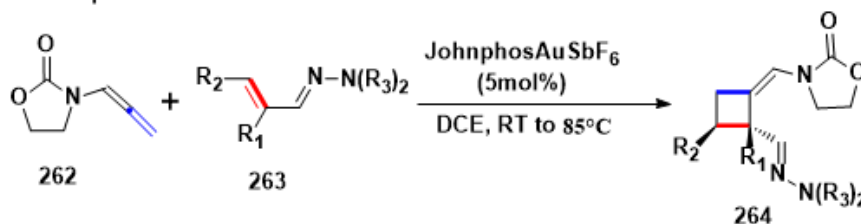
Zili Chen/JoseM. Gonzalez 2012



JoseM. Gonzalez 2012



Fernando Lopez 2014



Scheme 53. [2+2] cyclized addition

ligand showed the best yield (from 63% to 89%) and good regioselectivity. Besides high tolerance of alkenes substrates, various substituents were also tested on the allenamides including electronic donating group and electronic withdrawing group and approved the application of this catalytic system.

Although the previous work on the [2+2] cyclization of allenamides have obtained great success, to obtain high enantioselectivity of the cyclized cyclobutane bearing one chiral carbon center was still a challenge. To solve this problem^[115], JoseM. Gonzalez group (Scheme 53) applied the chiral (S)-SIPHOS-PE ligand **L₂** to construct the chiral environment and control the stereo position. Fortunately, the yield and ee could arrive to 95% and 90% respectively.

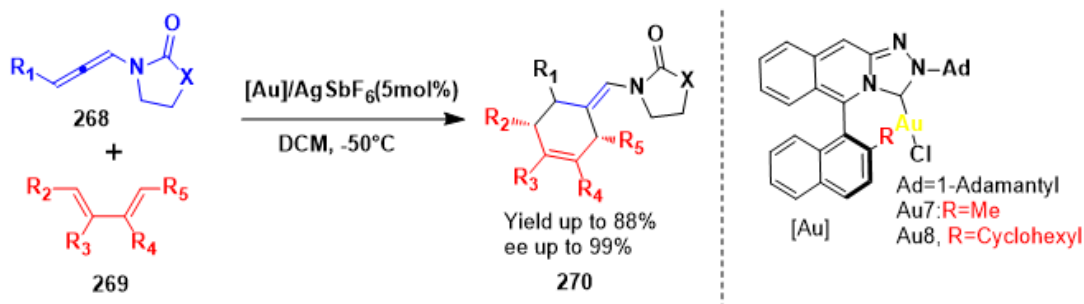
To expand the substrates for [2+2] cyclization of allenamides, Fernando López and Jose M. Gonzalez kept looking for new partners for allenamides. In 2014, they designed α , β -unsaturated hydrazones^[116] **263** which improved the nucleophilic capability of alkenes (Scheme 53). In the meantime, the existence of N-N bond could avoid the [4+2] process and only afforded [2+2] cyclized product **264** catalyzed by Johnphosgold in moderate reaction. In addition, the yield was still great (from 41% to 97%) equipped with high regio- and chem- selectivity.

Accompanied with [2+2] cyclization of allenamides, [4+2] cyclization with allenamides also becomes a popular research area to construct six member ring compounds. In 2011, José L. Mascareñas and Fernando López group^[117] published gold catalyzed [4+2] cyclization between

Fernando Lopez/Jose L. Mascareñas 2011



Fernando Lopez/Jose L. Mascareñas 2012



Scheme 54. [4+2] cyclized addition

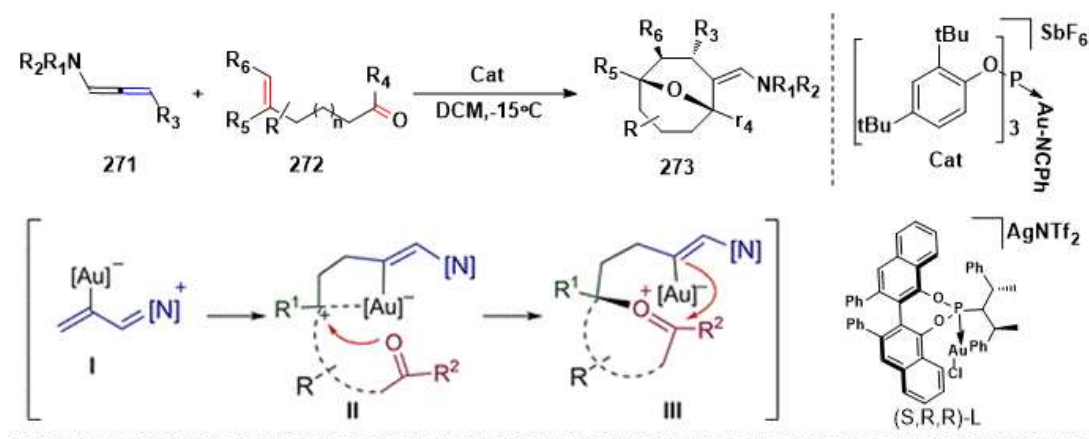
allenamides **265** and acyclic conjugated dienes **266**. Cyclohexene derivatives **267** were obtained in good to excellent yield (from 44% to 99%) and great diastereoselectivity. In the meantime, besides the high scope of dienes substrates, colorful substituents could also be featured on allenamides (R_1 , R_2 , R_3) and did not affect the yield and selectivity (Scheme 54).

Next year in 2012, they synthesized axially chiral triazoloisoquinolin-3-ylidene ligand (Scheme 54, [Au]) and applied it into [4+2] cyclization above^[118]. Promisingly, under the assistance of

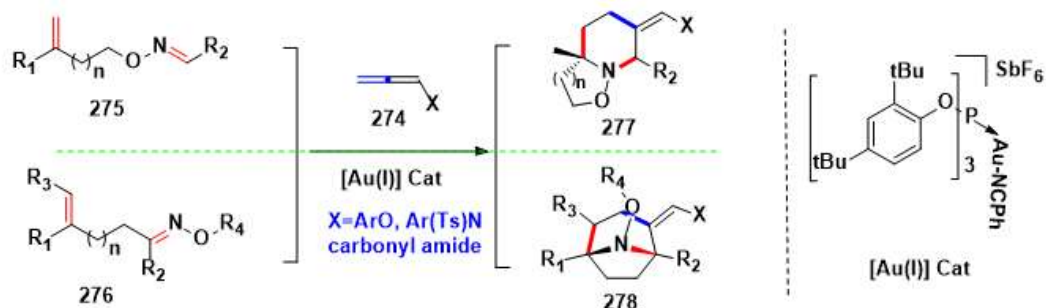
AgSbF₆, high yield (up to 88) and great enantioselectivity (up to 99) were obtained in DCM at low temperature via constructing two chiral carbon centers.

On the other hand, José L. Mascareñas and Fernando López group also extended the dienes to uncoujugated system by replacing one double bond with another electrophiles to trap alkenyl gold intermediate. In 2011, they^[119] put attention on carbonyl-tethered alkenes **272** and used it as the starting material to proceed cyclization with allenamides **271**. Followed the intermediate **I** (Scheme 55) from traditional activation of allenamides via gold catalyst, the alkene then interacted with it and form the intermediate **II** bearing a carbon cation which could receive the attack of oxygen in carbonyl group. Finally intermediate **II** quenched alkenyl-gold by forming oxa-bridged product **273** whose size could be adjusted by changing the carbon number between alkene and carbonyl group. In addition, the tolerance of allenamides was also very high with

Fernando Lopez/Jose L. Mascarenas 2011



Fernando Lopez/Jose L. Mascarenas 2018

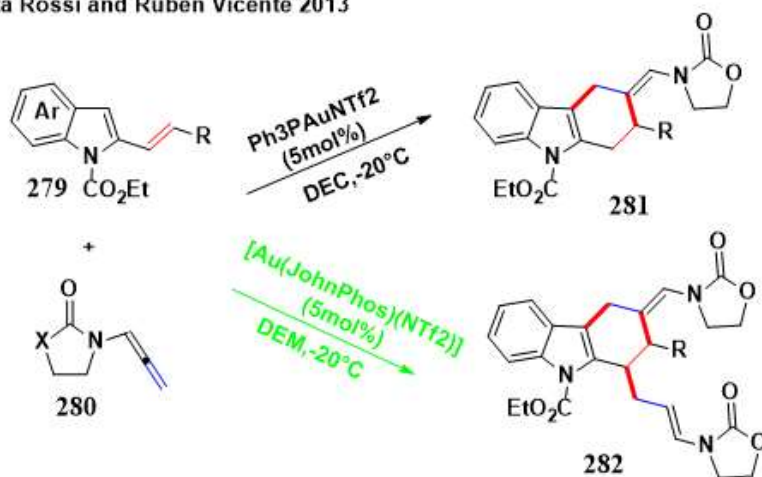


Scheme 55.

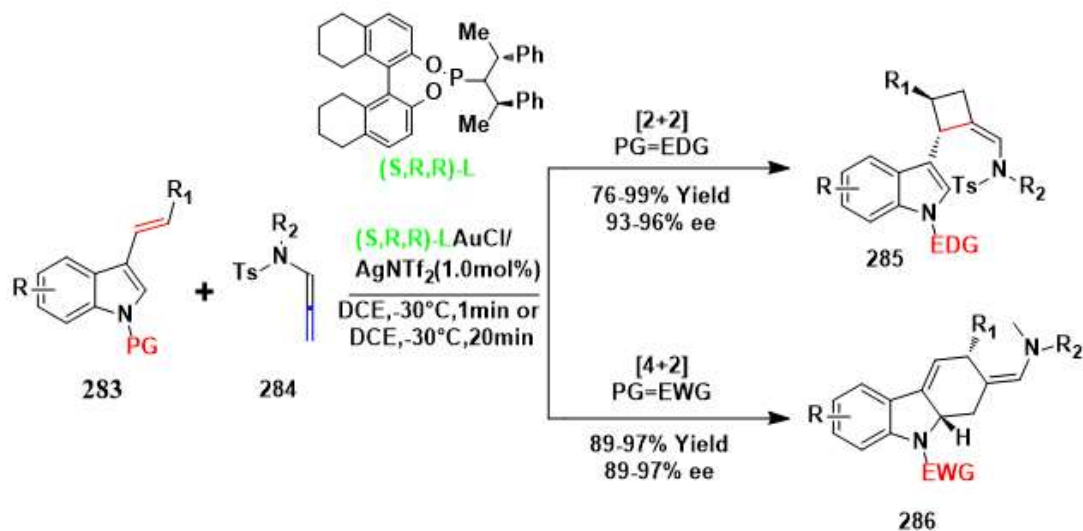
yield (from 31% to 96%). Moreover, they also applied chiral phosphine ligand (S,R,R)-L and AgNTf₂ and successfully improved the diastereoselectivity up to 90:10 with good yield(72%).

In 2018, Fernando López and Jose M. Gonzalez group^[120] together built another alkene-tethered oxime ethers **275** and **276** (Scheme 55) as starting material to construct more decorated products(including substituted piperidines **277** and aza-bridged carbocycles **278**) in good yield (from 40% to 94%) which was affected by the substituents of starting material, which made use of the same strategy with carbonyl-tethered alkenes. This work also demonstrated the advantages of oxime derivatives compared with imine derivatives since its high affinity to gold complex. At last, same chiral phosphine ligand (S,R,R)-L was used to successfully collect diastereoselectivity up to 95:5 with 51% yield.

Elisabetta Rossi and Ruben Vicente 2013



Junliang Zhang 2015



Scheme 56

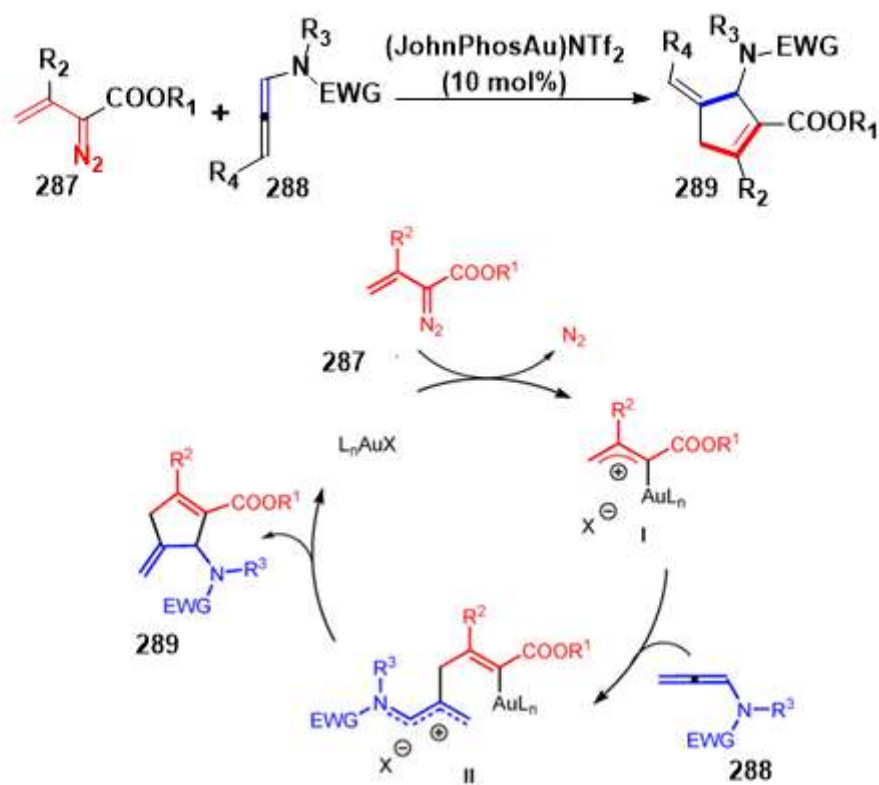
In 2013, Ruben Vicente group^[121] kept studying the applicable of suitable candidates to performed the cyclization with allenamides. They paid their attention on 2-vinyl indoles **279** (**Scheme 56**). At first, by introducing a carbamate at N-1 catalyzed by triphenyl phosphine gold complex, the desired tetrahydrocarbazole **281** was formed by cyclization process and proton transfer. But interestingly, new product of **282** was also collected partly which meant that the second allenamides was involved to replace the protodeauration process. By screening the condition, when Johnphos ligand was used, the yield of **282** was increased to 95% in DCE at low temperature. This unexpected transformation strongly approved the high applied potential to form complicated compounds.

Dependent on the data collected previously, Junliang Zhang group^[122] designed 3-vinyl indol derivatives **283** to perform the cyclization with allenamides **284**. They directly used the chiral ligand (S,R,R-L) (**Scheme 56**). As shown by Ruben Vicente group, the substituents on N-1 of indol could divert the reaction into different direction. Surprisingly, in this work, when the substituent was electron donating group, the [2+2] cyclization with allenamides happened to form cyclobutane products **285** in great yield (up 99%) and enantioselectivity (up 96%). However, when the substituent was electron withdrawing group, the reaction went to [4+2] cyclization with allenamides which afforded product **286** with also high yield (up 99%) and excellent enantioselectivity (up 97%). Moreover, the reaction condition is very moderate and the reaction ratio could step into 20 mins.

Among the cyclization reaction of allenamides, it mainly is activated by gold complex at first and interact with a nucleophile. However, in 2016, Luis A. Lopez group^[123] brought vinyl diazo compounds **287** which is easy to form carbene gold complex **I** as an electrophile (**Scheme 57**). In this condition, allenamides **288** become the nucleophile to attack carbene gold complex **I** and form the intermediate **II** which, at last, undergoes cyclization process to give the cyclopentene derivatives **289** in yield of 42% to 66%. The performance of allenamides in this work further expands chemists' impression and opens a wide research area to fully utilize allenamides to construct more useful moleculars.

Beyond the cyclization of allenamides happened between two molecules, three components involved cyclization addition reaction including allenamides catalyzed by gold complex also were reported in the past decades.

Luis A. Lopez 2016

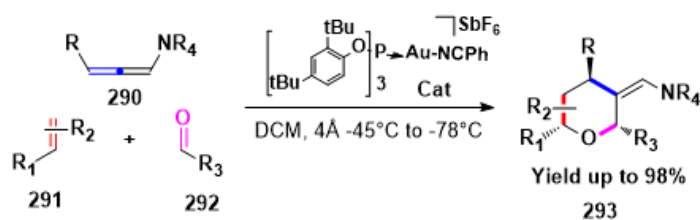


Scheme 57

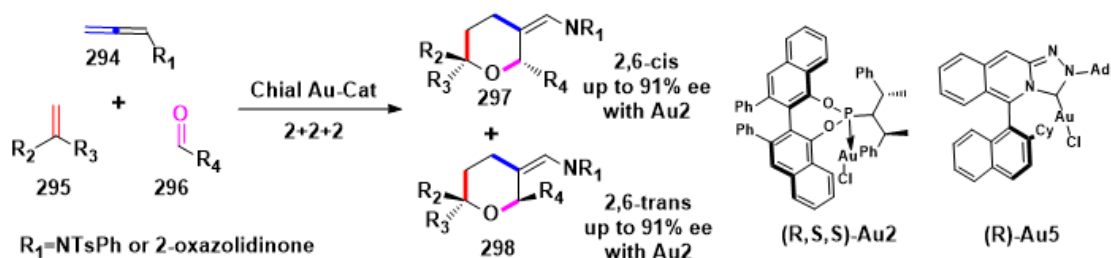
In 2015, Fernando Lopez group^[124] successfully forced three components: allenamides **290**, alkenes **291** and aldehydes **292** into one pot and formed the cyclized tetrahydropyrans **293** under minus 45 °C in DCM assisted by phosphite gold complex **Cat** (Scheme 58). Besides good to excellent yield (from 43% to 98%), highly regio- and chemoselective is also got in this reaction system. On the basis of this work, two years later, Fernando Lopez group^[125] published their another work by working on the enantioselective version (Scheme 58). In this work, by using chiral ligand **Au2** and **Au5**, more substrates were tested and gave good yield (up to 93%). Besides high regioselectivity, high enantioselectivity of products **297** and **298** were also collected which were both up to 91%.

Instead of reacting with other compounds, allenamides also can react with themselves since its

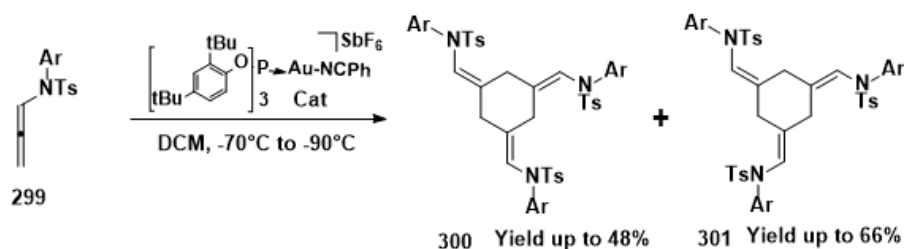
Fernando Lopez 2015



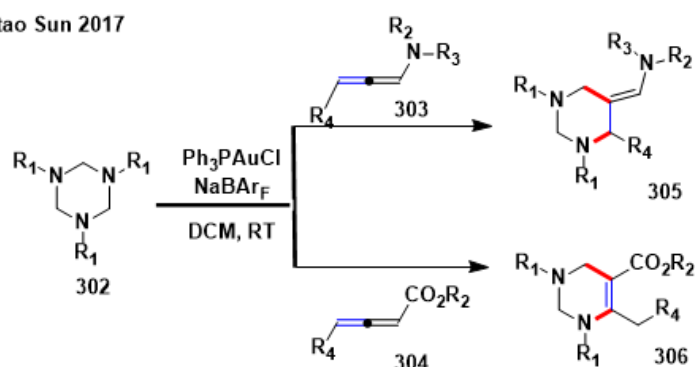
Fernando Lopez 2017



Jose. M. Gonzalez 2016



Jiangtao Sun 2017



Scheme 58. [2+2+2] cyclized addition

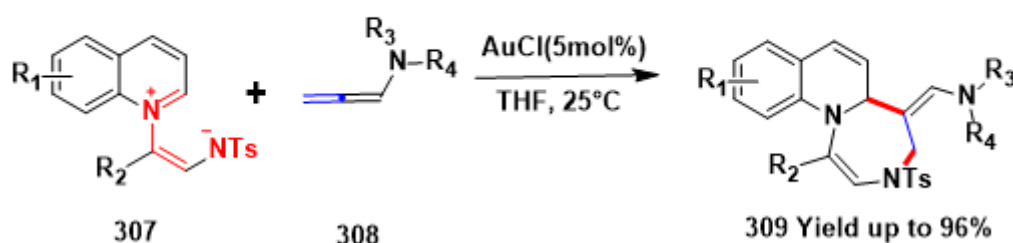
electrophilic property brought by gold and the essential nucleophilicity. In 2016, Jos éM. Gonz áez group^[126] developed a strategy to synthesize trimethylene cyclohexane **300** and **301** through [2+2+2]-cyclotrimerization catalyzed by Cat (Scheme 58). Although the whole yield was promising which was up to 90%, the regioselectivity was not high to give two isomers **300** and **301** with almost equal ratio.

In 2017, Jiangtao Sun group^[127] reported PhPAuBAR₄^F complex induced regiodivergent [2 + 2 + 2]-cycloadditions of allenes (**303** or **304**) and triazines **302** to form the six-membered N-heterocycles products (**305** and **306**) (Scheme 58). With the optimized condition, allenamides afforded the product of **305** while allenates gave the corresponding product of **306** with triazines **302** in good yield up to 92%.

Allenamides are not limited to synthesize the mediate or small cyclic compounds by cyclization addition reaction catalyzed by gold catalyst. It also accesses to preparing macrocyclic compounds by cyclization addition strategy of allenamides with proper partners forced by gold catalysis.

In 2018, Eun Jeong Yoo group^[128] made it possible by utilizing quinolinium zwitterions **307** and allenamides **308** catalyzed AuCl(5mol%) to prepared fused seven-member ring 1,4-diazepines **309**. This methodology is very mild and efficient in THF without extra ligand and shows great functional group tolerance in good to excellent yield (up to 96%)(Scheme 59).

Eun Jeong Yoo 2018



Scheme 59

In summary, allenamides showed its great advantages like various reaction sites and electron property while it is also easy to modify into different valuable compounds. Especially after cooperating with gold catalyst, its advantages and applications are magnified in many kinds synthetic chemistry. In the past decades, it has been used to build tons of useful compounds catalyzed by gold catalyst. Along with the accumulation about relative knowledge, there must be more creative ideas and work which will be published soon.

1.2. Catalytic asymmetric dearomatization reaction

Aromatic compounds are well utilized greatly in organic synthetic chemistry since they played great function in bio-active and natural compounds ^[129]. On the other hand, they are greatly abundant and easy to be decorated like Friedel-Crafts reaction, C-H activation which introduced various substituents. Among those modifications of aromatic compounds, dearomatization of aromatic compounds is also important strategy to achieve ring-including compounds including heterocyclic blocks in efficient, economic process. In the past, it met greatly challenge to destroy the aromaticity of aromatic compounds since the high resonance energy. So to dearomatize the aromatic compounds usually needs harsh reaction condition like sensitive catalyst, high temperature and high pressure such as Birch reduction reaction^[130], Oxiditive dearomatization^[131], hydrogenation of aromatic compounds^[132], nucleophilic dearomation^[133] and hypervalent iodine-mediated dearomatization^[134]. However, not limiting to only dearomatization of aromatic compounds, in front of condition of serious environment pollution, to develop more environment-friendly and atom-economic approaches also becomes a target of chemists. Facing with these problem, in recent years, catalytic transition metal catalysis has been developed to a very promising strategy to construct new C-X (X= C, N, O, S, Halogen) bonds in organic synthesis and has also become the hot research area all over the world. Along with this trend, chemists then brought this strategy into the dearomatization of aromatic compounds and then inspiringly open a new world to access to the construction of complicated tridimensional compounds ^[135]. In addition, Chemists also designed and developed various chiral ligands to complete the asymmetric transformation during the dearomatization process ^[136].

Catalytic asymmetric dearomatization (CADA) reactions have become one of the most efficient strategies in organic chemistry and shown great contribution to construct ring-including new molecules. Next, it is divided into two major sections including dearomatization of heteroaromatic compounds and phenols compounds collecting from 2005 to now.

1.2.1. Dearomatization of Heteroaromatic Compounds

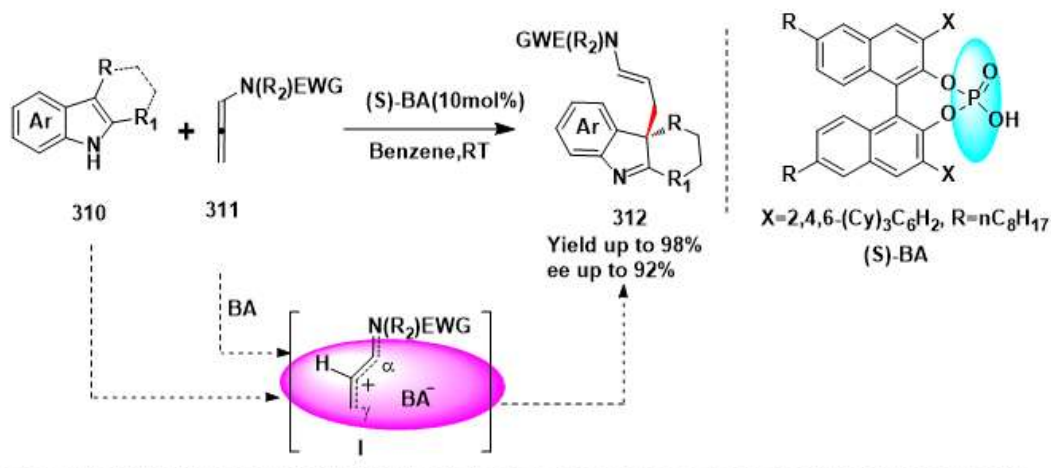
Heteroaromatic compounds which include heteroatom like N, O, S exist abundantly in nature and have shown great bioactivity leading in curing diseases^[129]. In this background, the synthesis of relative functional compounds attracts great attention from chemistry community. So far, various new reaction types were developed such as C-H bond activation and coupling reaction. Besides functionalizing the heteroaromatic compounds^[134] by various functional substituents to construct new molecules, dearomatization of heteroaromatic compounds also become more and more important strategy to synthesize the bioactive molecules which contributed greatly to human health. In the meantime, it also satisfied the requirement about constructing more specified and stereo-diverse compounds to conquer increasingly challenging disease happened currently.

On the catalytic dearomatization of heteroaromatic compounds, chemists have developed many different strategies by using different catalytic version and it is divided into organo-catalytic and transition metal catalytic dearomatization by highly making use of those catalysts' advantages in this part.

Organic catalysts have become a very strong tool in synthetic chemistry because organic catalysts are easy to prepare and the cost is very low compared with transition metal catalyst. On the other hand, for the catalytic activity, the result is also very promising and even shows great chem-, regio- and stereoselectivity in synthetic chemistry by its easy modification advantage.

By utilizing organic catalysts, in 2014, our group^[137] successfully applied chiral BINOL phosphoric acid catalyst (**Scheme 60**) in dearomatization of indol compounds and its derivatives **310** by combining with allenamides **311** leading to allylation of indol. By interacting with allenamides tightly, Brønsted acids ((**S**)-**BA**) produced an electrophilic intermediate **I** by constructing the stereochemical environment leading to high enantioselectivity of the corresponding N-heteroring compounds **312** in good to excellent yield and promising enantioselectivity (up to 94%). The carbon chain on the back of BINOL skeleton helped the solubility and could force substrates and catalyst stay closer assisted the hydrogen bond between catalyst and substrates and speed up the reaction rate. In addition, high substrates scope tolerance was also achieved under moderate reaction condition.

Marco Bandini 2014



Feng Shi 2014



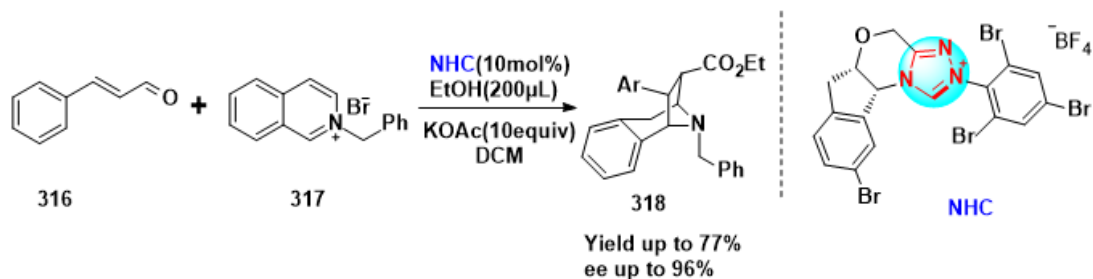
Scheme 60. Dearomatization of indol

Realizing the potential application of phosphoric acid catalyst on the dearomatization of indol derivatives, in the same year (2014), Feng Shi group^[139] (Scheme 60) enriched the strategy of phosphoric acid catalyzed dearomatization of indol compounds. In this work, quinone imine ketals **314** derivatives were chosen as the electrophile transferred by phosphoric acid catalyst **BA**. More inspiringly, this reaction did not stop after the addition and followed by alcohol elimination process to give the arylative product **315** of dearomatized indol and its derivatives in great yield and high enantioselectivity. Identically, hydrogen bond forming between **BH** and substrates played a greatly function on the connection and activation of substrates synergistically.

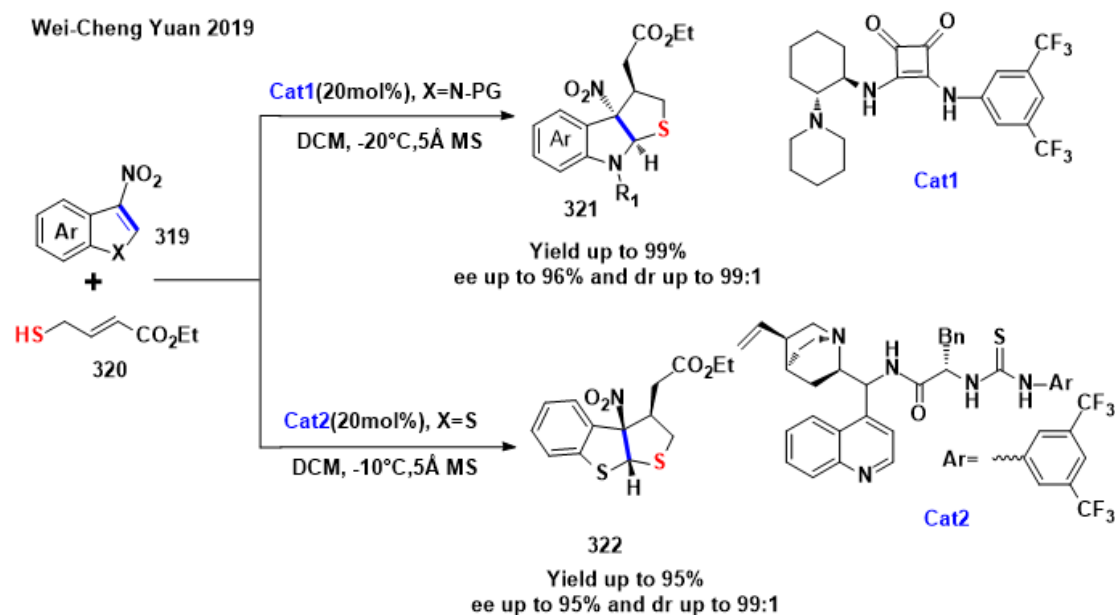
Beyond catalysts of phosphoric acid and derivatives, carbene catalysts also possessed a vital position among organo-catalyst catalyzed synthesis. In 2016, Bin Tan group^[139] successfully dearomatized the isoquinolines **317** via chiral-NHC catalysis using the aldehydes **316** through a Stetter reaction type^[140] (Scheme 61). Driven by the NHC catalyst, aldehyde was transferred an

intermediate including nucleophile and electrophile. Then isoquinolines got involved to form the cyclized tropane **318** and derivatives in good yield and high enantioselectivity.

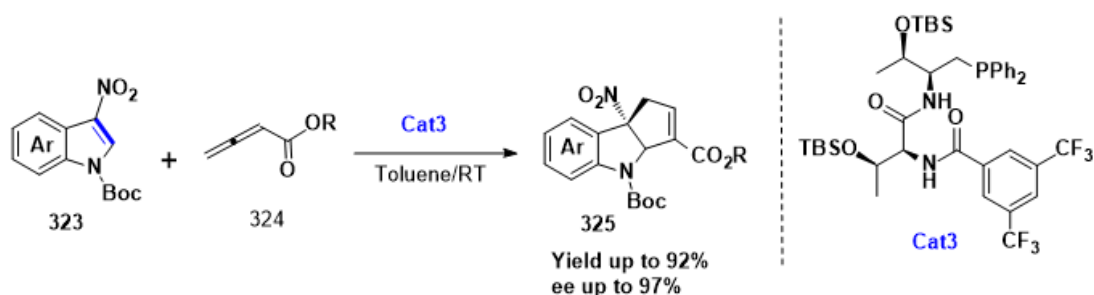
Bin Tan 2016



Wei-Cheng Yuan 2019



Yixin Lu 2019



Scheme 61. Organocatalyzed dearomatization of heteroaromatic compounds

Dearomatization of indol compounds usually made use of the **C3** as nucleophile to interact firstly with electrophile. However, **C2** of indol could also react firstly receive the attack of nucleophile by decreasing the nucleophilicity of **C3** via featuring the strong electron withdrawing group on **C3**. On the other hand, squaramides catalyst is also one major member of organo-catalysts in organic

Chapter 1

synthesis by activating the substrates via forming N-H hydrogen bond. Based on this theory, Wei-Cheng Yuan group^[141] achieved asymmetric dearomatization of 3-Nitroindols and 3-Nitrobenzothiophenes **319** with allyl thiol **320** triggered by amino squaramides catalysts **cat1** and **cat2** (Scheme 61). This reaction started from indol compounds as an electrophile at C2 and received the attack of allyl thiol which was activated by hydrogen bond activation mode with **cat1** and **cat2** and end up with another Michael addition from C3 nucleophile of indol to the allyl group. In the optimized reaction condition, A series of chiral tetrahydrothiopheneindolines **321** and tetrahydro -thiophene-benzothiophenes **322** featured three chiral carbon centers were obtained in high yields with good diastereoselectivities and excellent enantioselectivities.

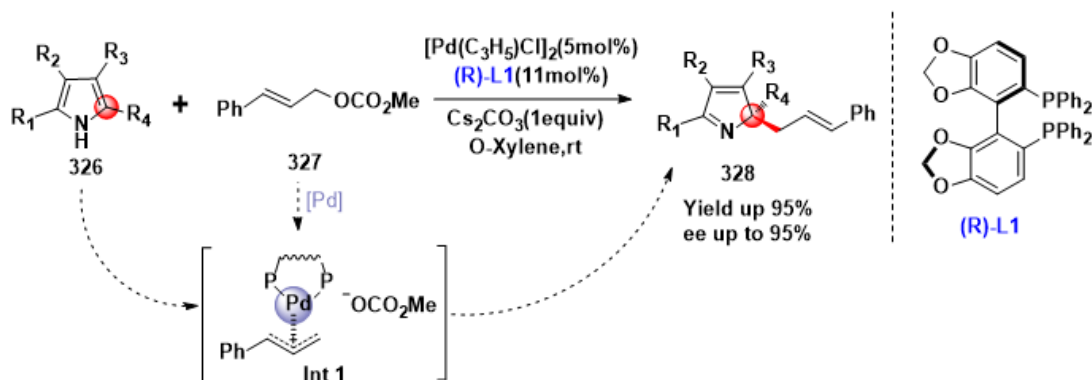
Keeping in pace with Wei-Cheng Yuan's work, Yixin Lu group^[142] (Scheme 61) developed phosphine-catalyzed dearomatization of 3-Nitroindol **323** with allene derivatives **324** co-assisted with squaramides **cat3** by the hydrogen bond. In this reaction, allene **324** received the attack of phosphine of **cat3** which was converted into a nucleophile to attack the electrophile C2 of indol starting material. Then the phosphinated allene accepted the attack of C3 of indol to form the final [3+2] annulated product with high enantioselectivity (up to 97%).

All the work showed above strongly approved the capability of organocatalyst in the dearomatization of heteroaromatic compounds. By its highly easy modification, great stereoselectivity could be obtained accompanied with high yield in very moderate condition efficiently. In addition, the cost was also decreased greatly on the organic synthesis compared to noble metal catalyst.

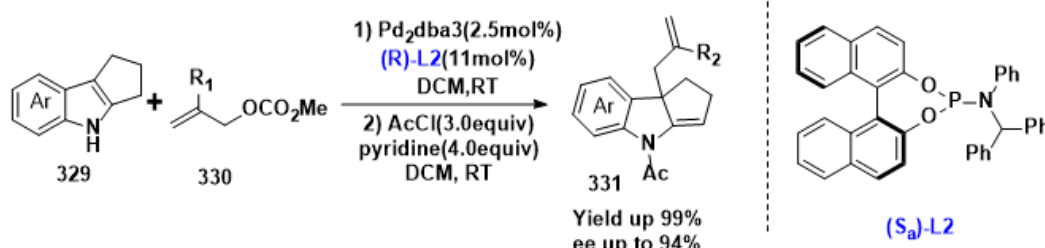
Even sometime the transition metal catalysis costs more than organocatalyst, the study of transition metal catalyzed transformation in organic chemistry is greatly necessary since their high activity on chemical bond which organocatalyst is not as good as metal catalyst like redox reaction and radical reaction. On the other hand, their catalytic amount and higher functional tolerance also make chemist absorbed. As a result, many works about transition metal catalyzed dearomatization of heteroaromatic starting materials.

On the palladium catalyzed dearomatization of heteroaromatic compounds, Shuli You group have made great contribution to the chemistry community. Pyrrol and derivatives is a kind of very

Shu-Li You 2014



Shu-Li You 2018



Scheme 62. Palladium catalyzed dearomatization of heteroaromatic compounds

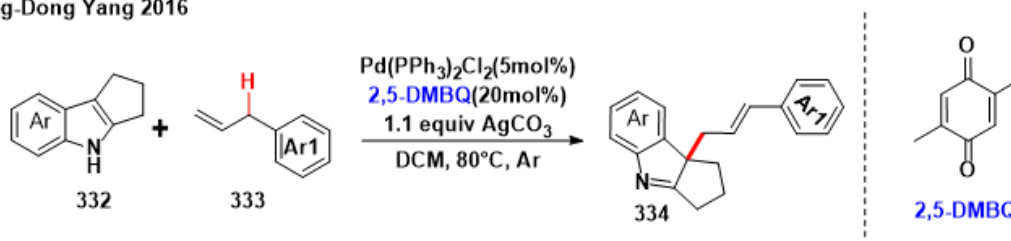
stable aromatic compounds and to functionalize this kind of motif is a very challenging task since the regio-selectivity due to the similar reactivity^[143] between C2 and C3. In 2014, they conquered this challenge by Pd catalyst^[144] (**Scheme 62**). In this work, polysubstituted 2H-Pyrroles and derivatives **328** were synthesized through Pd catalyzed dearomatization of pyrroles **326** with cinnamyl carbonate derivatives **327**. Carbonate group is a very great leaving group and is easy to form the allyl palladium **int1** which is a very good electrophile. By adjusting the ligand, $(R)\text{-L1}$ showed highly regio- and enantioselectivity on the dearomatized product with promising yield and constructed chiral quaternary carbon center.

Based on the work of dearomatization of pyrroles, allyl palladium intermediate was though a good reaction intermediate which could trap nucleophiles efficiently. With this idea, in 2018, Shuli you designed another allylic dearomatization of polycyclic indol derivatives^[145]. In this work (**Scheme 62**), β -substituted allyl carbonate **330** was chose to produce the allyl palladium complex and polycyclic indol **329** got involved as a nucleophile. On the other hand, chiral phosphoramidite ligand $(S_a)\text{-L2}$ was the best ligand which could give excellent yields (up to 99%) with excellent

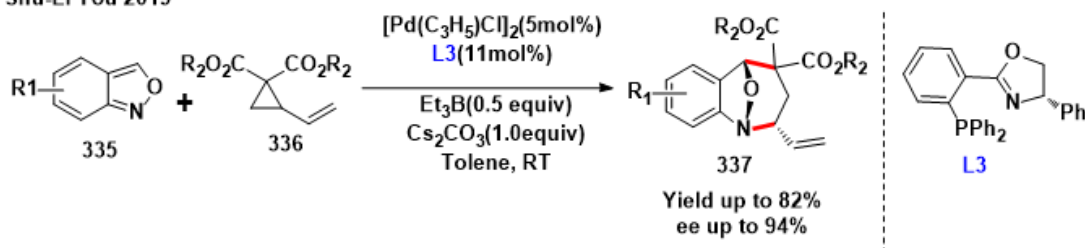
enantioselectivity (up to 98% ee) and was also applicable to synthesize various polycyclic indoline and indolenine derivatives **331**.

To make the transformation more atom-economic, in 2016, Shang Dong Yan group^[146] applied palladium catalyzed C-H activation into dearomatization of indols. In this work (Scheme 63), allylbenzene **333** was selected as the electrophile produced by palladium catalyzed C-H bond activation excluding the leaving group. 1,3-substituted indols **332** was smoothly dearomatized and functionalized to form the product **334** in good yield (up to 84%). During the catalytic cycle, Pd(II) was reduced to Pd(0) by forming the product and then Pd(0) was oxidized into Pd(II) by 2,5-DMBQ to get involved in the next catalytic cycle. This work provides a more atom economic way to access to the aimed product and also leave another task to obtain high enantioselectivity.

Shang-Dong Yang 2016



Shu-Li You 2019

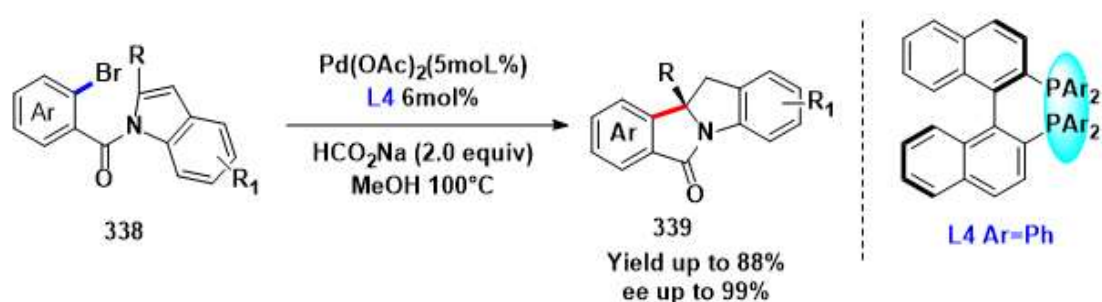


Scheme 63. Palladium catalyzed dearomatization of heteroaromatic compounds

Besides the strategy of dearomatization through C-H bond activation, in 2019, Shuli You group^[147] developed another pathway to dearomatize Anthranils **335** via palladium catalyzed C-C activation of vinylcyclopropanes **336** (Scheme 63). By making use of the high strain energy of cyclopropanes, palladium could open this ring by informing a nucleophile and an electrophile. Assisted by the triethyl boron, Nitrogen of **335** could become more nucleophilic which drove the reaction to proceed [4+3] cyclization with anthranils and gave the bridged cyclic products in high yields accompanied with excellent stereoselectivities.

To expand the palladium catalyst on dearomatization research, Yi xia Jia group^[148] successfully applied Pd-Catalyzed intramolecular reductive Heck reactions on the dearomatization of indol by designing proper substrates **338** (Scheme 64). By featuring the Bromo group at β position of aryl group, the reaction started from oxidative addition to palladium and followed by insertion from indol unite to give the dearomatized product **339** C2-quaternary stereogenic centers. On the other hand, L4 ligand showed the best activity by offering excellent yield and high enantioselectivity.

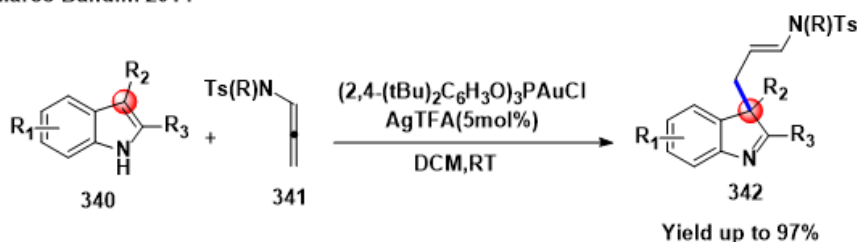
Yi-Xia Jia 2015



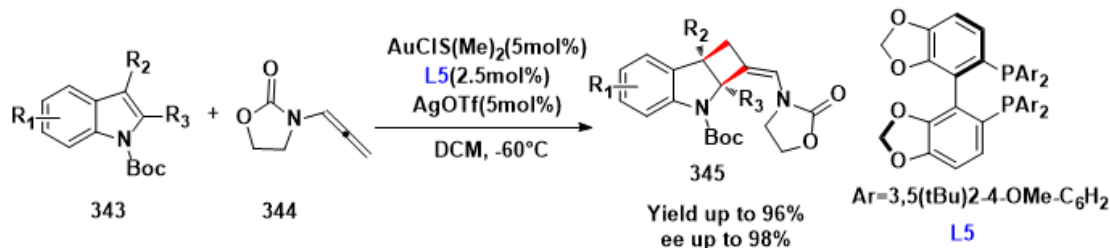
Scheme 64. Palladium catalyzed dearomatization of indol

Instead of Pd catalyzed dearomatization of aromatic compounds, gold catalyst also performed very well leading to become another useful tool to achieve the target of dearomatization and functionalization of aromatic compounds.

Marco Bandini 2014



Marco Bandini 2015



Scheme 65. Gold catalyzed dearomatization of indol

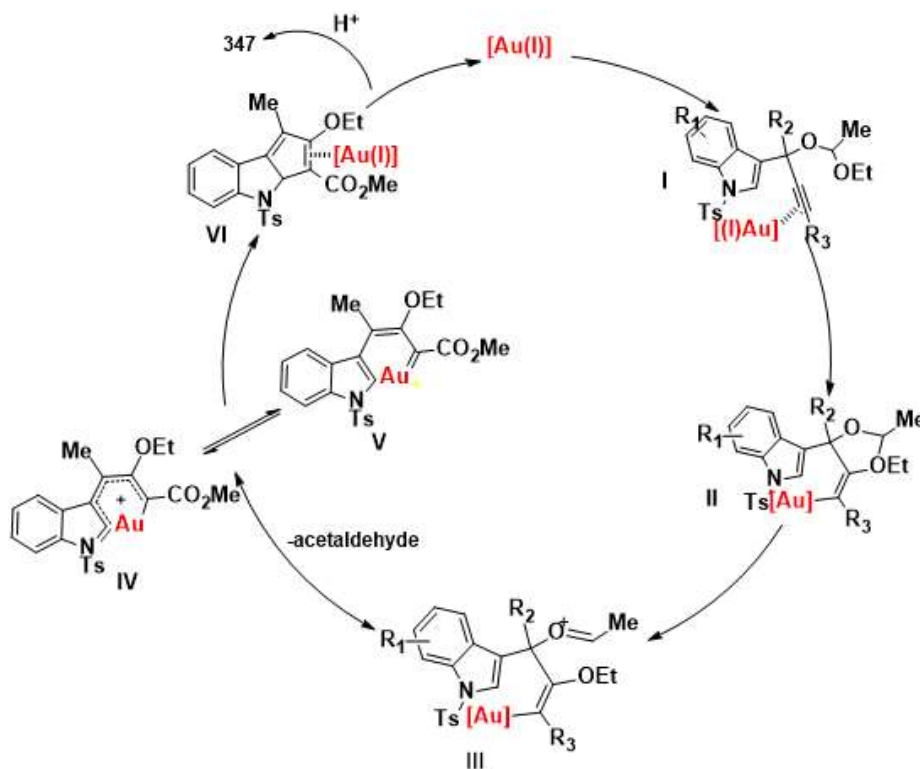
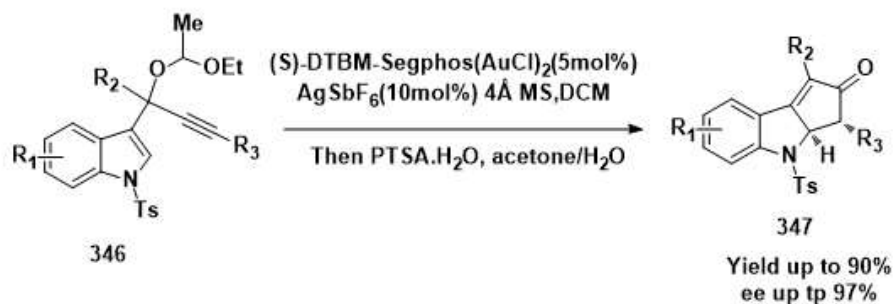
In this area, our group has developed several strategies to dearomatize indol and derivatives. In 2014, our group^[149] chose allenamides **341** as the suitable potential electrophile which was easy to coordinate to gold catalyst via π -activation (**Scheme 65**). By forming the gold complex intermediate, 2, 3-substituted indol **340** and derivatives got involved to interact with this intermediate as a nucleophile. in situ catalyst (2,4-(tBu)₂C₆H₃O)₃PAuCl/AgTFA was the best one even under air condition which gave the high yield and also tolerated various function group. On the other hand, quaternary carbon center in product **342** was obtained by functionalization of allylation and featured a new imine group which could be further modified.

Based on this work, next year in 2015, our group developed another strategy^[150] to dearomatize indols **345** via trapping the alkyl gold intermediate to form dearomatized [2+2]-cycloaddition between indol and allenamides. In this work, chiral ligand was used to attempt to obtain high enantioselectivity. Delightfully, when **L5** ligand (**Scheme 65**) was tested and contributed promising enantioselectivity (up to 98%) with excellent yield. However, besides the devotion of ligand, low temperature was also necessary to reduce the flexibility after the allenamides coordinated with gold catalyst.

On the gold catalyzed dearomatization of heteroaromatic compounds, F. Dean Toste group^[151] also developed new strategies by combining alkyne functional group **346**. In 2015, they came up with gold(I)-catalyzed dearomative rautenstrauch rearrangement on indol derivatives to obtain cyclopenta[*b*]indoles **347**(**Scheme 66**). indole-derived propargyl acetate **346** was designed which could be forced to go through rautenstrauch rearrangement (**Scheme 66**) catalyzed by cationic (S)-DTBM-Segphos gold(I) assisted with AgSbF₆. The reaction started from π -activation of alkyne by gold cation and accepted the anti-attack of the ethoxyl ether resulting in the formation of oxonium species **II**. Then consecutive cleavage of C-O bond and elimination of aceta -ldehyde happened to form the gold-substituted 1-aminopentadienyl intermediate **IV** which also might exist as carbenoid resonance structure **V**. At last, chiral phosphine

gold-controlled Enantiodetermining C–C bond formation occurred via Imino-Nazarov cyclization of **IV** to afford **VI** which could afford the final Cyclopenta [*b*]indoles **347** through protonation process in excellent yield and enantioselectivity.

F. Dean Toste 2015



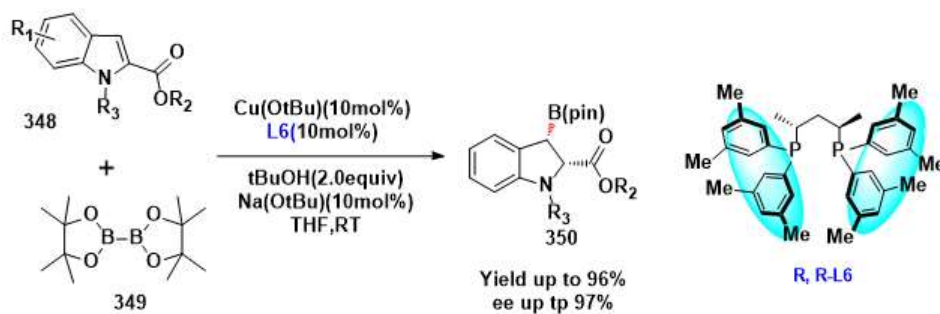
Scheme 66. Gold catalyzed dearomatization of indol via tandem [3, 3]-sigmatropic rearrangement

On the basis of this work, they continued to develop new acyclic diaminocarbene ligands which enable gold catalyzed cascade dearomatization of indol derivatives via tandem [3, 3]-sigmatropic rearrangement-[2+2]-cyclization process to give the polycyclic dearomatized indol product.

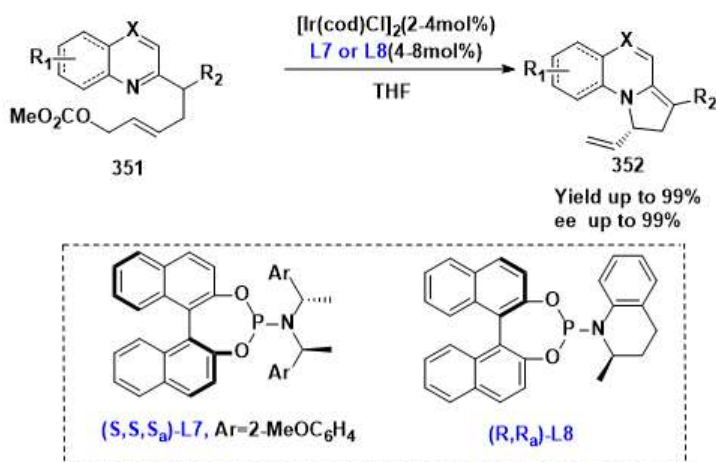
Beyond the catalysts talked about above, various other transition metal catalysts are also used to achieve dearomatization of heteroaromatic compounds along introducing different function group.

In 2015, Hajime Ito group^[152] reported copper catalyzed the borylative dearomatization of indole-2-carboxylate **348** with bis(pinacolato)diboron **349**. This work not only obtained dearomatized indol motif, C-B bond which is mainly used to perform coupling reaction was also constructed in high yield and diastereoselectivity by using **L6** chiral ligand (**Scheme 67**). In the

Hajime Ito 2015



Shu-Li You 2015



Scheme 67.

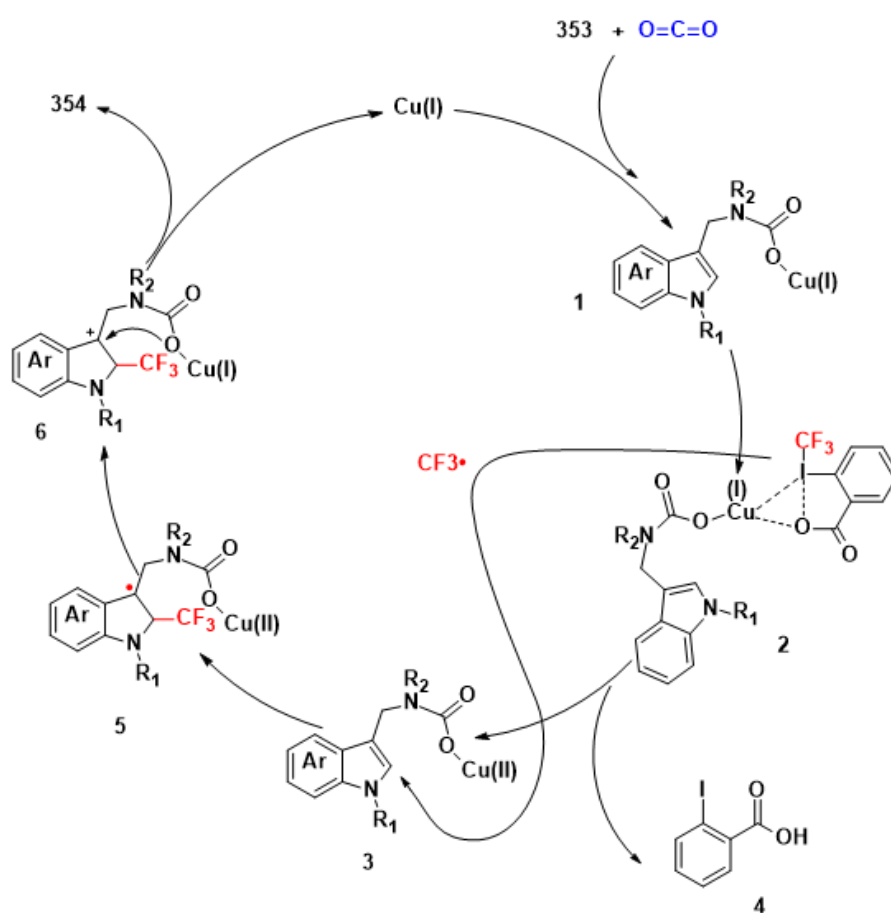
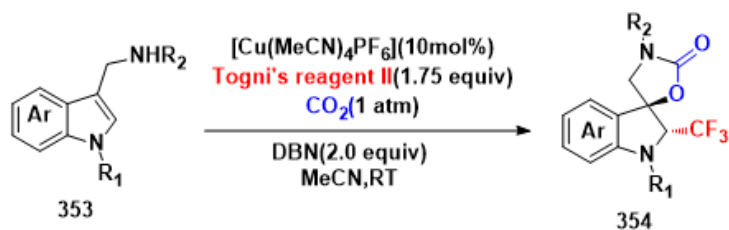
same year, Shuli you group^[153] used copper to successfully dearomatize indol and derivatives with propargylic acetate and collected asymmetric dearomatized indol products. In this work, versatile furoindoline and pyrroloindoline derivatives bearing a quaternary carbon stereogenic center (up to 98%) and a terminal alkyne moiety in good yield up to 86%.

In the meantime, Iridium catalyst was also applied to dearomatization reaction and achieved promising result. For instance, in 2015, Shuli You group^[154] used Iridium catalyst (**Scheme 67**) to dearomatize successfully Pyridines, Pyrazines, Quinolines, and Iso-quinolines **351** at the same time through cyclized allylation. By utilizing **L7** and **L8** ligands, the corresponding dearomatized products **352** were isolated in high levels of yield (up to 99% yield) and enantioselectivity (up to 99% ee).

In addition, in 2017 Dagang Yu^[155] group combined the radical reaction with dearomatization accompanied with carboxylation reaction via copper catalyzed redox reaction (**Scheme 68**). It is

known that amino group has a strong capability of trapping CO₂. Inspired by this theory, Yu group designed the substrate **353** featuring

Da-Gang Yu 2017

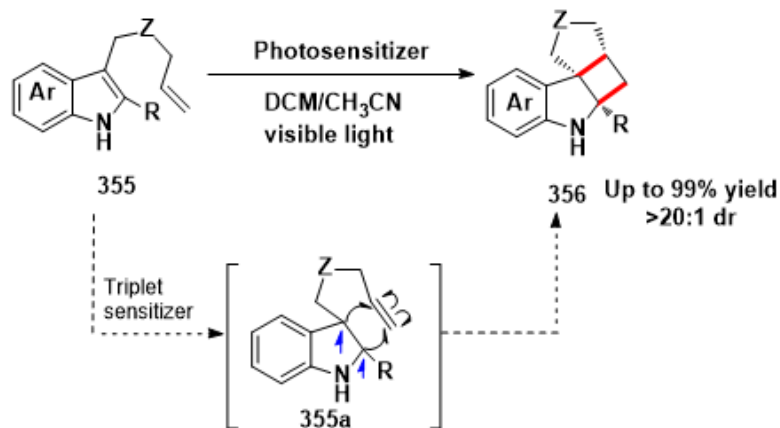


Scheme 68. Dearomatization via trapping CO₂

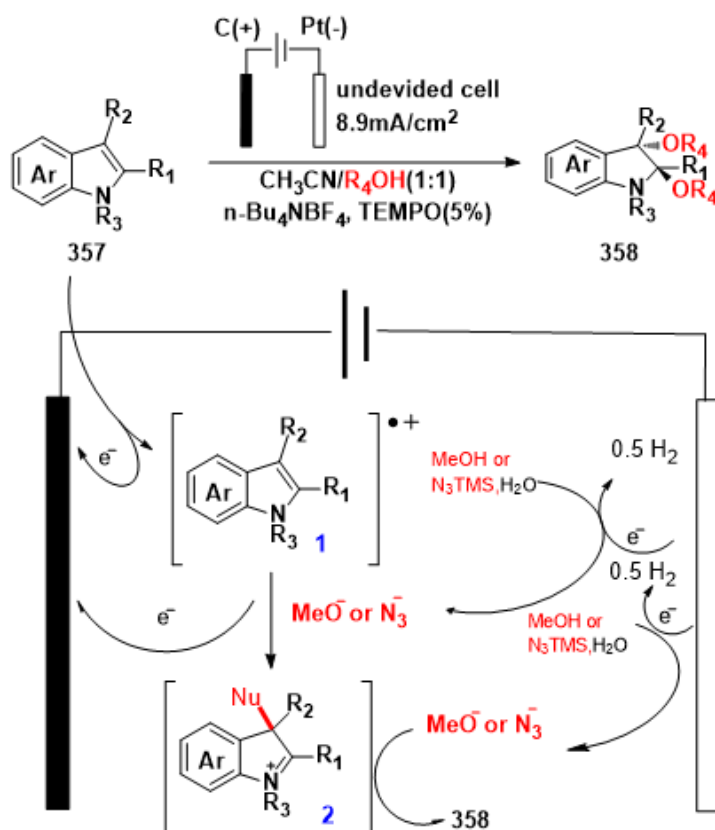
amino group as an anchor to fix CO₂. By trapping the CO₂, the copper stabilized carboxylate intermediate **1** formed and went through the oxidative process to form the Cu(II) intermediate **3** which trapped the CF₃ radical formed also by oxidative process of Cu(I) leading to intermediate **5**. Moreover, intermediate **5** was oxidized into carbon cation by Cu(II) and caught the nucleophile of

oxygen formed by releasing the Cu(I) catalyst to produce the dearomatized indol products featured trifluoro methylation and carboxylation in good yield.

Shu-Li You 2019



Guillaume Vincent 2019



Scheme 69. Photo and electronic catalyzed dearomatization

Along with the development of photocatalysis and electronic catalysis, chemists also try to apply those strategies to dearomatization of aromatic compounds. Under this ambition, in 2019, Shuli You group^[156] made the access to synthesize the cyclobutane-fused tetracyclic spiroindolines **356**

(**Scheme 69**) via visible-light-promoted intramolecular dearomatization of indole derivatives **335**. By promoting the electron of β , γ carbon of indole to the triplet excited state **335a**, intramolecular [2+2] cycloaddition of indole-tethered terminal olefin occurred to give the product **356** in good to excellent yield (up to 99%) and high selectivity (dr up to 20:1).

On the other hand, in this year (2019), Guillaume Vincent group ^[157] published their electrochemical dearomative 2,3-difunctionalization of indoles **357** (**Scheme 69**). The application of undivided electrolytic conditions avoided the use of an extra oxidant to force the catalytic cycle to complete. And it was proposed that indole derivatives likely were oxidized by losing one electron into a radical cation which could be trapped by alcohols or azide compounds formed by obtaining one electron leading to three-dimensional 2,3-dialkoxyindolines or 2,3-diazidoindolines **358** which also was applicable to various substituted starting material.

In summary, the catalytic asymmetric dearomatization of heteroaromatic compounds has been well developed and on this basis, more advanced and environment-friendly methodology will be further developed to provide more efficient approaches to natural compounds and pharmaceuticals.

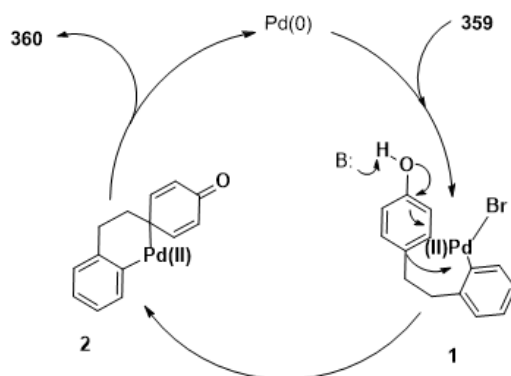
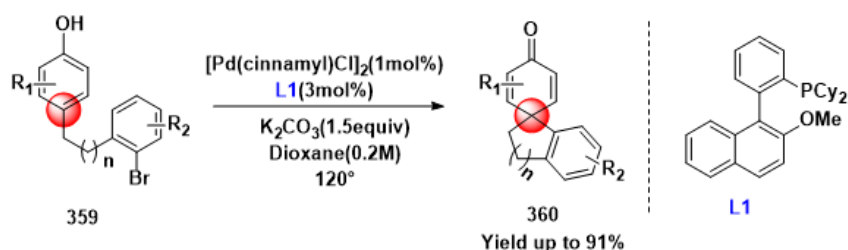
1.2.2. Dearomatization of Phenols

The dearomatization of phenol and derivatives has also grown up to a mature and strong strategy which already been used to access to various functionalized bio-active natural compounds and pharmaceutical ^[158]. It not only provides more tools to prepare useful and valuable compounds, it can also greatly decrease the cost of money and time since the abundant existence of phenol and its derivatives and the polyring structure property. On the other hand, attributing to dearomatization process, two-dimensional starting material can be converted to three-dimensional products which increases the potential bioactive value. In addition, chiral carbon centers will also be constructed and by designing and using chiral ligand, high enantioselectivity can also be collected.

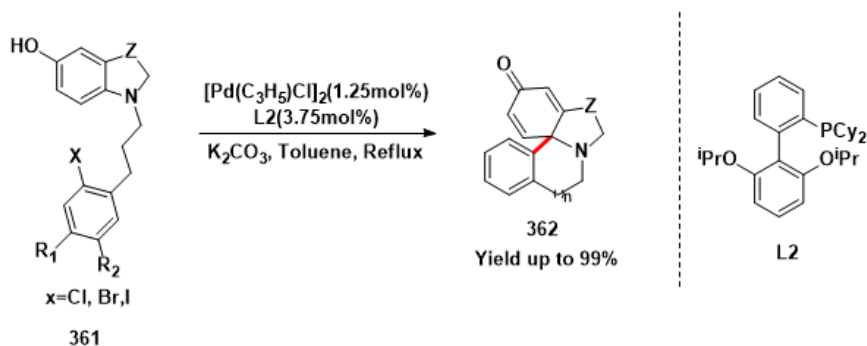
On these advantages of dearomatization strategy, chemists from all over the world have paid tons of attention on the catalytic asymmetric dearomatization of phenols to satisfy the requirement from the industry, economy and environment-friendly. Even though many strategies have been developed so far, catalytic asymmetric dearomatization of phenols will be mainly talked here and transition metal catalyzed dearomatization of phenols occupied large position. In the meantime, the dearomatization of phenols also majorly focused on phenols and naphthols.

In 2011, Stephen L. Buchwald group came up with the strategy^[159] of palladium(0) catalyzed redox arylyative dearomatization of phenols (Scheme 70). By featuring a aliphatic carbon chain bearing a terminal bromoaryl group at the *para* position of phenol **359**, It provides an entry to go through redox of Pd(0) process. Synergistic with tautomerism between enol and keto form promoted by external base K_2CO_3 , *para* carbon of phenol become more nucleophilic and could replace the bromo at Pd(II) to form the new Pd(II) intermediate **2**. At last, intermediate **2** performed reductive elimination to release the Pd(0) catalyst which got involved in the next

Stephen L. Buchwald 2011



Shu-Li You 2014



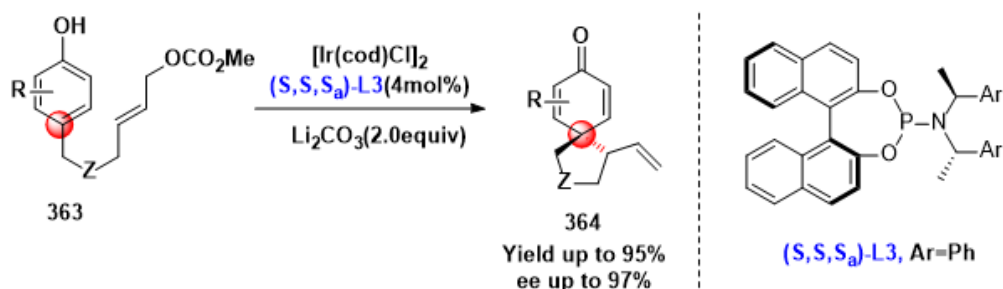
Scheme 70. Dearomatization of phenol

catalytic cycle and gave the final dearomatized phenol product **360** in good to excellent yield. The success was guaranteed by the ligand **L1**, however, this strategy was more applicable on electron rich substrates which could promote the oxidative process.

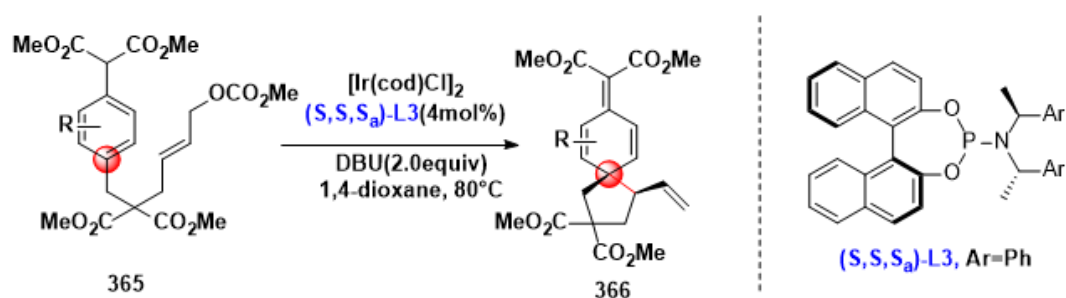
With same catalytic strategy, in 2014, Shuli You group^[160] built erythrinane skeleton **362** via Pd(0) catalyzed dearomatization of para-aminophenols **361**(Scheme 70) and increased the efficiency greatly. In this work, more heteroatom like N was introduced into starting material and tetracyclic sterically congested spiroamines bearing a quaternary carbon were synthesized in excellent yield (up to 99%) with the optimized ligand(L2).

In addition to Pd catalyzed dearomatization, Iridium also showed its strong power to dearomatize phenol compounds. In 2011, Shuli You group^[161] used Iridium catalyst to activate the allyl carbonate functional group to form the η^3 allyl-Ir(I) electrophile. By combining this electrophile with phenol as the nucleophile **363** (Scheme 71), the dearomatization of **363** was successfully

Shu-Li You 2011



Shu-Li You 2018



Scheme 71. Iridium catalyzed dearomatization of phenol

Chapter 1

achieved driven by Iridium activated via chiral ligand (**S,S,S_a-L3**) and afforded the spirocyclohexadienone derivatives with up to 97% ee.

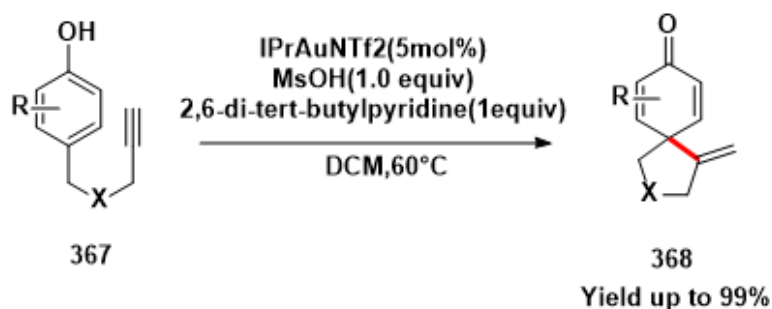
Being different with studying various electrophiles, in 2018, Shuli You group^[162] turned to another strategy by modifying the nucleophile tethered allylic carbonate **365** (**Scheme 71**). In this work, the electron donating hydroxyl group was replaced by dimethyl malonate group whose methylene was a kind of carbon donating group. Before testing this substrate, computations were firstly run to compare two model systems of asymmetric allylic dearomatization reactions between phenol and malonate diester substituted benzene. Delightfully, the result encouraged them to launch experimental studies with the same condition catalyzed by [Ir(cod)Cl]₂ and chiral ligand (**S,S,S_a-L3**). Finally, a series of spiro[4.5]cyclohexadiene compounds **366** were obtained in reasonable yields (up to 61%) and good enantioselectivity (up to 97%).

In other aspects, gold catalyst also contributed several strategies to dearomatize phenols compounds. In 2014, Yasumasa Hamada group^[163] tethered terminal alkyne in phenol **367** by carbon chain and proposed that the alkyne could accept the attack of para carbon of phenol to form the spiro[4.5]cyclohexadienones **368** activated by gold catalyst IPrAuNTf₂ (IPr=1,3-bis(2,6-diisopropylphenyl)imidazol-2-ylidene) via π -activation (**Scheme 72**). By launching the experiment to approve their idea, results was encouraging and strictly consistent with the original idea to obtain the aimed spiro[4.5]cyclohexadienones **368** products with good to excellent yield (up to 99%) and good functional group tolerance.

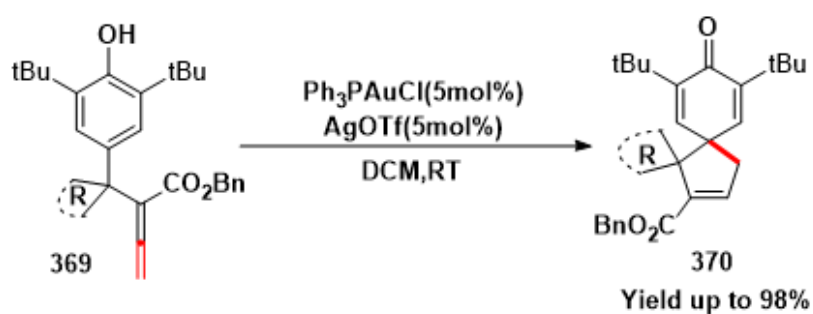
Gold catalyst is a kind of π -electron addicted Lewis Acid which is good at activating electron rich compounds such as alkyne and allene. Followed Hamada's work, Bo Tang group^[164] tethered terminal allene to para position of phenol as the starting material **369** (**Scheme 72**) and delightfully obtained the addition reaction between phenol and allene forced by Ph₃PAuCl/AgOTf in situ catalysis and also gave the corresponding spiro-polycyclic products **370** in excellent yield (up to 99%).

Moreover, Rhodium catalysis also provide the possibility to access to the dearomatization of phenols. In 2014, Moisés Gulías^[165] group applied Rh(III) catalyst to dearomatize the 2-vinylphenol **371** through cleavage of the terminal C–H bond of vinyl group and insertion of

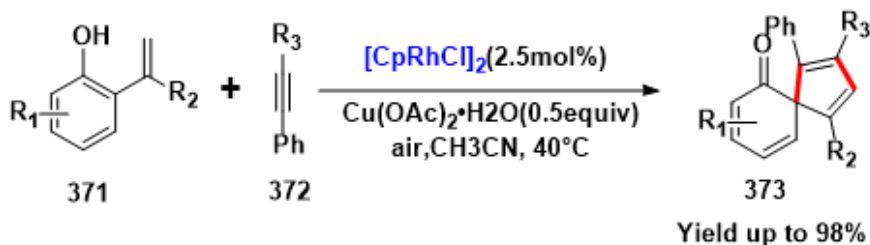
Yasumasa Hamada 2014



Bo Tang 2018



Moises Gulias 2014

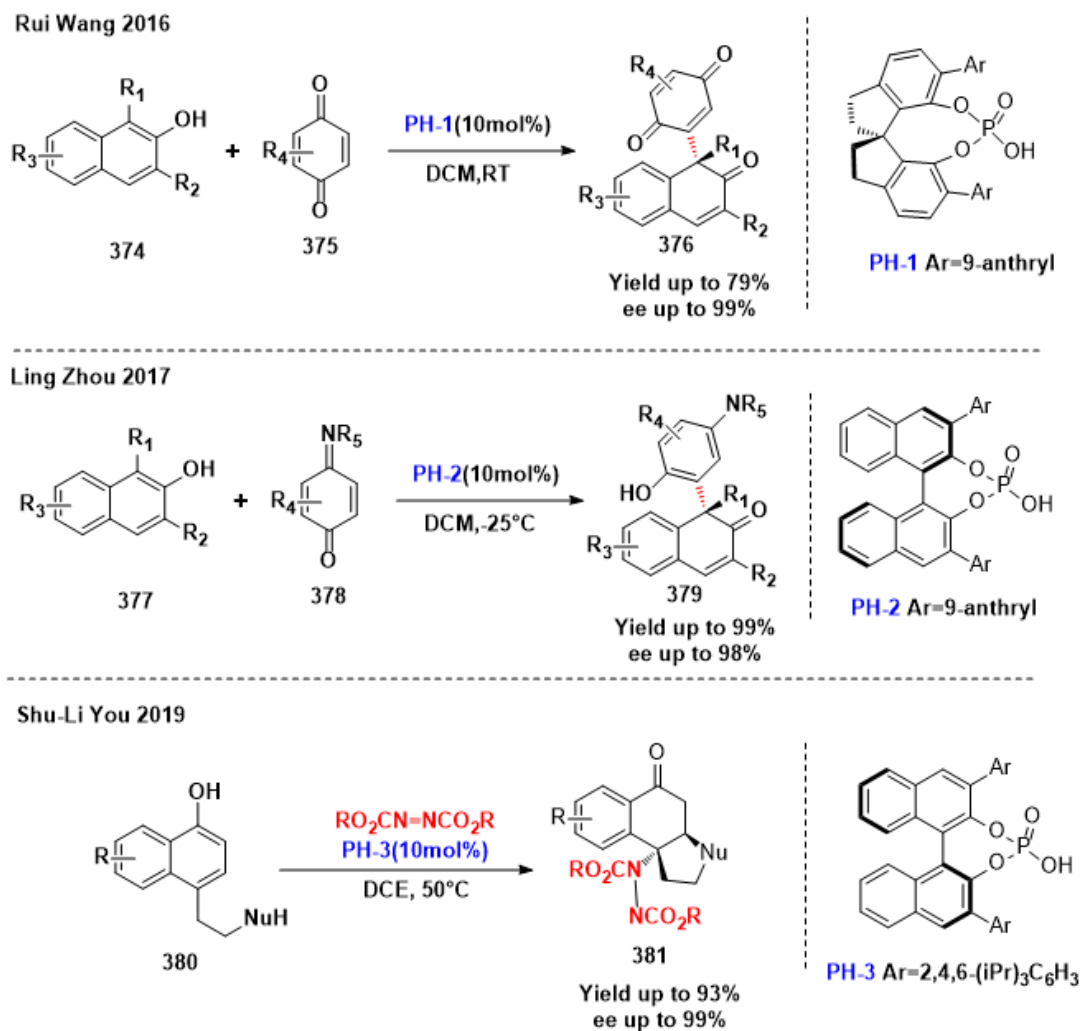


Scheme 72. Gold catalyzed dearomatization of phenol

alkynes **372** successfully (Scheme 72). Delightfully, [3 + 2] Annulation occurred between 2-alkenylphenols and alkynes under also mild reaction condition and with high atom economic character. Finally the products **373** with highly appealing spirocyclic skeletons were collected in good to excellent yield (up to 99%).

Besides phenols, naphthol compound also is one very important kind of phenols which is also abundant and widely applicable in people life. To promote its value for life, various modification based on naphthol have been developed like Fried-Crafts reaction. Among the modifications,

dearomatization of naphthol is also a useful strategy to provide polycyclic three dimensional compounds by featuring vary functional group.



Scheme 73. Organocatalyzed dearomatization of naphthol

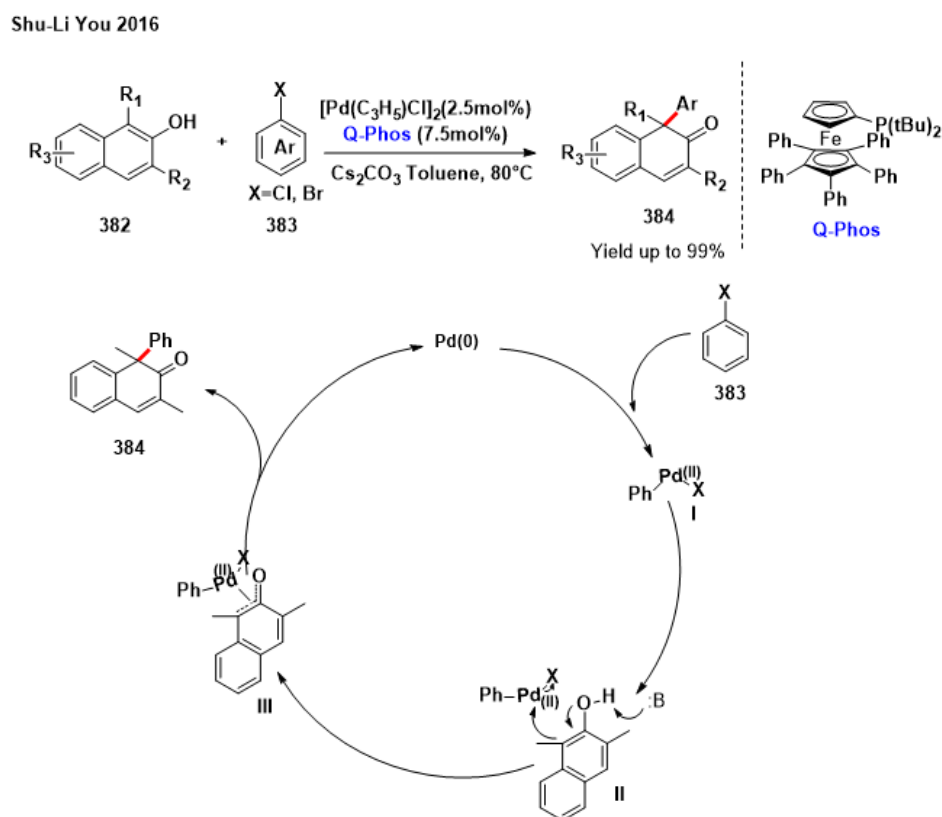
In the tool box of dearomatization of naphthols, organocatalysis has occupied a very important role and already abstracted large attention all over the world. In 2016, Rui Wang group^[166] chose quinones **375** (**Scheme 73**) as the electrophile which was activated by chiral spirocyclic phosphoric acid (**PH-1**) by hydrogen bond. On the other hand, naphthol **374** was activated also by the hydrogen bond with **PH-1** and was dragged to interact with quinones **375** via the hydrogen bond. Two starting material reacted with each other in the chiral space constructed by the chiral spirocyclic phosphoric acid which finally gave cyclohexadienones with a quinone moiety **376** in good yield and excellent enantioselectivity. Relying on this strategy, in 2017, Ling Zhou group^[167]

also successfully got their target to dearomatize the naphthol **377** catalyzed by chiral phosphoric acid (**PH-2**) by introducing the quinone monoimide **378**(**Scheme 73**). The aimed enantioenriched cyclohexadienones **379** were obtained also in excellent yield via an domino Michael addition procedure and the products bearing various functional group also could be collected without big influence of on the yield and selectivity.

From the results above, naphthol was dearomatized and left a free double bond inside the cyclohexadienone skeleton. The existence of free double leaves various possibility for further decoration and new reaction model. In 2019, Shouli You group^[168] noticed this opportunity and reported chiral phosphoric acid catalyzed aminative dearomatization of α -naphthols followed cascade Michael addition reaction. In this work (**Scheme 73**), 1-naphthol tethered a second nucleophile at the C4 position **380** was chose as the starting material to interact with diethyl azodicarboxylate catalyzed by chiral phosphoric acid (**PH-3**). A series of polycyclic ketones **381** in good yields with excellent enantioselectivity were synthesized under mild reaction condition. Under the support of DFT calculations and mechanistic investigations, the whole procedures included two steps which were stereochemistry-determining aminative dearomatization and rate-limiting Michael addition. This work inspired chemists that the possibility that the dearomatization could be a new flat to perform other transformation.

Like dearomatizing the phenol molecules, transition metal catalyst Pd could also be applied to dearomatize the naphthol compounds. Consistent with the Pd(0) catalyzed dearomatization of phenol^[159], in 2016, Shu-Li You group^[169] carried up this strategy to dearomatize naphthol **382** (**Scheme 74**). They successfully developed palladium(0) catalyzed intermolecular arylyative dearomatization of β -Naphthols by combining the aryl halides **383**. This reaction worked very well under assistance of **Q-Phos** ligand to give the arylyative and dearomatized naphthols in excellent yield. After this work, in 2018, they developed another palladium(0) catalyzed intermolecular cascade dearomatization reaction on naphthol (**Scheme 74**). In starting material **385**, another amino group was featured at C1 which was ready for the cascade procedure. Firstly the propargyl carbonates **386** were activated by **Binap** coordinated Palladium by releasing one CO₂ to form allene intermediate. Then the amino and the C1 carbon nucleophile continually attack the electrophilic allene intermediate which finally afforded β -naphthalenones featuring an all

carbon quaternary stereogenic center at the α -position in good to excellent yields and chemoselectivity.



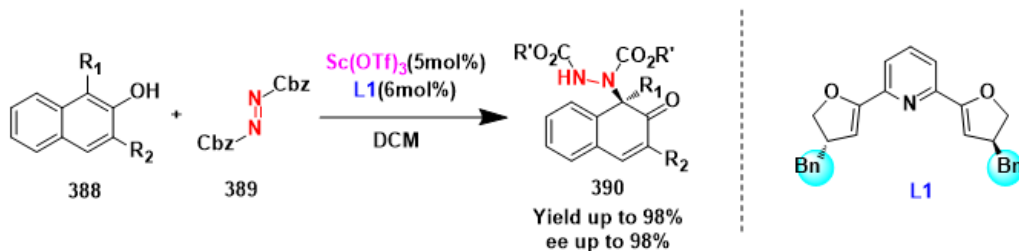
Shu-Li You 2018



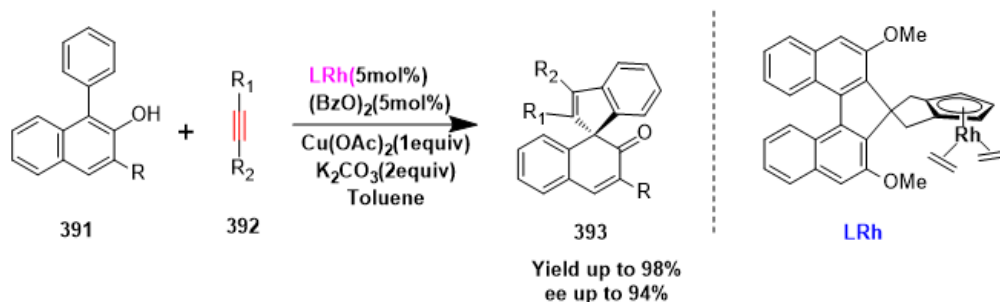
Scheme 74. Palladium catalyzed dearomatization of phenol

In the same way, other transition metal catalysts are also developed by using their unique advantages on dearomatization of naphthols. In 2015, Xinjun Luan group^[170] developed the scandium catalyzed asymmetric dearomative amination of naphthol **388** with azodicarboxylates **389**. By using the chiral ligand **L1** (**Scheme 75a**), high yield and great enantioselectivity of product **390** were collected under mild condition. In the same year(2015), Shuli You group^[171] found Rh(**LRh**)-Catalyzed asymmetric dearomatization of naphthols **391** by cascade C(sp²)-H bond activation and annulation procedures with alkynes **392**(**Scheme 75b**). This work gave

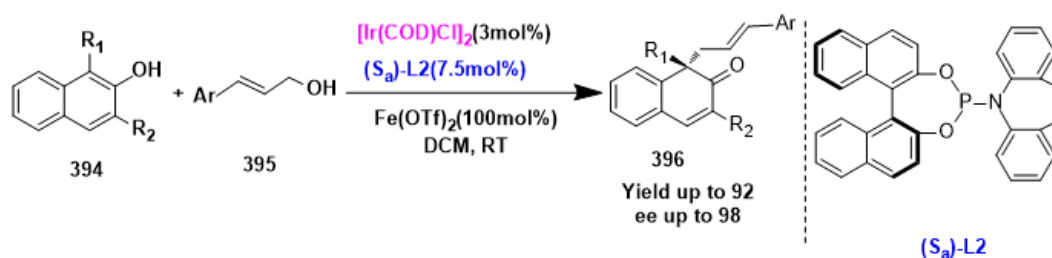
a) Xinjun Luan 2015



b) Shu-Li You 2015



c) Shu-Li You 2017



Scheme 75

another simple and efficient method to synthesize chiral spirocyclic β -naphthalenones **395** and its derivatives in excellent yield and enantioselectivity (both up to 99%).

In 2017, Shuli You group continued to pay attention on the dearomatization of naphthol and derivatives by Iridium catalyst^[172]. By testing and screening many reaction condition, when (*S_a*)-**L2** was the ligand and [Ir(COD)]₂ was the Iridium source, allyl alcohol **395** being the electrophile could be directly activated without featuring the strong leaving group like carbonate group and accepted the attack of naphthols **394** to form the dearomatized product bearing quaternary carbon in excellent yield and enantioselectivity (Scheme 75c).

In summary, dearomatization of aromatic compounds has become a very powerful strategy to approach more functionalized molecules. Recently, more and more great works on dearomatization of aromatic compounds and relative knowledge has also been accumulated

Chapter 1

increasingly. However, there are still a lot of problem such as the cost and easy prepared starting material. In addition, in front of more and more challenges in humans' health and living condition, great valued and creative molecules by introducing more functional group which is easy modified or has bioactive property should be synthesized through more efficient and greener way. In conjunction with the research in our group on gold catalyzed dearomatization of indol and derivatives, we started to propose the research target of my PhD life. Next, the results of my research on gold catalyzed functionalization of alkyne and allenamides during my PhD life will be presented in the following chapter.

Reference

- [1] a) Shaw, C. F., III. Uses, *Inorg. Chem. Med.* **1999**, 26; b) Demann, E. T. K.; Stein, P. S.; Haubenrich, J. E. J. Long-Term Effects, *Med. Implants*, **2005**, 15, 687; c) Messori, L.; Gabbiani, C. Met., *Comp. Cancer Chemother.* **2005**, 355; d) Kostova, I. *Anti-Cancer Agents Med. Chem.* **2006**, 6, 19.
- [2] a) M. Bandini, *Chem. Soc. Rev.* **2011**, 40, 1358-1367; b) M. Rudolph, A. Stephen K. Hashmi, *Chem. Soc. Rev.* **2012**, 41, 2448-2462; c) W. Zi, F. Dean Toste, *Chem. Soc. Rev.* **2016**, 45, 4567-4589; d) D. Pflaterer, A. Stephen K. Hashmi, *Chem. Soc. Rev.* **2016**, 45, 1331.
- [3] a) M. Dub: Organometallic Compounds. 2nd Edit., *Springer*, New York **1966**. ; b) M. L. H. Green in G. E. Coates, M. L. H. Green, and K. Wade: *Organometallic Compounds. Methuen, London* **1968**, Vol. 2, p. 28, 208, 255-257, 274, 277-280; c) G. E. Coates, F. Gfocking in H. H. Zeiss: *Organometallic Chemistry. Reinhold, New York*, **1960**, 426.
- [4] a) L. A. Woods, H. Gilman, *Proc. Iowa Acad. Sci.* **1943**, 49, 286; b) H. Gilman, L. A. Woods, *J. Am. Chem. Soc.* **1948** 70, 550-552.
- [5] G. E. Coates and C. Parkin, *J. Chem. Soc.* **1962**, 3220-3226
- [6] B. Armerr, H. Schmidbaur, *Angew. Chem. internat. Edit.* **1970**, 9, 2, 101-113.
- [7] D. Thompson, *Gold Bull.* **1988**, 32, 111-118.
- [8] a) G. C. Bond, D. Thompson, *Catal. Rev. Sci. Eng.* **1999**, 41, 319 – 388; b)) T. Aida, R. Higuchi, H. Niiyama, *Chem. Lett.* **1990**, 2247 – 2250; c) T. M. Salama, T. Shido, R. Ohnishi, M. Ichikawa, *J. Chem. Soc. Chem. Commun.* **1994**, 2749 – 2750.
- [9] L. U. Meyer, A. de Meijere, *Tetrahedron Lett.* **1976**, 497 – 500.
- [10] A. Stephen K. Hashmi, *Gold Bulletin*, **2004**, 37/1-2, 51-65.
- [11] Norman, R. O. C.; Parr, W. J. E.; Thomas, C. B., *J. Chem. Soc. Perkin Trans.* **1976**, 1, 1983-1987.
- [12] a) Fukuda, Y.; Utimoto, K.; Nozaki, H. *Heterocycles*, **1987**, 25, 297; b) Fukuda, Y.; Utimoto, K. *Synthesis*, 1991, 975.
- [13] A. K. Hashmi, L. Schwarz, J. Choi, T. M. Frost, *Angew. Chem. Int. Ed.* **2000**, 39, 2285-2288
- [14] J. A. Marshall, E. D. Robinson, *J. Org. Chem.* **1990**, 55, 3450 – 3451.
- [15] S. K. Hashmi, *Angew. Chem. Int. Ed. Engl.* **1995**, 34, 1581 – 158.
- [16] Enrico Muth L., G. Dyker, Ding, A.S. K. Hashmi, *Adv. Synth. Catal.* 2003, 345, 1247 - 1252
- [17] a) Y. Ito, M. Sawamura, T. Hayashi, *J. Am. Chem. Soc.* **1986**, 108, 6405 - 6406; b) T. Hayashi, M. Sawamura, Y. Ito, *Tetrahedron*, **1992**, 48, 1999 – 201.
- [14] David J. Gorin, Benjamin D. Sherry, and F. Dean Toste, *Chem. Rev.* **2008**, 108, 3351–3378.
- [15] Y. Fukuda, K. Utimoto, *synthesis*, **1991**, 11, 975-978.
- [16] T. E. Muller, M. Grosche, E. Herdtweck, A. Pleier, E. Walter, Y. Yan, *Organometallics*, **2000**, 19, 170-183.
- [17] a) J. Henrique Teles, S. Brode, M. Chabanas, *Angew. Chem. Int. Ed.* **1998**, 37, 1415-1418; b) E. Mizushima, T. Hayashi, M. Tanaka, *Org. Lett.* **2003**, 5, 18, 3349-3352.
- [18] a) J. S. Reichert, J. H. Bailey, J. A. Niewland, *J. Am. Chem. Soc.* **1923**, 45, 1553-1557; b) H. D. Hinton, J. A. Niewland, *J. Am. Chem. Soc.* 1930, 52, 2892-2896.
- [19] a) Y. Fukuda, K. Utimoto, *J. Org. Chem.* **1991**, 56, 3729-3731; b) Y. Fukuda, K. Utimoto, *Bull. Chem. Soc. Jpn.* **1991**, 64, 2013-2015.

Chapter 1

- [20] a) E. J. Nunez, Antonio M. Echavarren, *Chem. Rev.* **2008**, 108, 3326–3350; b) W. Zi, F. Dean Toste, *Chem. Soc. Rev.* **2016**, 45, 4567–4589.
- [21] A. Stephen K. Hashmi, *Gold Bulletin*, **2004**, 37/1–2, 51–65.
- [22] D. J. Gorin, F. Dean Toste, *Nature*, **2007**, 446, 395–403.
- [23] A. Furstner, Paul W. Davies, *Angew. Chem. Int. Ed.* **2007**, 46, 3410–3449.
- [24] D. Pflasterer, A. Stephen K. Hashmi, *Chem. Soc. Rev.* **2016**, 45, 1331–1367.
- [25] a) P. Schwerdtfeger, H.L. Hermann, H. Schmidbaur, *Inorg. Chem.* **2003**, 42, 1334–1342. b) P. Pyykk, *Chem. Rev.* **1988**, 88, 563–594.
- [26] G. A. Bowmaker, C. L. Brown, R. D. Hart, P. C. Healy, C. E. F. Rickard, A. H. White, *J. Chem. Soc. Dalton Trans.* **1999**, 881–889.
- [27] a) M. J. S. Dewar, *Bull. Soc. Chim. Fr.* **1951**, 18, C71–C79; b) J. Chatt, L. A. Duncanson, *J. Chem. Soc.* **1953**, 2939–2947.
- [28] a) R. H. Hertwig, W. Koch, D. Schröder, H. Schwarz, J. Hrusk, P. Schwerdtfeger, *J. Phys. Chem.* **1996**, 100, 12253–12260; b) M. S. Nechaev, V. M. Rayn, G. Frenking, *J. Phys. Chem. A.* **2004**, 108, 3134–3142.
- [29] *Curr. Methods Inorg. Chem.*, Vol. 3 (Eds.: H. Kurosawa, A. Yamamoto), *Elsevier*, Amsterdam, **2003**.
- [30] a) Irikura, K. K. & Goddard, W. A., *J. Am. Chem. Soc.* **1994**, 116, 8733–8740; b) D. J. Gorin, F. Dean Toste, *Nature*, **2007**, 446, 395–403.
- [31] Hertwig, R. H. et al., *J. Phys. Chem.* **1996**, 100, 12253–12260.
- [32] a) Irikura, K. K. & Goddard III, W. A. *J. Am. Chem. Soc.* **1994**, 116, 8733–8740; b) D. Benitez, N. D. Shapiro, E. Tkatchouk, Y. Wang, W. A. Goddard III, F. D. Toste, *Nat Chem.* **2009**, 1(6):482–486.
- [33] a) C. N. Oberhuber, M. Paz Muñoz, E. Buñuel, C. Nevado, D. J. Cardenas, Antonio M. Echavarren, *Angew. Chem. Int. Ed.* **2004**, 43, 2402–2406; b) C. N. Oberhuber, M. P. Muñoz, S. Lopez, E. J. Nuñez, C. Nevado, E. H. Gomez, M. Raducan, A. M. Echavarren, *Chem. Eur. J.* **2006**, 12, 1677–1693.
- [34] Mamane, V., Gress, T., Krause, H. & Furstner, A. P., *J. Am. Chem. Soc.* **2004**, 126, 8654–8655.
- [35] a) X. Shi, D. J. Gorin, F. Dean Toste, *J. Am. Chem. Soc.* **2005**, 127, 5802–5803; b) M. J. Johansson, D. J. Gorin, S. T. Staben, F. Dean Toste, *J. Am. Chem. Soc.* **2005**, 127, 18002–18003.
- [36] a) Michael C. Willis, *Chem. Rev.* **2010**, 110, 725–748; b) X. Du, Z. Huang, *ACS Catal.* **2017**, 7, 1227–1243; c) B. Walker, C. S. Sevov, *ACS Catal.* **2019**, 9, 7197–7203; d) S. Lucks, H. Brunner, *Org. Process Res. Dev.* **2017**, 21, 1835–1842.
- [37] a) G. Desimoni, G. Faita, P. Quadrelli, *Chem. Rev.* **2013**, 113, 5924–5988; b) C. M. R. Volla, I. Atodiresei, M. Rueping, *Chem. Rev.* **2014**, 114, 2390–2431; c) G. Desimoni, G. Faita, P. Quadrelli, *Chem. Rev.* **2018**, 118, 2080–2248.
- [38] G. Kovacs, A. Lledos, G. Ujaque, *Organometallics* **2010**, 29, 5919–5926.
- [39] a) M. Chiarucci, M. Bandini, *Beilstein J. Org. Chem.* **2013**, 9, 2586–2614; b) Bandini, M.; Cera, G.; Chiarucci, M. *Synthesis*, **2012**, 504–512; c) A. Corma, A. L.-Pérez, M. J. Sabater. *Chemical Reviews* **2011**, 111, 1657–1712.

Chapter 1

- [40] Yang, C., C. He, *J. Am. Chem. Soc.* **2005**, 127, 6966–6967.
- [41] C. Palo-Nieto, A. Sau, M. C. Galan, *J. Am. Chem. Soc.* **2017**, 139, 14041–14044.
- [42] a) J. Zhang, C. Yang, C. He, *J. Am. Chem. Soc.* **2006**, 128, 1798–1799; b) C. Brouwer, C. He, *Angew. Chem. Int. Ed.* **2006**, 45, 1744–1747.
- [43] a) C. F. Bender, R. A. Widenhoefer, *Chem. Commun.* **2006**, 4143–4144; b) C. F. Bender, R. A. Widenhoefer, *Org. Lett.*, **2006**, 8, 5303–5305; c) X. Han, R. A. Widenhoefer, *Angew. Chem. Int. Ed.* **2006**, 45, 1747–1749; d) C. F. Bender, R. A. Widenhoefer, *Chem. Commun.*, **2008**, 2741–2743.
- [44] Z. Zhang, S. D. Lee, R. A. Widenhoefer, *J. Am. Chem. Soc.* **2009**, 131, 5372–5373.
- [45] J. C. Timmerman, B. D. Robertson, R. A. Widenhoefer, *Angew. Chem. Int. Ed.* **2015**, 54, 2251–2254.
- [46] a) G. Kovacs, G. Ujaque, and A. Lledos, *J. Am. Chem. Soc.* **2008**, 130, 853–864; b) R. E. M. Brooner, R. A. Widenhoefer, *Organometallics*, **2011**, 30, 3182–3193.
- [47] R. L. LaLonde, W. E. Brenzovich, Jr., D. Benitez, E. Tkatchouk, K. Kelley, W. A. Goddard, F. De Toste, *Chem. Sci.*, **2010**, 1, 226–233.
- [48] O. Kanno, W. Kuriyama, Z. J. Wang, F. Dean Toste, *Angew. Chem. Int. Ed.* **2011**, 50, 9919–9922.
- [49] S. D. Lee, J. C. Timmerman, R. A. Widenhoefer, *Adv. Synth. Catal.* **2014**, 356, 3187–3192.
- [50] M. Abadie, M. Kouach, P. Roussel, Bernhard Linden, I. Rosal, X. Trivelli, Laurent Maron, E. Gnin, F. Medina, M. Vandewalle, Nathalie D., F. A. Niedercorn, F. Capet, C. Michon, *Chem. Eur. J.* **2017**, 23, 10777–10788.
- [51] X. Yao, C. J. Li, *J. Am. Chem. Soc.* **2004**, 126, 6884–6885.
- [52] R. V. Nguyen, X. Yao, D. Scott Bohle, C. Li, *Org. Lett.* **2005**, 7, 673–675.
- [53] C. Zhou, C. Che, *J. Am. Chem. Soc.* **2007**, 129, 5828–5829.
- [54] Y. Xiao, X. Liu, C. Che, *Angew. Chem. Int. Ed.* **2011**, 50, 4937–4941.
- [55] M. Wang, M. Wong, C. Che, *Chem. Eur. J.* **2008**, 14, 8353–8364.
- [56] J. C. Timmerman, W. W. Schmitt, R. A. Widenhoefer, *Org. Lett.* **2016**, 18, 4966–4969.
- [57] T. Tamai, K. Fujiwara, S. Higashimae, A. Nomoto, A. Ogawa, *Org. Lett.* **2016**, 18, 2114–2117.
- [58] S. K. Kristensen, S. L. R. Laursen, E. Taarning, T. Skrydstrup, *Angew. Chem.* **2018**, 130, 14083–14087.
- [59] a) D. J. Gorin, F. Dean Toste, *Nature*, **2007**, 446, 395–403; b) M. Hopkinson, A. Tlahuext-Aca and F. Glorius, *Acc. Chem. Res.*, **2016**, 49, 2261–2272.
- [60] a) M. O. Akram, S. Banerjee, S. S. Saswade, V. Bedib, N. T. Patil, *Chem. Commun.*, **2018**, 54, 11069–11083; b) M. Hopkinson, A. Tlahuext-Aca and F. Glorius, *Acc. Chem. Res.*, **2016**, 49, 2261–2272.
- [61] W. E. Brenzovich, Jr., D. Benitez, A. D. Lackner, H. P. Shunatona, E. Tkatchouk, W. A. Goddard, III, F. Dean Toste, *Angew. Chem. Int. Ed.* **2010**, 49, 5519–5522.
- [62] C. Gonzalez-Arellano, A. Abad, A. Corma, H. Garca, M. Iglesias, F. Snchez, *Angew. Chem. Int. Ed.* **2007**, 46, 1536–1538.
- [63] T. de Haro, C. Nevado, *Angew. Chem. Int. Ed.* **2011**, 50, 906–910.
- [64] G. Zhang, Y. Luo, Y. Wang, L. Zhang, *Angew. Chem. Int. Ed.* **2011**, 50, 4450–4454.
- [65] B. Sahoo, M. N. Hopkinson, F. Glorius, *J. Am. Chem. Soc.* **2013**, 135, 5505–5508.

Chapter 1

- [66] a) M. N. Hopkinson, B. Sahoo, Frank Glorius, *Adv. Synth. Catal.* **2014**, 356, 2794 – 2800; b) M.O. Akram, S. Banerjee, S. S. Saswade, V. Bedib, N.T. Patil, *Chem. Commun.*, **2018**, 54, 11069–11083; c) M. Hopkinson, A. Tlahuext-Aca and F. Glorius, *Acc. Chem. Res.*, **2016**, 49, 2261 – 2272.
- [67] a) William D. G. Brittain, B. R. Buckley, J. S. Fossey, *ACS Catal.* **2016**, 6, 3629–3636; b) Igor V. Alabugin, B. Gold, *J. Org. Chem.* **2013**, 78, 7777–7784; c) E. Jimenez-Nunez, A.M. Echavarren, *Chem. Rev.* **2008**, 108, 3326–3350; d) Y. Wei, M. Shi, *ACS Catal.* **2016**, 6, 2515–2524; M. C. Willis, *Chem. Rev.* **2010**, 110, 725–748.
- [68] P. H-Y. Cheong, P. Morganelli, M. R. Luzung, K. N. Houk, F. D. Toste, *J. Am. Chem. Soc.* **2008**, 130, 4517–4626.
- [69] a) A. S. K. Hashmi, I. Braun, P. Nösel, J. Schädlich, M. Wietek; M. Rudolph, F. Rominger, *Angew. Chem., Int. Ed.* **2012**, 51, 4456–4460. b) M. M. Hansmann, M. Rudolph, F. Rominger, A. S. K. Hashmi, *Angew. Chem., Int. Ed.* **2013**, 52, 2593–2598.; c) L. Ye, Y. Wang, D. H. Aue, L. Zhang, *J. Am. Chem. Soc.* **2012**, 134, 31–34; d) Y. Wang, A. Yepremyan, S. Ghorai, R. Todd, D. H. Aue, L. Zhang, *Angew. Chem., Int. Ed.* **2013**, 52, 7795–7799.
- [70] J. Bucher, T. Wurm, K. S. Nalivela, M. Rudolph, F. Rominger, A. S. K. Hashmi, *Angew. Chem., Int. Ed.* **2014**, 53, 3854–3858.
- [71] P. W. Davies, N. Martin, *Org. Lett.* **2009**, 11, 11, 2293–2296.
- [72] a) A. Gimeno, M. Medio-Simon, C. Ramirez de Arellano, A.B. Cuenca, Gregorio Asensio, *Org. Lett.* **2010**, 12, 9, 1900–1903; b) S. Fustero, I. Ibáñez†, P. Barrio, M. A. Maestro, S. Catalán, *Org. Lett.* **2013**, 15, 4, 832–835.
- [73] L. Zhu, Y. Yu, Z. Mao, X. Huang, *Org. Lett.* **2015**, 17, 30–33.
- [74] R. Miller, J. Carreras, M. E. Muratore, M. Gaydou, F. Camponovo, A. M. Echavarren, *J. Org. Chem.* **2016**, 81, 1839–1849.
- [75] a) Z. Zeng, H. Jin, J. Xie, B. Tian, M. Rudolph, F. Rominger, A. Stephen K. Hashmi, *Org. Lett.* **2017**, 19, 1020–1023; b) X. Tian, L. Song, M. Rudolph, F. Rominger, A. Stephen K. Hashmi, *Org. Lett.* **2019**, 21, 4327–4330; c) X. Tian, L. Song, M. Rudolph, Q. Wang, X. Song, F. Rominger, A. Stephen K. Hashmi, *Org. Lett.* **2019**, 21, 1598–1601.
- [76] H. Jin, B. Tian, X. Song, J. Xie, M. Rudolph, F. Rominger, A. S. K. Hashmi, *Angew. Chem., Int. Ed.* **2016**, 55, 12688–12692.
- [77] Y. Yu, G. Chen, L. Zhu, Y. Liao, Y. Wu, X. Huang, *J. Org. Chem.* **2016**, 81, 8142–8154.
- [78] a) R. L. Sahani, R. Liu, *Angew. Chem., Int. Ed.* **2017**, 56, 1026–1030; b) W. B. Shen, X. Xiao, Q. Sun, B. Zhou, X. Zhu, J. u Yan, X. Lu, L. Ye, *Angew. Chem., Int. Ed.* **2017**, 56, 605–609; c) R. L. Sahani, R. Liu, *Angew. Chem., Int. Ed.* **2017**, 56, 12736–12740.
- [79] a) K. Sugimoto, K. Toyoshima, S. Nonaka, K. Kotaki, H. Ueda, H. Tokuyama, *Angew. Chem., Int. Ed.* **2013**, 52, 7168–7171; b) J. Zhang, Q. Zhang, B. Xia, J. Wu, X. Wang, J. Chang, *Org. Lett.* **2016**, 18, 3390–3393. c) D. Zheng, S. Li, J. Wu, *Org. Lett.* **2012**, 14, 2655–2657; c) G. Chen, X. Zhang, X. Wei, Tang, M. Shi, *Angew. Chem., Int. Ed.* **2014**, 53, 8492–8497.
- [80] S. Antoniotti, E. Genin, V. Michelet, J. Genet, *J. Am. Chem. Soc.* **2005**, 127, 9976–9977.
- [81] V. Belting, N. Krause, *Org. Lett.* **2006**, 8, 4489–4492.

- [82] a) A. Aponick, C. Li, J. Malinge, E. F. Marques, *Org. Lett.* **2009**, 20, 4624-4627; b) M. Egi, K. Azechi, S. Akai, *Org. Lett.* **2009**, 11, 5002-5005.
- [83] V. Laserna, C. J. Rojas, T. D. Sheppard, *Org. Lett.* **2019**, 21, 4443-4447.
- [84] a) X. Cheng, Z. Wang, C. D. Quintanilla, L. Zhang, *J. Am. Chem. Soc.* **2019**, 141, 3787-3791; b) J. Zhang, Y. Liu, X. Wang, L. Zhang, *Organometallics*, **2019**, 38, 20, 3931-3938; c) T. Li, L. Zhang, *J. Am. Chem. Soc.* **2018**, 140, 17439-17443.
- [85] a) A. Martinez, P. G. Garca, M. A. F. Rodriguez, F. Rodriguez, R. Sanz, *Angew. Chem. Int. Ed.* **2010**, 49, 4633-4637; b) C. Michou, S. Liu, S. Hiragushi, J. Uenishi, M. Uemura, *Synlett*, **2008**, 1321-1324; c) T. Shibata, Y. Ueno, K. Kanda, *Synlett*, **2006**, 411-414; d) M. R. Luzung, J. P. Markham, F.D. Toste, *J. Am. Chem. Soc.* **2004**, 126, 10858-10859; e) Y. Horino, T. Yamamoto, K. Ueda, S. Kuroda, F.D. Toste, *J. Am. Chem. Soc.* **2009**, 131, 2809-2811; f) A. K. Buzas, F.M. Istrate, F. Gagosz, *Angew. Chem. Int. Ed.* **2007**, 46, 1141-1144; g) E. J. Nunez, Antonio M. Echavarren, *Chem. Rev.* **2008**, 108, 8, 3326-3350; h) P. Zhang, Y. Wang, Z. Zhang, J. Zhang, *Org. Lett.* **2018**, 20, 7049-7052; i) W. Zi, H. Wu, F. Dean Toste, *J. Am. Chem. Soc.* **2015**, 137, 3225-3228; j) C. Zhang, H. Li, C. Pei, L. Qiu, W. Hu, X. Bao, X. Xu, *ACS Catal.* **2019**, 9, 2440-2447.
- [86] a) I. Braun, P. Nşel, J. Schdlich, M. Wieteck, M. Rudolph, F. Rominger, A. S. K. Hashmi, *Angew. Chem. Int. Ed.* **2012**, 51, 4456-4460; b) M. Wieteck, I. Braun, M. Rudolph, F. Rominger, A. S. K. Hashmi, *Angew. Chem. Int. Ed.* **2012**, 51, 10633-10637.
- [87] a) M. Wieteck, I. Braun, P. Nşel, L. Jongbloed, M. Rudolph, F. Rominger, A. S. K. Hashmi, *Adv. Synth. Catal.* **2012**, 354, 555-562; b) I. Braun, M. Rudolph, F. Rominger, A. S. K. Hashmi, *Organometallics* **2012**, 31, 644-661.
- [88] C. J. Jones, R. Periana, D. Taube, V. Ziatdinov, R. Nielsen, J. Oxgaard, W. Goddard III, *Angew. Chem. Int. Ed.* **2004**, 43, 4626-4629.
- [89] a) L. Ye, Y. Wang, D. H. Aue, L. g Zhang, *J. Am. Chem. Soc.* **2012**, 134, 31-34; b) Y. Wang, A. Yepremyan, S. Ghorai, R. Todd, D. H. Aue, L. Zhang, *Angew. Chem. Int. Ed.* **2013**, 52, 7795-7799.
- [90] J. Bucher, T. Wurm, K. S. Nalivela, M. Rudolph, F. Rominger, A. Stephen K. Hashmi, *Angew. Chem. Int. Ed.* **2014**, 53, 3854-3858.
- [91] a) C. J. Evans, A. Lesarri, M. C. L. Gerry, *J. Am. Chem. Soc.* **2000**, 122, 6100-6105; b) J. R. Brown, P. Schwerdtfeger, D. Schröder, H. Schwarz, *J. Am. Soc. Mass Spectrom.* **2002**, 13, 485-492.
- [92] A. L.-Pérez, Paula Rubio-Marqués, S. S. Al-Deyab, S. I. Al-Resayes, A. Corma, *ACS Catal.* **2011**, 1, 601-606.
- [93] R. Ebule, S. Liang, G. B. Hammond, B. Xu, *ACS Catal.* **2017**, 7, 6798-6801.
- [94] J. M. Ketcham, B. Biannic, Aaron Aponick, *Chem. Commun.*, **2013**, 49, 4157-4159.
- [95] A. Gómez-Suárez, D. Gasperini, S. V. C. Vummaleti, A. Poater, L. Cavallo, S. P. Nolan, *ACS Catal.* **2014**, 4, 2701-2705.
- [96] a) Z. Wang, Y. Wang, L. Zhang, *J. Am. Chem. Soc.* **2014**, 136, 8887-8890; b) X. Li, Z. Wang, X. Ma, P. Liu, L. Zhang, *Org. Lett.* **2017**, 19, 5744-5747; c) A. Liao, A. Porta, X. Cheng, X. Ma, G. Zanoni, L. Zhang, *Angew. Chem., Int. Ed.* **2018**, 57, 8250-8254; d) Z. Wang, C. Nicolini, C. Hervieu, Y.-F. Wong, G. Zanoni, L. Zhang, *J. Am. Chem. Soc.* **2017**, 139, 16064-16067; e) Y. Wang, Z. Wang, Y. Li, G. Wu, Z. Cao, L. Zhang, *Nature Communications*, **2014**, DOI: 10.1038/ncomms4470.
- [97] T. Li, L. Zhang, *J. Am. Chem. Soc.* **2018**, 140, 17439-17443.

- [98] M. E. Muratore, A. Konovalov, H. Armengol-Relats, A. M. Echavarren, *Chem. Eur.J.* **2018**, 24, 15613–15621.
- [99] R. Pertschi, P. Wagner, N. Ghosh, V. Gandon, G. Blond, *Org. Lett.* **2019**, 21, 6084–6088.
- [100] J. Qi, Q. Teng, N. Thirupathi, C. Tung, Z. Xu, *Org. Lett.* **2019**, 21, 692–695.
- [101] J. Cai, X. Wang, Y. Qian, L. Qiu, W. Hu, X. Xu, *Org. Lett.* **2019**, 21, 369–372.
- [102] a) S. B. Wagh, R. R. Singh, R. L. Sahani, R. Liu, *Org. Lett.* **2019**, 21, 2755–2758; b) R. L. Sahani, R. Liu, *ACS Catal.* **2019**, 9, 5890–5896.
- [103] C. Zhang, H. Li, C. Pei, L. Qiu, W. Hu, X. Bao, X. Xu, *ACS Catal.* **2019**, 9, 2440–2447.
- [104] a) T. Lu, Z. Lu, Z. Ma, Y. Zhang, R.P. Hsung, *Chem. Rev.* **2013**, 113, 4862–4904; b) E. Manoni, M. Bandini, *Eur. J. Org. Chem.* **2016**, 3135–3142.
- [105] A. J. Hubert, H. G. Viehe, *J. Chem. Soc. C* **1968**, 228.
- [106] Z. Ma, S. He, W. Song, R. P. Hsung, *Org. Lett.* **2012**, 14, 5736–5739.
- [107] N. H. Slater, N. J. Brown, M. R. J. Elsegood, M. C. Kimber, *Org. Lett.* **2014**, 16, 4606–4609.
- [108] Y. Wang, P. Zhang, X. Di, Q. Dai, Z. Zhang, J. Zhang, *Angew.Chem. Int. Ed.* **2017**, 56, 15905 – 15909.
- [109] M. M. Mastandrea, N. Mellonie, P. Giacinto, A. Collado, S. P. Nolan, G. P. Miscione, A. Bottoni, M. Bandini, *Angew.Chem. Int. Ed.* **2015**, 54, 14885 –14889.
- [110] P. N. Bagle, M. V. Mane, K. Vanka, D. R. Shinde, S. R. Shaikh, R. G. Gonnadebe, N. T. Patil, *Chem. Commun.*, **2016**, 52, 14462—14465.
- [111] a) A. W. Hill, Mark R. J. Elsegood, M. C. Kimber, *J. Org. Chem.* **2010**, 75, 5406–5409; b) M. C. Kimber, *Org. Lett.* **2010**, 12, 5, 1128–1131.
- [112] a) T. Lu, Z. Lu, Z. Ma, Y. Zhang, R. P. Hsung, *Chem. Rev.* **2013**, 113, 4862–4904; b) J. L. Mascareñas, I. Varela, F. López, *Acc. Chem. Res.* **2019**, 52, 465–479.
- [113] H. Faustino, P. Bernal, L. Castedo, F. Lopez, J. Mascareñas, *Adv. Synth. Catal.* **2012**, 354, 1658–1664.
- [114] a) X. Li, L. Zhu, W. Zhou, Z. Chen, *Org. Lett.* **2012**, 14, 2, 436–439; b) S. S. Pantiga, C. He. Diaz, M. Piedrafita, E. Rubio, J. Gonzalez, *Adv. Synth. Catal.* **2012**, 354, 1651 – 1657.
- [115] Sa. Surez-Pantiga, C. Hernandez-Diaz, E. Rubio, JoseM. Gonzalez, *Angew. Chem. Int. Ed.* **2012**, 51, 11552 –11555.
- [116] P. Bernal-Albert, H. Faustino, A. Gimeno, G. Asensio, J. L. Mascareñas, F. López, *Org. Lett.* **2014**, 16, 6196–6199.
- [117] H. Faustino, F. López, L. Castedo, J. L. Mascareñas, *Chem. Sci.*, **2011**, 2, 633–637.
- [118] J. Francos, F. Grande-Carmona, H. Faustino, J. Iglesias-Sigüenza, E. Díez, I. Alonso, R. Fernández, J.M. Lassaletta, F. López, J. L. Mascareñas, *J. Am. Chem. Soc.* **2012**, 134, 14322–14325.
- [119] H. Faustino, I. Alonso, J. L. Mascareñas, F. Lopez, *Angew. Chem. Int. Ed.* **2013**, 52, 6526 –6530.
- [120] D. C. Marcote, I. Varela, J. Fernández-Casado, J. L. Mascareñas, F. López, *J. Am. Chem. Soc.* **2018**, 140, 16821–16833.
- [121] a) M. C. Kimber, *Org. Lett.*, 2010, 12, 1128–1131; b) V. Pirovano, L. Decataldo, E. Rossi, R. Vicente, *Chem. Commun.*, **2013**, 49, 3594—3596.
- [122] Y. Wang, P. Zhang, Y. Liu, F. Xia, J. Zhang, *Chem. Sci.*, **2015**, 6, 5564–5570.
- [123] E. Lopez, J. Gonzalez, L. A. Lopez, *Adv. Synth. Catal.* **2016**, 358, 1428–1432.
- [124] H. Faustino, I. Varela, J. L. Mascareñas, F. López, *Chem. Sci.*, **2015**, 6, 2903–2908.
- [125] I. Varela, H. Faustino, E. Díez, J. Iglesias-Sigüenza, F. Grande-Carmona, R. Fernández, J. M.

- Lassaletta, J. L. Mascareñas, F. López, *ACS Catal.* **2017**, 7, 2397–2402.
- [126] C. Hernández-Díaz, E. Rubio, J. M. González, *Eur. J. Org. Chem.* **2016**, 265–269.
- [127] S. Peng, S. Cao, J. Sun, *Org. Lett.* **2017**, 19, 524–527.
- [128] N. De, C. Eui Song, D. H. Ryu, E. J. Yoo, *Chem. Commun.*, **2018**, 54, 6911–6914.
- [129] S. P. Roche, J. A. Porco Jr., *Angew. Chem. Int. Ed.* **2011**, 50, 4068 – 4093.
- [130] Arthur J. Birch, *Pure & Appl. Chem.*, **1996**, 68, 553-556,
- [131] a) T.Dohi, A. Maruyama, N. Takenaga, K. Senami, Y. Minamitsuji, H. Fujioka, S. B. Caemmerer, Y. Kita, *Angew. Chem. Int. Ed.* **2008**, 47, 3787 –3790; b) K. Volp, A. M. Harned, *Chem. Commun.*, 2013, 49, 3001-3003; c) C. Bosset, R. Coffinier, P. A. Peixoto, M. E. Assal, K. Miqueu, J.-M. Sotiropoulos, L. Pouysegu and S. Quideau, *Angew. Chem., Int. Ed.*, 2014, 53, 9860-9864.
- [132] a) Y.-G. Zhou, *Acc. Chem. Res.* **2007**, 40, 1357 –1366; b) D.-S. Wang, Q.-A. Chen, S.-M. Lu, Y.-G. Zhou, *Chem.Rev.* **2012**, 112, 2557 – 2590.
- [133] F. López Ortiz, M. J. Iglesias, I. Fernández, C. M. A. Sánchez, G. R. Gómez, *Chem. Rev.*, 2007, 107, 1580–1691.
- [134] L. Pouységu, D. Deffieux and S. Quideau, *Tetrahedron*, 2010, 66, 2235–2261.
- [135] a) S. P. Roche, John A. Porco Jr, *Angew. Chem. Int. Ed.* **2011**, 50, 4068 – 4093; b) C. Zhuo, C. Zheng, S. You, *Acc. Chem. Res.* **2014**, 47, 2558–2573; c) C. Zhuo, W. Zhang, S. You, *Angew. Chem. Int. Ed.* **2012**, 51, 12662 – 12686.
- [136] I. V. Seregina, V. Gevorgyan, *Chem. Soc. Rev.*, **2007**, 36, 1173-1193.
- [137] C. Romano, M., M. Monari, E. Manoni, M. Bandini, *Angew. Chem. Int. Ed.* **2014**, 53, 13854 – 13857.
- [138] Y. Zhang, J. Zhao, F. Jiang, S. Sun, F. Shi, *Angew. Chem. Int. Ed.* **2014**, 53, 13912 –13915.
- [139] J. Xu, S. Zheng, J. Zhang, X. Liu, B. Tan, *Angew. Chem. Int. Ed.* **2016**, 55, 11834 –11839
- [140] D. Enders, O. Niemeier, T. Balensiefer, *Angew. Chem. Int. Ed.*, **2006**, 45, 1463-1467.
- [141] X. Chen, C. Lei, D. Yue, J. Zhao, Z. Wang, X. Zhang, X. Xu, W. Yuan, *Org. Lett.* **2019**, 21, 5452–5456.
- [142] K. Li, T. Alves, K. Huang, Y. Lu, *Angew. Chem. Int. Ed.* **2019**, 58, 5427 –5431.
- [143] a) Fleming, I. In *Frontier Orbitals and Organic Chemical Reactions*; Wiley: New York, **1976**; p 58. b) Saracoglu, N. *Top.Heterocycl. Chem.* **2007**, 11, 1-61; c) C. Zheng, C. Zhuo, S. You, *J. Am. Chem. Soc.* **2014**, 136, 16251–16259.
- [144] C. Zhuo, Y. Zhou, S. You, *J. Am. Chem. Soc.* **2014**, 136, 6590–6593.
- [145] R. Gao, L. Ding, C. Zheng, L. Dai, S. You, *Org. Lett.* **2018**, 20, 748–751.
- [146] H. Zhang, R. Hu, N. Liu, S. Li, S. Yang, *Org. Lett.* **2016**, 18, 28–31.
- [147] Q. Cheng, J. Xie, Y. Weng, S. You, *Angew. Chem. Int. Ed.* **2019**, 58, 5739 –5743.
- [148] C. Shen, R. Liu, R. Fan, Y. Li, T. Xu, J. Gao, Y. Jia, *J. Am. Chem. Soc.* **2015**, 137, 4936–4939.
- [149] M. Jia, G. Cera, D. Perrotta, M. Monari, M. Bandini, *Chem. Eur. J.* **2014**, 20, 9875 – 9878.
- [150] M. Jia, M. Monari, Q. Yang, M. Bandini, *Chem. Commun.*, **2015**, 51, 2320–2323.
- [151] a) W. Zi, H. Wu, F. Dean Toste, *J. Am. Chem. Soc.* **2015**, 137, 3225–3228; b) Z. L. Niemeyer, S. Pindi, D. A. Khrakovsky, C.N. Kuzniewski, C. M. Hong, L. A. Joyce, M. S. Sigman, F. Dean Toste, *J. Am. Chem. Soc.* **2017**, 139, 12943–12946.
- [152] K. Kubota, K. Hayama, H. Iwamoto, H. Ito, *Angew. Chem. Int. Ed.* **2015**, 54, 8809 –8813.
- [153] W. Shao, H. Li, C. Liu, C. Liu, S. You, *Angew. Chem. Int. Ed.* **2015**, 54, 7684 –7687.
- [154] Z. Yang, Q. Wu, W. Shao, S. You, *J. Am. Chem. Soc.* **2015**, 137, 15899–15906.

Chapter 1

- [155] J. Ye, L. Zhu, S. Yan, M. Miao, X. Zhang, W. Zhou, J. Li, Y. Lan, D. Yu, *ACS Catal.* **2017**, 7, 8324–8330.
- [156] M. Zhu, C. Zheng, X. Zhang, S. You, *J. Am. Chem. Soc.* **2019**, 141, 2636–2644.
- [157] J. Wu, Y. Dou, R. Guillot, C. Kouklovsky, G. Vincent, *J. Am. Chem. Soc.* **2019**, 141, 2832–2837.
- [158] a) W. Sun, G. Li, L. Hong, R. Wang, *Org. Biomol. Chem.*, **2016**, 14, 2164–2176; b) W. Wu, L. Zhang, S. You, *Chem. Soc. Rev.*, **2016**, 45, 1570–1580.
- [159] S. Rousseaux, J. Garc á-Fortanet, M. A. D. A. Sanchez, S. L. Buchwald, *J. Am. Chem. Soc.* **2011**, 133, 9282–9285.
- [160] R. Xu, Q. Gu, W. Wu, Z. Zhao, S. You, *J. Am. Chem. Soc.* **2014**, 136, 15469–15472.
- [161] Q. Wu, W. Liu, C. Zhuo, Z. Rong, K. Ye, S. You, *Angew. Chem. Int. Ed.* **2011**, 50, 4455–4458.
- [162] Z. Yang, R. Jiang, Q. Wu, Lin, L. Huang, C. Zheng, S. You, *Angew. Chem. Int. Ed.* **2018**, 57, 16190–16193.
- [163] T. Nemoto, N. Matsuo, Y. Hamada, *Adv. Synth. Catal.* **2014**, 356, 2417–2421.
- [164] H. Wang, K. Wang, Y. Xiang, H. Jiang, X. Wan, N. Li, B. Tang, *Adv. Synth. Catal.* **2018**, 360, 2352–2357.
- [165] A. Seoane, N. Casanova, N. Quiñones, J. L. Mascareñas, M. Gulías, *J. Am. Chem. Soc.* **2014**, 136, 7607–7610.
- [166] G. Zhu, G. Bao, Y. Li, J. Yang, W. Sun, J. Li, L. Hong, R. Wang, *Org. Lett.* **2016**, 18, 5288–5291.
- [167] X. Li, H. Yang, J. Wang, B. Gou, J. Chen, L. Zhou, *Chem. Eur. J.* **2017**, 23, 5381–5385.
- [168] Z. Xia, C. Zheng, R. Xu, S. You, *NATURE COMMUNICATIONS* (**2019**) 10:3150
<https://doi.org/10.1038/s41467-019-11109-9>.
- [169] R. Xu, P. Yang, H. Tu, S. Wang, S. You, *Angew. Chem. Int. Ed.* **2016**, 55, 15137–15141.
- [170] J. Nan, J. Liu, H. Zheng, Z. Zuo, L. Hou, H. Hu, Y. Wang, X. Luan, *Angew. Chem. Int. Ed.* **2015**, 54, 2356–2360.
- [171] J. Zheng, S. Wang, C. Zheng, S. You, *J. Am. Chem. Soc.* **2015**, 137, 4880–4883.

Chapter 1

Gold(I) Catalyzed Dearomatization of 2-Naphthols with Alkynes

2.1 Abstract: The gold(I)-catalyzed chemoselective dearomatization of β -naphthols is reported through a straightforward approach via [3,3]-sigmatropic rearrangement /allene-cyclyzation cascade processes. Easily accessed naphthyl-propargyl ethers and derivatives in this work are employed as starting materials. Delightfully, an array of dearomatized dyhydrofuryl-naphthalen-2(*IH*)-ones featured densely functional groups are obtained in high yields (up to 98%) in 10 min reaction time under extremely mild reaction conditions like reagent grade solvent and exposure to air. The potential of accessing to high enantioselectivity on the dearomatized dyhydrofuryl-naphthalen-2(*IH*)-ones is also approved by the good ee (65%) relying on (*R*)-xylyl-BINAP(AuCl)₂. In addition, complete theoretical elucidation of the reaction pathway is also proposed which addresses a rationale for essential motivation such as regio- and chemoselectivity.

2.2 Introduction: The catalytic dearomatization of aromatic compounds accompanied with constructing C-X bond processes is a desirable and powerful synthetic tool to access the target of preparing complex organic molecular due to the large availability and bioactivity of variously functionalized arenes as well as heteroarenes.^[1] In the past decades, the dearomatization of nitrogen-containing arenes such as indoles and pyrroles have been widely achieved, leading to a variety of site-selective dearomatized azacycles which have greatly potential application of the natural and bioactive compounds. Dependent on this basis, fully carbon-based aromatics materials starts attracting increasing attention in chemistry community since dearomatization on them still faces minor success mainly attributed to connatural nature such as: high conjugate system, lower nucleophilicity and regioselectivity issues.

Among all the candidates of fully carbon-based aromatics compounds which are target to perform catalytic dearomatization reactions, phenol and naphthol derivatives are facing increasing attention since the abundant and economic-saving advantages, rleading to the construction of densely functionalized naphthalones featuring also stereogenic centers in a asymmertric manner.^[2] In other aspect, Naphthalene -2(*IH*)-one is also major molecular motif of particular interest, which has been embedded into numerous naturally molecules as well as bioactive compounds (**Figure 1**). Under this background, the catalytic dearomatization of 2-naphthols offers an efficient and direct synthetic methodology to this framework. This approach found elegant applications with the use of strongly activated electrophiles through the establishment of new C-X (X: oxidative approach, *e.g.* hydroxylation,^[3a] amination,^[3b,c] thiolation^[3d,e] and halogenation^[3f]) as well as C-C bonds.^[4] In the latter one, the strongly activated carbon-based electrophiles is usually required in order to access acceptably mild reaction conditions and consequently obtain the controllable and useful selectivity. However, more eco-friendly, readily available and unsaturated hydrocarbons electrophiles which benefit to the site-specific dearomatization of naphthols derivatives are still undeveloped and face far less success.^[5] In conjunction with our interests on gold catalyzed catalytic manipulation of arenes and heteroarenes, especially indol derivatives,^[6,7] an unprecedented gold-catalyzed dearomatization stratedy of β -naphthols through a cascade reaction sequence including [3,3]-propargylic Claisen

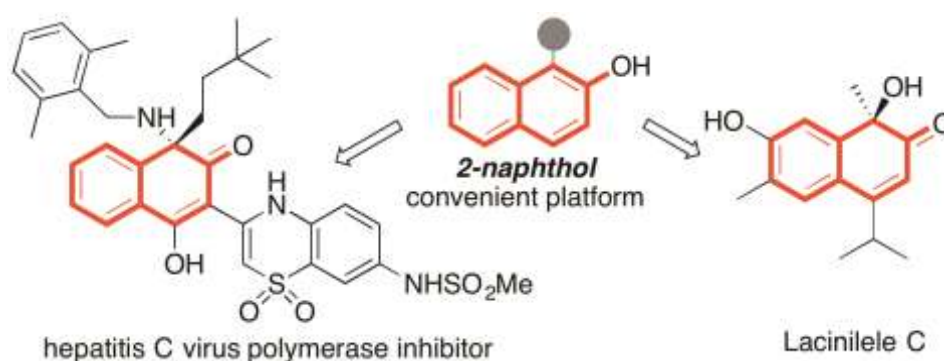
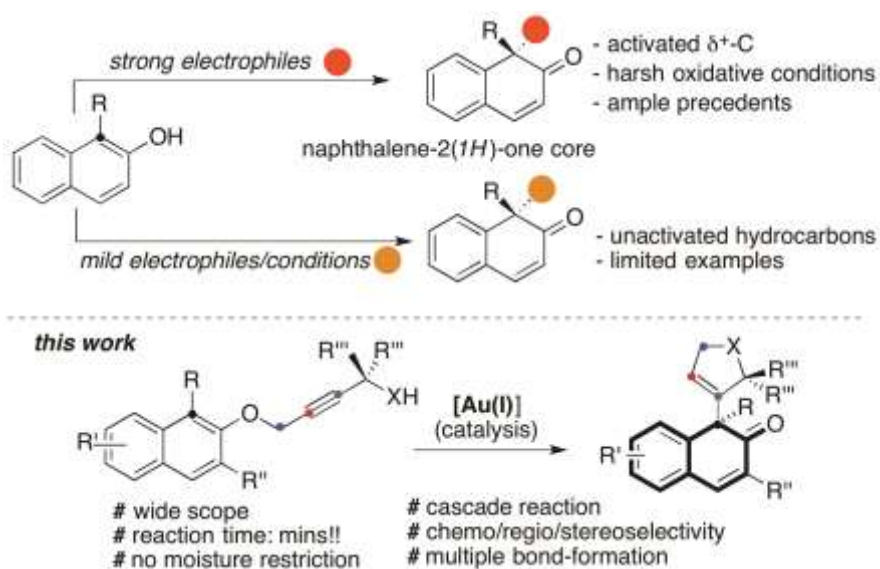


Figure 1 Dearomatization of 2-naphthols as direct synthetic entry to the naphthalen-2(1H)-one core. Biologically relevant compounds featuring dearomatized 2-naphthyl units.

rearrangement^[8] and successive nucleophilic annulation of the resulted allenyl intermediate^[9] is presented by our group. This cascade sequence of dearomatization process rewards the entitative attitude of [Au(I)] species on performing powerful electrophilic activation of alkynes^[10] and allenes^[11] towards nucleophilic additions, leading to efficient dearomatization of the naphthol and derivatives accompanied with construction of naphthalene -2(1H)-one core and elaborated side-chains in one pot (Scheme 1).^[12]

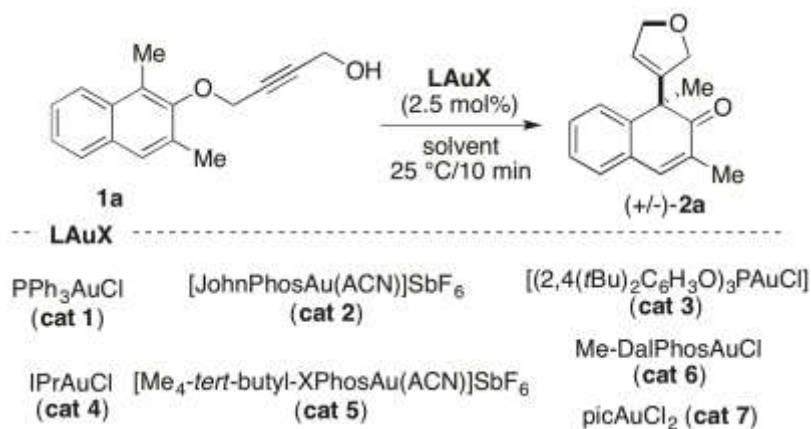
2.3 Experiments and results: To approve the reliability of our proposed idea, a initiatory survey on reaction parameter was carried out by using the easily accessible naphthyl-



Scheme 1. Working hypothesis of the present gold catalyzed cascade sequence.

propyn-ol **1a** as starting material. Fortunately, the treatment of **1a** with *in situ* PPh₃AuCl/AgSbF₆

Table 1. Screening of reaction conditions.^[a]



Entry	Cat	Solvent	Yield(%)
1	cat 1/AgSbF ₆	toluene	28
2	cat 2	toluene	98
3	cat 3/AgSbF ₆	toluene	30
4 ^[c]	cat 4/AgSbF ₆	toluene	58
5	cat 5	toluene	67
6	cat 6/AgSbF ₆	toluene	NR
7 ^[d]	cat 7/AgSbF ₆	toluene	40
8 ^[e]	cat 2	toluene	97
9	JohnPhosAuCl/AgNTf ₂	toluene	83
10	JohnPhosAuCl/AgTFA	toluene	traces
11	JohnPhosAuCl/AgOTs	toluene	NR
12	cat 2	DCM	73
13	cat 2	THF	90
14	cat 2	Et ₂ O	50
15 ^[f]	-/AgSbF ₆	toluene	21
16	JohnPhosAuCl/-	toluene	NR

Chapter 2

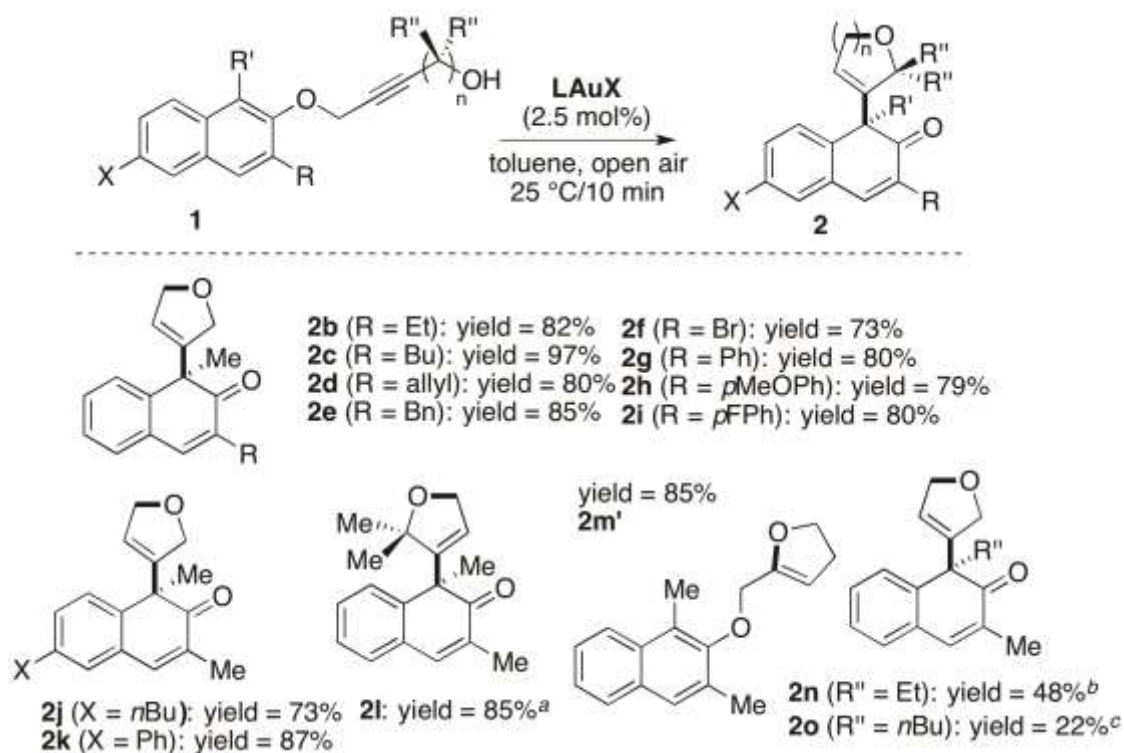
[a] All the reactions were run under nitrogen on 0.05 mmol scale of **1a** (0.5 M) in the presence of AgX 2.5 mol%, unless otherwise specified. [b] Isolated yield after flash chromatography. [c] Reaction time 40 min. [d] AgSbF₆ was used 5 mol%. [e] With reagent grade solvent, open air vial. [f] A series of unknown compounds was detected in the reaction crude. NR: no reaction.

(2.5 mol%) in dry toluene at room temperature offered successfully the desired and targeted dearomatized naphthalene-one **2a** in inspiring yield (28%) along with a complicated mixture of byproducts.

A series of gold(I)-complexes bearing different substituents which can affect the electronic and steric effect on ligand were then examined respectively (entries 2-7, Table 1) and consequently **cat 2** ([JohnPhosAu(ACN)]SbF₆, entry 2) was chosen as the optimal promoting catalyst by providing **2a** in almost quantitative yield (98%) within 10 min reaction time. With this delightful result, we were also encouraged to approve that when reagent grade toluene in an open air-vial conditions was employed, no decrease in catalytic performance was observed by still obtaining excellent yield (entry 8, yield = 97%). Even excellent yield was obtained in hand, different stabilizing counterions (entries 9-11) were also used to inspect the function and result in this transformation. Except ⁻NTf₂ counter anion which gave good yield (83%, entry 9), both ⁻TFA and ⁻OTf failed to offer the final product **2a**. Moreover, different from aromatic solvent like toluene, DCM, THF and Diethyl Ether were also tested separately (entry 12-14) and the decrease of product **2a** was found which means that aromatic solvent is helpful on this transformation. Additionally, single JohnPhosAuCl (entry 16) and AgSbF₆ (entry 15) were also tested individually and the result excluded the effects from Silver salts during the catalytic process and highlight the function of Au(I) and ⁻SbF₆, which have to be integrated in one pot.

Having achieved the optimized reaction conditions in hand, we next turned our attention onto the exploration of the substrate scope to test the tolerance of functional group. To obtain this purpose, numerous of differently substituted β-naphtholyl ethers (**1b-t**) were synthesized (see SI for details) and treated with the optimal condition of using **cat 2** (2.5 mol%) as the best catalyst in toluene at room temperature without moisture precautions.

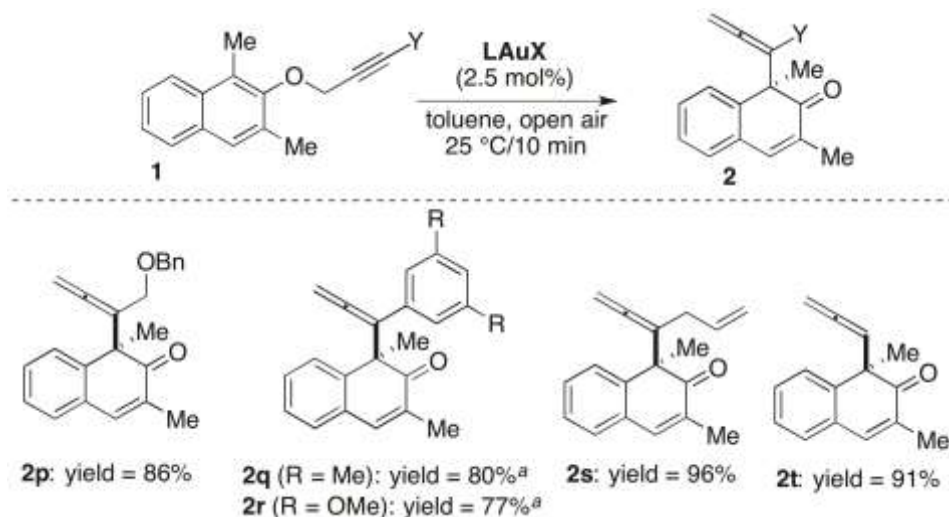
As summarized in **Scheme 2**, the protocol showed high stability and kept the efficiency with variously modified C(3)-substituted precursors (R = Et, nBu, allyl, Bn, Br and arenes **1b-i**) and



Scheme 2. Scope of the reaction. All compounds were obtained in racemic form. a Reaction time = 15 h. b Reaction time = 50 min at $-15\text{ }^\circ\text{C}$ (NMR conversion). c Reaction time = 30 min at rt.

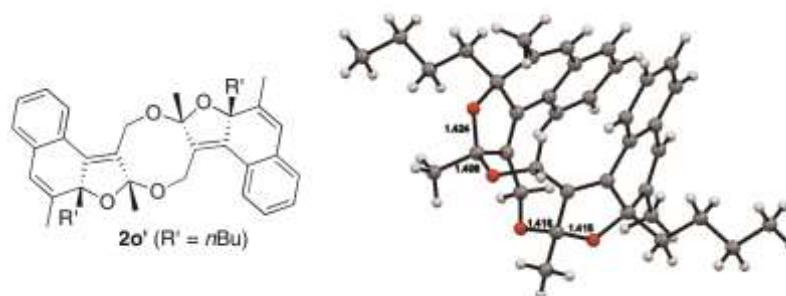
furnished the corresponding dearomatized and cyclized dihydrofuryl naphthalenone product in good to excellent yield (up to 97%). Additionally, when the functional group including EDG and EWG were introduced to C6, the corresponding dearomatized compounds were still promisingly obtained (**1j** and **k**: $x = n\text{Bu}$ and Ph) in high yields (73 and 87%). Identically, this protocol also was friend greatly with the substrates when the alkyne chain was decorated by substituent (**1l**) by offering excellent yield (85%) even though the reaction time was prolonged. However, when homopropargylic side-chains was extent to longer (**1m** with $n = 2$), this catalytic system lost its control on the pathway of dearomatization. In this case, under best reaction conditions, the formation of the dihydrofuryl compound **2m'** was collected (yield = 85%)^[12] rather than the normal dearomatization reaction since gold promoted intramolecular -OH addition to the triple bond was more competitive than the carbon nucleophile which form the target product.

In order to further detect the ultimately accessible substrates diversity in this catalytic strategy, modification on the terminal hydroxyl unit was considered. With this consideration, other moieties such as benzyloxy-, aryl and allyl moieties (**1p-t**) were used to replace the hydroxyl group which



Scheme 3. Examples of gold catalyzed synthesis of C(1)-allenyl dearomatized naphthalone cores (**2p-t**). All compounds were obtained in racemic form. ^a Reaction carried out at 0 °C for 2 h.

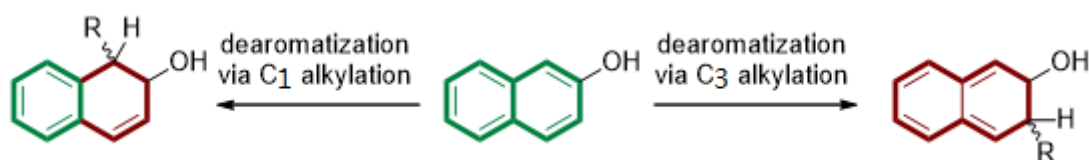
could stop the cyclization process by affording the corresponding allenyl dearomatized product. Inspiringly, in all cases we designed, all the corresponding dearomatized allenyl compounds (**2p-t**) were harvested in good to excellent yields (62-96%) under optimal reaction conditions (**Scheme 3**). Interestingly, terminal propargylic ether **1t** exhibited great competence in this catalytic system via offering the corresponding monosubstituted allenyl naphthalenone **1t** in excellent yield (91%). In this moment, It is worthy to highlight that the existence of ethyl (**1n**) and n-butyl (**1o**) groups at C1 instead of methyl group exploited another reaction pathway to form an unexpected by-product that were isolated in significant amounts (28% and 29%, respectively) along with producing the desired dearomatized species in moderate yield (**2n** 48% and **2o** 22%). Moreover, The structure of byproduct **2o'** (R' = nBu) was proved to be the diastereomerically pure



Scheme 4. Dimeric structure of the byproduct encountered with substrates **1o**.

dimeric compound depicted in **Scheme 4**. Mechanistically, the reaction result brought several interesting interrogatives such as: 1) the regiochemistry between C(1) and C(3) in the dearomatization event; 2) Concerted or stepwise Claisen rearrangement? 3) Mechanistically driving force on the divergence between C(1)-Me and C(1)-Bu of naphthol derivatives.

To scatter the light into these aspects we resorted to assistance of computational simulation. Firstly we focused our attention on the regioselectivity issue. We computed the diverted reaction profiles for the alternative sigmatropic rearrangements onto positions **1** and **3** of the naphthol respectively and the results told us that the reaction pathway toward C3 was energetically less favoured since the associated energy penalty was significant (between 6 and 20 kcal/mol, becoming larger than the reaction evolved towards products, see SI). We tried to trace this energy penalty back to aromaticity. The sigmatropic rearrangement onto C1 implies the loss of aromaticity at one of the rings of the naphthol system was lower than while the same migration onto C3 broke the conjugation in an o-quinodimethane form which resulted in the complete loss of aromaticity across the entire naphthol structure as shown in **Scheme 5**. Both structural (bond length alternation) and magnetic (ACID, NICS) parameters were consistent with this interpretation (see SI).

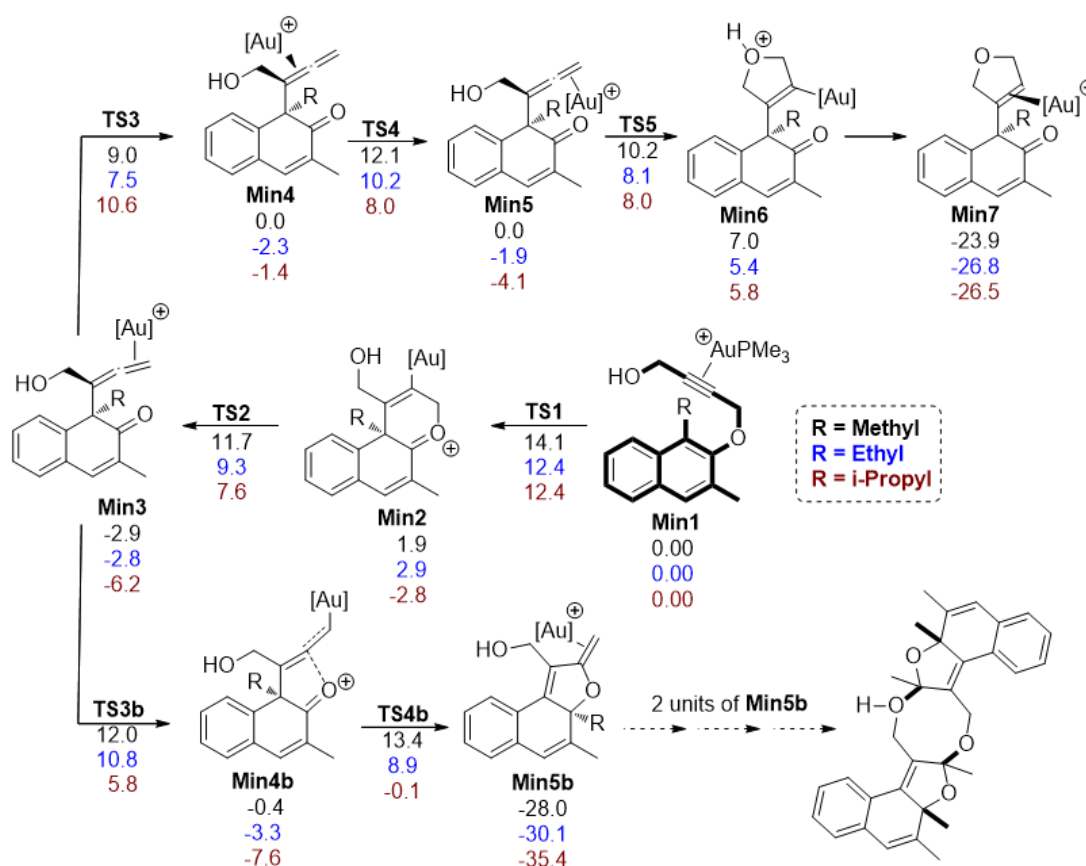


Scheme 5. [3,3]-Sigmatropic rearrangement selectivity governed by aromaticity. Fragments showing aromaticity highlighted with bold green bonds, those losing aromaticity in bold red.

Then we turned our attention on the mechanism of affording the favoured regioisomer. The major characteristic of the proposed mechanism on where we started this work were confirmed by our simulations. However, it is worth noting that the [3,3]-sigmatropic rearrangement happened in a step-wise method through a six membered ring intermediate^[8a] while the naphthol has already lost the aromaticity at one ring by tautomerization process which formed a naphthalenone isomer whose carbonyl oxygen can then stabilize the activated allene via a dative bond (**Min2** in **Scheme 6**). The subsequent allene intermediate arrived at the key and important step which has two available pathways respectively to form the expected product in dimethyl-naphthols and the

unexpected ones in ethyl and butyl naphthol derivatives. The activated allene fragment in **Min3** can be attacked by two internal nucleophiles including the allenyl alcohol or ketene group. The first approach requires a rotation of the gold catalyst (**Min3** vs **Min5**) along the allenyl axis because when the allene was formed in **TS2**, the catalyst was oriented syn direction to the alcohol. In another direction, the second way required an alkyl 1,2-migration to transfer the ketone back into an alkoxyde that stabilized the final fused furan system.

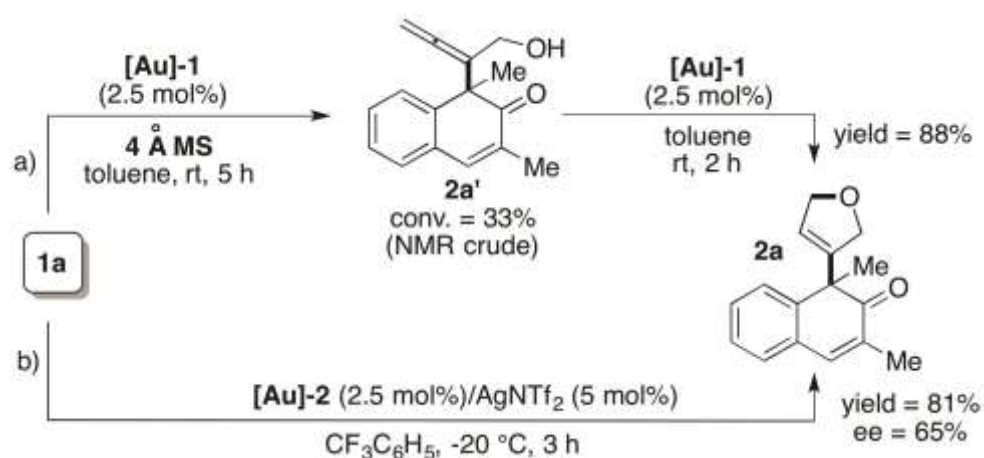
To understand this competitive transformation in depth, we computed the reaction profiles for systems containing groups bearing different migrating ability. Substrates with methyl and ethyl groups at C1 position since they have been experimentally tested were selected as model sample, and isopropyl group was also additionally considered to explore the influence of group along with increased migratory ability.



Scheme 6. Computed mechanistic alternatives for the formation of the expected furanyl naphthalenone (**Min7**) and the unexpected dimer (via **Min5b**). Free energies in kcal/mol⁻¹ computed at the M06/Def2SVPP level with toluene parameters in the PCM solvation model (1atm,298 K).^[13] For a detailed description of the computational methodology see the Supporting Information.

The obtained results are consistent exceptionally well with the experimental observations and are summarized in **Scheme 6**. The methyl group showed lower migratory ability so that the favoured path was the attack of the allenyl alcohol (10.2 kcal/mol) from the allene intermediate **Min3**. Moreover, calculation showed that the C-O bond formation was not the selectivity determining step in this pathway, since the rotation of the gold complex to the anti position is slightly more energy demanding (12.1 kcal/mol). Dependent on our calculations, once the initial barrier is overcome, the formation of the key allene intermediate (**Min3**) is quite favourable. In the experimental parameter, this intermediate can actually be detected in the TLC plate which has priority to form product. To certify that our computed mechanism is in agreement with this finding, stochastic kinetic simulations (see the SI for details) was run, which verified that, within our computed mechanism, **Min3** was accumulates significantly on concentration before the second reacting site of the mechanism got involved into the reaction. Despite the essential reluctance of the methyl group to participate in a migration process, the energy gap between mono-dearomatization and the alternative path yielding the dimer(higher) is only 1.3 kcal/mol (13.4 kcal/mol for the transition state involving the migration). This is a rather small energy difference which is enough to guarantee selectivity due to the mild thermal conditions utilized in this experiment. However, it is also possible to divert the reaction pathway. When an ethyl group was featured, the energy requirements for the migration step were significantly reduced so that migration process became easier since it was no longer the determining step in this branch, resulting in that the 5 membered ring formation of **Min5b** becomes the determining step. In the meantime, for the route leading to the expected product, all barriers were holistically reduced by about 2 kcal/mol, adjusting energy barrier of the determining step to 10.2 kcal/mol. This small energy difference (10.8 vs 10.2 kcal/mol) can be almost ignored among both branches resulting in the experimental findings of significant amounts of both kinds of products. In addition, the energy difference between two pathways becomes smaller along with increasing migration ability of the alkyl group. When the alkyl group is isopropyl derivative, the competitive situation completely reverts and the formation of the unexpected product seems to become obviously preferred (5.8 vs 10.6 kcal/mol). Additionally, the formation of **2m'** by using homopropargyl alcohol **1m** is also explained on the grounds of aromaticity loss (see the SI).

Finally, to strongly corroborate the mechanistic outcome resulting from the computational investigation, the allenyl-ol intermediate **2a'** (33% conversion, $^1\text{H-NMR}$) was detected and isolated successfully by running the classic dearomatization reaction in the presence of dried 4 Å MS whose abundant hydroxyl group prevented the final C-O bond forming transformation (**Scheme 7a**).^[14] Then, the formation of **2a'** in the whole catalytic cycle was unambiguously proved. In other hand, by treating **2a'** with fresh [JohnPhosAu(CH₃CN)]SbF₆ (2.5 mol%) in toluene without MS, as expected, it was completely converted into **2a** in 2h, similarly to the one-pot protocol (Table 1, entry 8).



Scheme 7. a) Proving the step-wise cascade mechanism involving allenyl-ol **2a'** the key intermediate, [Au]-1: JohnPhosAu(CH₃CN)SbF₆. b) Stereoselective dearomatization reaction with chiral gold complex, [Au]-2: (*R*)-xylyl-BINAP(AuCl)₂.

Moreover, the step-wise sigmatropic rearrangement resulting from computations encouraged us to further investigate an enantioselective transformation by means of chiral gold(I) complexes that are directly engaged in the stereoselection of the sequent process. Interestingly, the use of *in situ* (*R*)-xylyl-BINAP(AuCl)₂/AgNTf₂ (5 mol%) in reagent grade CF₃-C₆H₅ at -20 °C enabled the isolation of **2a** in 81% yield and 65% ee, proving the suitability of our methodology to be implemented into a stereoselective variant (**Scheme 7b**).

2.4 Summary

In conclusion, we have successfully presented a novel and efficient strategy for the site-selective dearomatization of β -naphthols via gold catalysis. Benefiting from unique advantages of gold(I) complex, readily availability of the starting material is converted to varied dearomatized naphthalenone skeleton including products via a cascade process involving an initial [3,3]-rearrangement followed cyclized addition on resulted allenyl-ol derivatives. In the meantime, a computational investigation spreads light on the whole stepwise reaction machinery and provides important theoretical support for the high regioselectivity observed as well as for the chemical divergence relating to substrates **2n** and **2o**. Further studies on the stereoselective dearomatization of different aromatic rings are undergoing and will be presented in near future.

2.5 Reference

- [1] a) A. R. Pape, K. P. Kaliappan and E. P. Kündig, *Chem. Rev.* **2000**, *100*, 2917-2940; b) S. P. Roche, J. A. Porco, Jr. *Angew. Chem. Int. Ed.* **2011**, *50*, 4068-4093; c) C.-X. Zhuo, W. Zhang, S.-L. You, *Angew. Chem. Int. Ed.* **2012**, *51*, 12662-12686; d) C. Zheng and S.-L. You, *Chem.* **2016**, *1*, 830-857; e) *Asymmetric Dearomatization Reactions* (Ed. S.-L. You), Wiley-VCH, **2016**; f) W.-T. Wu, L. Zhang and S.-L. You, *Chem. Soc. Rev.* **2016**, *45*, 1570-1580; g) h) X.-W. Liang, C. Zheng and S.-L. You, *Chem. Eur. J.* **2016**, *22*, 11918-11933; h) S. Park, S. Chang, *Angew. Chem. Int. Ed.* **2017**, *56*, 7720-7738.
- [2] For some representative catalytic and enantioselective examples see: a) T. Oguma, T. Katsuki, *J. Am. Chem. Soc.* **2012**, *134*, 20017-20034; b) C.-X. Zhuo, S.-L. You, *Angew. Chem. Int. Ed.* **2013**, *52*, 10056-10059; c) R.J. Phipps, F. D. Toste, *J. Am. Chem. Soc.* **2013**, *135*, 1268-1271; d) S.-G. Wang, X.-J. Liu, Q.-C. Zhao, C. Zheng, S.-B. Wang, S.-L. You, *Angew. Chem., Int. Ed.* **2015**, *54*, 14929-14932; e) Q. Yin, S.-G. Wang, X.-W. Liang, D.-W. Gao, J. Zheng, S.-L. You, *Chem. Sci.* **2015**, *6*, 4179-4183; f) G. Zhu, G. Bao, Y. Li, J. Yang, W. Sun, J. Li, L. Hong, R. Wang, *Org. Lett.* **2016**, *18*, 5288-5291; g) Q. Cheng, Y. Wang, S.-L. You, *Angew. Chem. Int. Ed.* **2016**, *55*, 3496-3499; h) L. Wang, D. Yang, D. Li, P. Wang, K. Wang, J. Wang, X. Jiang and R. Wang, *Chem. Eur. J.* **2016**, *22*, 8483-8487; i) H.-F. Tu, C. Zheng, R.-Q. Xu, X.-J. Liu, S.-L. You, *Angew. Chem. Int. Ed.* **2017**, *56*, 3237-3241; j) D. Shen, Q. Chen, P. Yan, X. Zeng, and G. Zhong, *Angew. Chem. Int. Ed.* **2017**, *56*, 3290-3294.
- [3] For some representative examples see: C-O bond formation: a) C. Grandclaoudon and P. Y. Toullec, *Eur. J. Org. Chem.* **2016**, 260-264; C-N bond formation: b) J. Dhineshkumar, P. Samaddar and K. Ramaiah Prabhu, *Chem. Commun.* **2016**, *52*, 11084-11087; c) A. Changotra, S. Das and R. B. Sunoj, *Org. Lett.* **2017**, *19*, 2354-2357; C-S bond formation: d) P. Zhang, M. Li, X.-S. Xue, C. Xu, Q. Zhao, Y. Liu, H. Wang, Y. Guo, L. Lu and Q. Shen, *J. Org. Chem.* **2016**, *81*, 7486-7509; e) J. Li, M. Wang, Y. Zhang, Z. Fan, W. Zhang, F. Sun, N. Ma, *ACS Sustainable Chem. Eng.*, **2016**, *4*, 3189-3195; C-halogen bond formation: f) Z. Zhang, Q. Sun, D. Xu, C. Xia and W. Sun, *Green Chem.* **2016**, *18*, 5485-5492.
- [4] a) C.-X. Zhuo, S.-L. You, *Adv. Synth. Catal.* **2014**, *356*, 2020-2028; b) D. Yang, L. Wang, M. Kai, D. Li, X. Yao, R. Wang, *Angew. Chem. Int. Ed.* **2015**, *54*, 95239527; c) R.-Q. Xu, P. Yang, H.-F. Tu, S.-G. Wang, S.-L. You, *Angew. Chem. Int. Ed.* **2016**, *55*, 15137-15141; d) B. Heid and B. Plietker, *Synthesis*, **2016**, *48*, 340-350; d) L. Shao, X.-P. Hu, *Chem. Commun.* **2017**, *53*, 8192-8195; e) H. Nakayama, S. Harada, M. Kono, T. Nemoto, *J. Am. Chem. Soc.* **2017**, *139*, 10188-10191; f) R.-Q. Xu, P. Yang, S.-L. You, *Chem. Commun.* **2017**, *53*, 7553-7556; g) R.-Q. Xu, Q. Gu, S.-L. You, *Angew. Chem. Int. Ed.* **2017**, *56*, 7252-7256.
- [5] For elegant examples: a) J. Nan, Z. Zuo, L. Luo, L. Bai, H. Zheng, Y. Yuan, J. Liu, X. Luan, Y. Wang, *J. Am. Chem. Soc.* **2013**, *135*, 17306-17309; b) J. Zheng, S.-B. Wang, C. Zheng and S.-L. You, *J. Am. Chem. Soc.* **2015**, *137*, 4880-4883 and references therein; c) C. Zheng, J. Zheng, S.-L. You, *ACS, Catal.* **2016**, *6*, 262-271; d) W.-T. Wu, R.-Q. Xu, L. Zhang, S.-L. You, *Chem. Sci.* **2016**, *7*, 3427-3431.
- [6] a) M. Bandini, M. Tragni and A. Umani-Ronchi, *Adv. Synth. Catal.* **2009**, *351*, 2521-2524; b) M. Bandini, A. Eichholzer, *Angew. Chem. Int. Ed.* **2009**, *48*, 9533-9537; c) M. Bandini, A. Eichholzer, A. Gualandi, T. Quinto, D. Savoia, *ChemCatChem.* **2010**, *2*, 661-665; d) M. Bandini, A. Gualandi, M. Tragni, D. Savoia, *J. Organomet. Chem.* **2011**, *696*, 338-347; e) G. Cera, P.

- Crispino, M. Monari, M. Bandini, *Chem. Commun.* **2011**, 47, 7803-7805; f) G. Cera, S. Piscitelli, M. Chiarucci, G. Fabrizi, A. Goggiamani, R. S. Ramón, S. P. Nolan, M. Bandini, *Angew. Chem. Int. Ed.* **2012**, 51, 9891-9895; g) M. Bandini, A. Bottoni, M. Chiarucci, G. Cera, G. Miscione, *J. Am. Chem. Soc.* **2012**, 134, 20690-20700; j) M. Chiarucci, E. Matteucci, G. Cera, G. Fabrizi, M. Bandini, *Chem. Asian J.* **2013**, 8, 1776-1779; k) M. Chiarucci, R. Mocci, L.-D. Syntrivanis, G. Cera, A. Mazzanti, M. Bandini, *Angew. Chem. Int. Ed.* **2013**, 52, 10850-10853; l) P. Giacinto, G. Cera, A. Bottoni, M. Bandini, G. P. Miscione, *ChemCatChem.* **2015**, 7, 2480-2484.
- [7] M. Bandini, *Chem. Soc. Rev.* **2011**, 40, 1358-1367.
- [8] a) Benjamin D. Sherry, F. Dean Toste, *J. Am. Chem. Soc.* **2004**, 126, 15978-15979; b) T. Cao, J. Deitch, E. C. Linton, M. C. Kozlowski, *Angew. Chem. Int. Ed.* **2012**, 51, 2448-2451; c) D. Tejedor, G. Méndez-Abt, L. Cotos, F. García-Tellado, *Chem. Soc. Rev.* **2013**, 42, 458-471; d) J. Li, L. Lin, B. Hu, P. Zhou, T. Huang, X. Liu, X. Feng, *Angew. Chem.* **2017**, 129, 903-906; *Angew. Chem. Int. Ed.* **2017**, 56, 885-888.
- [9] a) M. Jia, G. Cera, D. Perrotta, M. Bandini, *Chem. Eur. J.* **2014**, 20, 9875-9878; b) M. Jia, M. Monari, Q.-Q. Yang, M. Bandini, *Chem. Commun.* **2015**, 51, 2320-2323; c) R. Ocello, A. De Nisi, M. Jia, Q.-Q. Yang, P. Giacinto, A. Bottoni, G. P. Miscione, M. Bandini, *Chem. Eur. J.* **2015**, 21, 18445-18453; d) L. Rocchigiani, M. Jia, M. Bandini, A. Macchioni, *ACS Catalysis* **2015**, 5, 3911-3915.
- [10] For general review articles on the gold catalyzed functionalization of alkynes and rearrangement reaction see: a) C. Obradors, A. M. Echavarren, *Acc. Chem. Res.* **2014**, 47, 902-912; b) B. Alcaide, P. Almendros, *Acc. Chem. Res.* 2014, 47, 939-952; c) R. Dorel, A. E. Echavarren, *Chem. Rev.* 2015, 115, 9028-9072.
- [11] M. Chiarucci, M. Bandini, *Beilstein J. Org. Chem.* 2013, 9, 2586-2614.
- [12] For representative examples of gold catalyzed dearomatization of nitrogen-containing arenes with alkynes see: a) C. Ferrer, A. M. Echavarren, *Angew. Chem. Int. Ed.* **2006**, 45, 1105-1109; b) C. Ferrer, C. H. M. Amijs, A. M. Echavarren, *Chem. Eur. J.* **2007**, 13, 1358-1373. c) G. Cera, P. Crispino, M. Monari, M. Bandini, *Chem. Commun.* **2011**, 47, 7803-7805; d) G. Cera, M. Chiarucci, A. Mazzanti, M. Mancinelli, M. Bandini, *Org. Lett.* **2012**, 14, 1350-1353; e) J. D. Podoll, Y. Liu, L. Chang, S. Walls, W. Wang, X. Wang, *Proc. Natl. Acad. Sci.* **2013**, 110, 15573-15778; f) L. Zhang, Y. Wang, Z.-J. Yao, S. Wang, Z.-X. Yu, *J. Am. Chem. Soc.* **2015**, 137, 13290-13300; g) V. Magné, F. Blanchard, A. Marinetti, A. Voituriez, X. Guinchard, *Adv. Synth. Catal.* **2016**, 358, 3355-3361.
- [13] a) Y. Zhao and D. G. Truhlar, *Theor. Chem. Acc.* **2008**, 120, 215-241; b) F. Weigend, R. Ahlrichs, *Phys. Chem. Chem. Phys.*, **2005**, 7, 3297-305; c) O. N. Faza, R. A. Rodríguez, C. S. López, *Theor. Chem. Acc.* **2011**, 128, 647-661; d) O. N. Faza, C. S. López, *Top. Curr. Chem.* **2014**, 357, 213-284.
- [14] Although the role of the MS at the present is still unclear, we could speculate that both inclusion phenomena and specific absorption of the more polar **2a'** with respect to **2a** on the additive could account for the observed trapping action exerted on the allenyl-ol intermediate **2a'**.

Supporting Information

Table of Contents

General methods.....	107
Computational methods.....	108
Synthesis of 4-((naphthalen-2-yl)oxy)but-2-yn-1-ol derivatives 1a-o	109
Synthesis of 4-((naphthalen-2-yl)oxy)but-2-yn-1-ol derivatives 1p,q	113
Synthesis of 4-((naphthalen-2-yl)oxy)but-2-yn-1-ol derivatives 1r,s	114
Synthesis of 4-((naphthalen-2-yl)oxy)but-2-yn-1-ol derivatives 1u,v	115
General procedure for Gold-catalyzed intramolecular dearomatization reaction of naphthol derivatives:	116
Interrupted dearomatization process.....	122
Table S1: Enantioselective dearomatization of 1a	123
Crystal data and structure refinement for compound 2o'	125
Aromaticity governing regioselectivity	126
Table of Energies.....	128
Kinetic simulation.....	130
References.....	131

General Methods.

¹H-NMR spectra were recorded on Varian 400 (400 MHz) spectrometers. Chemical shifts are reported in ppm from TMS with the solvent resonance as the internal standard (deuteriochloroform: 7.24 ppm). Data are reported as follows: chemical shift, multiplicity (s = singlet, d = doublet, t = triplet, q = quartet, sext = sextet, sept = septet, p = pseudo, b = broad, m = multiplet), coupling constants (Hz). ¹³C-NMR spectra were recorded on a Varian 400 (100 MHz) spectrometers with complete proton decoupling. Chemical shifts are reported in ppm from TMS with the solvent as the internal standard (deuteriochloroform: 77.0 ppm). GC-MS spectra were taken by EI ionization at 70 eV on a Hewlett-Packard 5971 with GC injection. They are reported as: *m/z* (rel. intense). LC-electrospray ionization mass spectra were obtained with Agilent Technologies MSD1100 single-quadrupole mass spectrometer. Chromatographic purification was done with 240-400 mesh silica gel. Other anhydrous solvents were supplied by Sigma Aldrich in Sureseal® bottles and used without any further purification. Commercially available chemicals were purchased from Sigma Aldrich, Stream and TCI and used without any further purification. Analytical high performance liquid chromatography (HPLC) was performed on a liquid chromatograph equipped with a variable wave-length UV detector (deuterium lamp 190-600 nm), using a Daicel Chiracel™OD-H, (0.46 cm I.D. x 25 cm Daicel Inc). HPLC grade isopropanol and *n*-hexane were used as the eluting solvents. Melting points were determined with Bibby Stuart Scientific Melting Point Apparatus SMP 3 and are not corrected. Agilent Technologies LC/MSD Trap 1100 series (nebulizer: 15.0 PSI, dry Gas: 5.0 L/min, dry Temperature: 325 °C, capillary voltage positive scan: 4000 mA, capillary voltage negative scan: 3500 mA).

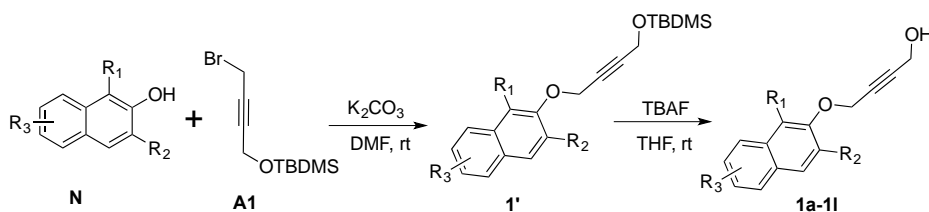
The X-ray intensity data for **2o'** were measured on a Bruker Apex II CCD diffractometer. Cell dimensions and the orientation matrix were initially determined from a least-squares refinement on reflections measured in three sets of 20 exposures, collected in three different ω regions, and eventually refined against all data. A full sphere of reciprocal space was scanned by 0.3° ω steps. The software SMART^[1] as used for collecting frames of data, indexing reflections and determination of lattice parameters. The collected frames were then processed for integration by the SAINT program, and an empirical absorption correction was applied using SADABS.^[2] The structures were solved by direct methods (SIR 97)^[3] and subsequent Fourier syntheses and refined by full-matrix least-squares on F^2 (SHELXTL),^[4] using anisotropic thermal parameters for all non-hydrogen atoms. All the hydrogen atoms were located in difference Fourier maps. The aromatic, methyl and methylene hydrogen atoms were placed in calculated positions and refined with isotropic thermal parameters $U(H) = 1.2 Ueq(C)$ or $U(H) = 1.5 Ueq(C)$ (methyl H), respectively and allowed to ride on their carrier carbons. The molecular graphics were generated by using ORTEP.^[5] Color codes for the molecular graphics: red (O), grey (C), white (H). Crystal data

and other experimental details for **2o'** are reported in Table S3 whereas bond lengths [Å] and angles (deg) are shown in Table S4. CCDC- 1575784 contains the supplementary crystallographic data for this paper. These data can be obtained free of charge at www.ccdc.cam.ac.uk/conts/retrieving.html (or from the Cambridge Crystallographic Data Centre, 12 Union Road, Cambridge CB2 1EZ, UK; Fax: +44-1223-336-033; e-mail: deposit@ccdc.cam.ac.uk).

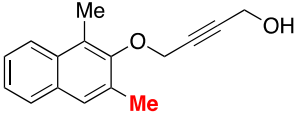
Computational Methods

Throughout this work the Density Functional Theory has been employed in its Kohn-Sham formulation^[6] The *meta*-GGA exchange-correlation functional, M06, by Zhao and Truhlar^[7] was used with the double- ζ quality Def2SVPP basis set. This modern basis set is well balanced and densely populated which, in terms of size and number of Gaussian functions, makes it comparable with popular triple- ζ quality options like the 6-311+G(3df,2p) basis set by Pople. This model chemistry has been tested in a thorough benchmark focused on [Au(I)]/alkyne chemistry and renders improved results with respect to other density functional/basis set combinations.^[8] All geometry optimizations have been carried out using tight convergence criteria in order to obtain accurate stationary points. Such accuracy in the geometries also required a pruned grid for numerical integration with 99 radial shells and 590 angular points per shell. In difficult-to-converge cases the discretization of the numerical integration grid was further improved to 175 radial shells and 974 angular points per shell for first-row atoms and 250/974 for atoms in the second and later rows. Analysis of the normal modes obtained via diagonalization of the Hessian matrix was used to confirm the topological nature of each stationary point. The wave function stability for each optimized structure has also been checked.^[9] The ACID surfaces and vectorial field were computed using the continuous set of gauge transformations, (CSGT)^[10]. All the calculations reported in this manuscript were performed with Gaussian 09.^[11]

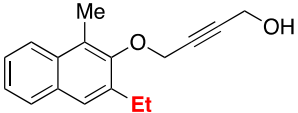
Preparation of β -naphthols (**N**)^[12], propargyl bromide(**A1**),^[13] propargyl bromides(**A2/A3**),^[14] propargyl bromides(**A4/A5**)^[15] and 6-bromohex-1-en-4-yne(**A7**)^[16] were accomplished following the reported procedures. 3-Bromoprop-1-yne(**A6**) was purchased from Sigma-Aldrich.

Synthesis of 4-((naphthalen-2-yl)oxy)but-2-yn-1-ol derivatives **1a-o**

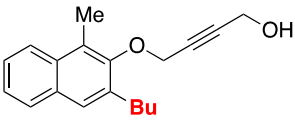
To a flamed two-necked flask was added DMF(15ml), the desired 2-naphthol **N**(1mmol) and **A1**(1.5 mmol, 1.5 equiv.). Then K_2CO_3 (2 mmol, 2 equiv.) was added under N_2 atmosphere and keep stirring at room temperature. After the reaction was complete(monitored by TLC), the solution was quenched with water and extracted with EtOAc three times. Then the combined organic layers were washed with brine, dried with Na_2SO_4 , filtered and concentrated by rotary evaporation. The residue (**1'**) was directly hydrolyzed by tetrabutylammonium fluoride (TBAF, 1.5mmol) in reagent grade THF at room temperature for 2h. After quenching with water, the solution was extracted with EtOAc three times. Next the combined organic layers were washed with brine, dried with Na_2SO_4 , filtered and concentrated by rotary evaporation. The residue was purified with silica gel column chromatography to afford the **1**.

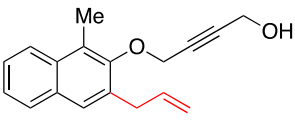


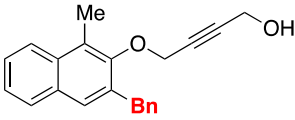
1a. Light yellow oil, cHex:EtOAc = 20:1→8:1, yield = 83%. 1H NMR (400 MHz, $CDCl_3$) δ = 7.90 (d, $J=8.0$ Hz, 1H), 7.71 (d, $J=4.0$ Hz, 1H), 7.51 (s, 1H), 7.47-7.38 (m, 2H), 4.57 (t, $J=2.0$ Hz, 2H), 4.32 (t, $J=2.0$ Hz, 2H), 2.63 (s, 3H), 2.48 (s, 3H). ^{13}C NMR (100 MHz, $CDCl_3$) δ = 153.09, 132.44, 131.14, 130.98, 127.57, 127.49, 125.23, 125.13, 124.87, 123.92, 85.33, 81.19, 60.82, 51.01, 17.42, 11.99. GC-MS (m/z): 240. Anal. Calc. for ($C_{16}H_{16}O_2$: 240.12): C, 79.97; H, 6.71; found: C, 80.03, H, 6.59.

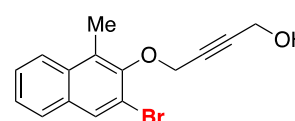


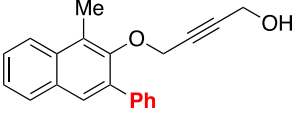
1b. Light yellow oil, cHex:EtOAc = 20:1→8:1, yield = 73%. 1H NMR (400 MHz, $CDCl_3$) δ = 7.90 (d, $J=8.0$ Hz, 1H), 7.73 (d, $J=8.0$ Hz, 1H), 7.53 (s, 1H), 7.46-7.37 (m, 2H), 4.57 (t, $J=3.2$ Hz, 2H), 4.32 (t, $J=3.2$ Hz, 2H), 2.86 (q, $J=7.2$ Hz, 2H), 2.63 (s, 3H), 1.33 (t, $J=7.6$ Hz, 3H). ^{13}C NMR (100 MHz, $CDCl_3$) δ = 152.90, 136.94, 132.33, 131.22, 127.77, 125.67, 125.23, 125.07, 124.81, 123.83, 85.22, 81.32, 61.26, 51.12, 23.67, 14.54, 12.06. GC-MS (m/z): 254. Anal. Calc. for ($C_{17}H_{18}O_2$: 254.13): C, 80.28; H, 7.13; found: C, 80.11, H, 7.21.

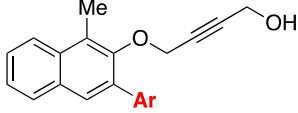

1c. Light yellow oil, cHex:EtOAc = 20:1→10:1, yield = 68%. ¹H NMR (400 MHz, CDCl₃) δ = 7.91 (d, *J*=8.0 Hz, 1H), 7.74 (d, *J*=8.0 Hz, 1H), 7.52 (s, 1H), 7.46 – 7.38 (m, 2H), 4.57 (s, 2H), 4.32 (s, 2H), 2.80 – 2.84 (t, *J*=16.0 Hz, 2H), 2.63 (s, 3H), 1.74-1.66 (m, 2H), 1.51 – 1.36 (m, 2H), 0.97 (t, *J*=7.2 Hz, 3H). ¹³C NMR (100 MHz, CDCl₃) δ = 153.09, 135.68, 132.35, 131.15, 127.74, 126.51, 125.21, 125.12, 124.80, 123.84, 85.25, 81.32, 61.36, 51.11, 32.70, 30.60, 22.75, 14.01, 12.11. GC-MS (*m/z*): 282. Anal. Calc. for (C₁₉H₂₂O₂: 282.16): C, 80.82; H, 7.85; found: C, 80.65, H, 7.70.

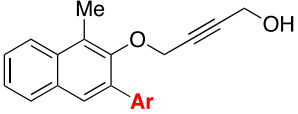

1d. Light yellow oil, cHex:EtOAc = 20:1→8:1, yield = 65%. ¹H NMR (400 MHz, CDCl₃) δ = 7.92 (d, *J*=8.0 Hz, 1H), 7.76 (d, *J*=8.0 Hz, 1H), 7.53 (s, 1H), 7.48-7.39 (m, 2H), 6.14-6.04 (m, 1H), 5.18-5.14 (m, 2H), 4.58 (s, 2H), 4.32 (s, 2H), 3.63 (d, *J*=8.0 Hz, 2H), 2.64 (s, 3H). ¹³C NMR (100 MHz, CDCl₃) δ = 152.67, 137.06, 133.01, 132.61, 131.11, 127.87, 127.09, 125.51, 125.38, 124.93, 123.88, 116.26, 85.48, 81.09, 61.44, 51.01, 34.91, 12.11. GC-MS (*m/z*): 266. Anal. Calc. for (C₁₈H₁₈O₂: 266.13): C, 81.17; H, 6.81; found: C, 81.01, H, 6.70.

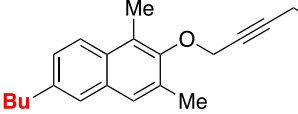

1e. Light yellow oil, cHex:EtOAc = 20:1→8:1, yield = 63%. ¹H NMR (400 MHz, CDCl₃) δ = 7.92 (d, *J*=8.0, 1H), 7.70 (d, *J*=8.0, 1H), 7.50 – 7.36 (m, 3H), 7.34 – 7.17 (m, 5H), 4.45 (t, *J*=1.6, 2H), 4.30 (t, *J*=1.6, 2H), 4.22 (s, 2H), 2.64 (s, 3H). ¹³C NMR (100 MHz, CDCl₃) δ = 152.96, 140.66, 134.15, 132.72, 131.02, 129.04(2C), 128.41(2C), 127.94, 127.78, 126.09, 125.54, 125.42, 124.91, 123.83, 85.34, 81.30, 61.41, 51.12, 37.00, 12.18. GC-MS (*m/z*): 316. Anal. Calc. for (C₂₂H₂₀O₂: 316.15): C, 83.52; H, 6.37; found: C, 83.40, H, 6.21.

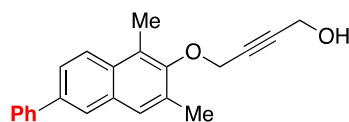

1f. Light yellow oil, cHex:EtOAc = 20:1→10:1, yield = 80%. ¹H NMR (400 MHz, CDCl₃) δ = 7.91 – 7.95 (m, 2H), 7.70 (d, *J*=8.0 Hz, 1H), 7.52 (t, *J*=8.0 Hz, 1H), 7.43 (t, *J*=4.0 Hz, 1H), 4.73 (s, 2H), 4.31 (s, 2H), 2.70 (s, 3H). ¹³C NMR (100 MHz, CDCl₃) δ = 149.61, 132.68, 131.74, 130.39, 128.18, 127.40, 126.44, 125.83, 124.31, 116.93, 85.64, 80.94, 61.29, 51.16, 12.82. GC-MS (*m/z*): 304/306. Anal. Calc. for (C₁₅H₁₃BrO₂: 304.01): C, 59.04; H, 4.29; found: C, 58.89, H, 4.12.


1g. Light yellowoil, cHex:EtOAc = 20:1→10:1, yield = 76%. ¹H NMR (400 MHz, CDCl₃) δ = 7.99 (d, *J*=8.0 Hz, 1H), 7.82 (d, *J*=8.0 Hz, 1H), 7.69-7.66 (m, 3H), 7.54-7.50 (m, 1H), 7.47 – 7.43 (m, 3H), 7.40 – 7.36 (m, 1H), 4.18 (t, *J*=4.0 Hz, 2H), 4.15 (t, *J*=4.0 Hz, 2H), 2.72 (s, 3H). ¹³C NMR (100 MHz, CDCl₃) δ = 151.20, 138.79, 134.71, 133.01, 131.00, 129.33(2C), 128.43, 128.34(3C), 127.33, 126.38, 126.11, 125.14, 124.09, 84.96, 81.23, 60.68, 50.98, 12.19. GC-MS (*m/z*): 302. Anal. Calc. for (C₂₁H₁₈O₂: 302.13): C, 83.42; H, 6.00; found: C, 83.31, H, 6.89.

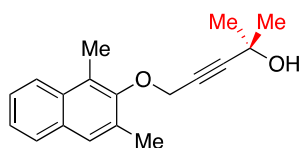

1h(Ar = *p*OMe-C₆H₄). Light yellowoil, cHex:EtOAc = 20:1→10:1, yield = 77%. ¹H NMR (400 MHz, CDCl₃) δ = 7.97 (d, *J*=8.0 Hz, 1H), 7.80 (d, *J*=8.0 Hz, 1H), 7.65 (s, 1H), 7.62 – 7.59 (m, 2H), 7.52 – 7.48 (m, 1H), 7.45 – 7.41 (m, 1H), 7.0-6.9 (m, 2H), 4.18-4.17 (m, 4H), 3.86 (s, 3H), 2.71 (s, 3H). ¹³C NMR (100 MHz, CDCl₃) δ = 159.04, 151.29, 134.26, 132.78, 131.08, 131.05, 130.39, 128.29, 127.91, 126.30, 125.89, 125.06, 124.06, 113.81, 84.85, 81.36, 60.48, 55.29, 51.04, 12.17. GC-MS (*m/z*): 332. Anal. Calc. for (C₂₂H₂₀O₃: 332.14): C, 79.50; H, 6.07; found: C, 79.31, H, 6.00.


1i(Ar = *p*F-C₆H₄). Light yellowoil, cHex:EtOAc = 20:1→10:1, yield = 73%. ¹H NMR (400 MHz, CDCl₃) δ = 7.98 (d, *J*=8.0 Hz, 1H), 7.81 (d, *J*=8.0 Hz, 1H), 7.65 – 7.62 (m, 3H), 7.50 – 7.54 (m, 1H), 7.47 – 7.43 (m, 1H), 7.16 – 7.10 (m, 2H), 4.17 – 4.16 (m, 4H), 2.71 (s, 3H). ¹³C NMR (100 MHz, CDCl₃) δ = 163.56, 161.11, 151.01, 134.65, 133.67, 133.03, 130.96, 130.88, 128.36, 128.15, 126.53, 126.19, 125.24, 124.09, 115.36, 115.15, 84.98, 81.09, 60.61, 51.02, 12.17. ¹⁹F NMR (377 MHz, CDCl₃) δ = -115.06 (m). GC-MS (*m/z*): 320. Anal. Calc. for (C₂₁H₁₇FO₂: 320.12): C, 78.73; H, 5.35; found: C, 78.61, H, 5.14.

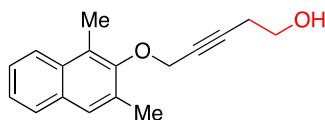

1j. Light yellowoil, cHex:EtOAc = 20:1 →10:1, yield = 65%. ¹H NMR (400 MHz, CDCl₃) δ = 7.82 (d, *J*=8.8, 1H), 7.48 (s, 1H), 7.44 (s, 1H), 7.29 (dd, *J*=8.4, 1.6, 1H), 4.55 (t, *J*=2.0, 2H), 4.31 (s, 2H), 2.83 – 2.68 (m, 2H), 2.61 (s, 3H), 2.46 (s, 3H), 1.71 – 1.60 (m, 2H), 1.37 (m, 2H), 0.93 (t, *J*=7.2, 3H). ¹³C NMR (100 MHz, CDCl₃) δ = 152.51, 139.37, 131.28, 130.84, 130.78, 126.95, 126.79, 126.04, 124.90, 123.80, 85.12, 81.41, 60.76, 51.12, 35.51, 33.51, 22.32, 17.39, 13.95, 11.96. GC-MS (*m/z*): 296, Anal. Calc. for (C₂₀H₂₄O₂: 296.18): C, 81.04; H, 8.16; found: C, 81.21, H, 8.01.



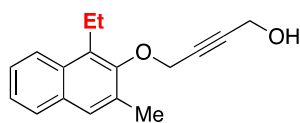
1k. White solid, cHex:EtOAc = 20:1→10:1, yield = 60%. ^1H NMR (400 MHz, CDCl_3) δ = 7.97 (d, J =8.0, 1H), 7.91 (d, J =1.2, 1H), 7.72 – 7.63 (m, 3H), 7.57 (s, 1H), 7.47 (t, J =7.6, 3H), 7.36 (t, J =6.8, 1H), 4.59 (d, J =1.6, 2H), 4.33 (t, J =1.2, 2H), 2.65 (s, 3H), 2.49 (s, 3H). ^{13}C NMR (100 MHz, CDCl_3) δ = 153.22, 141.02, 137.51, 131.62, 131.49, 131.36, 128.79(**2C**), 127.74, 127.25, 127.21(**2C**), 125.41, 125.07, 124.83, 124.51, 85.22, 81.33, 60.79, 51.14, 17.45, 12.03. GC-MS (m/z): 316. Anal. Calc. for ($\text{C}_{22}\text{H}_{20}\text{O}_2$: 316.15): C, 83.52; H, 6.37; found: C, 83.35, H, 6.18.



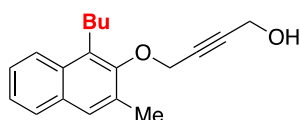
1l. Light yellow oil, cHex:EtOAc = 20:1→8:1, yield = 69%. ^1H NMR (400 MHz, CDCl_3) δ = 7.90 (d, J =8.0 Hz, 1H), 7.71 (d, J =8.0 Hz, 1H), 7.51 (s, 1H), 7.41 (m, 2H), 4.57 (s, 2H), 2.63 (s, 3H), 2.48 (s, 3H), 1.49 (s, 6H). ^{13}C NMR (100 MHz, CDCl_3) δ = 153.19, 132.43, 131.12, 131.09, 127.52, 127.35, 125.15, 125.11, 124.77, 123.86, 91.61, 77.61, 65.12, 60.82, 31.14, 17.49, 12.06. GC-MS (m/z): 268. Anal. Calc. for ($\text{C}_{18}\text{H}_{20}\text{O}_2$: 268.15): C, 80.56; H, 7.51; found: C, 80.42, H, 7.38.



1m. Light yellow oil, cHex:EtOAc = 20:1 →10:1, yield = 70%. ^1H NMR (400 MHz, CDCl_3) δ = 7.90 (d, J =8.0 Hz, 1H), 7.71 (m, 1H), 7.51 (s, 1H), 7.46-7.37 (m, 2H), 4.54 (t, J =2.4 Hz, 2H), 3.69 (t, J =8.0 Hz, 2H), 2.62 (s, 3H), 2.51-2.49 (m, 2H), 2.48 (s, 3H). ^{13}C NMR (100 MHz, CDCl_3) δ = 153.11, 132.43, 131.13, 131.07, 127.53, 127.36, 125.17, 125.13, 124.79, 123.86, 84.29, 77.46, 61.03, 60.86, 23.19, 17.44, 11.98. GC-MS (m/z): 254. Anal. Calc. for ($\text{C}_{17}\text{H}_{18}\text{O}_2$: 254.13): C, 80.28; H, 7.13; found: C, 80.35, H, 7.05.



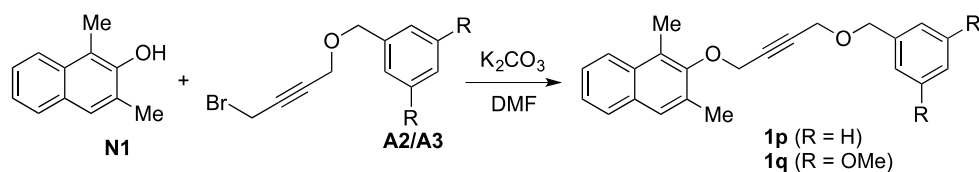
1n. Colorless oil, cHex:EtOAc = 20:1 →10:1, yield = 65%. ^1H NMR (400 MHz, CDCl_3) δ = 7.94 (d, J =8.0, 1H), 7.71 (d, J =8.0, 1H), 7.51 (s, 1H), 7.40 (m, 2H), 4.59 (t, J =1.6, 2H), 4.34 (t, J =1.6, 2H), 3.15 (q, J =7.2, 2H), 2.48 (s, 3H), 1.30 (t, J =7.6, 3H). ^{13}C NMR (100 MHz, CDCl_3) δ = 152.62, 131.57, 131.55, 131.42, 130.90, 127.84, 127.76, 125.20, 124.73, 123.87, 85.28, 81.27, 61.17, 51.13, 19.21, 17.44, 15.42. GC-MS (m/z): 254. Anal. Calc. for ($\text{C}_{17}\text{H}_{18}\text{O}_2$: 254.13): C, 80.28; H, 7.13; found: C, 80.31, H, 7.00.



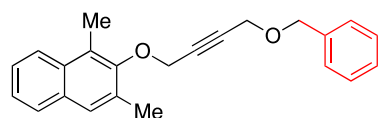
1o. Colorless oil, cHex:EtOAc = 20:1 →10:1, yield = 61%. ^1H NMR (400 MHz, CDCl_3) δ = 7.92 (d, J =8.0, 1H), 7.71 (d, J =7.0, 1H),

7.51 (s, 1H), 7.47 – 7.34 (t, 2H), 4.58 (t, $J=2.0$, 2H), 4.33 (t, $J=2.0$, 2H), 3.1 (t, $J=8.0$, 2H), 2.47 (s, 3H), 1.69 – 1.61 (m, 2H), 1.56 – 1.45 (m, 2H), 0.98 (t, $J=7.2$, 3H). ^{13}C NMR (100 MHz, CDCl_3) δ = 152.94, 131.68, 131.50, 130.83, 130.33, 127.80, 127.72, 125.13, 124.69, 123.97, 85.21, 81.34, 61.11, 51.16, 33.15, 25.96, 23.27, 17.46, 13.97. GC-MS (m/z): 282. Anal. Calc. for ($\text{C}_{19}\text{H}_{22}\text{O}_2$: 282.16): C, 80.82; H, 7.85; found: C, 80.70, H, 7.72.

Synthesis of 4-((naphthalen-2-yl)oxy)but-2-yn-1-ol derivatives **1p,q**

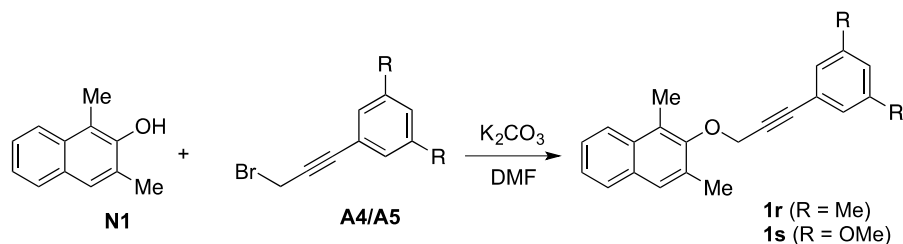


To a flamed two-necked flask was added DMF(15ml), **N1**(1mmol) and bromides **A2** or **A3**(1.5 mmol, 1.5 equiv.). Then K_2CO_3 (2 mmol, 2 equiv.) was added under N_2 atmosphere and kept stirring at room temperature. After the reaction was complete(monitored by TLC), the solution was quenched with water and extracted with EtOAc three times. Then the combined organic layers were washed with brine, dried with Na_2SO_4 , filtered and concentrated by rotary evaporation. The residue was purified with silica gel column chromatography to afford **1o** and **1p**.

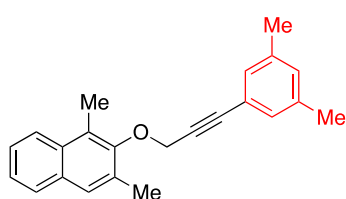


1p. Light yellow oil, $c\text{Hex:EtOAc} = 80:1 \rightarrow 15:1$, yield = 80%. ^1H NMR (400 MHz, CDCl_3) δ = 7.92 (d, $J=8.0$ Hz, 1H), 7.72 (d, $J=8.0$ Hz, 1H), 7.52 (s, 1H), 7.47 – 7.38 (m, 2H), 7.36 – 7.26 (m, 5H), 4.64 (t, $J=2.0$ Hz, 2H), 4.54 (s, 2H), 4.23 (t, $J=1.6$ Hz, 2H), 2.65 (s, 3H), 2.50 (s, 3H). ^{13}C NMR (100 MHz, CDCl_3) δ = 153.14, 137.31, 132.48, 131.13, 131.07, 128.39(2C), 128.00(2C), 127.82, 127.55, 127.45, 125.17, 125.15, 124.80, 123.90, 83.09, 82.05, 71.57, 60.82, 57.37, 17.48, 12.05. GC-MS (m/z): 330. Anal. Calc. for ($\text{C}_{23}\text{H}_{22}\text{O}_2$: 330.16): C, 83.60; H, 6.71; found: C, 83.51, H, 6.58.

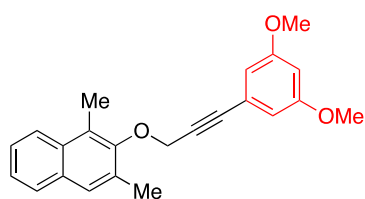
Synthesis of 4-((naphthalen-2-yl)oxy)but-2-yn-1-ol derivatives **1r,s**



To a flamed two-necked flask was added DMF(15ml), **N1** (1mmol), **A4** or **A5**(1.5 mmol, 1.5 equiv.). Then, K_2CO_3 (2 mmol, 2 equiv.) was added under N_2 atmosphere and kept stirring at room temperature. After the reaction was complete(monitored by TLC), the solution was quenched with water and extracted with EtOAc three times. Then the combined organic layer was washed with brine, dried with Na_2SO_4 , filtered and concentrated by rotary evaporation. The residue was purified with silica gel column chromatography (cHex:EtOAc = 80:1) to afford the **1r** or **1s**.

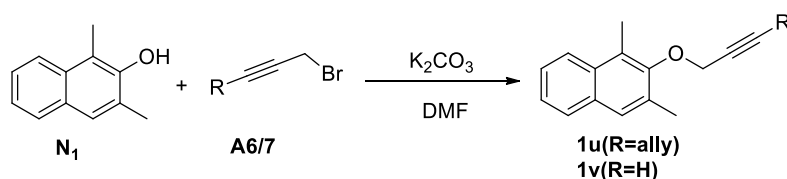


1r. Light yellow oil, yield = 75%. ^1H NMR (400 MHz, CDCl_3) δ = 7.94 (d, $J=8.0$ Hz, 1H), 7.72 (d, $J=8.0$ Hz, 1H), 7.53 (s, 1H), 7.46-7.37 (m, 2H), 7.03 (s, 2H), 6.95 (s, 1H), 4.77 (s, 2H), 2.68 (s, 3H), 2.53 (s, 3H), 2.26 (s, 6H). ^{13}C NMR (100 MHz, CDCl_3) δ = 153.36, 137.83(2C), 132.49, 131.26, 131.12, 130.42, 129.33(2C), 127.52, 127.38, 125.26, 125.09, 124.72, 123.92, 122.05, 87.24, 83.90, 61.49, 21.04(2C), 17.53, 12.11. GC-MS (m/z): 314. Anal. Calc. for ($\text{C}_{23}\text{H}_{22}\text{O}$: 314.17): C, 87.86; H, 7.05; found: C, 87.71, H, 6.90.

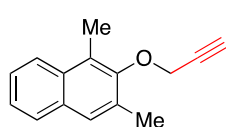


1s. Light yellow oil, yield = 70%. ^1H NMR (400 MHz, CDCl_3) δ = 7.92 (d, $J=8.0$ Hz, 1H), 7.72 (d, $J=8.0$ Hz, 1H), 7.53 (s, 1H), 7.46 – 7.37 (m, 2H), 6.55 (d, $J=2.4$ Hz, 2H), 6.43 (t, $J=2.0$ Hz, 1H), 4.78 (s, 2H), 3.72 (s, 6H), 2.68 (s, 3H), 2.53 (s, 3H). ^{13}C NMR (100 MHz, CDCl_3) δ = 160.46(2C), 153.22, 132.48, 131.21, 131.13, 127.53, 127.41, 125.27, 125.13, 124.77, 123.92, 123.70, 109.40(2C), 101.99, 86.95, 84.20, 61.32, 55.36(2C), 17.52, 12.11. GC-MS (m/z): 346. Anal. Calc. for ($\text{C}_{23}\text{H}_{22}\text{O}_3$: 346.16): C, 79.74; H, 6.40; found: C, 79.69, H, 6.29.

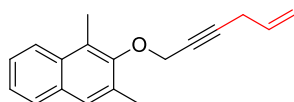
Synthesis of 4-((naphthalen-2-yl)oxy)but-2-yn-1-ol derivatives **1u,v**



To a flamed two-necked flask was added DMF(15ml), **N1** (1mmol), **A6** or **A7**(1.5 mmol, 1.5 equiv.). Then, K_2CO_3 (2 mmol, 2 equiv.) was added under N_2 atmosphere and kept stirring at room temperature. After the reaction was complete(monitored by TLC), the solution was quenched with water and extracted with EtOAc three times. Then the combined organic layer was washed with brine, dried with Na_2SO_4 , filtered and concentrated by rotary evaporation. The residue was purified with silica gel column chromatography (cHex:EtOAc = 80:1) to afford the **1u** or **1v**.

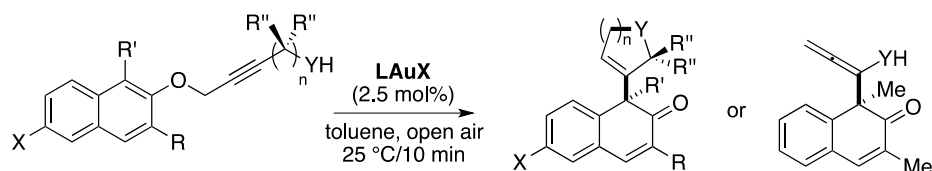


1u. Colorless oil, yield = 70%. $^1\text{H NMR}$ (400 MHz, CDCl_3) δ = 7.93 (d, $J=8.0$ Hz, 1H), 7.73 (d, $J=8.0$ Hz, 1H), 7.53 (s, 1H), 7.48 – 7.40 (m, 2H), 4.57 (d, $J=2.8$, 2H), 2.66 (s, 3H), 2.51 (s, 3H). $^{13}\text{C NMR}$ (100 MHz, CDCl_3) δ = 153.23, 132.47, 131.16, 131.01, 127.57, 127.48, 125.19, 125.13, 124.84, 123.93, 79.23, 75.15, 60.57, 17.45, 12.02. GC-MS (m/z): 210. Anal. Calc. for ($\text{C}_{15}\text{H}_{14}\text{O}$: 210.10): C, 85.68; H, 6.71; found: C, 85.76, H, 6.48.

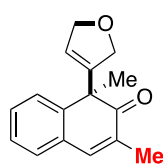


1v. Colorless oil, yield = 75%. $^1\text{H NMR}$ (400 MHz, CDCl_3) δ = 7.90 (d, $J=8.0$, 1H), 7.71 (d, $J=8.0$, 1H), 7.51 (s, 1H), 7.45 – 7.36 (m, 2H), 5.84-5.75 (m, 1H), 5.28 (dq, $J=17.3$, 1.6, 1H), 5.09 (dq, $J=10.0$, 1.6, 1H), 4.56 (t, $J=2.0$, 2H), 3.03 – 3.00 (m, 2H), 2.63 (s, 3H), 2.48 (s, 3H). $^{13}\text{C NMR}$ (100 MHz, CDCl_3) δ = 153.32, 132.47, 131.97, 131.19, 131.07, 127.50, 127.34, 125.12, 125.07, 124.69, 123.88, 116.34, 84.17, 77.83, 61.18, 23.13, 17.42, 11.97. GC-MS (m/z): 250. Anal. Calc. for ($\text{C}_{15}\text{H}_{14}\text{O}$: 250.33): C, 86.36; H, 7.25; found: C, 86.02, H, 7.12.

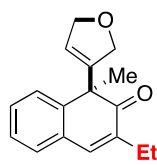
General procedure for Gold-catalyzed intramolecular dearomatization reaction of naphthol derivatives:



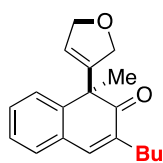
Ascrew-top vialwas chargedwith reagent grade toluene (1 ml), substrate **1a-s**(0.05mmol) and **cat 2**(2.5mol%, 0.9 mg). Then,the reactionwas kept stirring at room temperature for 10min (unless otherwise specified) when judged completeby TLC.To the mixture 2 mL of water were added, the layers separated and the aqueousphase and extracted with three times EtOAc. The combined organic layer was washed with brine, dried with Na₂SO₄, filtered and concentrated by rotary evaporation. The residue was purified with silica gel column chromatography (cHex:EtOAc = 20:1→15:1) to afford thedearomatized compounds**2**.



(+/-)-**2a**. Light yellowoil, yield = 97%. ¹H NMR (400 MHz, CDCl₃) δ = 7.33 – 7.24 (m, 5H), 5.76 (m, 1H), 4.68 – 4.64 (m, 2H), 4.30-4.26 (m, 1H), 4.16-4.11 (m, 1H), 1.98 (s, 3H), 1.63 (s, 3H). ¹³C NMR (100 MHz, CDCl₃) δ = 200.49, 143.22, 142.14, 141.53, 131.97, 129.43, 129.13, 128.60, 127.34, 127.14, 123.13, 75.68, 74.41, 51.72, 26.26, 15.95. GC-MS (m/z): 240. Anal. Calc. for (C₁₆H₁₆O₂: 240.12): C, 79.97; H, 6.71; found: C, 79.88, H, 6.65.

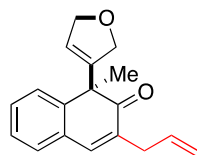


(+/-)-**2b**. Light yellowoil, yield =82%. ¹H NMR (400 MHz, CDCl₃) δ = 7.34 – 7.25 (m, 4H), 7.19 (s, 1H), 5.83 – 5.72 (m, 1H), 4.73 – 4.62 (m, 2H), 4.33-4.27(m, 1H), 4.15 – 4.10 (m, 1H), 2.40 (q, J=3.2 Hz, 2H), 1.63 (s, 3H), 1.12 (t, J=3.2 Hz, 3H). ¹³C NMR (100 MHz, CDCl₃) δ = 200.12, 143.03, 142.12, 139.75, 137.48, 129.52, 129.11, 128.79, 127.34, 127.07, 123.13, 75.67, 74.40, 51.88, 26.09, 22.47, 12.52. GC-MS (m/z): 254. Anal. Calc. for (C₁₇H₁₈O₂: 254.13): C, 80.28; H, 7.13; found: C, 80.20, H, 7.01.

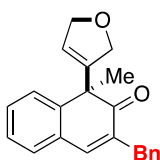


(+/-)-**2c**. Light yellowoil, yield =97%. ¹H NMR (400 MHz, CDCl₃) δ = 7.32 – 7.25 (m, 4H), 7.19(s, 1H), 5.77 – 5.75 (m, 1H), 4.68 – 4.61 (m, 2H), 4.32 – 4.26 (m, 1H), 4.15-4.09 (m, 1H), 2.37 (t, J=7.6 Hz 2H), 1.62 (s, 3H), 1.51 – 1.44 (m, 2H), 1.40-1.30 (m, 2H), 0.91 (t, J=3.2 Hz, 3H). ¹³C NMR (100 MHz,

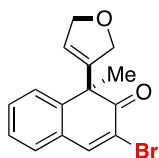
CDCl_3) δ = 200.16, 143.09, 142.12, 140.58, 136.20, 129.52, 129.10, 128.74, 127.34, 127.06, 123.14, 75.67, 74.40, 51.92, 30.54, 29.18, 26.08, 22.46, 13.87. GC-MS (m/z): 282. Anal. Calc. for ($\text{C}_{19}\text{H}_{22}\text{O}_2$: 282.16): C, 80.82; H, 7.85; found: C, 80.55, H, 7.72.



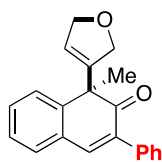
(+/-)-**2d**. Light yellow oil, yield = 80%. ^1H NMR (400 MHz, CDCl_3) δ = 7.34 – 7.25 (m, 4H), 7.22 (s, 1H), 5.93–5.83 (m, 1H), 5.76 – 5.75 (m, 1H), 5.15–5.10 (m, 2H), 4.67 – 4.61 (m, 2H), 4.31 – 4.27 (m, 1H), 4.16–4.09 (m, 1H), 3.13 (d, J =8.0 Hz, 2H), 1.63 (s, 3H). ^{13}C NMR (100 MHz, CDCl_3) δ = 199.66, 143.19, 142.01, 141.31, 134.89, 134.06, 129.39, 129.31, 129.00, 127.39, 127.13, 123.27, 117.14, 75.67, 74.38, 51.93, 33.34, 26.15. GC-MS (m/z): 266. Anal. Calc. for ($\text{C}_{18}\text{H}_{18}\text{O}_2$: 266.13): C, 81.17; H, 6.81; found: C, 81.09, H, 6.75.



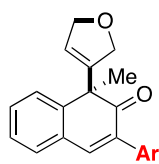
(+/-)-**2e**. Light yellow oil, yield = 85%. ^1H NMR (400 MHz, CDCl_3) δ = 7.33 – 7.14 (m, 9H), 7.07 (s, 1H), 6.71 – 6.70 (m, 1H), 4.70 – 4.59 (m, 2H), 4.28 – 4.22 (m, 1H), 4.11–4.05 (m, 1H), 3.71 (s, 2H), 1.61 (s, 3H). ^{13}C NMR (100 MHz, CDCl_3) δ = 199.71, 143.13, 141.86, 141.60, 138.84, 135.45, 129.42, 129.31, 129.11, 129.08, 128.48, 127.37, 127.08, 126.32, 123.35, 75.66, 74.33, 52.06, 35.51, 25.89. GC-MS (m/z): 316. Anal. Calc. for ($\text{C}_{22}\text{H}_{20}\text{O}_2$: 316.15): C, 83.52; H, 6.37; found: C, 83.35, H, 6.29.



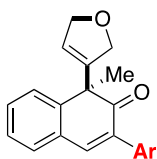
(+/-)-**2f**. Light yellow oil, yield = 73%. ^1H NMR (400 MHz, CDCl_3) δ = 7.90 (s, 1H), 7.43 – 7.39 (m, 1H), 7.34 – 7.28 (m, 3H), 5.77–5.75 (m, 1H), 4.72 – 4.61 (m, 2H), 4.36–4.30 (m, 1H), 4.20–4.14 (m, 1H), 1.69 (s, 3H). ^{13}C NMR (100 MHz, CDCl_3) δ = 192.95, 146.57, 143.18, 141.12, 130.65, 129.22, 129.08, 127.87, 127.52, 124.17, 120.97, 75.70, 74.24, 53.54, 26.43. GC-MS (m/z): 304/306. Anal. Calc. for ($\text{C}_{15}\text{H}_{13}\text{BrO}_2$: 304.01): C, 59.04; H, 4.29; found: C, 58.99, H, 4.18.



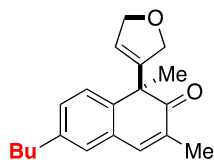
(+/-)-**2g**. Light yellow oil, yield = 80%. ^1H NMR (400 MHz, CDCl_3) δ = 7.53 (s, 1H), 7.50 – 7.47 (m, 2H), 7.41–7.35 (m, 4H), 7.34 – 7.30 (m, 3H), 5.82 – 5.80 (m, 1H), 4.75 – 4.64 (m, 2H), 4.45 – 4.39 (m, 1H), 4.26–4.20 (m, 1H), 1.75 (s, 3H). ^{13}C NMR (100 MHz, CDCl_3) δ = 199.03, 143.44, 141.90, 141.81, 135.45, 134.82, 129.92, 129.74, 129.52, 128.55(2C), 128.21(3C), 127.60, 127.11, 123.71, 75.73, 74.49, 52.96, 25.86. GC-MS (m/z): 302. Anal. Calc. for ($\text{C}_{21}\text{H}_{18}\text{O}_2$: 302.13): C, 83.42; H, 6.00; found: C, 83.31, H, 5.85.



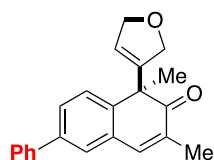
(+/-)-**2h** (Ar = *p*OMe-C₆H₄). Light yellow oil, yield = 79%. ¹H NMR (400 MHz, CDCl₃) δ = 7.48 – 7.43 (m, 3H), 7.38 – 7.29 (m, 4H), 6.94– 6.90 (m, 2H), 5.81 – 5.80 (m, 1H), 4.75 – 4.64 (m, 2H), 4.43 – 4.37 (m, 1H), 4.24 – 4.19 (m, 1H), 3.82 (s, 3H), 1.73 (s, 3H). ¹³C NMR (100 MHz, CDCl₃) δ = 199.40, 159.70, 143.21, 141.89, 140.68, 134.27, 129.78(2C), 129.72, 129.61, 129.52, 127.82, 127.56, 127.03, 123.62, 113.71(2C), 75.72, 74.50, 55.31, 52.96, 25.89. GC-MS (m/z): 332. Anal. Calc. for (C₂₂H₂₀O₃: 332.14): C, 79.50; H, 6.07; found: C, 79.25, H, 6.19.



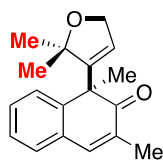
(+/-)-**2i** (Ar = *p*F-C₆H₄). Light yellow oil, yield = 80%. ¹H NMR (400 MHz, CDCl₃) δ = 7.50 – 7.45 (m, 3H), 7.40 – 7.37 (m, 2H), 7.35–7.31 (m, 2H), 7.10 – 7.00 (m, 2H), 5.82–5.80 (m, 1H), 4.75 – 4.64 (m, 2H), 4.43–4.37 (m, 1H), 4.25 – 4.19 (m, 1H), 1.74 (s, 3H). ¹³C NMR (100 MHz, CDCl₃) δ = 199.02, 163.97, 161.51, 143.41, 141.88, 141.73, 133.75, 130.37, 130.29, 130.03, 129.76, 129.34, 127.65, 127.15, 123.78, 115.27, 115.06, 75.72, 74.45, 52.93, 25.91. ¹⁹F NMR (377 MHz, CDCl₃) δ = -113.49 (m). GC-MS (m/z): 320. Anal. Calc. for (C₂₁H₁₇FO₂: 320.12): C, 78.73; H, 5.35; found: C, 78.51, H, 5.21.



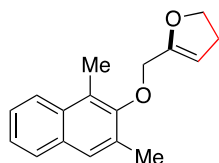
(+/-)-**2j**. Light yellow oil, yield = 73%. ¹H NMR (400 MHz, CDCl₃) δ = 7.22 (s, 1H), 7.16–7.10 (m, 2H), 7.05 (s, 1H), 5.74 – 5.73 (m, 1H), 4.72 – 4.60 (m, 2H), 4.31–4.25 (m, 1H), 4.16–4.10 (m, 1H), 2.59 (t, *J* = 8.0 Hz, 2H), 1.97 (s, 3H), 1.66 – 1.51 (m, 2H), 1.61 (s, 3H), 1.39–1.30 (m, 3H), 0.92 (t, *J* = 8.0 Hz, 3H). ¹³C NMR (100 MHz, CDCl₃) δ = 200.78, 142.39, 142.03, 141.86, 140.45, 131.77, 129.32, 129.23, 128.53, 127.06, 122.81, 75.68, 74.43, 51.43, 35.00, 33.38, 26.17, 22.28, 15.98, 13.89. GC-MS (m/z): 296. Anal. Calc. for (C₂₀H₂₄O₂: 296.18): C, 81.04; H, 8.16; found: C, 80.85, H, 8.00.



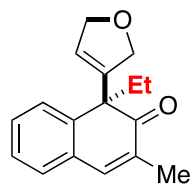
(+/-)-**2k**. Light yellow oil, yield = 87%. ¹H NMR (400 MHz, CDCl₃) δ = 7.59 – 7.57 (m, 2H), 7.54–7.52 (dd, *J* = 8.0 Hz, *J* = 4.0 Hz, 1H), 7.46 – 7.43 (m, 3H), 7.38–7.32 (m, 3H), 5.89 – 5.80 (m, 1H), 4.72 – 4.63 (m, 2H), 4.36 – 4.30 (m, 1H), 4.22 – 4.16 (m, 1H), 2.01 (s, 3H), 1.67 (s, 3H). ¹³C NMR (100 MHz, CDCl₃) δ = 200.44, 142.09, 142.06, 141.48, 140.42, 139.97, 132.38, 129.83, 128.87(2C), 127.76, 127.66, 127.65, 127.19, 126.94(2C), 123.22, 75.71, 74.44, 51.56, 26.21, 16.04. GC-MS (m/z): 316. Anal. Calc. for (C₂₂H₂₀O₂: 316.15): C, 83.52; H, 6.37; found: C, 83.41, H, 6.21.



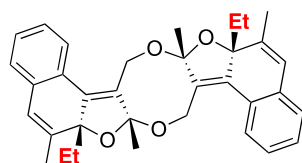
(+/-)-**2l**. Light yellow oil, yield = 85%. ^1H NMR (400 MHz, CDCl_3) δ = 7.90 (d, J =8.0, 1H), 7.71 (d, J =8.0, 1H), 7.51 (s, 1H), 7.41 (m, 2H), 6.45 (s, 1H), 4.39 (s, 2H), 2.58 (s, 3H), 2.43 (s, 3H), 2.28 (s, 3H), 1.99 (s, 3H). ^{13}C NMR (100 MHz, CDCl_3) δ = 195.53, 159.13, 153.23, 132.50, 131.03, 130.60, 127.54, 125.18, 124.74, 124.51, 123.80, 119.39, 77.71, 28.10, 21.37, 17.19, 11.54. GC-MS (m/z): 268. Anal. Calc. for ($\text{C}_{18}\text{H}_{20}\text{O}_2$: 268.15): C, 80.56; H, 7.51; found: C, 80.68, H, 7.41.



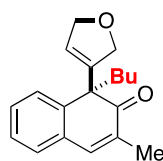
(+/-)-**2m'**. Colorless oil, yield = 85%. ^1H NMR (400 MHz, CDCl_3) δ = 7.91 (d, J =8.3 Hz, 1H), 7.71 (d, J =7.9 Hz, 1H), 7.51 (s, 1H), 7.40 (m, 2H), 5.05 (t, J =2.5 Hz, 1H), 4.46 (t, J =9.5 Hz, 2H), 4.35 (d, J =0.9 Hz, 2H), 2.62 (s, 3H), 2.47 (s, 3H). GC-MS (m/z): 254. Anal. Calc. for ($\text{C}_{17}\text{H}_{18}\text{O}_2$: 254.13): C, 80.28; H, 7.13; found: C, 80.13, H, 7.25.



(+/-)-**2n**. Colorless oil, yield = 48%. ^1H NMR (400 MHz, CDCl_3) δ = 7.34 – 7.23 (m, 5H), 5.67-5.66 (m, 1H), 4.68 – 4.56 (m, 2H), 4.32-4.26 (m, 1H), 4.16-4.10 (m, 1H), 2.55-2.46 (m, 1H), 2.10 – 2.00 (m, 1H), 1.97 (s, 3H), 0.51 (t, J =7.6, 3H). GC-MS (m/z): 254. Anal. Calc. for ($\text{C}_{17}\text{H}_{18}\text{O}_2$: 254.13): C, 80.28; H, 7.13; found: C, 80.10, H, 6.99.

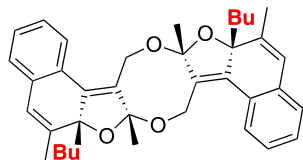


(+/-)-**2n'**. White solid, yield = 28%. ^1H NMR (400 MHz, CDCl_3) δ = 7.17 (dt, J =1.2 Hz, 7.2 Hz, 2H), 7.04 (dt, J =1.2 Hz, 7.2 Hz, 2H), 6.79 (d, J =7.2 Hz, 2H), 6.58 (d, J =7.2 Hz, 2H), 4.95 (d, J =1.2 Hz, 2H), 4.50 (d, J =15.6 Hz, 2H), 4.38 (d, J =15.6 Hz, 2H), 1.75 (d, J =1.2 Hz, 6H), 1.73 (s, 6H), 1.29-1.20 (m, 4H), 0.60 (t, J =7.2 Hz, 6H). ^{13}C NMR (100 MHz, CDCl_3) δ = 142.43, 139.40, 145.10, 135.82, 128.53, 127.71, 126.75, 126.59, 125.24, 121.50, 111.95, 90.94, 77.16, 57.31, 32.03, 25.90, 16.91, 8.95. Anal. Calc. for ($\text{C}_{34}\text{H}_{36}\text{O}_4$: 508.26): C, 80.28; H, 7.13; found: C, 80.41, H, 7.12.

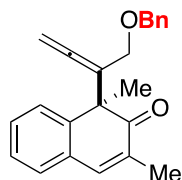


(+/-)-**2o**. Colorless oil, yield = 22%. ^1H NMR (400 MHz, CDCl_3) δ = 7.34 – 7.24 (m, 5H), 5.66 – 5.65 (m, 1H), 4.67 – 4.55 (m, 2H), 4.32-4.26 (m, 1H), 4.16-4.10 (1H), 2.49-2.42 (m, 1H), 2.10 – 1.96 (m, 1H), 1.97 (s, 3H), 1.21 – 1.09 (m, 2H), 0.89 – 0.80 (m, 2H), 0.72 (t, J =7.6, 3H), 1.74 (d, J =1.2 Hz, 6H),

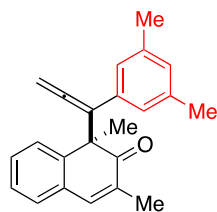
1.72 (s, 6H), 1.08-1.00 (m, 8H), 0.69 (t, $J=7.2$ Hz, 6H). GC-MS (m/z): 282. Anal. Calc. for ($C_{19}H_{22}O_2$: 282.16): C, 80.82; H, 7.85; found: C, 80.95, H, 7.71.



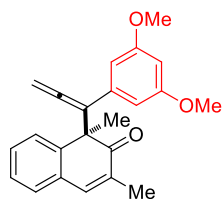
(+/-)-**2o'**. White solid, yield = 29%. 1H NMR (400 MHz, $CDCl_3$) δ = 7.18 (dt, $J=1.2$ Hz, 7.2 Hz, 2H), 7.04 (dt, $J=1.2$ Hz, 7.2 Hz, 2H), 6.78 (d, $J=7.2$ Hz, 2H), 6.56 (d, $J=7.2$ Hz, 2H), 4.93 (d, $J=1.6$ Hz, 2H), 4.49 (d, $J=16.0$ Hz, 2H), 4.37 (d, $J=16.0$ Hz, 2H). ^{13}C NMR (100 MHz, $CDCl_3$) δ = 142.60, 139.79, 135.05, 133.49, 128.49, 127.77, 126.81, 126.58, 125.23, 121.37, 111.92, 90.55, 57.33, 39.14, 26.49, 25.93, 22.85, 17.05, 13.82. Anal. Calc. for ($C_{38}H_{44}O_4$: 564.32): C, 80.82; H, 7.85; found: C, 80.75, H, 7.72.



(+/-)-**2p**. Colorless oil, cHex:EtOAc = 40:1 \rightarrow 20:1, yield = 86%. 1H NMR (400 MHz, $CDCl_3$) δ = 7.33 – 7.26 (m, 2H), 7.22 – 7.16 (m, 6H), 7.08 – 7.06 (m, 2H), 5.20 – 5.17 (m, 1H), 5.10 – 5.07 (m, 1H), 4.21 (d, $J=12.0$ Hz, 2H), 4.07 (d, $J=12.0$ Hz, 2H), 3.66 – 3.76 (m, 2H), 1.87 (s, 3H), 1.45 (s, 3H). ^{13}C NMR (100 MHz, $CDCl_3$) δ = 207.77, 200.83, 144.48, 140.73, 137.93, 132.43, 130.12, 128.70, 128.40, 127.98(2C), 127.75(2C), 127.33, 127.24, 126.90, 105.52, 78.90, 71.59, 69.21, 51.71, 28.93, 16.06. GC-MS (m/z): 330. Anal. Calc. for ($C_{23}H_{22}O_2$: 330.16): C, 83.60; H, 6.71; found: C, 83.75, H, 6.51.

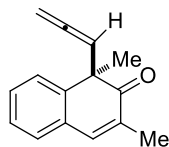


(+/-)-**2r**. Colorless oil, cHex:EtOAc = 40:1 \rightarrow 20:1, yield = 80%. 1H NMR (400 MHz, $CDCl_3$) δ = 7.39 – 7.29 (m, 3H), 7.25 – 7.21 (m, 2H), 6.62 (s, 1H), 6.45 (s, 2H), 5.40 (dd, $J=16, 11.6$, 2H), 2.05 (s, 6H), 2.02 (d, $J=1.2, 3H$), 1.48 (s, 3H). ^{13}C NMR (100 MHz, $CDCl_3$) δ = 210.30, 201.75, 146.21, 140.73, 137.34, 134.28, 132.43, 129.33, 129.16, 128.63, 128.25, 126.87, 126.63, 124.54(2C), 80.53, 77.16, 53.73, 31.37, 21.21(2C), 16.03. MS (m/z): 314. Anal. Calc. for ($C_{23}H_{22}O$: 314.17): C, 87.86; H, 7.05; found: C, 87.77, H, 7.18.

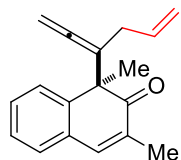


(+/-)-**2s**. Colorless oil, cHex:EtOAc = 40:1 \rightarrow 20:1, yield = 87%. 1H NMR (400 MHz, $CDCl_3$) δ = 7.38 (s, 1H), 7.35 (dd, $J=5.7, 3.3$, 1H), 7.31 (dd, $J=6.2, 2.7$, 2H), 7.27 – 7.22 (m, 1H), 6.12 (t, $J=2.2$ Hz, 2H), 6.03 (d, $J=2.2$, 1H), 5.44 (q, $J=12.0$ Hz, 2H), 3.52 (s, 2H), 2.02 (s, 3H), 1.49 (s, 3H). ^{13}C NMR (100 MHz, $CDCl_3$) δ = 210.37, 201.54, 160.33, 146.18, 140.79,

136.64, 132.43, 129.48, 129.05, 128.72, 127.04, 126.63, 109.83, 104.68, 99.39, 80.97, 54.94, 53.75, 31.37, 16.06. GC-MS (m/z):346. Anal. Calc.for (C₂₃H₂₂O₃: 346.16): C, 79.74; H, 6.40; found: C, 79.60, H, 6.22.

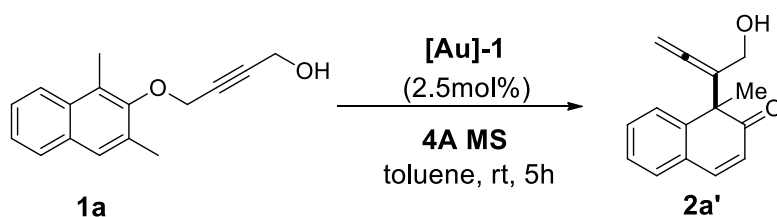


(+/-)-**2u**. Colorless oil, cHex:EtOAc = 40:1→20:1, yield = 91%. ¹H NMR (400 MHz, CDCl₃) δ = 7.38 (d, *J*=8.0 Hz, 1H), 7.33 – 7.29 (m, 1H), 7.27 – 7.20 (m, 4H), 5.25 (t, *J*=6.8 Hz, 1H), 4.90-4.79 (m, 2H), 1.99 (s, 3H), 1.53 (s, 3H). ¹³C NMR (100 MHz, CDCl₃) δ = 208.03, 202.04, 144.53, 141.21, 131.85, 129.51, 128.74, 128.40, 127.52, 127.03, 96.13, 78.55, 51.06, 26.22, 16.01. GC-MS (m/z): 210. Anal. Calc. for (C₁₅H₁₄O: 210.27): C, 85.68; H, 6.71; found: C, 85.51, H, 6.50.

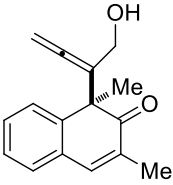


(+/-)-**2v**. Colorless oil, cHex:EtOAc = 40:1→20:1, yield = 96%. ¹H NMR (400 MHz, CDCl₃) δ = 7.35 – 7.24 (m, 5H), 5.65-5.54 (m, 1H), 5.10 – 5.00 (m, 2H), 4.84 – 4.74 (m, 2H), 2.41 – 2.30 (m, 1H), 2.25 – 2.13 (m, 1H), 2.00 (s, 3H), 1.42 (s, 3H). ¹³C NMR (100 MHz, CDCl₃) δ = 207.38, 202.35, 144.95, 141.37, 135.39, 132.53, 130.07, 128.98, 128.38, 127.30, 127.01, 115.66, 106.86, 79.55, 54.29, 34.24, 28.85, 15.96. GC-MS (m/z): 250. Anal. Calc. for (C₁₈H₁₈O: 250.14): C, 86.36; H, 7.25; found: C, 86.15, H, 7.09.

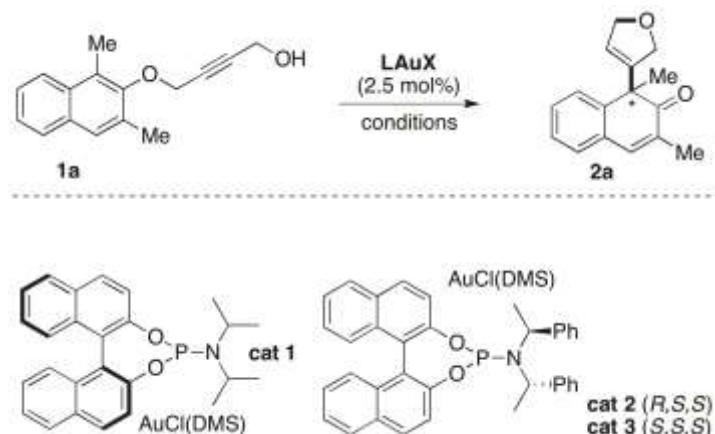
Interrupted dearomatization process



Ascrew-top vialwas chargedwith reagent grade toluene (1 ml), substrate **1a** (0.05mmol), **cat** **2**(2.5mol%, 0.9 mg) and 4 ÅMS. Then,the reactionwas kept stirring at room temperature for 6h.To the mixture 2 mL of water were added, the layers separated and the aqueousphase and extracted with three times EtOAc. The combined organic layer was washed with brine, dried with Na₂SO₄, filtered and concentrated by rotary evaporation. The residue was purified with silica gel column chromatography (cHex:EtOAc = 20:1→10:1) to afford thedearomatized compounds**2a'**.



(+/-)-**2a'**. White solid, cHex:EtOAc = 40:1→20:1, yield = 33%. ¹H NMR (400 MHz, CDCl₃) = 7.33 – 7.25 (m, 5H), 5.22 – 5.11 (m, 2H), 3.87-3.70 (m, 2H), 2.00 (d, *J*=1.2, 3H), 1.45 (s, 1H). ¹³C NMR (100 MHz, CDCl₃) δ = 206.65, 202.77, 144.37, 141.38, 132.14, 129.85, 129.08, 128.69, 127.18, 127.09, 108.64, 80.50, 61.64, 52.91, 29.00, 16.05. GC-MS (*m/z*): 240. Anal. Calc. for (C₁₆H₁₆O₂: 240.30): C, 79.97; H, 6.71; found: C, 79.85, H, 6.85.

Table S1: Enantioselective dearomatization of **1a**.^[a]

Run	LAuX	Conditions	Yield (%) ^[b]	Ee (%) ^[c]
1	Cat 1	AgNTf ₂ (5 mol%), toluene, rt	89	0
2	Cat 2	AgSbF ₆ (5 mol%), toluene, rt	88	0
3	Cat 2	AgSbF ₆ (5 mol%), toluene, - 15 °C	75	0
4	Cat 3	AgSbF ₆ (5 mol%), toluene, rt	74	0
5	(<i>R</i>)-xylyl-BINAP(AuCl) ₂	AgNTf ₂ (5 mol%), toluene, rt	72	50
6	(<i>R</i>)-xylyl-BINAP(AuCl) ₂	AgNTf ₂ (5 mol%), dry toluene, rt	69	52
7	(<i>R</i>)-xylyl-BINAP(AuCl) ₂	AgNTf ₂ (5 mol%), ClC ₆ H ₅ , rt	49	36
8	(<i>R</i>)-xylyl-BINAP(AuCl) ₂	AgNTf ₂ (5 mol%), CH ₂ Cl ₂ , rt	60	43
9	(<i>R</i>)-xylyl-BINAP(AuCl) ₂	AgNTf ₂ (5 mol%), CF ₃ C ₆ H ₅ , rt	82	58
10	(<i>R</i>)-DTBM-MeO-biphep(AuCl) ₂	AgNTf ₂ (5 mol%), CF ₃ C ₆ H ₅ , rt	67	20
11 ^[d]	(<i>R</i>)-xyl-SDP(AuCl) ₂	AgNTf ₂ (5 mol%), CF ₃ C ₆ H ₅ , rt	65	5
12 ^[d]	(<i>R</i>)-Josiphos(AuCl) ₂	AgNTf ₂ (5 mol%), CF ₃ C ₆ H ₅ , rt	33	13
13 ^[e]	(<i>R</i>)-xylyl-BINAP(AuCl) ₂	AgNTf ₂ (5 mol%), CF ₃ C ₆ H ₅ , - 20 °C	81	65
14 ^[f]	(<i>R</i>)-xylyl-BINAP(AuCl) ₂	AgNTf ₂ (5 mol%), CF ₃ C ₆ H ₅ , rt, 4Å MS	66	50
15	(<i>R</i>)-xylyl-BINAP(AuCl) ₂	AgNTf ₂ (5 mol%), dry CF ₃ C ₆ H ₅ , rt	79	56

Chapter 2

^[a]All the reactions were carried out in reagent grade solvent and 10 min reaction time, unless otherwise specified. ^[b]Isolated yield after flash chromatography. ^[c] Determined by chiral HPLC analysis. ^[d] Chiral gold chloride precursor was prepared *in situ*. ^[e] Reaction time 3 h. ^[f] Referred to the allenyl-ol **2a'** (24 h reaction time).

2a-(Entry 13). Yield = 81%. *Ee* = 65%. HPLC: Chiralcel-OD-H: eluent: *n*Hex:IPA = 90:10, flow = 0.5 mL/min, T = 30 °C, $R_{t_{major}}$ (12.3 min), $R_{t_{minor}}$ (12.9 min). $[\alpha]_D = -35.7^\circ$ ($c = 0.35$, CHCl_3).

Table S2. Crystal data and structure refinement for compound **2o'**.

Compound	2o'
Formula	C ₃₈ H ₄₄ O ₄
Fw	564.73
T, K	293
λ , Å	0.71073
Crystal symmetry	Triclinic
Space group	<i>P</i> -1
<i>a</i> , Å	11.317(3)
<i>b</i> , Å	11.631(2)
<i>c</i> , Å	13.464(3)
α	107.861(4)
β	90.899(5)
γ	112.091(4)
<i>V</i> , Å ³	1545.7(6)
<i>Z</i>	2
D_x , Mg m ⁻³	1.213
μ (Mo-K α), mm ⁻¹	0.077
F(000)	608
Crystal size/ mm	0.30 x 0.27 x 0.25
θ limits, °	1.607 - 24.704
Reflections collected	14840
Unique obs. Reflections [$F_o > 4\sigma(F_o)$]	5169 [R(int) = 0.0854]
Goodness-of-fit-on F ²	1.029
R ₁ (F) ^a , wR ₂ (F ²) [$I > 2\sigma(I)$]	0.0782, 0.1681
Largest diff. peak and hole, e. Å ⁻³	0.285 and -0.275

$$a) R_1 = \frac{\sum ||F_o| - |F_c||}{\sum |F_o|}, b) wR_2 = \frac{[\sum w(F_o^2 - F_c^2)^2 / \sum w(F_o^2)^2]^{1/2}}{[\sigma^2(F_o^2) + (aP)^2 + bP]^{1/2}}$$

where $P = (F_o^2 + F_c^2)/3$.

Table S3. Selected bond lengths (Å) and angles (deg) for **2o'**

O(1)-C(1)	1.408(4)	C(1)-C(12)	1.503(4)
O(1)-C(26)	1.412(4)	C(11)-C(12)	1.316(4)
O(3)-C(13)	1.416(4)	C(24)-C(25)	1.310(4)
O(3)-C(14)	1.416(4)	C(25)-C(26)	1.485(4)
O(2)-C(1)	1.424(4)	C(1)-C(12)	1.503(4)
O(2)-C(2)	1.433(4)	C(12)-C(13)	1.474(4)
O(4)-C(14)	1.415(4)	C(14)-C(25)	1.494(4)
O(4)-C(15)	1.429(4)	C(5)-C(4)	1.444(5)
C(1)-O(1)-C(26)	116.1(2)	C(13)-O(3)-C(14)	115.7(2)
O(3)-C(13)-C(12)	113.3(3)	O(1)-C(26)-C(25)	113.8(3)

C(1)-C(12)-C(13)	122.5(3)	C(14)-C(25)-C(26)	123.1(3)
------------------	----------	-------------------	----------

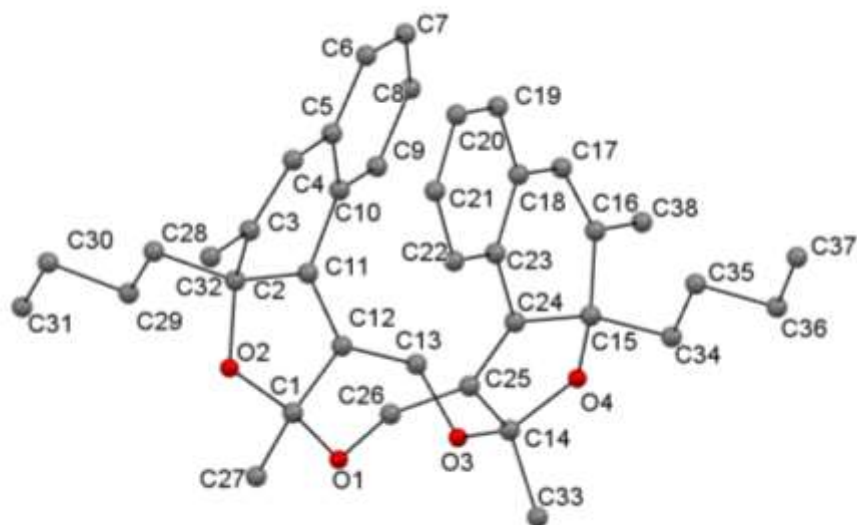


Figure S4. Molecular structure of **2o'**. Hydrogen atoms have been omitted for clarity.

Cartesian Coordinates

Aromaticity governing regioselectivity

Figure S5 illustrates the reaction profiles computed for the pathways leading to regioisomeric naphthalenones via [3,3]-sigmatropic rearrangement of the propargyl alcohol attached to the oxygen in position 2. It can be observed that the pathway involving position 3 (red in Figure S5) is consistently higher in energy and renders a very unfavourable product devoid of aromaticity in the entire structure. On the contrary, dearomatization through position 1 (blue in Figure S5) does not affect the aromaticity of half of the naphthol system, and renders a product that is more stable (by more than 20 kcal/mol) before protodeauration.

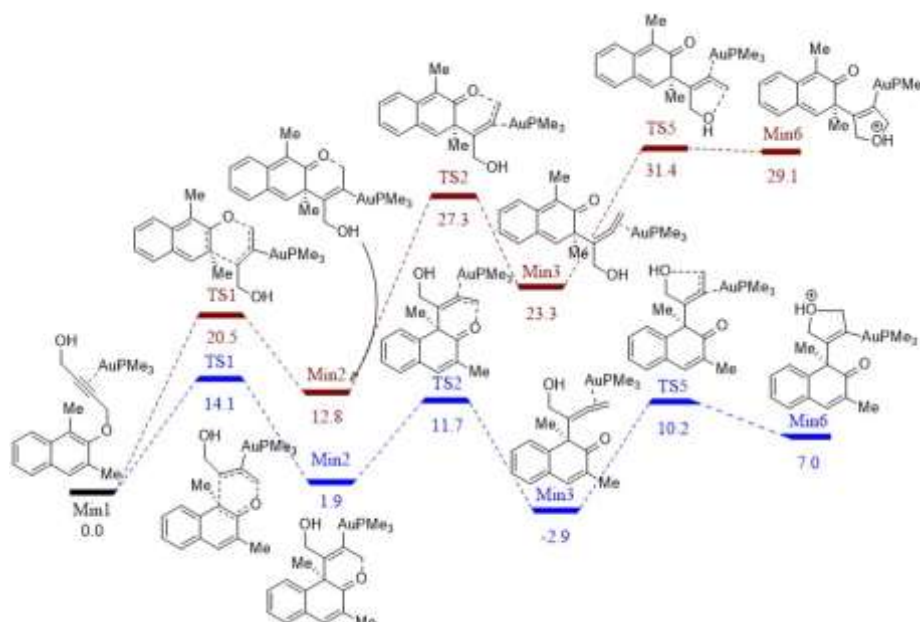
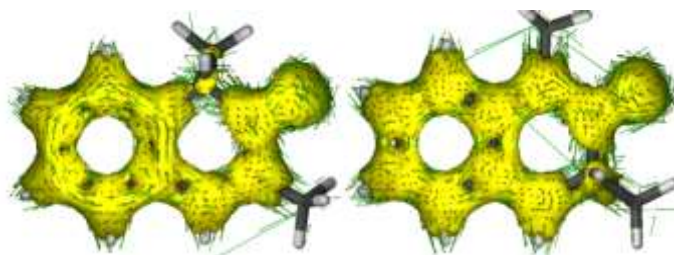


Figure S5. Alternative regioisomeric profiles for the gold mediated dearomatization of naphthols.

These findings are compatible with results obtained with the ACID method.^[17] This methodology reveals regions of delocalized electron density, and it is particularly sensitive for aromatic areas, where diatropic currents can be observed through a vectorial field of flux



(Figure S6).

FigureS6. ACID isosurface (0.05 au) for two simple phenols dearomatized at positions 1 (left) and 3 (right). The flux field shows clear aromatic currents in one (left) whereas currents vanished in the second (right). The external magnetic field is directed down into the paper plane.

Table of Energies

Table S4. Computed energies for the competing reactions

Structure	Methyl		Ethyl		i-Propyl	
	Expect. prod.	Unexp. prod.	Expect. prod.	Unexp. prod.	Expect. prod.	Unexp. prod.
Min1	0.0		0.0		0.0	
TS1	14.1		12.4		12.4	
Min2	1.9		2.9		-2.8	
TS2	11.7		9.3		7.6	
Min3	-2.9		-2.8		-6.2	
TS3a/b	9.0	12.0	7.5	10.8	10.6	5.8
Min4a/b	0.0	-0.4	-2.3	-3.3	-1.4	-7.6
TS4a/b	12.1	13.4	10.2	8.9	8.0	-0.1
Min5a/b	0.0	-20.8	-1.9	-30.1	-4.1	-35.4
TS5a	10.2		8.1		8.0	
Min6a	7.0		5.4		5.8	
Min7a	-23.9		-26.8		-26.5	

Free energies in kcal/mol computed at the M06/Def2SVPP level with toluene parameters in the PCM solvation model (1 atm, 298 K). For a detailed description of the computational methodology see the SI.

Formation of 2m'

We decided to also explore the formation of **2m'**, obtained when homopropargyl alcohol **1m** is used. In this case the reaction pathway bifurcation occurs right at the beginning of the computed mechanism. **TS1** initiates the sigmatropic rearrangement and, due to the extended chain, another transition state (**TS1c**) is associated with the direct nucleophilic attack of the homopropargyl alcohol onto the activated alkyne. Satisfyingly, when we

Chapter 2

computed both alternative transition states for this system, we observed that the activation energy to reach **TS1c** was 1.3 kcal/mol lower than that to reach **TS1**. Due to the comparable ring strain and electronic stability of the rings being formed in both alternatives (a dihydrofuran ring) the explanation for the favoured formation of **2m'** must reside elsewhere. It seems reasonable that, again, the partial loss of aromaticity required in the sigmatropic rearrangement is the reason for the formation of **2m** via a direct nucleophilic attack that maintains the entire aromatic character of the naphthol ring intact

Kinetic simulation

To simulate concentration vs time in the dearomatization reaction and identify which intermediates may be detectable in the experiment we computed rate constants, using activation free energies derived from the values in Table S4 and applying the Eyring equation. Then we used these rate constants as inputs in a stochastic kinetic simulator. Due to the limitations of the numerical integrator we had to multiply all the rate constants by 10E-6. The reaction is artificially slowed in this way, however, the relative concentration of products vs time is maintained since the ratio between each pair of rate constants is held constant with this operation. The mechanism therefore used as input is as follows:

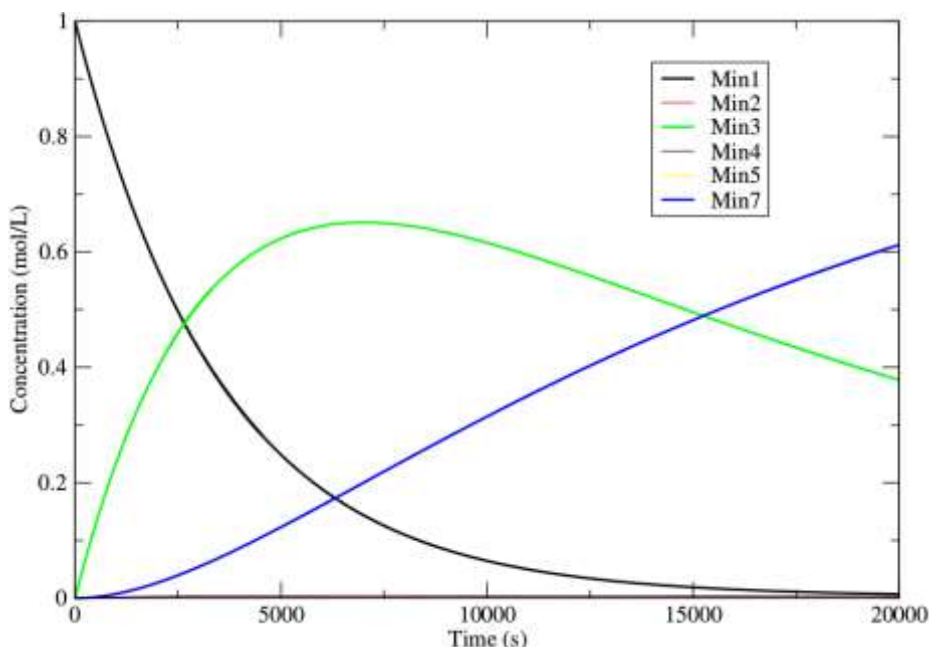
```

Min1 <==> Min2      k1=0.000283  k-1=0.007
Min2 <==> Min3      k2=0.43    k-2=0.000122
Min3 <==> Min4      k3=0.0116  k-3=1.56
Min4 <==> Min5      k4=0.00829 k-4=0.00829
Min5 --> Min6      k5=0.205

```

[Min1]=1

The last step was considered to be irreversible since it involves protodeauration and,

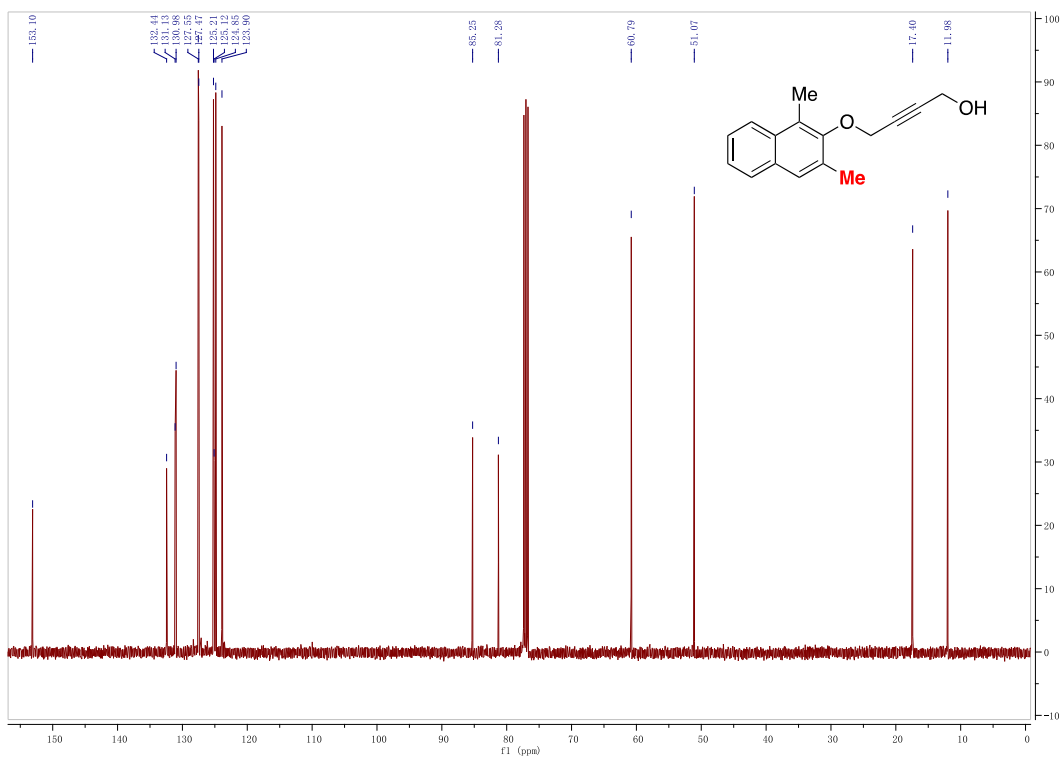
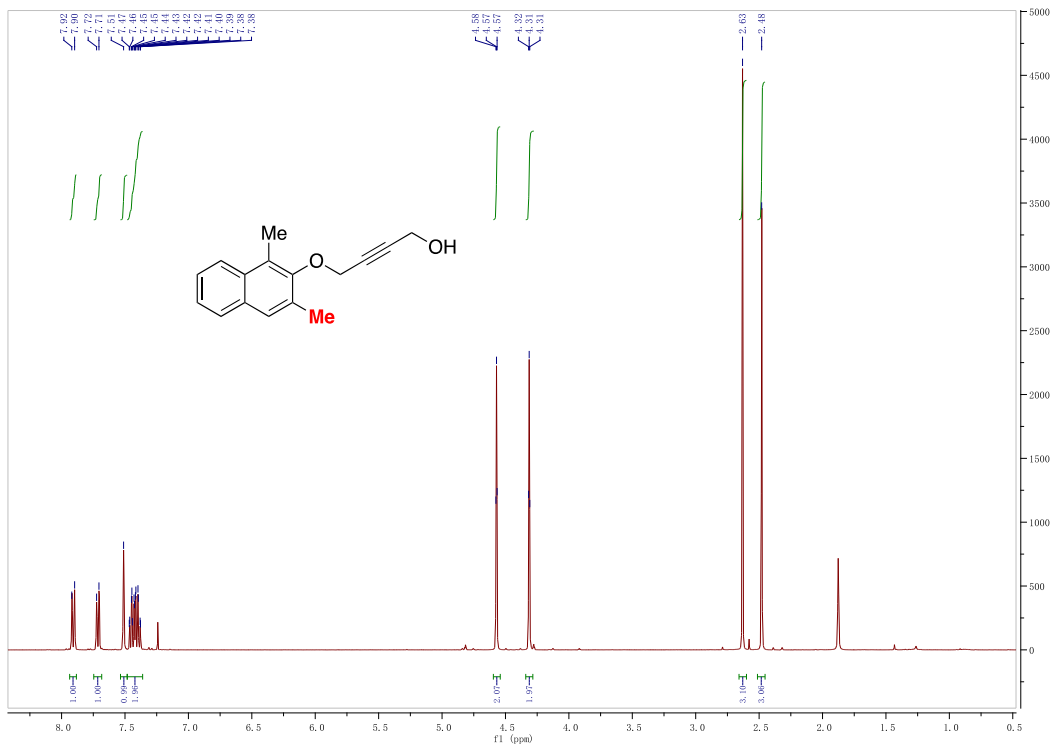


according to our calculations, the final product is stable with respect to the reactant by more than 20 kcal/mol. The results of this simulation confirm that the key allene intermediate (Min3) is accumulated before product formation occurs, and could be detected experimentally. **FigureS7.** Kinetic simulation for the dearomatization of **Min1**.

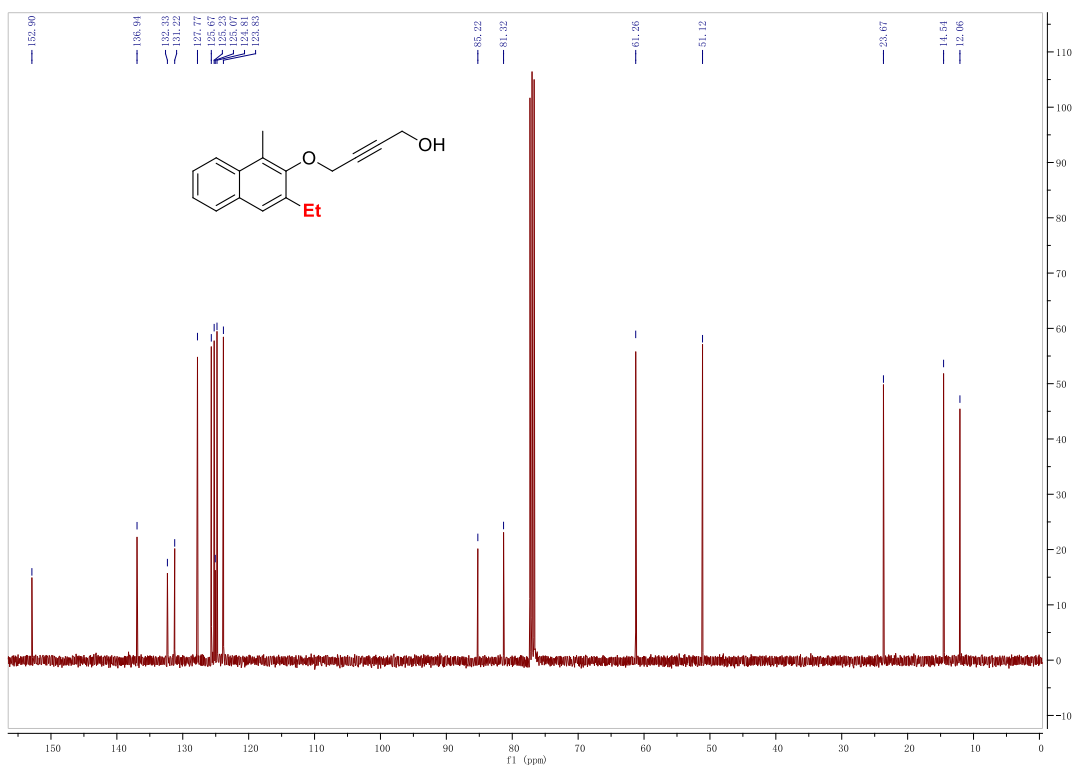
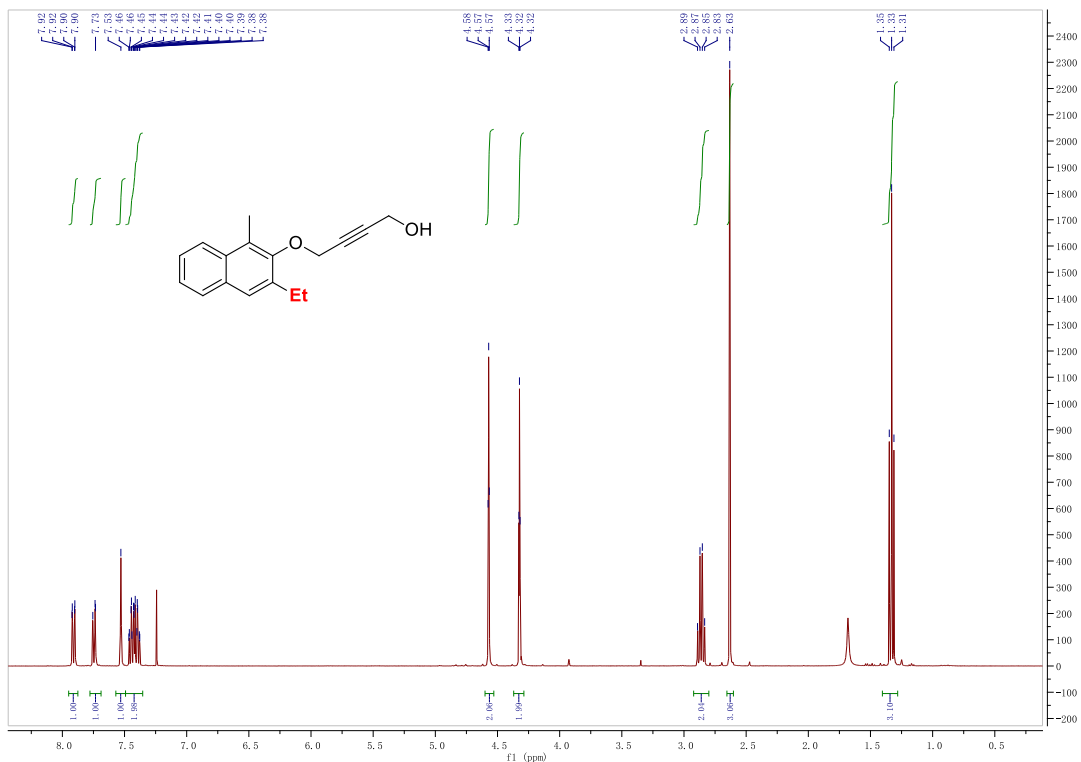
References

- [1] SMART & SAINT Software Reference Manuals, Version 5.051 (Windows NT Version), Bruker Analytical X-ray Instruments Inc. Madison, WI, 1998.
- [2] Sheldrick, G. M. SADABS, program for empirical absorption correction, University of Göttingen, Germany, 1996.
- [3] A. Altomare, M.C. Burla, M. Camalli, G.L. Cascarano, C. Giacovazzo, A. Guagliardi, A.G.G. Moliterni, G. Polidori, R. Spagna, *J. Appl. Crystallogr.* 1999, 32, 115-119.
- [4] G.M. Sheldrick, SHELXTLplus Version 5.1 (Windows NT version) Structure Determination Package; Bruker Analytical X-ray Instruments Inc.: Madison, WI, 1998.
- [5] L. Farrugia, ORTEP-3, *J. Appl. Cryst.* 2012, 45, 849-854.
- [6] W. Kohn, L. Sham, *Phys. Rev.* 1965, 140, A1133-A1138.
- [7] Y. Zhao, D.G. Truhlar, *Theor. Chem. Acc.* 2008, 120, 215-241.
- [8] a) O.N. Faza, R.A. Rodríguez, C.S. López, *Theor. Chem. Acc.* 2011, 128, 647-661; d) O.N. Faza, C.S. López, *Top. Curr. Chem.* 2014, 357, 213-284.
- [9] R. Bauernschmitt, R. Ahlrichs, *J. Chem. Phys.* 1996, 104, 9047-9052.
- [10] T.A. Keith, R.F.W. Bader, *Chem. Phys. Lett.* 1993, 210, 223-231.
- [11] M.J. Frisch, Gaussian09, revision D.01; Gaussian, Inc.: Wallingford, CT, 2013.
- [12] T. Oguma, T. Katsuki, *J. Am. Chem. Soc.* 2012, 134, 20017-20020.
- [13] G. Cera, P. Crispino, M. Monari, M. Bandini, *Chem. Commun.*, 2011, 47, 7803-7805
- [14] N. Kern, A. Blanc, J.M. Weibel, P. Pale, *Chem. Commun.*, 2011, 47, 6665-6667.
- [15] a) F. Kleinbeck, F. D. Toste, *J. Am. Chem. Soc.* 2009, 131, 9178-9179. b) R. E. M. Brooner, T. J. Brown, R. A. Widenhofer, *Angew. Chem. Int. Ed.* 2013, 52, 6259-6261
- [16] N. Eleftheriadis, S. A. Thee, M. R. H. Zwinderman, N. G. J. Leus, F. J. Dekker, *Angew. Chem. Int. Ed.* 2016, 55, 12300-12305
- [17] D. Geuenich, K. Hess, F. Köhler, R. Herges, *Chem. Rev.* 2005, 105, 3758-3772.

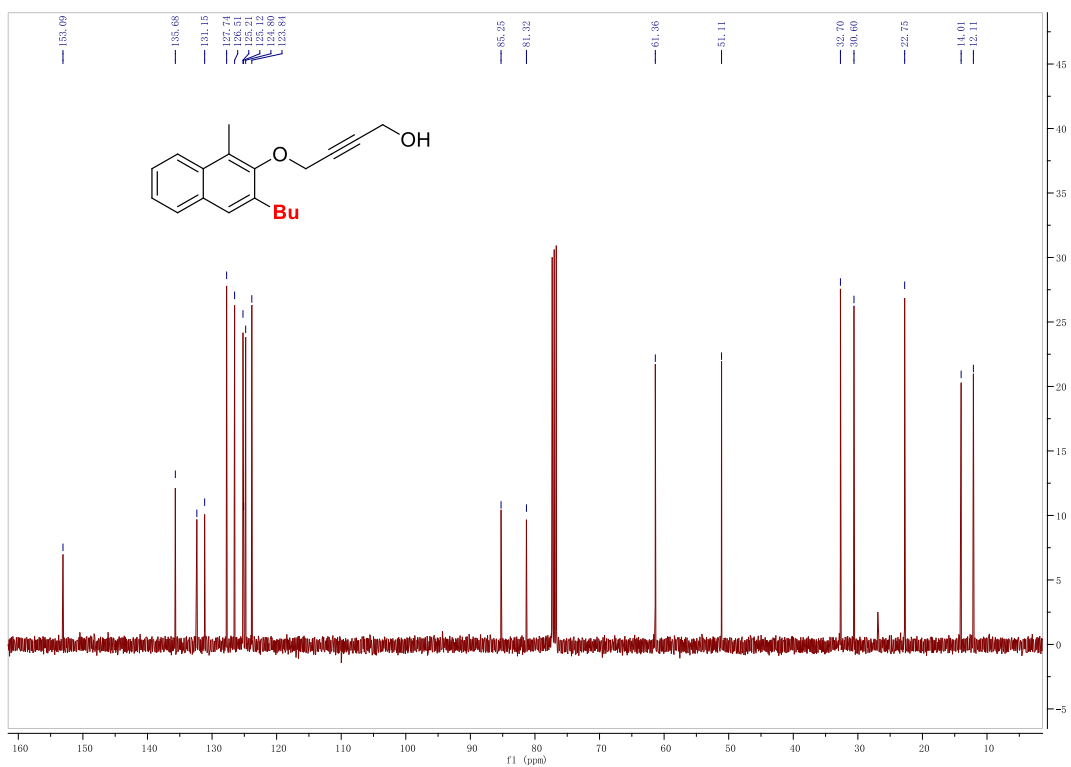
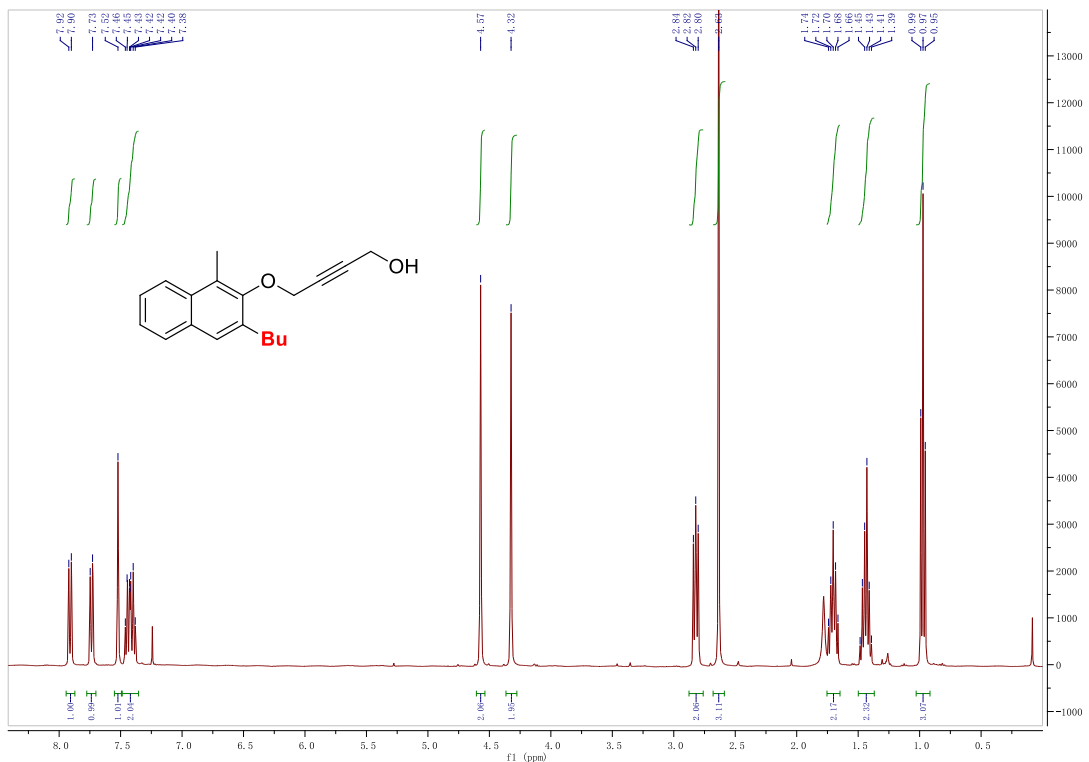
Chapter 2



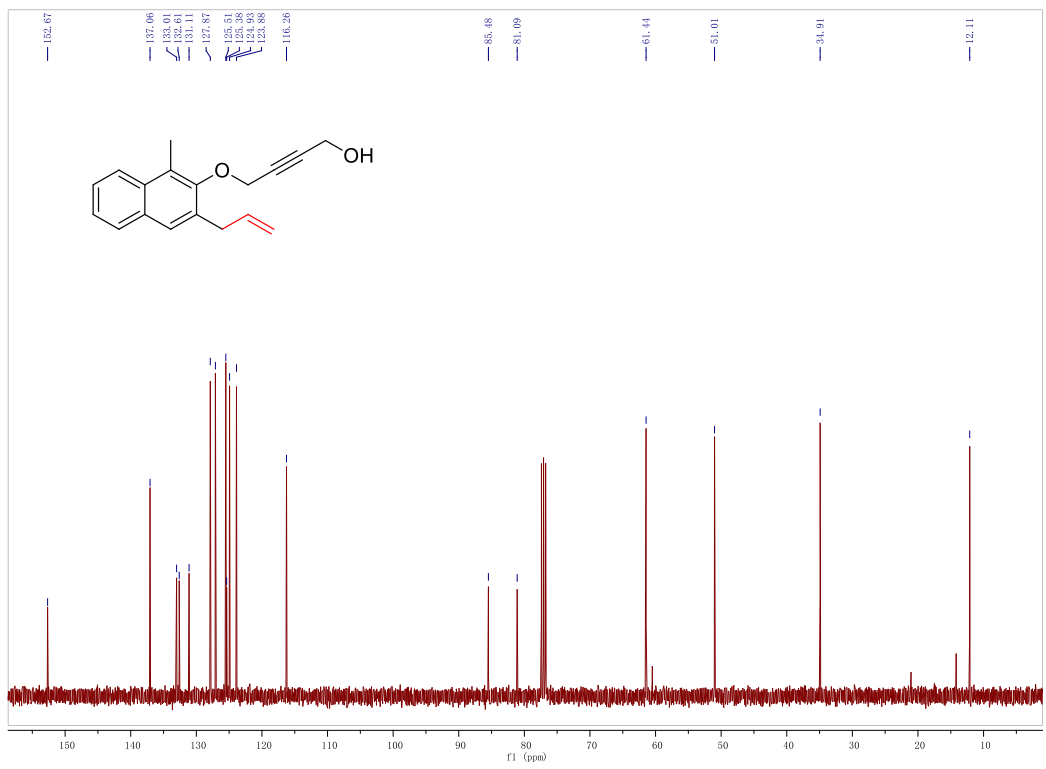
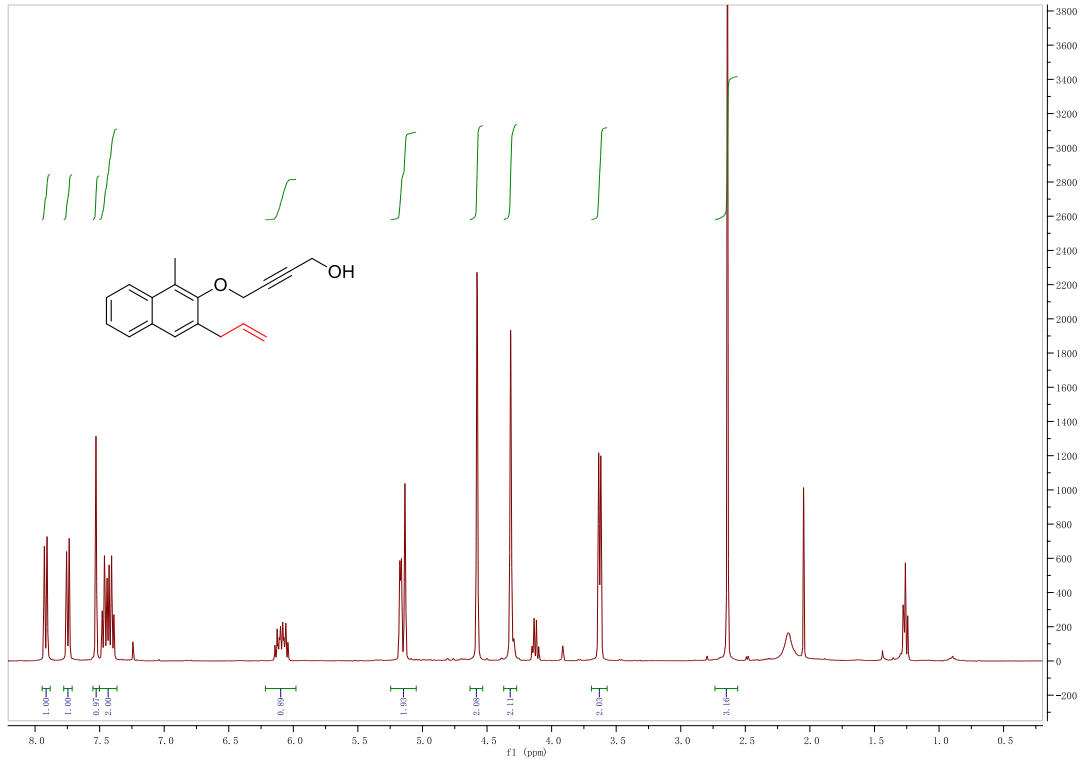
Chapter 2



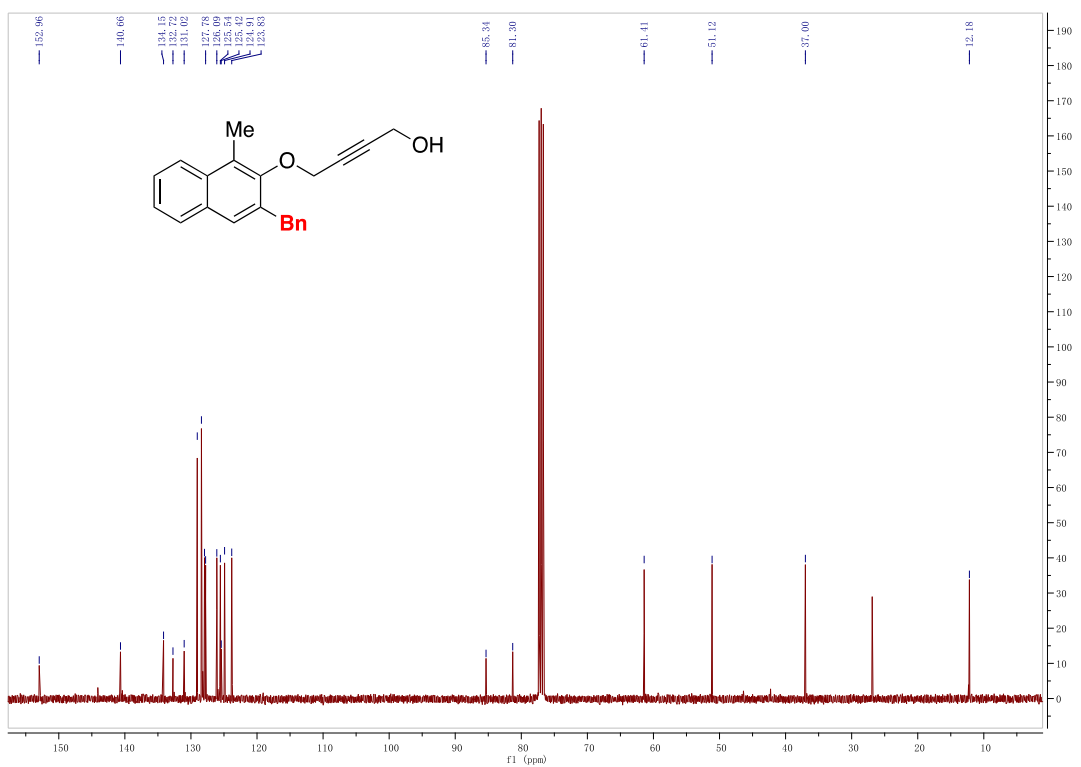
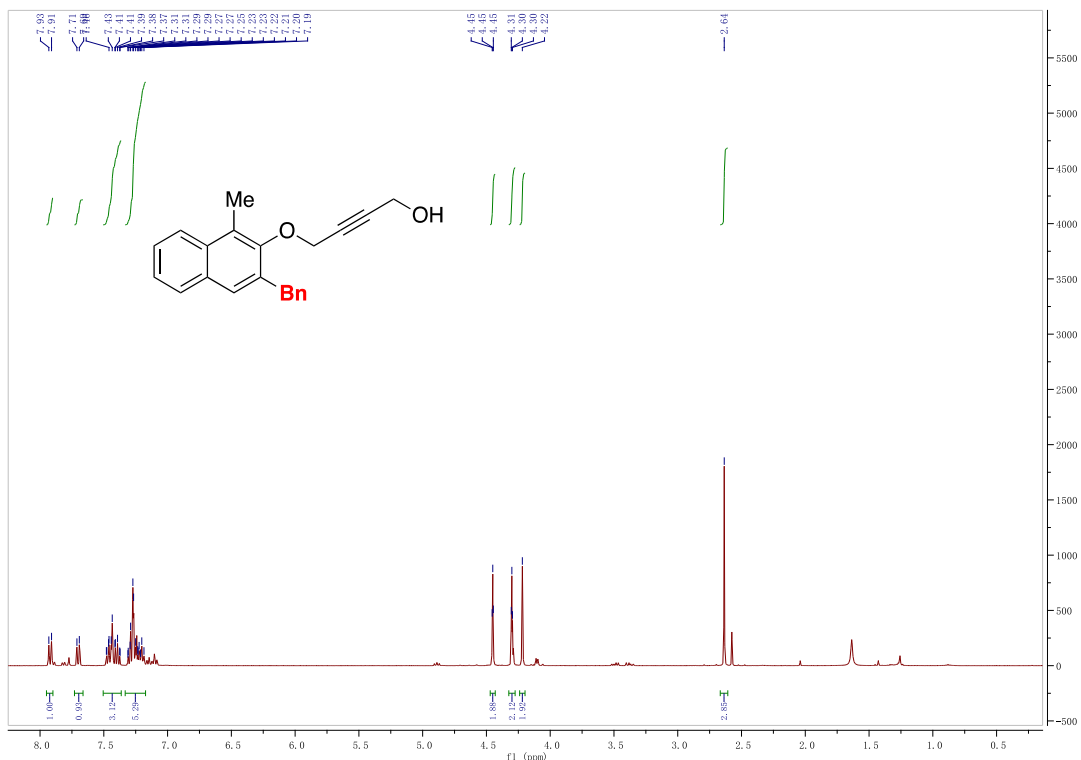
Chapter 2



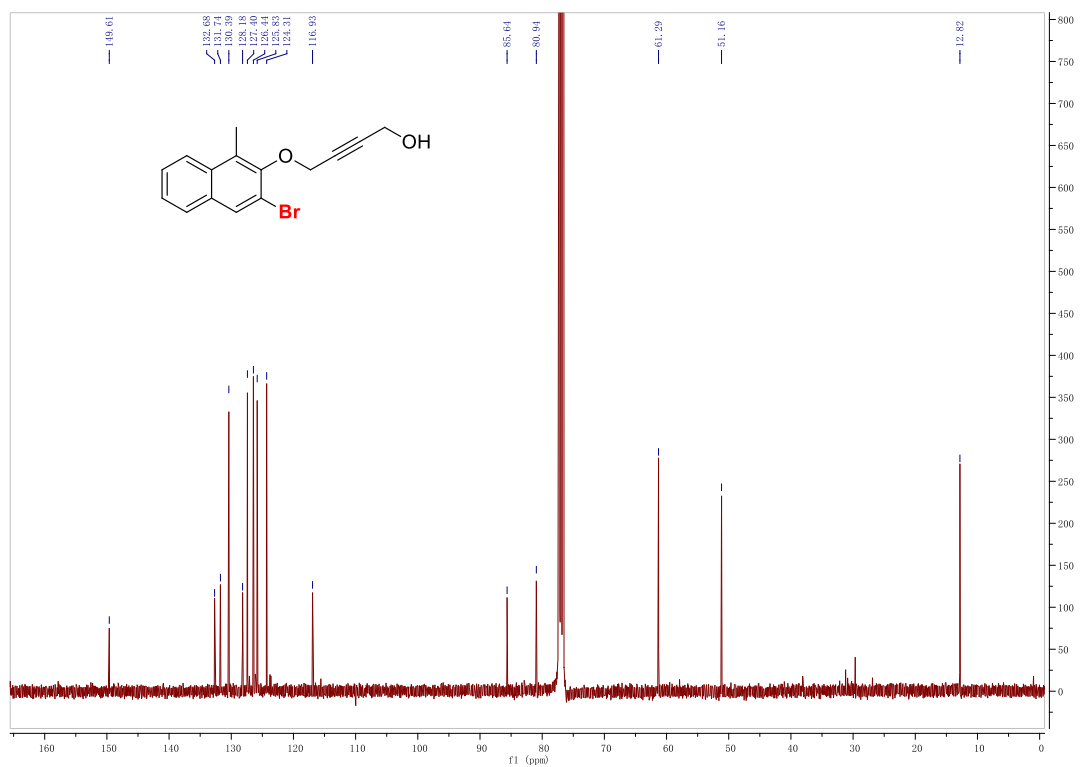
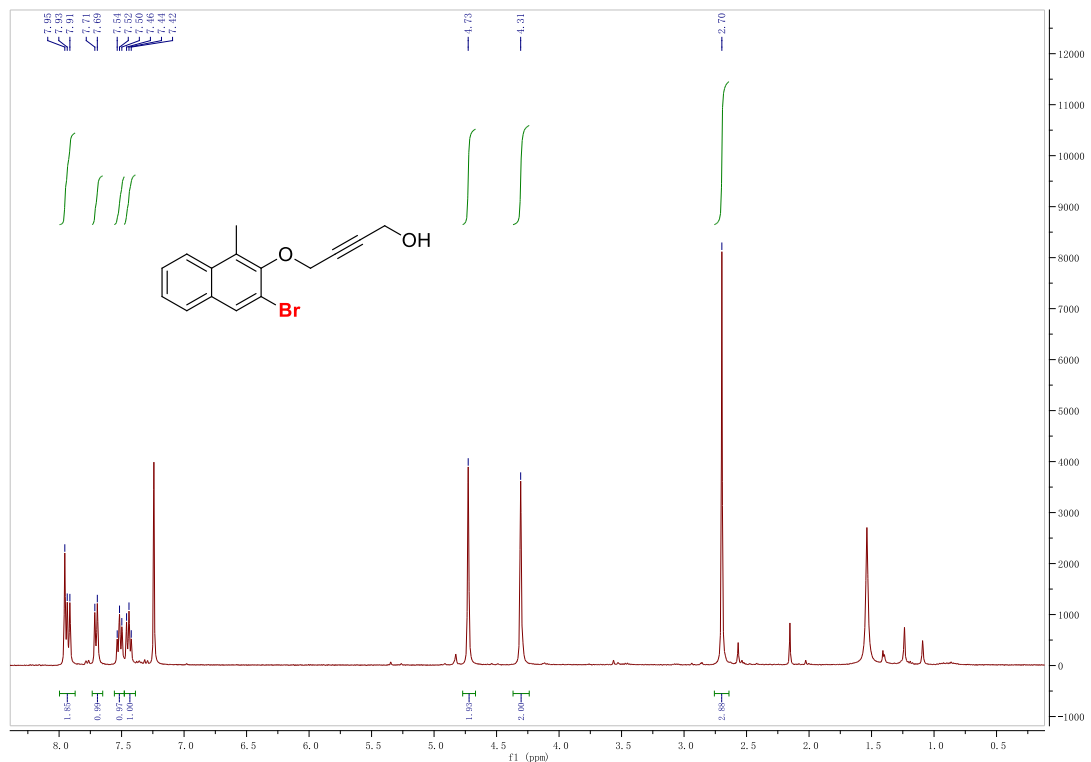
Chapter 2



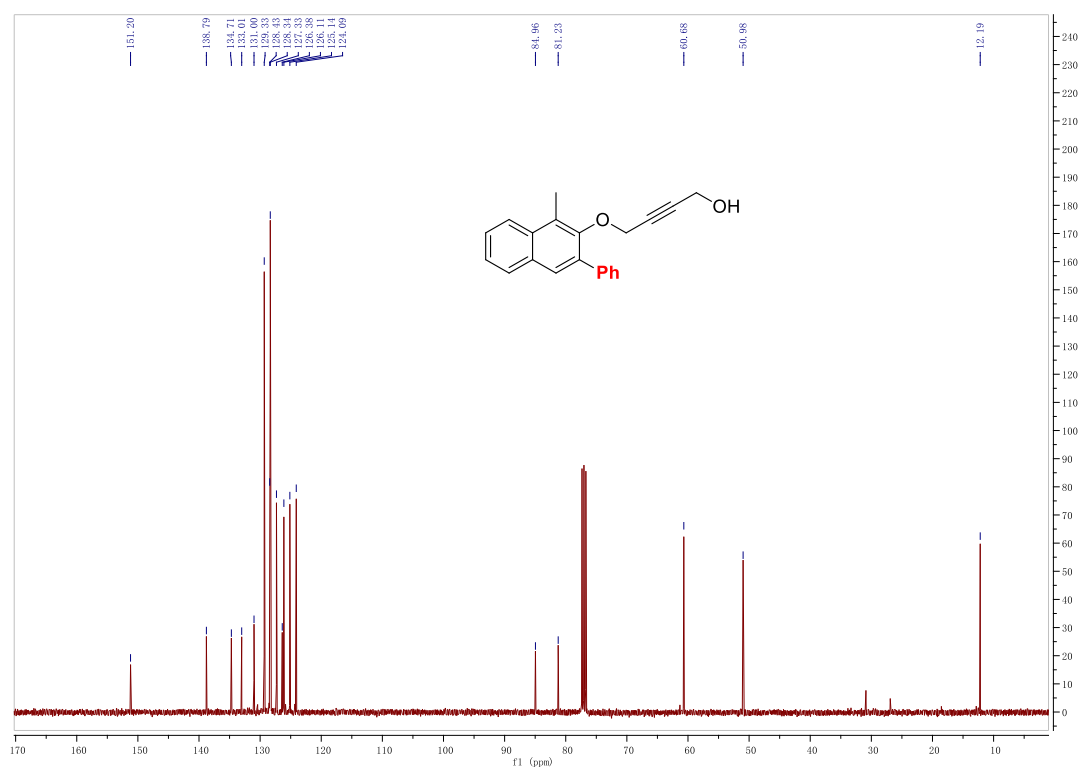
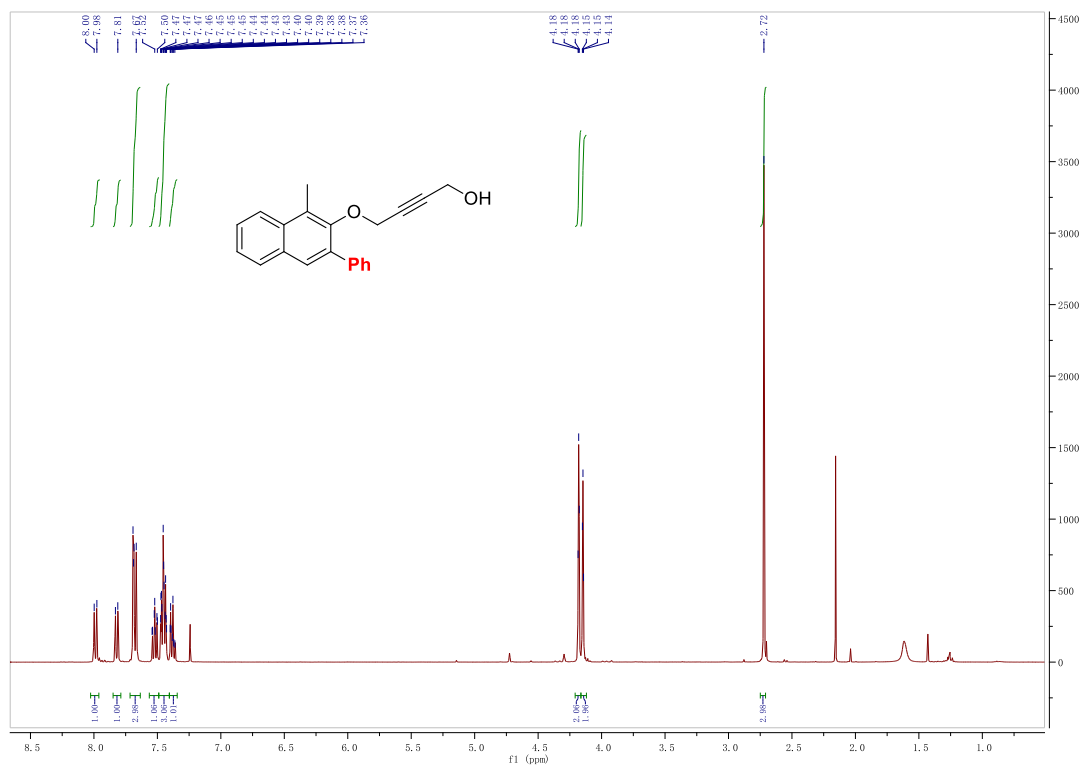
Chapter 2



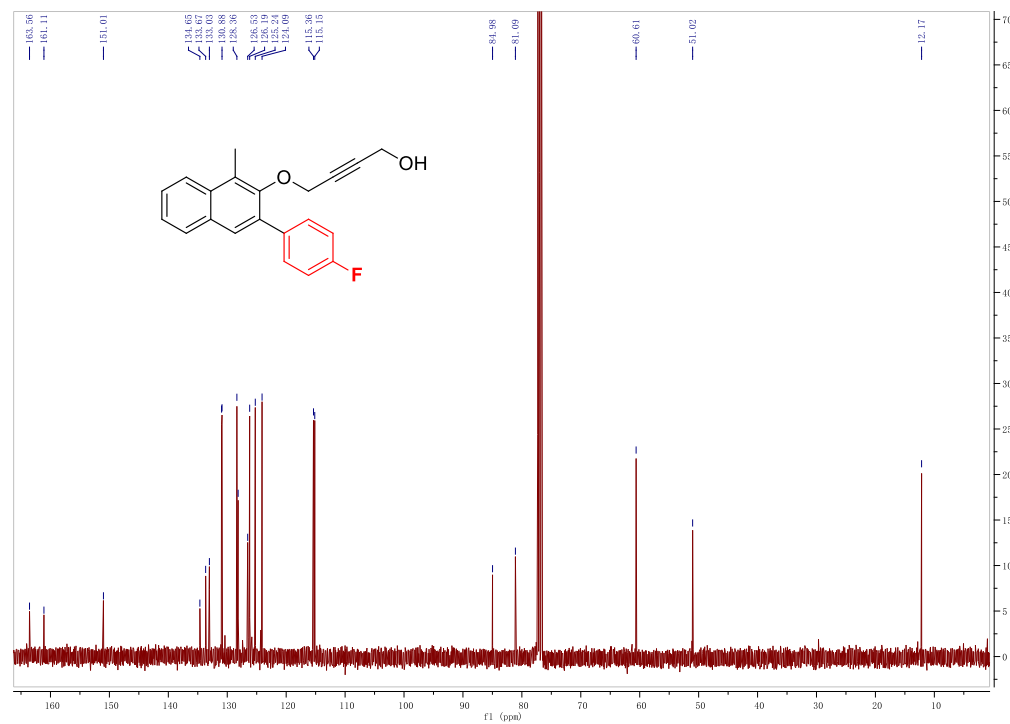
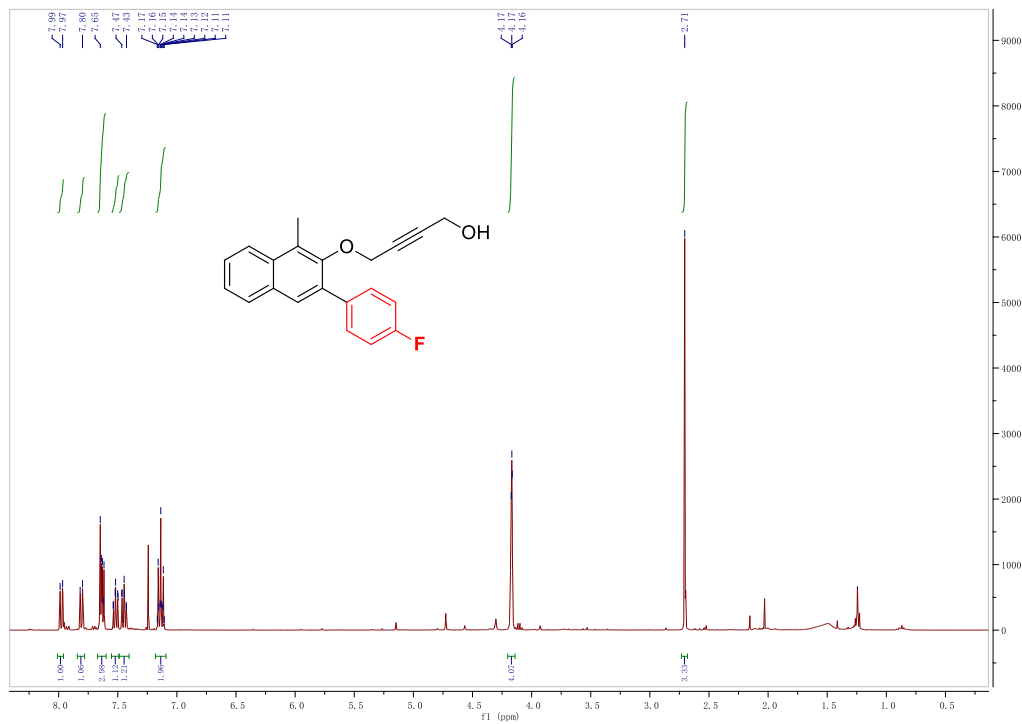
Chapter 2



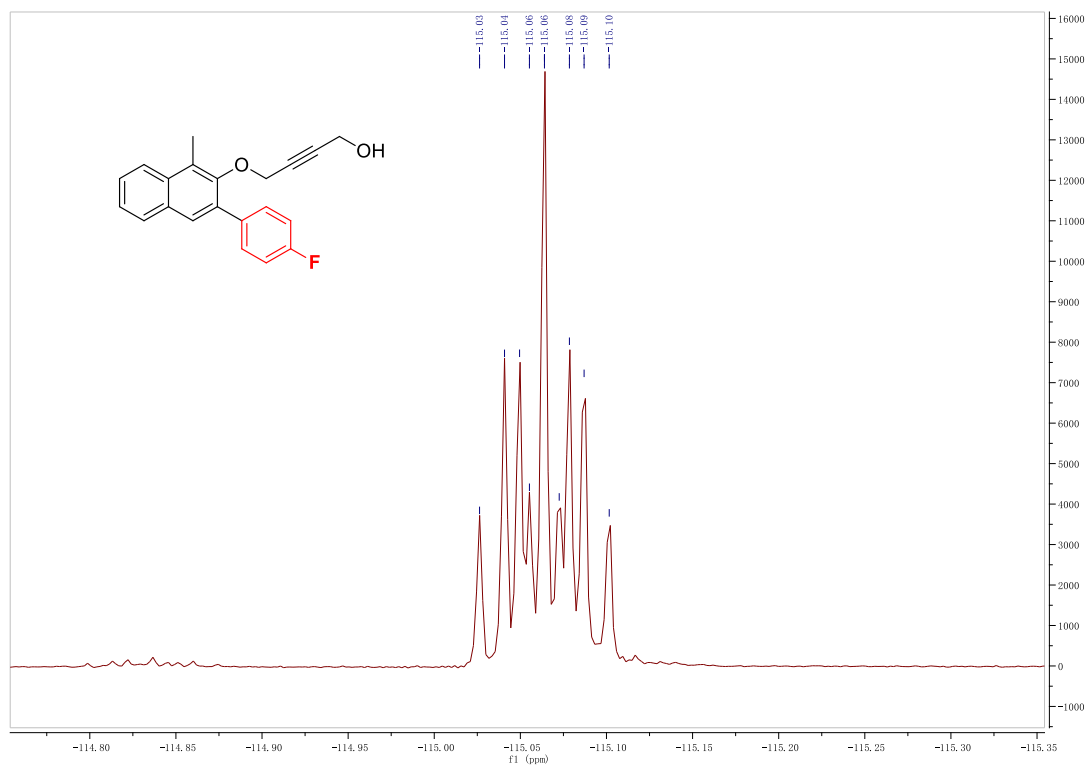
Chapter 2



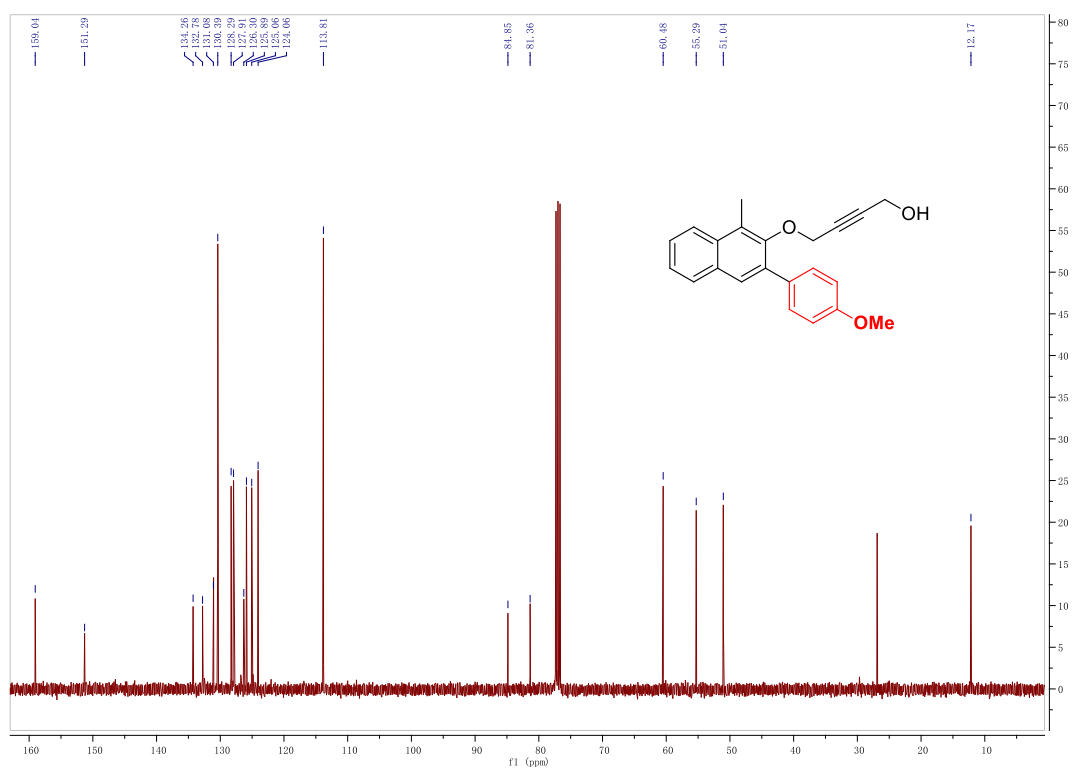
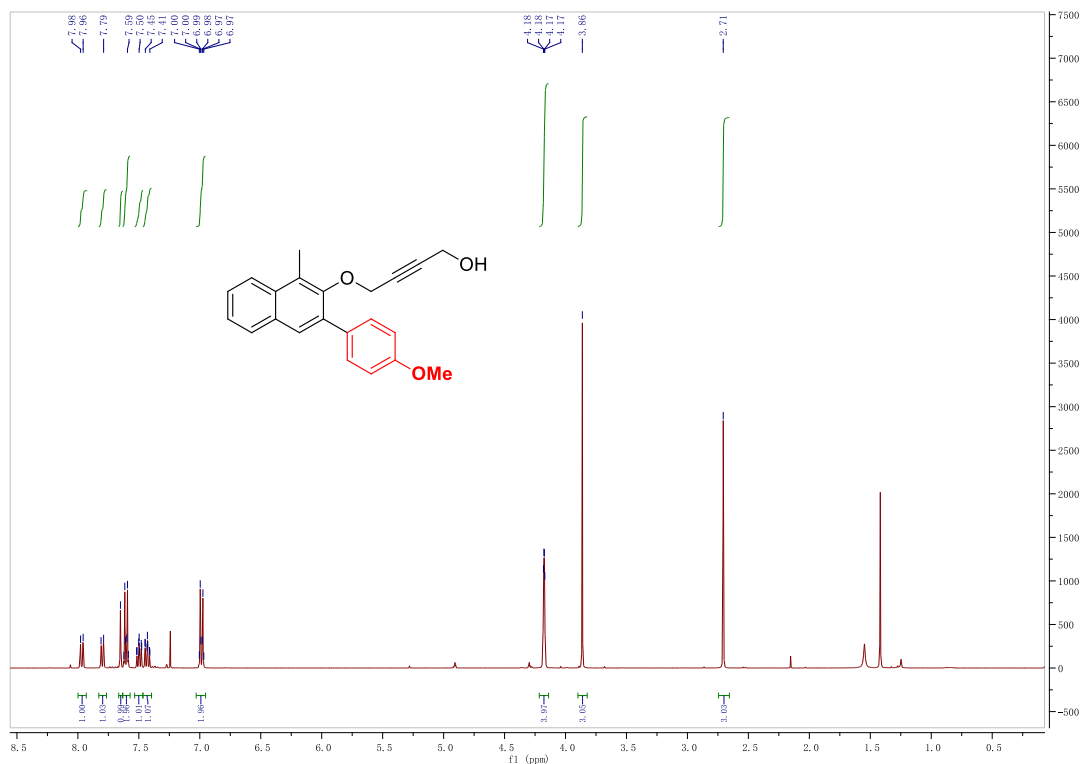
Chapter 2



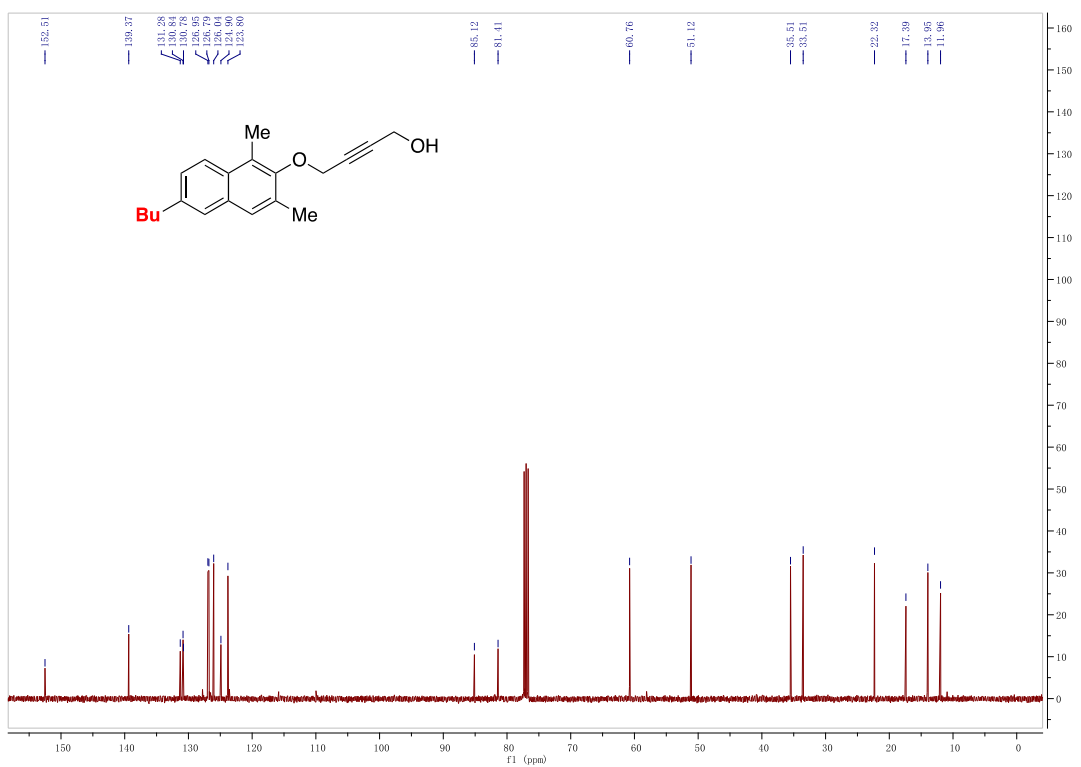
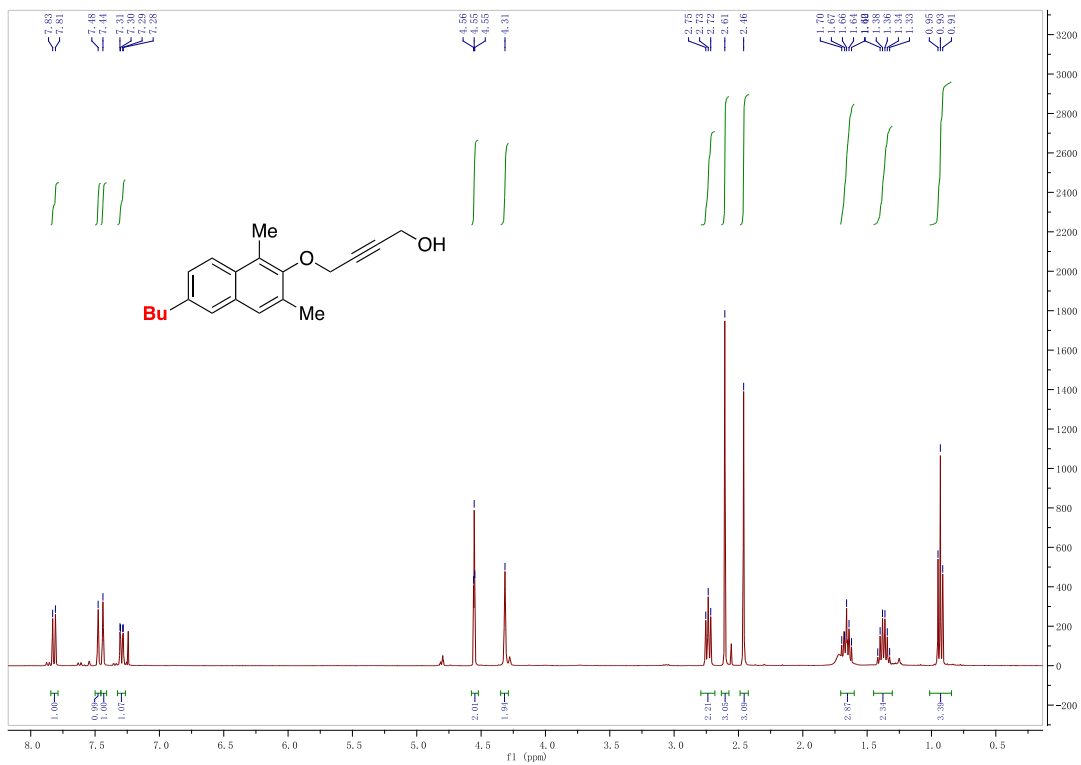
Chapter 2



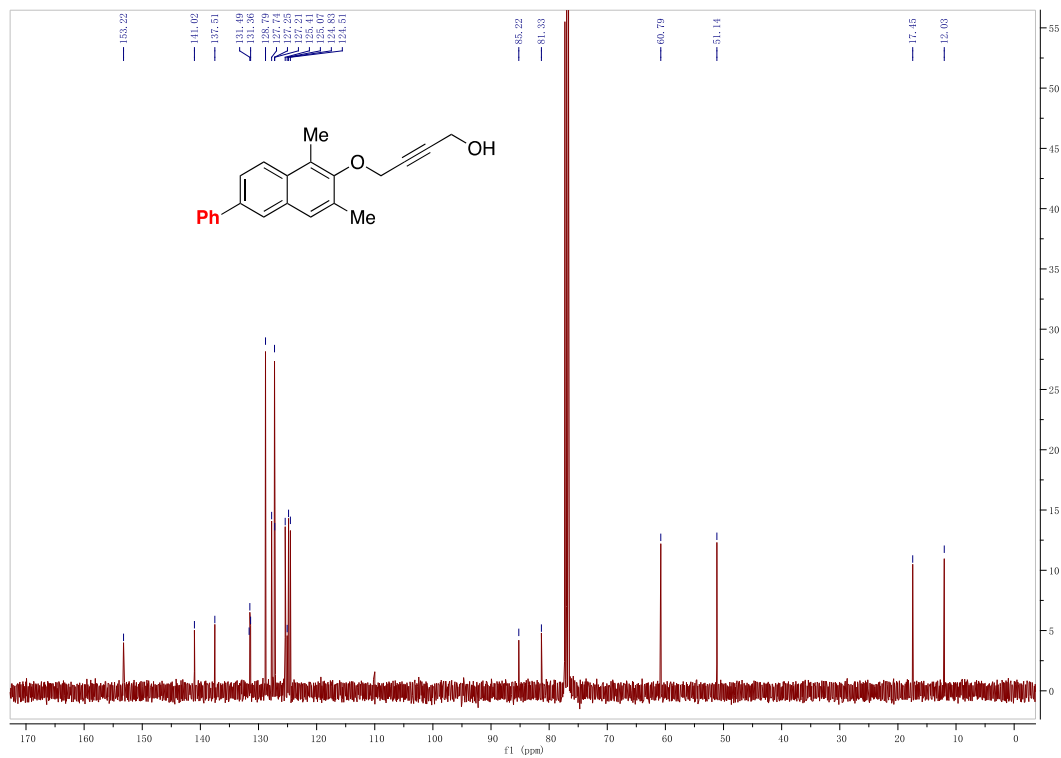
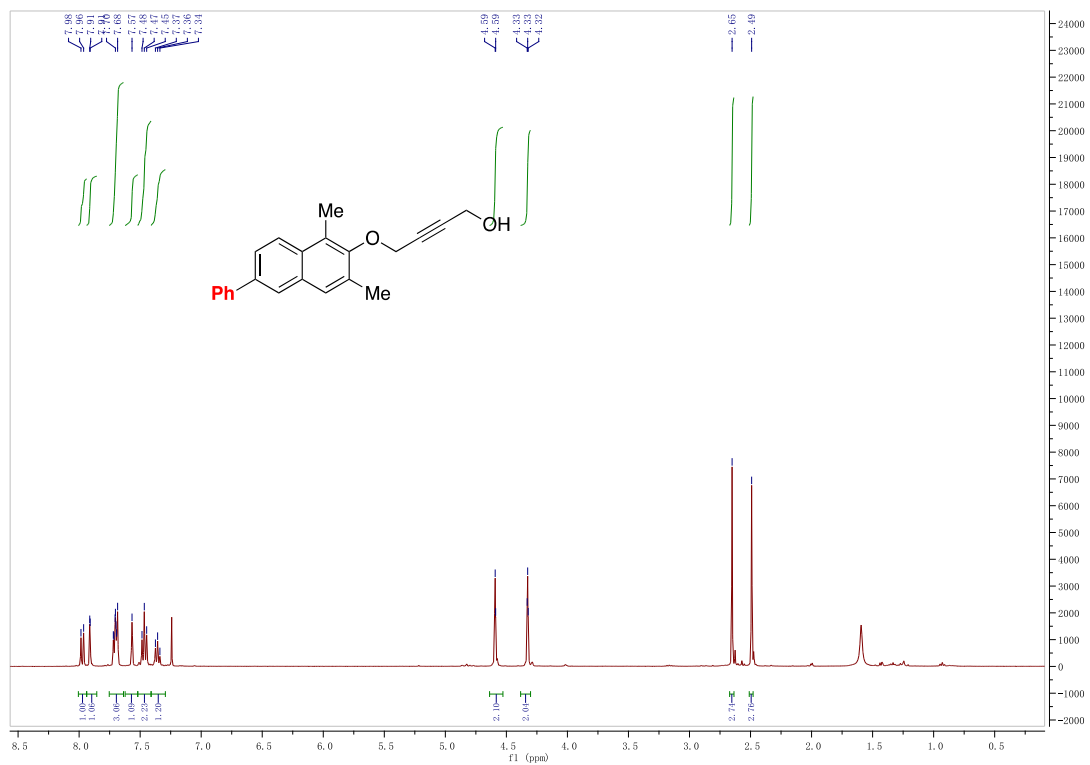
Chapter 2



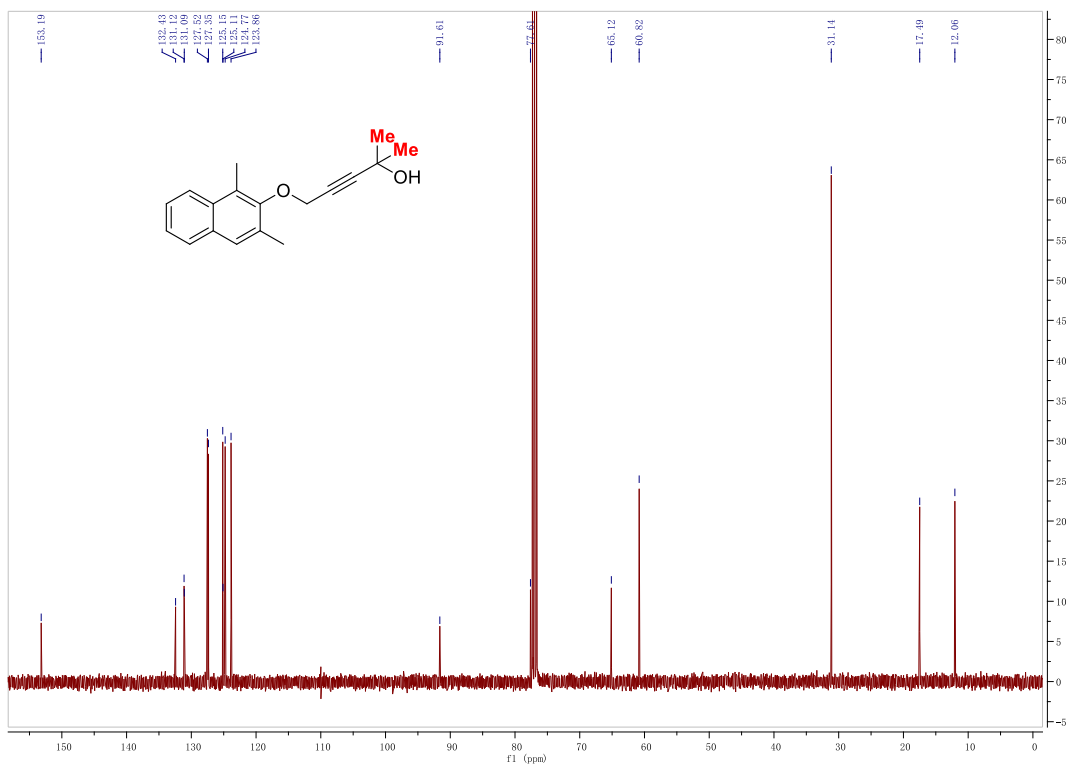
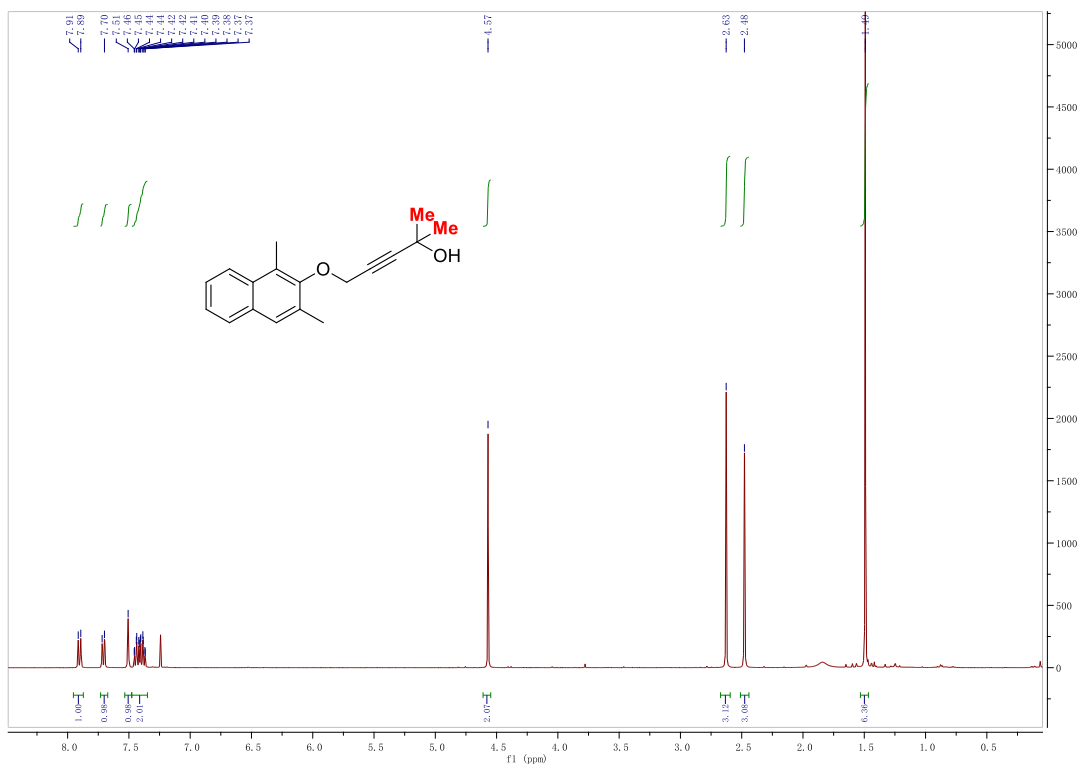
Chapter 2



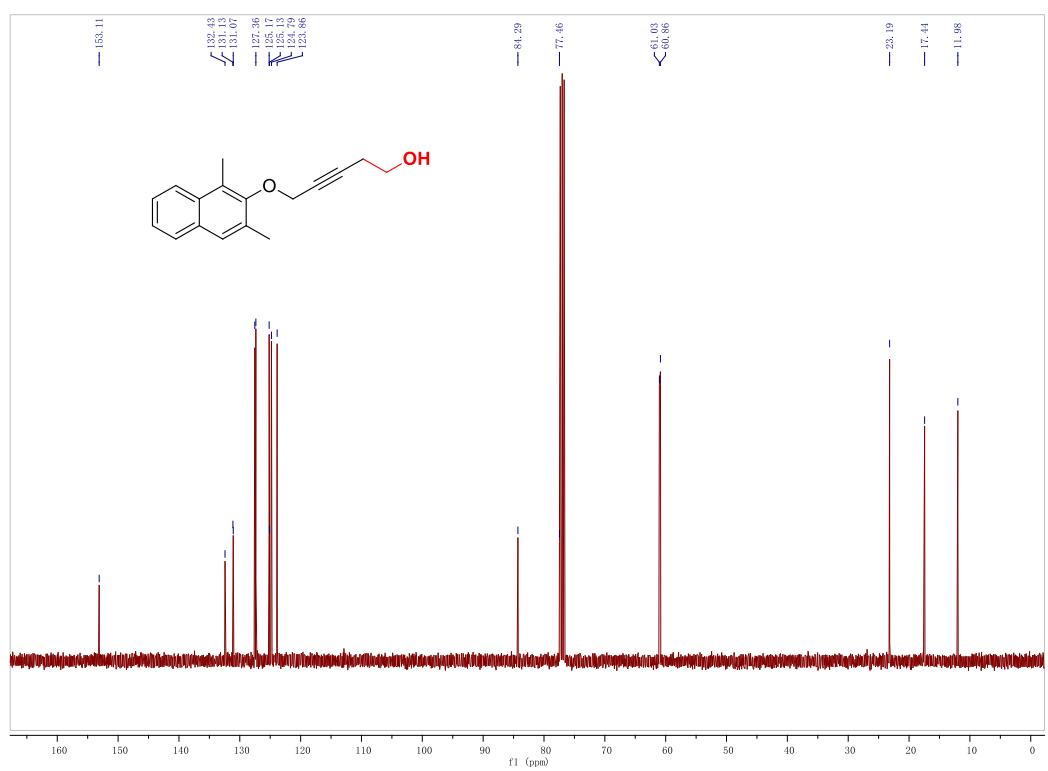
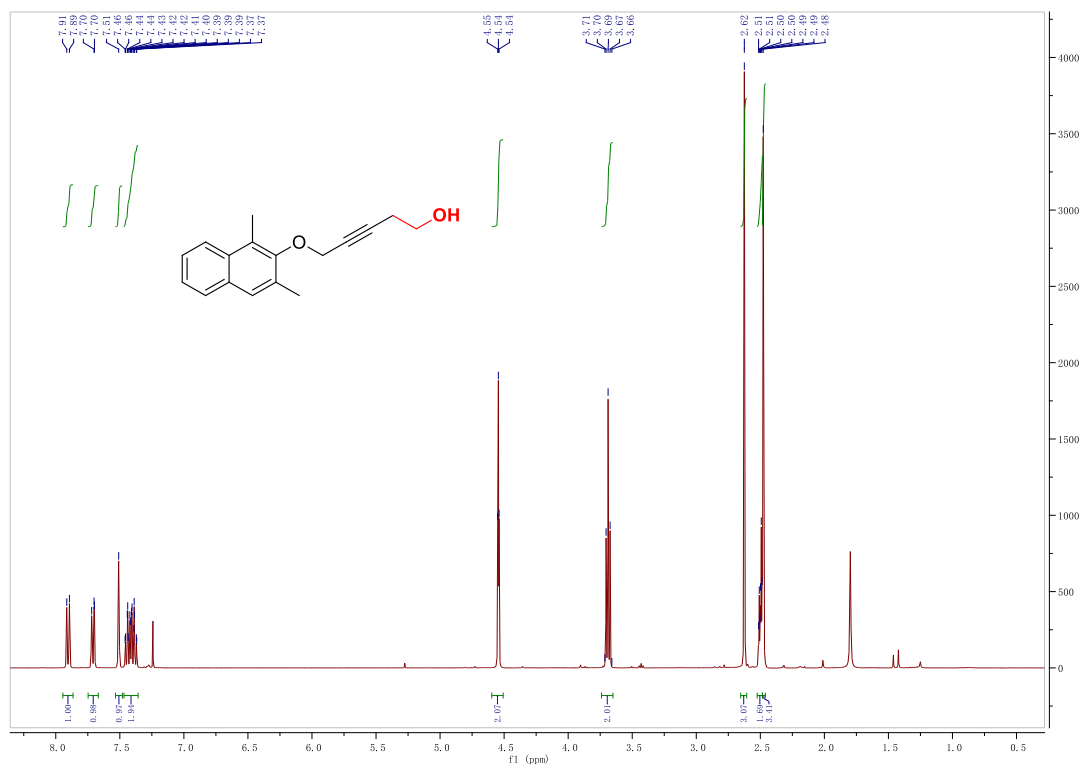
Chapter 2



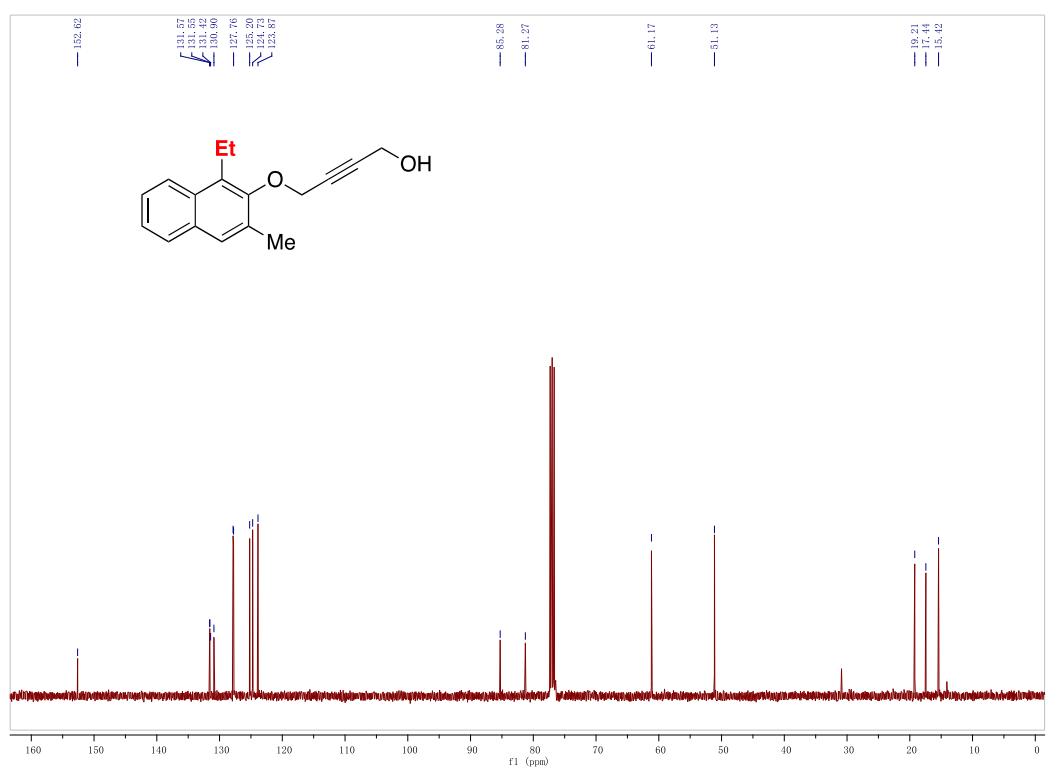
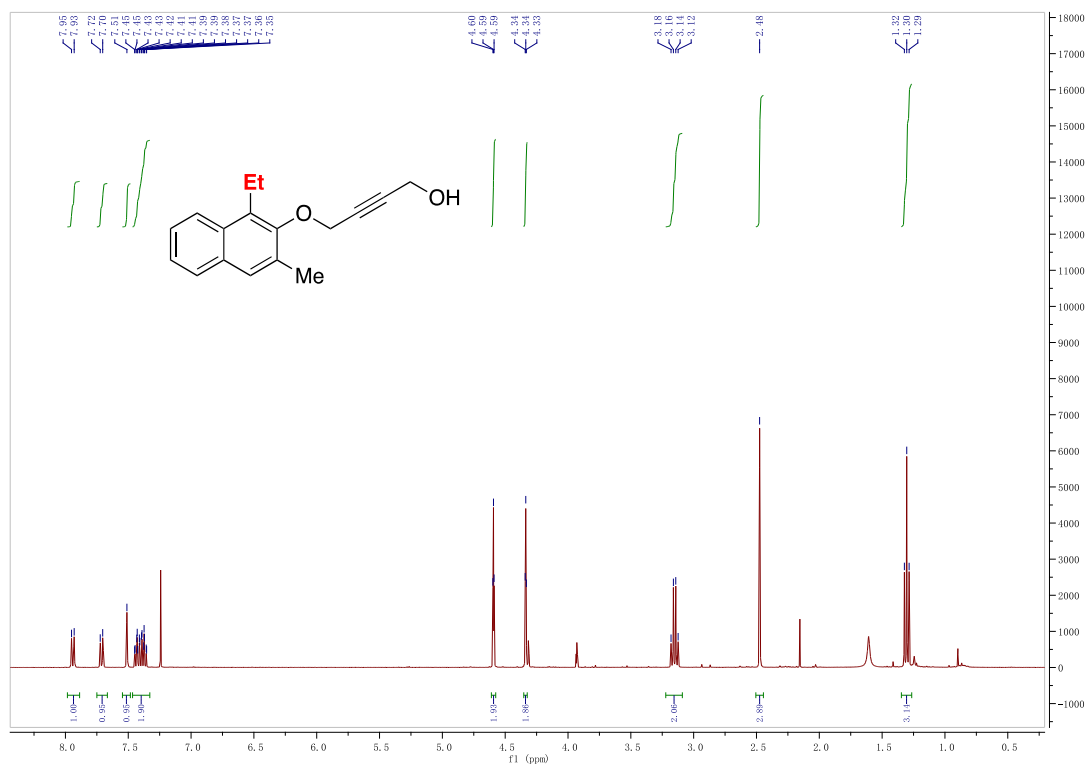
Chapter 2



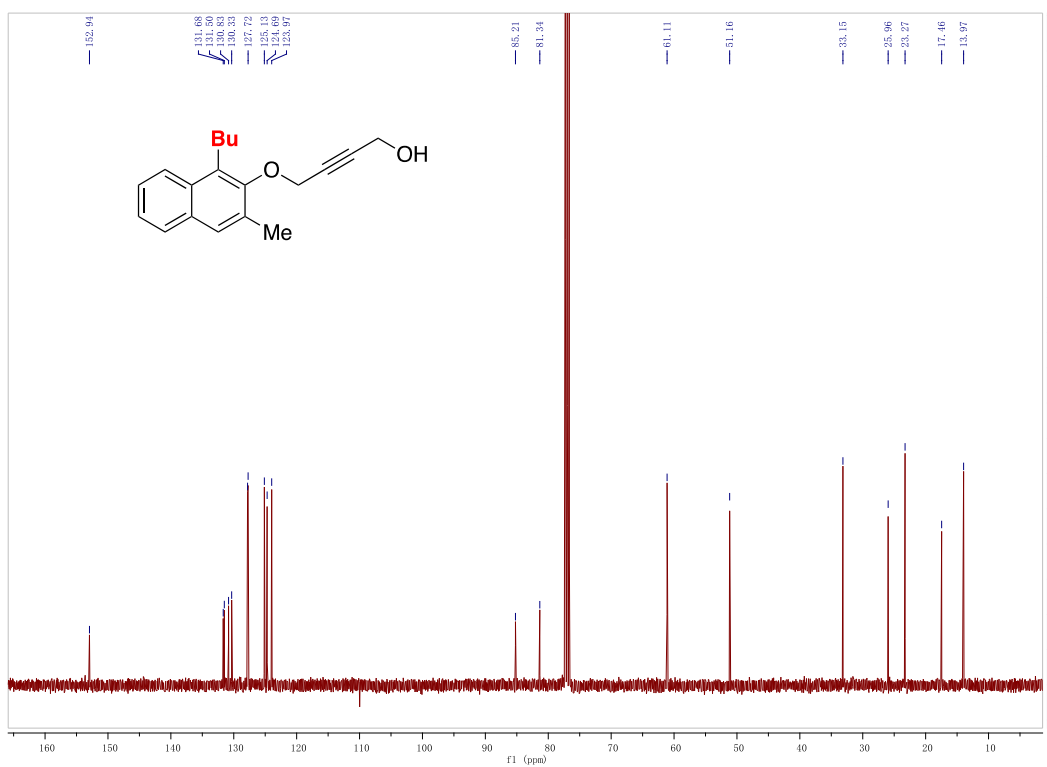
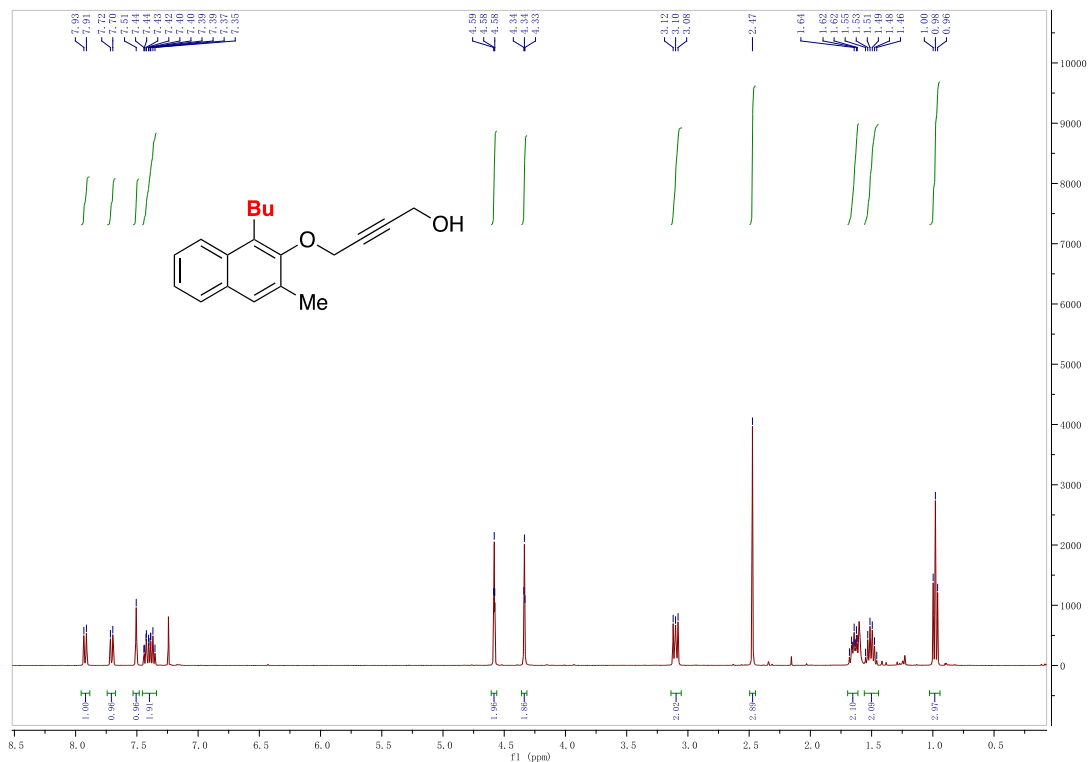
Chapter 2



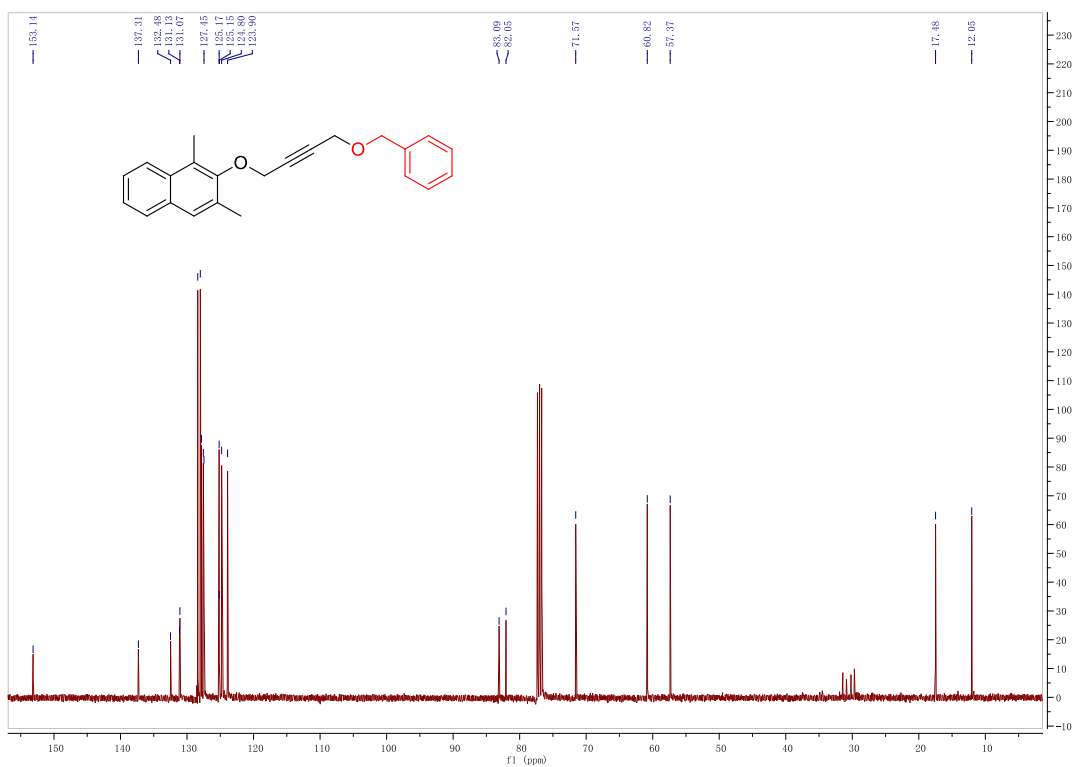
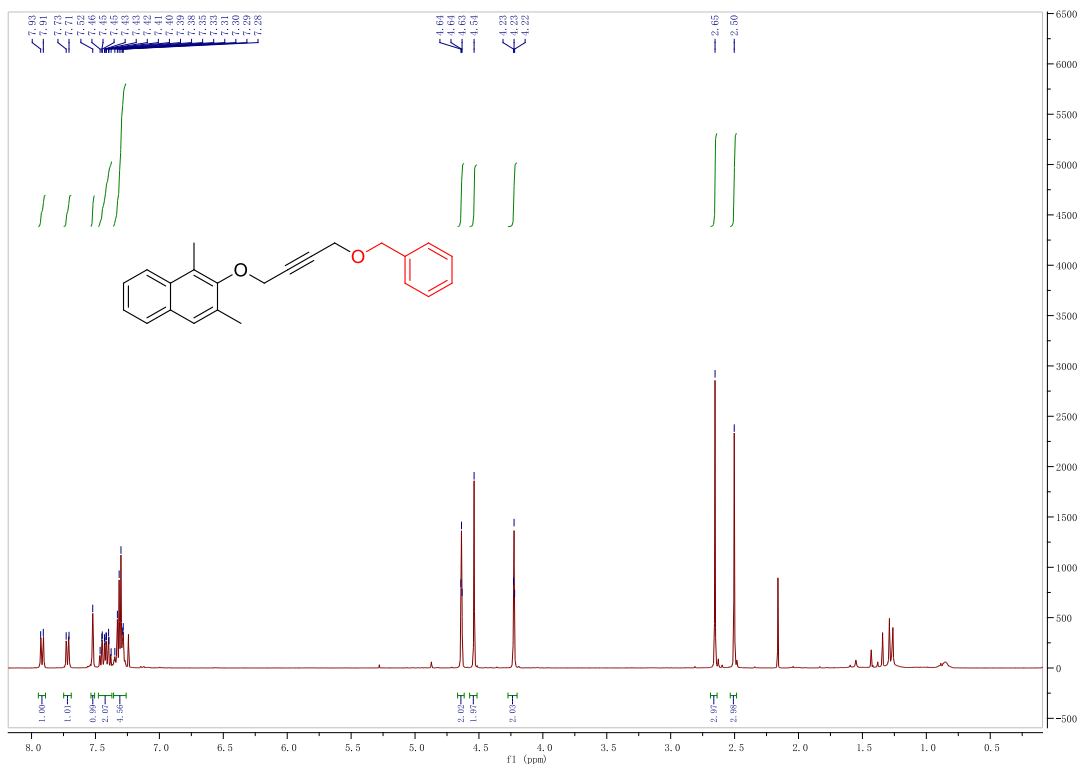
Chapter 2



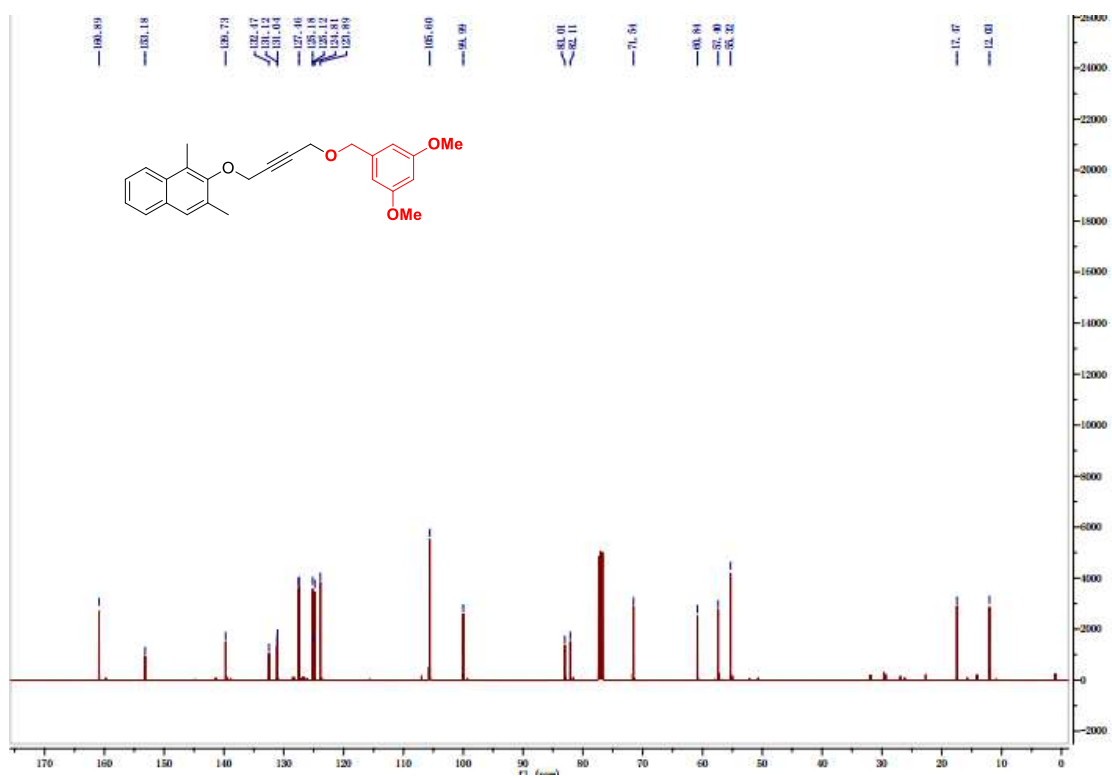
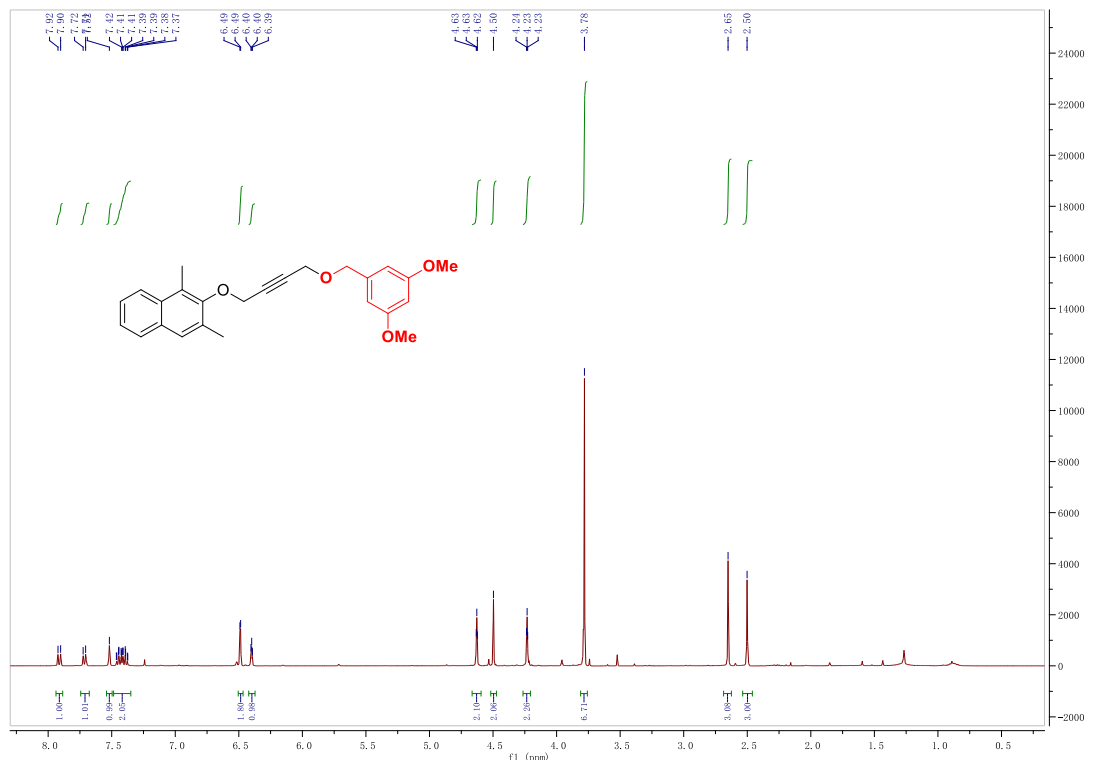
Chapter 2



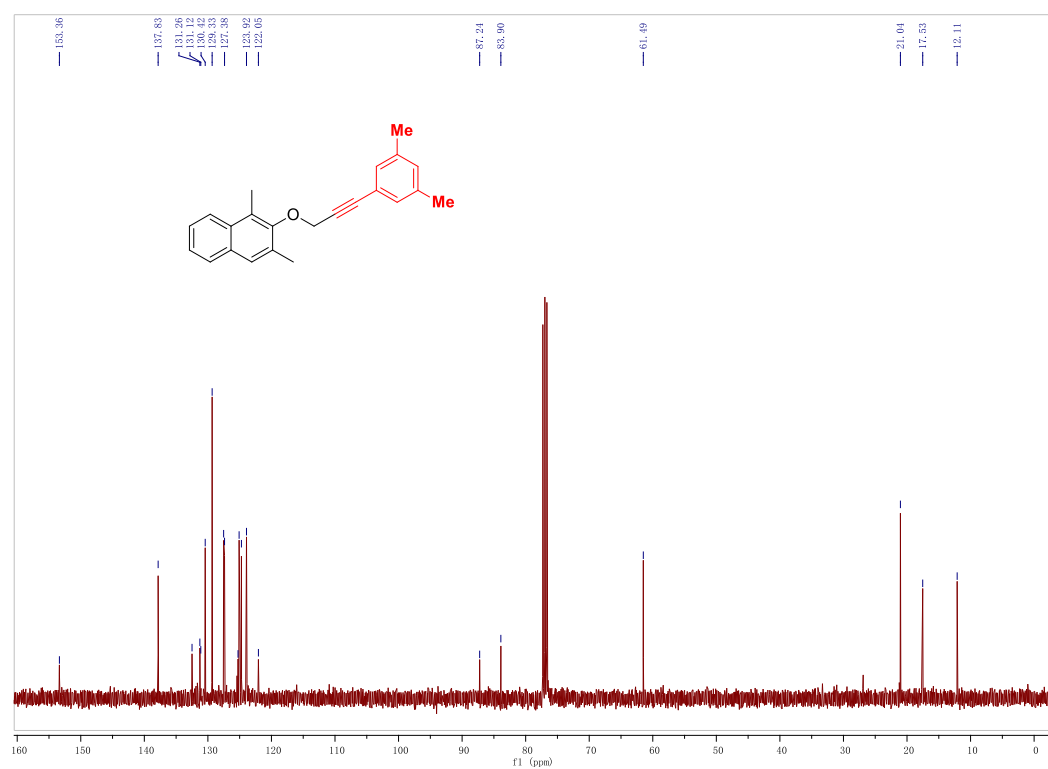
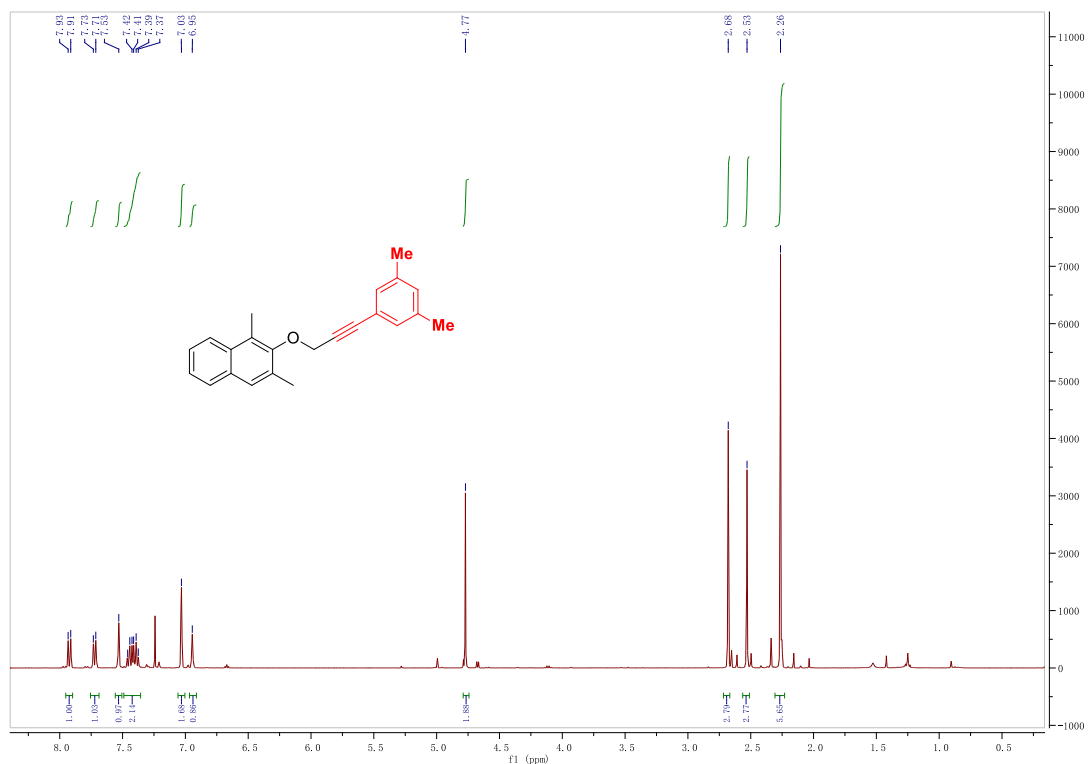
Chapter 2



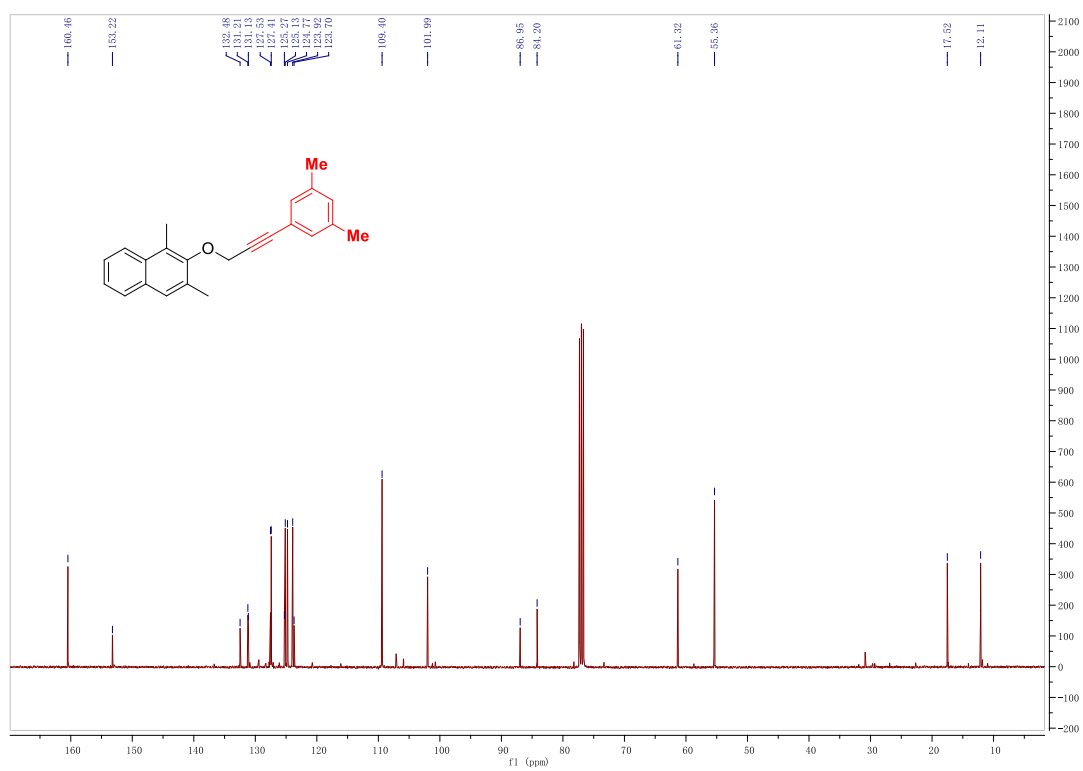
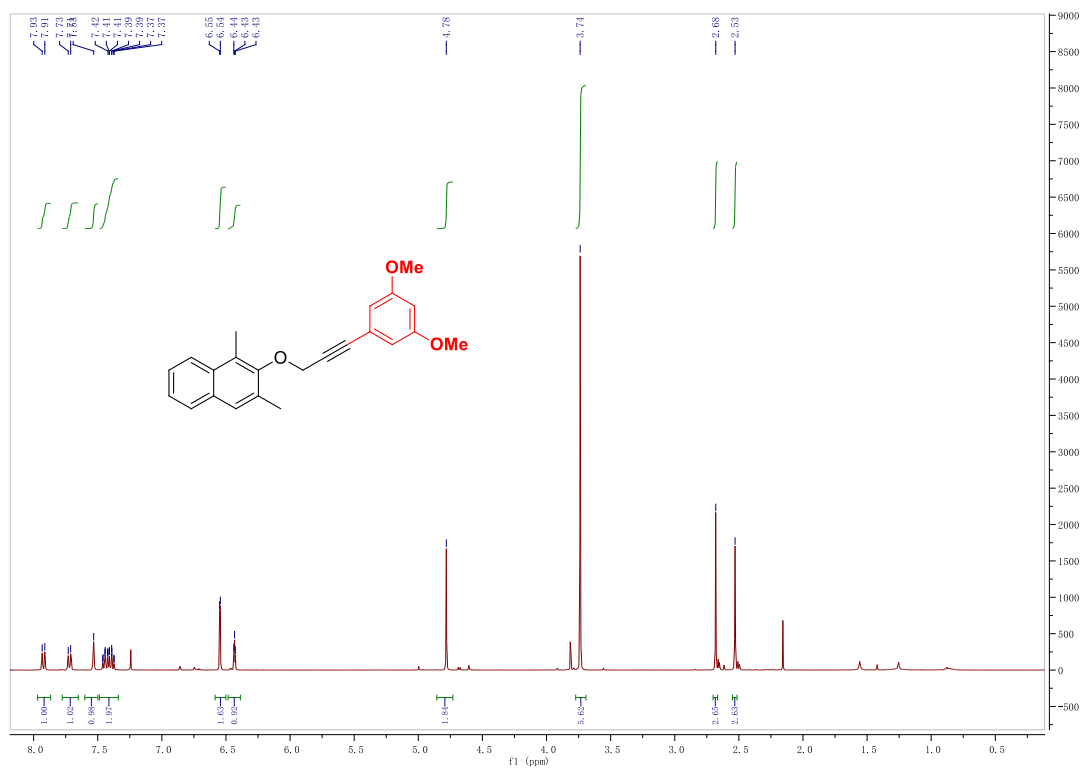
Chapter 2



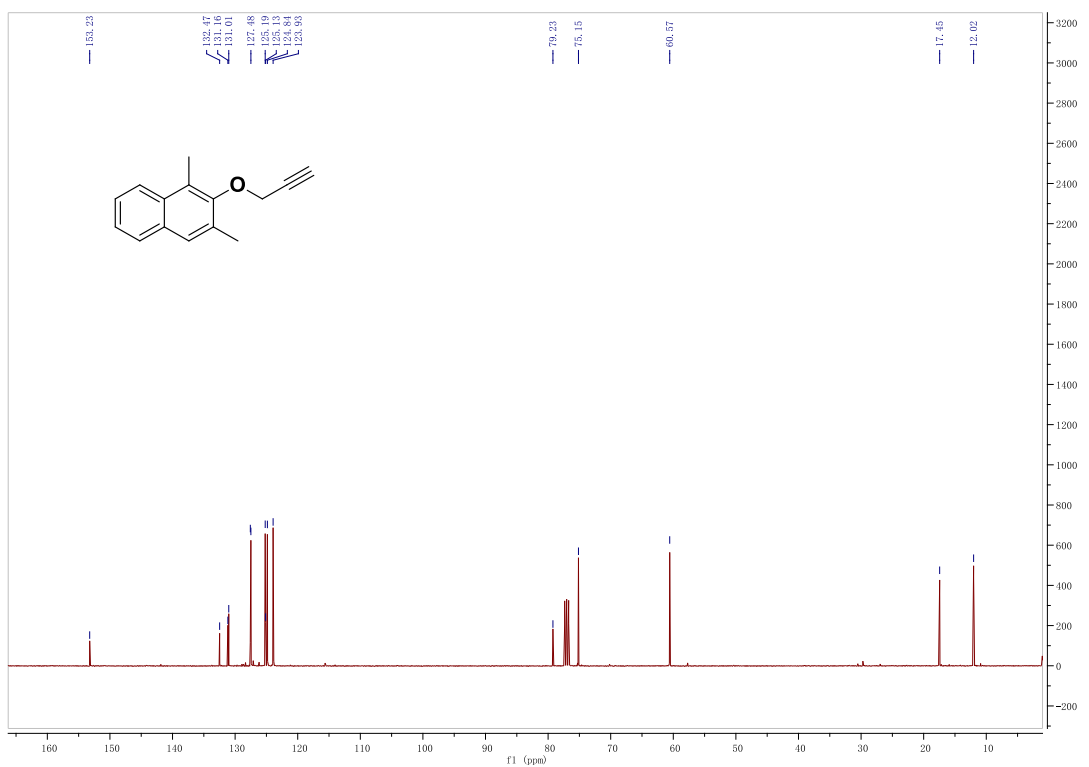
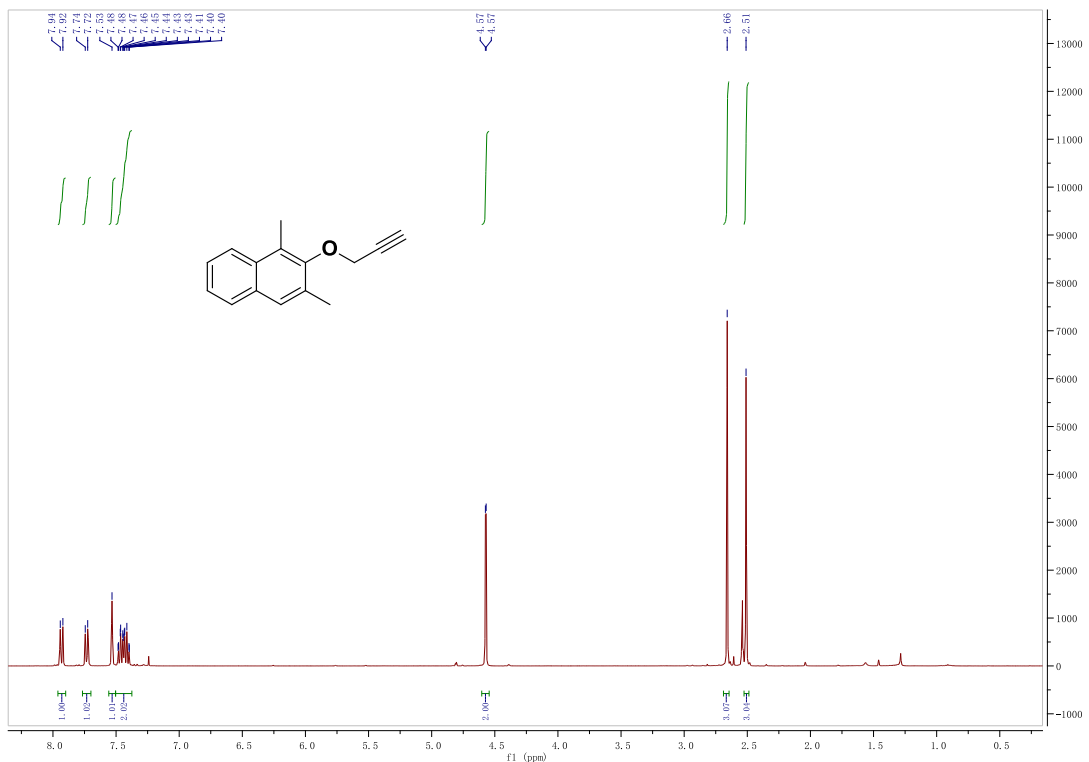
Chapter 2



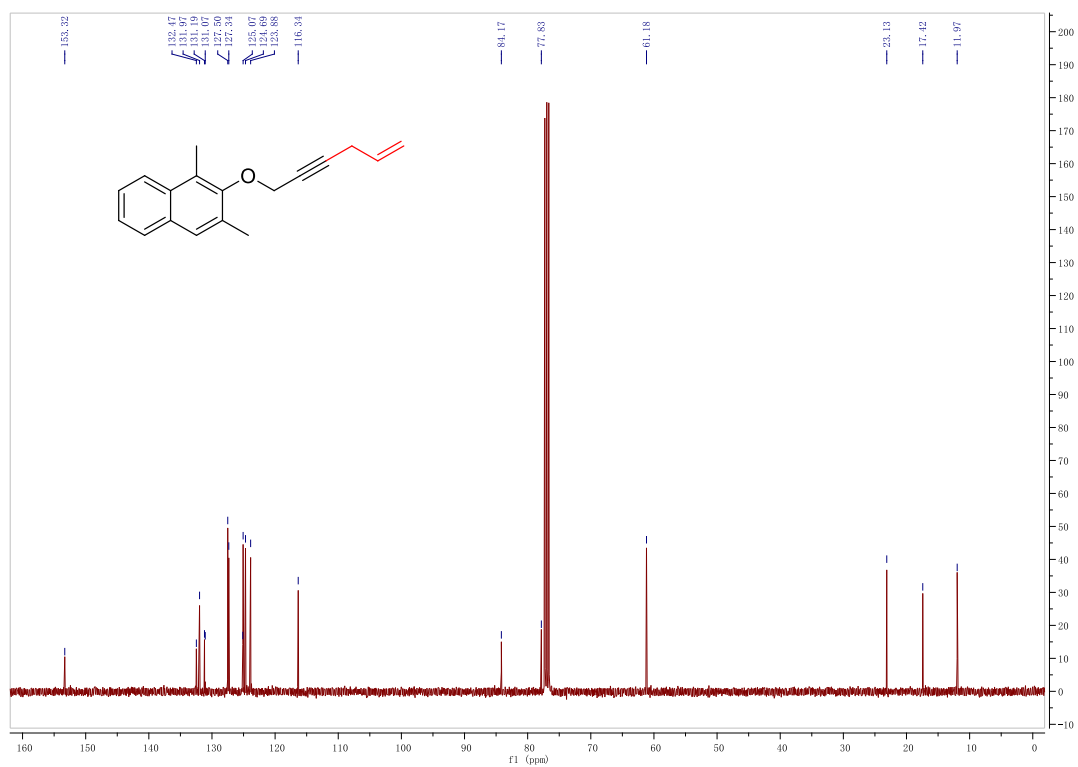
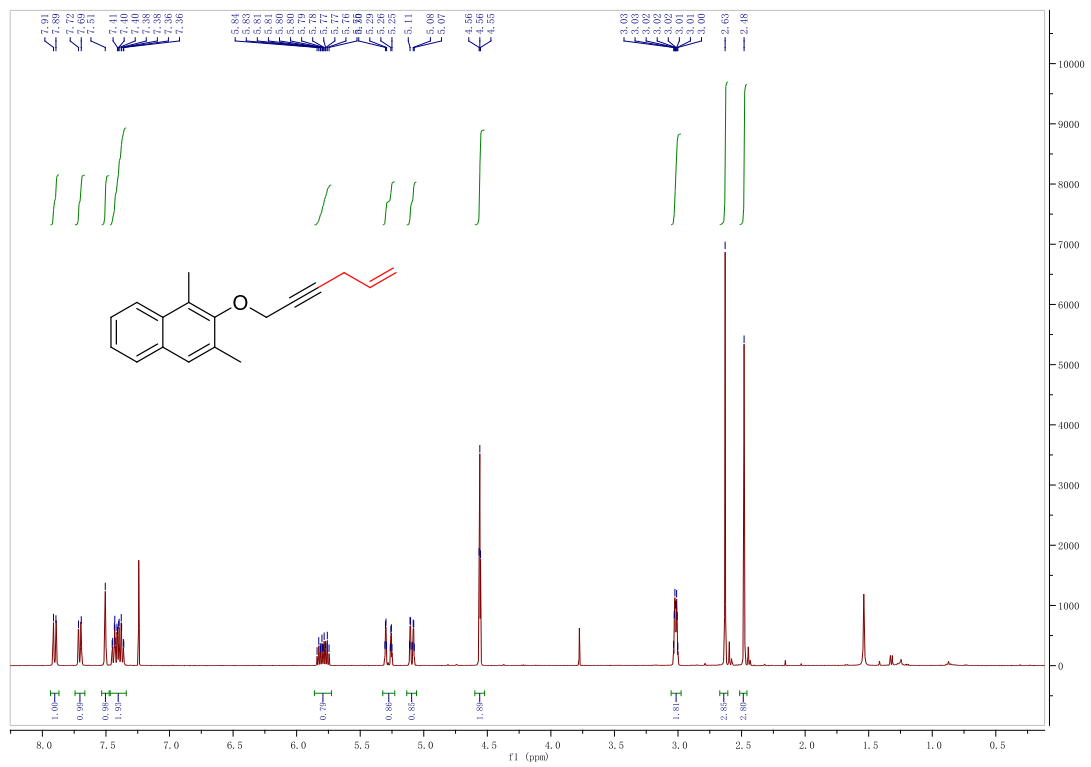
Chapter 2



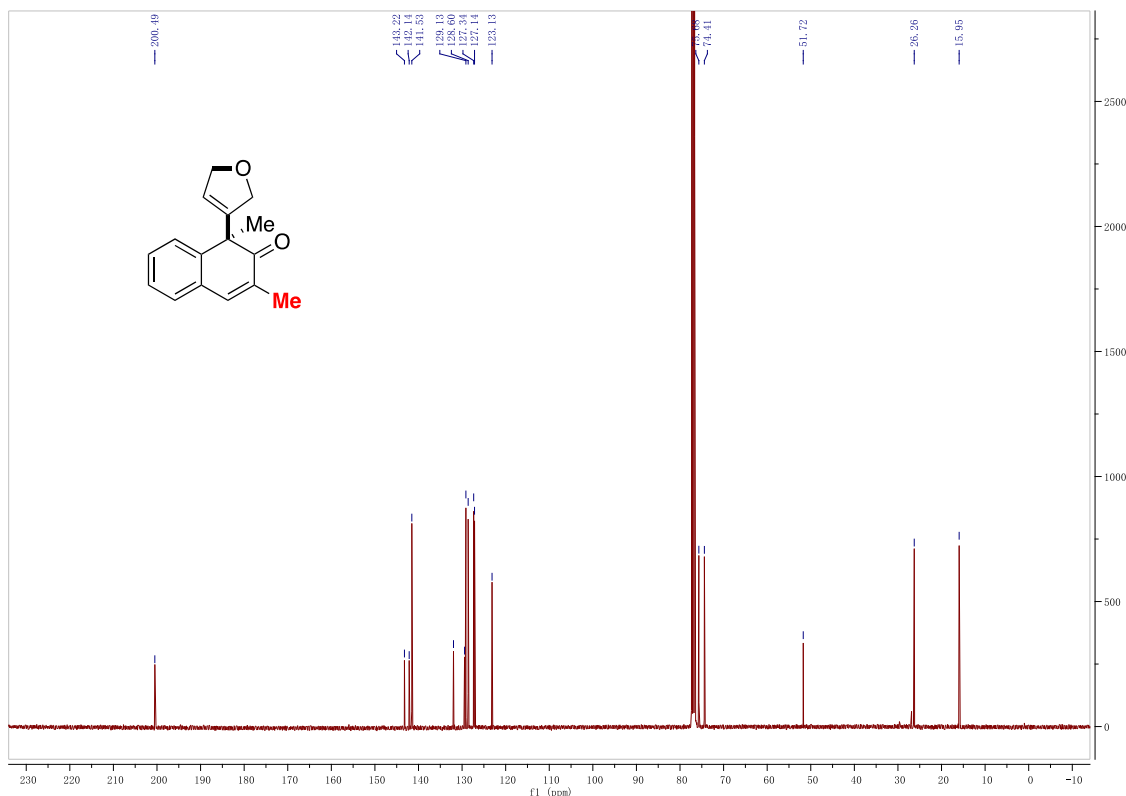
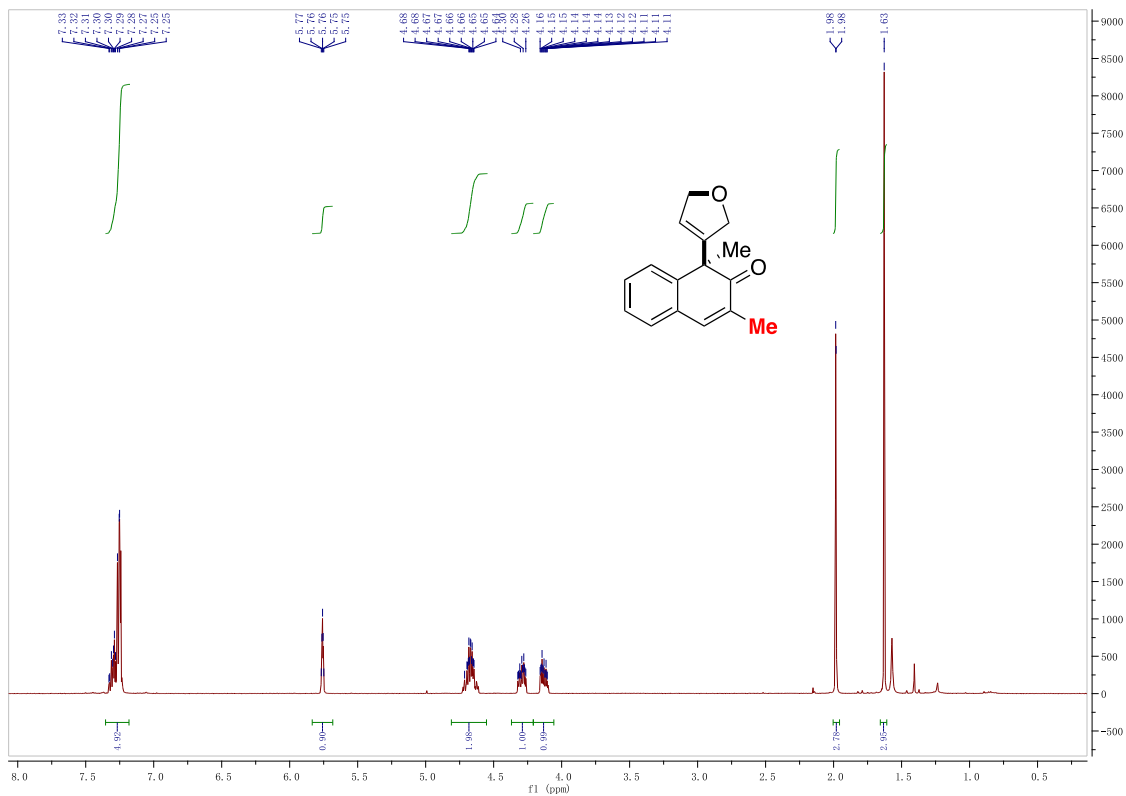
Chapter 2



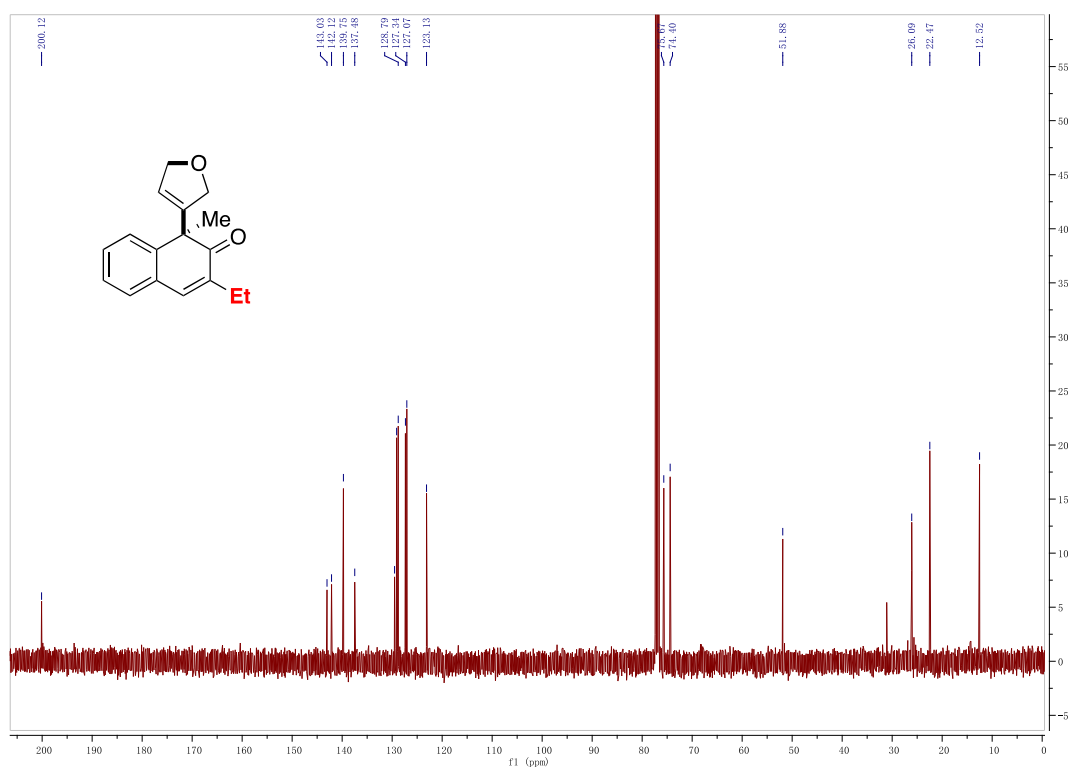
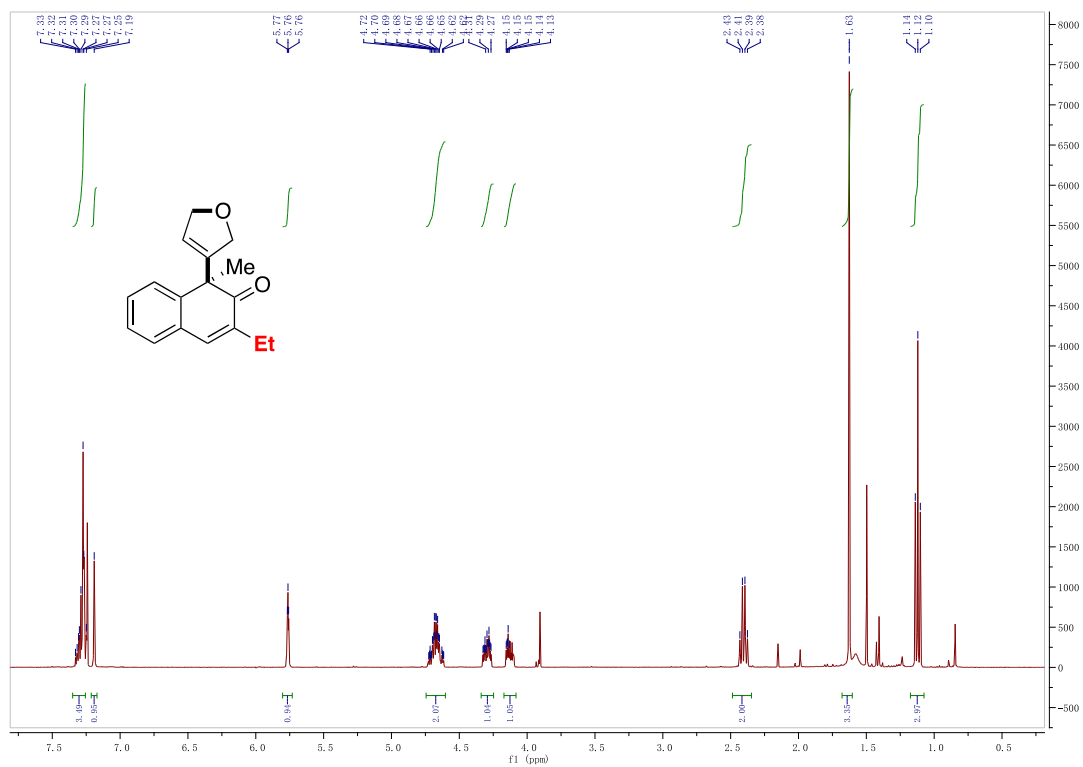
Chapter 2



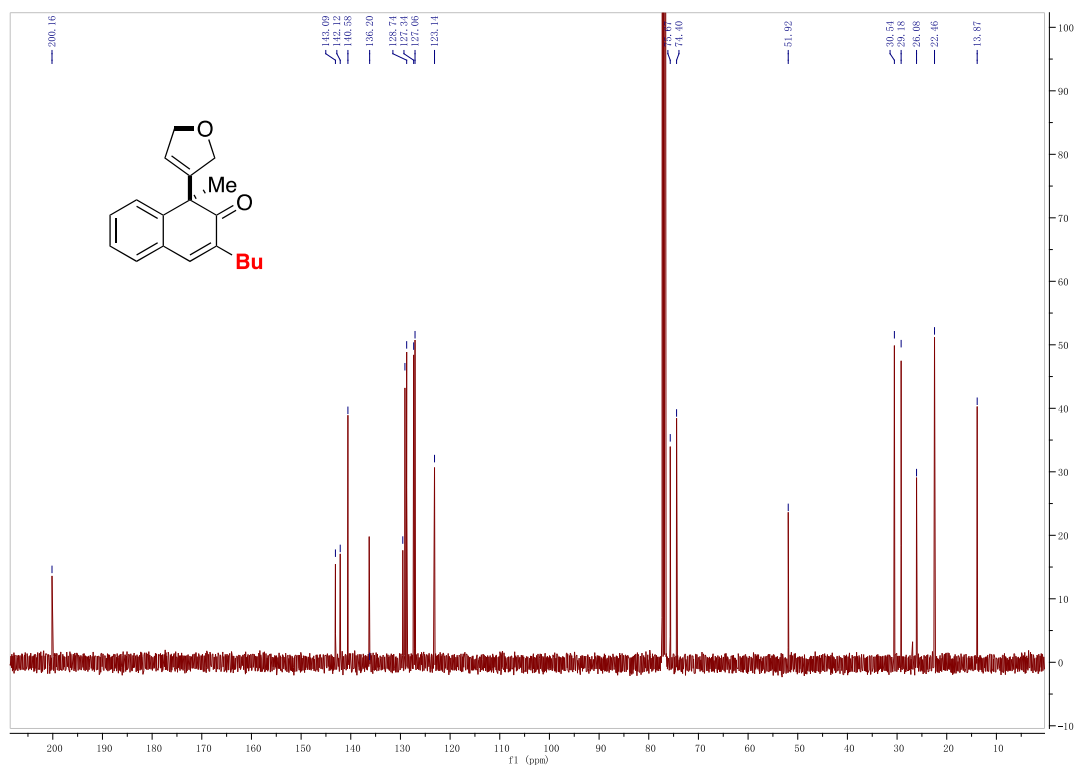
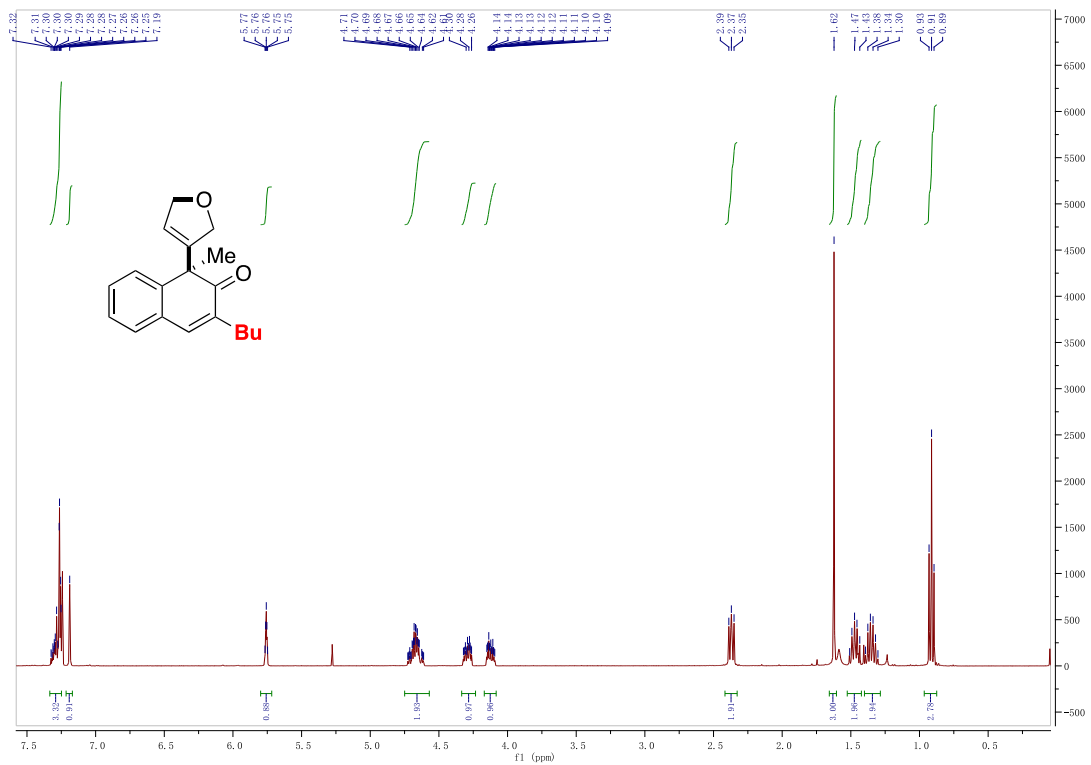
Chapter 2



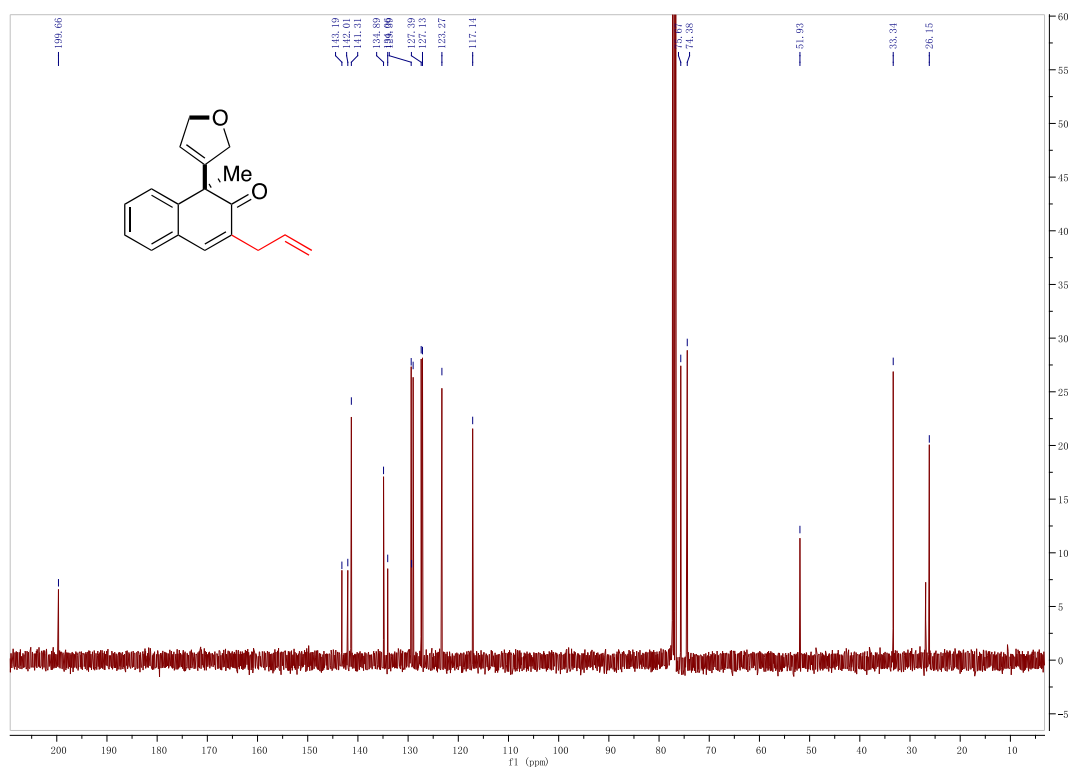
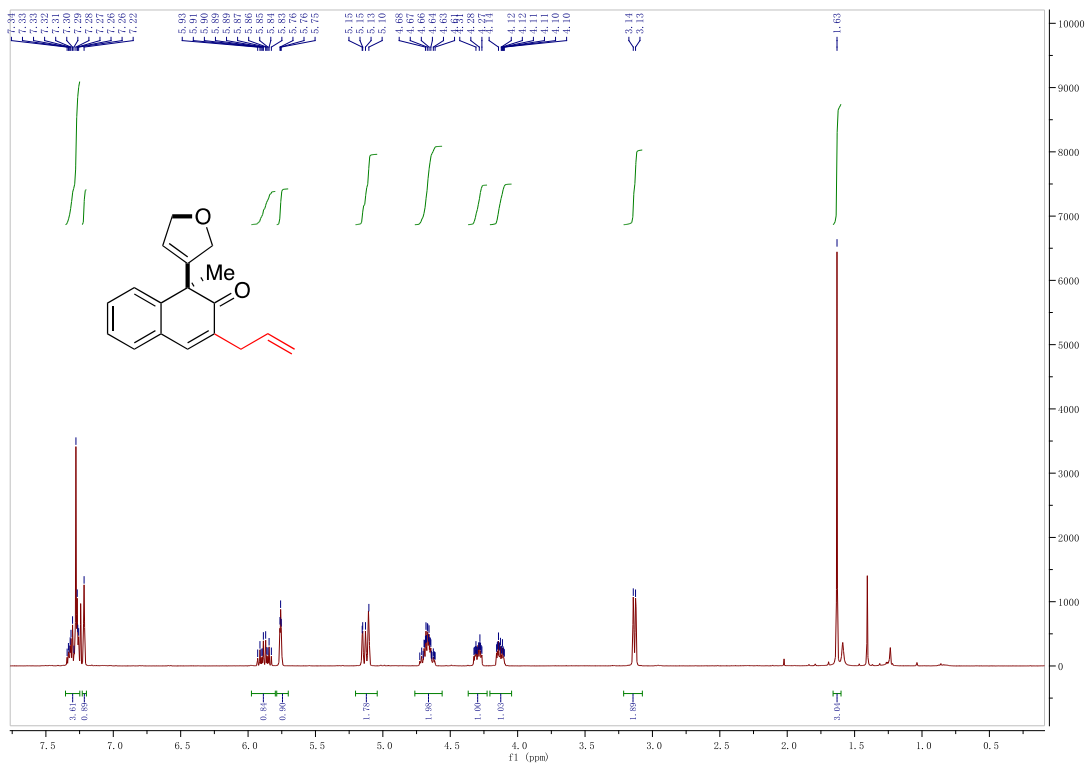
Chapter 2



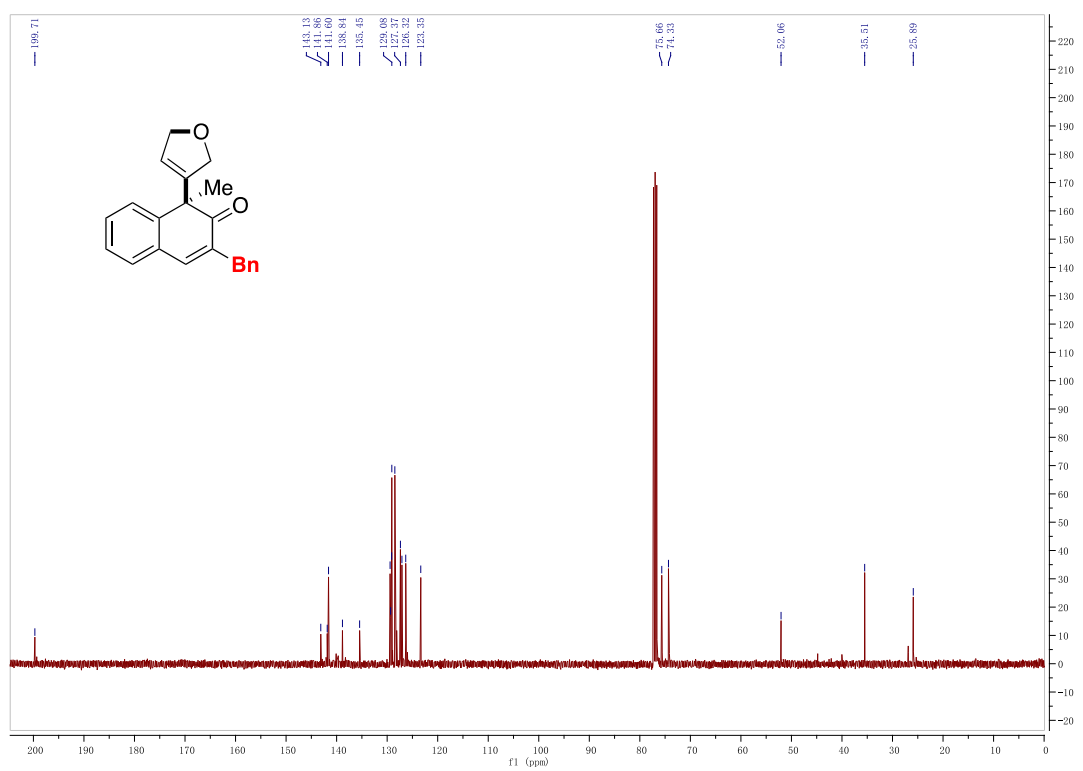
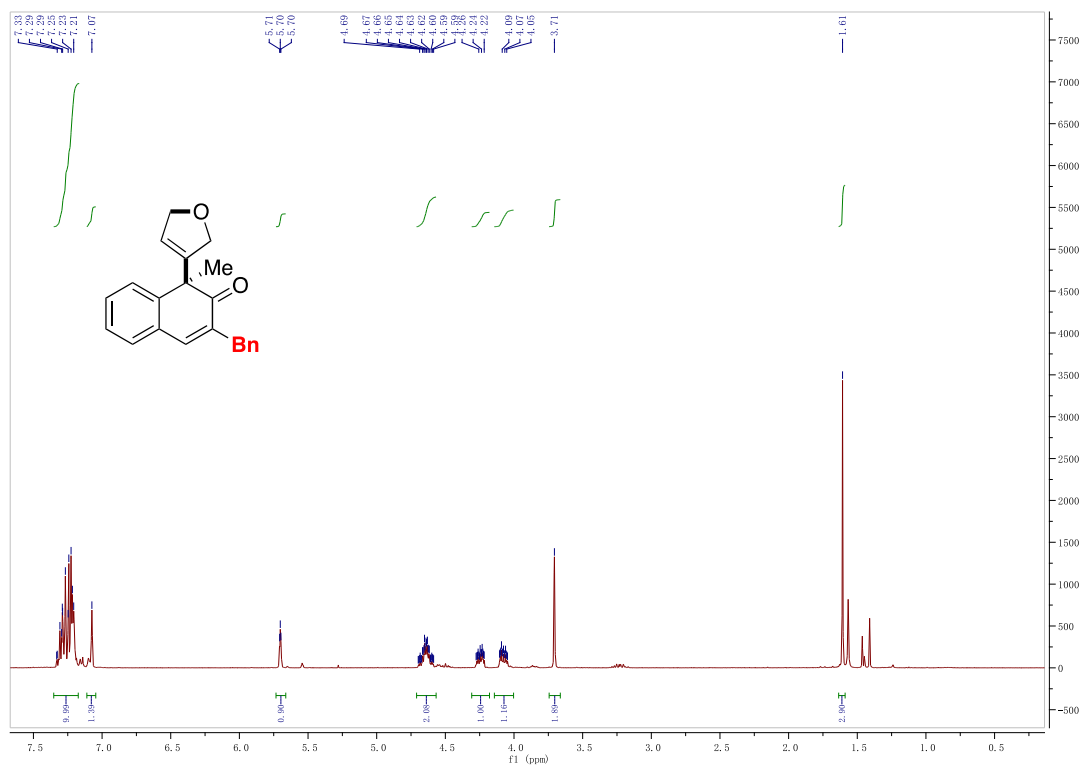
Chapter 2



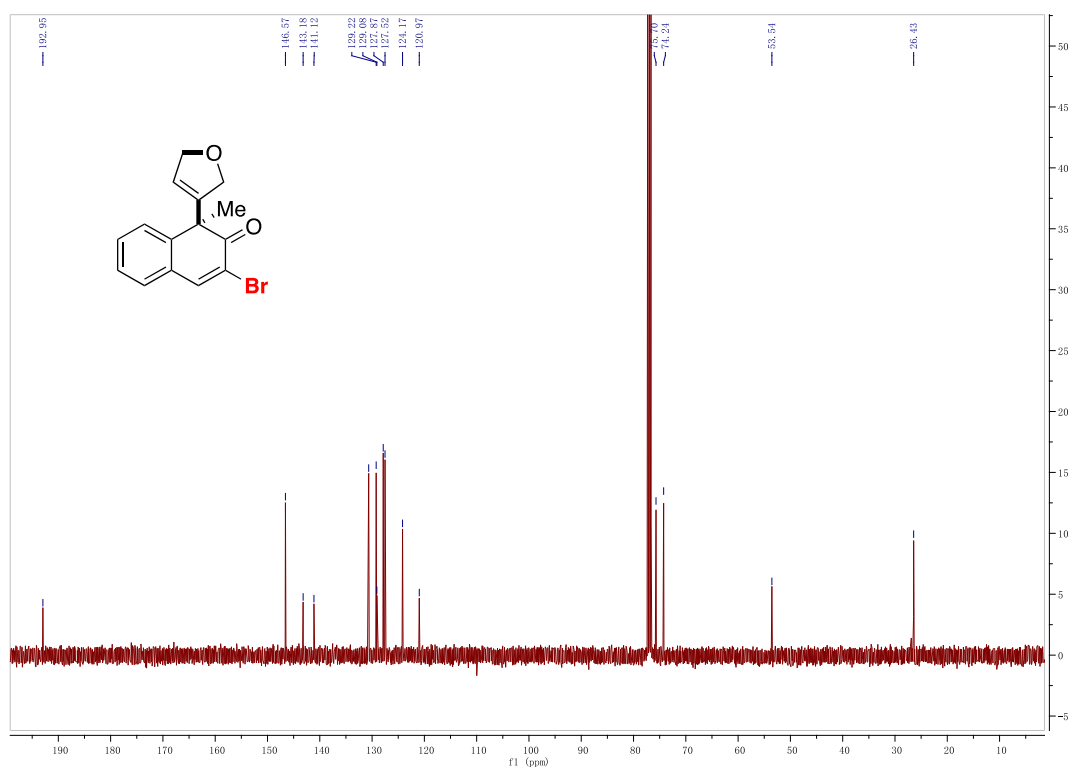
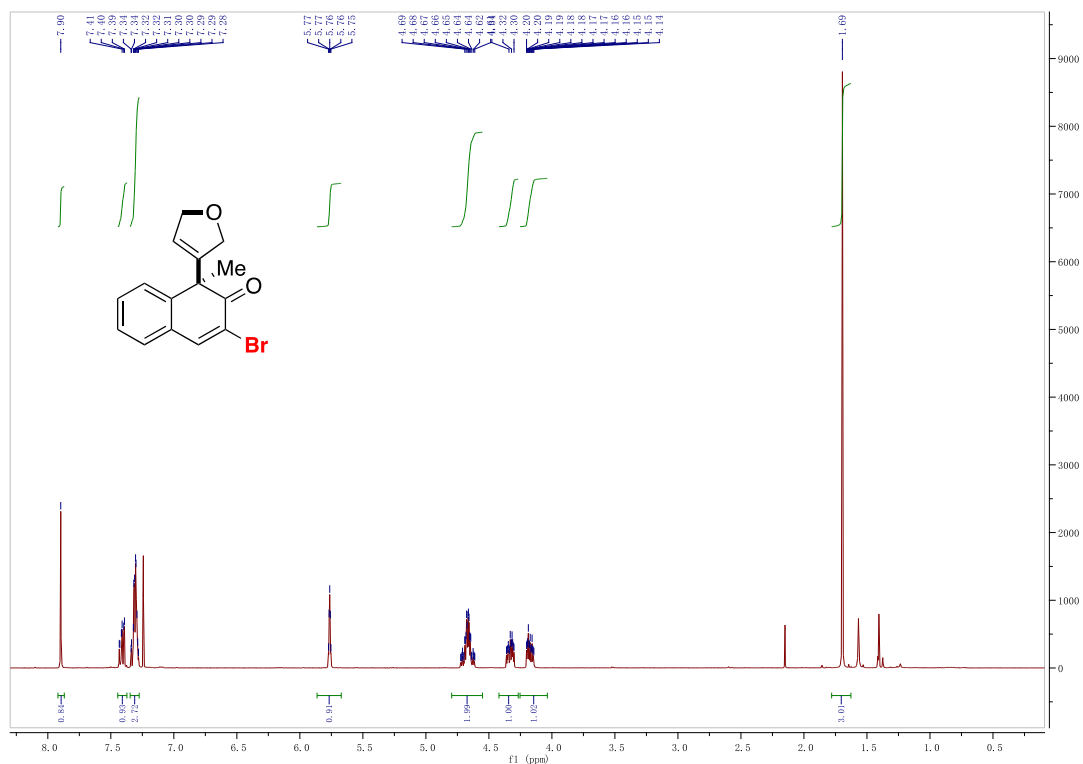
Chapter 2



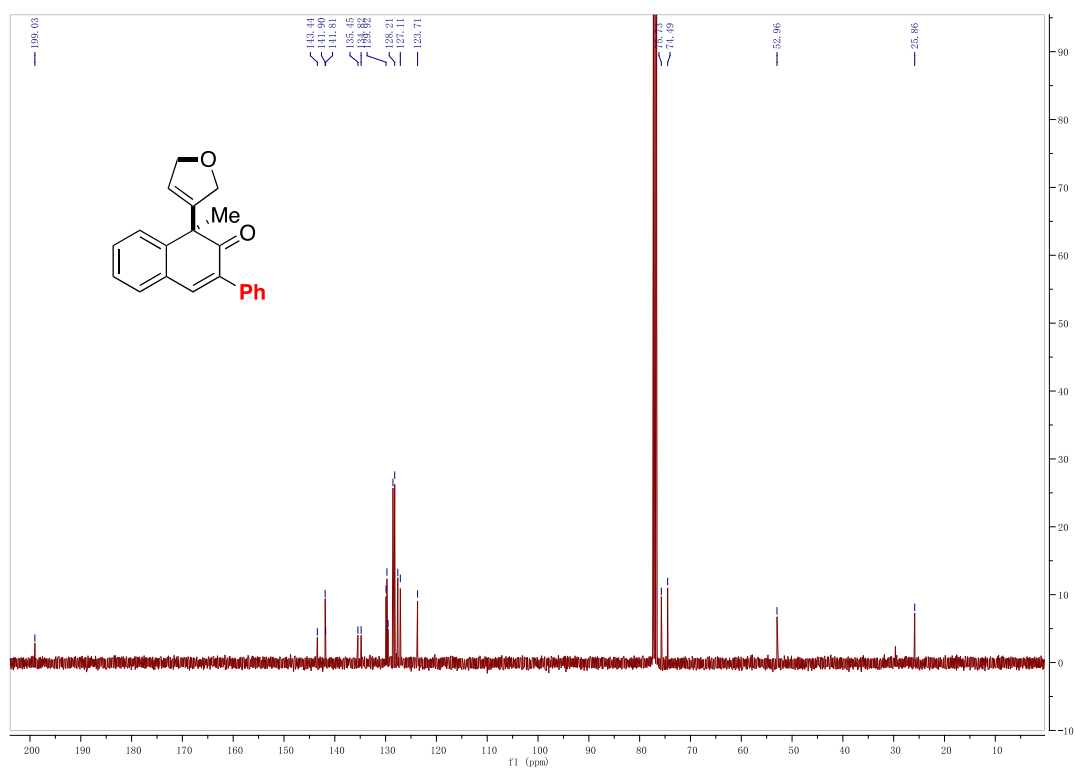
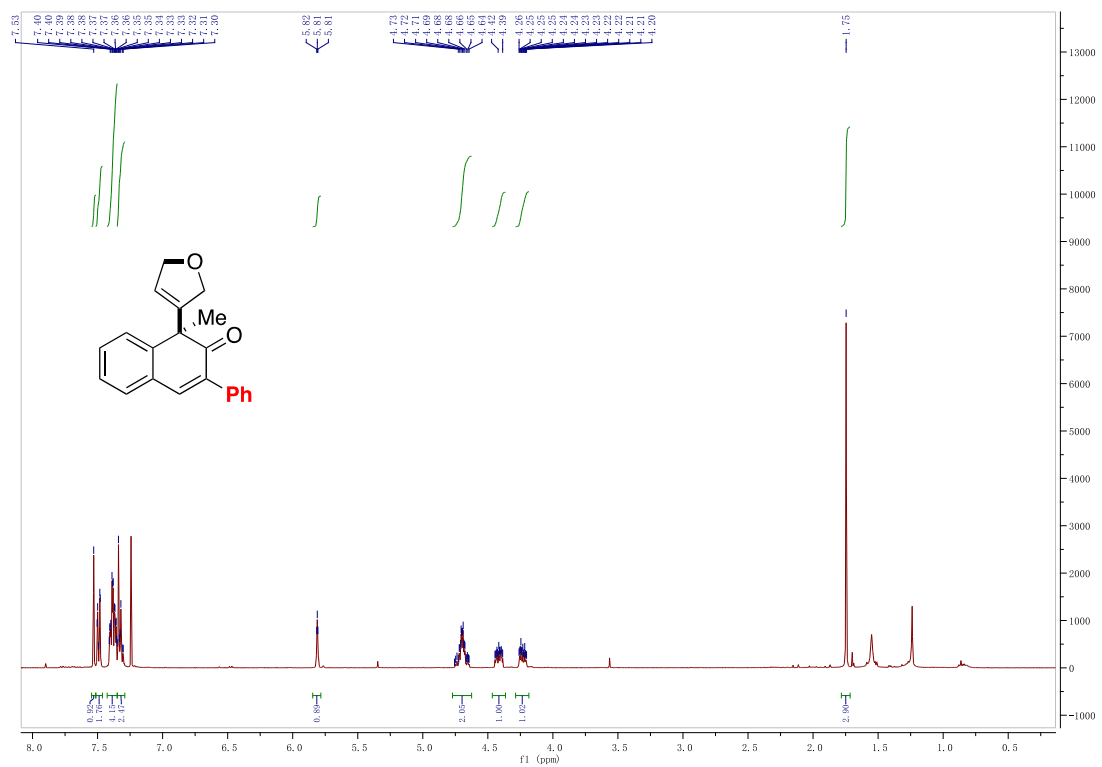
Chapter 2



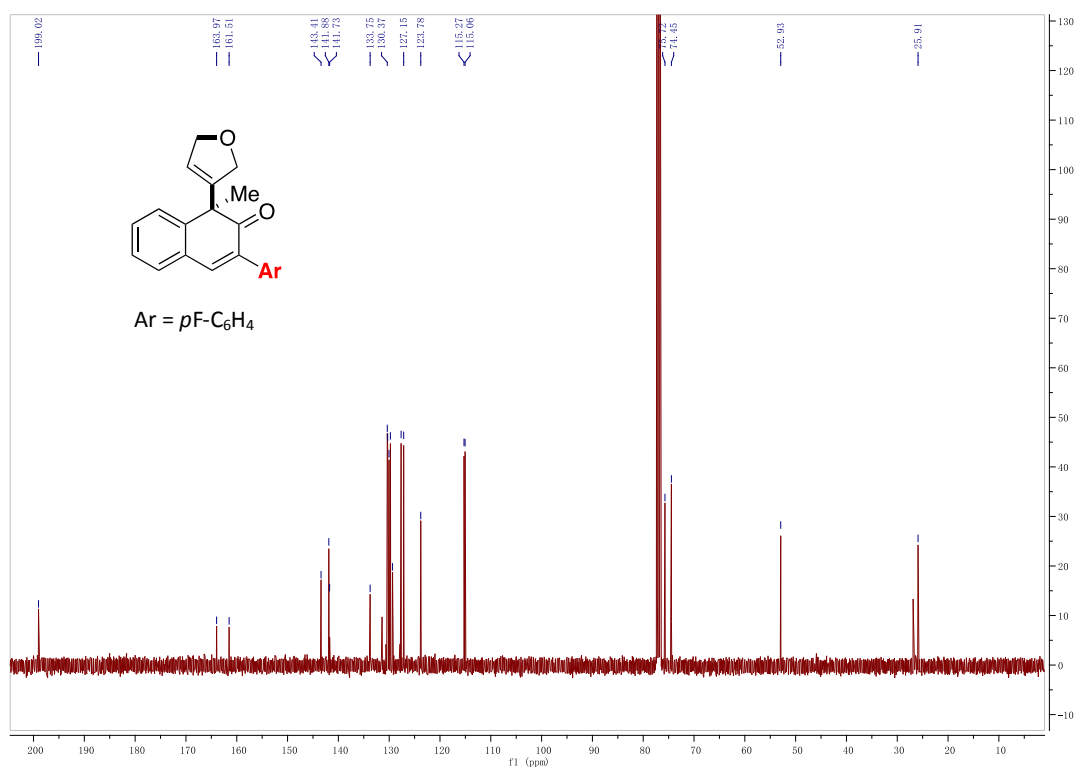
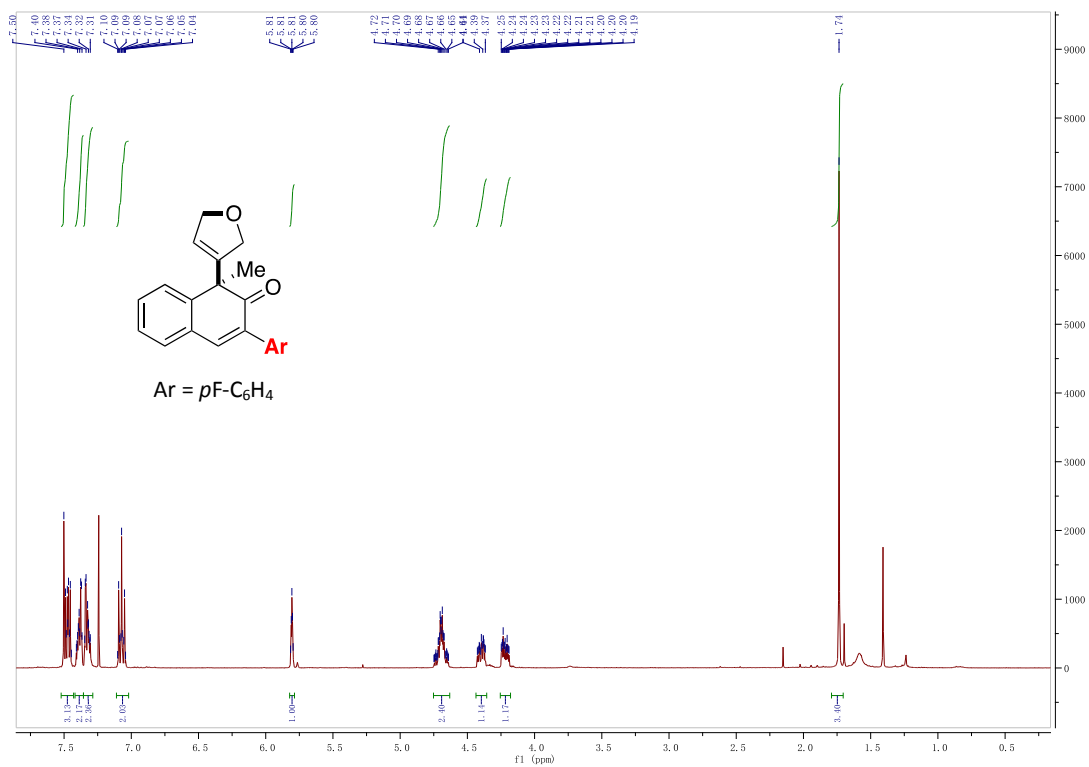
Chapter 2



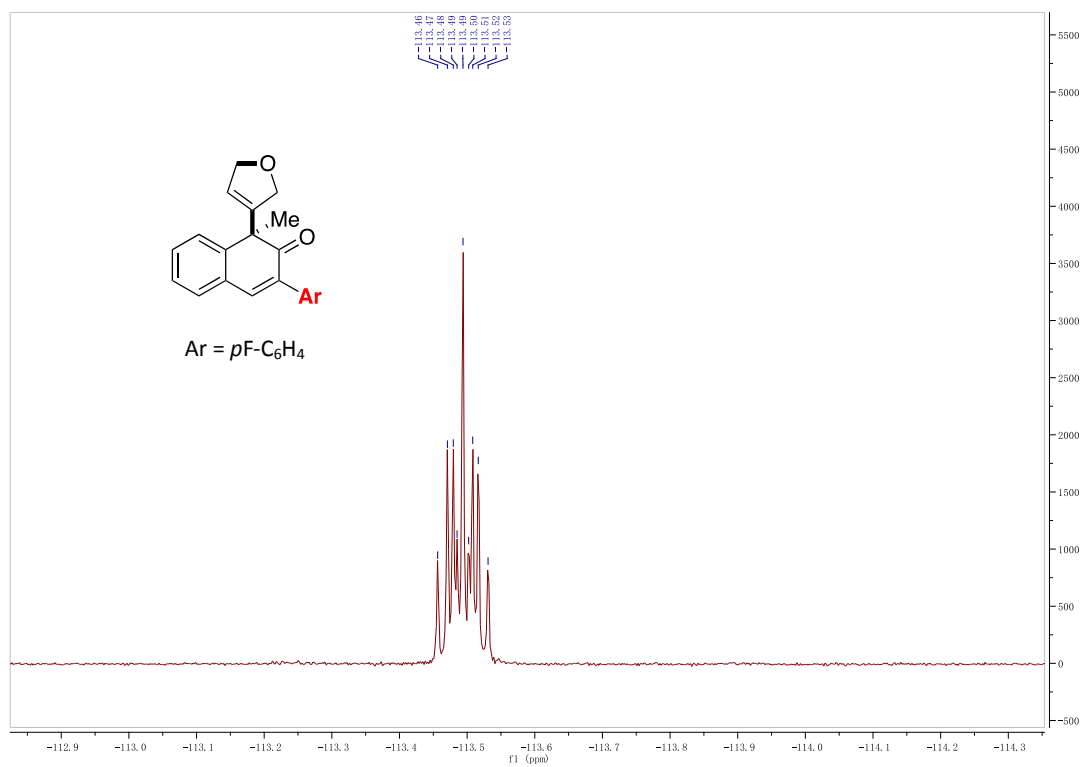
Chapter 2



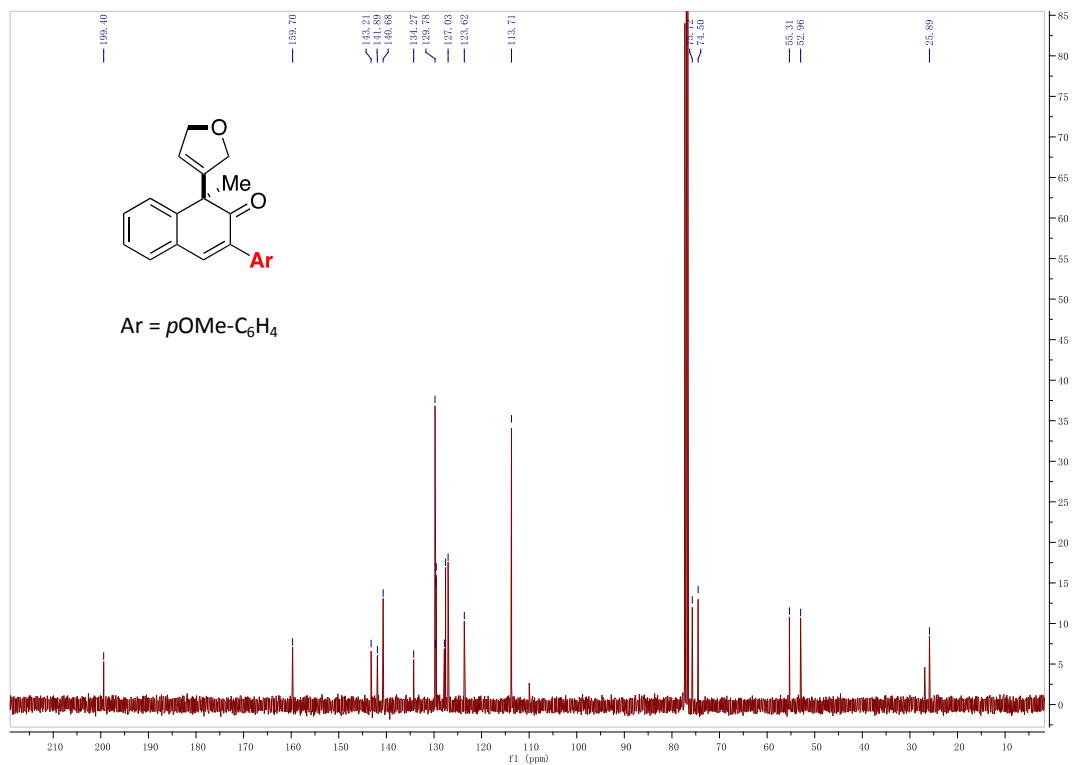
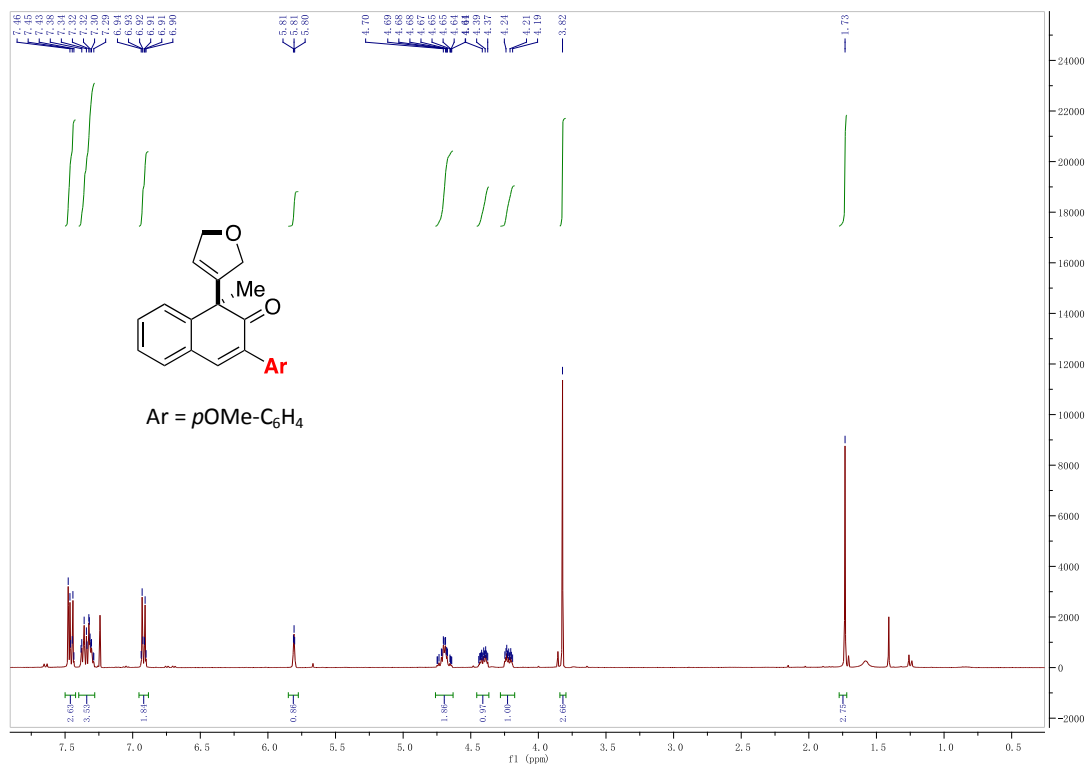
Chapter 2



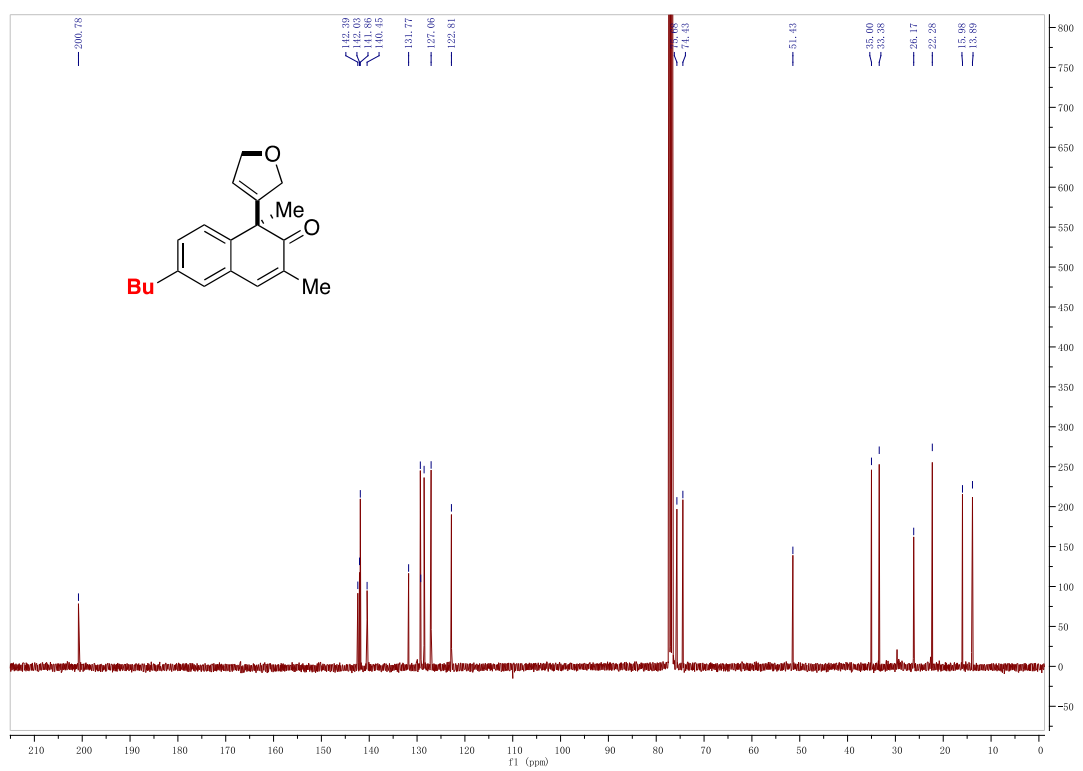
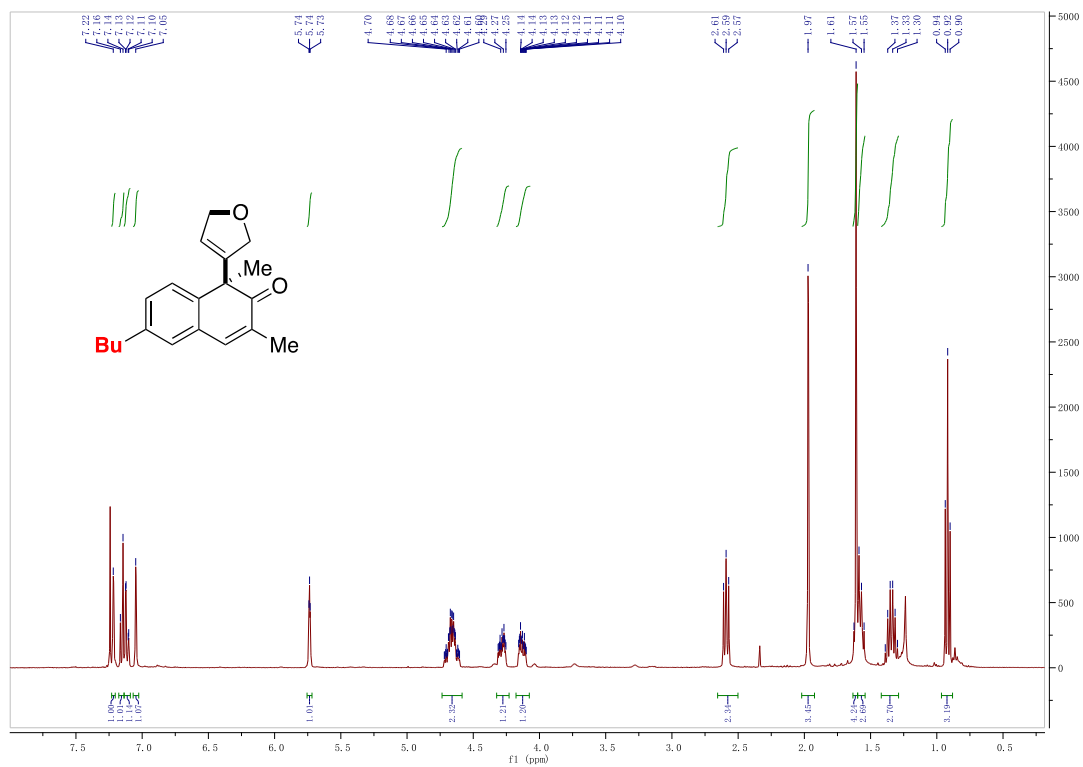
Chapter 2



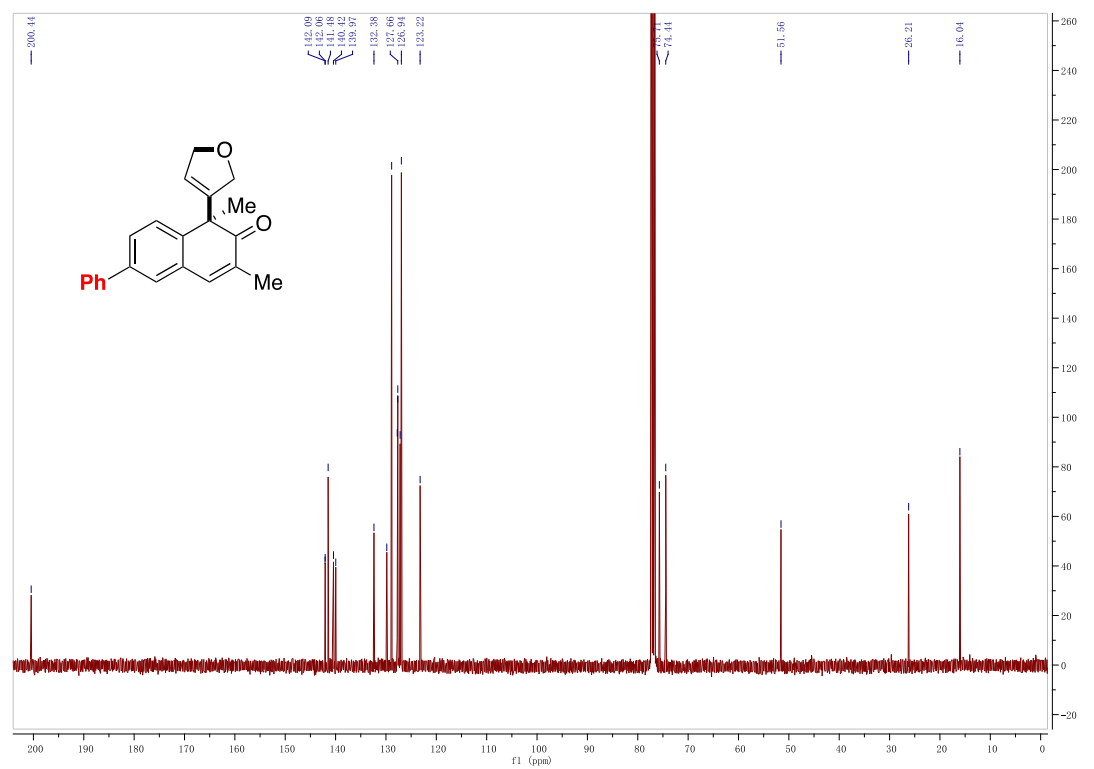
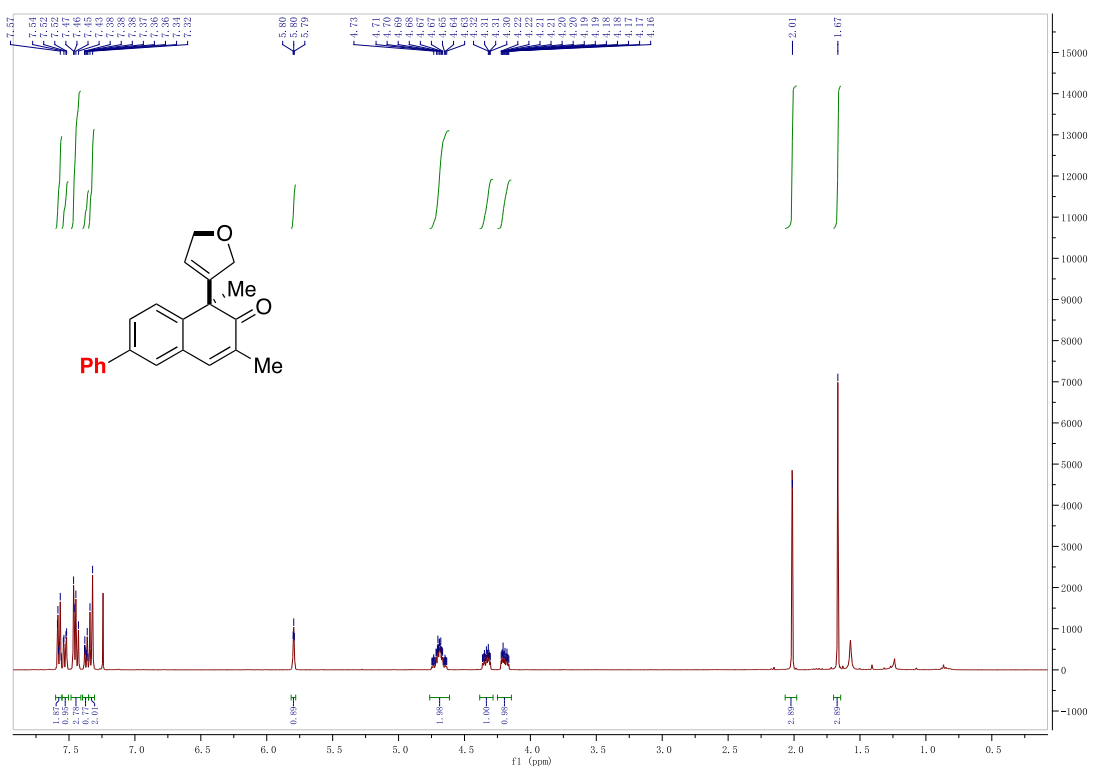
Chapter 2



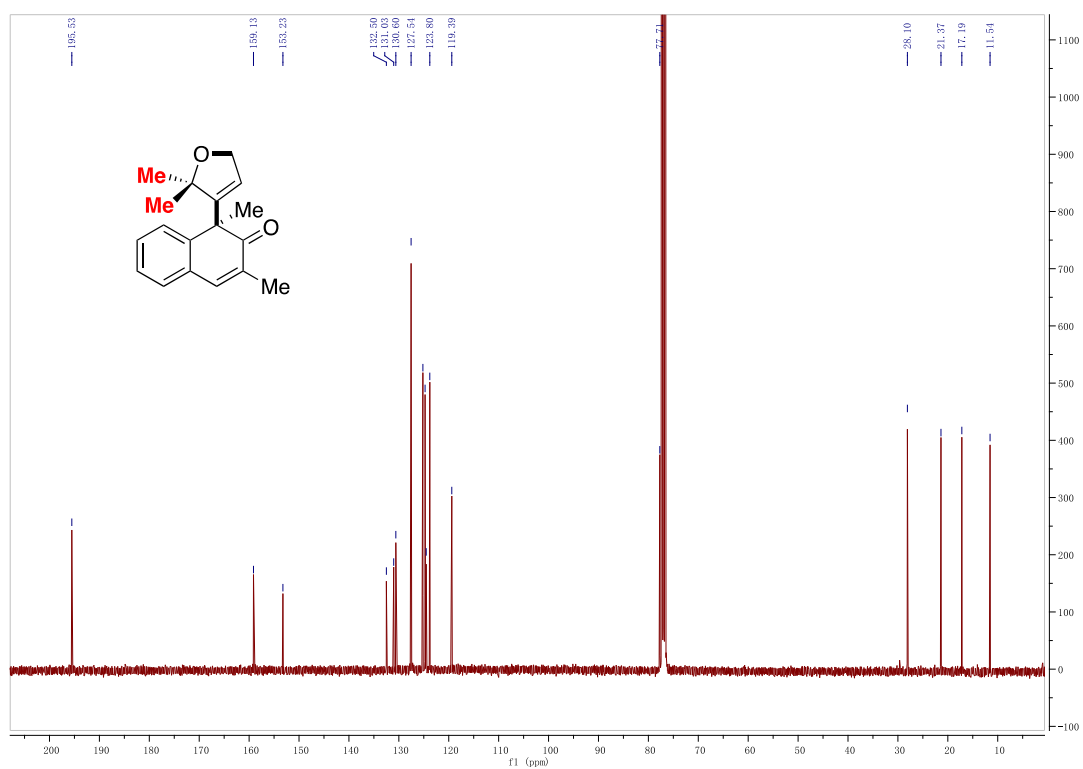
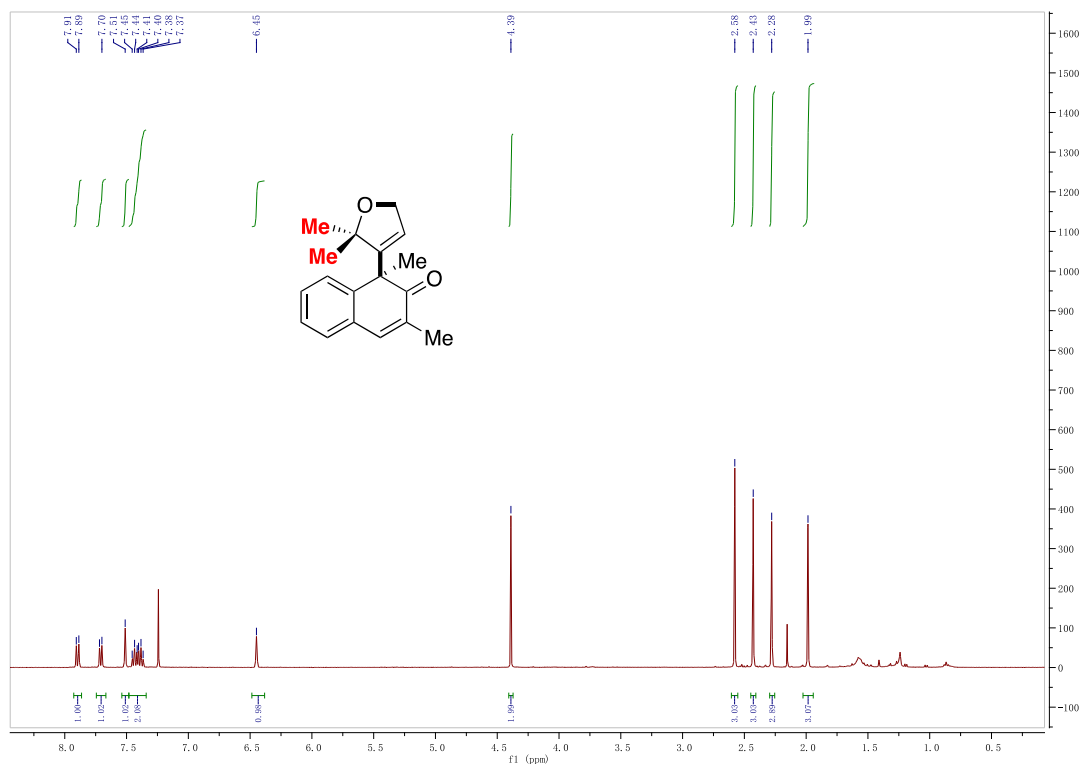
Chapter 2



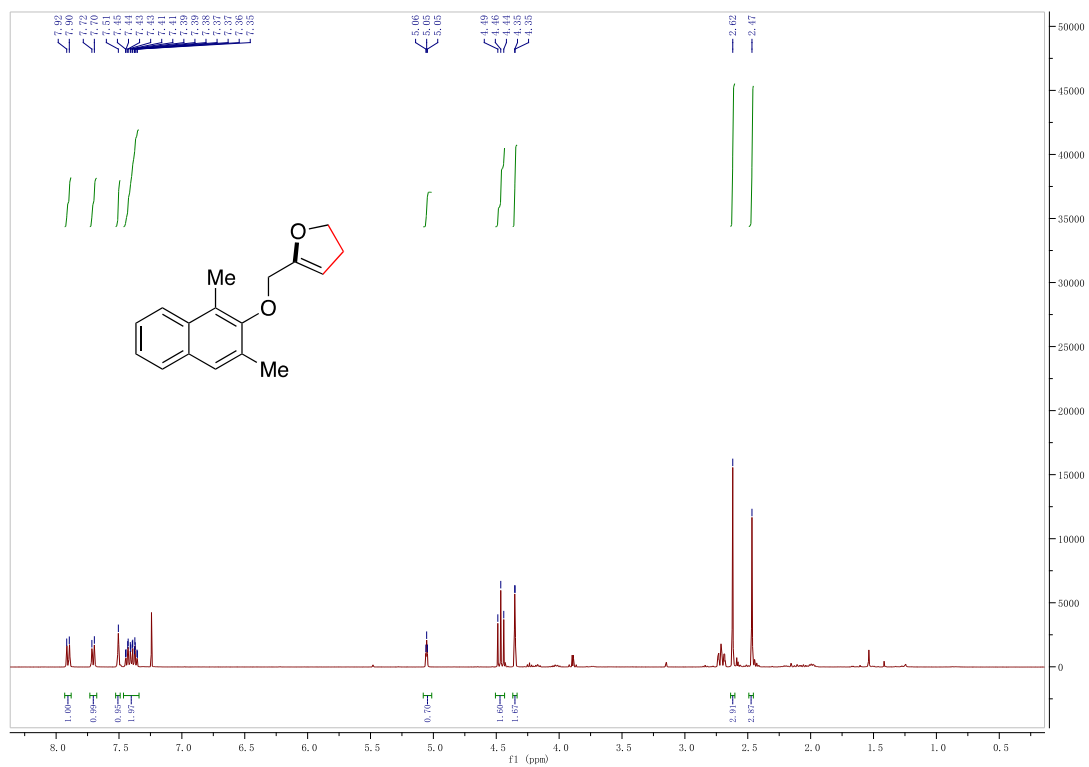
Chapter 2



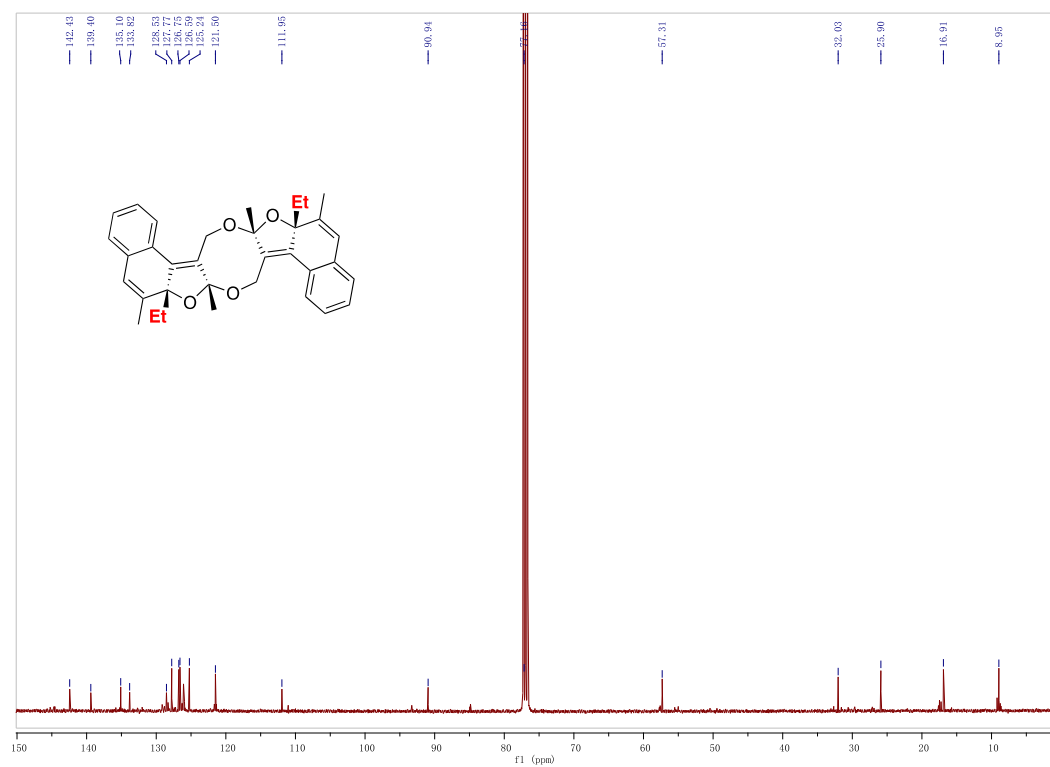
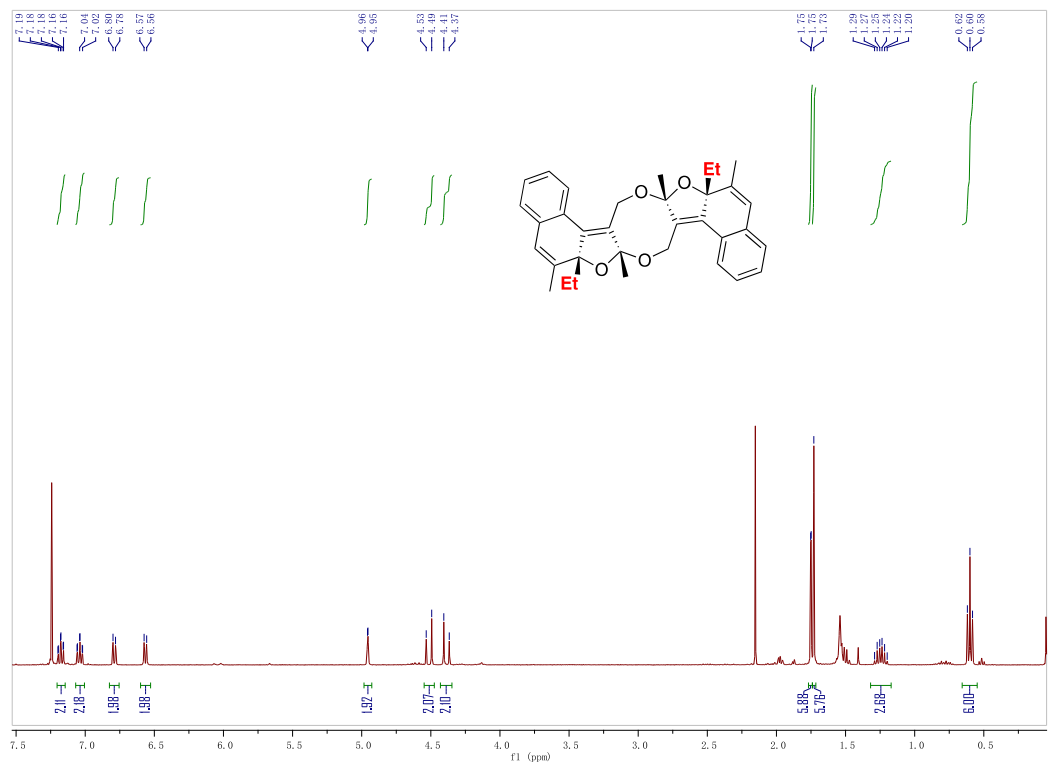
Chapter 2



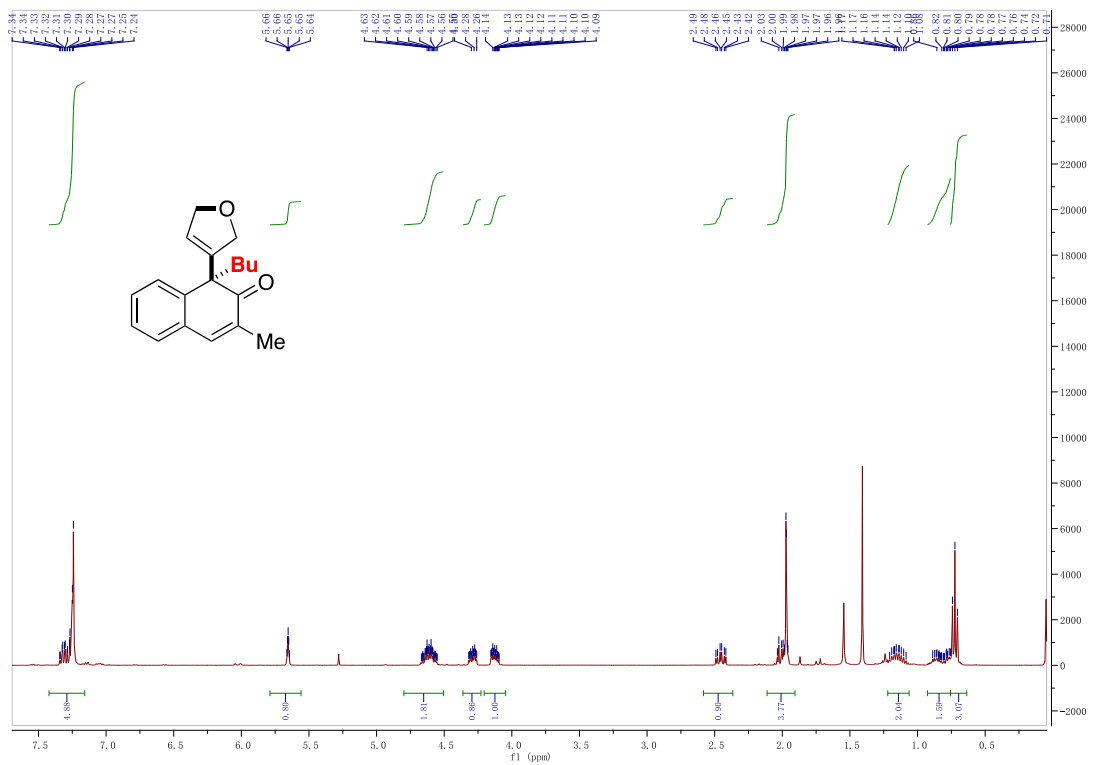
Chapter 2



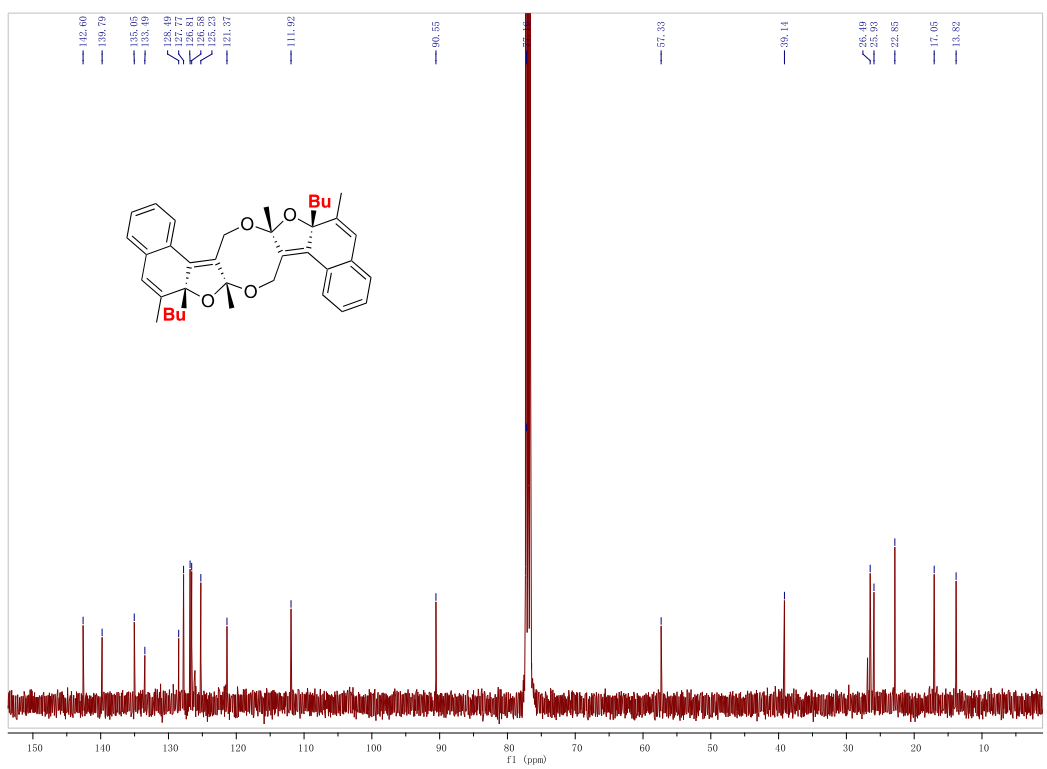
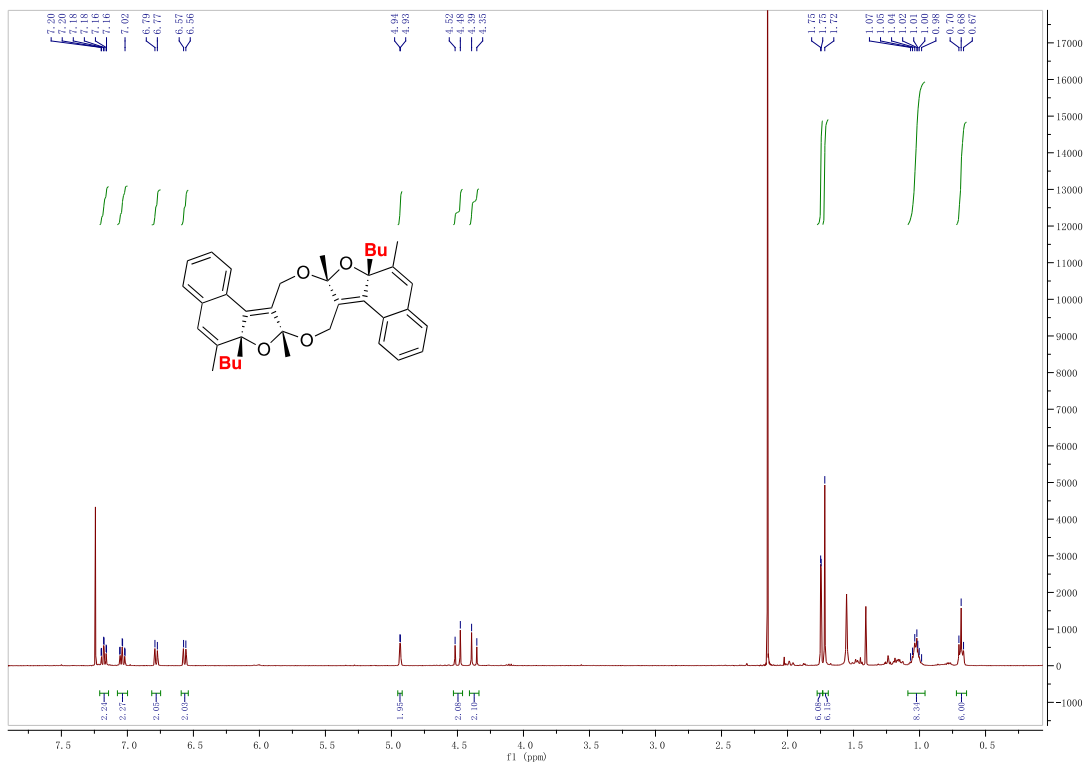
Chapter 2



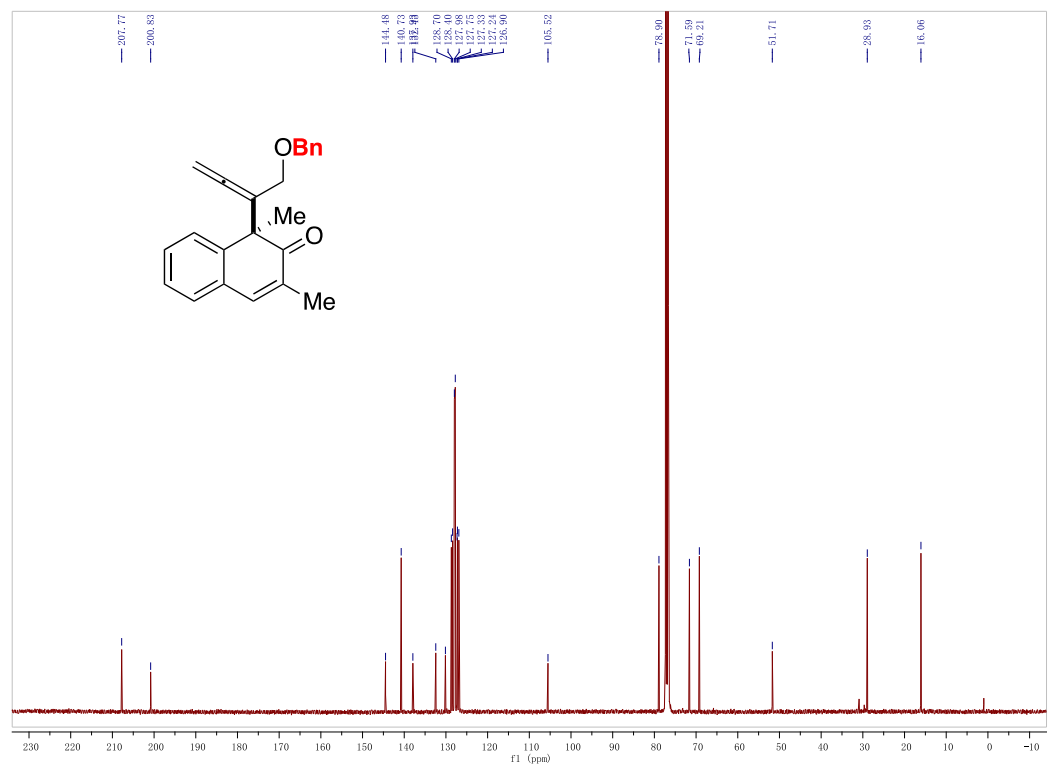
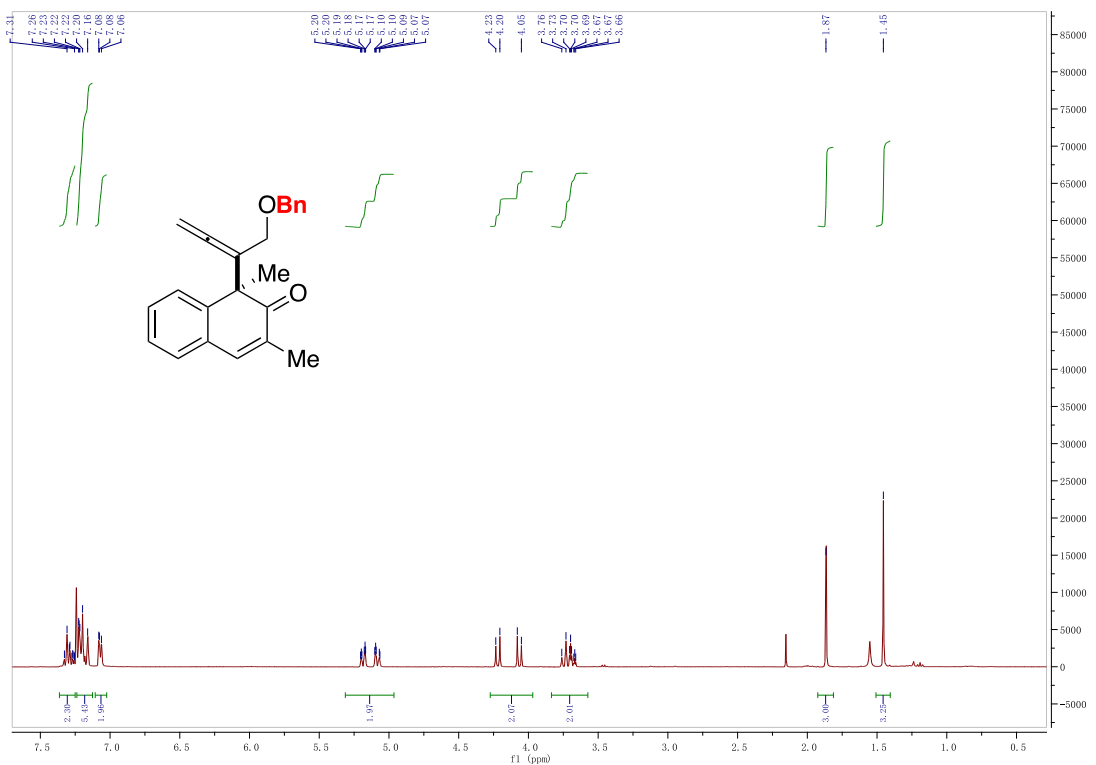
Chapter 2



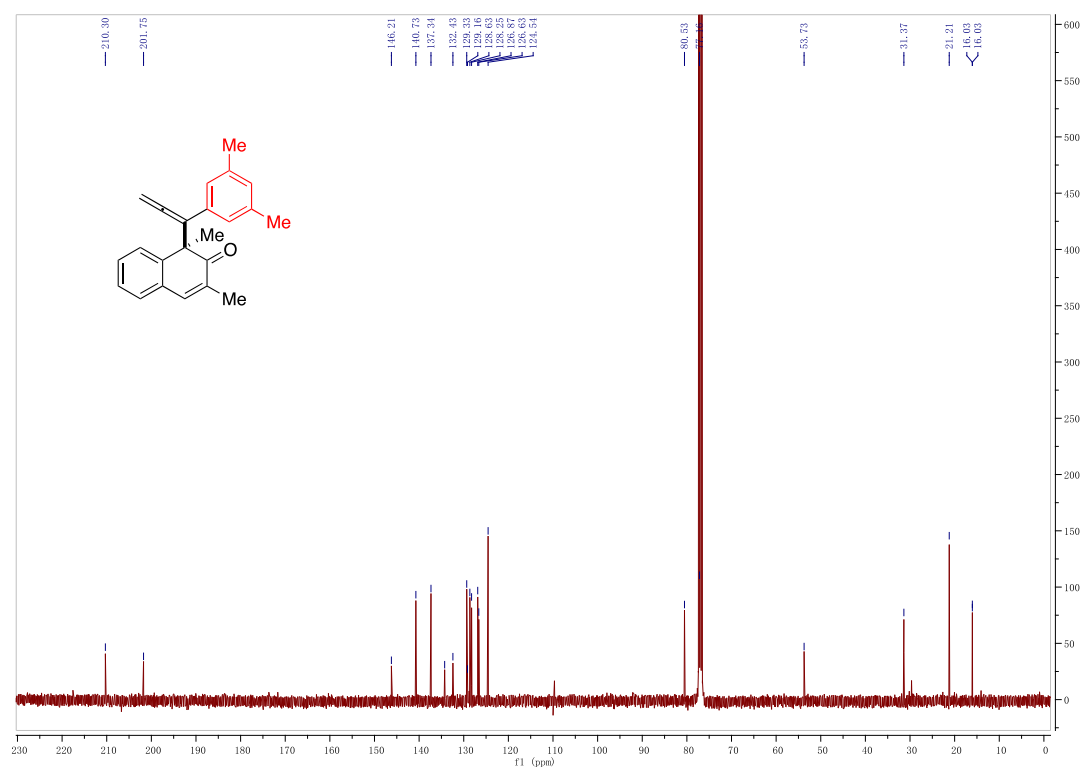
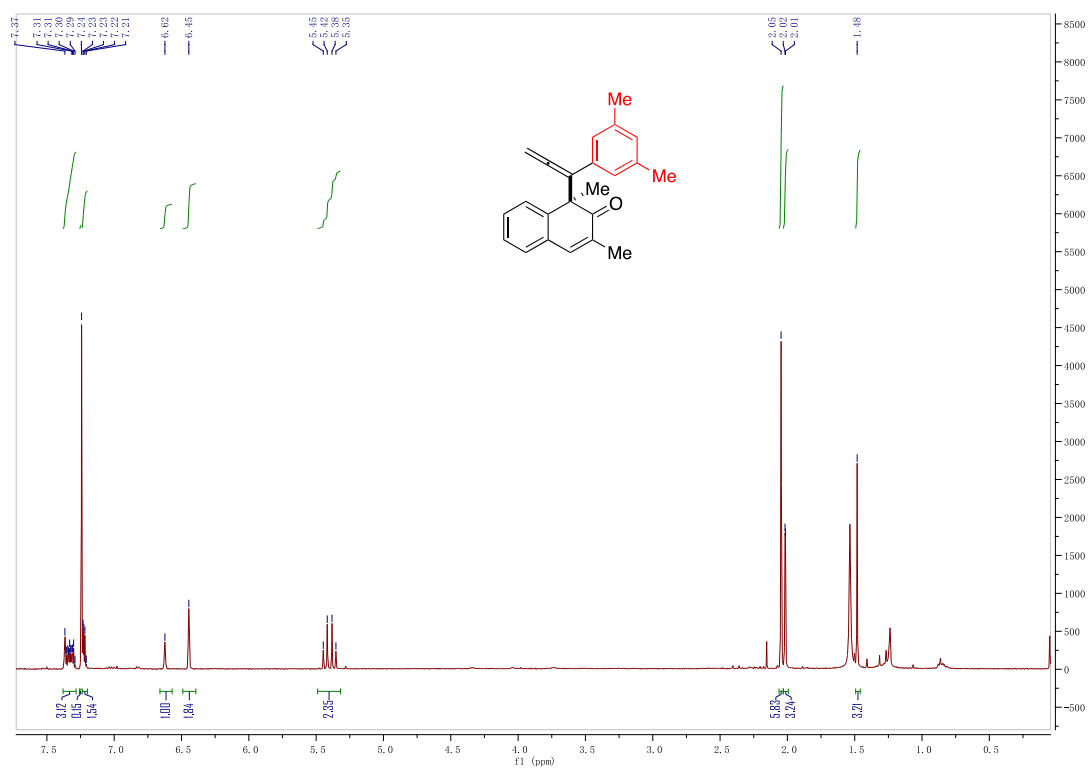
Chapter 2



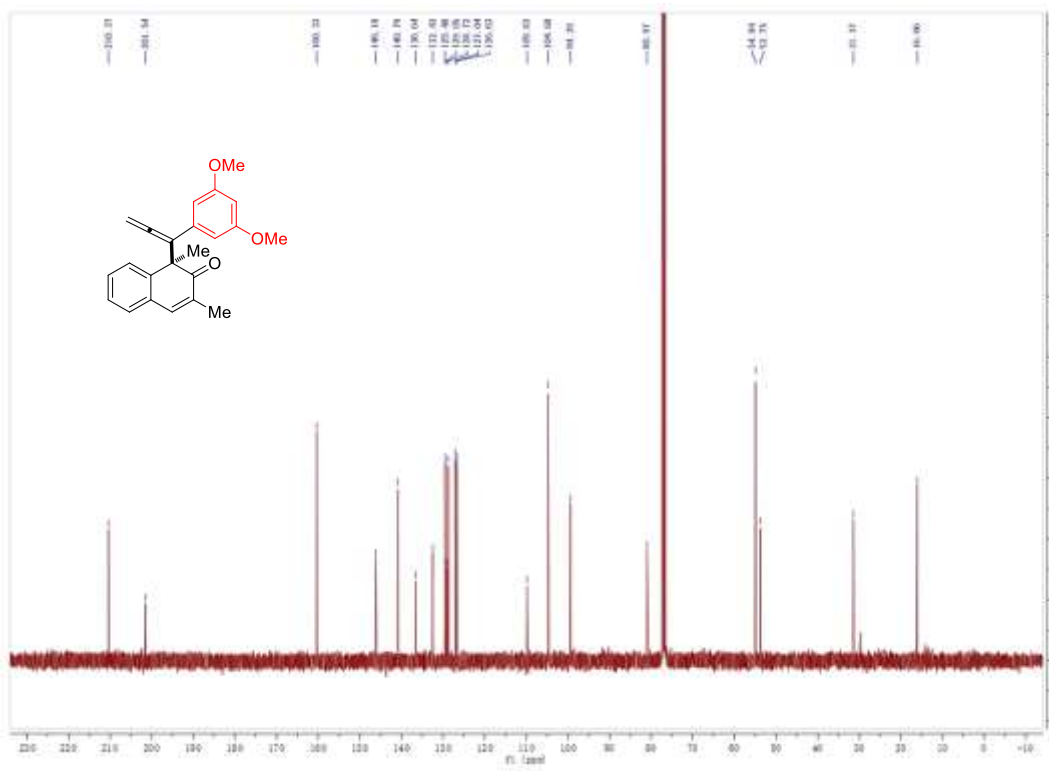
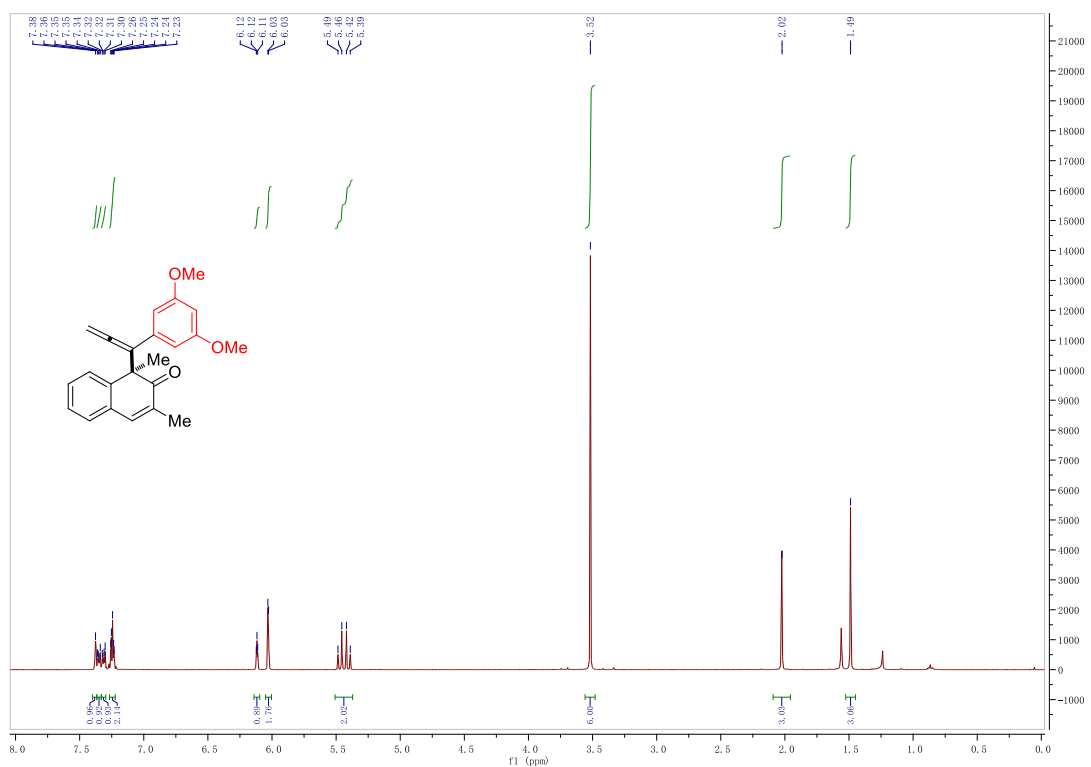
Chapter 2



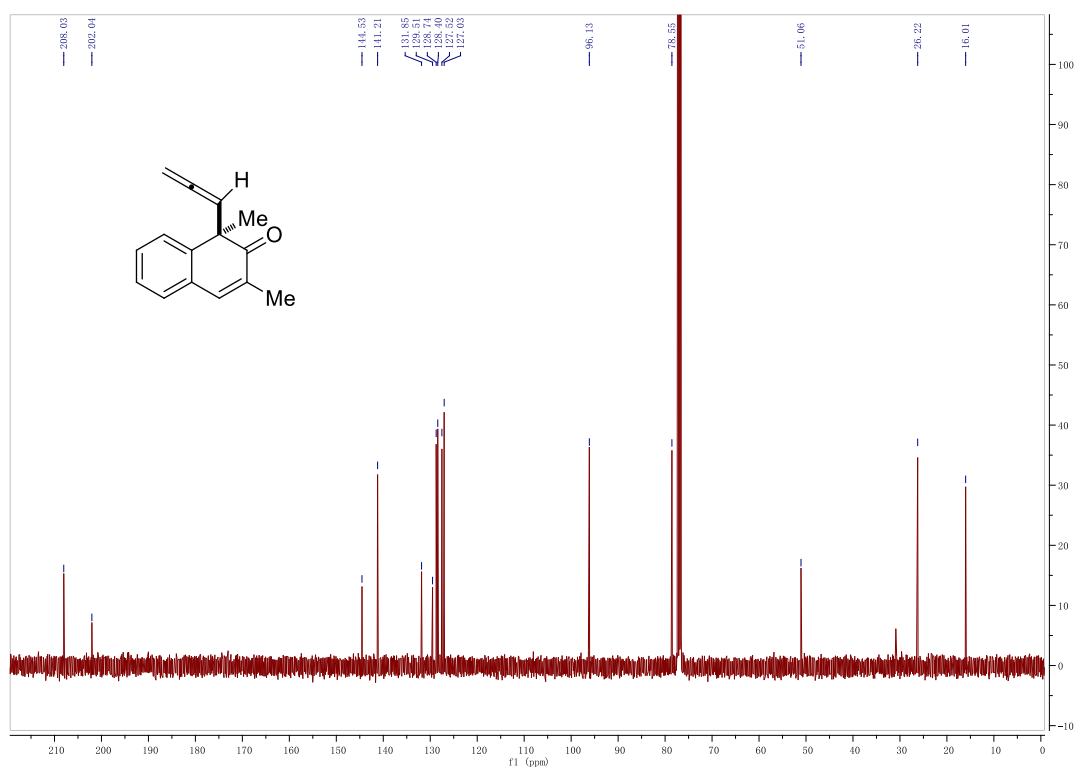
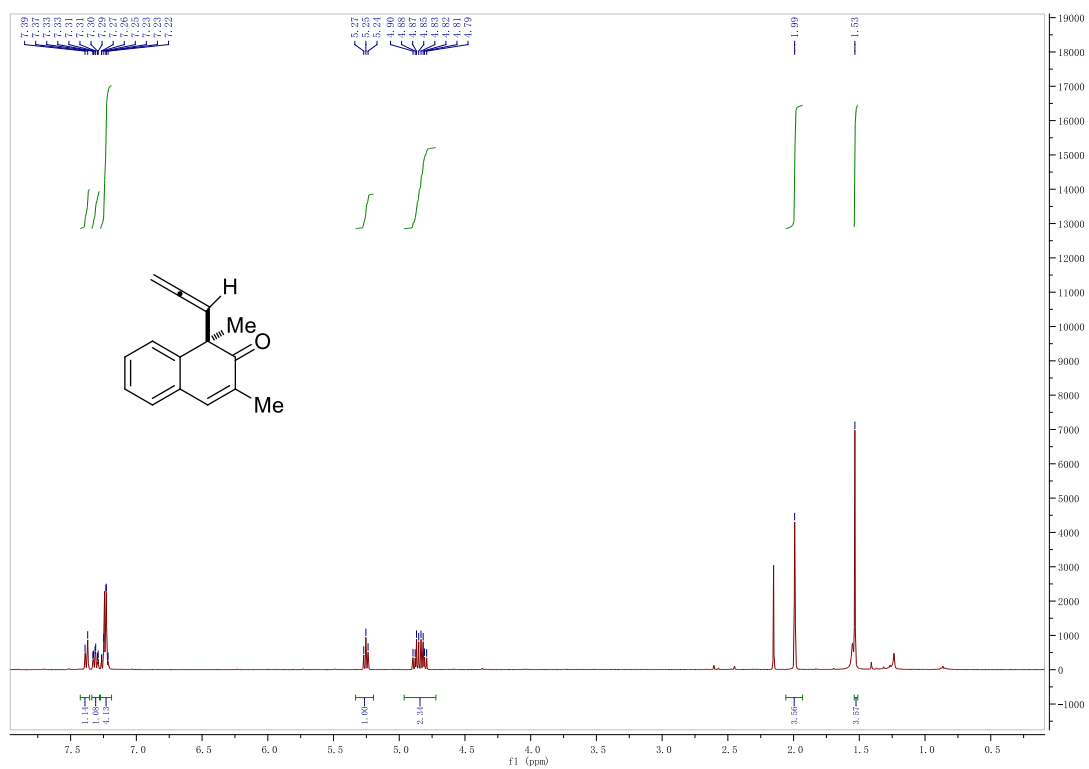
Chapter 2



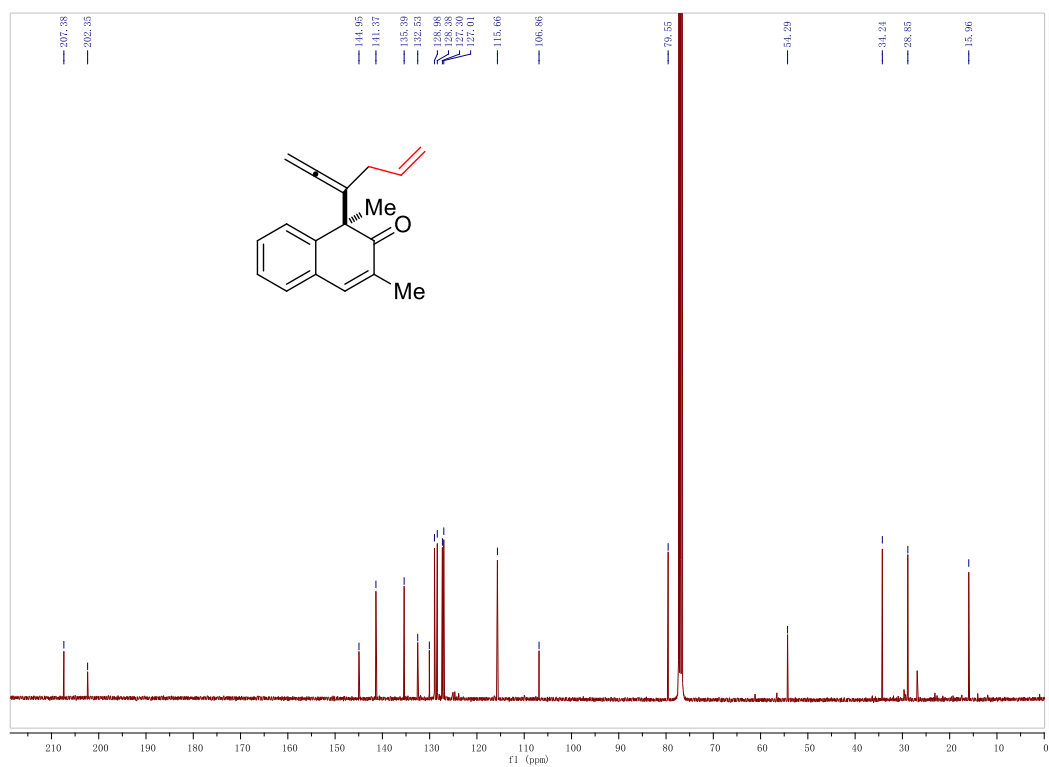
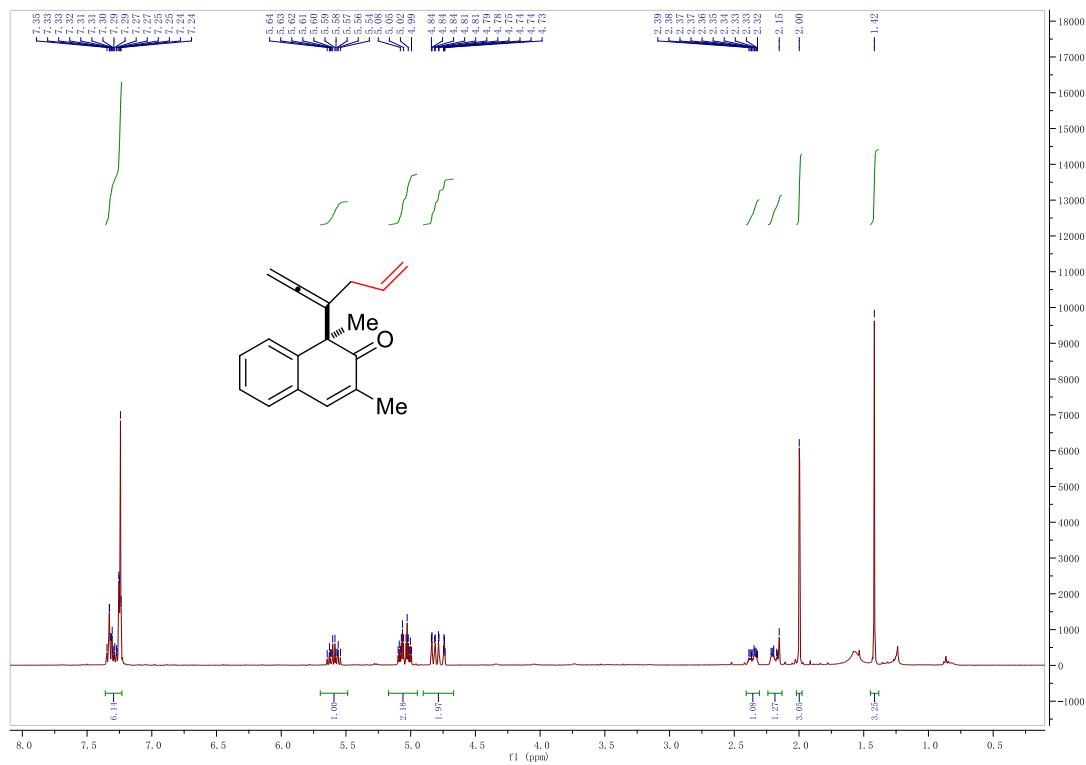
Chapter 2



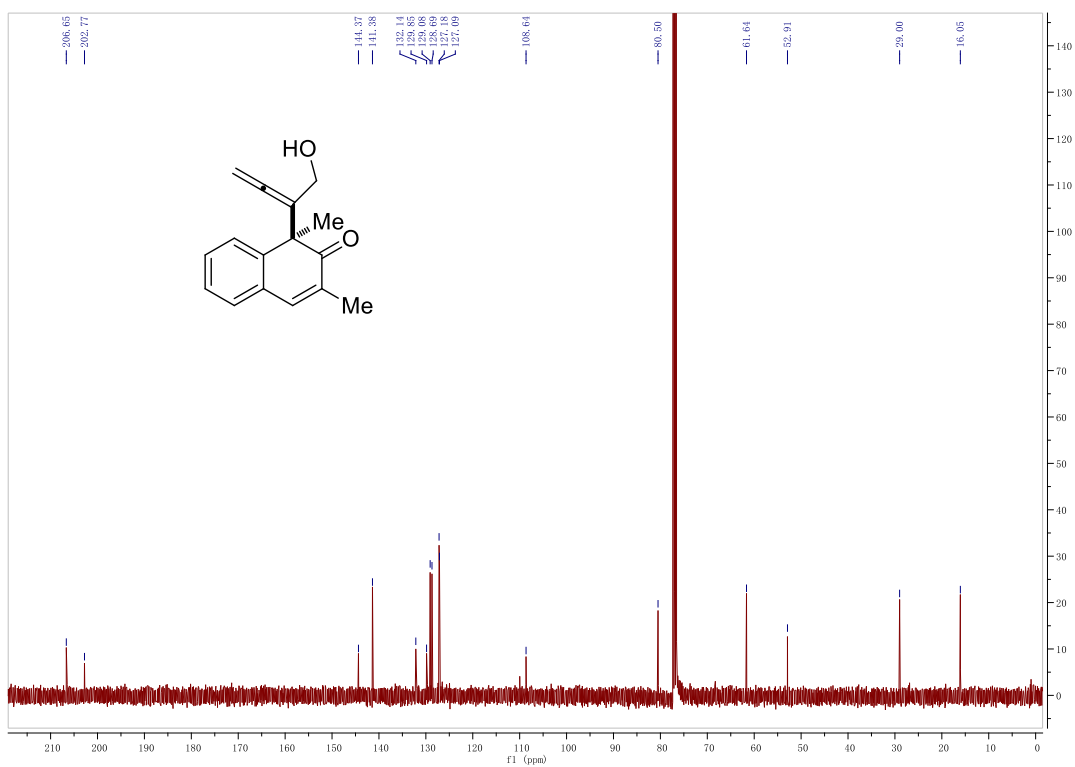
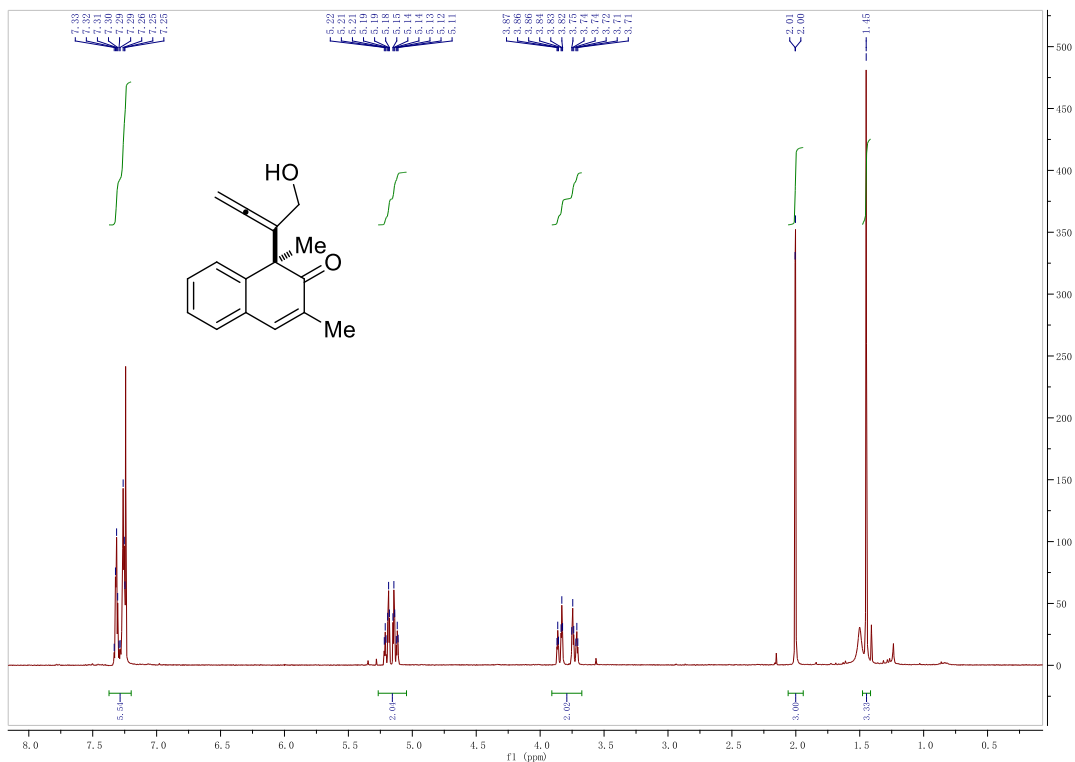
Chapter 2



Chapter 2



Chapter 2



PPh₃AuTFA Catalyzed Intermolecular Dearomatization of 2-Naphthols with Allenamides

3.1 Abstract: An efficient gold catalyzed intermolecular dearomatization of substituted β -naphthols with allenamides is presented here. PPh₃AuTFA (5 mol %) approves the efficient dearomatively allylation protocol under mild conditions and exhibits high tolerance on substrates scope (24 examples) in good to excellent yield accompanied with high regioselectivity and stereoselectivity. Moreover, the synergistic catalytic system also highlight the synergistic function between the [PPh₃Au]⁺ (π -acid) and TFA⁻ (Lewis base). At last, a new chiral BINOL phosphoric acid silver salt is successfully synthesized and used as the chiral counter anion, which strongly promotes the enantioselectivity (up to 92%).

3.2 Introduction: The catalytic dearomatization of 2-naphthols has been recognized to be a desirable and practical synthetic methodology to structurally various three dimensional functional molecules from readily accessible dimensional fragment.^[1] The construction of a novel naphthalenone core featured a stereogenic center at the C(1) position acts as a powerful platform to obtain the realization of numerous of important molecular skeleton widely exists in tons of natural and bio-active molecules^[2] (**Figure 1** upper). In general, catalytic dearomatization of naphthols is mainly divided into oxidative and non-oxidative strategies. As mentioned in our previous work, the formation of C-X (X: O, N, halide) linkage is majorly obtained through oxidative pathway,^[3] the latter methodology commonly contributes the formation of new C-C bond via a desirable carbon-based decoration of the arene cells.^[4] In the latter approach, the use of atom economic and easily accessible unsaturated hydrocarbons deserve a unique and large attention due to the easy modification and low-cost to approach diverse chemical compounds.^[5] Based on the first project in **chapter 2** on gold catalyzed intramolecular dearomatization of 2-naphthols, To develop another methodology which enhances the selectivity, diversity tolerance of functional group on starting material and makes the starting

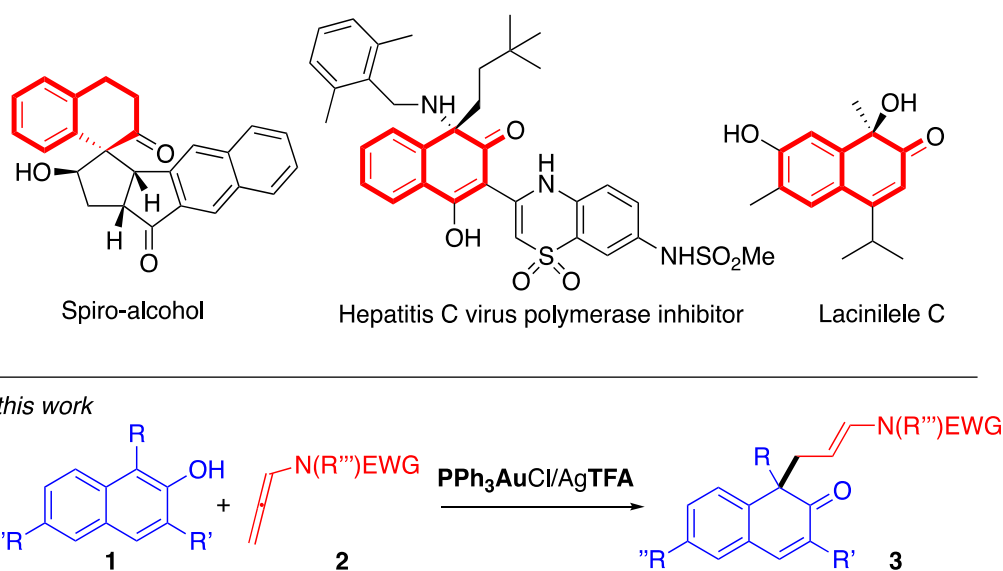


Figure 1. Examples of naturally occurring compounds comprising partially dearomatized naphthyl cores (upper panel). The present work representation of dearomatization protocols (lower panel).

easier to obtain, our group are encouraged to design the gold catalyzed intermolecular dearomatization of naphthol derivatives. On the other hand, dependent on our ongoing interests in

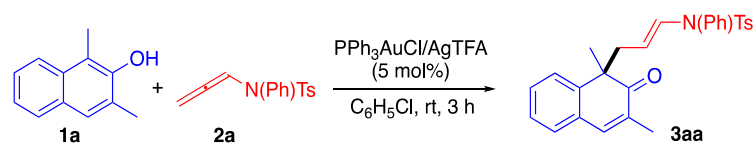
the metal and organo-catalyzed dearomatization of electron-rich aromatic compounds^[6], we have recently realized and present the important impact of the gold counterion^[7] on the overall chemo-, regio- and stereochemical parameters of the condensation of C2,3-disubstituted indoles with allenamides.^[8,9]

As the result showed, the use of TFA anion (TFA: trifluoroacetate) switched the site-selective C(3)-allylation of N(H)-indoles via consequent dearomatization of the pyrrolyl ring.^[6b] The formation of hydrogen-bond interactions between the indole and the TFA anion was proposed and certified assisted by NMR analysis, providing a concrete theoretical support for the final regiochemical outcome.^[6e]

In this work, we present the implementation of this adaptive concept by achieving Ph₃PAuCl/AgTFA synergistically catalyzed intermolecular dearomatization of β -naphthols **1** with allenamides **2** to furnish selectively C(1)-allylated naphthalene -2(1H)-ones **3** among three competitive C(1), C(3) and hydroxyl group.

3.3 Experiment and Results: Firstly, 1,3-dimethyl-2-naphthol **1a** and allenamide **2a** were selected as the model starting material and were treated with the catalyst of Ph₃PAuCl/AgTFA (5 mol%) in chlorobenzene at room temperature. Fortunately, the dearomatized product **3a** in high regio- and stereoselectivity was collected via condensation of 1,3-dimethyl-2-naphthol **1a** to allenamide **2a** in excellent yield (98%, Table 1, entry 1). Even this inspiring result was obtained, deviations from the optimal conditions generally were also tested and a drop in catalytic performance was listed in Table 1.

From the table 1, in solvent aspect, the aromatic solvent were benefit to drive the transformation compared with other kinds of solvent (entry 2-5), particularly, chloro -benzene via electron density fine tuning was approved to be most suitable solvent giving the highest yield (98%, entry 1) in short reaction times (3 h). Next, different counter anions (entry 6-10) which showed different affinity to gold and basicity were also examined respectively. Interestingly, strongly coordinating anions such as OTs⁻ and AcO⁻ and OPNB⁻ were examined and did not enhance the reaction in any extent (entries 7, 8). In other aspect, the employment of poorly coordinating analogous like SbF₆⁻, OTf⁻ and NTf₂⁻(entries 6, 10, 11) caused complete decomposition of **2a** even at lower temperature.

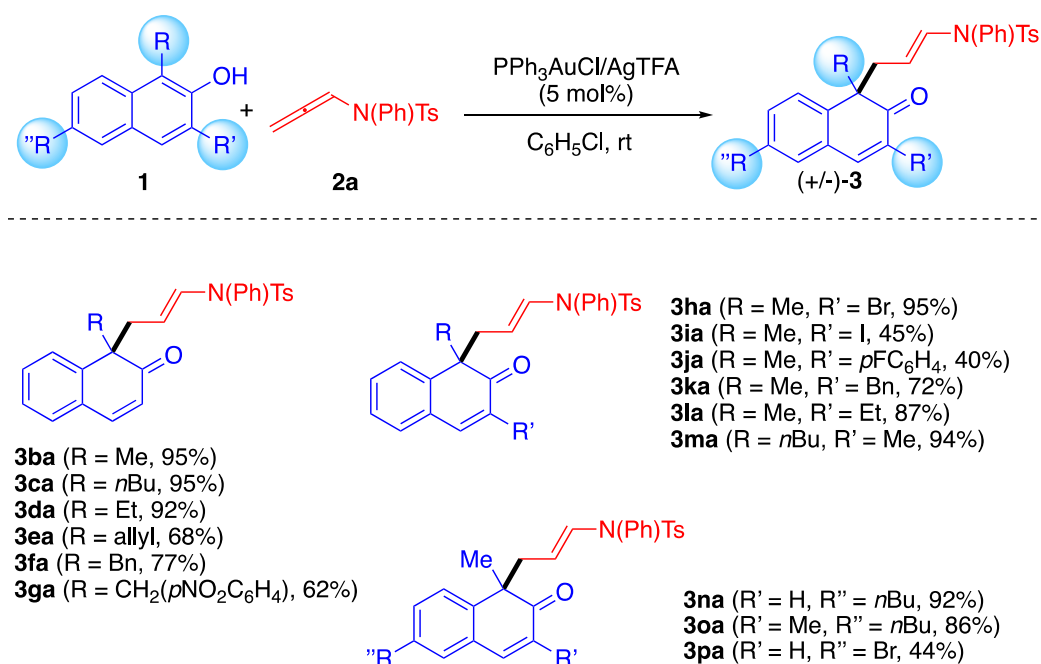
Table 1. Optimization of the reaction conditions^a

Run	Deviation from optimal	Yield 3aa (%) ^b
1	--	98
2	CH ₃ CN as the solvent	NR
3	Toluene as the solvent	50
4	THF as the solvent	traces
5	CH ₂ Cl ₂ as the solvent	62
6	AgOTf	decomposition ^c
7	AgOTs	10
8	AgOAc	traces
9	AgOPNB ^d	traces
10	AgSbF ₆ ^d	decomposition ^c
11	AgNTf ₂	decomposition ^c
12	Reagent grade C ₆ H ₅ Cl	65
13	JohnPhosAuCl/AgTFA	66
14	IPrAuCl/AgTFA	55
15	picAuCl ₂ /AgTFA ^e	71
16	without AgTFA	NR
17	without PPh ₃ AuCl	29
18	PPh ₃ AuTFA ^f	92

^aReaction conditions: **1a** (0.05 M). **1a:2a:PPh₃AuCl:AgTFA** = 1/2/0.05/0.05 under anhydrous conditions, unless otherwise specified. In all cases, only the (E)-**3aa** isomer was isolated. ^bDetermined after flash chromatography. ^cWith reference to **2a**. ^dOPNB = p-NO₂-benzoate. ^eReaction temperatures: 0 °C. ^fWith picAuCl (5 mol %) and AgTFA (10 mol %). ^gNR = no reaction. ^hPreformed complex was employed.

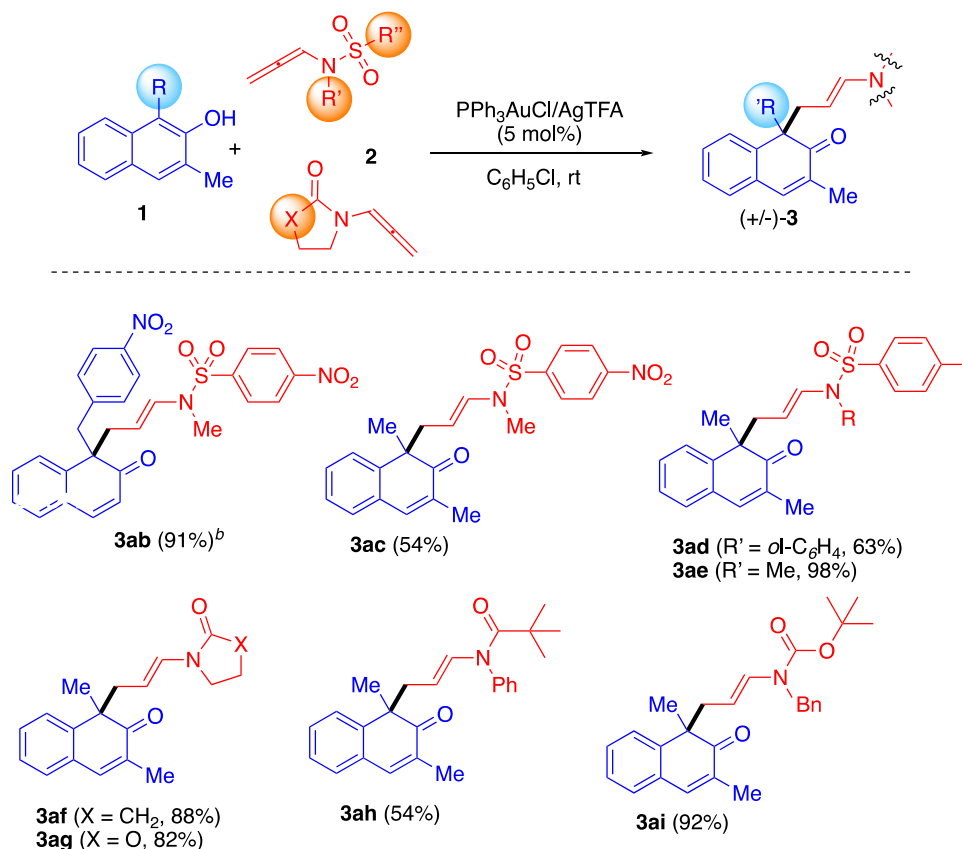
Moreover, by testing reagent grade C₆H₅Cl (entry 12 vs entry 1), anhydrous conditions was verified to be necessary to achieve excellent yield. Besides influence of solvent and counter anion, different

gold(I) and gold(III) sources were also compared and the use of gold(III) caused significant drop on offering the corresponding product (entries 13-15). Then control experiment was also performed by applying PPh_3AuCl and AgTFA individually to expel the affection of silver metal and address the necessity of TFA^- (entries 16-17). At last, the preformed PPh_3AuTFA complex^[10] was isolated to be applied in performing the titled dearomatization and the synergistic function of gold(I) complex and TFA^- was proved (yield = 92%, entry 18)^[11].



Scheme 1. Screening of Substituted Naphthols **1a**, ^aReaction conditions: **1** (0.05 M) under anhydrous conditions (also see the Supporting Information (SI)).

With the optimized desirable catalytic conditions, we then turned our attention on the expansion of this catalytic system on the scope of substrates by variously functional group in different position in both kinds of starting material. Firstly, we started from the decoration on naphthol (**Scheme 1**). When C3 has not substitutions, no matter what kinds of substituents, EDG or EWG (R=Me, Et, *n*Bu, allyl and aryl), all the corresponding dearomatized products were obtained (**3ba-3ga**) in good to excellent yield with high site-selectivity. Next, different kinds of substituents were also introduced respectively at C3 and C6 positions of the naphthyl core and the promising results (**3ha-3pa**) proved high practical application of this catalysis system by good to excellent yield.

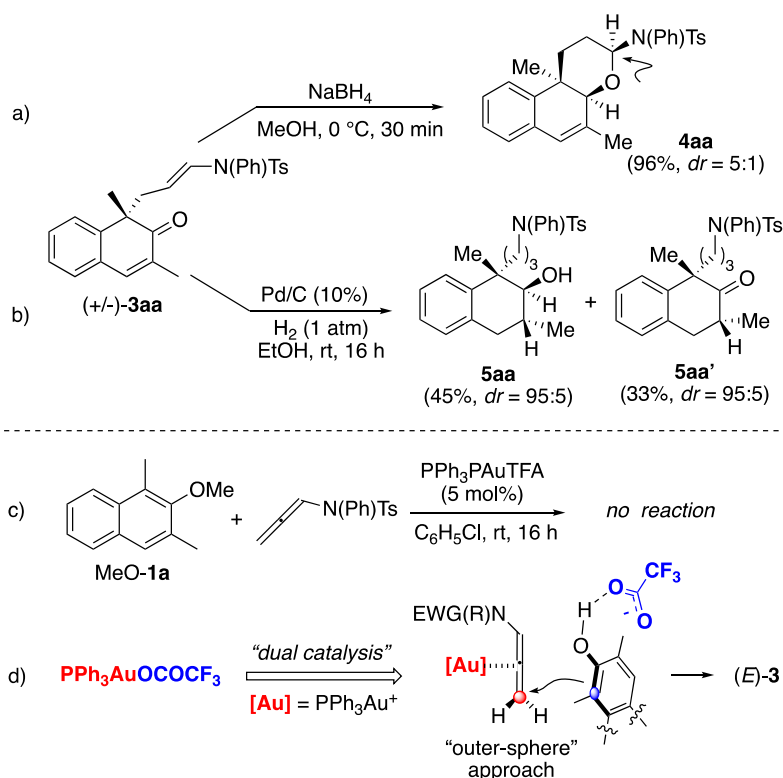


Scheme 2. Screening of Substituted Allenamides **2a**, ^aReaction conditions: **1** (0.05 M) under anhydrous conditions (also see the SI), ^b1:2 = 1:3.

Further, a wide range of cyclic and acyclic allenamides (**2b–2h**) were also subjected to examine the catalytic system (Table 1, entry1) and the corresponding results are summarized in **Scheme 2**. In all cases, a wide of modification on nitrogen was performed and the desired dearomatized naphthalen-2(1H)-one **3** (**3ab–3ai**) were separated in good to excellent yields (56%–96%) and high stereoselectivity preferring the E-enamide moiety. However, the process faced also some limitations that when the α - and γ -substituted allenamides^[12] were subjected to the optimal condition, the corresponding product were not collected since mostly the inertness of allenamides.^[12]

In addition, the synthetic application of the dearomatized products **3** was verified via further modification based on compound **3aa** through the chemoselective reduction of the carbonyl moiety with NaBH_4 in MeOH at room temperature. Surprisingly, this transformation did not stop at simple reduction. And the 1H-benzochromene **4aa** was finally isolated in high yield (96%) and good diastereoisomeric control (5:1) via subsequent cyclized trapping of the newly formed

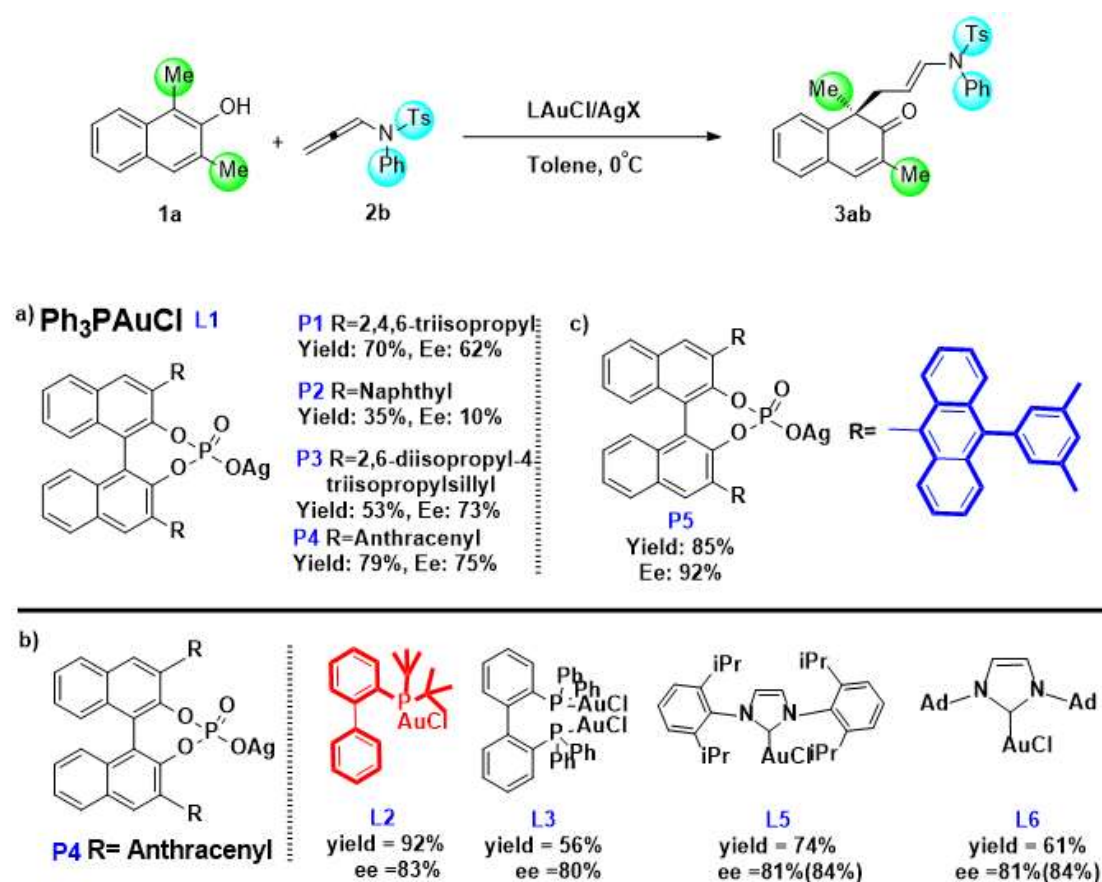
secondary alcohol by the enamide group (see **Scheme 3a**). In addition, the Pd/C (10 wt %, 10 mol %) catalyzed hydrogenation of **3aa** (H_2 , 1 atm) was performed in EtOH at room temperature leading to a isolatable mixture of diastereomerically pure 1,2,3,4- tetrahydronaphthalene derivatives **5aa** and **5aa'** (1.4:1, **Scheme 3b**).



Scheme 3. Chemical Manipulation of the Dearomatized Naphthalenone Compounds **3** and Mechanism Proposal^a: ^aThe outer-sphere approach was shown. Attempts to isolate the corresponding aldehyde via acidic hydrolysis of **3aa** were nfruitful, leading to the complete decomposition of the starting material.

Mechanistically, a synergistic π -acid and Lewis base catalysis is proposed for the observed transformation^[13] here. Besides the normal electrophilic activation of the allenyl core^[14] coordinated by the gold(I) complex,^[15] the “relatively” basic $CF_3CO_2^-$ anion, on one hand, was used to stabilize the gold cation. On the other hand, it played simultaneous activating and directing action on the naphthol which also would guarantee the optimal electronic/spatial arrangement for the C-C bond forming process (**Scheme 1d**, outer-sphere-type approach is shown).^[16] The pKa of the corresponding Trifluoroacetic acid (pKa of TFAH ca. 0) can provide a rough indication of the desirable compromise among metal-coordination attitude and basicity of the anionic species^[17]. In particular, while stronger coordinating anions like AcO^- and $OPNB^-$ (pKa ca. 5 and 3.4, respectively) resulting in not being replaced by the allenamide did not promote the

reaction, poorly coordinating analogous such as SbF_6^- and OTf caused the decomposition of the allenyl unit, probably via polymerization processes or hydrolysis^[18]. It is worthy to mention that direct interaction signal among PPh_3AuTFA and **1a** was not detected via ^1H , ^{19}F and ^{31}P -NMR investigation (CD_2Cl_2 , rt, see SI) without allenamide^[19] fragment that reasonably explained the process of replacing the TFA- from the coordination sphere of the metal. Additionally, experiment was also performed by using the inertness of **OMe-1a** under optimal condition, and the result was in agreement with the postulated TFA-/naphthol hydrogen-bond interaction during the reaction process.



Scheme 4. Ligand and chiral phosphoric acid silver salts screening

Finally, we paid our attention on achieving the asymmetric transformation on this basis by adjusting the ligand. However, it is well known^[20] that the coordination of gold catalyst with π -electron rich group is the η linear coordination and accepts the attack of nucleophile from opposite sides of the metal center in out-sphere way. In the meantime, the size of gold atom also contributed to increase the difficulty of embracing the substrates into a chiral atmosphere. To

solve this problem, we changed the direction by using chiral counterion^[21] to assist gold complex to construct the chiral space. On the basis of the optimal condition, Ph₃P (triphenyl phosphine) was firstly elected as the gold ligand accompanied with adjusting the chiral silver phosphate (**Scheme 4a**, P1-P4). Inspiringly, the *in situ* catalyst formed from Ph₃PAuCl and chiral silver phosphate **P4** offered the best ee (75%) among the four chiral silver phosphates. To enhance the enantioselectivity, different ligands on gold complex (**Scheme 4b**, L2-L6) were respectively screened by interacting with chiral silver phosphate **P4** to form the corresponding catalysts. JohnPhosAuCl **L2** ((2-biphenyl)di-tert-butylphosphine) successfully promoted the ee to 83% in excellent yield (92%). These results exhibit the signal that the ee could be improved more through adjustment on the substituent of silver phosphate. Then we designed and successfully synthesized a new chiral silver phosphate **P5** bearing 9-(3,5-dimethyl) anthracenyl group. Through the cooperation of JohnPhosAuCl **L2** and chiral silver phosphate **P5** (**Scheme 4c**, L5), fortunately, the dearomatized naphthalenone **3ab** was obtained in excellent yield (85%) and enantioselectivity (92%). Next, this strategy will be directly to examine the scope of substrates.

3.4 Summary

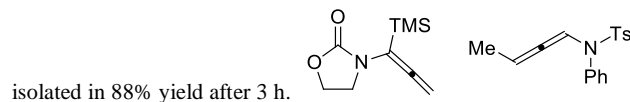
In conclusion, the gold(I)·TFA catalysed intermolecular dearomatization of 2-naphthols with allenamides is documented and a range of C1-allylated naphthalene -2(1H)-ones are obtained in high yields. Besides this catalytic system showed more excellent region, chemo and stereoselectivity than previous work, this work also strengthened the function of chiral counter anion on the asymmetric transformation.

3.5 Reference

- [1] a) Pape, A.R.; Kaliappan, K.P.; Kündig, E.P. *Chem.Rev.* **2000**, *100*, 2917-2940; b) Roche, S.P.; Porco, Jr. J.A. *Angew. Chem. Int. Ed.* **2011**, *50*, 4068-4093; c) Zhuo, C.-X.; Zhang, W.; You, S.-L. *Angew. Chem. Int. Ed. Engl.* **2012**, *51*, 12662-12686; d) Zheng, C.; You, S.-L. *Chem.* **2016**, *1*, 830-857; e) *Asymmetric Dearomatization Reactions* (Ed. S.-L. You), Wiley-VCH, **2016**; f) Wu, W.-T.; Zhang, L.; You, S.-L. *Chem. Soc. Rev.* **2016**, *45*, 1570-1580; g) Liang, X.-W.; Zheng, C.; You, S.-L. *Chem. Eur. J.* **2016**, *22*, 11918-11933; h) Park, S.; Chang, S. *Angew. Chem. Int. Ed.* **2017**, *56*, 7720-7738; i) Bariwal, J.; Voskressensky, L.G.; Van del Eucken, E.V. *Chem. Soc. Rev.* **2018**, *47*, 3831-3848.
- [2] a) Fang, X.; Zeng, Y.; Li, Q.; Wu, Z.; Yao, H.; Lin, A. *Org. Lett.* **2018**, *20*, 2530-2533; b) Krueger, A. C.; Madigan, D. L.; Green, B. E.; Hutchinson, D. K.; Jiang, W. W.; Kati, W. M.; Liu, Y.; Maring, C. J.; Masse, S. V.; McDaniel, K. F.; Middleton, T. R.; Mo, H.; Molla, A.; Montgomery, D. A.; Ng, T. I.; Kempf, D. J. *Bioorg. Med. Chem. Lett.* **2007**, *17*, 2289-292. c) Krohn, K.; Zimmermann, G. *J. Org. Chem.* **1998**, *63*, 4140-4142.
- [3] For some representative examples of C-X bond forming dearomatization of naphthols see: a) Dhineshkumar, J.; Samaddar, P.; Ramaiah Prabhu, K. *Chem. Commun.* **2016**, *52*, 11084; b) Zhang, P.; Li, M.; Xue, X.-S.; Xu, C.; Zhao, Q.; Liu, Y.; Wang, H.; Guo, Y.; Lu, L.; Shen, Q. *J. Org. Chem.* **2016**, *81*, 7486-7509; c) Li, J.; Wang, M.; Zhang, Y.; Fan, Z.; Zhang, W.; Sun, F.; Ma, N. *ACS Sustainable Chem. Eng.*, **2016**, *4*, 3189-3195; d) Zhang, Z.; Sun, Q.; Xu, D.; Xia, C.; Sun, W. *Green Chem.* **2016**, *18*, 5485-5492; e) Changotra, A.; Das, S.; Sunoj, R. B. *Org. Lett.* **2017**, *19*, 2354-2357; f) Wang, Y.-F.; Shao, J.-J.; Wang, B.; Chu, M.-M.; Qi, S.-S.; Du, X.-H.; Xu, D.-Q. *Adv. Synth. Catal.* **2018**, *360*, 2285-2290.
- [4] a) Zhuo, C.-X.; You, S.-L. *Adv. Synth. Catal.* **2014**, *356*, 2020-2028; b) Yang, D.; Wang, L.; Kai, M.; Li, D.; Yao, X.; Wang, R. *Angew. Chem. Int. Ed.* **2015**, *54*, 9523-9527; c) Xu, R.-Q.; Yang, P.; Tu, H.-F. Wang, S.-G.; You, S.-L. *Angew. Chem. Int. Ed. Engl.* **2016**, *55*, 15137-15365; d) Heid, B.; Plietker, B. *Synthesis*, **2016**, *48*, 340-350; e) Shao, L.; Hu, X.-P. *Chem. Commun.* **2017**, *53*, 8192- 8195; e) Nakayama, H.; Harada, S.; Kono, M.; Nemoto, T. *J. Am. Chem. Soc.* **2017**, *139*, 10188-10191; f) Xu, R.-Q.; Yang, P.; You, S.-L. *Chem. Commun.* **2017**, *53*, 7553-7556; g) Xu, R.-Q.; Gu, Q.; You, S.-L. *Angew. Chem. Int. Ed.* **2017**, *56*, 7252-7256.
- [5] a) Nan, J.; Zuo, Z.; Luo, L.; Bai, L.; Zheng, H.; Yuan, Y.; Liu, J.; Luan, X.; Wang, Y. *J. Am. Chem. Soc.* **2013**, *135*, 17306-17309; b) Zheng, J.; Wang, S.-B.; Zheng, C.; You, S.-L. *J. Am. Chem. Soc.* **2015**, *137*, 4880- 4883; c) Zheng, C.; Zheng, J.; You, S.-L. *ACS Catal.* **2016**, *6*, 262-271; d) Wu, W.-T.; Xu, R.-Q.; Zhang, L.; You, S.-L. *Chem. Sci.* **2016**, *7*, 3427-3431.
- [6] a) Cera, G.; Chiarucci, M.; Mazzanti, A.; Mancinelli, M.; Bandini, M. *Org. Lett.* **2012**, *14*, 1350-1353; b) Jia, M.; Cera, G.; Perrotta, D.; Bandini, M. *Chem. Eur. J.* **2014**, *20*, 9875-9878; c) Romano, C.; Jia, M.; Monari, M.; Manoni, E.; Bandini, M. *Angew. Chem. Int. Ed.* **2014**, *53*, 13854-13857; d) Jia, M.; Monari, M.; Yang, Q.-Q.; Bandini, M. *Chem. Commun.* **2015**, *51*, 2320-2323; e) Rocchigiani, L.; Jia, M.; Bandini, M.; Macchioni, A. *ACS Catalysis* **2015**, *5*, 3911-3915; f) Ocello, R.; De Nisi, A.; Jia, M.; Yang, Q.-Q.; Giacinto, P.; Bottoni, A.; Miscione, G. P.; Bandini, M. *Chem. Eur. J.* **2015**, *21*, 18445-18453; g) Manoni, E.; De Nisi, A.; Bandini, M. *Pure & Appl. Chem.* **2016**, *88*, 207-214; h) An, J.; Parodi, A.; Monari, M.; Castiñeira Reis, M.; Silva Lopez, C.; Bandini, M. *Chem. Eur. J.* **2017**, *23*, 17473-17477.
- [7] For general reviews on the topic see: a) Jia, M.; Bandini, M. *ACS Catal.* **2015**, *5*, 1638-1652; b) Ranieri, B.; Escofet, I.; Echavarren, A.E. *Org. Biomol. Chem.* **2015**, *13*, 7103-7118 c) Schiebl, J.; Schulmeister, J.; Doppiu, A.; Wörner, E.; Rudolph, M.; Karch, R.; Hashmi, A. S. K. *Adv. Synth. Catal.* **2018**, *360*, 2493-2502.
- [8] For general reviews on the use of N-allenyl amides in organic synthesis see: a) Wei, L.-L.; Xiong, H.; Hsung, R. P. *Acc. Chem. Res.* **2003**, *36*, 773-782. b) Lu, T.; Lu, Z.; Ma, Z.-X.; Zhang, Y.; Hsung, R. P. *Chem. Rev.* **2013**, *113*, 4862-4904. c) Manoni, A.; Bandini, M. *Eur. J. Org. Chem.* **2016**, *2016*, 3135-3142.

Chapter 3

- [9] For general reviews on gold-catalyzed dearomatization reaction see: a) Wu, W.-T.; Zhang, L.; You, S.-L. *Huaxue Xuebao* 2017, 75,419. b) An, J.; Bandini, M. *Chimia* 2018, 72, 610–613.
- [10] a) Zhang, Z.-Y.; Szlyk, E.; Palenik, G. J.; Colgate, S. O. *Acta Crystallogr., Sect. C: Cryst. Struct. Commun.* 1988, 44, 2197. b) Guo, R.; Li, K.-N.; Gong, L.-Z. *Org. Biomol. Chem.* 2013, 11, 6707-6712.
- [11] Performing the model reaction on 1 mmol scale of 1a in the presence of PPh₃AuCl/AgOTf (2.5 mol%), 3aa was



- [12] The following allenamides proven ineffective under optimal conditions.
- [13] a) Hashmi, A. S. K.; Hubbert, C. *Angew. Chem., Int. Ed.* 2010, 49, 1010–1012. b) Hashmi, A. S. K. *Angew. Chem., Int. Ed.* 2010, 49, 232–5241.
- [14] For a selection of reviews/monographs on the use of allenes in organic synthesis, see: a) Yu, S.; Ma, S. M. *Angew. Chem., Int. Ed.* 2012, 51, 3074-3112. b) Muñoz, M. P. *Chem. Soc. Rev.* 2014, 43, 3164-3183. c) López, F.; Mascareñas, J. L. *Chem. Soc. Rev.* 2014, 43, 2904-2915. d) Kitagaki, S.; Inagaki, F.; Mukai, C. *Chem. Soc. Rev.* 2014, 43, 2956-2978; e) Le Bras, J.; Muzart, S. *Chem. Soc. Rev.* 2014, 43, 3003-3040. f) Neff, R. K.; Frantz, D. E. *Tetrahedron* 2015, 71, 7-18; g) Lledó, A.; Pla-Quintana, A.; Roglans, A. *Chem. Soc. Rev.* 2016, 45, 2010-2023.
- [15] For general reviews on gold-catalyzed manipulation of allenes, see: a) Krause, N.; Hashmi, A. S. K. *Modern Allene Chemistry*; Wiley-VCH: Weinheim, Germany, 2004;. b) Morita, N.; Krause, N. *Angew. Chem., Int. Ed.* 2006, 45, 1897-1899; c) Yang, W.; Hashmi, A. S. K. *Chem. Soc. Rev.* 2014, 43, 2941-2955; d) Winter, C.; Krause, N. *Wiley-VCH: Weinheim, Germany*, 2012, 363. e) Muñoz, M. P. *Org. Biomol. Chem.* 2012, 10, 3584. f) Hashmi, A. S. K.; Buehrle, M. *Aldrichimica Acta* 2010, 43, 7380-7383; Also see: g) Hashmi, A. S. K.; Schwarz, L.; Choi, J.-H.; Frost, T. M. *Angew. Chem., Int. Ed.* 2000, 39, 2285–2288; h) Hashmi, A. S. K.; Frost, T. M.; Bats, J. W. *J. Am. Chem. Soc.* 2000, 122, 11553–11554.
- [16] At the present, the “inner-sphere type” approach deriving from the simultaneous interaction of counterion with naphthol, as well as metal center, cannot be excluded.
- [17] a) Laurence, C.; Brameld, K. A.; Graton, J. r. m.; Le Questel, J.-Y.; Renault, E. *J. Med. Chem.* 2009, 52, 4073–4086. b) Pike, S. J.; Hutchinson, J. J.; Hunter, C. A. *J. Am. Chem. Soc.* 2017, 139, 6700– 6706. c) Lu, Z.; Han, J.; Okoromoba, O. E.; Shimizu, N.; Amii, H.; Tormena, C. F.; Hammond, G. B.; Xu, B. *Org. Lett.* 2017, 19, 5848–5841.
- [18] The presence of the in situ formed PPh₃Au-O-naphthyl adduct was ruled out by NMR analysis (see the Supporting Information).
- [19] Adventitious traces of water in the NMR analyses led to the formation of α -[PPh₃Au]-acrolein intermediate: Mastandrea, M. M.; Mellonie, N.; Giacinto, P.; Collado, A.; Nolan, S. P.; Miscione, G. P.; Bottoni, A.; Bandini, M. *Angew. Chem., Int. Ed.* 2015, 54, 14885 (also see ref 6e).
- [20] W. Zi, F. Dean Toste, *Chem.Soc.Rev.*, **2016**, 45, 4567—4589.
- [21] G. L. Hamilton, E. J. Kang, M. Mba, F. D. Toste, *science*, **2007**, 137, 486-499.

3.6 Supplement

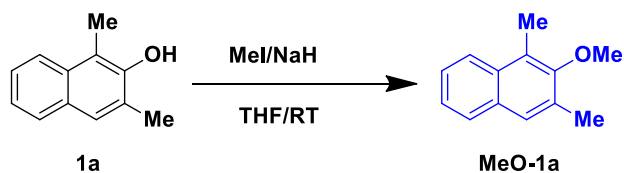
Table of Contents

General methods.....	191
Preparation of MeO- 1a	192
General procedure for gold-catalyzed dearomatization of 2-naphthols with <i>N</i> -allenyl amides.....	192
Synthesis of the <i>1H</i> -benzochromene 4aa	200
Hydrogenation of 3aa	201
References.....	202

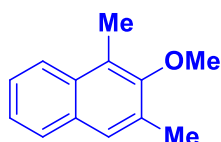
General Methods.

^1H -NMR spectra were recorded on Varian 400 (400 MHz) spectrometers. Chemical shifts are reported in ppm from TMS with the solvent resonance as the internal standard (deuteriochloroform: 7.24 ppm). Data are reported as follows: chemical shift, multiplicity (s = singlet, d = doublet, t = triplet, q = quartet, sext = sextet, sept = septet, p = pseudo, b = broad, m = multiplet), coupling constants (Hz). ^{13}C -NMR spectra were recorded on a Varian 400 (100 MHz) spectrometers with complete proton decoupling. Chemical shifts are reported in ppm from TMS with the solvent as the internal standard (deuteriochloroform: 77.0 ppm). GC-MS spectra were taken by EI ionization at 70 eV on a Hewlett-Packard 5971 with GC injection. They are reported as: m/z (rel. intense). LC-electrospray ionization mass spectra were obtained with Agilent Technologies MSD1100 single-quadrupole mass spectrometer. Chromatographic purification was done with 240-400 mesh silica gel. Other anhydrous solvents were supplied by Sigma Aldrich in Sureseal[®] bottles and used without any further purification. Commercially available chemicals were purchased from Sigma Aldrich, Stream and TCI and used without any further purification. Melting points were determined with Bibby Stuart Scientific Melting Point Apparatus SMP 3 and are not corrected. Agilent Technologies LC/MSD Trap 1100 series (nebulizer: 15.0 PSI, dry Gas: 5.0 L/min, dry Temperature: 325 °C, capillary voltage positive scan: 4000 mA, capillary voltage negative scan: 3500 mA). Preparation of β -naphthols **1**^[1] and *N*-allenyl amides^[2] were accomplished following the reported procedures.

Preparation of MeO-1a

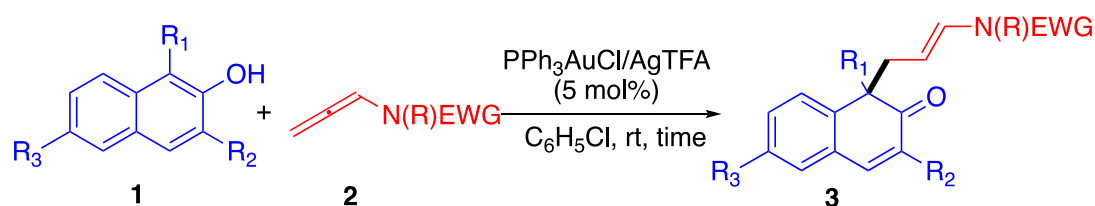


An oven-dried two-necked flask was charged with **1a** (80 mg, 0.5 mmol) and **NaH** (37 mg, 2.0 equiv) in a sequence and left stirring for 30 min at 0 °C. **MeI** (85.6 mg, 1.2 equiv) was then added and the mixture kept stirring until **1a** was completely converted (monitored by TLC). Then, water was added and the mixture extracted with ethyl acetate. At last, organic phase was collected and dried with anhydrous sodium sulfate. After removing the organic solvent under vacuum, the reaction crude was transferred to silica gel column chromatography (cHex:EtOAc = 40:1) to afford compounds **MeO-1a**.

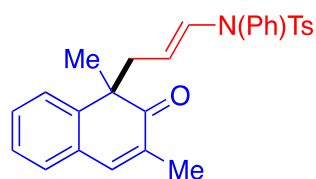


MeO-1a. Colorless oil, yield = 75%. ^1H NMR (400 MHz, CDCl_3) δ = 7.93 (d, J = 8.4 Hz, 1H), 7.74 (d, J = 7.6 Hz, 1H), 7.54 (s, 1H), 7.48 – 7.39 (m, 1H), 3.81 (s, 3H), 2.63 (s, 3H), 2.49 (s, 3H). ^{13}C NMR (100 MHz, CDCl_3) δ = 155.14, 132.77, 131.20, 131.04, 127.69, 127.51, 125.20, 124.68, 124.61, 123.93, 60.65, 17.19, 11.51. GC-MS (m/z): 186. Anal. Calc. for ($\text{C}_{13}\text{H}_{14}\text{O}$: 186.25): C, 83.83; H, 7.58; found: C, 83.65, H, 7.41.

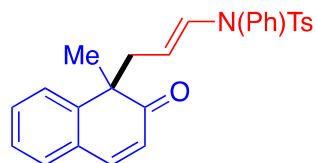
General procedure for gold-catalyzed dearomatization of 2-naphthols with *N*-allenyl amides.



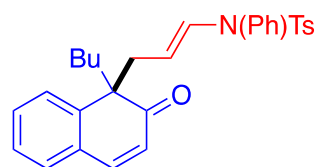
An oven dried two-necked flask was charged with anhydrous chlorobenzene (1 ml), Ph_3PAuCl (1.2 mg, 5 mol%) and AgTFA (0.6 mg, 5 mol%). After stirring for 15 min, substrate **1** (0.05 mmol) and **2** (0.1 mmol) were added under dark atmosphere. Then, the reaction was kept stirring at room temperature until **1** was completely consumed (TLC). At last, the solution was directly transferred into silica gel column chromatography (cHex:EtOAc = 40:1 → 15:1) to afford compounds **3**.



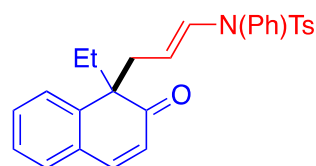
(+/-)-**3aa**. Colorless oil, yield = 98% (3 h). ^1H NMR (400 MHz, CDCl_3) δ = 7.32 – 7.18 (m, 10H), 7.13 (d, J = 8 Hz, 1H), 7.08 (s, 1H), 6.67 – 6.65 (m, 2H), 6.58 (d, J = 12.0 Hz, 1H), 3.85–3.78 (m, 1H), 2.63 (dd, J = 12, 6.4 Hz, 1H), 2.42 (s, 3H), 2.35 (dd, J = 8.4, 4.8 Hz, 1H), 1.78 (d, J = 1.2 Hz, 3H), 1.39 (s, 3H). ^{13}C NMR (100 MHz, CDCl_3) δ = 203.90, 145.09, 143.69, 141.68, 136.65, 135.98, 132.56, 131.15, 130.33, 130.11(2C), 129.61(2C), 129.23(2C), 128.95, 128.80, 128.37, 127.50(2C), 126.75, 126.56, 106.73, 51.85, 45.04, 25.53, 21.74, 15.76. LC-MS (m/z): 481. Anal. Calc. for ($\text{C}_{28}\text{H}_{27}\text{NO}_3\text{S}$: 457.59): C, 73.50; H, 5.95; found: C, 73.66, H, 6.05.



(+/-)-**3ba**. Colorless oil, yield = 95% (2 h). ^1H NMR (400 MHz, CDCl_3) δ = 7.38 – 7.29 (m, 4H), 7.26 – 7.16 (m, 8H), 6.65 (d, J = 8.0 Hz, 1H), 6.65 (d, J = 8.0 Hz, 2H), 6.63 (d, J = 6.4 Hz, 1H), 3.90 – 3.83 (m, 1H), 2.67 (dd, J = 13.2, 7.2 Hz, 1H), 2.42 (s, 3H), 2.37 (dd, J = 8.0, 3.2 Hz, 1H), 1.40 (s, 3H). ^{13}C NMR (100 MHz, CDCl_3) δ = 203.91, 145.78, 145.03, 143.71, 136.60, 135.94, 131.53, 130.10, 130.06(2C), 129.60(2C), 129.34, 129.27(2C), 128.86, 127.54(2C), 126.88, 126.84, 125.24, 121.87, 106.59, 52.24, 44.42, 25.63, 21.7. LC-MS (m/z): 288, 155. Anal. Calc. for ($\text{C}_{27}\text{H}_{25}\text{NO}_3\text{S}$: 443.56): C, 73.11; H, 5.68; found: C, 73.00, H, 5.89.

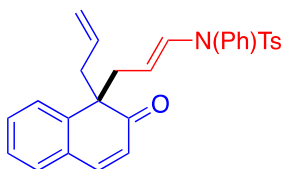


(+/-)-**3ca**. Colorless oil, yield = 95% (3 h). ^1H NMR (400 MHz, CDCl_3) δ = 7.41 – 7.36 (m, 1H), 7.32–7.29 (m, 3H), 7.24 – 7.14 (m, 8H), 6.60 (d, J = 8.0 Hz, 2H), 6.59 (d, J = 3.6 Hz, 1H), 5.93 (d, J = 10.0 Hz, 1H), 3.85–3.37 (m, 1H), 2.68 (dd, J = 10, 7.2 Hz, 1H), 2.42 (s, 2H), 2.35 (dd, J = 12.8, 8.4 Hz, 1H), 2.16 (td, J = 12.4, 8.8 Hz, 1H), 1.76 (td, J = 12.4, 4.4 Hz, 1H), 1.41 (s, 3H), 1.55–0.98 (m, 2H), 0.87 – 0.73 (m, 2H), 0.68 (t, J = 7.2 Hz, 3H). ^{13}C NMR (100 MHz, CDCl_3) δ = 204.20, 145.19, 144.79, 143.65, 136.63, 136.00, 131.37, 131.05, 130.18, 130.05(2C), 129.58(2C), 129.27, 129.21(2C), 128.80, 127.55(2C), 126.76, 126.71, 126.20, 106.32, 56.91, 45.07, 41.38, 27.07, 23.11, 21.75, 13.86. LC-MS (m/z): 485.6. Anal. Calc. for ($\text{C}_{30}\text{H}_{31}\text{NO}_3\text{S}$: 485.64): C, 74.20; H, 6.43; found: C, 74.01, H, 6.21.

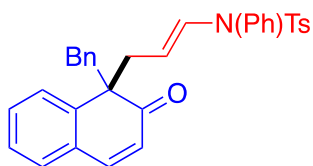


(+/-)-**3da**. Colorless oil, yield = 92% (3 h). ^1H NMR (400 MHz, CDCl_3) δ = 7.41 – 7.36 (m, 1H), 7.31–7.28 (dd, J = 7.6, 4.7 Hz, 3H), 7.23 – 7.14 (m, 7H), 6.62 – 6.59 (m, 3H), 5.95 (d, J = 10.0 Hz, 1H), 3.86 – 3.78 (m, 1H), 2.69 (dd, J = 13.2, 7.2 Hz, 1H), 2.42 (s, 3H), 2.36 (dd, J = 13.2, 7.2 Hz, 1H), 2.24 – 2.15 (m, 1H), 1.85 – 1.76 (m, 1H), 0.43 (t, J = 7.2 Hz, 3H).

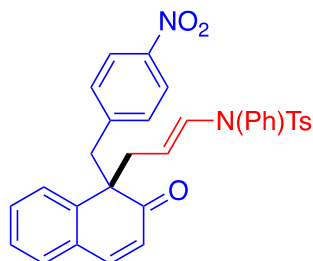
^{13}C NMR (100 MHz, CDCl_3) δ = 204.24, 145.26, 144.39, 143.65, 136.61, 135.95, 131.35, 130.18, 130.03(2C), 129.58(2C), 129.29, 129.22(2C), 128.80, 127.53(2C), 126.79, 126.75, 126.27, 121.88, 106.42, 57.59, 44.65, 34.48, 21.75, 9.19. LC-MS (m/z): 480.5. Anal. Calc. for ($\text{C}_{28}\text{H}_{27}\text{NO}_3\text{S}$: 457.59): C, 73.50; H, 5.95; found: C, 73.21, H, 5.69.



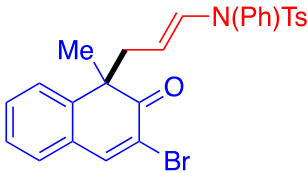
(+/-)-**3ea**. Colorless oil, yield = 68% (24 h). ^1H NMR (400 MHz, CDCl_3) δ = 7.41 – 7.37 (m, 1H), 7.33 – 7.30 (m, 3H), 7.24 – 7.14 (m, 8H), 6.65 – 6.59 (m, 3H), 5.93 (d, J = 10.0 Hz, 1H), 5.23 – 5.13 (m, 1H), 4.81 – 4.70 (m, 2H), 3.86–3.78 (m, 1H), 2.87 (dd, J = 13.6, 7.2 Hz, 1H), 2.73 (dd, J = 13.2, 7.3 Hz, 1H), 2.53 (dd, J = 13.6, 7.2 Hz, 1H), 2.42 (s, 3H), 2.42–2.38 (m, 2H). ^{13}C NMR (100 MHz, CDCl_3) δ = 203.26, 145.22, 143.93, 143.69, 136.58, 135.93, 132.81, 131.62, 130.10, 130.02(2C), 129.59(2C), 129.38, 129.24(2C), 128.84, 127.54(2C), 127.15, 126.88, 126.00, 121.90, 118.11, 106.07, 56.66, 45.35, 43.92, 21.76. LC-MS (m/z): 492. Anal. Calc. for ($\text{C}_{29}\text{H}_{27}\text{NO}_3\text{S}$: 469.60): C, 74.17; H, 5.80; found: C, 74.25, H, 5.45.

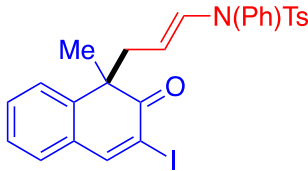


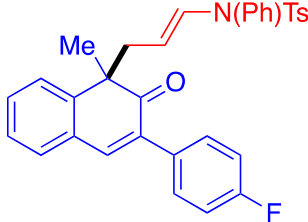
(+/-)-**3fa**. Colorless oil, yield = 77% (5 h). ^1H NMR (400 MHz, CDCl_3) δ = 7.62 (d, J = 8.0 Hz, 1H), 7.45–7.39 (m, 2H), 7.30–7.03 (m, 10H), 6.98–6.91 (m, 3H), 6.66–6.70 (d, J = 16 Hz, 1H), 6.57 (t, J = 8.0 Hz, 3H), 5.77 (d, J = 10.0 Hz, 1H), 3.87 – 3.79 (m, 1H), 3.40 (d, J = 13.2 Hz, 1H), 3.06 (d, J = 12.8 Hz, 1H), 2.96 (dd, J = 13.2, 7.2 Hz, 1H), 2.58 (dd, J = 13.2, 8.4 Hz, 1H), 2.40 (s, 3H). ^{13}C NMR (100 MHz, CDCl_3) δ = 203.35, 145.06, 143.64, 136.59, 136.42, 135.88, 131.71, 131.12, 129.94(2C), 129.85, 129.64(2C), 129.56(2C), 129.32, 129.19(2C), 128.77, 127.71(2C), 127.64, 127.51(2C), 126.89, 126.37, 126.02, 121.88, 106.33, 57.93, 48.04, 43.33, 21.73. LC-MS (m/z): 542.2. Anal. Calc. for ($\text{C}_{33}\text{H}_{29}\text{NO}_3\text{S}$: 519.66): C, 76.27; H, 5.63; found: C, 76.12, H, 5.35.

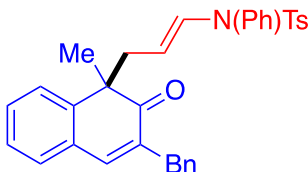


(+/-)-**3ga**. Yellow solid, yield = 62% (3 h). Mp = 78–82 °C ^1H NMR (400 MHz, CDCl_3) δ = 7.78 (d, J = 8.8 Hz, 2H), 7.49 – 7.44 (m, 2H), 7.30 – 7.14 (m, 9H), 6.99 (d, J = 9.6 Hz, 1H), 6.74 (d, J = 8.8 Hz, 2H), 6.70 (d, J = 13.6 Hz, 1H), 6.57–6.55 (m, 2H), 5.77 (d, J = 8.0 Hz, 1H), 3.84–3.76 (m, 1H), 3.54 (d, J = 13.2 Hz, 1H), 3.14 (d, J = 13.2 Hz, 1H), 2.94 (dd, J = 13.2, 7.2 Hz, 1H), 2.60 (dd, J = 13.2, 8.4 Hz, 1H), 2.41 (s, 2H). ^{13}C NMR (100 MHz, CDCl_3) δ = 202.60, 146.69, 145.43, 144.41, 143.79, 142.93, 136.45, 135.86, 132.14, 131.03, 130.38(2C), 130.25, 129.96(2C), 129.69, 129.60(2C), 129.27(2C), 128.90, 127.53(2C), 127.44, 127.38, 126.03, 122.96(2C), 105.23, 57.72, 47.03, 44.17, 21.75. LC-MS (m/z): 587. Anal. Calc. for ($\text{C}_{33}\text{H}_{28}\text{NO}_3\text{S}$: 564.66): C, 70.20; H, 5.00; found: C, 70.41, H, 5.21.

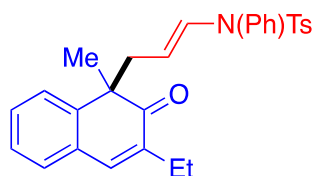

 (+/-)-**3ha**. Colorless oil, yield = 95% (3 h). ^1H NMR (400 MHz, CDCl_3) δ = 7.36 -7.16 (m, 11H), 6.65 (d, J = 6.8, 2H), 6.63 (d, J = 5.6, 1H), 5.94 (d, J = 9.6 Hz, 1H), 3.90-3.83 (m, 1H), 2.67-2.65 (m, 1H), 2.42 (s, 3H), 2.42-2.40 (m, 1H), 1.40 (s, 3H). ^{13}C NMR (100 MHz, CDCl_3) δ = 203.90, 145.78, 145.02, 143.71, 136.61, 135.95, 131.53, 130.09, 130.06(2C), 129.59(2C), 129.34, 129.26(2C), 128.85, 127.54(2C), 126.87, 126.83, 125.24, 121.87, 106.60, 52.24, 44.41, 25.63, 21.75. LC-MS (m/z): 546. Anal. Calc. for ($\text{C}_{27}\text{H}_{24}\text{BrNO}_3\text{S}$: 522.46): C, 62.07; H, 4.63; found: C, 61.96, H, 4.51.


 (+/-)-**3ia**. Light yellow oil, yield = 45% (15 h). ^1H NMR (400 MHz, CDCl_3) δ = 8.02 (s, 1H), 7.40 (td, J = 8.0, 1.6 Hz, 1H), 7.35-7.20 (m, 9H), 7.3 (d, J =7.6 Hz, 1H), 6.71 (dd, J = 8.4, 1.6 Hz, 2H), 6.61 (d, J = 14.0 Hz, 1H), 3.82-3.75 (m, 1H), 2.63 (dd, J = 13.6, 7.6 Hz, 1H), 2.42 (s, 3H), 2.35 (dd, J = 13.2, 8.0 Hz, 1H), 1.46 (s, 3H). ^{13}C NMR (100 MHz, CDCl_3) δ = 197.32, 154.22, 145.60, 143.78, 136.47, 135.87, 131.82, 131.14, 130.68, 130.14(2C), 129.73(2C), 129.44(2C), 128.95, 128.75, 127.56(2C), 127.15, 126.86, 105.48, 101.93, 53.33, 45.81, 25.84, 21.79. LC-MS (m/z): 592. Anal. Calc. for ($\text{C}_{27}\text{H}_{24}\text{INO}_3\text{S}$: 569.46): C, 56.95; H, 4.25; found: C, 56.70, H, 4.31.

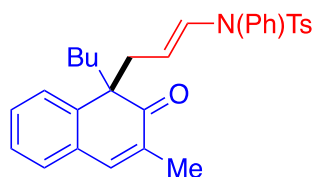

 (+/-)-**3ja**. Light yellow oil, yield = 40% (24 h). ^1H NMR (400 MHz, CDCl_3) δ = 7.48 – 7.47 (m, 1H), 7.38 – 7.36 (m, 1H), 7.34 – 7.22 (m, 9H), 7.12- 7.17 (m, 4H), 7.01 (t, J = 8.8 Hz, 2H), 6.67 – 6.63 (m, 3H), 3.97 – 3.90 (m, 1H), 2.70 (dd, J = 13.2, 7.2 Hz, 1H), 2.40 (s, 3H), 2.03 – 1.98 (m, 1H), 1.48 (s, 3H). ^{13}C NMR (100 MHz, CDCl_3) δ = 202.23, 163.98, 145.40, 143.74, 142.47, 136.58, 135.98, 134.42, 131.51, 130.49(d, $^1J_{\text{CF}}$ =8.0 Hz, 1C), 130.22, 130.11(2C), 129.97, 129.88, 129.61(2C), 129.56, 129.54, 129.34(2C), 128.83, 127.47(2C), 126.84 (d, $^2J_{\text{CF}}$ =43 Hz, 2C), 115.16(d, $^3J_{\text{CF}}$ =22 Hz, 2C), 106.35, 52.83, 45.26, 25.12, 21.75. ^{19}F NMR (376 MHz, CDCl_3) δ -113.87 – -113.93 (m, 1 F). LC-MS (m/z): 560. Anal. Calc. for ($\text{C}_{33}\text{H}_{28}\text{FNO}_3\text{S}$: 537.65): C, 73.72; H, 5.25; found: C, 73.62, H, 5.11.


 (+/-)-**3ka**. Colorless oil, yield =72% (6 h). ^1H NMR (400 MHz, CDCl_3) δ = 7.56 – 7.51 (m, 1H), 7.48 – 7.441 (m, 1H), 7.33 (d, J = 8.0 Hz, 2H), 7.30 – 7.14 (m, 10H), 7.11 – 7.04 (m, 4H), 6.83 (s, 1H), 6.66 – 6.62 (m, 3H), 3.85 – 3.77 (m, 1H), 3.51 (dd, J = 72.0,

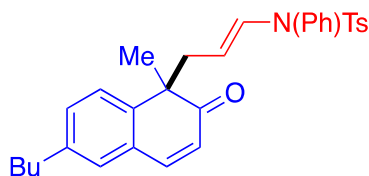
16.0 Hz, 2H), 2.64 (dd, $J = 13.6, 7.6$ Hz, 1H), 2.40 – 2.31 (m, 1H), 2.38 (s, 3H), 1.39 (s, 3H). ^{13}C NMR (100 MHz, CDCl_3) $\delta = 203.03, 144.96, 143.79, 141.88, 139.02, 136.69, 135.90, 135.89, 134.55, 134.42, 131.41(2\text{C}), 130.07(2\text{C}), 129.64(2\text{C}), 129.34(2\text{C}), 129.26(2\text{C}), 129.19, 128.92, 128.81, 128.64(2\text{C}), 127.53(2\text{C}), 126.74, 126.53, 126.41, 106.70, 52.08, 44.81, 35.22, 25.52, 21.72$. LC-MS (m/z): 556.2. Anal. Calc. for ($\text{C}_{34}\text{H}_{31}\text{NO}_3\text{S}$: 533.69): C, 76.52; H, 5.86; found: C, 76.31, H, 5.65.



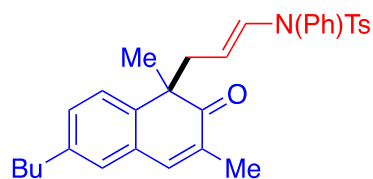
(+/-)-**3la**. Colorless oil, yield = 87% (4 h). ^1H NMR (400 MHz, CDCl_3) $\delta = 7.32 - 7.15$ (m, 11H), 7.02 (s, 1H), 6.67 – 6.64 (m, 2H), 6.58 (d, $J = 12$ Hz, 1H), 3.86-3.78 (m, 1H), 2.66-2.60 (m, 1H), 2.42 (s, 3H), 2.35 (dd, $J = 8.0, 4.0$ Hz, 1H), 2.26-2.15 (m, 2H), 1.39 (s, 3H), 0.95 (t, $J = 8.0$ Hz, 3H). ^{13}C NMR (100 MHz, CDCl_3) $\delta = 203.45, 144.92, 143.68, 139.95, 137.91, 136.64, 135.97, 131.20, 130.38, 130.11(2\text{C}), 129.60(2\text{C}), 129.24(2\text{C}), 128.92, 128.81, 128.57, 127.50(2\text{C}), 126.75, 126.50, 106.66, 51.87, 45.04, 25.43, 22.27, 21.74, 12.60$. LC-MS (m/z): 494.2. Anal. Calc. for ($\text{C}_{29}\text{H}_{29}\text{NO}_3\text{S}$: 471.62): C, 73.86; H, 6.20; found: C, 73.70, H, 6.09.



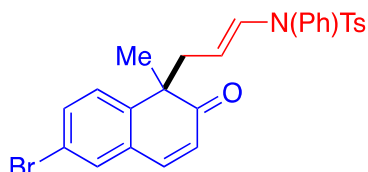
(+/-)-**3ma**. Colorless oil, yield = 94% (6 h). ^1H NMR (400 MHz, CDCl_3) $\delta = 7.34 - 7.11$ (m, 11H), 7.06 (s, 1H), 6.61 (d, $J = 8.0$ Hz, 1H), 6.54 (d, $J = 14$ Hz, 1H), 3.78-3.71 (m, 1H), 2.63 (dd, $J = 13.2, 7.2$ Hz, 1H), 2.42 (s, 3H), 2.34 (dd, $J = 13.2, 4.8$ Hz, 1H), 2.20 – 2.13 (m, 1H), 1.80 – 1.72 (m, 1H), 1.75 (s, 3H), 1.13-1.01 (m, 2H), 0.76 – 0.61 (m, 1H), 0.67 (t, $J = 7.2$ Hz, 3H). ^{13}C NMR (100 MHz, CDCl_3) $\delta = 207.07, 204.10, 144.01, 143.63, 141.98, 136.63, 135.95, 133.32, 131.53, 130.97, 130.07(2\text{C}), 129.59(2\text{C}), 129.17(2\text{C}), 129.04, 128.74, 128.31, 127.46(2\text{C}), 126.59, 126.43, 106.48, 56.50, 45.45, 41.25, 31.06, 23.10, 21.73, 15.58, 13.87$. LC-MS (m/z): 522.6. Anal. Calc. for ($\text{C}_{31}\text{H}_{33}\text{NO}_3\text{S}$: 499.67): C, 74.52; H, 6.66; found: C, 74.27, H, 6.35.



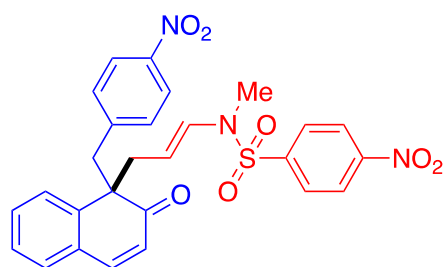
(+/-)-**3na**. Colorless oil, yield = 92% (3 h). ^1H NMR (400 MHz, CDCl_3) $\delta = 7.37$ (d, $J = 8.0$ Hz, 2H), 7.22 – 7.13 (m, 8H), 7.02 (m, 1H), 6.68 – 6.64 (m, 3H), 5.92 (d, $J = 9.6$ Hz, 1H), 3.89-3.82 (m, 1H), 2.67-2.61 (m, 1H), 2.59 (t, $J = 8.0$ Hz, 2H), 2.42 (s, 3H), 2.35 (dd, $J = 11.6, 7.6$ Hz, 1H), 1.61 – 1.54 (m, 2H), 1.37 (s, 3H), 1.37 – 1.30 (m, 2H), 0.93 (t, $J = 7.2$ Hz, 3H). ^{13}C NMR (100 MHz, CDCl_3) $\delta = 204.23, 145.29, 143.71, 142.93, 141.46, 136.69, 135.98, 131.36, 130.28, 130.06(2\text{C}), 129.59, 129.57(2\text{C}), 129.25, 129.22(2\text{C}), 128.77, 127.56(2\text{C}), 126.76, 125.11, 107.07, 51.93, 44.21, 35.12, 33.58, 25.60, 22.46, 21.75, 14.09$. LC-MS (m/z): 523. Anal. Calc. for ($\text{C}_{31}\text{H}_{33}\text{NO}_3\text{S}$: 499.67): C, 74.52; H, 6.66; found: C, 74.31, H, 6.41.



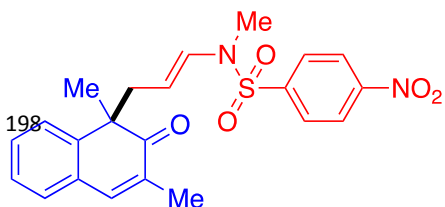
(+/-)-**3oa**. Colorless oil, yield = 86% (3 h). ^1H NMR (400 MHz, CDCl_3) δ = 7.36 (d, J = 8.4 Hz, 2H), 7.25 – 7.13 (m, 6H), 7.08 (dd, J = 8.0, 1.6 Hz, 1H), 7.04 (s, 1H), 6.94 (s, 1H), 6.67 (dd, J = 8.0, 1.6 Hz, 2H), 6.61 (d, J = 14.0 Hz, 1H), 3.85–3.78 (m, 1H), 2.62 – 2.56 (m, 3H), 2.41 (s, 3H), 2.32 (dd, J = 13.2, 7.6 Hz, 1H), 1.78 (d, J = 1.2 Hz, 3H), 1.53 – 1.41 (m, 2H), 1.36 (s, 3H), 1.36–1.28 (m, 2H), 0.92 (t, J = 7.2 Hz, 3H). ^{13}C NMR (100 MHz, CDCl_3) δ = 204.19, 143.70, 142.26, 141.94, 141.30, 136.75, 136.05, 132.35, 130.98, 130.11(2C), 130.09, 129.58(2C), 129.20(2C), 129.14, 128.72, 128.31, 127.53(2C), 126.45, 107.25, 51.56, 44.84, 35.20, 33.60, 25.49, 22.46, 21.74, 15.81, 14.11. LC-MS (m/z): 536.7. Anal. Calc. for ($\text{C}_{32}\text{H}_{35}\text{NO}_3\text{S}$: 513.70): C, 74.82; H, 6.87; found: C, 74.62, H, 6.61.



(+/-)-**3pa**. Colorless oil, yield = 44% (6 h). ^1H NMR (400 MHz, CDCl_3) δ = 7.47 (dd, J = 8.4, 2.0 Hz, 1H), 7.36 (d, J = 2.0 Hz, 1H), 7.31 (d, J = 8.4 Hz, 2H), 7.26 – 7.15 (m, 7H), 6.68 – 6.63 (m, 3H), 5.98 (d, J = 10.0 Hz, 1H), 3.88 – 3.80 (m, 1H), 3.88 – 3.80 (dd, J = 13.2, 6.8 Hz, 1H), 2.44 (s, 3H), 3.37 – 3.32 (dd, J = 13.6, 8.8 Hz, 1H), 1.37 (s, 3H). ^{13}C NMR (100 MHz, CDCl_3) δ = 203.05, 144.53, 143.93, 143.28, 136.53, 135.80, 132.67, 131.81, 131.76, 130.04(2C), 129.67(2C), 129.36(2C), 129.00, 128.68, 127.48(2C), 126.39, 121.91, 120.50, 106.08, 52.15, 44.09, 25.69, 21.80. LC-MS (m/z): 287, 155, 80. Anal. Calc. for ($\text{C}_{27}\text{H}_{24}\text{NO}_3\text{S}$: 522.46): C, 62.07; H, 4.63; found: C, 62.21, H, 4.42.

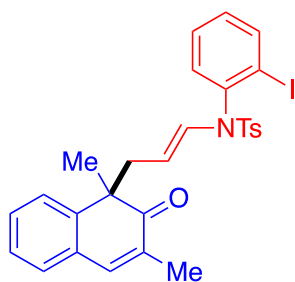


(+/-)-**3ba**. Yellow solid, yield = 91% (30 h). Mp = 62–67 °C. ^1H NMR (400 MHz, CDCl_3) δ = 8.23 (d, J = 8.4 Hz, 2H), 7.81 (d, J = 8.4 Hz, 2H), 7.64 (d, J = 8.4 Hz, 2H), 7.55 (d, J = 3.2 Hz, 2H), 7.37 – 7.33 (m, 1H), 7.15 (d, J = 7.6 Hz, 1H), 7.03 (d, J = 9.6 Hz, 1H), 6.71 (d, J = 8.8 Hz, 2H), 6.56 (d, J = 14.0 Hz, 1H), 5.85 (d, J = 10.0 Hz, 1H), 4.27–4.20 (m, 1H), 3.30 (dd, J = 14.0, 1.4 Hz, 2H), 3.15 – 3.09 (m, 1H), 2.75 (dd, J = 13.6, 7.6 Hz, 1H), 2.57 (s, 3H). ^{13}C NMR (100 MHz, CDCl_3) δ = 202.33, 145.60, 143.65, 142.88, 142.57, 131.19, 130.44, 130.42(2C), 130.15, 130.00, 128.59, 128.21(2C), 127.77, 127.25, 126.21, 124.54, 124.43(2C), 122.97(2C), 106.36, 57.54, 48.83, 42.36, 32.32. LC-MS = 412, 136. Anal. Calc. for ($\text{C}_{32}\text{H}_{25}\text{N}_3\text{O}_7\text{S}$: 595.63): C, 64.53; H, 4.23; found: C, 64.31, H, 4.00.

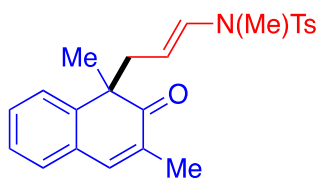


(+/-)-**3ac**. Colorless oil, $c\text{Hex}:\text{EtOAc}$ = 40:1→20:1, yield = 54% (24 h). ^1H NMR (400 MHz, CDCl_3) δ = 8.25

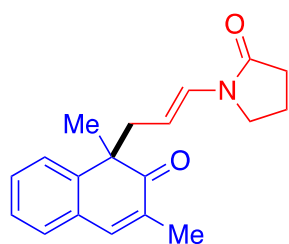
– 8.22 (m, 2H), 7.65 – 7.62 (m, 2H), 7.40 – 7.35 (m, 2H), 7.31 – 7.27 (m, 1H), 7.23-7.18 (m, 2H), 6.48 (d, $J = 14.0$ Hz, 1H), 4.33 – 4.25 (m, 1H), 2.87 (ddd, $J = 14.0, 7.2, 1.2$ Hz, 1H), 2.61 (s, 3H), 2.52 (ddd, $J = 14.0, 8.0, 1.2$ Hz, 1H), 1.91 (d, $J = 1.6$ Hz, 3H), 1.40 (s, 3H). ^{13}C NMR (100 MHz, CDCl_3) $\delta = 203.54, 150.13, 144.88, 143.07, 141.66, 132.61, 130.38, 129.34, 129.18, 128.84, 128.20(2\text{C}), 127.01, 126.40, 124.43(2\text{C}), 108.05, 51.88, 42.39, 32.40, 27.81, 15.93$. LC-MS (m/z): 449.0. Anal. Calc. for ($\text{C}_{22}\text{H}_{22}\text{N}_2\text{O}_5\text{S}$: 426.49): C, 61.86; H, 5.20; found: C, 61.61, H, 5.01.



(+/-)-3ad. Yellow solid, cHex:EtOAc = 40:1, yield = 63% (10 h) Mp = 57-63 °C. ^1H NMR (400 MHz, CDCl_3) $\delta = 7.85 - 7.83$ (m, 1H), 7.50 (d, $J = 8.8$ Hz, 1H), 7.35 (d, $J = 8.8$ Hz, 1H), 7.30 – 7.25 (m, 5H), 7.16 – 7.09 (m, 3H), 6.98 – 6.94 (m, 1H), 6.54 (dd, $J = 36.0, 14.0$ Hz, 1H), 6.36 (ddd, $J = 59.2, 8.0, 1.6$ Hz, 1H), 3.70 – 3.58 (m, 1H), 2.70 - 2.57 (m, 1H), 2.43 (d, $J = 5.2$ Hz, 3H), 2.40 – 2.33 (m, 1H), 1.78 (dd, $J = 27.2, 0.8$ Hz, 3H), 1.38 (d, $J = 4.4$ Hz, 1H). ^{13}C NMR (100 MHz, CDCl_3) $\delta = 203.99$ (203.79), 145.03 (144.75), 144.11 (143.91), 142.06 (141.85), 140.83 (140.73), 139.41, 136.43, 132.54 (132.22), 130.41(2C), 130.38 (130.24), 130.28 (130.15), 129.88 (129.72), 129.80(2C) (129.76(2C)), 128.89(2C), 128.68, 128.42, 127.84 (127.73), 126.76 (126.70), 126.68 (126.55), 107.67 (107.21), 102.48 (102.34), 51.77 (51.67), 44.39 (44.04), 25.88, 21.80 (21.76), 15.98 (15.74). LC-MS (m/z): 606.6. Anal. Calc. for ($\text{C}_{28}\text{H}_{26}\text{INO}_3\text{S}$: 538.48): C, 57.64; H, 4.49; found: C, 57.41, H, 4.31.

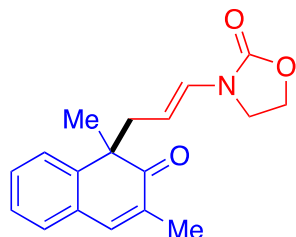


(+/-)-3ae. Colorless oil, cHex:EtOAc = 40:1→20:1, yield = 98% (3 h). ^1H NMR (400 MHz, CDCl_3) $\delta = 7.39$ (d, $J = 8.0$ Hz, 2H), 7.34-7.33 (m, 2H), 7.27-7.17 (m, 5H), 6.50 (d, $J = 14.0$ Hz, 3H), 4.20 – 4.13 (m, 1H), 2.79 – 2.74 (m, 1H), 2.56 (s, 3H), 2.50 – 2.44 (m, 1H), 2.38 (s, 3H), 1.89 (d, $J = 1.2$ Hz, 3H), 1.41 (s, 3H). ^{13}C NMR (100 MHz, CDCl_3) $\delta = 203.81, 145.05, 143.61, 141.57, 134.76, 132.64, 130.34, 130.22, 129.76(2\text{C}), 129.06, 128.67, 127.03(2\text{C}), 126.87, 126.46, 105.49, 51.88, 43.48, 32.15, 26.63, 21.67, 15.91$. LC-MS (m/z): 418.0. Anal. Calc. for ($\text{C}_{28}\text{H}_{27}\text{NO}_3\text{S}$: 457.59): C, 73.50; H, 5.95; found: C, 73.26, H, 5.78.



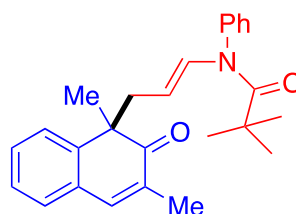
(+/-)-3af. Colorless oil, cHex:EtOAc = 40:1→20:1, yield = 82% (15 h). ^1H NMR (400 MHz, CDCl_3) $\delta = 7.34 - 7.32$ (m, 2H), 7.25 – 7.20 (m, 3H), 6.65 (d, $J = 14.4$ Hz, 1H), 4.45-4.37 (m, 1H), 3.28 – 3.17 (m, 2H), 2.77 (dd, $J = 13.6, 7.2$ Hz, 1H), 2.49 (dd, $J = 15.6, 8.0$ Hz, 1H), 2.37 (t, $J = 8.8$ Hz, 2H), 2.00 – 1.92 (m, 2H), 1.96 (s, 3H), 1.43 (s, 3H). ^{13}C NMR (100 MHz, CDCl_3) $\delta = 203.95, 172.91, 145.14, 141.58,$

132.56, 130.26, 129.10, 128.67, 126.90, 126.48, 125.97, 106.60, 51.91, 45.21, 43.60, 31.28, 26.08, 17.37, 16.04. LC-MS (m/z): 318.0. Anal. Calc. for (C₁₉H₂₁NO₂: 295.38): C, 77.26; H, 7.17; found: C, 77.01, H, 7.31.



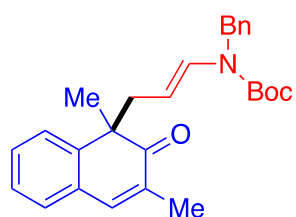
(+/-)-**3ag**. Colorless oil, cHex:EtOAc = 40:1→20:1, yield = 88% (10 h). ¹H NMR (400 MHz, CDCl₃) δ = 7.34 (d, *J* = 3.2 Hz, 2H), 7.26 – 7.21(m, 3H), 6.43 (d, *J* = 14.4 Hz, 1H), 4.32 – 4.25(m, 3H), 3.47 – 3.36 (m, 2H), 2.79 (dd, *J* = 14.0, 8.0Hz, 1H), 2.49 (dd, *J* = 10.0, 8.0 Hz, 1H), 1.97 (s, 3H), 1.43 (s, 3H). ¹³C NMR (100 MHz, CDCl₃) δ = 203.84, 155.23, 145.02, 141.64, 132.57, 130.27, 129.17, 128.73,

126.98, 126.44, 126.23, 105.55, 62.09, 51.88, 43.04, 42.53, 26.42, 16.03. LC-MS (m/z): 320.2. Anal. Calc. for (C₁₈H₁₉NO₃: 297.35): C, 72.71; H, 6.44; found: C, 72.55, H, 6.21.



(+/-)-**3ah**. Yellow oil, yield = 54% (48 h). ¹H NMR (400 MHz, CDCl₃) δ = 7.30 – 7.13 (m, 7H), 7.08 (s, 1H), 7.00 (d, *J* = 16.0 Hz, 1H), 6.87 – 6.85 (m, 2H), 3.73 – 3.65 (m, 1H), 2.59 (dd, *J* = 13.2, 6.8 Hz, 1H), 2.32 (dd, *J* = 12.0, 8.4 Hz, 1H), 1.83 (s, 3H), 1.39 (s, 3H), 0.98 (s, 9H). ¹³C NMR (100 MHz, CDCl₃) δ = 204.13, 176.02, 145.11,

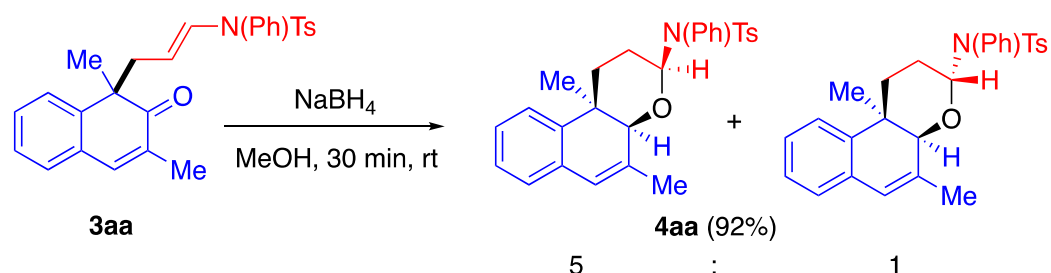
141.78, 140.32, 133.70, 132.51, 130.25(2C), 129.04(2C), 128.90, 128.30, 128.16, 126.73, 126.60, 120.08, 108.99, 51.81, 45.75, 29.13, 27.80, 24.88, 15.86. LC-MS (m/z): 410. Anal. Calc. for (C₂₆H₂₉NO₂: 387.52): C, 80.59; H, 7.54; found: C, 80.50, H, 7.22.



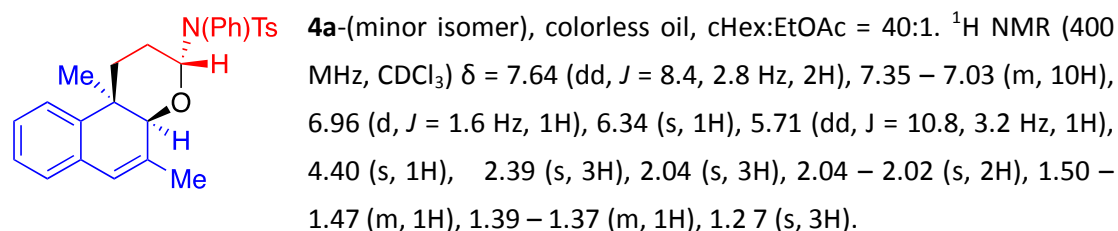
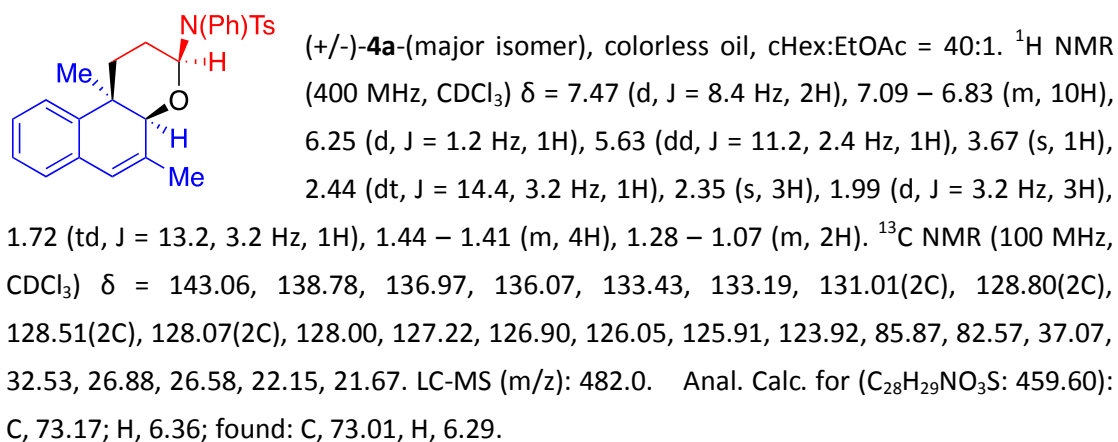
(+/-)-**3aj**. Colorless oil, yield = 92% (3 h). ¹H NMR (400 MHz, CDCl₃) δ = 7.33 – 7.14 (m, 5H), 7.15 (d, *J* = 7.6 Hz, 1H), 7.09 (d, *J* = 7.2 Hz, 1H), 6.87 (d, *J* = 7.6 Hz, 3H), 6.49 (d, *J* = 13.2 Hz, 1H), 4.44 (s, 2H), 4.12 (s, 1H), 2.59 (s, 1H), 2.35 (s, 1H), 1.46 (s, 3H), 1.36 (s, 9H). ¹³C NMR (100 MHz, CDCl₃) δ = 204.28, 201.33, 153.21, 145.03, 141.77,

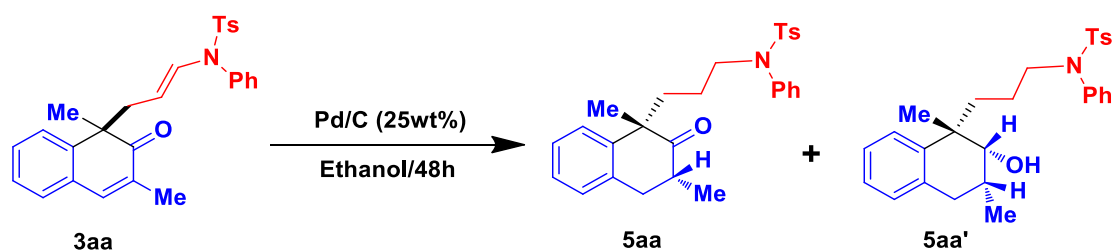
132.31, 130.37, 129.42, 128.72, 128.51(2C), 126.76, 126.53(2C), 126.47, 103.82, 103.42, 81.36, 51.81, 39.85, 33.91, 29.83, 28.55, 28.35, 25.25. LC-MS (m/z): 440.2. Anal. Calc. for (C₂₇H₃₁NO₃: 417.55): C, 77.67; H, 7.48; found: C, 77.51, H, 7.37.

Synthesis of the 1*H*-benzochromene **4aa**:

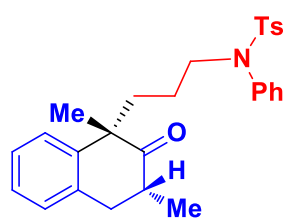


A one-necked flash was charged with reagent grade methanol (2 ml), racemic **3aa** (0.1 mmol) and NaBH_4 (0.15 mmol) in a sequence. The reaction was stirred at rt for 0.5 h at rt. The solvent was removed under vacuum, then water was added and the product extract three times with AcOEt. After dryness with Na_2SO_4 the volatiles were removed under vacuum. $^1\text{H-NMR}$ spectrum was collected on the crude mixture (*dr* = 5:1). Finally, the product was purified by flash chromatography (combined yield = 92%).

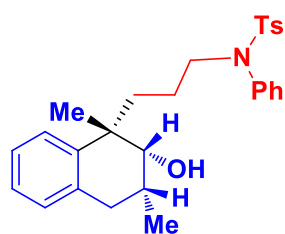


Hydrogenation of **3aa**:

To an oven-dried two-necked flask with ethanol (3 ml) was charged **3aa** (27 mg, 0.06 mmol) and Pd/C (8.2 mg, 25 wt%) and the flask was subjected to H₂ atmosphere (1 atm, balloon). The reaction was stirred at room temperature for 48 h. Then, the reaction mixture was filtrated through celite and concentrated under reduced pressure. The residue was purified via flash-chromatography on silica gel (*c*-Hex:AcOEt = 20:1) to afford compound **5aa** and **5aa'**.

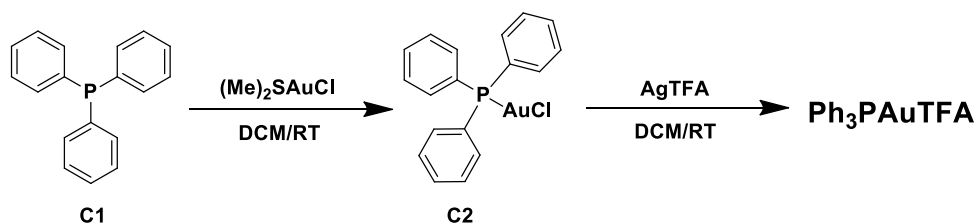


5aa, Colorless oil, yield = 33%, *c*Hex:EtOAc = 40:1. ¹H NMR (400 MHz, CDCl₃) δ = 7.37 (d, *J* = 8.0 Hz, 2H), 7.22 – 7.16 (m, 6H), 7.03 (d, *J* = 7.6 Hz, 1H), 6.85 – 6.82 (m, 2H), 3.42 – 3.35 (m, 1H), 3.26 – 3.20 (m, 1H), 2.88 (dd, *J* = 15.2, 5.6 Hz, 1H), 2.74 – 2.68 (m, 1H), 2.56 (d, *J* = 15.2 Hz, 1H), 2.38 (s, 3H), 2.25 (ddd, *J* = 16.0, 11.6, 5.6 Hz, 1H), 1.68 – 1.60 (m, 1H), 1.38 (s, 3H), 1.07 (d, *J* = 6.4 Hz, 3H), 1.01 – 0.91 (m, 1H), 0.84 – 0.71 (m, 1H). ¹³C NMR (100 MHz, CDCl₃) δ = 215.23, 143.12, 141.77, 138.75, 135.64, 135.37, 129.78, 129.35, 129.24(2C), 128.76(2C), 127.66(2C), 127.63(2C), 126.99, 126.54, 126.19, 51.56, 50.61, 40.51, 37.13, 36.89, 28.80, 23.64, 21.47, 14.33. LC-MS (*m/z*): 491.0. Anal. Calc. for (C₂₈H₃₁NO₃S: 461.62): C, 72.85; H, 6.77; found: C, 73.01, H, 6.29.



5aa', Colorless oil, yield = 45%, *c*Hex:EtOAc = 40:1. ¹H NMR (400 MHz, CDCl₃) δ = 7.45 (d, *J* = 8.4 Hz, 2H), 7.33 – 7.27 (m, 3H), 7.22 (d, *J* = 8.0 Hz, 3H), 7.12 (t, *J* = 7.2 Hz, 1H), 7.08 – 7.06 (m, 3H), 7.02 (d, *J* = 7.2 Hz, 1H), 3.63 – 3.43 (m, 2H), 3.44 (s, 1H), 2.64 – 2.60 (m, 2H), 2.40 (s, 3H), 2.12 – 2.06 (m, 1H), 1.91 – 1.81 (m, 2H), 1.67 – 1.51 (m, 2H), 1.05 (d, *J* = 6.8 Hz, 3H), 1.05 (s, 3H). ¹³C NMR (100 MHz, CDCl₃) δ = 143.42, 142.91, 139.46, 135.37, 135.00, 129.49(2C), 129.12(2C), 128.98, 128.89(2C), 127.95, 127.91(2C), 126.98, 126.50, 125.74, 75.98, 51.51, 42.00, 35.34, 32.49, 28.99, 28.96, 23.11, 21.69, 18.83. LC-MS (*m/z*): 463.1. Anal. Calc. for (C₂₈H₃₃NO₃S: 463.63): C, 72.54; H, 7.17; found: C, 73.01, H, 6.29.

The preparation of preformed catalyst($\text{Ph}_3\text{PAuOTf}_3$)



Preparation of C2: The following process was modified partly^[3]. A two-necked flask dried by heating gun was charged with anhydrous **DCM(3ml)** and **(Me)₂SAuCl(39.3mg, 0.15mmol)** under dark atmosphere. During solution was stirring, a solution of **Ph₃P(44.2 mg, 0.15mmol)** in DCM(3ml) was added dropwise. After keeping the reaction stirring for 5h, the solvent was removed under reduced pressure. The residue was washed with diethyl ether. After removing the diethyl ether under vacuum, **C2** was collected as a white power(59mg, 0.12mmol, 80%).

Preparation of C2: A dry two-necked flask was charged with **C2(59mg, 0.12mmol)** collected from above reaction, **AgTFA (26.4mg, 0.12mmol)** and anhydrous **DCM(3ml)** under dark atmosphere. After keeping this reaction stirring at room temperature for 3h, the solution was filtered through neutral alumina(ca. 5cm x 5cm). Then the solvent was removed under reduced pressure and the remains was washed with diethyl ether. After removing the diethyl ether under vacuum, **Cat** was collected as a white power(59mg, 0.10mmol, 83%).

Ph₃PAuTFA, white power, yield = 83%. ¹H NMR (400 MHz, CD₂Cl₂) δ = 7.59 – 7.51 (m, 15H). ¹⁹F NMR (400 MHz, CD₂Cl₂) δ = -74.31(s, 3F). ³¹P NMR (400 MHz, CD₂Cl₂) δ = 30.04(s).

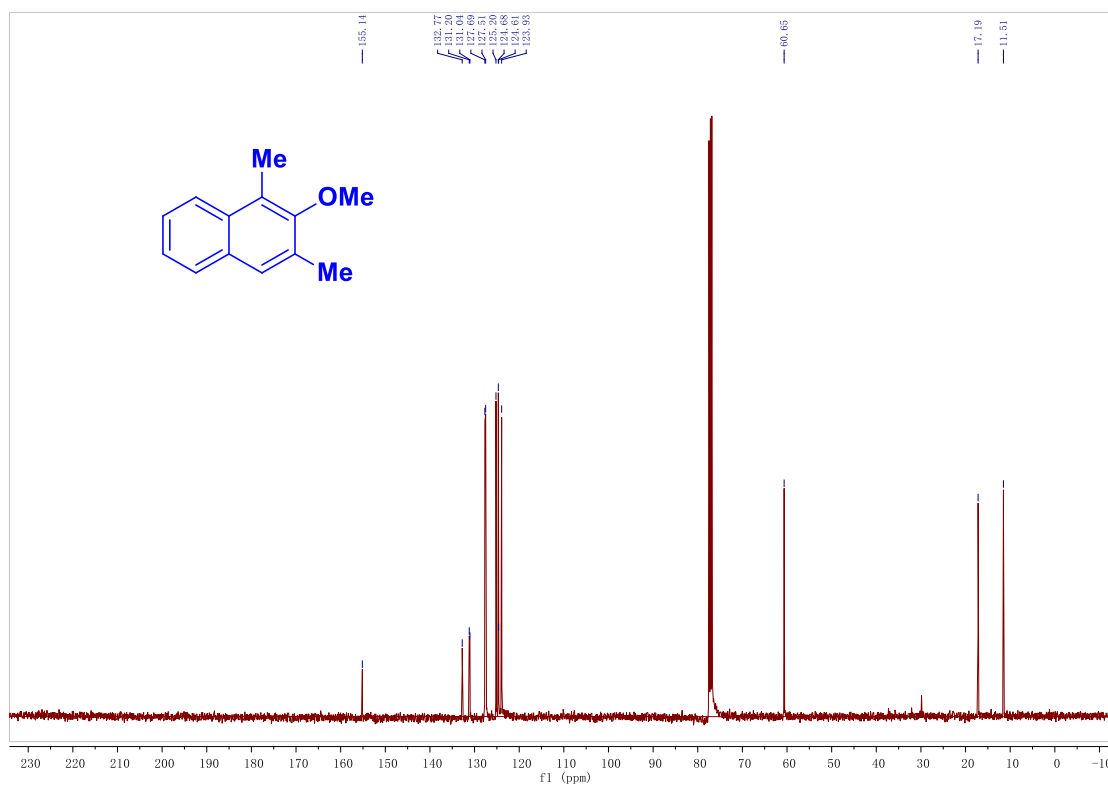
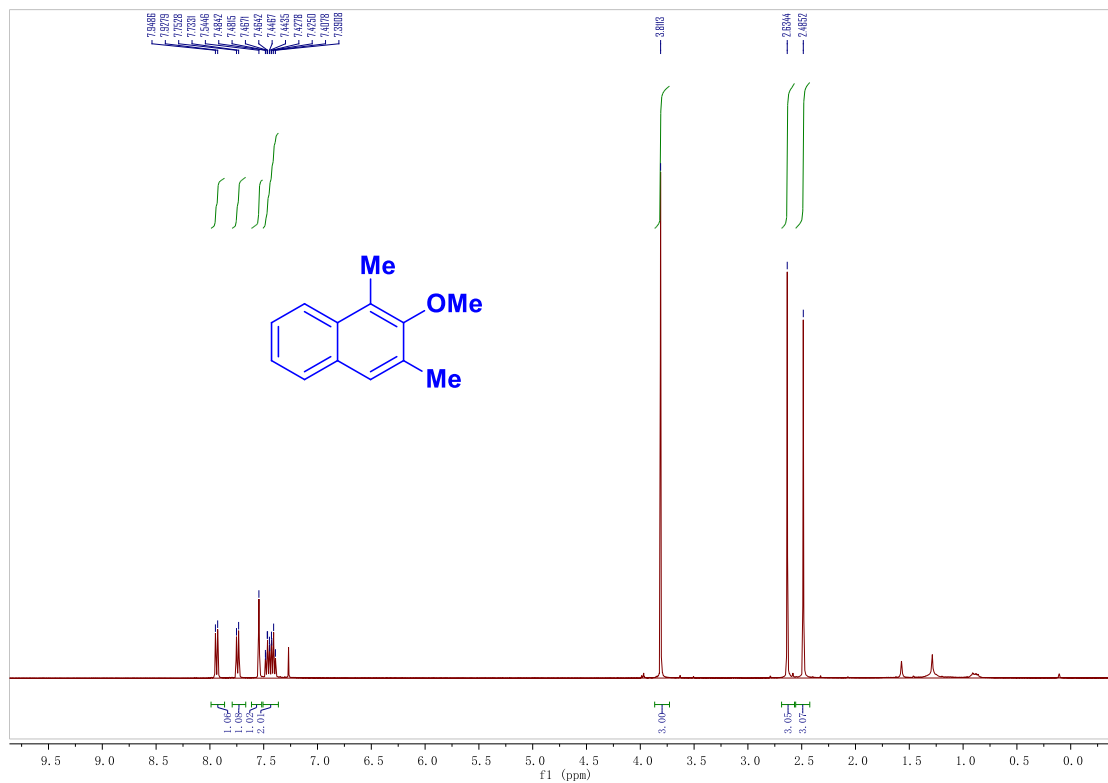
Mechanism study experiment

To a NMR tube was added **Ph₃PAuTFA (1.43mg, 10mol%)**, the proton, fluorine, phosphine NMR datas was collected. Next, **1a (4.3mg, 0.025mmol)** was added into NMR tube and keep obtaining the proton, fluorine, phosphine NMR. At last **2a (14.3mg, 0.025mmol)** was added and keep monitoring the NMR data continually at different time at room temperature.

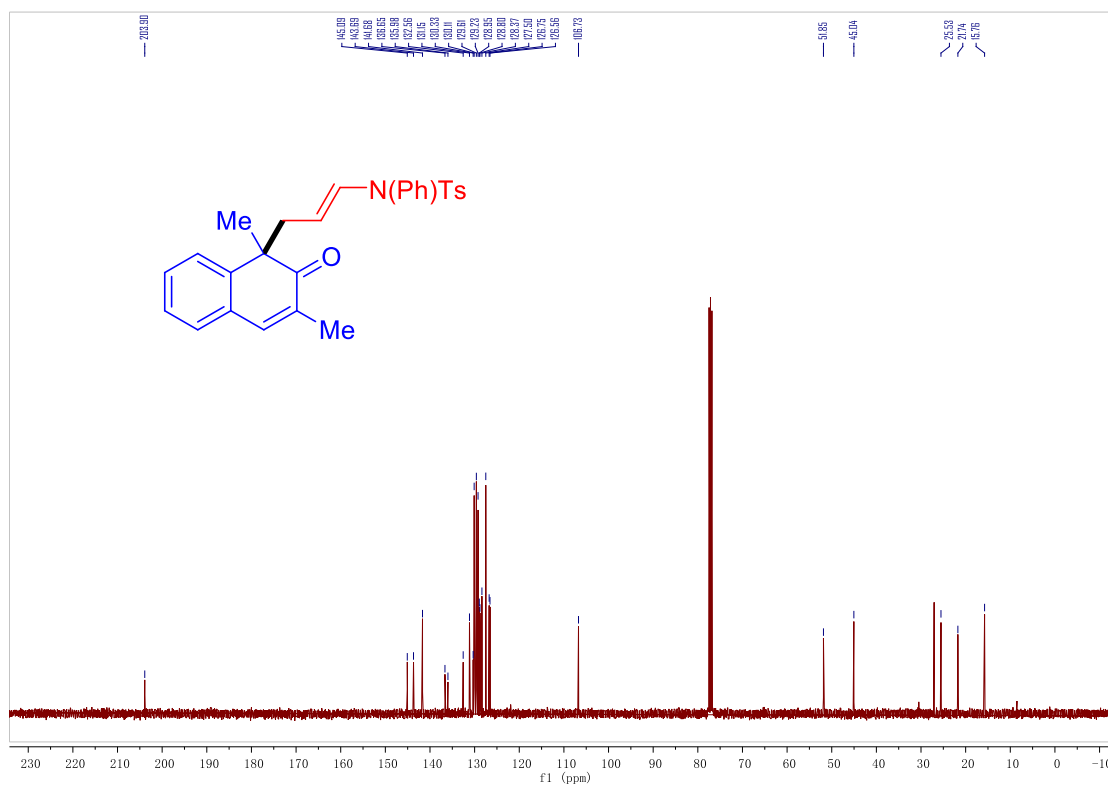
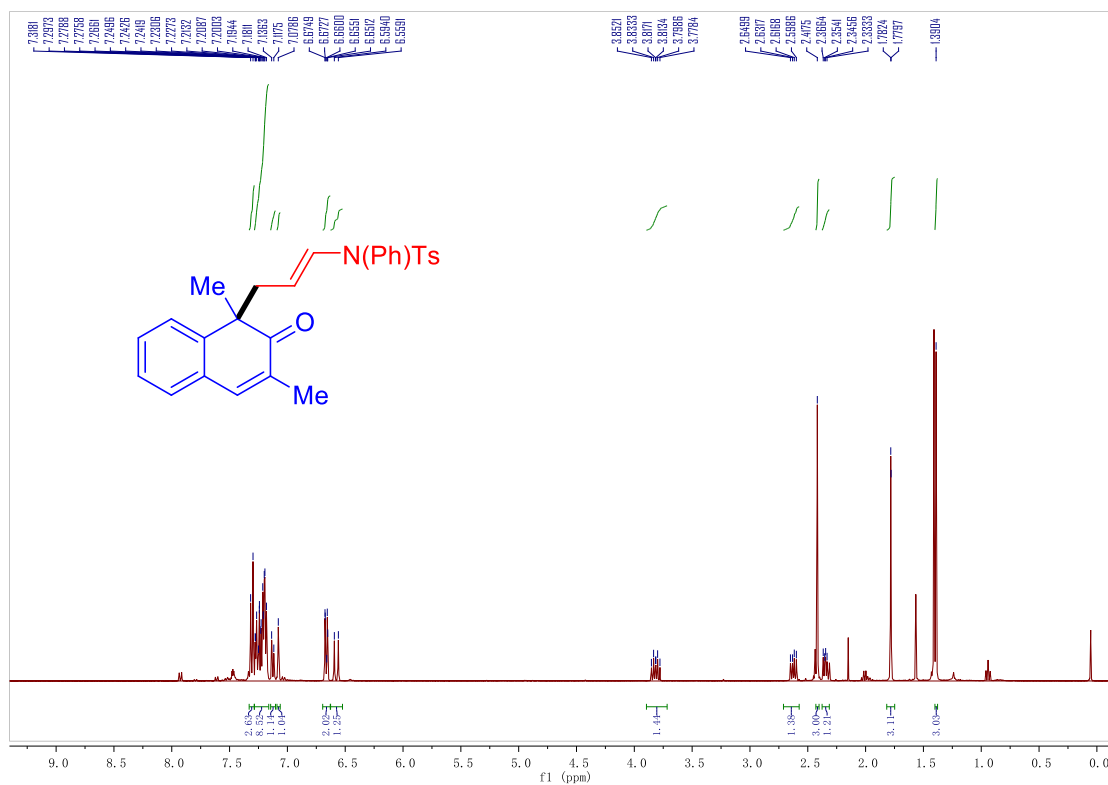
References

- [1] a) T. Oguma, T. Katsuki, J. Am. Chem. Soc. 2012, 134, 20017-20020. b) Y. Zhang, Y. Liao, X.hua Liu, X. Xu, L. Lin, X. Feng, Chem. Sci., 2017, 8, 6645–6649. c) J. Nan, J. Liu, H. Zheng, Z. Zuo, L. Hou, H. Hu, Y. Wang, X. Luan, Angew. Chem. Int. Ed. 2015, 54, 2356 -2360.
- [2] a) Y. Liu, A. De Nisi, A. Cerveri, M. Monari, M. Bandini, Org. Lett. 19, 19, 5034-5037. b) M. Jia, G. Cera, D. Perrotta, M. Monari, Marco Bandini, Chem. Eur. J. 2014, 20, 9875-9878.
- [3] a) M. Preisenberger, A. Schier and H. Schmidbaur, J. Chem. Soc., Dalton Trans., 1999, 1645–1650; b) Z.S Zhang, S. Edward; P. Gus J, Colgate, Sam O., Acta Crystallographica, Section C: Crystal Structure Communications, 1988, vol. 44, p. 2197 - 2198

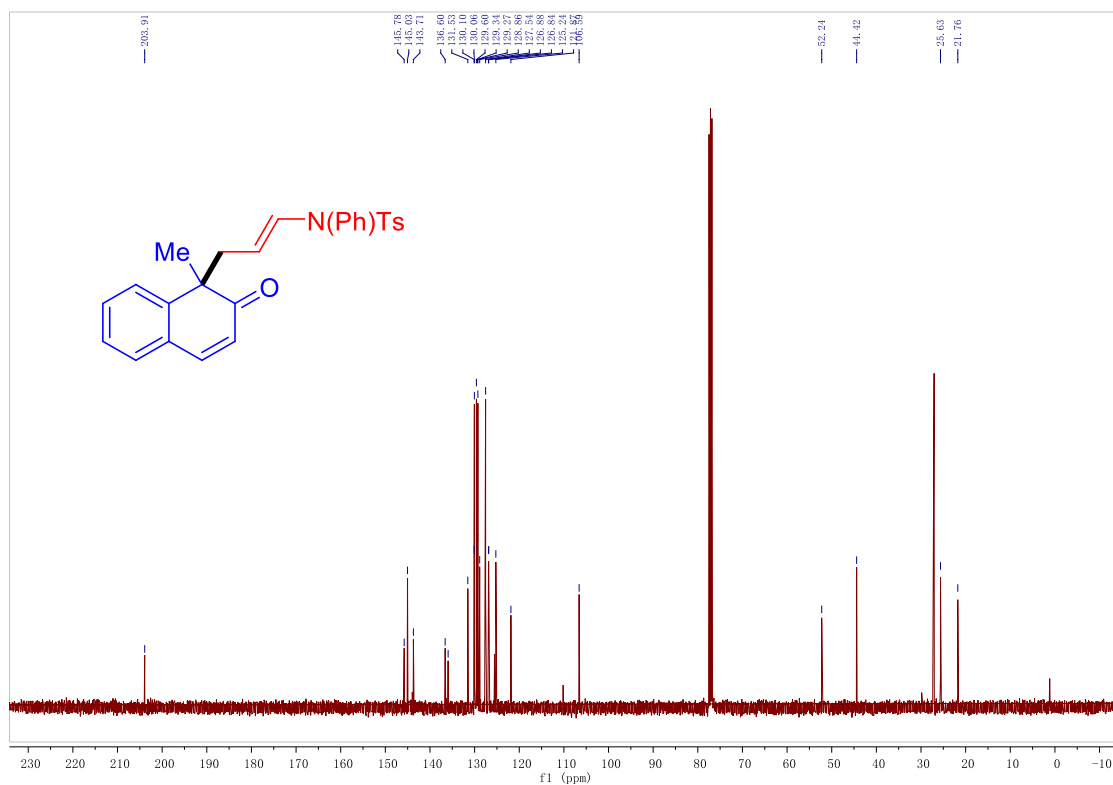
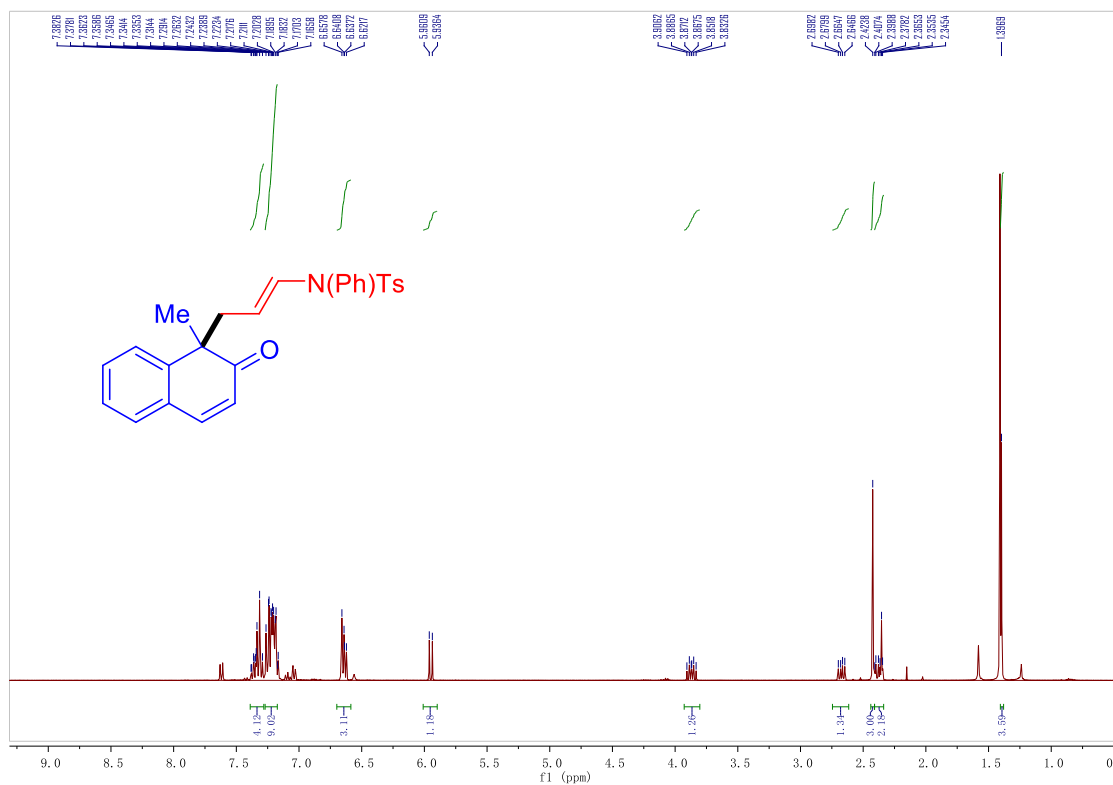
Chapter 3



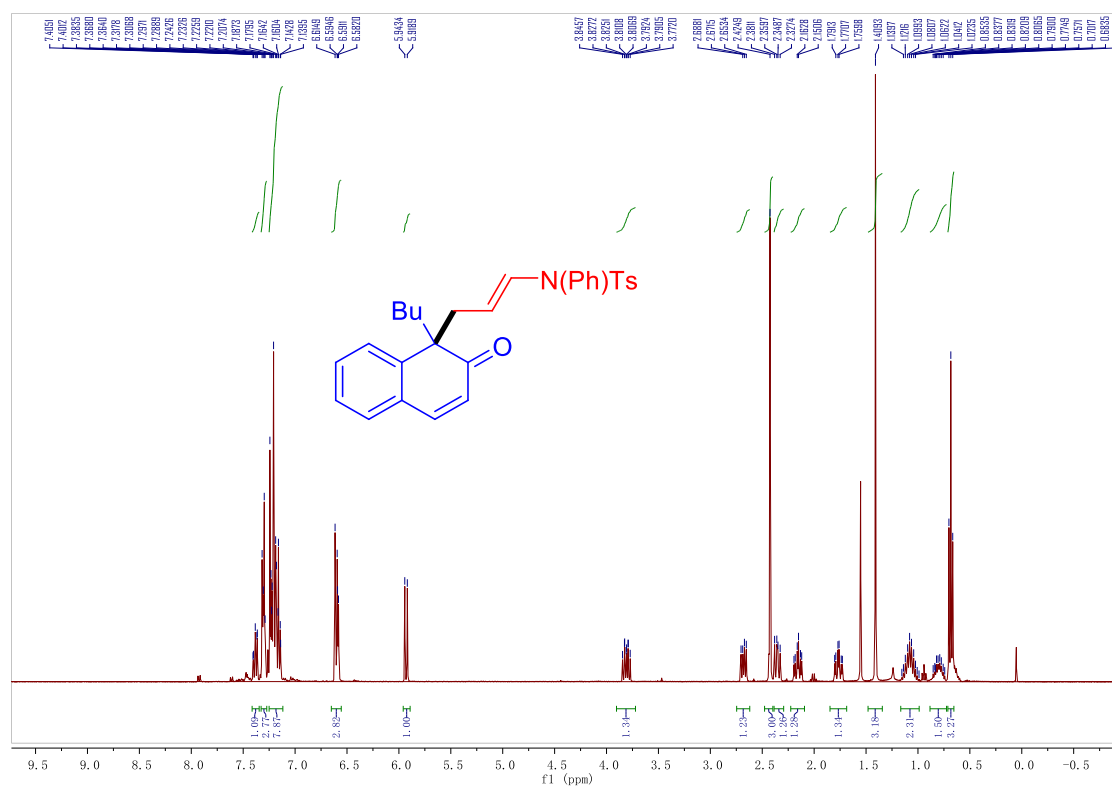
Chapter 3



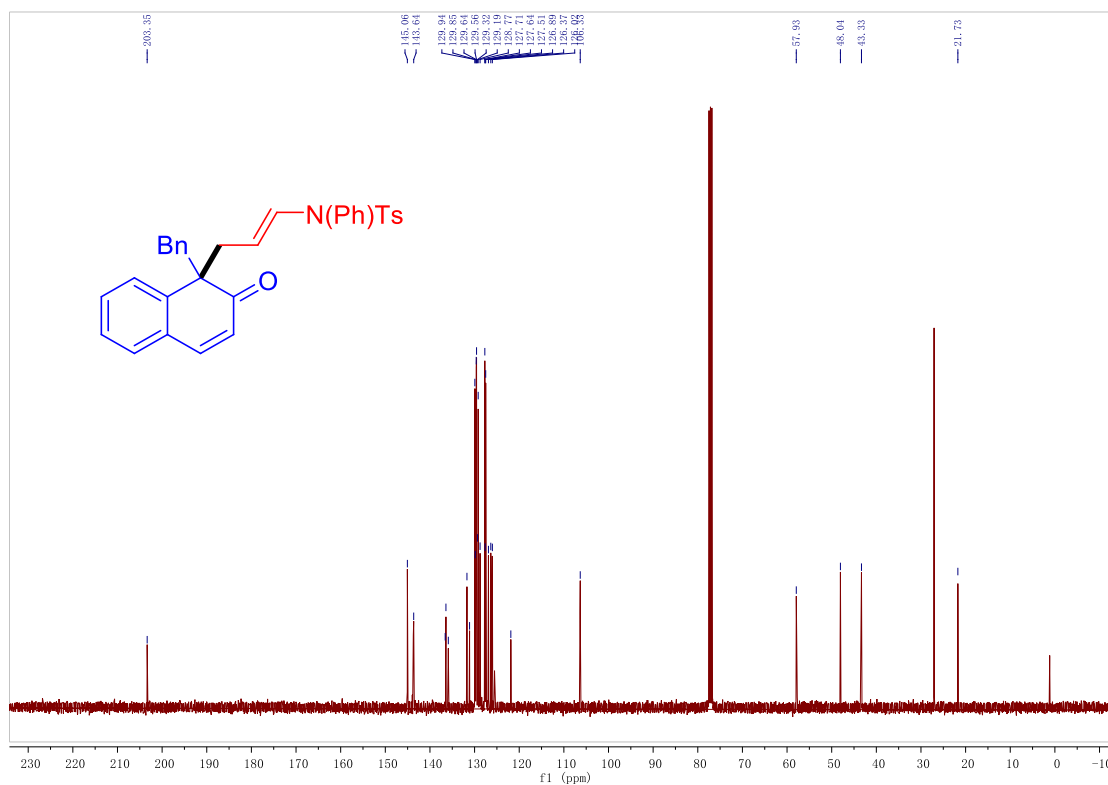
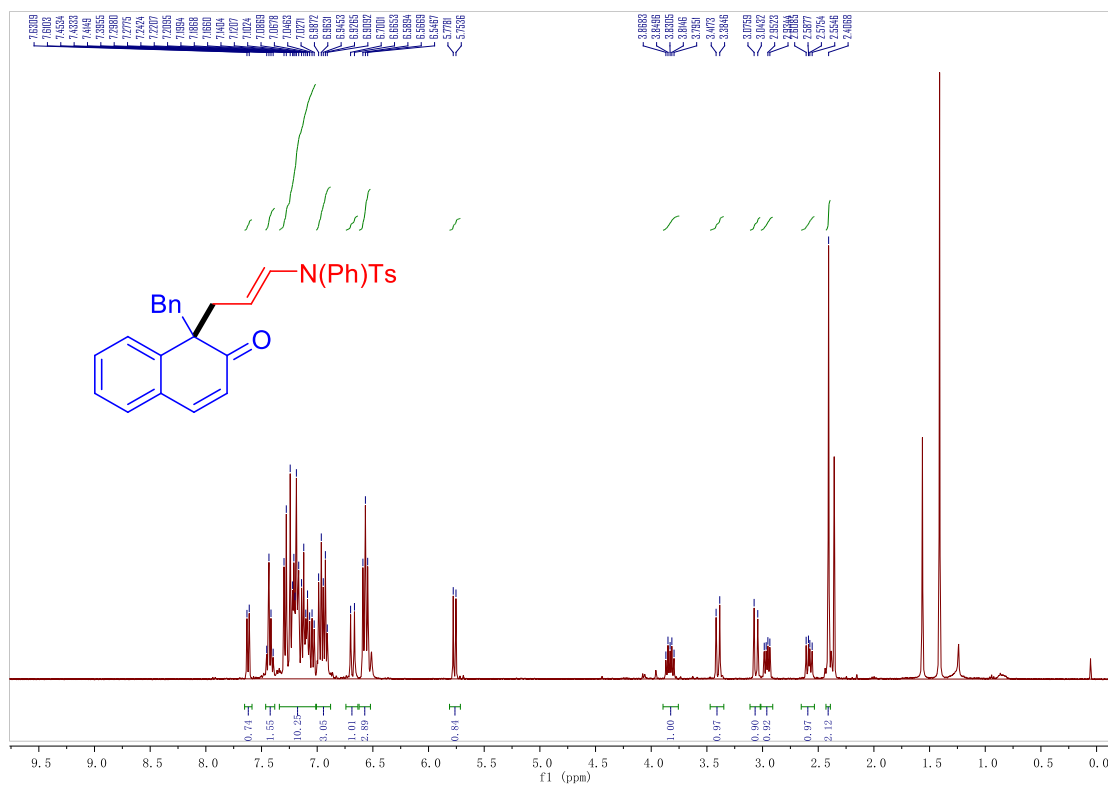
Chapter 3



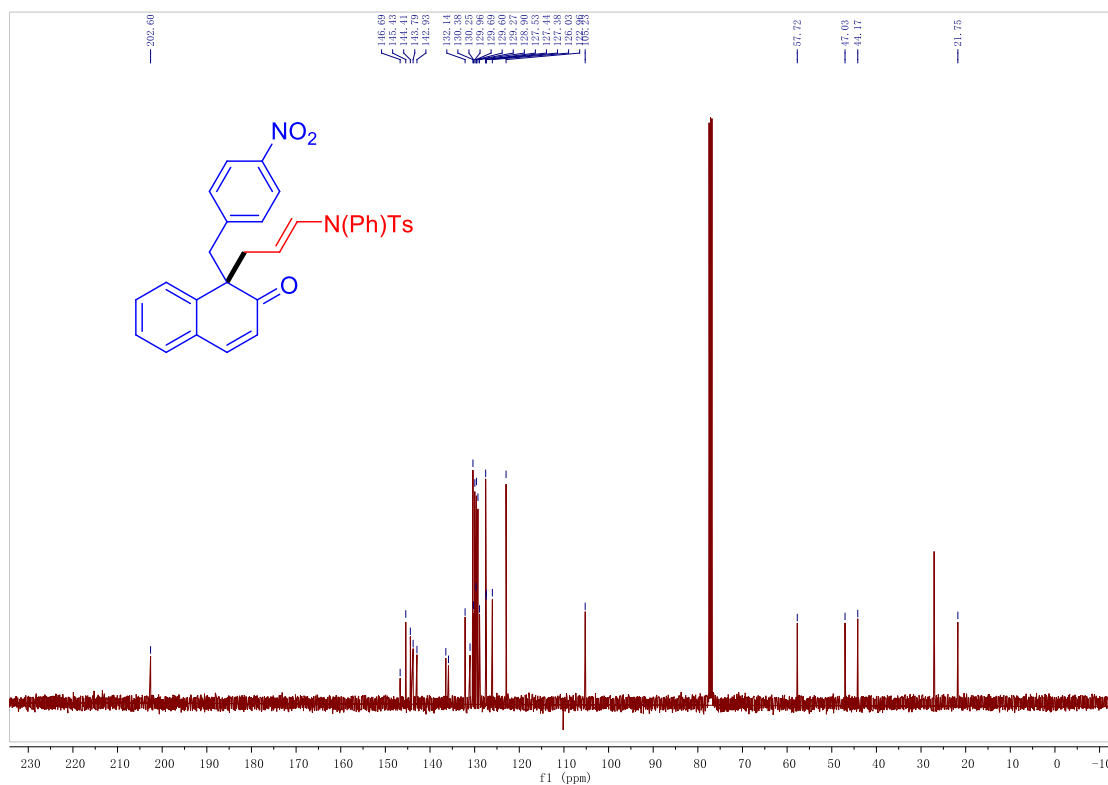
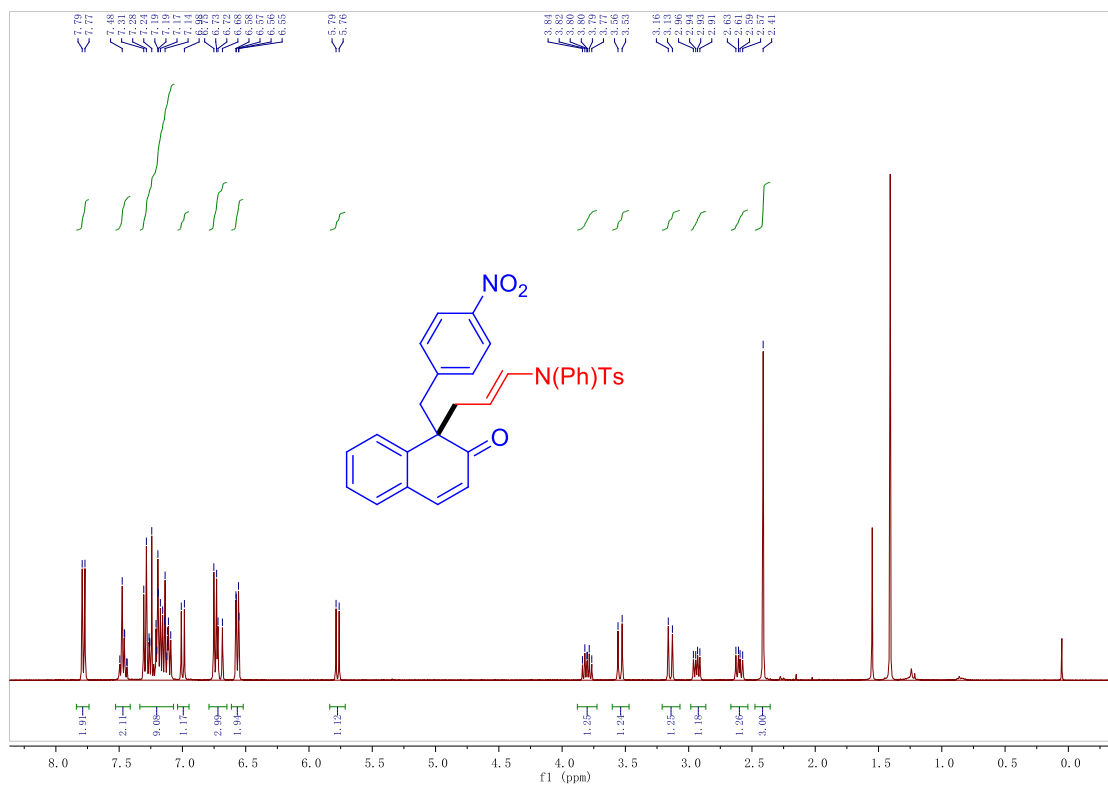
Chapter 3



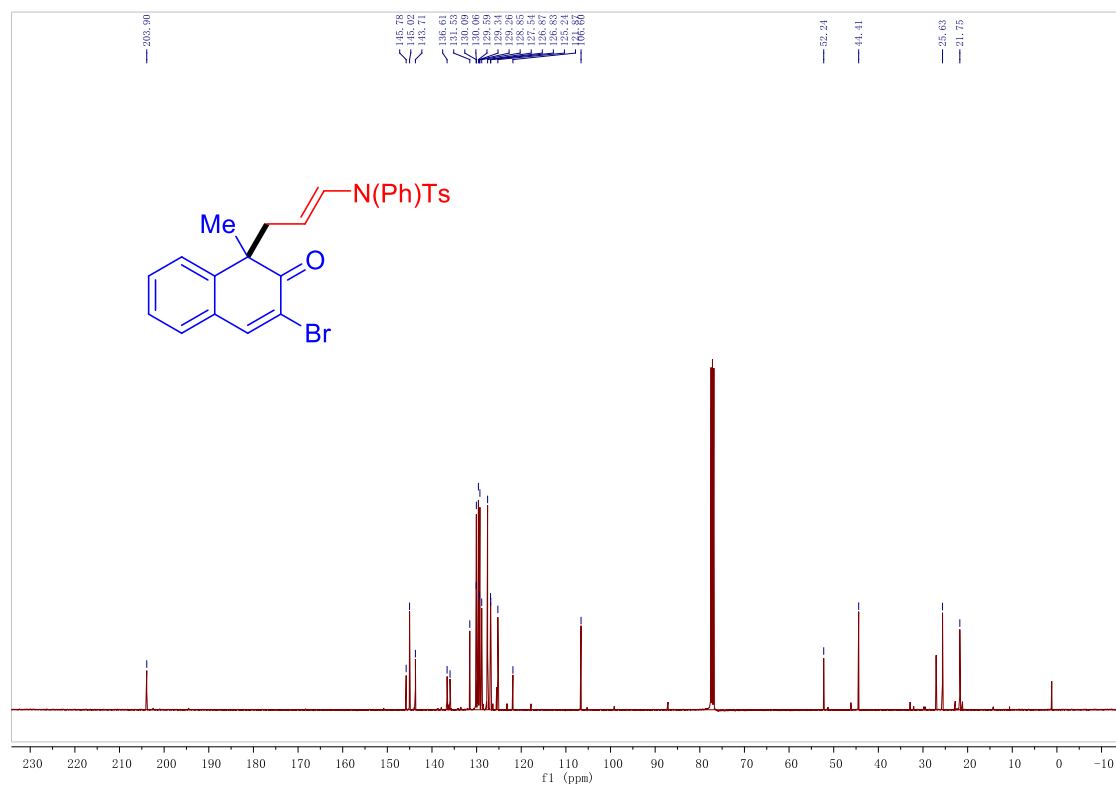
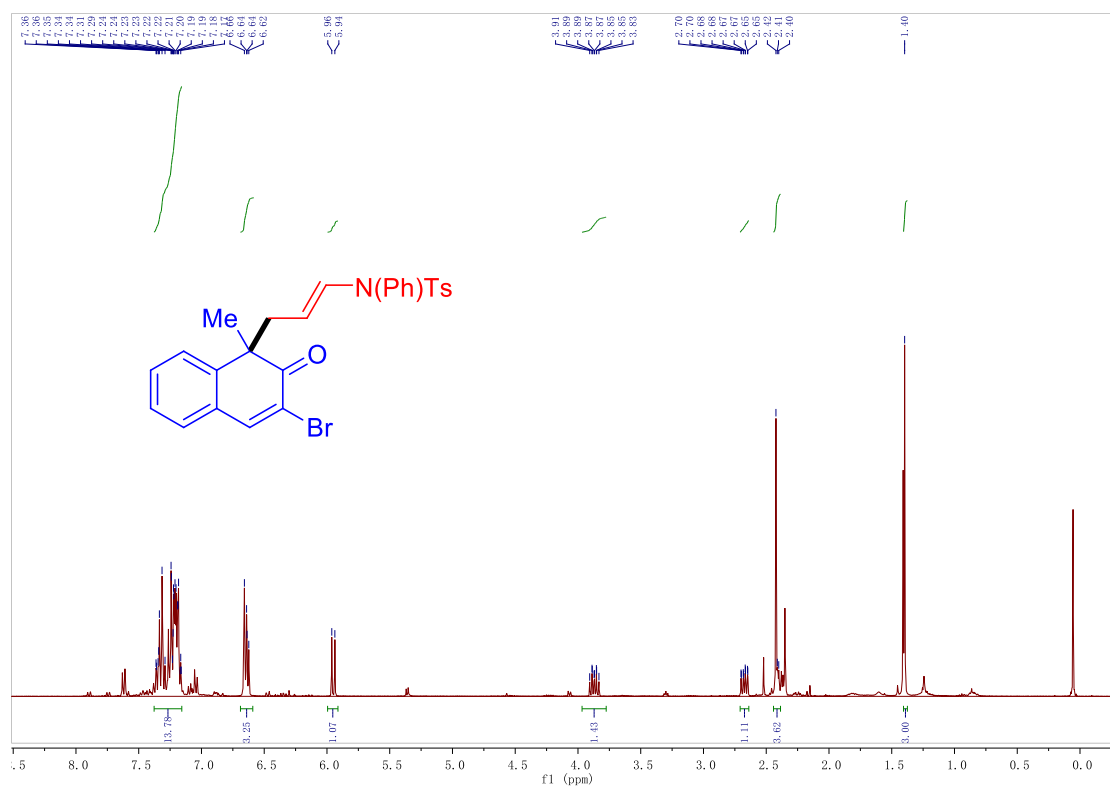
Chapter 3



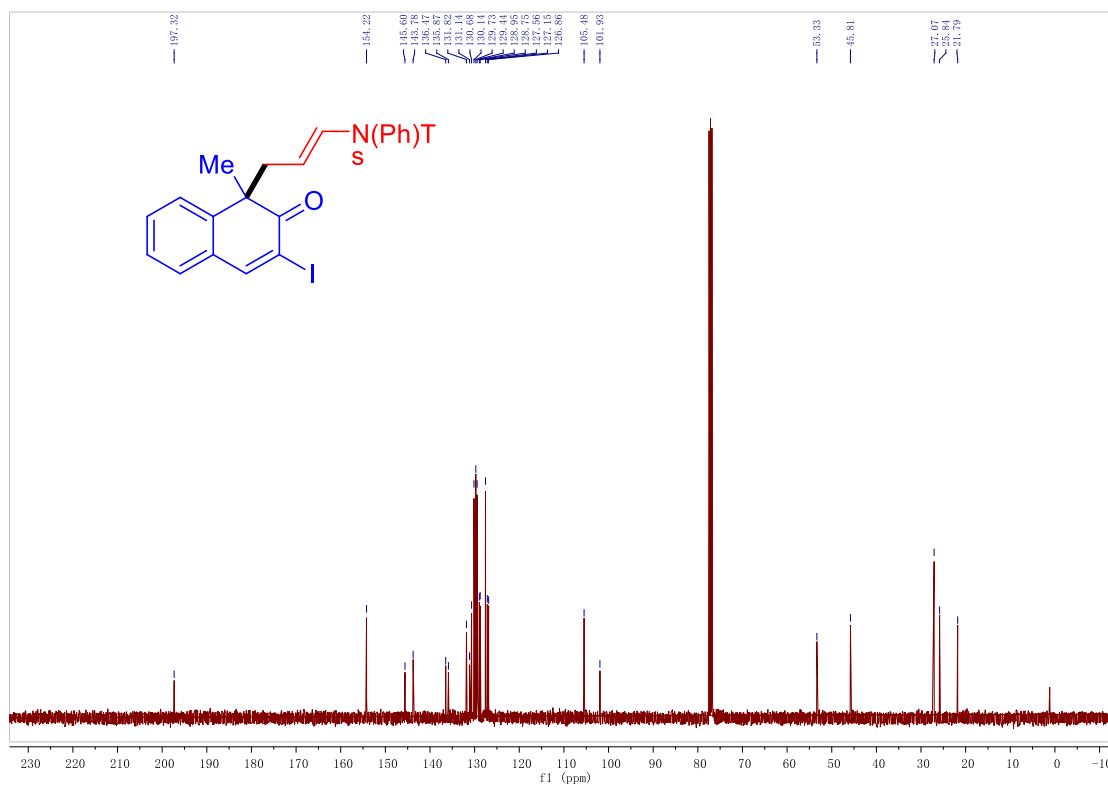
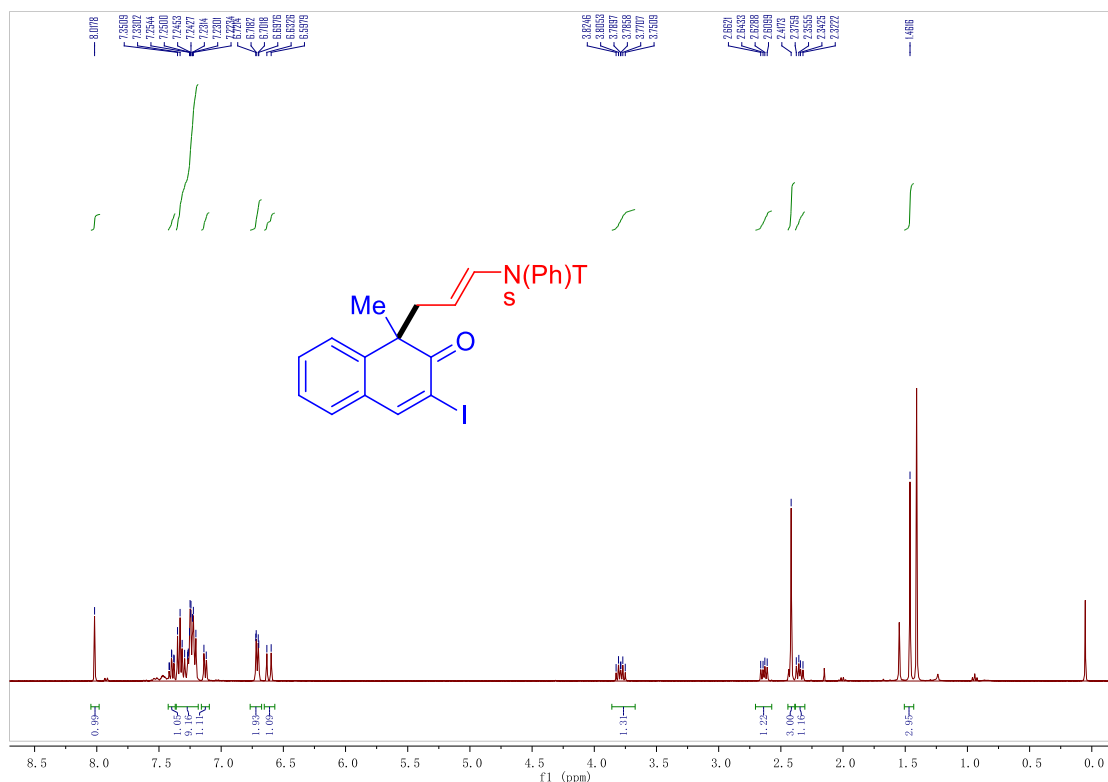
Chapter 3



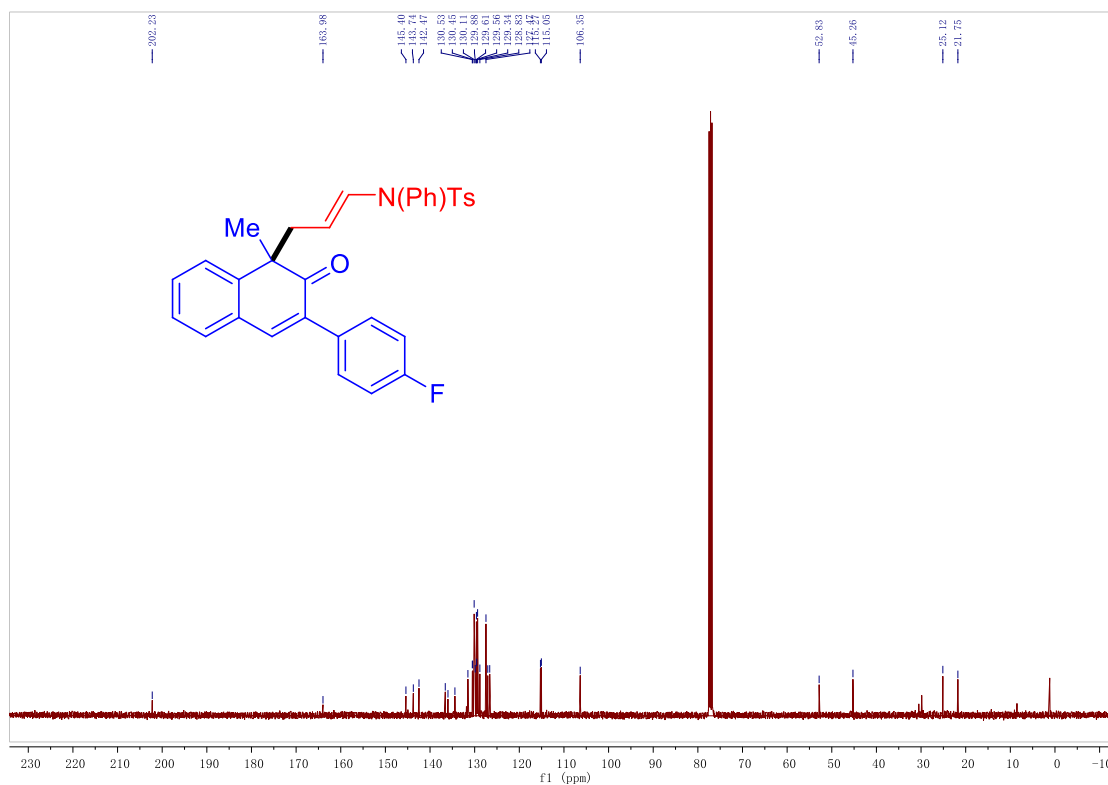
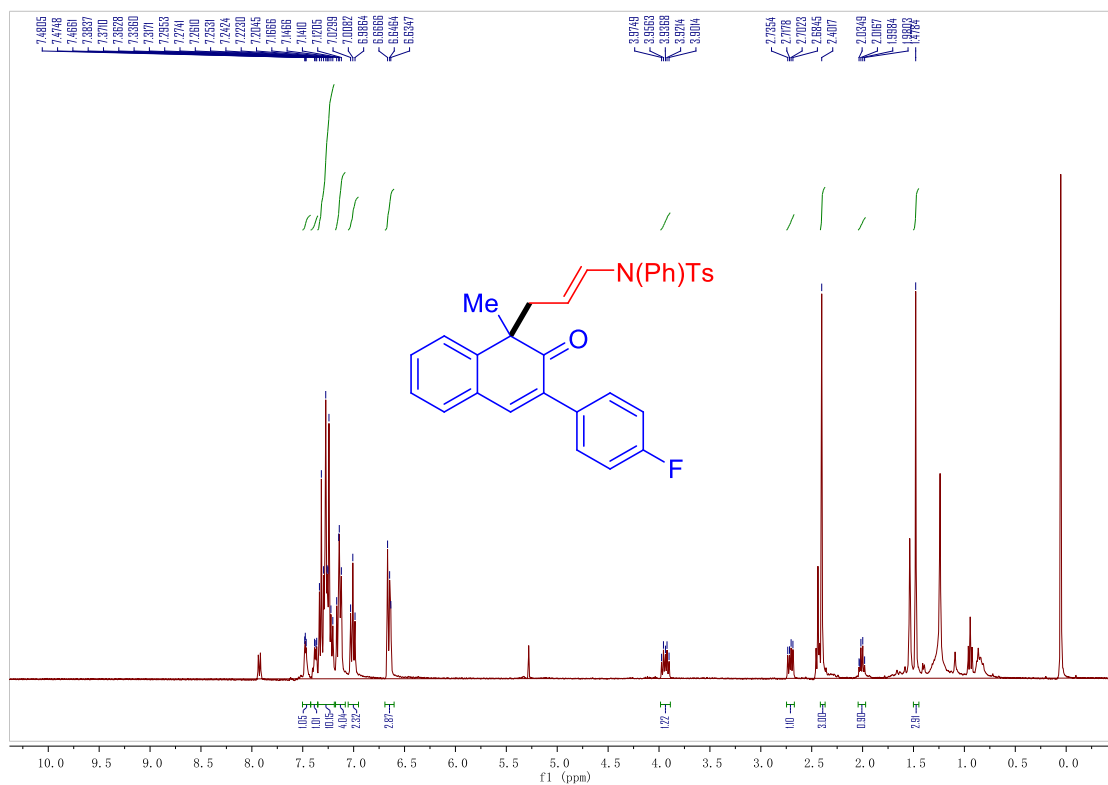
Chapter 3



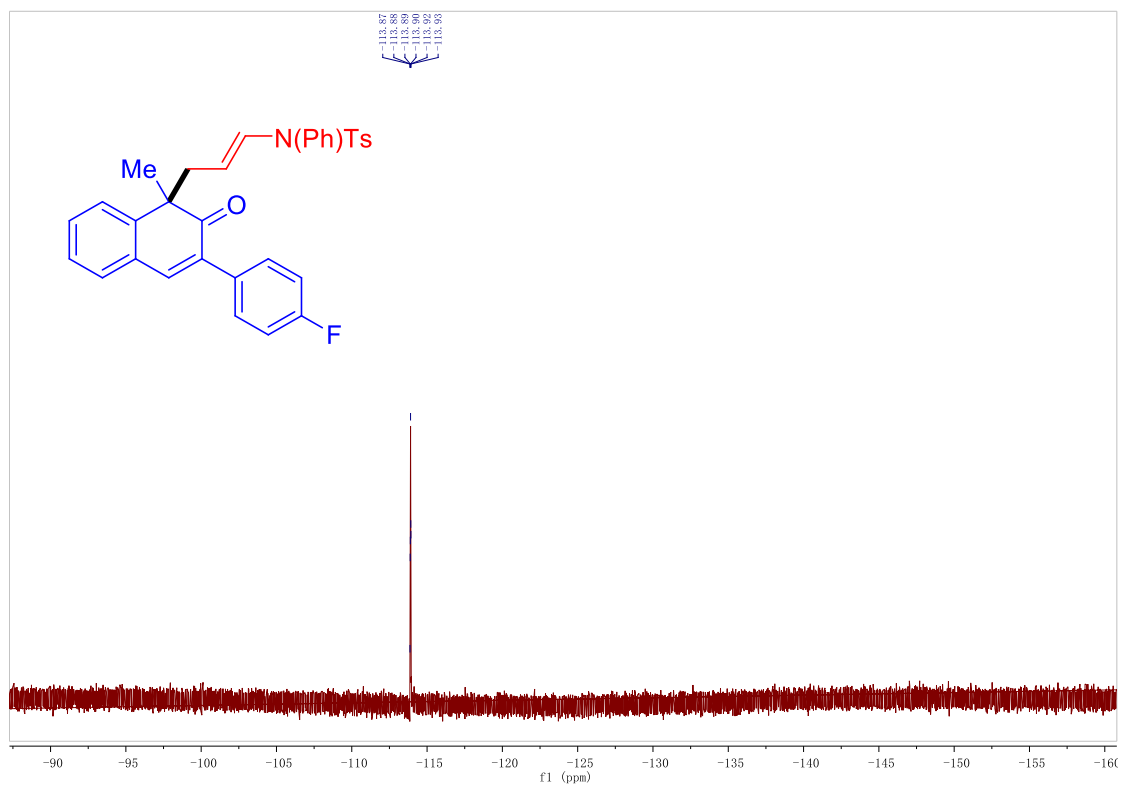
Chapter 3



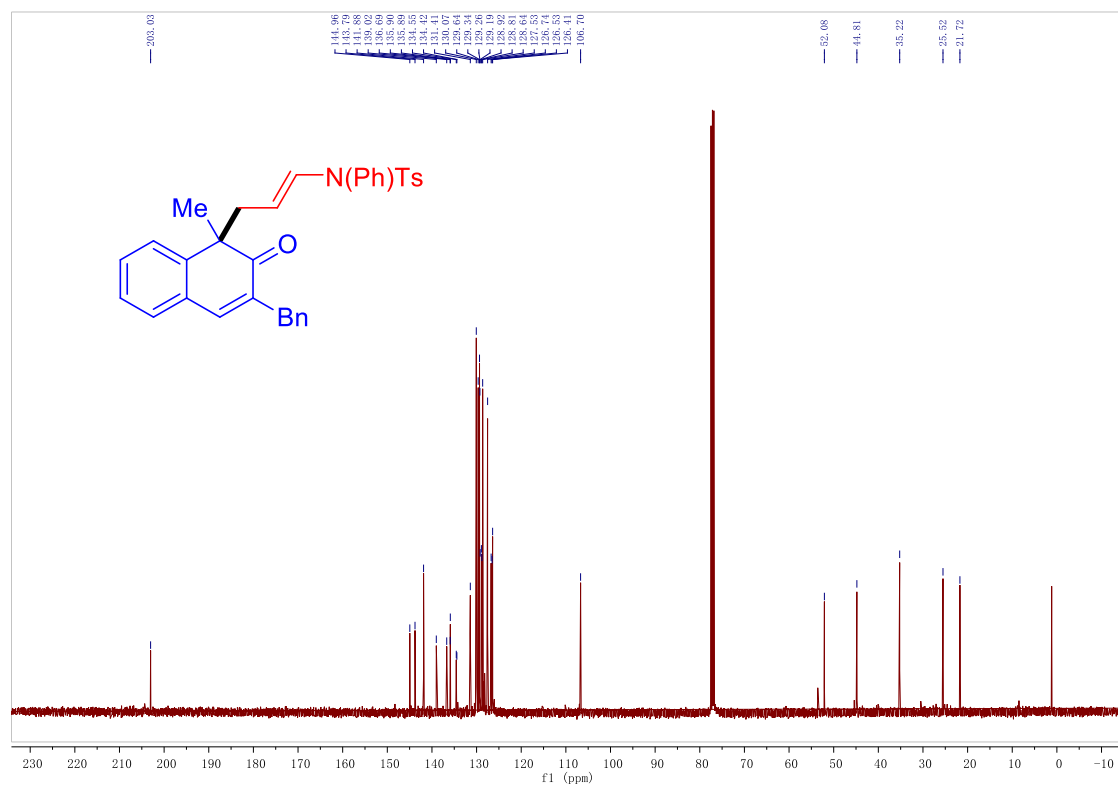
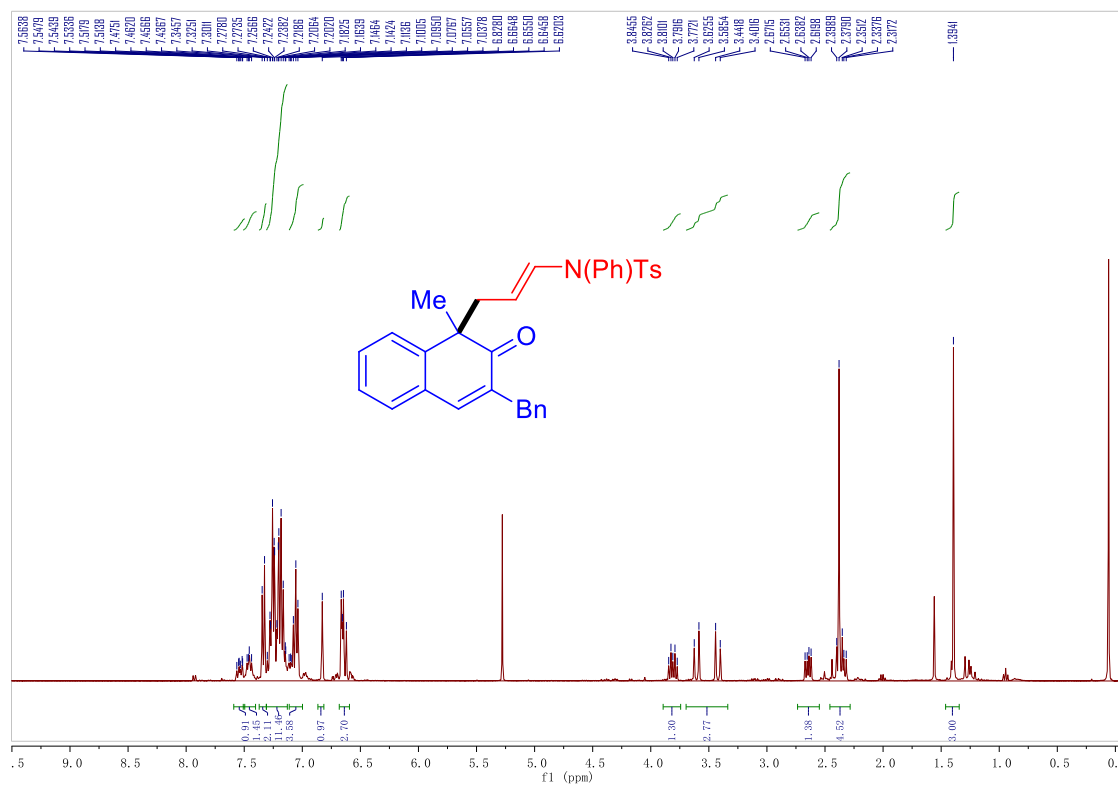
Chapter 3



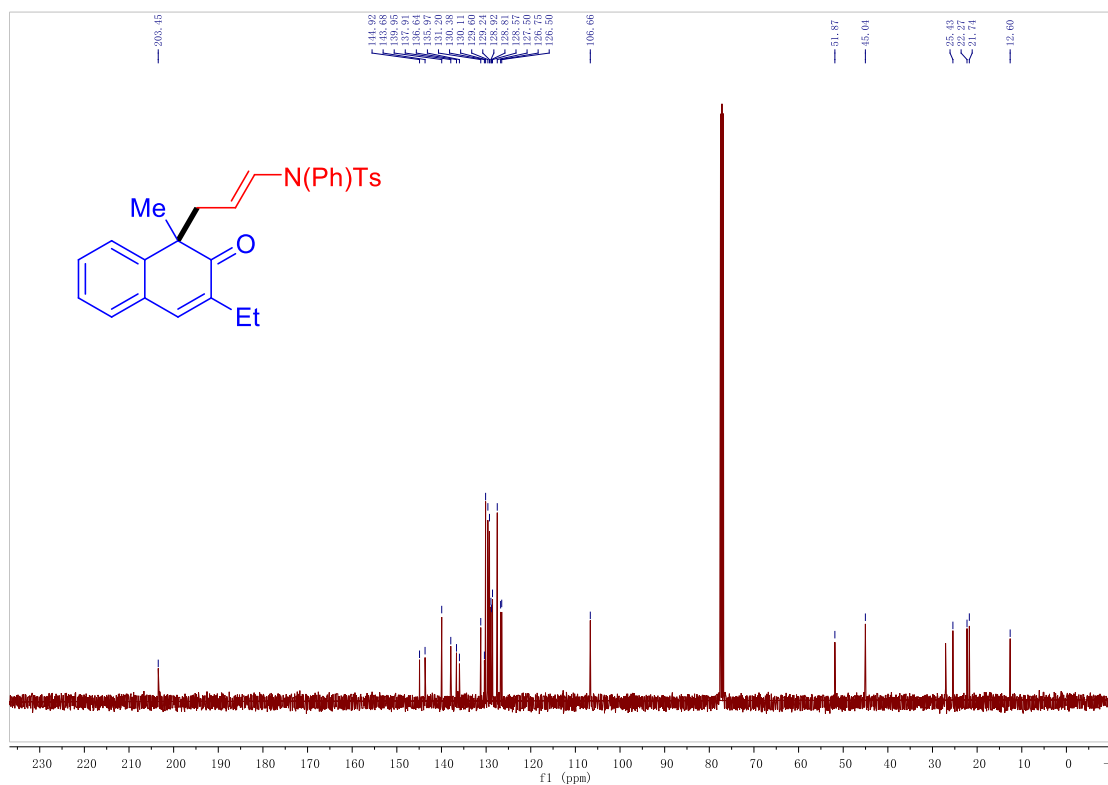
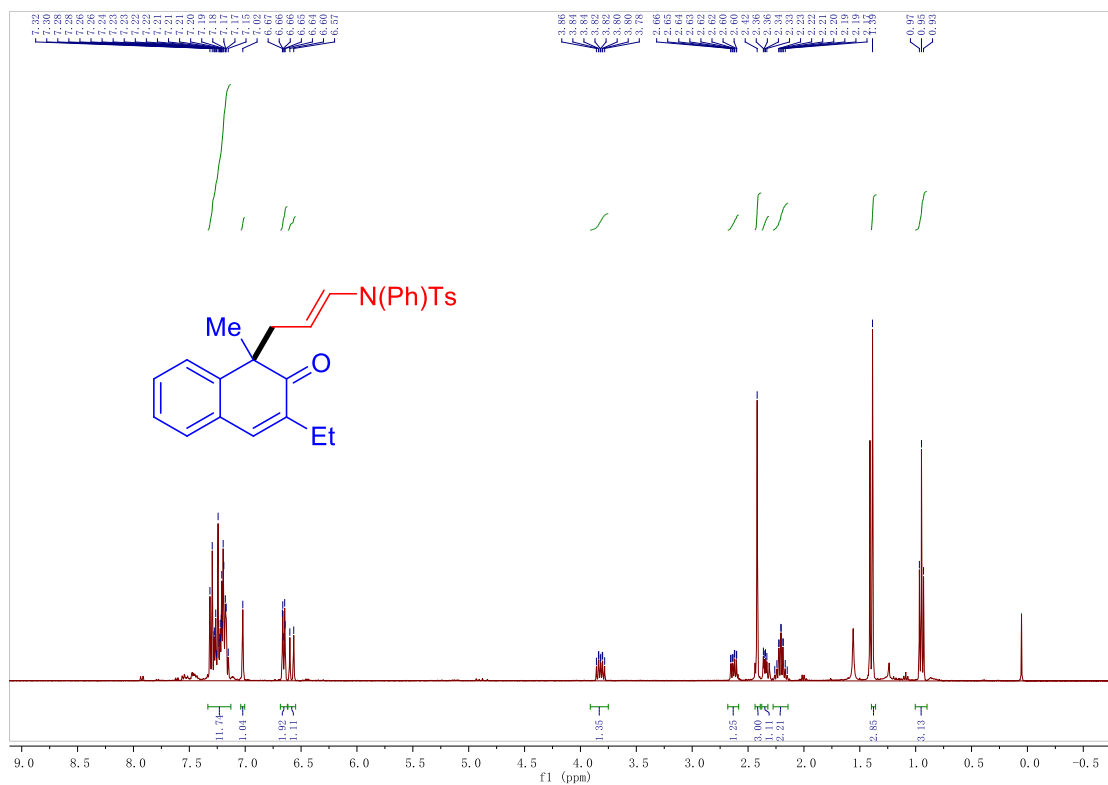
Chapter 3



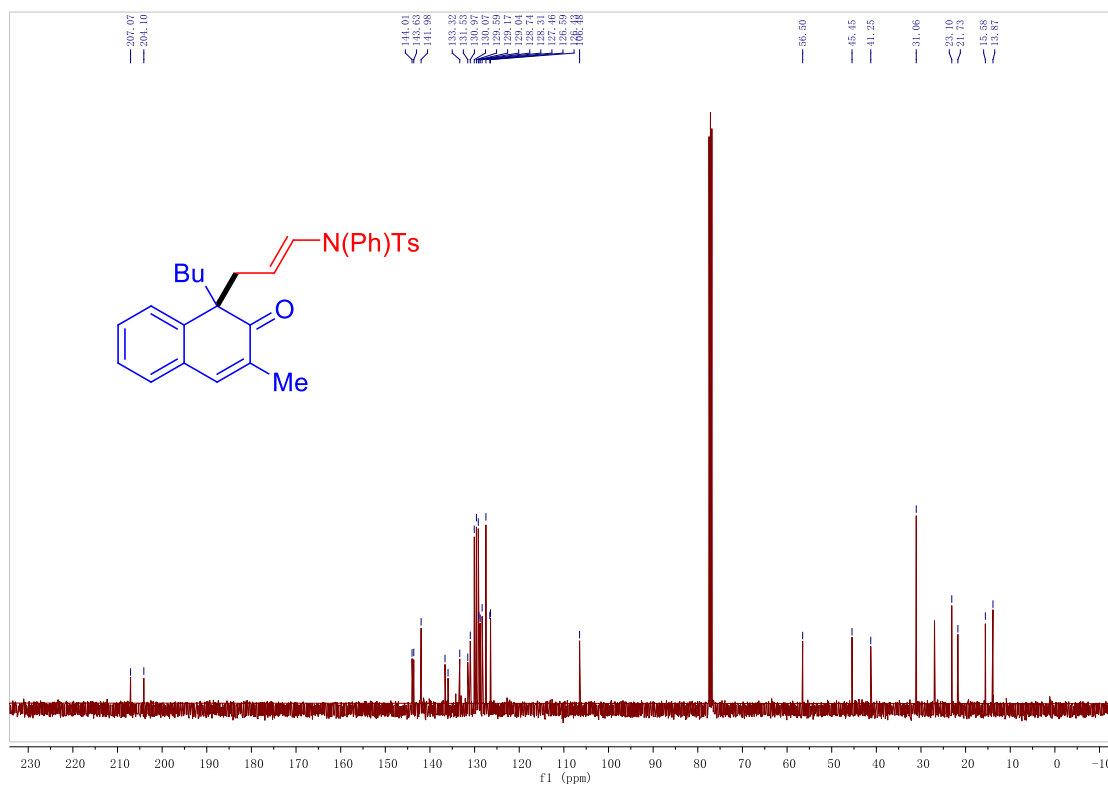
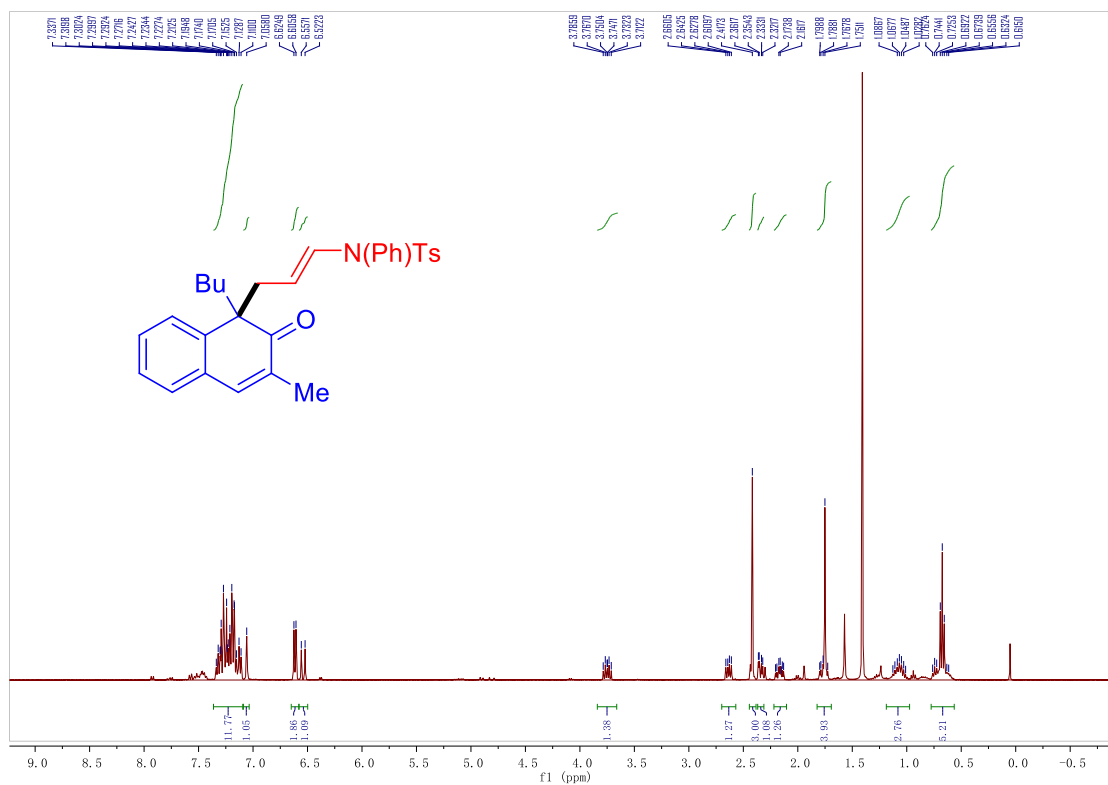
Chapter 3



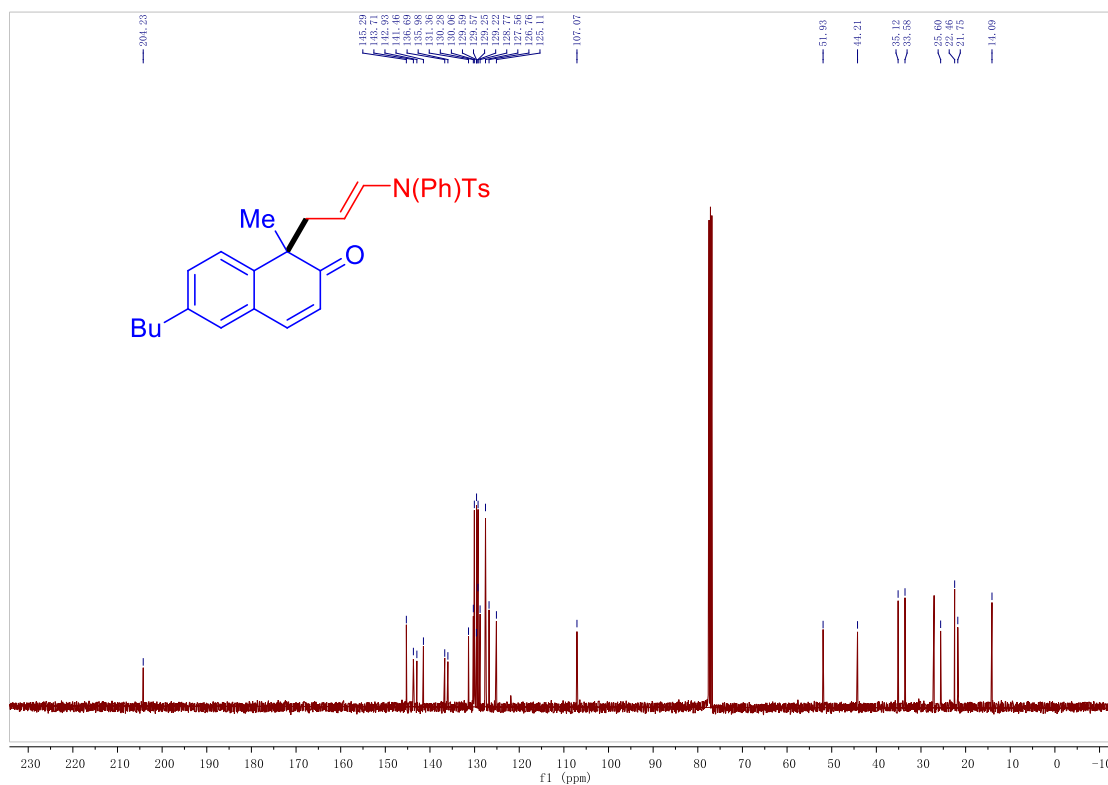
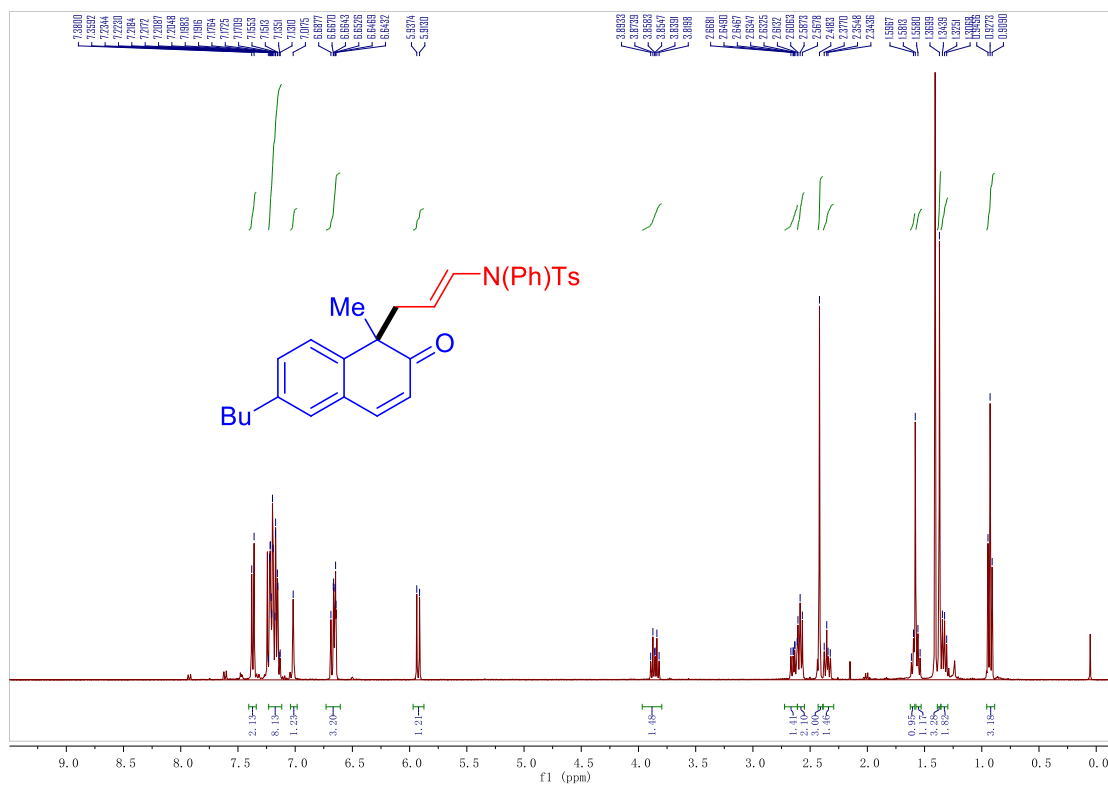
Chapter 3



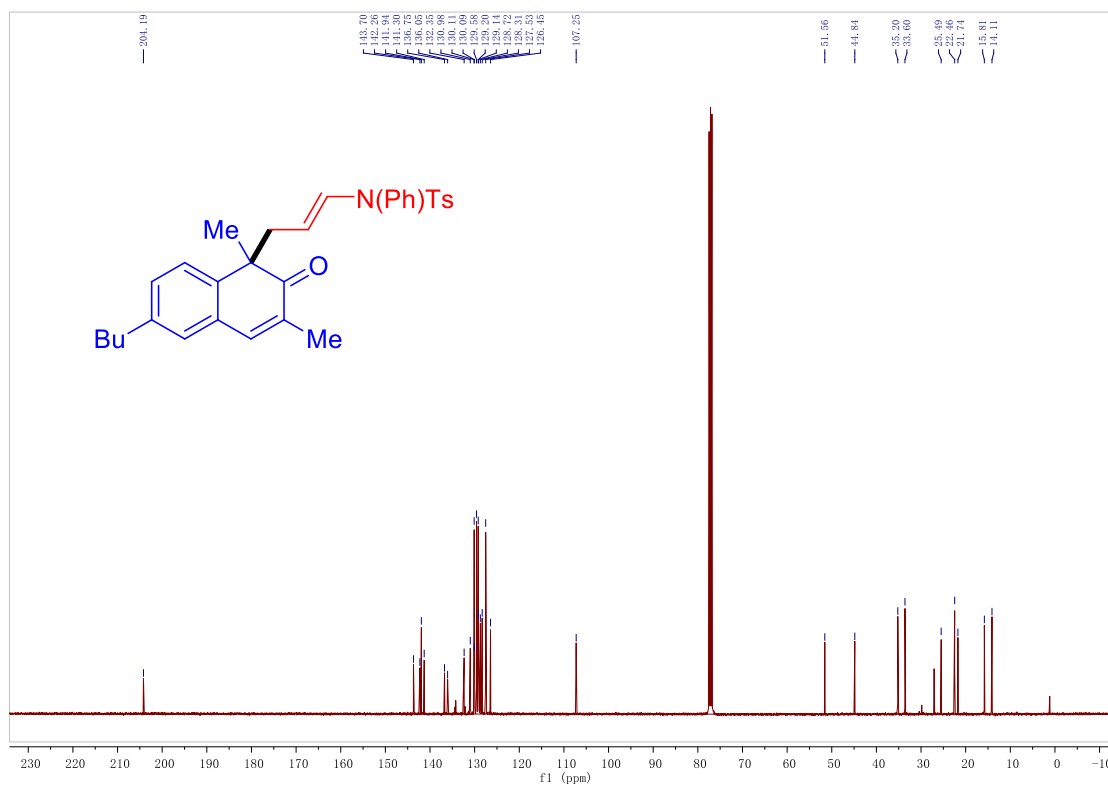
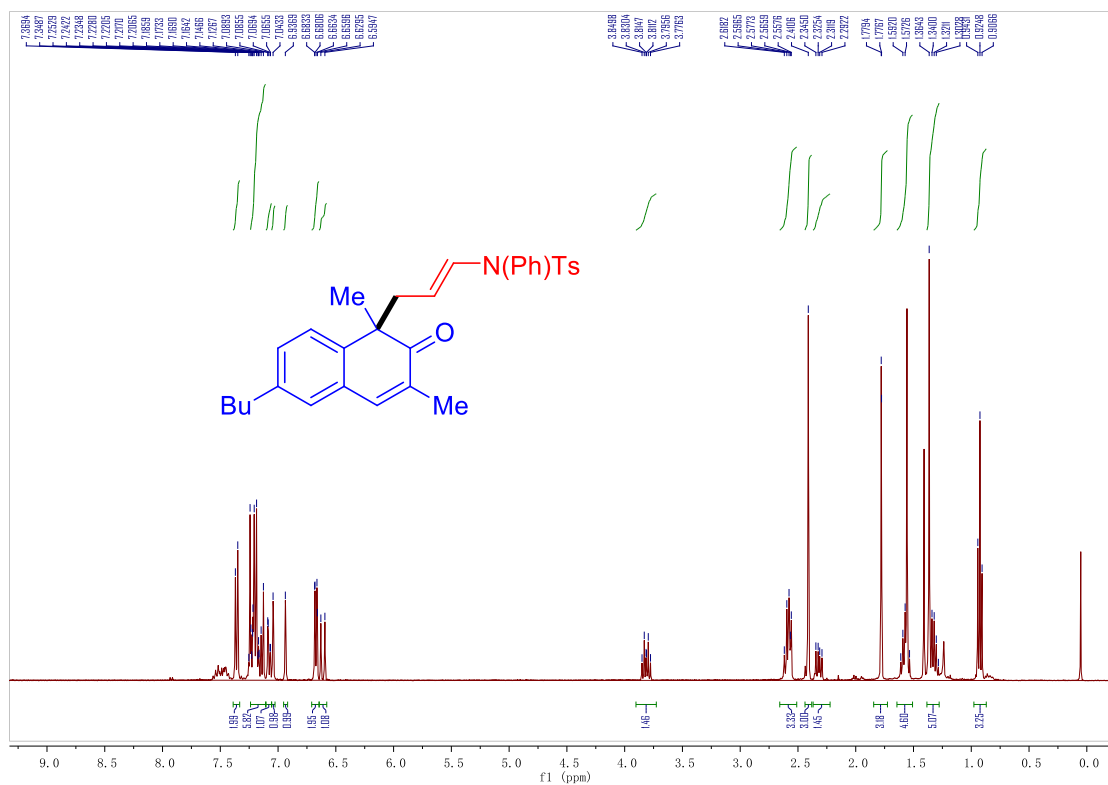
Chapter 3



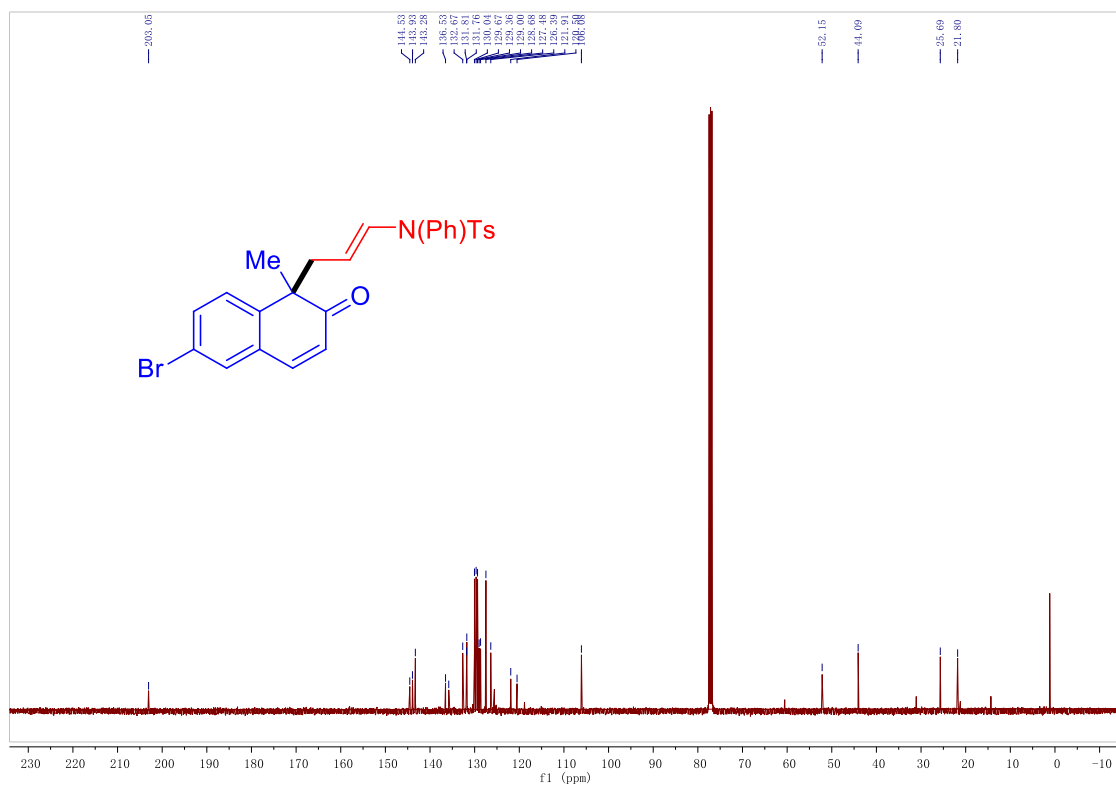
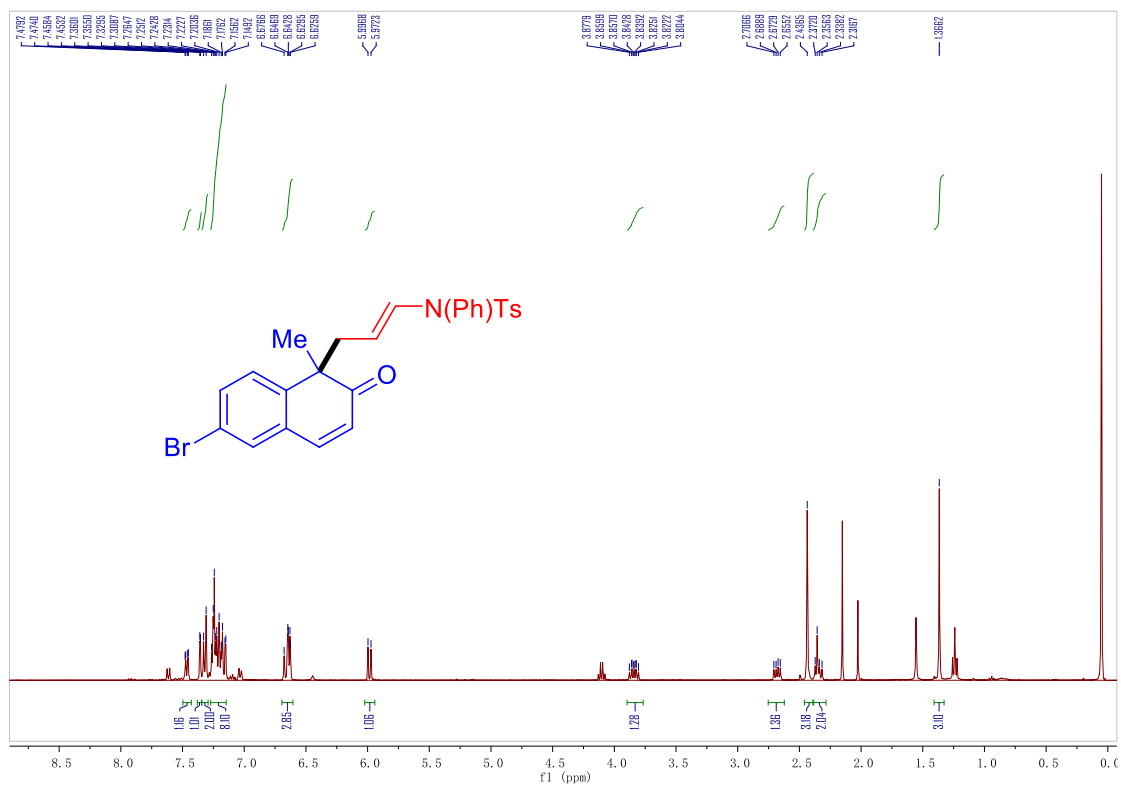
Chapter 3



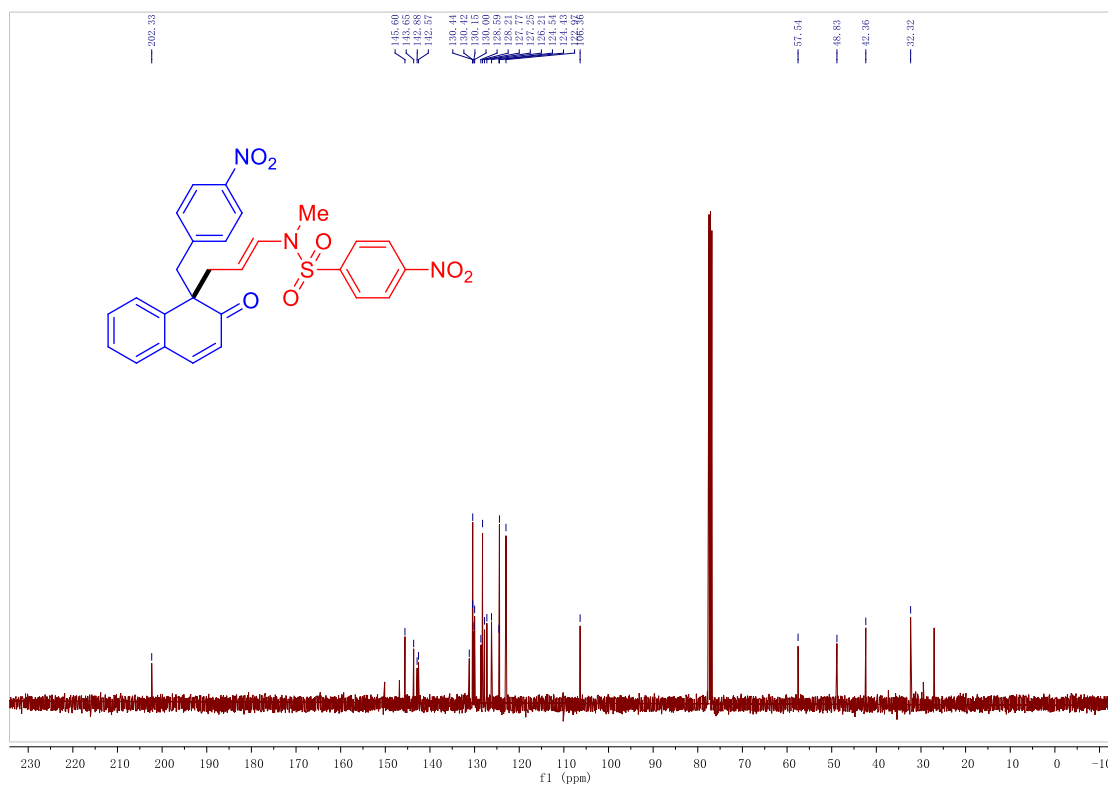
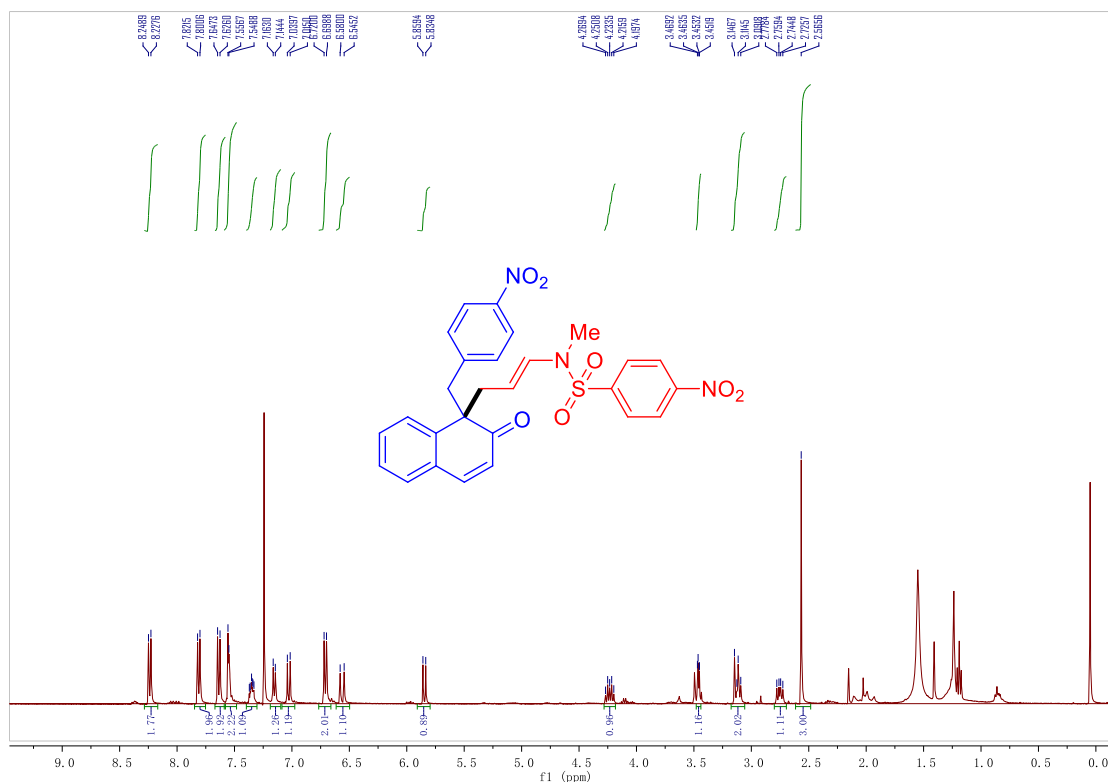
Chapter 3



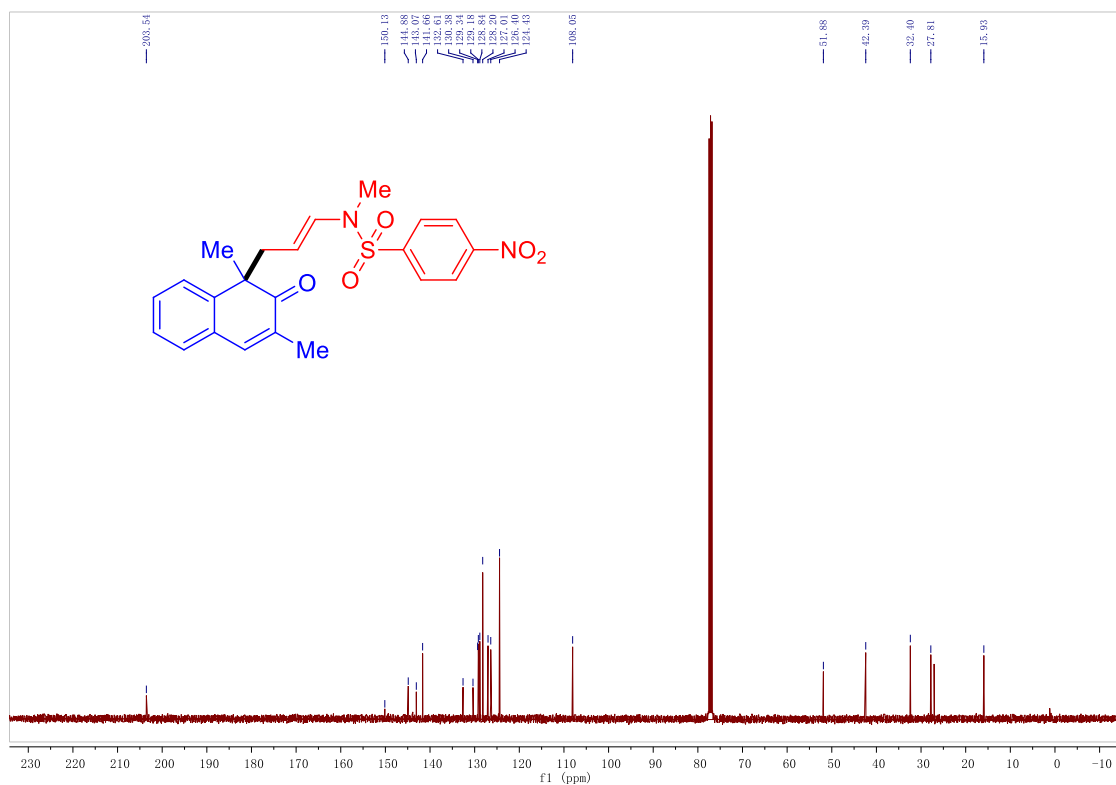
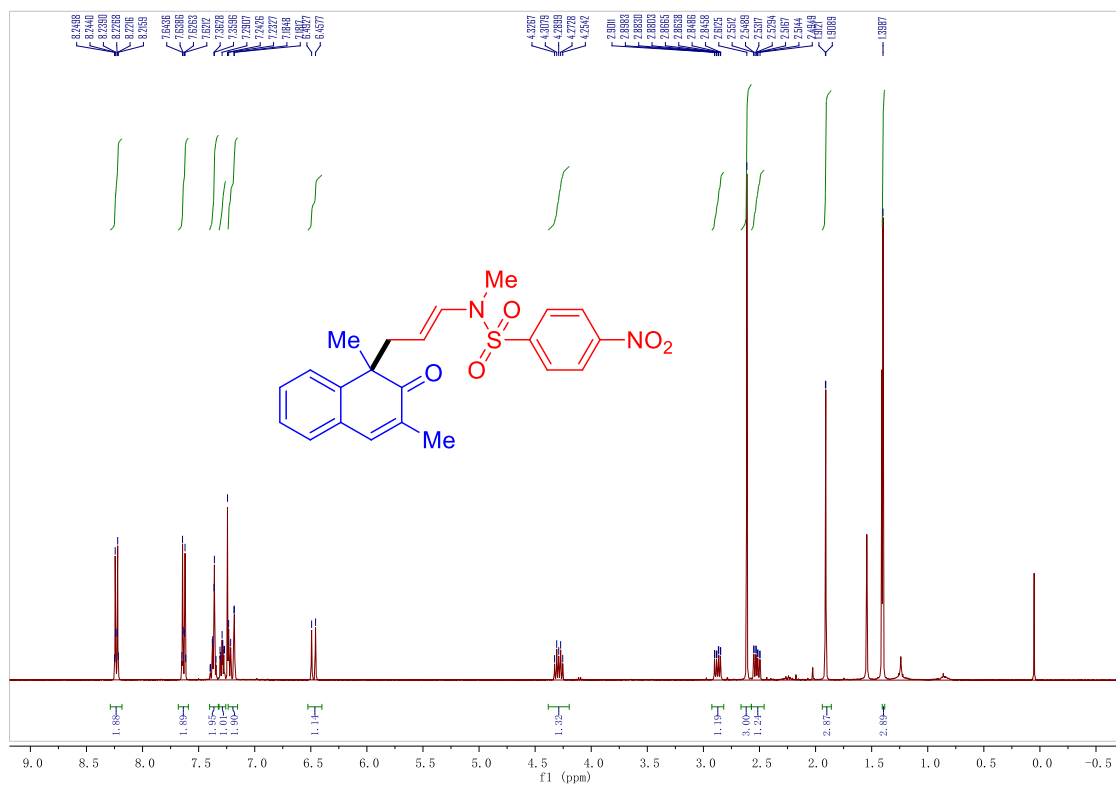
Chapter 3



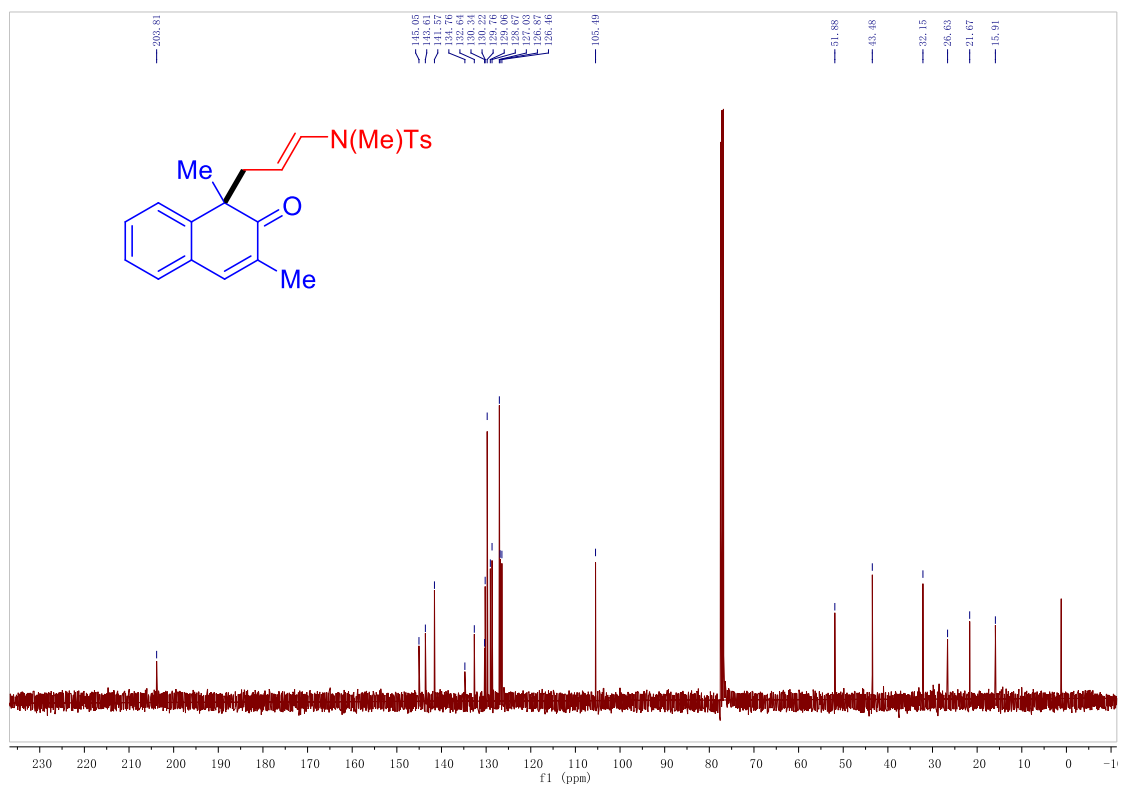
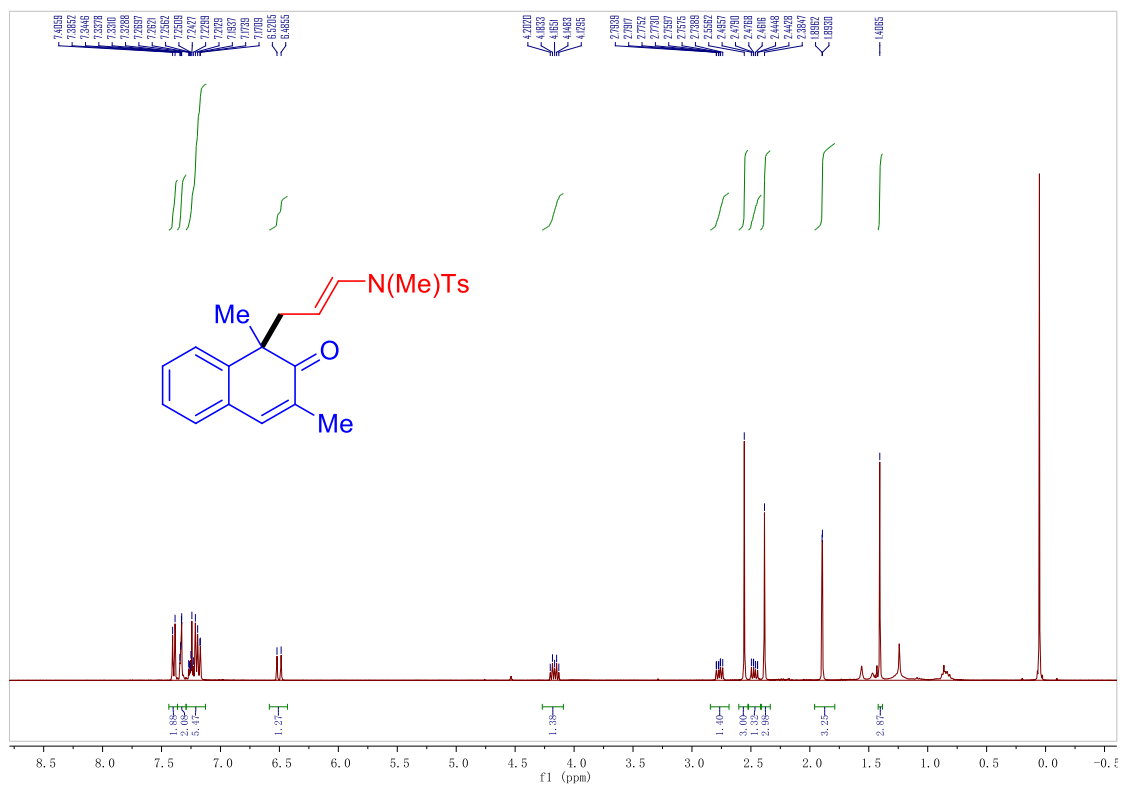
Chapter 3



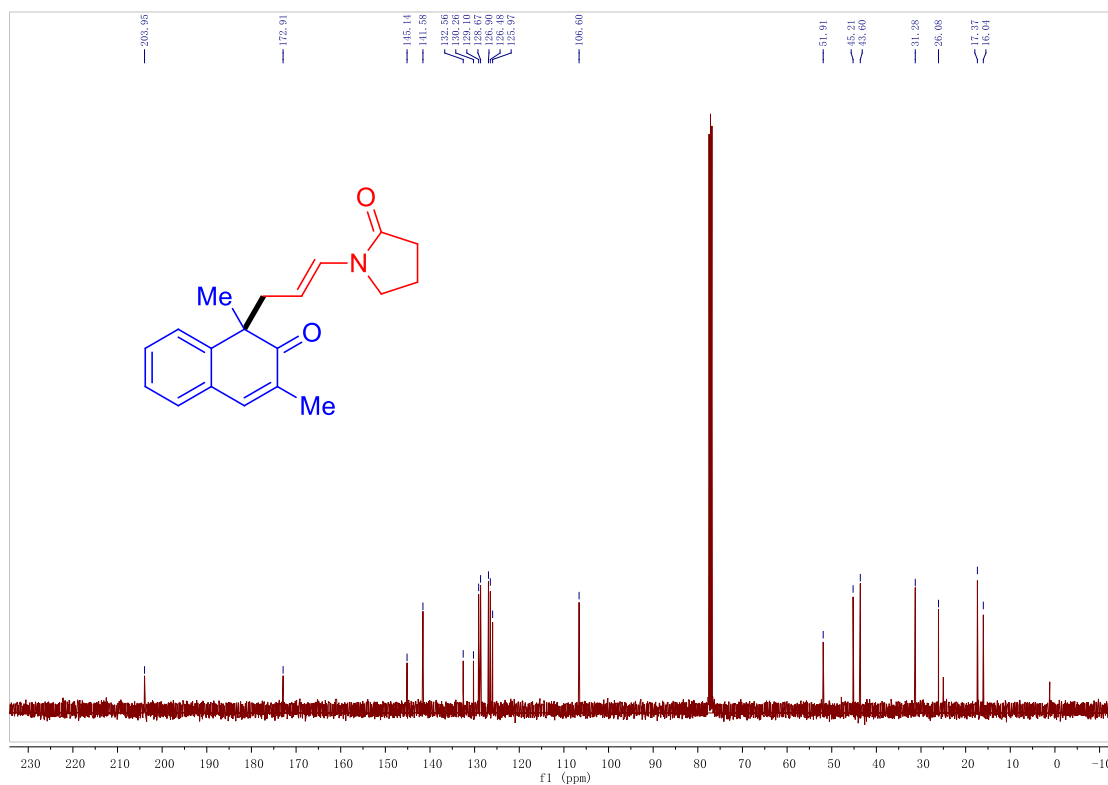
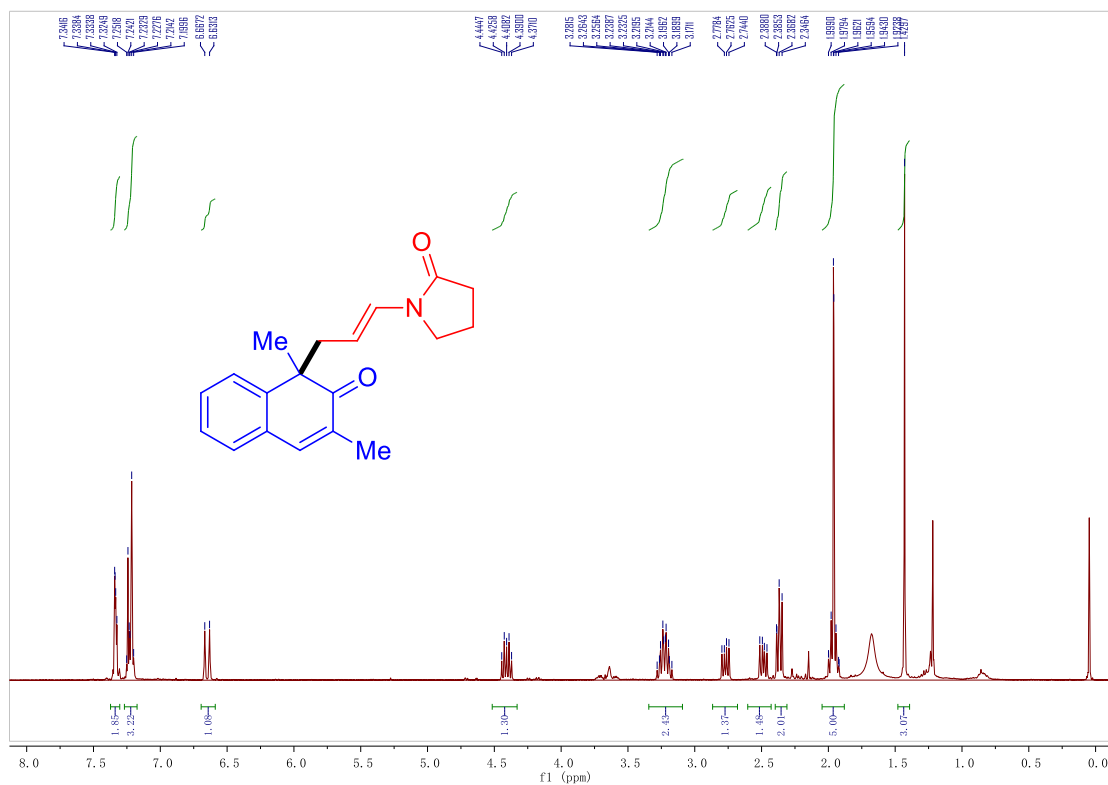
Chapter 3



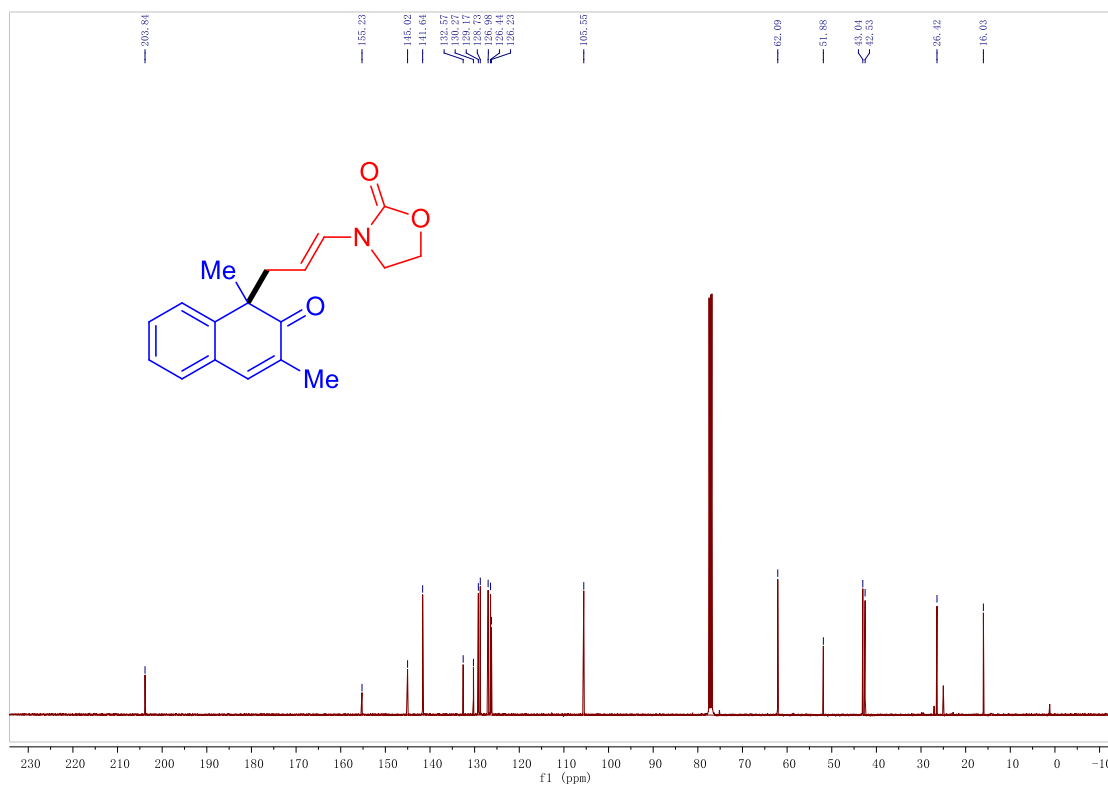
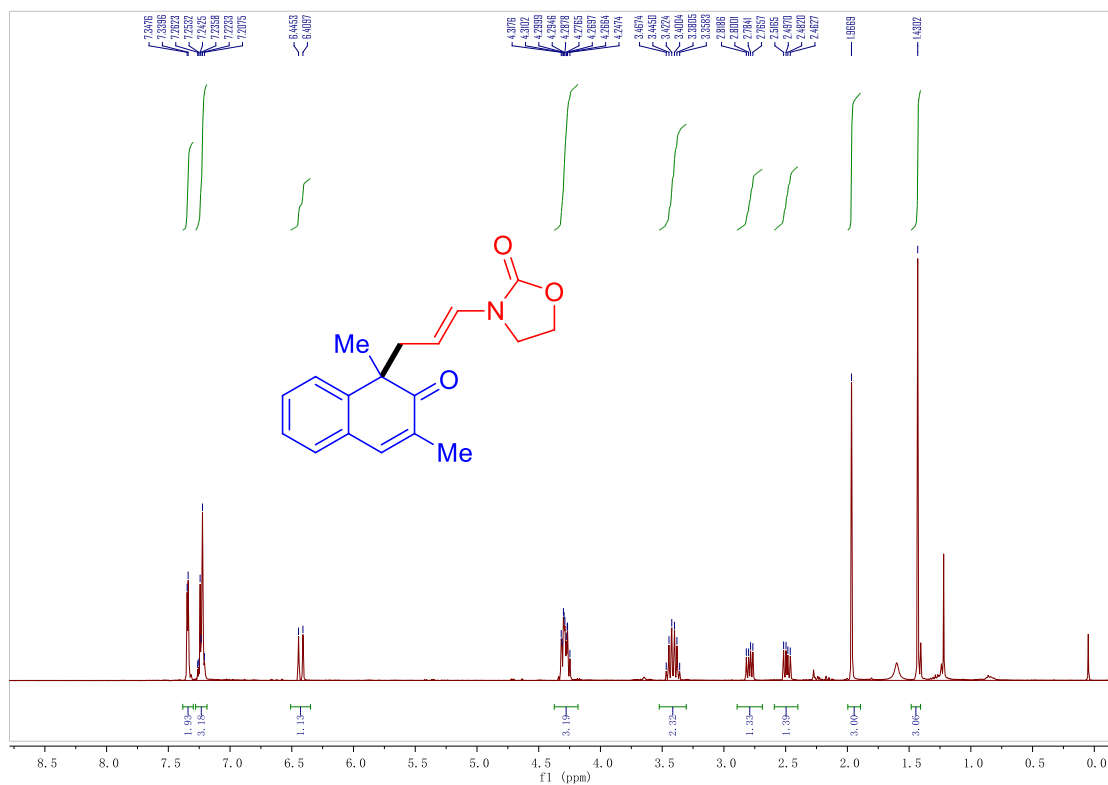
Chapter 3



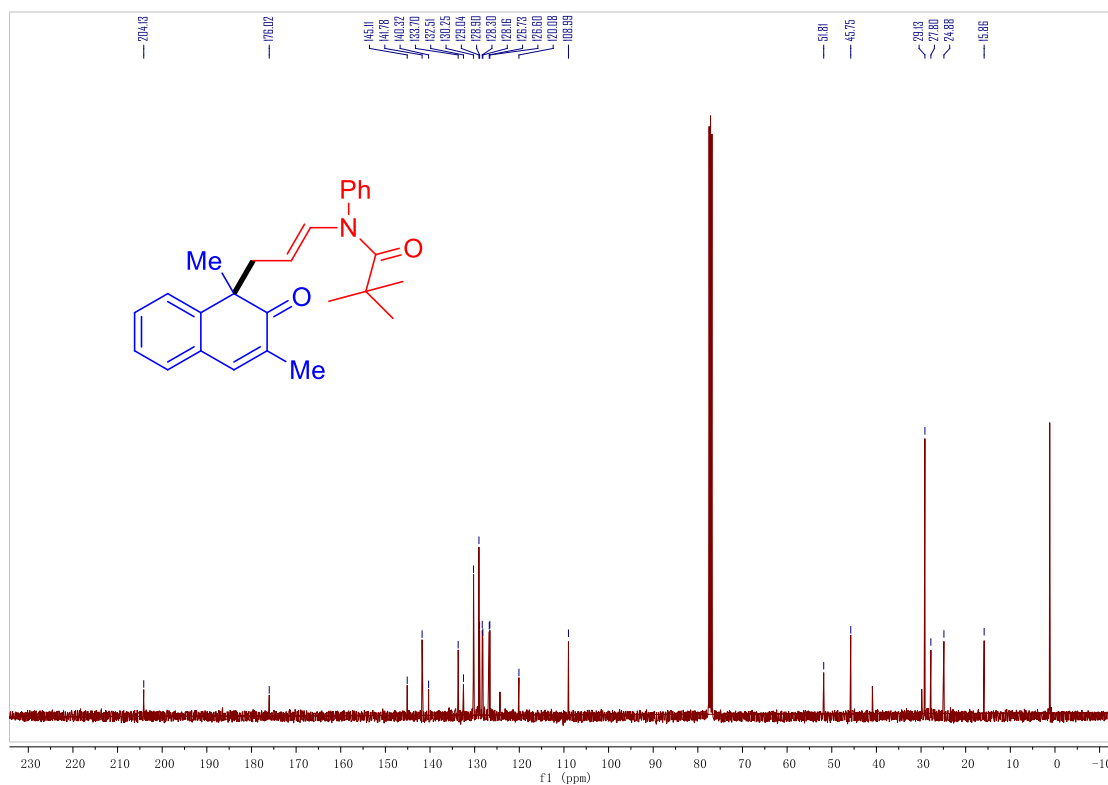
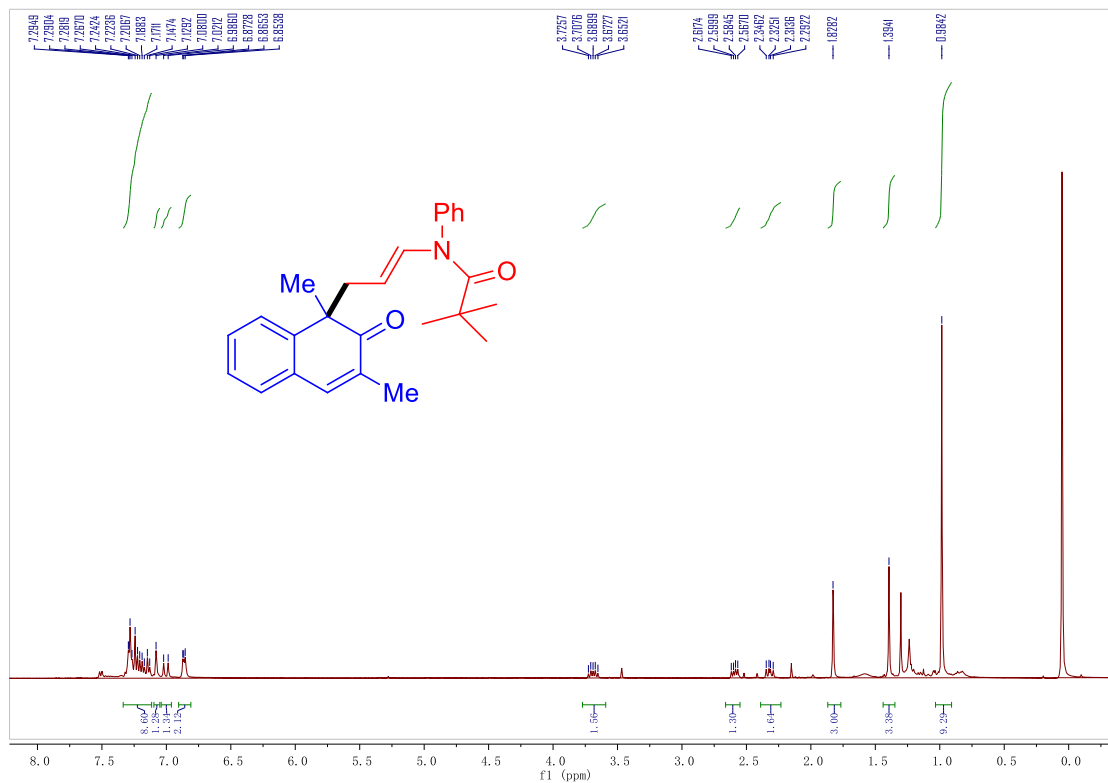
Chapter 3



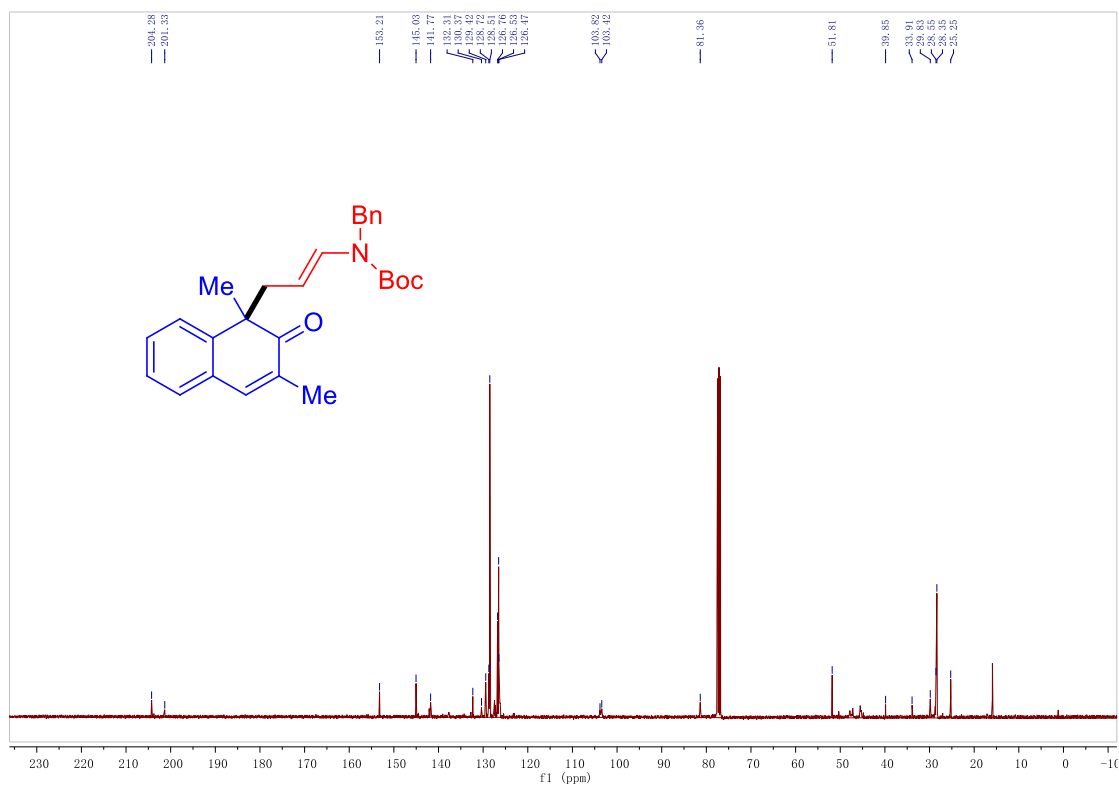
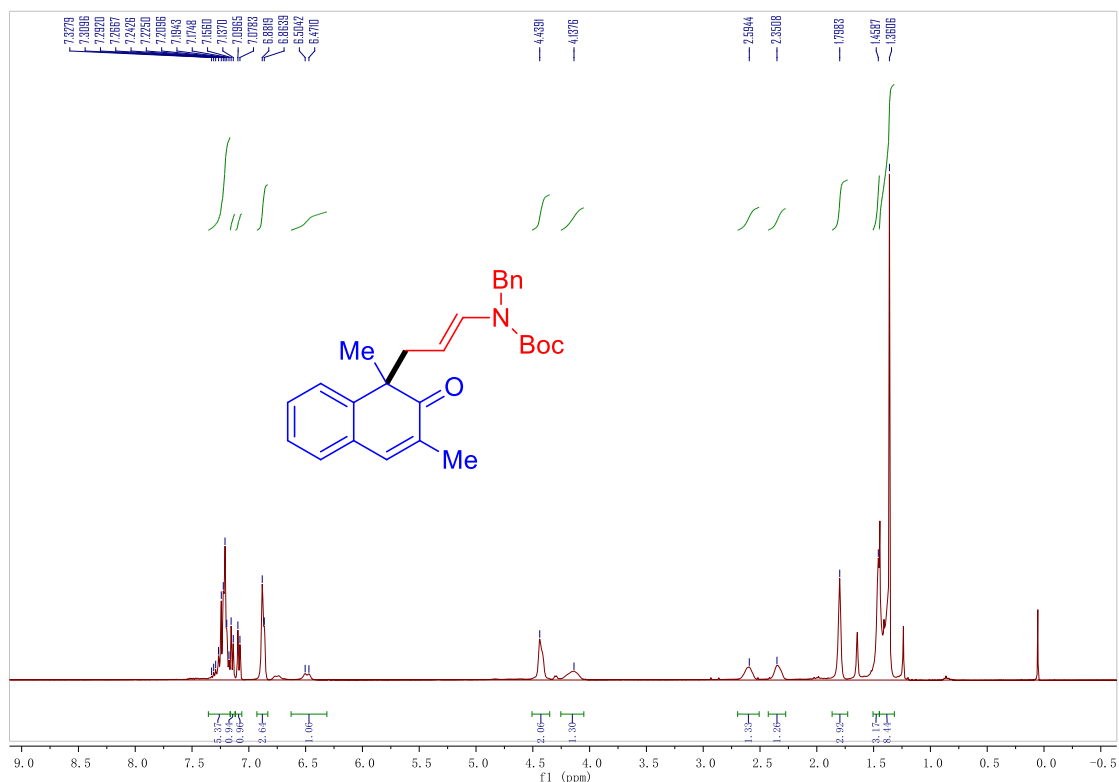
Chapter 3



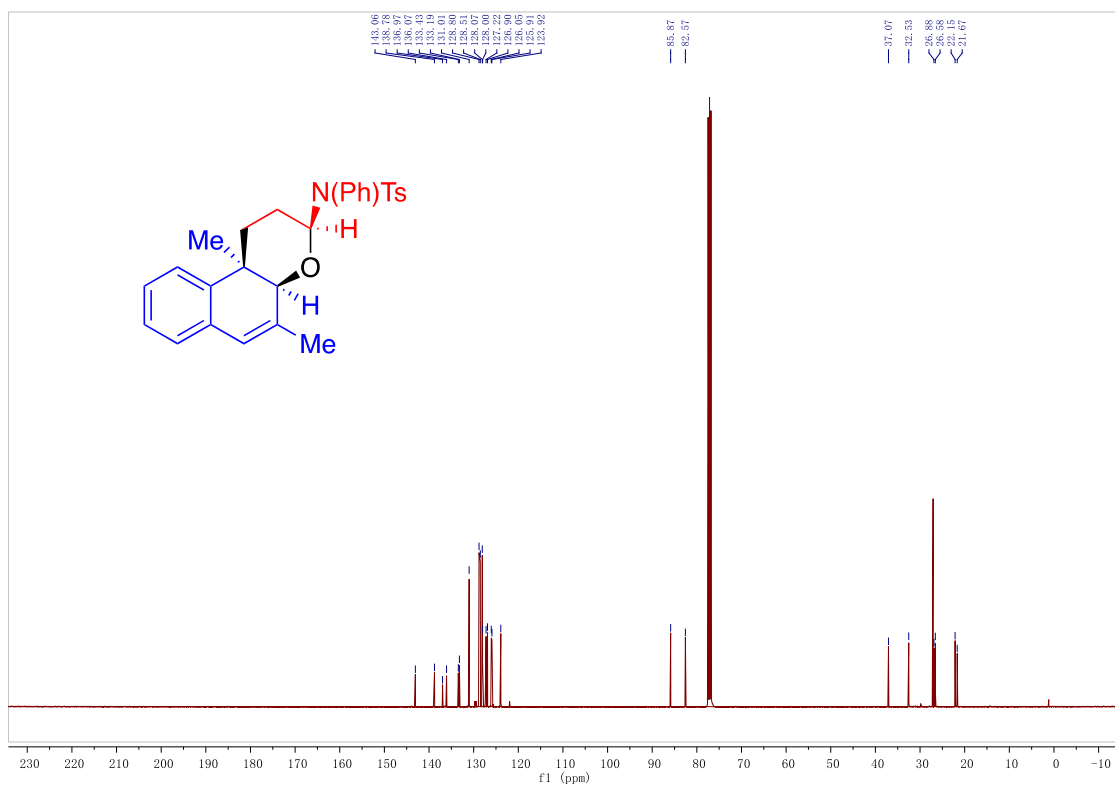
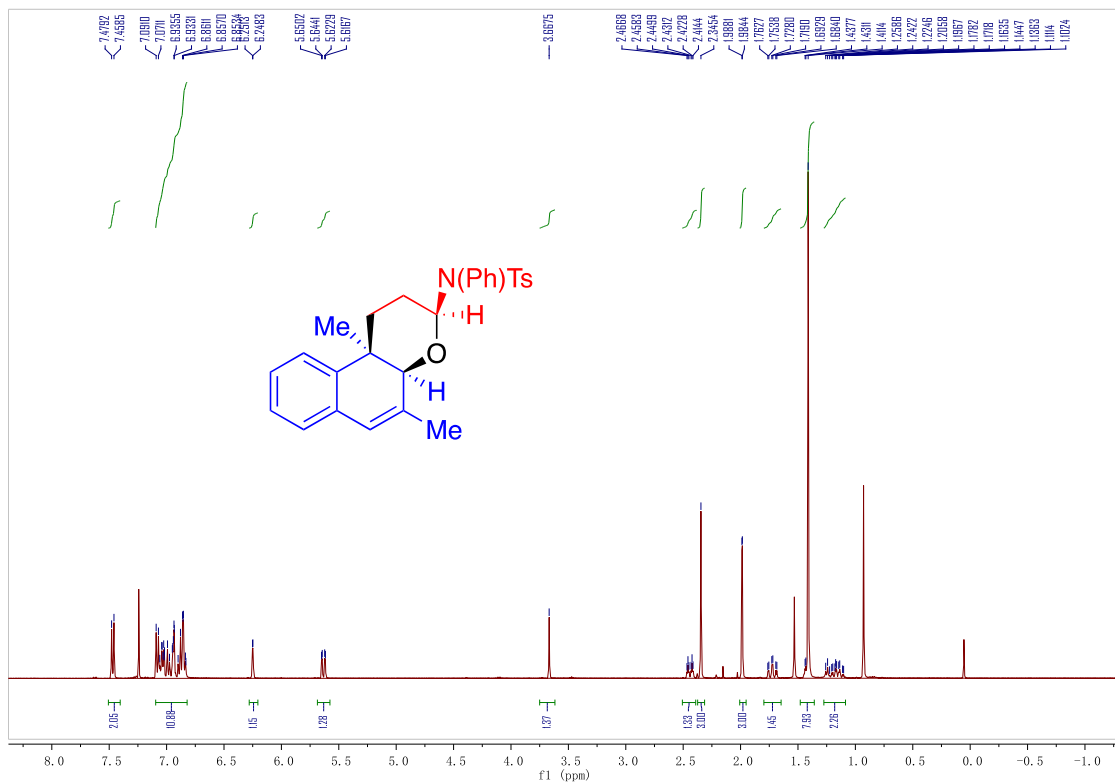
Chapter 3



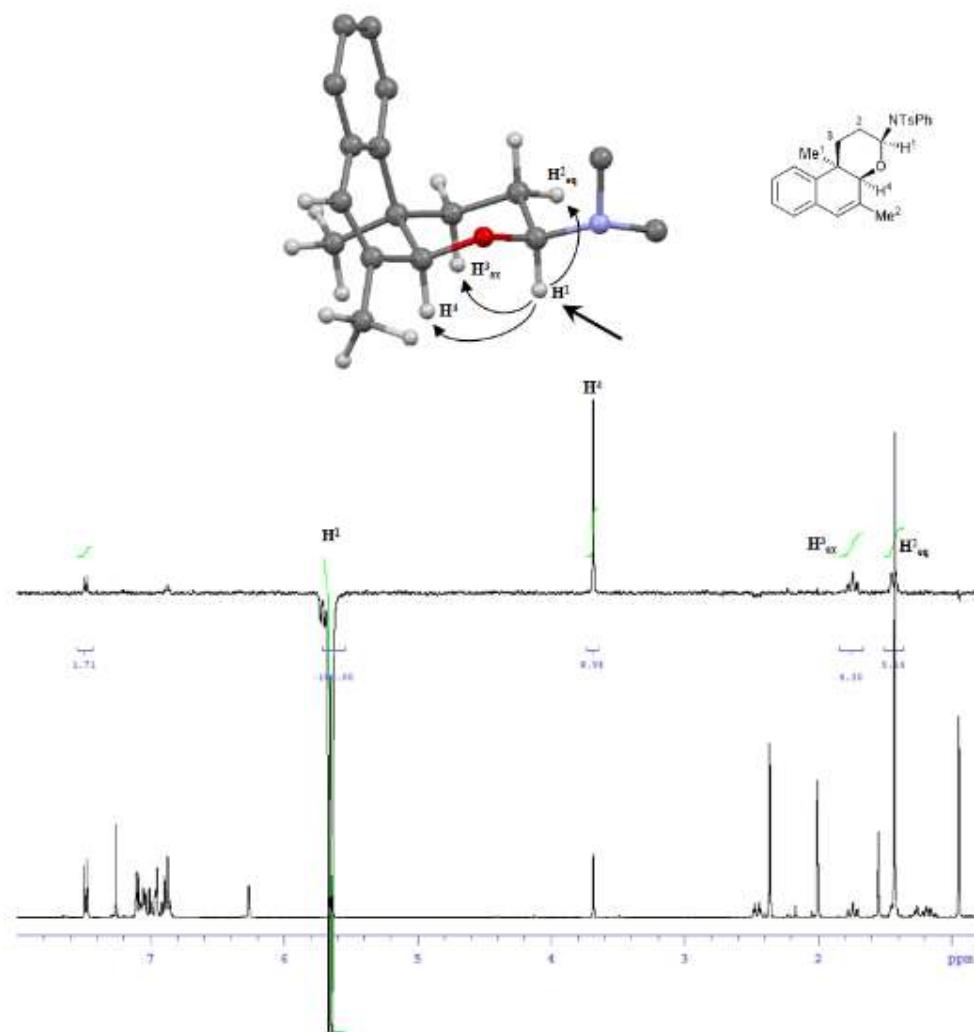
Chapter 3



Chapter 3



Chapter 3

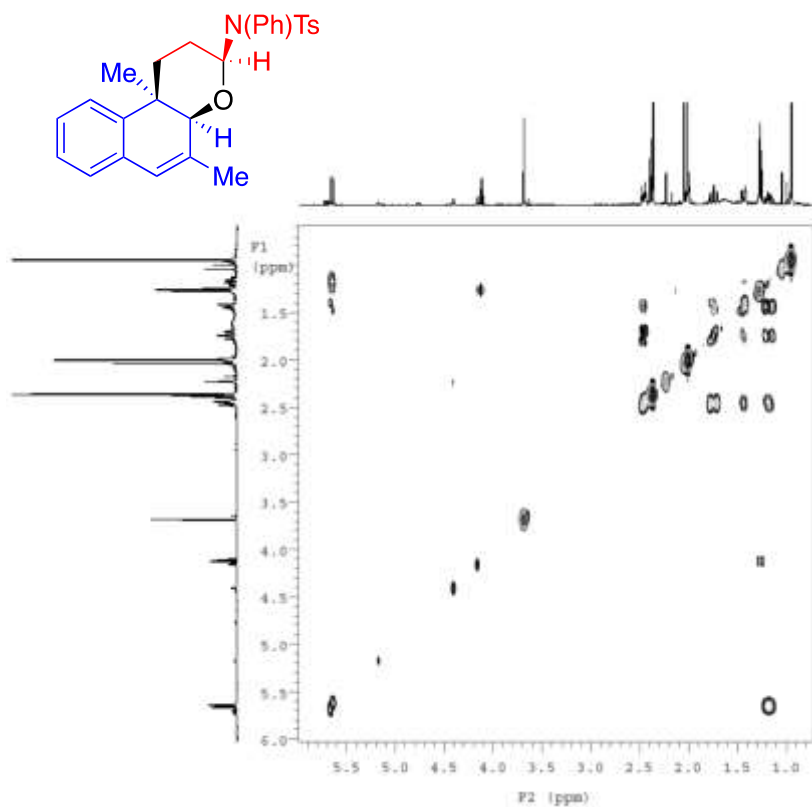


All the NMR experiments were acquired on a Varian MR 400 spectrometer.

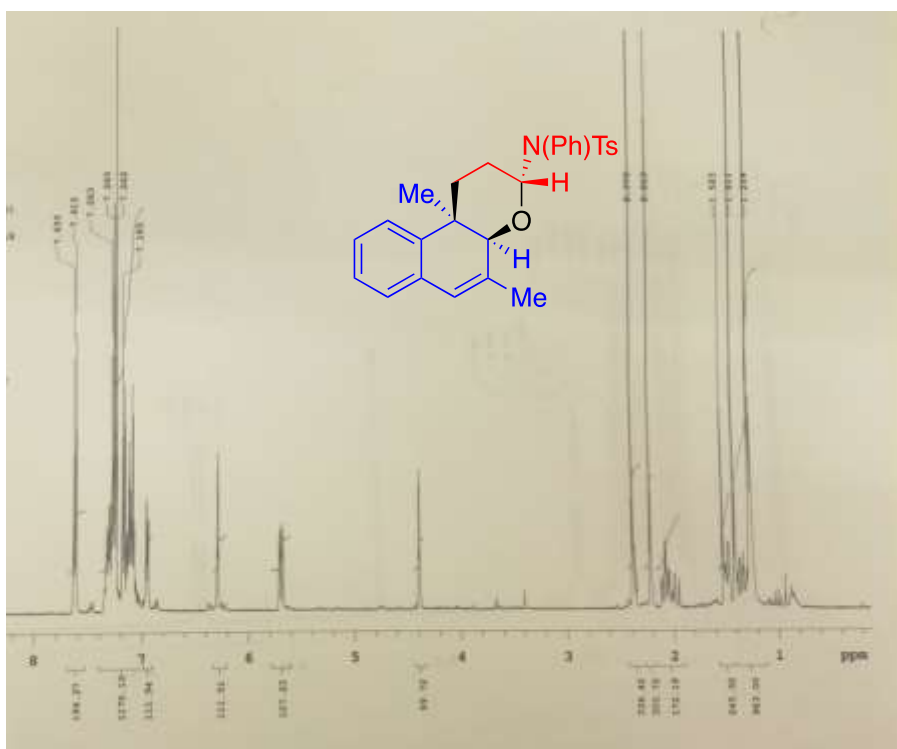
Monodimensional NOE experiment (400 MHz, CDCl₃, 25 °C) was performed by using a DPGSE-NOE sequence, with a 50 Hz pulse and a mixing time of 1.5 s.

Irradiation at the frequency of proton H¹ (5.65 ppm) showed strong positive NOE response of the H⁴ frequency, confirming the *syn*-relationship. Weaker NOE effects were also observed for the equatorial H² and the axial H³ protons.

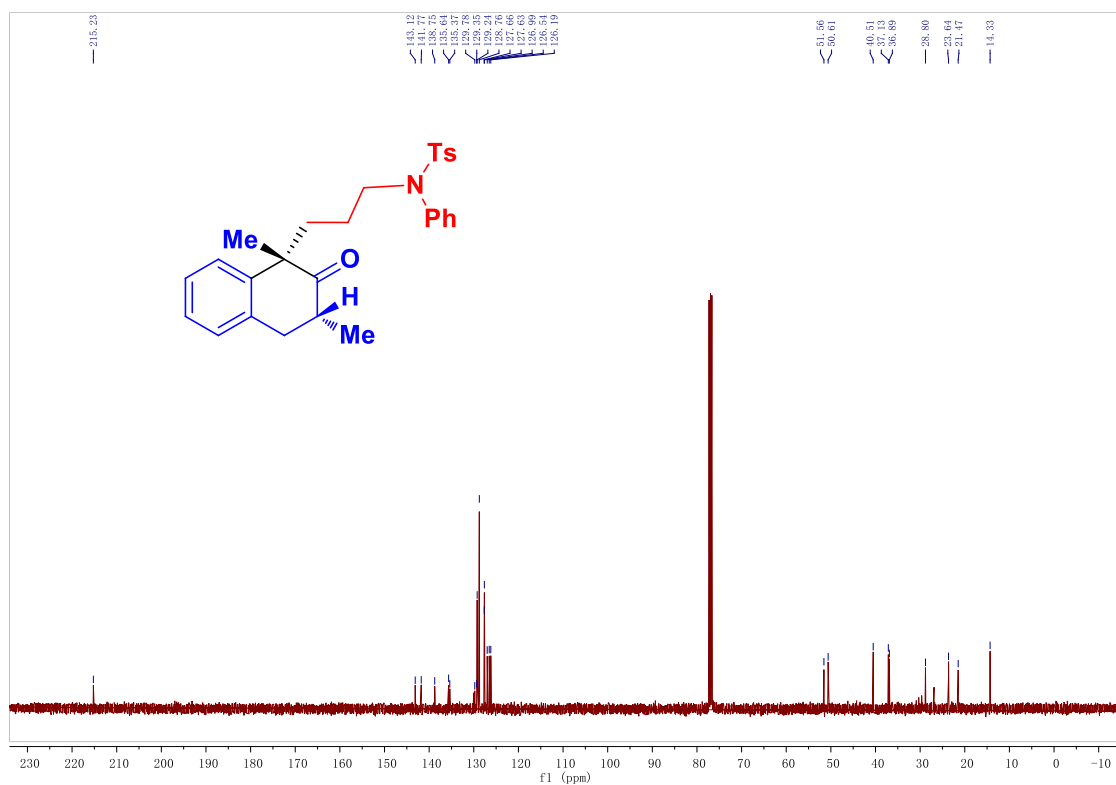
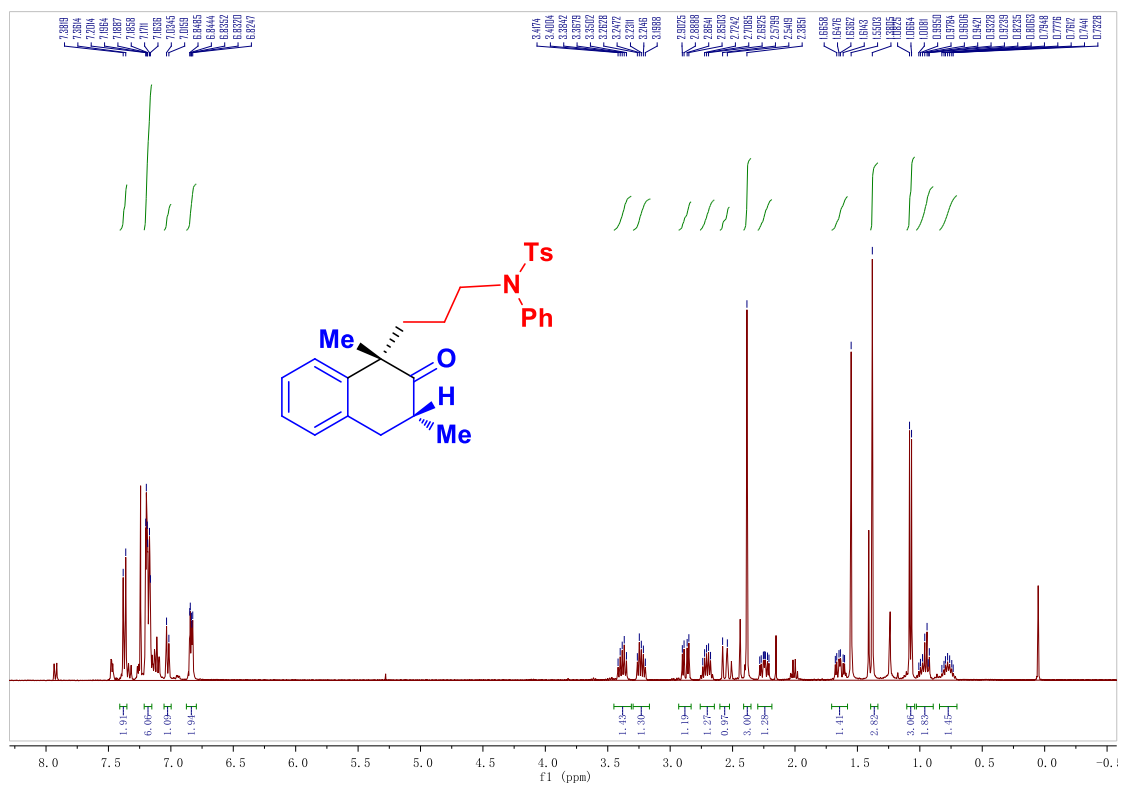
Chapter 3

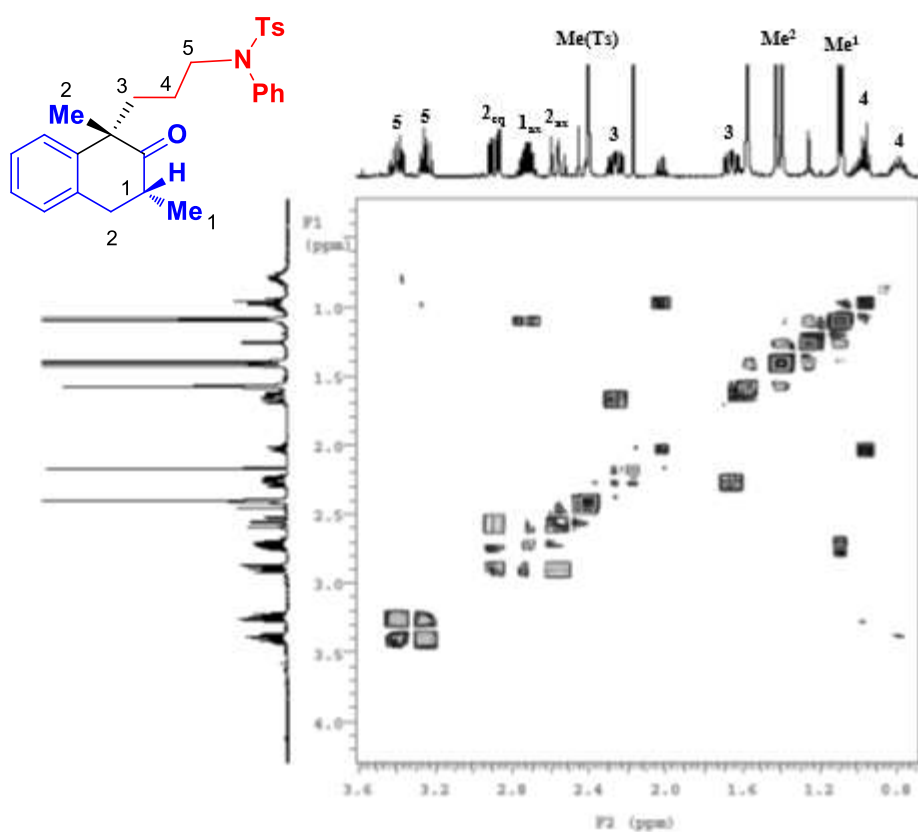


Gradient COSY (400 MHz, CDCl₃, 25 °C) expansion of the alifatic region.

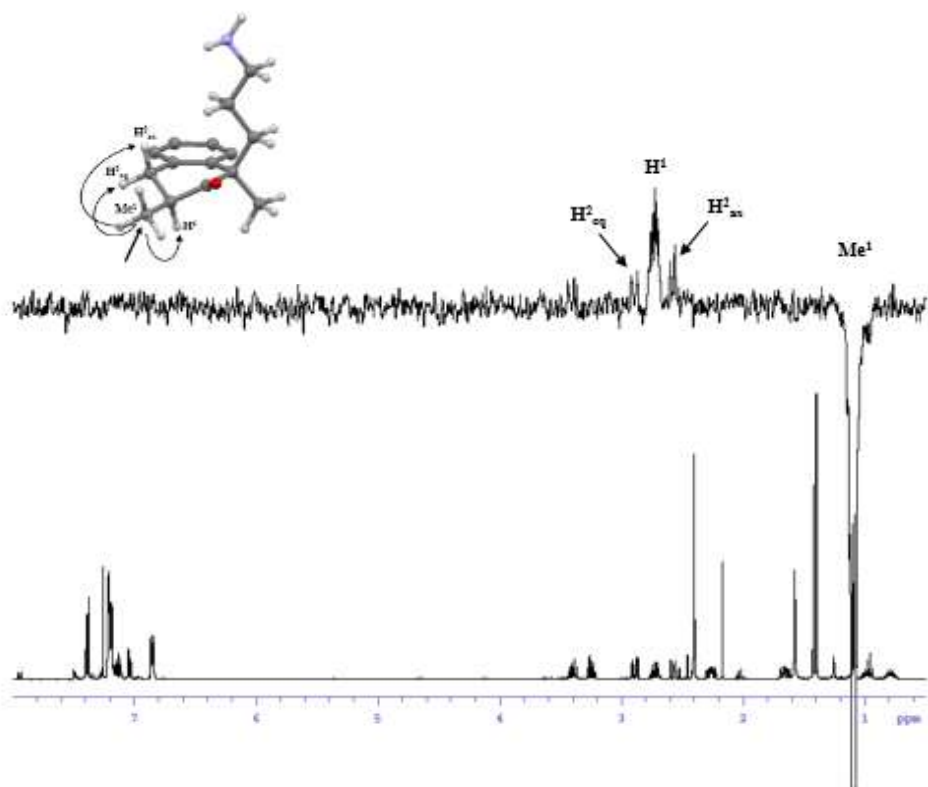


Chapter 3

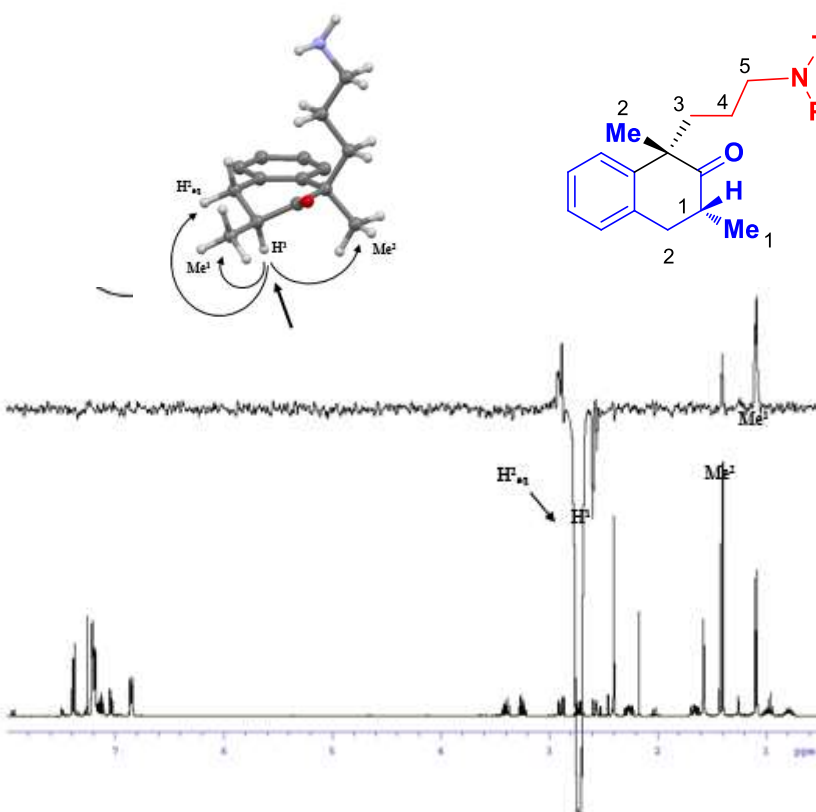
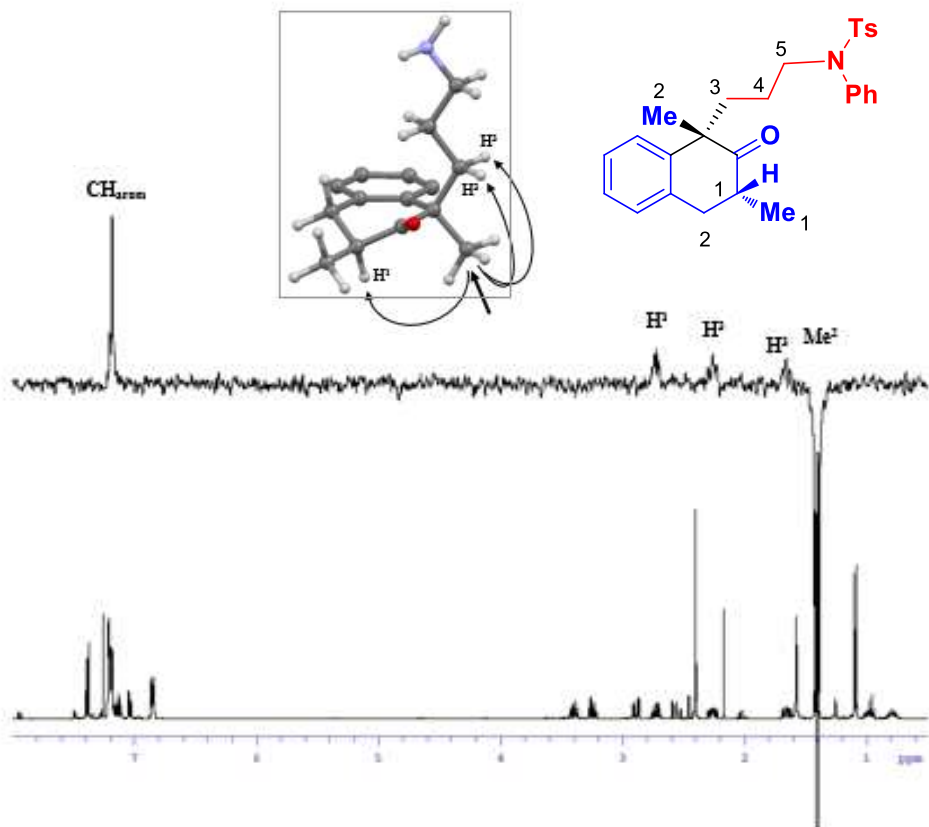




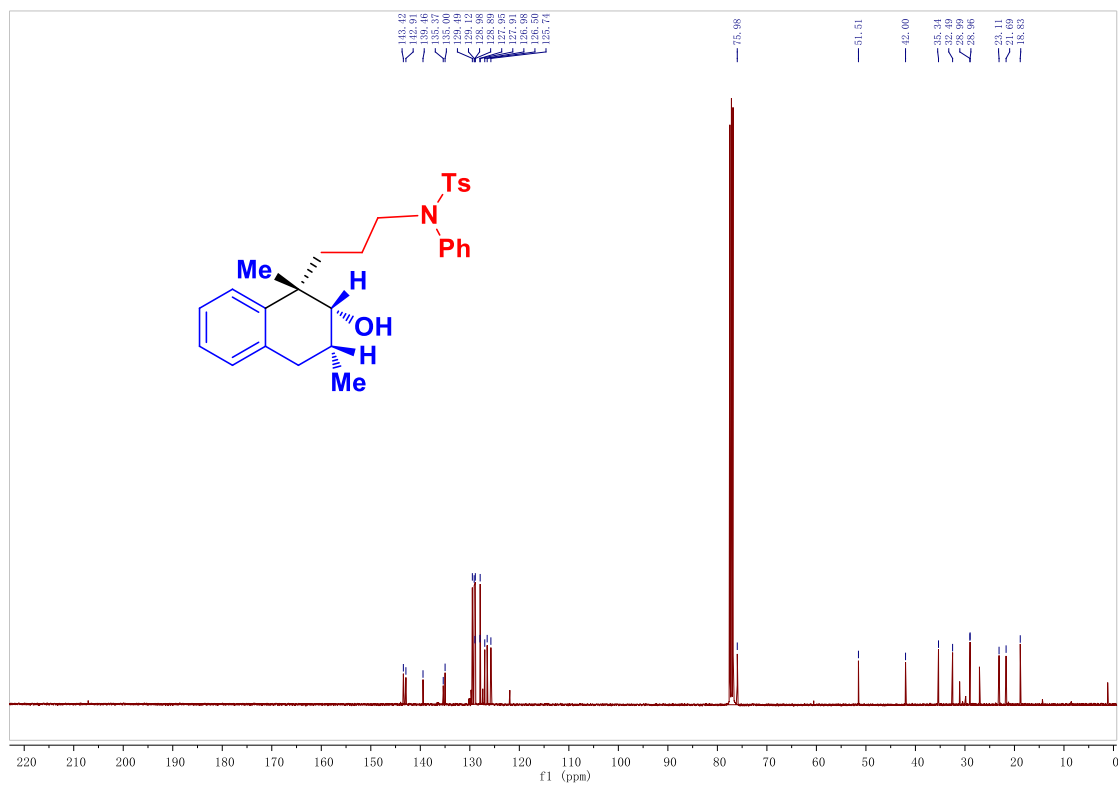
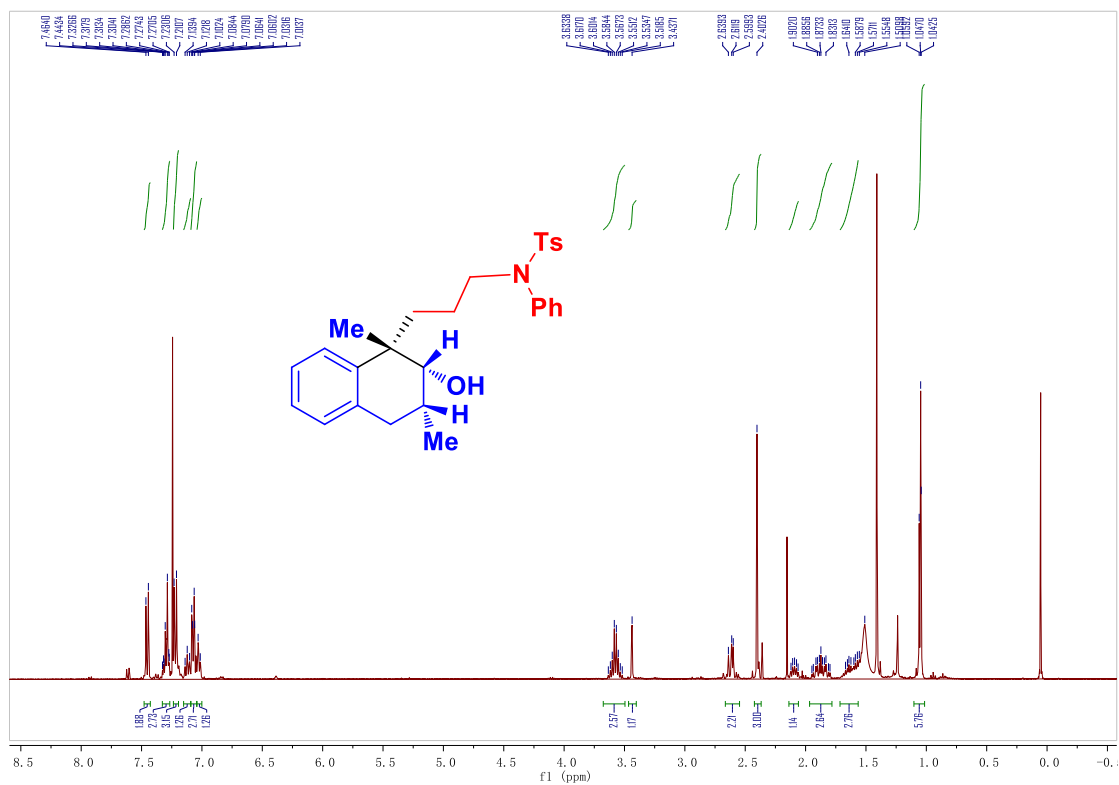
Gradient COSY (400 MHz, CDCl₃, 25 °C) expansion of the aliphatic region.



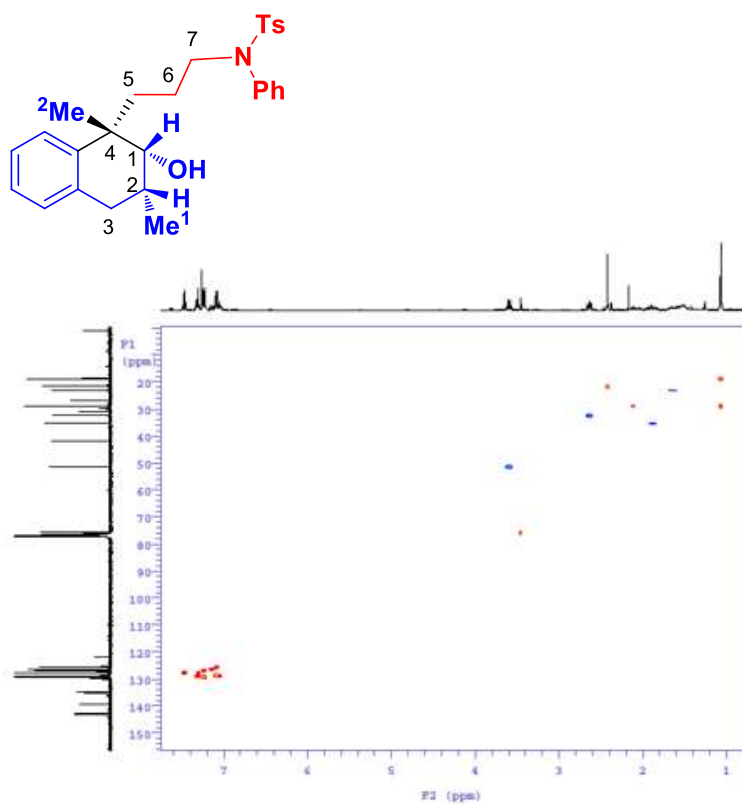
Monodimensional NOE experiment (400 MHz, CDCl₃, 25 °C) was performed by using a DPGSE-NOE sequence, with a 50 Hz pulse and a mixing time of 1.5 s.



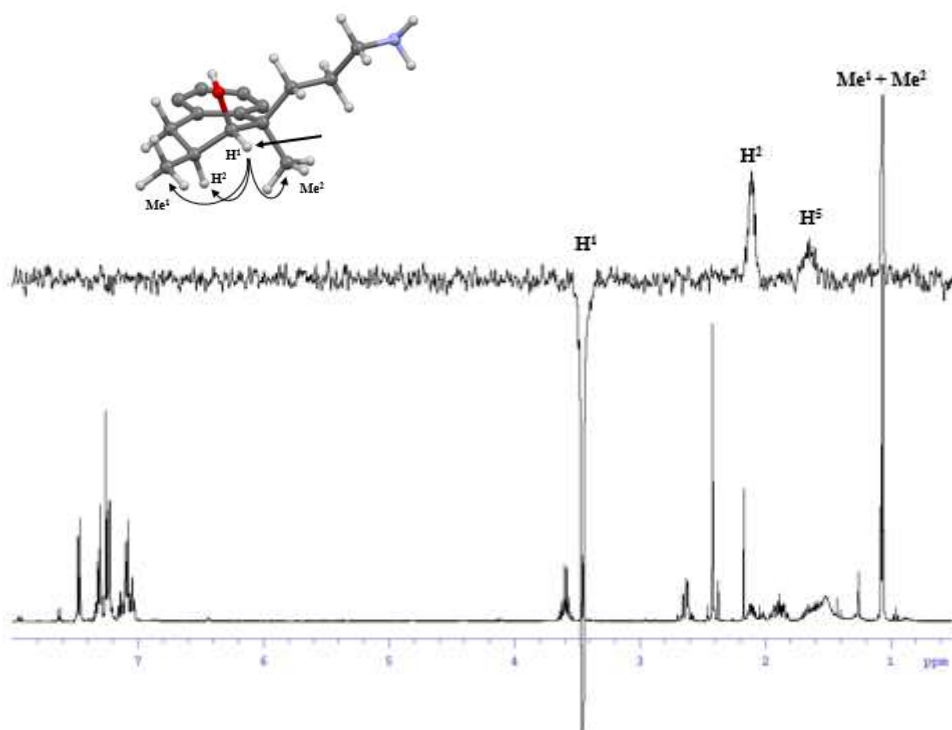
Chapter 3



Chapter 3



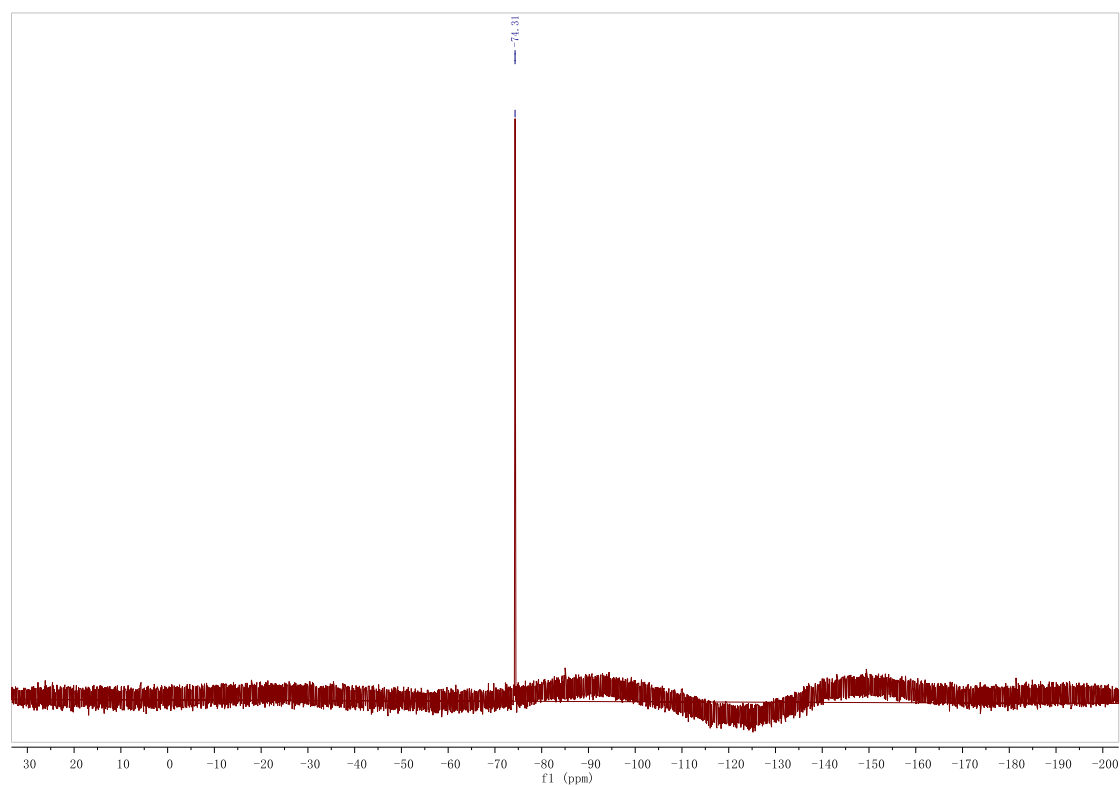
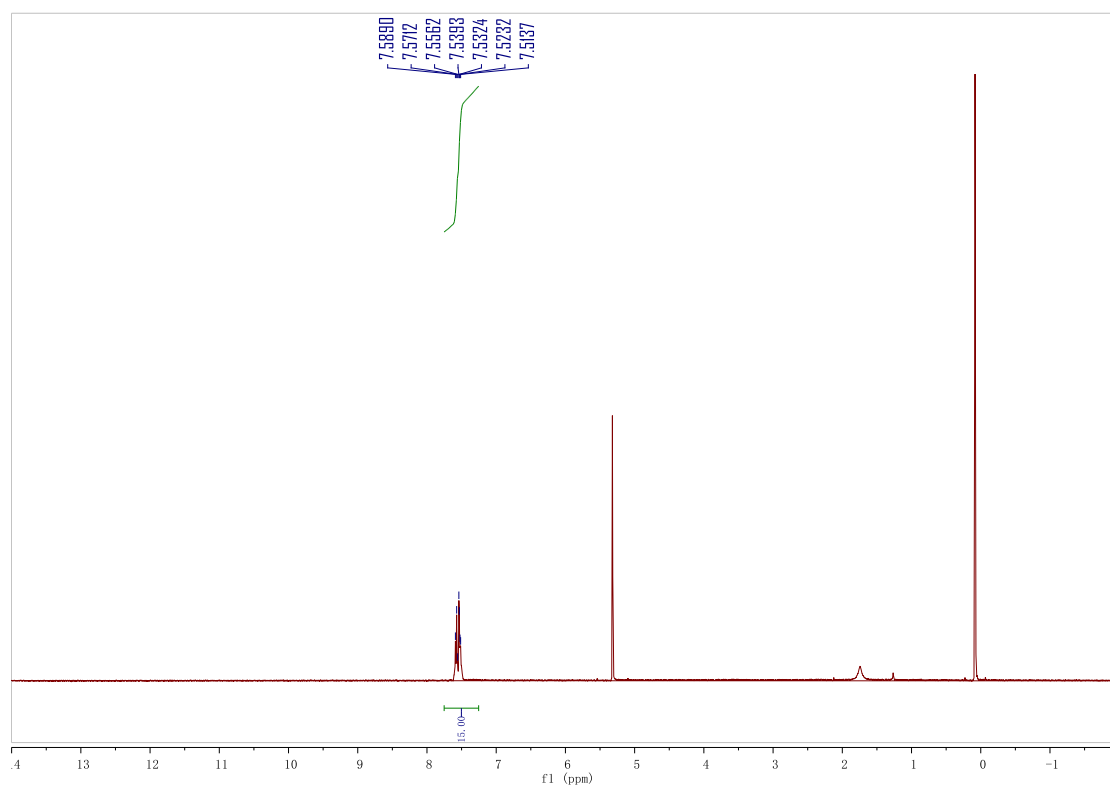
Gradient HSQC (400 MHz, CDCl₃, 25 °C)



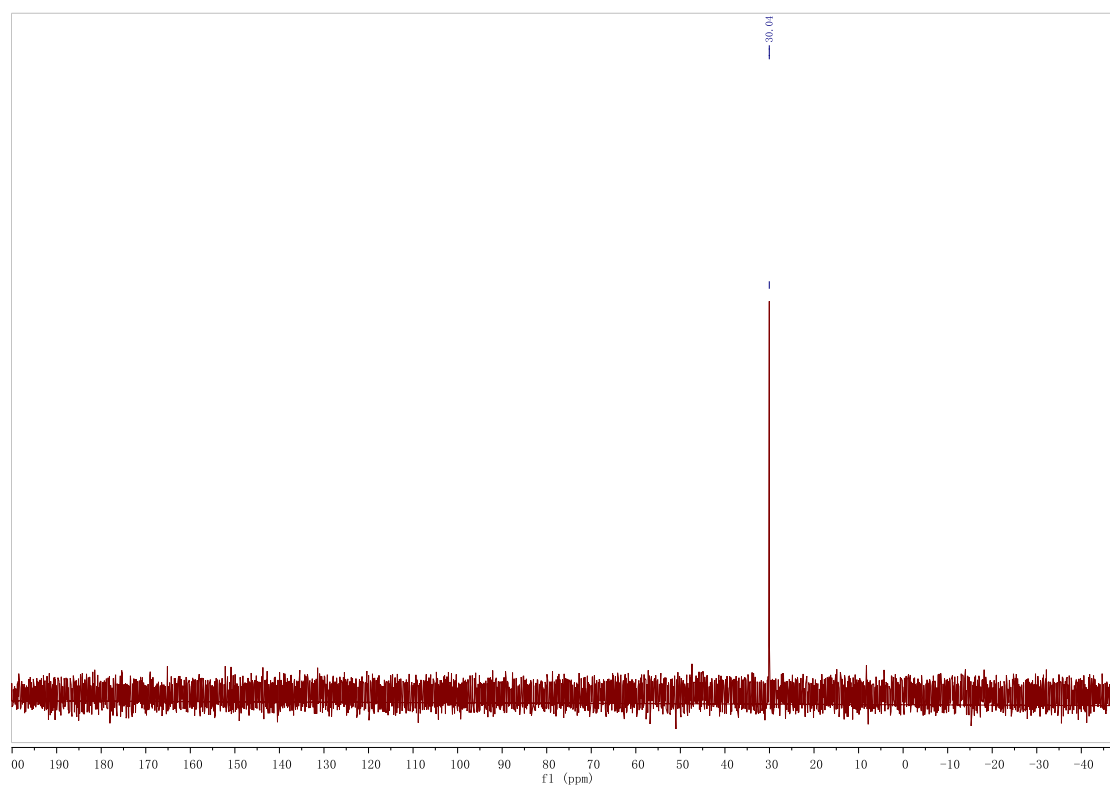
Monodimensional NOE experiment (400 MHz, CDCl₃, 25 °C) was performed by using a DPGSE-NOE sequence, with a 50 Hz pulse and a mixing time of 1.5 s.

Chapter 3

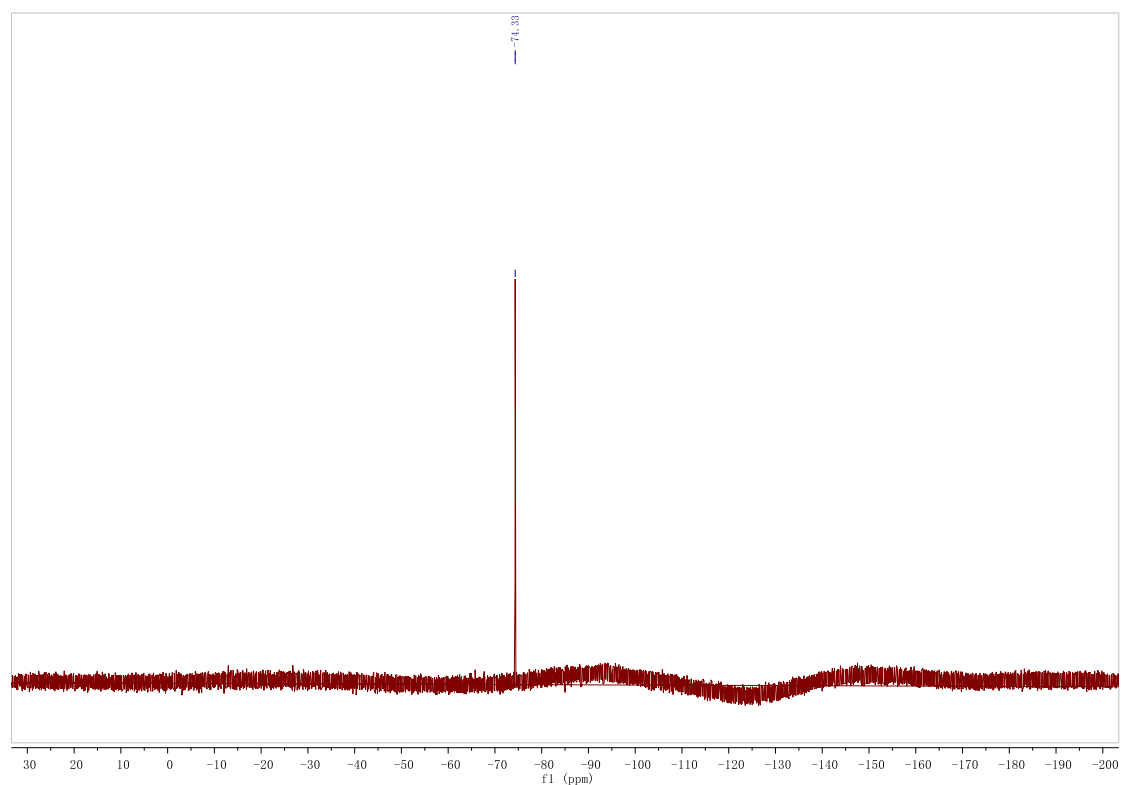
PPh₃AuTFA



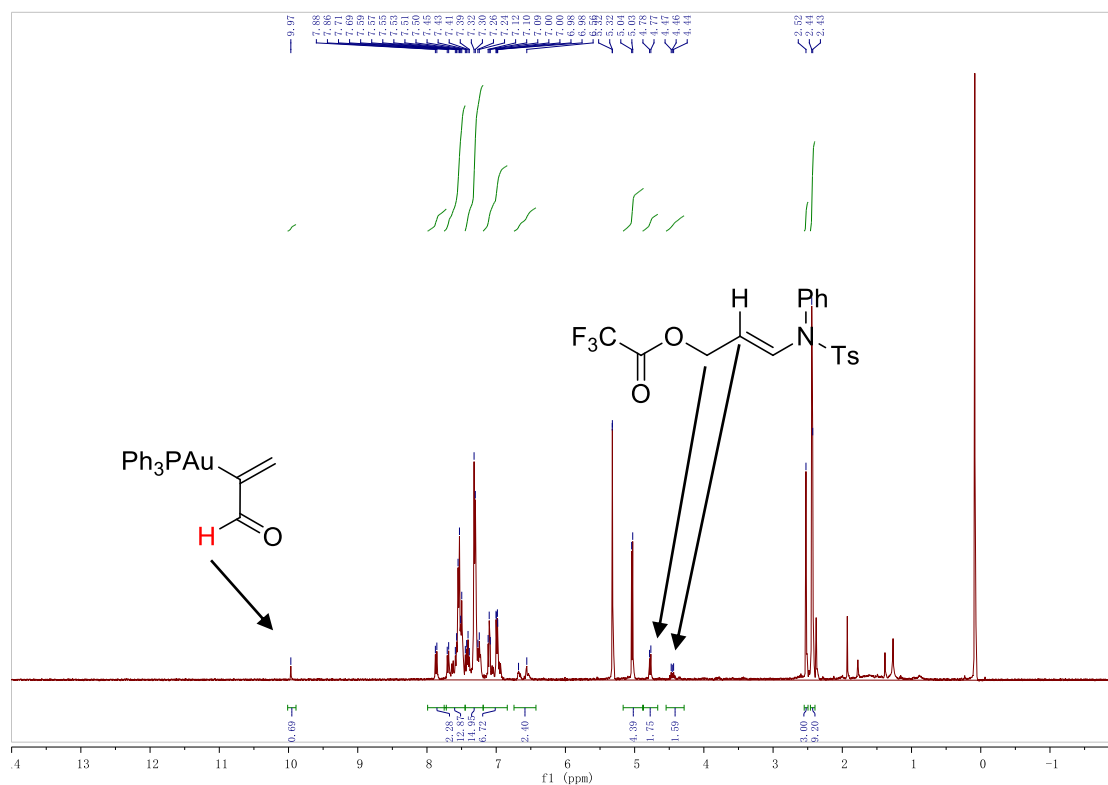
PPh₃AuTFA



PPh₃AuTFA(10mol%)+Naphthol (¹⁹F-NMR)



PPh₃AuTFA(10mol%)+Naphthol (H-NMR)

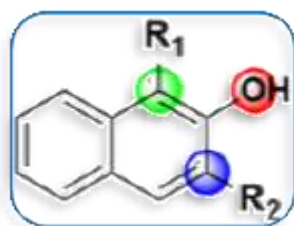


References

- [1] a) T. Oguma, T. Katsuki, *J. Am. Chem. Soc.* 2012, 134, 20017-20020. b) Y. Zhang, Y. Liao, X.hua Liu, X. Xu, L. Lin, X. Feng, *Chem. Sci.*, 2017, 8, 6645–6649. c) J. Nan, J. Liu, H. Zheng, Z. Zuo, L. Hou, H. Hu, Y. Wang, X. Luan, *Angew. Chem. Int. Ed.* 2015, 54, 2356 -2360.
- [2] a) Y. Liu, A. De Nisi, A. Cerveri, M. Monari, M. Bandini, *Org. Lett.* 19, 19, 5034-5037. b) M. Jia, G. Cera, D. Perrotta, M. Monari, Marco Bandini, *Chem. Eur. J.* 2014, 20, 9875-9878.
- [3] a) M. Preisenberger, A. Schier and H. Schmidbaur, *J. Chem. Soc., Dalton Trans.*, 1999, 1645–1650; b) Z.S Zhang, S. Edward; P. Gus J, Colgate, Sam O., *Acta Crystallographica, Section C: Crystal Structure Communications*, 1988, vol. 44, p. 2197 – 21

Conclusion

Gold catalysis has grown up to a greatly vital methodology on the organic synthesis which provides various access to new various natural compounds and pharmaceutical candidates. Being an unique Lewis acid, Gold catalyst makes great contribution via coordinating and activating electron rich functional group such as alkyne, alkene and allene. Based on this character, our group has started to applied gold catalysis into dearomatization of arene compounds which are abundant, economic and easy-obtained 2D molecules in nature. In conjunction with the experience on the dearomatization of indol derivatives in our group, we started to conquer another challenging work of dearomatization on naphthol derivatives under the background of transferring the 2D molecule to 3D molecule which will greatly increase the selectively potential application in the pharmaceutical.

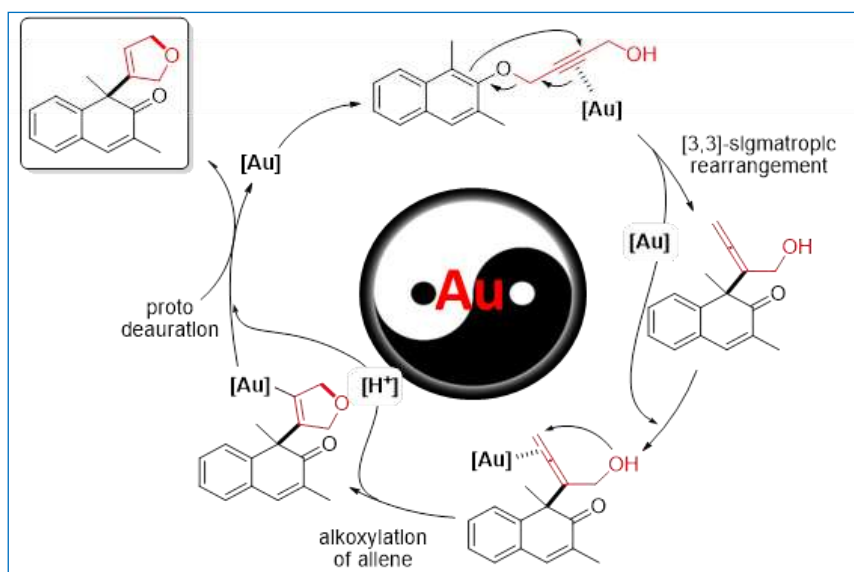
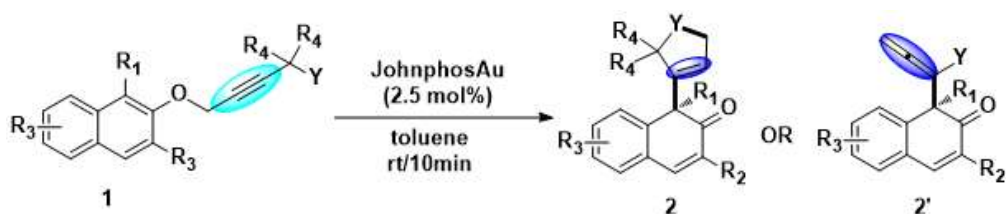


Scheme 1

However, numerous of challenge stands in front of us such as siteselectivity, stereoselectivity, enantioselectivity and suitable electrophile. For naphthol molecule, there are three nucleophiles including C1, hydroxyl group and C3 (Scheme1).

So firstly, to figure out this problem, we designed the substrate 1a as model substrate which expel the hydroxyl group nucleophile firstly. Using JohnphosAuSbF₆ as catalyst, the aimed 3D product 2a was obtained via [3,3]-propargylic Claisen rearrangement. Then several ligand, counter anion, and solvent were tested (scheme 1). With the optimised condition in hand, we expanded the scope of substrate. A wide range of substrates bearing an EDG or an EWG on the aromatic ring gave the corresponding 3D product in good yield and selectivity. Moreover, we also proposed

the catalytic mechanism (**Scheme 2**). A computational investigation strongly proved the whole step-wise reaction mechanism.



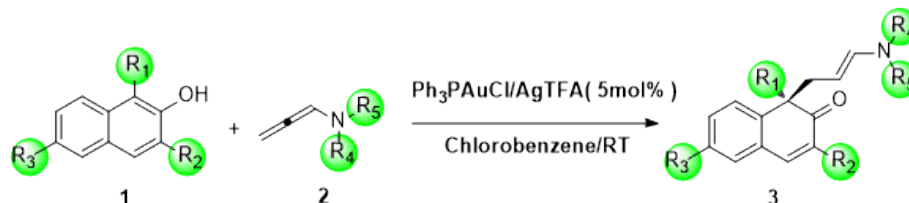
Scheme 2

In the meantime, chiral ligand was applied to achieve moderate enantioselectivity (65% ee). Eventhough the results were promising, there were still several drawbacks in this work such as when steric substituents were introduced to C1, dearomatized dimer product would be given.

Next, to conquire above problem and more fuctional group could be introduced, the intermolecular dearomatization came into our horizon even more nucleophiles get into the competence. However, on the other hand, it will also be more efficient as the substrates are easy to be obtained and decorated while more fuctional groups could also be introduced into the aimed 3D product.

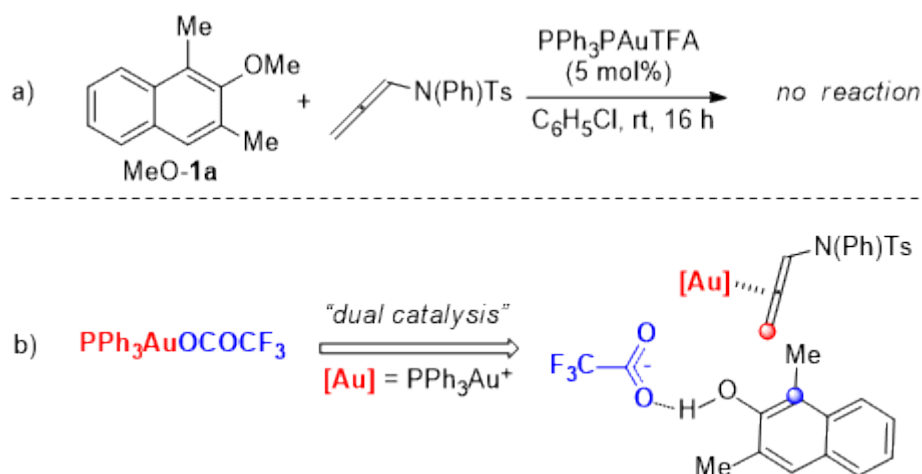
In this imaginaton, allenamide was chosed as the electrophile since its electron-rich characteristic. And allenamide including hetero-atom is also easy to be edited by

adding numerous of valued functional group. Fortunately, this idea came true via using $\text{Ph}_3\text{PAuCl}/\text{AgTFA}$ as in situ catalyst in chlorobenzene and this condition was also proved the best condition(**Scheme 3**).



Scheme 3

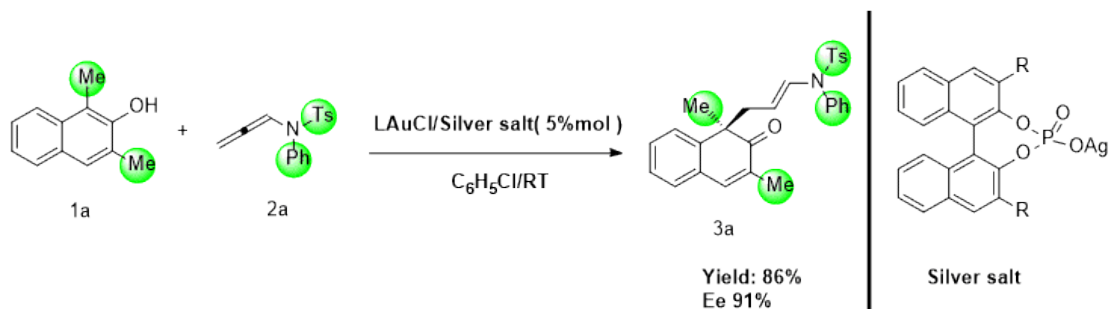
With this optimised condition, the functionalized tolerance was examined. The results showed that either EDG or EWG was introduced on the substrates, they did not affect the result. And even steric bulky substituents at C1 could still offer promising yield with high site-selectivity and stereoselectivity.



Scheme 4

In this work, counter anion was also proved great vital in catalysis process by doing control experiment (Scheme 4). TFA^- also needs to activate the hydroxyl group by removing proton and control the space position by stabilizing $\text{Au}(\text{I})$ so that provide the precise C1 reacting products and *Z*-isomer. At last, application experiment of product 3 was also carried out via hydrogenation and proved very well.

Being same with our previous project, a quarter chiral carbon center was constructed. However, to obtain high enantioselectivity via gold catalysis is a very huge challenge



Scheme 5

since the linear coordination version with electron-rich functional group and nucleophile can only attack the electrophile from back face which make it more difficult. Simply adjusting the ligand of gold could not offer promising enantioselectivity. To solve this problem, chiral phosphoric acid silver salt came into our horizon. We proposed that chiral counter anion and gold ligand could provide a suitable chiral atmosphere without decreasing the yield. Fortunately after we decorated the counter anion with different substituents, high ee was achieved at last (Scheme 5). This work is going to be finished and submitted.